

University of São Paulo
Institute of Astronomy, Geophysics and Atmospheric Sciences

Mariana Fadigatti Picolo

**Atmospheric conditions observed during severe weather occurrences in the area
of the SOS-CHUVA project**

São Paulo
2018

Mariana Fadigatti Picolo

**Atmospheric conditions observed during severe weather occurrences in the area
of the SOS-CHUVA project.**

Dissertation submitted to the Department of
Atmospheric Sciences of the Institute of
Astronomy, Geophysics and Atmospheric
Sciences in partial fulfilment of the requirements
for the degree of Master of Science

Area: Meteorology

Advisor: Prof. Dr. Edmilson Dias de Freitas

São Paulo

2018

Acknowledgments

To my family, especially my mother for all the support through the execution of this work.

To Yohan, for the love, support and comprehension through this period.

To Prof. Edmilson for the opportunity, support, and suggestions during the development of this project.

To Jean, from MASTER, for providing the data used in this research.

To CAPES for the financial support during the first years of work.

SUMÁRIO

LIST OF FIGURES.....	VII
LIST OF TABLES.....	XXVIII
LIST OF ABBREVIATIONS.....	XXIX
RESUMO.....	XXX
ABSTRACT	XXXI
1 INTRODUCTION	32
1.1 OBJECTIVES.....	34
1.2 REGION OF STUDY	35
2 SEVERE CONVECTIVE STORMS	36
2.1 BASIC CONCEPTS	36
2.1.1 <i>Buoyancy</i>	36
2.1.2 <i>Stages of development</i>	36
2.1.3 <i>Thermodynamic structure</i>	37
2.1.4 <i>Thermodynamic indices</i>	38
2.1.5 <i>Vertical wind shear</i>	40
2.2 BIBLIOGRAPHIC REVISION.....	41
2.2.1 <i>Mesoscale definition</i>	41
2.2.2 <i>Synoptic scale processes</i>	42
2.3 BIBLIOGRAPHIC REVISION FOR SÃO PAULO	44
3 METHODOLOGY	51
3.1 EVENTS	52
4 RESULTS	55
4.1 STRONG SYNOPTIC FORCING	55
4.1.1 <i>Category 1a</i>	55

4.1.2 <i>Partial conclusions for category 1a</i>	138
4.1.3 <i>Category 1b</i>	141
4.1.4 <i>Partial conclusions for category 1 b</i>	202
4.2 CATEGORY 2	204
4.2.1 <i>December, 18, 2016</i>	204
4.2.2 <i>December, 25, 2016</i>	225
4.2.3 <i>February, 22</i>	244
4.2.4 <i>December, 28, 2016</i>	269
4.2.5 <i>Partial conclusion for category 2</i>	292
5 CONCLUSION AND FUTURE STUDIES	295
5.1 SUGGESTIONS TO FUTURE STUDIES	298
6 REFERENCES	299

LIST OF FIGURES

Figure 2-1: Spatial and time scales of process that occurs in microscale and mesoscale. From Orlandi (1975).	42
Figure 4-1: Water vapor channel images at 00:00 UTC (a), and 12:00 UTC (b) for December, 3 rd , 2016.	56
Figure 4-2: Infrared satellite images at 00:00 UTC (a), and 06:00 UTC (b) for December, 03 rd , 2016.....	57
Figure 4-3: Infrared enhanced temperature satellite images at 09:30 UTC (a), 12:30 UTC (b), 14:30 UTC (c), 15:00 UTC (d), 16:30 UTC (e), 19:30 UTC (f), 23:30 UTC (g), 2:00 UTC (h.) for December, 03 rd , 2016.	57
Figure 4-4: IPMET radar reflectivity at 09:00 UTC (a), 10:30 UTC (b), 14:00 UTC (c), and 15:00 UTC (d) for December, 03 rd , 2016.).	59
Figure 4-5: São Roque (left) and Campinas (right) radar reflectivity at 16:00 UTC (a), 17:20 UTC (b), and 18:30 UTC for December, 03 rd , 2016.....	61
Figure 4-6: Streamline and isotachs ($m s^{-1}$) at 200 hPa at 00:00 UTC (a) and 12:00 UTC (b), mass divergence ($10^{-4} s^{-1}$) at 06:00 UTC (c), for December, 03, 2016.).....	63
Figure 4-7: Geopotential height and vorticity at 500 hPa, 12:00 UTC (a), and vorticity advection at 500 hPa, 12:00 UTC (b).	64
Figure 4-8: Streamlines and relative humidity at 850 hPa at 12:00 UTC (a) and 15:00 UTC (b).	64
Figure 4-9: Temperature advection at 850 hPa at 06:00 UTC (a), and 12:00 UTC (b) for December, 03 rd , 2016.	64

Figure 4-10: Mean sea level pressure (hPa) and wind (m s^{-1}) at 12:00 UTC (a), and 18:00 UTC (b) for December, 3 rd , 2016.....	65
Figure 4-11: Water vapor mixing ratio (g kg^{-1}) and wind (m s^{-1}) at 00:00 UTC (a), 03:00 UTC (b), 06:00 UTC (c), 09:00 UTC (d), 12:00 UTC (e), 15:00 UTC (f), 18:00 UTC (g), and 21:00 UTC (h) for December, 03 rd , 2016.....	66
Figure 4-12: Moisture divergence ($\text{g kg}^{-1} \text{ s}^{-1}$) at 12:00 UTC for December, 03, 2016.....	68
Figure 4-13: CAPE (J kg^{-1}) at 12:00 UTC (a), 15:00 UTC (b), 18:00 UTC (c), and 21:00 UTC (d) for December, 03 rd , 2016.....	69
Figure 4-14: CIN at 00:00 UTC (a), 09:00 UTC (b), 10 UTC (c), 11 UTC (d), 12:00 UTC (e) for December, 03 rd , 2016.	70
Figure 4-15: LI from GFS(K) at 12:00 UTC (a), 12:00 UTC (b) for December, 03 rd , 2016. ..	71
Figure 4-16: 700-500 hPa lapse rate at 00:00 UTC (a), 12:00 UTC (b), and 12:00 UTC (c), for December, 03, 2016.	72
Figure 4-17: CAPE from a surface parcel at 12:00 UTC (a), and at 12:00 UTC, for December, 03, 2016.....	73
Figure 4-18: Vertical cross section of relative humidity at 23.0°, at 00:00 UTC (a), 03:00 UTC (b), 06:00 UTC (c), 09:00 UTC (d), 12:00 UTC (e), 12:00 UTC (f), for December, 03, 2016.....	74
Figure 4-19: Vertical cross section of wind at 23.0° from BRAMS, at 00:00 UTC (a), 03:00 UTC (b), 06:00 UTC (c), 09:00 UTC (d), 12:00 UTC (e), 12:00 UTC (f) 18:00 UTC (g), and 21:00 UTC (h), for December, 03, 2016.	75
Figure 4-20: Vertical cross section of wind at 23.0° from GFS, at 12:00 UTC (a), 15:00 UTC (b), for December 03, 2016.....	77

Figure 4-21: Automatic surface station which recorded wind gust above 15 ms^{-1} , for December, 03, 2016.	78
Figure 4-22: Precipitation (mm), wind gust (ms^{-1}), and temperature ($^{\circ}\text{C}$) at stations A701 (a) and (b), A711 (c) and (d), A715 (e) and (f), A725 (g) and (h), A726 (i) and (j), A737 (k) and (l), A739 (m) and (n), A741 (o) and (p).	79
Figure 4-23: Infrared satellite images for January 15 at 00:00 UTC (a), 09:00 UTC (b), 18:00 UTC (c), and 22 UTC (d); January, 16 at 12:00 UTC (e), and 18:00 UTC (f); January, 17 at 12:00 UTC (g), and 18:00 UTC (h).	82
Figure 4-24: Enhanced infrared satellite images for January, 15 at 15:00 UTC (a), 16:30 UTC (b), 17:00 UTC (c), 17:30 UTC (d), 18:30 UTC (e), 20:30 UTC (f), 22:00 UTC (g); January, 16 at 00:00 UTC (h), 02:30 UTC (i), 09:00 UTC (j), 11:00 UTC (l), 18:00 UTC (m), 19:00 UTC (n), 20:30 UTC (o), 23:30 UTC (p); January, 17 at 05:00 UTC (r), 17:00 UTC (s).	85
Figure 4-25: Radar images from the São Roque radar at January, 15 at 15:00 UTC (a), 16:20 UTC (b), 17:10 UTC (c), 17:50 UTC (d), 19:00 (e), 20:20 UTC (f), 21:30 UTC (g), 23:50 UTC (h); January, 16, at 04:50 UTC (i), 08:00 UTC (j), 10:30 UTC (l), 15:00 UTC (m), 16:20 UTC (n), 17:40 UTC (o), 20:20 UTC (p), 21:10 UTC (q), 23:30 UTC (r), 23:50 UTC (s); January, 17 at 06:10 UTC (t), 12:10 UTC (u).	88
Figure 4-26: Streamlines and isotachs at 200 hPa at 00 and 12:00 UTC for January, 15 (a), (b), January, 16, (c), (d), January, 17 (e), (f).	92
Figure 4-27: Wind divergence at 200 hPa for January, 15 at 21:00 UTC (a), January, 16 at 00:00 UTC (b), and 06:00 UTC (c).	93

Figure 4-28: Streamlines, geopotential height and vorticity at 500 hPa for January, 15 th , at 00:00 UTC (a), 06:00 UTC (b), 12:00 UTC (c), 18:00 UTC (d).....	94
Figure 4-29: Streamlines, geopotential height and vorticity at 500 hPa for January, 16, at 00:00 UTC (a), 06:00 UTC (b), 12:00 UTC (c), 18:00 UTC (d).....	95
Figure 4-30: Streamlines and relative humidity at 850 hPa at January, 15 at 00:00 UTC (a), 06:00 UTC (b), 12:00 UTC (c), 18:00 UTC (d).....	96
Figure 4-31: Streamlines and relative humidity at 850 hPa at January, 16 th at 00:00 UTC (a), 06:00 UTC (b), 12:00 UTC (c), 18:00 UTC (d).....	97
Figure 4-32: Streamlines and relative humidity at 850 hPa at January, 17 th at 006:00 UTC (a), 12:00 UTC (b).....	97
Figure 4-33: Temperature advection at 850 hPa on January, 15 at 00:00 UTC (a), 06:00 UTC (b), 12:00 UTC (c), 18:00 UTC (d).....	98
Figure 4-34: Temperature advection at 850 hPa on January, 16 at 00:00 UTC (a), 06:00 UTC (b), 12:00 UTC (c), 18:00 UTC (d).....	99
Figure 4-35: Mean sea level pressure and wind on January, 15 th at 00:00 UTC (a), 06:00 UTC (b), 12:00 UTC (c), 18:00 UTC (d).....	99
Figure 4-36: Mean sea level pressure and wind on January, 16 th at 00:00 UTC (a), 06:00 UTC (b), 12:00 UTC (c), 18:00 UTC (d).....	100
Figure 4-37: CAPE at 12:00 UTC (a), 15:00 UTC (b), 18:00 (c); LI at 12:00 (d), 15:00 (e), 18:00 (f); 700-500 hPa lapse rate at 12:00 UTC (g), 15:00 UTC (h), 18:00 UTC (i) from GFS for January, 15 th , 2017.	102
Figure 4-38: CAPE at 12:00 UTC (a), 15:00 UTC (b), LI at 12:00 (c), 15:00 (d); 700-500 hPa lapse rate at 12:00 UTC (e), 15:00 UTC (f) from GFS for January, 16 th , 2017.....	103

Figure 4-39: CIN from GFS at January, 15 th (a), and January, 16 th (b), at 12:00 UTC.	104
Figure 4-40: Wind speed and direction, temperature and dew point temperature, temperature and relative humidity at stations A701 (a), (b), (c), A712 (d), (e), (f), A728 (g), (h), (i), A740 (j), (l), (m), A746 (n), (o), (p), A755 (q), (r).	107
Figure 4-41: Wind speed and direction and temperature, dew point temperature and relative humidity from METAR at stations SBMT (a), (d), SBSP (b), (e), SBGR (c), (f).	108
Figure 4-42: Wind speed and direction (a) and temperature, dew point temperature and relative humidity (b) from METAR at station SBTA.	109
Figure 4-43: Infrared images for South America at 00:00 UTC (a), 06:00 UTC (b), 12:00 UTC (c), 18:00 UTC (d) on February 24.	110
Figure 4-44: Infrared satellite images for February, 24 at 16:35 UTC (a), 17:35 UTC (b), 18:35 UTC (c), 19:35 UTC (d), 20:35 UTC (e), 21:35 UTC (f), 22:35 UTC (g), and 23:35 UTC (h).	111
Figure 4-45: Enhanced infrared satellite images for February, 24 at 19:00 UTC (a), and 21:00 UTC (b).	112
Figure 4-46: São Roque radar images from February, 24 th at 14:30 UTC (a), 15:30 UTC (b), 16:30 UTC (c), 17:40 UTC(d), 18:00 UTC (e), 19:10 UTC (f), 19:50 UTC (g), 20:10 UTC (h), 20:20 UTC (i), 21:20 UTC (j), 22:20 UTC (k), and 23:00 UTC (l).	114
Figure 4-47: Streamlines and isotach (m s^{-1}) for February, 24 at 00:00 UTC (a), 06:00 UTC (b), 12:00 UTC (c), and 18:00 UTC (d).	117
Figure 4-48: Mass divergence for February, 24 th at 00:00 UTC (a), 06:00 UTC (b), 12:00 UTC (c), and 18:00 UTC (d).	118

Figure 4-49: Geopotential height (gpm), vorticity ($1 \times 10^{-5} \text{ s}^{-1}$) and streamlines at 500 hPa from February, 24 th at 00:00 UTC (a), 06:00 UTC (b), 12:00 UTC (c), and 18:00 UTC (d).	119
Figure 4-50: Streamlines and relative humidity, streamlines and temperature at 850 hPa for February, 24 at 00:00 UTC (a) and (b), 06:00 UTC (c) and (d), 12:00 UTC (e) and (f), and 18:00 UTC (g) and (h).	120
Figure 4-51: Temperature advection (K s^{-1}) at 850 hPa for February, 24 at 18:00 UTC.	122
Figure 4-52: Mean sea level pressure (hPa) and winds (m s^{-1}) for February, 24 th at 00:00 UTC (a), 06:00 UTC (b), 12:00 UTC (c), and 18:00 UTC (d).	122
Figure 4-53: Sounding (a) and hodograph (b) for February, 24 th at 12:00 UTC. (source: http://weather.uwyo.edu/upperair/sounding.html).	123
Figure 4-54: Vertical variation of water vapor mixing ratio (g kg^{-1}) (a), relative humidity (%) (b), and equivalent potential temperature (K) (c) for February, 24 th at 12:00 UTC.	124
Figure 4-55: CAPE from BRAMS for February, 24 th at 06:00 UTC (a), 10:00 UTC (b), 11:00 UTC (c), 12:00 UTC (d), 15:00 UTC (e), and 16:00 UTC (f).	126
Figure 4-56: CAPE from GFS at 12:00 UTC (a), and 15:00 UTC (b) for February, 24, 2017.	128
Figure 4-57: CIN for a surface parcel at 12:00 UTC, for February, 24, 2017.	128
Figure 4-58: LI from GFS at 12:00 UTC (a), and at 12:00 UTC (b) for February, 24, 2017.	128
Figure 4-59: 700-500 hPa lapse rate from GFS at 12:00 UTC (a), and 15:00 (b), for February, 24, 2017.	129

- Figure 4-60: Vertical cross section of water vapor mixing ratio at 12:00 UTC (g kg^{-1}) (a), relative humidity at 12:00 UTC (%) (b), and 18:00 UTC (c), and wind at 12:00 UTC (ms^{-1}) (d) from BRAMS for February, 24th 130
- Figure 4-61: Vertical cross section of relative humidity (a) and winds (b) from GFS at 12:00 UTC for February, 24, 2017..... 131
- Figure 4-62: Moisture divergence for February, 24th at 14:00 UTC (a), 15:00 UTC (b), and 16:00 UTC (c). 132
- Figure 4-63: Water vapor mixing ratio and wind for February, 24 at 00:00 UTC (a), 03 UT (b), 06:00 UTC (c), 09:00 UTC (d), 12:00 UTC (e), 15:00 UTC (f), 18:00 UTC (g), and 21:00 UTC (h). 133
- Figure 4-64: Wind speed and direction (a), temperature and dew point temperature (b), temperature and relative humidity (c) for station A701, temperature and dew point temperature (d), and temperature and relative humidity (e) for station A755 for February, 24, 2017..... 136
- Figure 4-65: Wind speed (m s^{-1}) and direction (degrees), temperature, dew point temperature and relative humidity from METAR for stations SBMT (a), (d), SBSP (b), SBGR (c), (f), for February, 24th. 136
- Figure 4-66: Precipitation (mm) and wind gust (ms^{-1}) for February, 24th at stations A701 (a), A705 (b), A707 (c), A711 (d), A713 (e), A714 (f), A716 (g), A718 (h), A725 (i), A726 (j), A728 (l), A741 (m), A746 (n), and precipitation (mm) at station A755 (o). 137
- Figure 4-67: Infrared satellite image for January, 07 at 00:00 UTC (a), and 12:00 UTC (b). 142

Figure 4-68: Enhanced infrared satellite image for January, 07 at 16:30 UTC (a), 17:30 UTC (b), 18:30 UTC (c), 19:30 UTC (d), 20:30 UTC (e), 21:30 UTC (f), 22:30 UTC (g), 23:30 UTC (h).....	143
Figure 4-69: São Roque radar images for January, 07 at 17:00 UTC (a), 1740 (b), 1750 UTC (c), 18:00 UTC (d), 18:40 UTC (e), 1850 UTC (f), 20:00 UTC (g), 20:20 UTC (h), 2030 UTC (i), 22 UTC (j).	145
Figure 4-70: Streamlines and isotach (m s^{-1}) at 200 hPa for January, 07 th at 00:00 UTC (a), 06:00 UTC (b), 12:00 UTC (c), and 18:00 UTC (d).....	147
Figure 4-71: Wind divergence at 200 hPa for January, 07 at 00:00 UTC (a), 12:00 UTC (b), and 18:00 UTC (c).	148
Figure 4-72: Geopotential, vorticity and streamlines at 500 hPa for January, 07 at 00:00 UTC (a), 06:00 UTC (b), 12:00 UTC (c), and 18:00 UTC (d).	149
Figure 4-73: Streamlines and relative humidity (%) at 850 hPa for January, 07 th at 00:00 UTC (a), 06:00 UTC (b), 12:00 UTC (c), and 18:00 UTC (d).	150
Figure 4-74: Mean sea level pressure (hPa) and wind (m s^{-1}) for January, 07 th at 00:00 UTC (a), 06:00 UTC (b), 12:00 UTC (c), and 18:00 UTC (d).	151
Figure 4-75: CAPE (J kg^{-1}) from GFS for January, 07 th at 12:00 (a), and 15:00 UTC (b). ...	152
Figure 4-76: CIN (J kg^{-1}) from GFS for January, 07 th at 12:00 (a).	152
Figure 4-77: LI (K) from GFS for January, 07 th at 12:00 (a), and 15:00 UTC (b).....	153
Figure 4-78: 700-500 hPa lapse rate ($1 \times 10^{-3} \text{ K gpm}^{-1}$) from GFS at 12:00 UTC (a), and 15:00 UTC (b), for January, 07.....	154

Figure 4-79: Vertical cross section at 23.5°S of latitude from GFS of relative humidity at 12:00 UTC (a), and 12:00 UTC (b), and of winds at 12:00 UTC (c), and 12:00 UTC (d), for January, 07, 20171.....	154
Figure 4-80: Wind speed and direction, temperature and dewpoint temperature, temperature and relative humidity for January, 07 at station A701 (a), (b), (c); A712 (d), (e), (f); A713 (g), (h), (i); A746 (j), (k), (l).	156
Figure 4-81: Temperature (°C) and dewpoint temperature (°C) (a), temperature (°C) and relative humidity (%) (b), precipitation (mm) (c) at station A755 for January, 07 th	158
Figure 4-82: Wind gust (m s^{-1}) and precipitation (mm) for January, 07 th at station A701 (a), A728 (b), and A740 (c).	158
Figure 4-83: Wind speed and direction (a), relative humidity, temperature and dew point temperature from METAR at station SBSP (a), (b), and SBMT (c), (d), for January, 07 th , 2017.....	159
Figure 4-84: Infrared images for South America for January, 30 th at 12:00 UTC (a), and 15:00 UTC (b).	160
Figure 4-85: Visible channel satellite image for January, 30 th at 14:45 UTC.....	160
Figure 4-86: Infrared satellite images for January, 30 th , at 06:38 UTC (a), 16:08 UTC (b), 17:08 UTC (c), 17:38 UTC (d), 17:45 UTC (e), 18:38 UTC (f), 19:08 UTC (g), 19:38 UTC (h).	161
Figure 4-87: São Roque radar images for January, 30 th at 15:00 UTC (a), 16:00 UTC (b), 16:30 UTC (c), 17:00 UTC (d), 17:20 UTC (e), 17:30 UTC (f), 17:40 UTC (g), 18:00 UTC (h), 18:20 UTC (i), 18:40 UTC (j), 19:30 UTC (l), 19:40 UTC (m).	163

Figure 4-88: Streamlines and isotahcs at 200 hPa for January, 30 at 00:00 UTC (a), 06:00 UTC (b), 12:00 UTC (c), and 18:00 UTC (d).....	166
Figure 4-89: Wind divergence ($1 \times 10^{-4} \text{ s}^{-1}$) at 200 hPa for January, 30 th at 06:00 UTC (a), 09:00 UTC (b), 15:00 UTC (c), and 18:00 UTC (d).....	166
Figure 4-90: Geopotential (gpm) and vorticity ($1 \times 10^{-5} \text{ s}^{-1}$) at 500 hPa for January, 30 th at 00:00 UTC (a), 06:00 UTC (b), 12:00 UTC (c), 18:00 UTC (d).....	167
Figure 4-91: Streamlines and relative humidity (%) at 850 hPa for January, 30 th at 00:00 UTC (a), 06:00 UTC (b), 12:00 UTC (c), and 18:00 UTC (d).	168
Figure 4-92: Temperature advection (K s^{-1}) at 850 hPa for January, 30 th at 09:00 UTC (a), 12:00 UTC (b), 15:00 UTC (c).	169
Figure 4-93: Mean sea level pressure and wind for January, 30 at 00:00 UTC (a), 06:00 UTC (b), 12:00 UTC (c), and 18:00 UTC (d).....	170
Figure 4-94: Sounding and hodograph for January, 30 th at 12:00 UTC (source: http://weather.uwyo.edu/upperair/sounding.html).....	171
Figure 4-95: Vertical variation of water vapor mixing ratio (g kg^{-1}) (a), relative humidity (%) (b), and equivalent potential temperature (K) (c).	172
Figure 4-96: CAPE from GFS at 12:00 UTC (J kg^{-1}) (a) and 15:00 UTC (b) for January, 30 th , 2017.....	173
Figure 4-97: CIN from GFS at 12:00 UTC for January, 30, 2017.	174
Figure 4-98: 700-500 hPa lapse rate from GFS at 12:00 UTC (a), and 15:00 UTC (b).....	174
Figure 4-99: LI from GFS at 12:00 UTC (J kg^{-1}) (a) and 15:00 UTC (b) for January, 30 th , 2017.....	174

Figure 4-100: Vertical cross section of relative humidity (a), and wind (b), at the latitude of 23.5°S, at 12:00 UTC, for January, 30, 2017.	175
Figure 4-101: Vertical cross section of relative humidity (%) at 12:00 UTC (a), and 15:00 UTC (b), vertical cross section of wind (m s^{-1}) at 12:00 UTC (c), and 15:00 UTC (d) for the latitude of 23.0°S, from GFS for January, 30 th	176
Figure 4-102: Wind speed and direction, temperature and dew point temperature, temperature and relative humidity for January, 30 at station A701 (a), (b), (c); A728 (d), (e), (f); A740 (g), (h), (i); A746 (j), (l), (m); A755 (n), (o), for January, 30 th , 2017.....	178
Figure 4-103: Wind speed, temperature, relative humidity and dew point temperature from METAR at station SBSP (a), (d), SBMT (b), (e), and SBGR (c), (f), for January, 30, 2017.....	179
Figure 4-104: Infrared satellite image for South America at 00:00 UTC (a), 12:00 UTC (b), 16:30 UTC (c), 18:00 UTC (d), for February, 06 th	181
Figure 4-105: Visible channel satellite image for the State of São Paulo at 14:08 UTC for February, 06 th	182
Figure 4-106: Infrared satellite images for the State of São Paulo at 00:38 UTC (a), 14:08 UTC (b), 14:45 UTC (c), 16:08 UTC (d), 16:35 UTC (e), 18:38 UTC (f), for February, 06 th , 2017.....	182
Figure 4-107: Enhanced infrared satellite images for the southeast region at 18:30 UTC (a), 19:30 UTC (b), 21:00 UTC (c), 23:00 UTC (d), for February, 06 th , 2017.	183
Figure 4-108: Radar images from the São Roque radar at 16:00 UTC (a), 17:00 UTC (b), 18:00 UTC (c), 19:30 TC (d), 19:40 UTC (e), 20:40 UTC (f), 21:10 UTC (g), 21:40 UTC (h), 22:00 UTC (i), 22:40 UTC (j), 23:00 UTC (l), 23:40 UTC (m).	185

Figure 4-109: Streamlines and isotachs at 200 hPa at 00:00 UTC (a), 12:00 UTC (b), for February, 06, 2017.	187
Figure 4-110: Geopotential height (gpm), vorticity ($1e-5 \text{ s}^{-1}$) and streamlines at 500 hPa at 00:00 UTC (a), 06:00 UTC (b), 12:00 UTC (c), 18:00 UTC (d) for February, 06 th	188
Figure 4-111: Streamlines and relative humidity (%) at 850 hPa at 00:00 UTC (a), 06:00 UTC (b), 12:00 UTC (c), 18:00 UTC (d) for February, 06 th	189
Figure 4-112: Mean sea level pressure (hPa), and wind (m s^{-1}) at 00:00 UTC (a), 06:00 UTC (b), 12:00 UTC (c), 18:00 UTC (d) for February, 06 th	190
Figure 4-113: CAPE from BRAMS at 12:00 UTC (a), and 15:00 UTC (b) for February, 06 th	192
Figure 4-114: CIN from BRAMS at 12:00 UTC for February, 06 th	192
Figure 4-115: CAPE from GFS at 12:00 UTC (a), and 15:00 UTC (b) for February, 06 th	192
Figure 4-116: CIN from GFS at 12:00 UTC for February, 06 th	193
Figure 4-117: LI from GFS at 12:00 UTC (a), and 15:00 UTC (b) for February, 06 th	193
Figure 4-118: 700-500 hPa from GFS at 12:00 UTC (a), and 15:00 UTC (b) for February, 06 th	193
Figure 4-119: Water vapor mixing ratio and wind at 00:00 UTC (a), 03:00 UTC (b), 06:00 UTC (c), 09:00 UTC (d), 12:00 UTC (e), 15:00 UTC (f), 18:00 UTC (g), 21:00 UTC (h) for February, 06 th	194
Figure 4-120: Vertical cross section from BRAMS of relative humidity at 12:00 UTC (a), 15 UTC (b), and of winds at 12:00 UTC (c), and 15:00 UTC (d) at 23.5 °S for February, 06 th	196

Figure 4-121: Vertical cross section from GFS of relative humidity at 12:00 UTC (a), 15 UTC (b), and of winds at 12:00 UTC (c), and 15:00 UTC (d) at 23.5 °S for February, 06 th ..	197
Figure 4-122: Wind speed and direction, temperature and dew point temperature, temperature and relative humidity at stations A701 (a), (b), (c), A728 (d), (e), (f), A740 (g), (h), (i) for February, 06 th	199
Figure 4-123: Temperature and dewpoint temperature (a), temperature and relative humidity (b) at station A755 for February, 06 th	200
Figure 4-124: Wind speed and direction, temperature, dewpoint temperature and relative humidity from METAR at stations SBMT (a), (b), SBSP (c), (d), SBGR (e), (f), SBTA (g), (h) for February, 06 th	201
Figure 4-125: Precipitation (mm) and wind gust (m s^{-1}) at station A701 for February, 06 th	202
Figure 4-126: Infrared image at 12:00 UTC.....	205
Figure 4-127: Satellite 1 km visible images, at 15:00 UTC (a), 16:00 UTC (b), 17:00 UTC (c), 17:30 UTC (d), 18:00 UTC (e), and 19:00 UTC (f).....	206
Figure 4-128: Infrared enhanced temperature satellite images at 18:00 UTC.....	207
Figure 4-129: Images from the São Roque radar at 16:00 UTC (a), 17:00 UTC (b), 17:20 UTC (c), 1730 (d), 1740 (e), 18:00 UTC (f), 18:20 UTC (g), 18:40 UTC (h), 19:10 UTC (i), and 2030 UTC (j).....	208
Figure 4-130: Streamlines and isotachs (m s^{-1}) at 200 hPa at 00:00 UTC (a), 06:00 (b), 12:00 UTC (c), and 18:00 UTC (d) for December, 18 th	211
Figure 4-131: Geopotential and vorticity (a), vorticity advection (b) at 500 hPa at 12:00 UTC.....	212

Figure 4-132: Streamlines and relative humidity (a), temperature advection at 850 (b) , for December, 18 th	212
Figure 4-133: Mean sea level pressure (hPa) and wind (m s^{-1}) at 12:00 UTC for December, 18 th	213
Figure 4-134: CIN from BRAMS at 12:00 UTC, for December, 18 th	214
Figure 4-135: CAPE from BRAMS at 12:00 UTC (a), and 15:00 UTC (b), for December, 18 th	214
Figure 4-136: CAPE from GFS at 12:00 UTC (a), and 15:00 UTC (b), for December, 18 th .	214
Figure 4-137: LI at 12:00 UTC (a), and 15:00 UTC (b).	215
Figure 4-138: CIN from GFS at 12:00 UTC, for December, 18 th	215
Figure 4-139: 700-500 hPa lapse rate from GFS at 00:00 UTC (a), and 12:00 UTC (b), for December, 18 th	215
Figure 4-140: Moisture divergence at 13 UTC (a), 14:00 UTC (b), 15:00 UTC (c), and 16:00 UTC (d).....	216
Figure 4-141: Water vapor mixing ratio and wind at 00:00 UTC (a), 03 UTC (b), 06:00 UTC (c), 09:00 UTC (d), 12:00 UTC (e), 15:00 UTC (f), 18:00 UTC (g), 21:00 UTC (h). ..	217
Figure 4-142: Vertical cross section of relative humidity from BRAMS at 23.5° at 12:00 UTC (a), and 15:00 UTC (b), for December, 18 th	219
Figure 4-143: Vertical cross section of wind from BRAMS at 23.5° at 12:00 UTC (a), 15:00 UTC (b), for December, 18 th	219

Figure 4-144: Vertical cross section from GFS at 23.5°S of relative humidity at 12:00 UTC (a), 15:00 UTC (b); winds at 12:00 UTC (c), and 15:00 UTC (d), for December, 18 th , 2016.....	220
Figure 4-145: Wind speed and direction, temperature and dew point temperature at stations A712 (a) and (b), A701 (c) and (d), A740 (e) and (f), A755 (g), , for December, 18 th .	222
Figure 4-146: Wind speed and direction from METAR at SBSP (a), SBMT (c); temperature, relative humidity, and dew point temperature at SBSP (b), and SBMT (d).	223
Figure 4-147: Precipitation and wind gust at station A701 (a), A713 (b), A740 (c), and precipitations at station A755 (d), for December, 18 th	224
Figure 4-148: Infrared satellite image at 12:00 UTC.	225
Figure 4-149: Satellite 1 km visible images, at 13 UTC (a), 14:00 UTC (b), 15 UT (c), 16:00 UTC (d), 17:00 UTC (e), 18:00 UTC (f), 1830 UTC (g), and 19:00 UTC (h), for December, 25 th	226
Figure 4-150: Images from the São Roque radar at 14:00 UTC (a), 1650 UTC (b), 17:20 UTC (c), 1730 (d), 1740 (e), 18:00 UTC (f), 1850 UTC (g), 19:10 UTC (h), 19:40 UTC (i), and 20:00 UTC (j).....	228
Figure 4-151: Streamlines and isotachs (m s^{-1}) at 200 hPa (a), geopotential height (gpm) and vorticity at 500 hPa (b), streamlines and temperature ($^{\circ}\text{C}$) at 850 hPa (c), and streamlines and relative humidity (%) at 850 hPa (d) at 12:00 UTC.....	231
Figure 4-152: Vorticity advection at 500 hPa (a), wind divergence at 200 hPa (b), temperature advection at 850 hPa (c) at 12:00 UTC.....	232
Figure 4-153: Mean sea level pressure and winds at 00:00 UTC (a), 06:00 UTC (b), 12:00 UTC (c), 18:00 UTC (d).	233

Figure 4-154: CIN from the BRAMS model at 12:00 UTC.....	233
Figure 4-155: CAPE from BRAMS at 12:00 UTC (a), 15:00 UTC (b), and 17 UTC (c), for December, 25 th . From GFS, CAPE is between 400 and 500 J kg ⁻¹ near Campinas at 12:00 UTC. At 15:00 UTC, in the same region it is ranging from 800 to 1100 J kg ⁻¹ . These values indicate a marginally unstable condition at 12:00 UTC, and it is between a marginally and a moderately unstable condition at 15:00 UTC. LI is between -2 and -3 K at 12:00 UTC, and -3 and -4 K at 15:00 UTC. These ranges indicate an unstable condition with probable storm, even severe in the presence of some lifting mechanism. High values of CIN are seen in the region at 12:00 UTC, it is between -40 and -60 J kg ⁻¹ . However, other events were compared with the GFS output, and it was noted that, at 12:00 UTC, it is usually lower than expected, which makes it possible for this parameter to be even higher in reality. Considering this argument and the values of CAPE observed, also considering that the range is correctly, is possible to say that it does not seem likely that a storm would develop in the region. The 700-500 hPa lapse rate also from GFS, at 12:00 and 15:00 UTC is between 5.5 and 6.0 K km ⁻¹ , although values ranging from 6 to 6.5 K km ⁻¹ are seen nearby.	234
Figure 4-156: CAPE from GFS at 12:00 UTC (a), and 15:00 UTC (b), for December, 25, 2016.....	235
Figure 4-157: LI from GFS at 12:00 (a), and 15:00 UTC (b), for December, 25 th	235
Figure 4-158: CIN from GFS at 12:00 UTC for December, 25, 2016.	236
Figure 4-159: 700-500 hPa lapse rate from GFS at 12:00 UTC (a), and 15:00 UTC (b), for December, 25, 2016.	236
Figure 4-160: Vertical cross section from BRAMS at 23°S of relative humidity at 12:00 UTC (a), and 15:00 UTC, of wind at 12:00 UTC (c), and 15:00 UTC (d).	237

Figure 4-161: Vertical cross section from GFS at 23°S of relative humidity at 12:00 UTC (a), and 15:00 UTC, of wind at 12:00 UTC (c), and 15:00 UTC (d).	238
Figure 4-162: Moisture divergence at 15:00 UTC.	239
Figure 4-163: Water vapor mixing ratio and wind at 00:00 UTC (a), 03 UTC (b), 06:00 UTC (c), 09:00 UTC (d), 12:00 UTC (e), 15:00 UTC (f), 18:00 UTC (g), 21:00 UTC (h). ..	240
Figure 4-164: Wind speed and direction (a), temperature and dew point temperature (b) at station A712.	242
Figure 4-165: Wind speed and direction (a), temperature and dew point temperature (b) at station A701.	243
Figure 4-166: Temperature and dew point temperature at station A755, for December, 25 th	243
Figure 4-167: Precipitation and wind gust at Station A739 (a), and A726 (b).	243
Figure 4-168: Infrared images for South America for February, 22 at 00:00 UTC (a), and 12:00 UTC (b).	245
Figure 4-169: Visible channel satellite images at 16:00 UTC (a) and 177 UTC (b).	245
Figure 4-170: Enhanced infrared satellite image for February, 22 at 17:30 UTC (a), 18:00 UTC (b), 1830 UTC (c), 19:00 UTC (d), 19:30 UTC (e), 20:00 UTC (f), 2030 UTC (g), 2130 UTC (h).	246
Figure 4-171: São Roque radar images for February, 22 at 1710 UTC (a), 18:00 UTC (b), 1830 UTC (c), 1920 UTC (d), 1930 (e), 20:10 UTC (f).	248
Figure 4-172: Streamlines and isotachs at 200 hPa for February, 22 at 00:00 UTC (a), 06:00 UTC (b), 12:00 UTC (c), 18:00 UTC (d).	249

Figure 4-173: Wind divergence at 200 hPa for February, 22 at 12:00 UTC (a), 15:00 UTC (b), and 18:00 UTC (c).	250
Figure 4-174: Geopotential, vorticity and streamlines at 500 hPa for February, 22 at 00:00 UTC (a), 06:00 UTC (b), 12:00 UTC (c), and 18:00 UTC (d).	251
Figure 4-175: Streamlines and relative humidity at 850 hPa for February, 22 at 00:00 UTC (a), 06:00 UTC (b), 12:00 UTC (c), and 18:00 UTC (d).....	252
Figure 4-176: Warm advection at 850 hPa at 12:00 UTC, for February, 22, 2017.....	253
Figure 4-177: Mean sea level pressure and wind for February, 22 at 00:00 UTC (a), 06:00 UTC (b), 12:00 UTC (c), and 18:00 UTC (d).....	253
Figure 4-178: Sounding and hodograph for February, 22 at 12:00 UTC. (source: http://weather.uwyo.edu/upperair/sounding.html).	255
Figure 4-179: Vertical variation of water vapor mixing ratio (a), relative humidity (b), and equivalent potential temperature (c) derived from the sounding for February, 22 at 12:00 UTC.....	255
Figure 4-180: CAPE from BRAMS at 12:00 UTC (a) and 15:00 UTC (b) for February, 22.....	256
Figure 4-181: CIN from BRAMS at 11:00 UTC (a) and 12:00 UTC (b) for February, 22.....	257
Figure 4-182: CAPE at 12:00 UTC (a), 15:00 UTC (b); LI at 12:00 UTC (c), and 15:00 UTC (d); 700-500 hPa lapse rate at 12:00 UTC (e), and 15:00 UTC (f), from GFS for February, 22, 2017.	258
Figure 4-183: CIN from GFS at 12:00 UTC, for February, 22, 2017.	259
Figure 4-184: Vertical cross section from BRAMS at 23.0°S of relative humidity at 12:00 UTC (a), and 15:00 UTC (b), and winds at 12:00 UTC (c), and 15:00 UTC (d) for February, 22 th	260

Figure 4-185: Vertical cross section from GFS at 23.0°S of relative humidity at 12:00 UTC (a), and 15:00 UTC (b), and winds at 12:00 UTC (c), and 15:00 UTC (d) for February, 22th.....	261
Figure 4-186: Moisture divergence for February, 22 at 14:00 UTC (a), and at 15:00 UTC (b).	262
Figure 4-187: Water vapor mixing ratio and wind for February, 22 at 00:00 UTC (a), 03 UTC (b), 06:00 UTC (c), 09:00 UTC (d), 12:00 UTC (e), 15:00 UTC (f), 18:00 UTC (g), and 21:00 UTC (h).....	262
Figure 4-188: Wind speed and direction, temperature and dew point temperature, temperature and relative humidity for February, 22 at A701 (a), (b), (c); A713 (d), (e), (f); A726 (g), (h), (i); A728 (j), (l), (m); A739 (n), (o), (p); A740 (q), (r), (s); A746 (t), (u), (v).....	266
Figure 4-189: Wind speed and direction from METAR at station SBMT (a), SBSP (b), and SBGR (c); temperature, dew point temperature and relative humidity at stations SBMT (d), SBSP (e) and SBGR (f), for February, 22, 2017.....	268
Figure 4-190: Temperature and dew point temperature (a), temperature and relative humidity (b) at station A755 for February, 22.	268
Figure 4-191: Precipitation and wind gust at station A701 (a), and precipitation at station A755 (b) for February, 22.....	269
Figure 4-192: Infrared satellite images for South America for December, 28 at 00:00 UTC (a), 06:00 UTC (b), 11 UTC (c), 16:00 UTC (d).....	270
Figure 4-193: Visible channel satellite images for December, 28 at 1008 UTC (a), 1338 UTC (b), 1445 UTC (c), 1608 UTC (d), 1638 UTC (e), and 1738 UTC (f).....	271

Figure 4-194: Enhanced infrared satellite images for December, 28 at 16:00 UTC (a), 17:30 UTC (b), 1830 UTC (c), 19:30 UTC (d), 2030 UTC (e), 2130 UTC (f), 22 UTC (g), 23:00 UTC (h).....	272
Figure 4-195: São Roque radar images for December, 28 at 17:00 UTC (a), 17:40 UTC (b), 1750 UTC (c), 18:00 UTC (d), 1830 UTC (e), 1850 UTC (f), 1920 UTC (g), 20:00 UTC (h), 20:10 UTC (i), 2030 UTC (j), 2040 UTC (l), 21:00 UTC (m), 2150 UTC (n), 2250 UTC (o).....	275
Figure 4-196: Streamlines and isotachs at 200 hPa for December, 28 at 00:00 UTC (a), 06:00 UTC (b), 12:00 UTC (c), and 18:00 UTC (d).....	277
Figure 4-197: Wind divergence at 200 hPa for December, 28 at 00:00 UTC (a), 06:00 UTC (b), 12:00 UTC (c), and 18:00 UTC (d).....	278
Figure 4-198: Geopotential, vorticity and streamlines at 500 hPa for December, 28 at 00:00 UTC (a), 06:00 UTC (b), 12:00 UTC (c), and 18:00 UTC (d).	279
Figure 4-199: Streamlines and temperature, streamlines and relative humidity at 850 hPa for December, 28 at 00:00 UTC (a), (b), 06:00 UTC (c), (d), 12:00 UTC (e), (f), and 18:00 UTC (g), (h).	280
Figure 4-200: Mean sea level pressure and wind for December, 28 at 00:00 UTC (a), 06:00 UTC (b), 12:00 UTC (c), and 18:00 UTC (d).....	281
Figure 4-201: CAPE at 12:00 UTC (a), and 15:00 UTC (b); LI at 12:00 UTC (c), and 15:00 UTC (d); 700-500 hPa Lapse rate at 12:00 UTC (e), and 15:00 UTC (f), from GFS for December, 28, 2016.	283

- Figure 4-202: Vertical cross section of relative humidity from GFS at 23.5°S at 12:00 UTC (a), 15:00 UTC (b), of winds at 12:00 UTC (c), and 15:00 UTC, for December, 28, 2016.284
- Figure 4-203: Vertical cross section of relative humidity from GFS at 23°S at 12:00 UTC (a), 15:00 UTC (b), of winds at 12:00 UTC (c), and 15:00 UTC, for December, 28, 2016.285
- Figure 4-204: Wind speed and direction, temperature and dewpoint temperature, temperature and relative humidity for December, 28 at station A701 (a), (b), (c); A712 (d), (e), (f); A728 (g), (h), (i); A740 (j), (l), (m); A746 (n), (o), (p).289
- Figure 4-205: Temperature and dewpoint temperature (a), temperature relative humidity (b), and precipitation (c) for December, 28 at station A755.....290
- Figure 4-206: Wind speed, temperature, dew point temperature, and temperature for METAR at stations SBSP (a), (b), SBMT (c), (d), SBGR (e), (f), SBTA (g), (h), for December, 28, 2016.....290
- Figure 4-207: Precipitation and wind gust for December, 28 at station A701 (a), A714 (b), A718 (c), A726 (d), A728 (e), A739 (f), A741 (g).291

LIST OF TABLES

Table 2-1: Convective potential related to CAPE values.....	39
Table 2-2: Convective potential related to LI values.	40
Table 3-1: Description of the selected events.....	53

LIST OF ABBREVIATIONS

BRAMS – Brazilian developments on the Regional Atmospheric Modeling System

CAPE – Convective Available Potential Energy

CIN – Convective Inhibition

EL – Equilibrium Level

GDP – Gross Domestic Product

GFS – Global Forecast System

IBGE – Instituto Brasileiro de Geografia e Estatística

INMET – Instituto Nacional de Meteorologia

LCL – Lifting Condensation Level

LFC – Level of Free Convection

LI – Lifted Index

MCS – Mesoscale Convective Systems

QG – Quasi Geostrophic

SACZ - South Atlantic Convergence Zone

UTC - Universal Time Coordinated

RESUMO

PICOLO, M, F. **Condições atmosféricas observadas durante ocorrências de tempo severo na área do projeto SOS-CHUVA**. 2018. 307 f. Dissertação – Instituto de Astronomia, Geofísica e Ciências Atmosféricas, Universidade de São Paulo, São Paulo.

Neste trabalho, foram selecionados 10 eventos de ocorrências de tempo severo na região nordeste do estado de São Paulo, considerando os danos produzidos de acordo com as notícias locais no verão de 2016/2017. Os danos foram relacionados a inundações repentinas devido a fortes chuvas, tempestades de granizo e rajadas de vento. Os eventos foram separados em três categorias diferentes: condições sinóticas intensas relacionadas ao fluxo de noroeste (ZCAS ou zona de convergência de umidade), forte condição sinótica não relacionada ao fluxo de noroeste (por exemplo, frentes, vórtice ciclônico de altos níveis) e condições sinóticas de menor intensidade. Três eventos foram caracterizados como pertencendo à primeira categoria, três como da segunda, e quatro como a terceira. Isto indica que as condições sinóticas tiveram um papel relevante na produção de condições favoráveis à ocorrência de tempo severo na região durante o período analisado. Aspectos de superfície, como a topografia, e a circulação da brisa do mar, foram importantes na iniciação na maioria dos eventos, especialmente para aqueles na terceira categoria. Uma forte influência do aquecimento diurno também foi observada, considerando a hora de ocorrência dos eventos, sendo apenas um caso ocorrido no período noturno/amanhecer. A precipitação pareceu ser mais importante em eventos relacionados a fortes condições sinóticas, enquanto que a ocorrência de granizo foi mais relevante em eventos com fraca influência das condições sinóticas. A energia potencial convectiva disponível (CAPE) a partir das sondagens e das saídas do GFS indicaram condições entre marginalmente ($0-1000 \text{ J kg}^{-1}$) e moderadamente instável ($1000-2500 \text{ J kg}^{-1}$) e o índice levantado indicou uma condição instável com prováveis tempestades (-6 a -2 K). Apenas um evento, ocorrido em 3 de dezembro de 2016, que está na primeira categoria, ocorreu com CAPE indicando uma condição muito instável ($2500-3500 \text{ J kg}^{-1}$) e LI indicando uma condição muito instável com possível ocorrência de tempestade severa ($<-6 \text{ K}$).

Palavras chave: Tempo severo, tempestades, impactos econômicos, perdas humanas.

ABSTRACT

PICOLO, M, F. **Atmospheric conditions observed during severe weather occurrences in the area of the SOS-CHUVA Project.** 2018. 307 f. Dissertation – Institute of Astronomy, Geophysics and Atmospheric Sciences, University of São Paulo, São Paulo.

During the present work 10 events of severe weather occurrences in the northeast region of the State of São Paulo were selected considering damages produced according to the local news during summer of 2016/2017. Damages were related to flash floods due to heavy rain, hailstorm and wind gusts. They were separated into three different categories: strong synoptic conditions related to the northwest flow (SACZ or humidity convergence zone), strong synoptic condition not related to the northwest flow (e.g., fronts, upper level cyclonic vortex), and weak synoptic conditions. Three events were characterized as the first category, three as the second, and four as the third. This indicates that the synoptic conditions had a relevant role in producing a favorable condition for severe weather occurrences in the region during the period analyzed. The presence of the surface features such as topography and the sea breeze circulation were important in initiation on most of the events, especially for those in the third category. A strong relationship with the diurnal heating was also observed considering the hour of the occurrences, being only one case occurred in the night/dawn period. Precipitation appeared to be more important in events related to strong synoptic conditions, while hail occurrences were more relevant in events in the weak synoptic conditions. Convective available potential energy from soundings and the GFS output indicated conditions between marginally (0-1000 J kg⁻¹) and moderately unstable (1000-2500 J kg⁻¹), and lifted index indicated an unstable condition with probable storms (-6 to -2 K). Only one event, December, 3, 2016, which is in the first category, occurred with CAPE indicating a very unstable condition (2500-3500 J kg⁻¹) and LI indicating a very unstable condition with possible severe storm occurrence (< -6 K).

Key words: Severe Weather, Thunderstorms, Economic Impacts, Human Losses.

1 INTRODUCTION

Convective systems and clouds play important roles in several atmospheric processes, such as the general atmospheric circulation through the release of latent heat, chemical process with the sweep of pollutants in the boundary layer and the contribution of lightning to the creation of nitrates, earth's radiation budget through the reflection of incoming solar radiation by clouds (Cotton and Anthes, 1989). They are also major components on the hydrological cycle (Cotton and Anthes, 1989). The main problem with convective systems is that they produce severe weather phenomena, generating economic and social impacts (Doswell, 2003). Moller (2001) shows a table of severe local storms events around the world presenting the number of deaths and damages in U.S. dollars. Damages, in some events, sum up to billions of dollars and deaths go up to 500. In Brazil, during 1991-2012, 35% of the climatic disasters were related to heavy rain; flash floods, floods and landslides affecting over 46 million people (CEPED, 2013a). Young et al. (2015) estimated the loss in "brazilian Real" related to these three events during 2002-2012, in average, the loss was estimated to be around 278 billion "reais".

It is important to define what is considered severe weather, according to Johns and Doswell (1992) a storm must generate at least one of these phenomena to be considered severe: tornadoes, damaging wind or gusts exceeding 26 ms^{-1} , hail with diameters higher than 1.9 cm. This is the definition used in USA. In Australia, heavy rains or flash floods are also included in the definition (Mills and Colquhoun, 1998). It can be noticed that the definition of severe weather described by Mills and Colquhoun (1998) is more appropriate to São Paulo, since convective systems tend to generate heavy rain events, which lead to floods and landslides, generally observed in the region. In the State of São Paulo, during 1991-2012, 593 cases of flash floods occurred, affecting over 2.5 million people and produced damages in over 1000 buildings (CEPED, 2013b). Santos (2013) estimated losses related to floods in the

city of São Paulo in the year of 2008, and concluded that it produced, on average, damages of 226 millions “reais” to Brazil.

The State of São Paulo is extremely affected, especially during spring and summer, by severe weather that causes heavy rain, strong winds and hailstorms. The consequences of some of these storms are floods, landslides, fall of trees, which affect thousands of people (Pereira Filho et al., 2002). The State of Sao Paulo was identified as one of the regions with the most severe convective systems in the world and with favorable conditions to the development of those systems (Zipser et al. (2006), Brooks et al. (2003)). Zipser et al. (2006) used measurements made by the TRMM satellite to identify where are the most severe convective storms in the world, using the idea that the stronger the convective vertical velocity, the more intense the storm is (Doswell, 2001). He considered the maximum height of the 40 dBZ level, the minimum brightness temperature at 85 and 37 GHz and the flash rate. In the results, regions in the Southeast of South America (which includes South and Southeast regions of Brazil, northern Argentina and Uruguay) appear to be one of the locations with the most severe storms. Brooks et al. (2003) used reanalysis data from NCAR-NCEP to create soundings and find environments with favorable conditions to severe weather. Relationships between severe storms and sounding parameters were obtained for USA, and then applied to the rest of the world. Again, Southeast of South America showed high frequency of occurrence of days with favorable conditions to thunderstorms. In agreement with those results, Albrecht (2016) found the same regions to be the main lightning hotspots in South America.

Several authors studied severe weather in these regions, including the occurrences of tornados (Velasco and Fritsch, 1987; Altinger de Schwarzkopf and Rosso 1982; Silva Dias and Grammelsbacher 1991; Held et al, 2006; Massambani et al., 1992; Nascimento, 2004; Silva Dias, 1999; Nascimento and Marcelino 2005, among others). A factor that contributes to

the formation of storms is the urban heat island effect (Cotton and Pielke, 1995). According to Silva Dias et al., (2013), the urban heat island can interact with the sea breeze, in the Metropolitan Region of São Paulo, a result also observed by Freitas et al. (2007). Other types of local circulations can have an impact on the formation of storms in the region as mentioned by Freitas et al. (2009), like local circulations generated by topography.

The study of severe storms events is extremely important to understand the factors involving the conditions related to them to improve forecasting and alert systems, so damages and human losses can be reduced. This work is part of the FAPESP's Thematic project SOS-CHUVA (*“Sistema de Observação e previsão de tempo Severo - Previsão imediata de tempestades intensas e entendimento dos processos físicos no interior das nuvens”*), which the main goal is to better understand physical processes related to severe weather, in order to improve short term forecasting and mitigate effects on society related to these extreme events.

1.1 OBJECTIVES

The general objective of the present work is to analyze cases of severe weather that occurred during summer and autumn 2016-2017 in the state of São Paulo. To do so, we used atmospheric fields obtained from the Global Forecast System (GFS) model to understand the synoptic scale environment and atmospheric fields from the Brazilian developments on the Regional Atmospheric Modeling System (BRAMS) to analyze the mesoscale conditions during the occurrence of selected severe weather events. Also, surface stations data from “Instituto Nacional de Meteorologia“ (INMET), SYNOP, METAR from airports and radar data will were used in order to better understand the effects of each event and improve the analyses.

1.2 REGION OF STUDY

The State of São Paulo is localized in a climatic transition zone, between climates with a well-defined dry period, called Humid Tropical Highland Climate and the subtropical climates, that are permanently moist (Tarifa and Armani, 2001). It is affected by tropical meteorological systems and by baroclinic systems, originating in the North and Center-West regions and South regions, respectively. Some examples are: cold fronts (Silva Dias, 1987); mesoscale convective complexes (Velasco and Fritsch, 1987); squall lines (Sales and Pereira Filho, 2000; Bender, 2012); cyclonic vortices associated with cyclogenesis (Reboita, 2008; Gan and Rao, 1991); and the South Atlantic Convergence Zone (SACZ) (Carvalho et al., 2004; Jorgetti, 2009; Freitas et al., 2009).

The State of São Paulo is the most populous in Brazil with 41 million people, being almost 40 million of those living in urban areas, and covers an area of 24 thousand km² (IBGE, 2010). It is the number one GDP (gross domestic product) in the country; in 2015 around 39% of it came from industries and 58,9% was from services, less than 2% originated in farming (SEADE, 2016) The city of Campinas (in which the radar of the SOS-CHUVA project is installed) is the third most populous in the State of São Paulo (1 million of people) (IBGE, 2010), the third GDP of the State, contributing to 3.1% of it (SEADE, 2014). The highest contribution to the GDP of the State from Campinas comes from industries (3.3%) (SEADE, 2014). Campinas is also the 8th city in the country with the highest area of urban concentration, the city of São Paulo is the first (IBGE, 2015).

2 SEVERE CONVECTIVE STORMS

2.1 Basic Concepts

This topic was adapted from the COMET Program (<https://www.meted.ucar.edu/index.php><http://www.comet.ucar.edu/>), based on the topics related to Principles of Convection.

2.1.1 Buoyancy

The concept of buoyancy is one of the most basic to understand deep, moist convection. Buoyancy is the force that acts on an air parcel in response to the difference of densities between the parcel and the surrounding air, it may be positive (upward movement) or negative (downward movement). If an air parcel is hotter than the ambient air, and consequently less dense, it becomes positively buoyant and rises. It is the basic concept behind updrafts and downdrafts, which can lead to the formation of hail, or destructive winds on surface, respectively. Water loading and entrainment of dry mid-level air are both important to updraft and downdraft strength, for example, dry air entrainment would cause evaporation, which would make air denser and would increase downdraft strength.

2.1.2 Stages of development

a. Short-lived single cells

The stages of development of an ordinary cell, in the absence of vertical shear, are: a parcel of air in an unstable environment rises until it reaches its lifting condensation level (LCL), which is equal to or lower than the level of free convection (LFC) if the ambient is unstable or conditionally unstable, respectively. The parcel will, then, accelerate until its equilibrium level (EL). Moisture is condensing in the rising air, and eventually, the weight will be too much for the updraft to hold, and precipitation will occur. Precipitation will, then,

carry air downward, and will contribute to the strength of downdraft. When the downdraft reaches the surface it spreads out and forms the cold pool, this is the final stage of the life cycle of the cell. The cold pool spreads out and generates horizontal vorticity on its edges, causing lifting, it can, then, by itself, generate new cells, if the lifting is enough to reach the LFC. This is the short-lived single cells (Byers and Braham, 1949). The process usually takes 30 to 50 minutes. According to Weisman and Klemp (1986), the storm moves with the mean environmental wind over the lowest 5 to 7 km, and can produce high winds and hail.

b. Multicells

It is another basic model to describe types of storms. According to Weisman and Klemp (1986) “(...) multicell storm can be thought of as a cluster of short-lived single cells.” A large cold pool forms combining all of the outflows from each cell, and as it propagates it triggers new cells. Due to the constant redevelopment of new cells, the storm motion is usually different from the mean wind. Also due to this fact they last longer, and if their movement is very slow it can lead to heavy rain occurrences. It can also produce hail and short-lived tornadoes.

2.1.3 Thermodynamic structure

Analyze the vertical structure of the atmosphere is an important task in order to understand severe weather. This is done, usually, using soundings, to verify instability, presence of moisture or dry air, and to derive thermodynamic indices.

One relevant feature regarding the thermodynamic structure of the atmosphere is the presence of dry air above the boundary layer, which enhances evaporation leading to strong downdrafts (Johns and Doswell, 1992). Therefore the low values of environmental relative humidity may lead to the occurrence of strong downdrafts. The presence of dry air can also assist in the determination of the development of organized severe storms (Colquhoun, 1987).

The most common environment producing tornadoes in Fawbush and Miller (1954) analysis was type I, in which hot and dry air overlays moist air in the boundary layer.

Doswell et al (1985) suggests that the presence of dry air is important to maintain high lapse rates. According to the authors “(...) the dryness of the air is only critically important insofar as it allows the maintenance of high lapse rates.” Still according to the authors, the combination of low level moisture and high lapse rates in mid-levels lead to convective instability, and regions with potential for storms development.

According to James and Markowski (2010) differences in the literature is seen regarding the presence of dry air in mid-levels at midlatitudes and tropical convection. In tropical convection, dry air tends to be detrimental to strong updrafts.

Analyzing days with strong, weak and no convection in Florida Panhandle, Fuelberg and Biggar (1994), concluded that relative humidity was 20 % lower than days with weak or strong convection. They also concluded that, in average relative humidity varied from approximately 85 % near the surface to 35 % at 400 hPa. To which the authors concluded that “Although dryness is often associated with severe convection over the Midwest and Great Plains, the dryness inhibits typical summertime convection over Florida. “

2.1.4 Thermodynamic indices

Several thermodynamic indices were created in order to better evaluate the conditions that would lead to severe storms, like CAPE, CIN, LI, among others. An explanation of these three will be given here, considering they will be used to analyze the events.

a. CAPE

CAPE is the Convective Available Potential Energy, a measure of buoyancy energy available for a parcel. It is determined by the sum of all temperatures differences between the ascent path (parcel) and the environment from the LFC to the equilibrium level (EL) (Eq. 1).

$$\text{CAPE} = g \int_{Z_{LFC}}^{Z_{EL}} \left(\frac{Tv_p - Tv_a}{Tv_a} \right) dz \quad (\text{J kg}^{-1}) \quad (1)$$

Tv_p is the virtual temperature of the parcel, Tv_a is the virtual temperature of the ambient air, Z_{LFC} is the level of free convection, Z_{EL} is the equilibrium level and g is gravity. High values of CAPE are associated with severe storms.

Table 2-1: Convective potential related to CAPE values.

CAPE (J kg ⁻¹)	Convective potential
0	Stable
0-1000	Marginally unstable
1000-2500	Moderately unstable
2500-3500	Very unstable
>3500	Extremely unstable

b. CIN

CIN is the Convective Inhibition, is a measure of the strength of the capping inversion. The inversion can prevent parcels from reaching the LFC, preventing the formation of storms. To initiate convection, other mechanism is required.

$$\text{CIN} = g \int_{\text{sup}}^{Z_{LFC}} \left(\frac{Tv_p - Tv_a}{Tv_a} \right) dz \quad (\text{J kg}^{-1}) \quad (2)$$

c. LI

LI, the Lifted Index, determines the amount of instability in an environment and it is calculated as the difference between the temperature of the ambient air and of an air parcel (rising from the surface) at 500 hPa (Eq. 2).

$$\text{LI} = T_a - T_p \quad (^\circ\text{C}) \quad (3)$$

If the parcel is colder than the ambient air, and is negatively buoyant, LI is positive. LI is negative when the parcel is positively buoyant, hotter than the ambient air. As LI gets more negative, the potential for the formation of convective storms grows.

Table 2-2: Convective potential related to LI values.

LI (K)	Convective potential
> 6	Very stable
1 - 6	Stable, unlikely storm development
-2 – 0	Slightly unstable, with possible storm in the presence of some lifting mechanism
-6 to -2	Unstable, with probable storm, even severe, in the presence of some lifting mechanism
< -6	Very unstable, with probable severe storm, in the presence of some lifting mechanism

2.1.5 Vertical wind shear

The presence of vertical wind shear can affect storm evolution, structure and longevity, by interacting with the cold pool, updrafts and downdrafts. Vertical wind shear also generates horizontal vorticity in the atmosphere, and interacting with the vorticity produced by the cold pool, can enhance lifting, favoring the development of new cells. An interaction of this horizontal vorticity and the updraft can produce mid-level rotation and can generate new updrafts on the lateral sides of the cell. The rotating updraft is a characteristic of supercells, which are associated with severe weather. It also influences the supercell evolution, the shear profile is important in this case, for example, in an ambient with a straight shear (as seen in a

hodograph) it causes cell splitting, creating two equal cells. Another important point about vertical wind shear is that it affects the strength and organization of mesoscale convective systems (MCS) like squall lines.

Further details regarding the topics mentioned here will be discussed in the next topic, which also presents a revision of important literature on the matter.

2.2 Bibliographic Revision

The three necessary ingredients to deep, moist convection are: moisture, low-level instability and ascent of parcels to the level of free convection (LFC) (Doswell and Bosart, 2001). These conditions are provided by synoptic-scale and mesoscale processes. Johnson and Mapes (2001), focusing only on mesoscale processes, separate them in preconditioning, triggering and storm-generated that affect the evolution and growth of new cells.

2.2.1 Mesoscale definition

Some authors have discussed the definition of what is considered mesoscale (Emanuel, 1986; Markowki and Richardson, 2011). According to them, it is believed that term mesoscale was first introduced by Ligda (1951) in an article about weather radar, to represent phenomena that were smaller than the synoptic scale and larger than the microscale. The American Meteorological Society's Glossary of Meteorology defines mesoscale as "pertaining to atmospheric phenomena having horizontal scales raging from a few to several hundred kilometers (...)". It includes thunderstorm, squall lines, fronts, precipitation bands, sea and land breezes, among others. Orlanski (1975) created a subdivision of mesoscale systems into meso- α , meso- β and meso- γ . Meso- α have horizontal scales of 200-2000 km and temporal scales of 1 day to 1 week, it encompasses systems such as frontal systems and hurricanes. The meso- β scale have horizontal scales of 20-200 km and temporal scale of several hours to 1 day, it includes systems like squall lines, low-level jet, mountain and sea

circulations. The last one, meso- γ have horizontal scale of 2-20 km and temporal scales of half hour to several hours, it applies to systems such as clear air turbulence, thunderstorms, urban effects (Figure 2-1). This definition is used by Cotton and Anthes (1989). Markowki and Richardson, (2011) presents a different way of defining mesoscale; it is by the terms that are retained in the dynamical equations. On the mesoscale, frequently, terms cannot be neglect in the equations, differently from the synoptic scale (e.g., vertical accelerations, advection by the ageostrophic wind) and microscale (e.g., Coriolis force). This is also mentioned by Doswell, 1987, who proposes that mesoscale processes can be defined as “those which cannot be understood without considering large scale and microscale processes”.

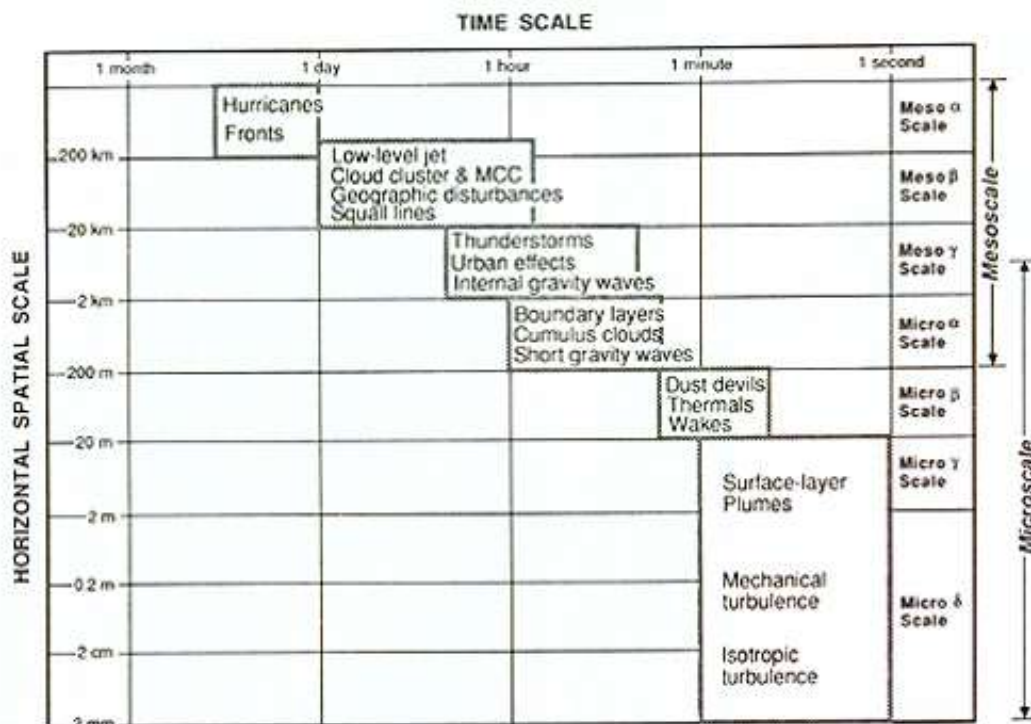


Figure 2-1: Spatial and time scales of process that occurs in microscale and mesoscale. From Orlandi (1975).

2.2.2 Synoptic scale processes

Doswell (1987) uses the idea that large-scale processes are those which are quasi-geostrophic (adiabatic, hydrostatic, mass continuity is satisfied, advection is dominated by the

geostrophic part of the wind, and the variation of Coriolis parameter is neglectable). These processes are important to the establishment of favorable conditions to the development of convection (Johnson and Mapes, 2011).

A process associated with synoptic-scale features that is mentioned as important to the development of severe storms is the vorticity advection. Miller (1972) mentions that positive vorticity advection (North Hemisphere) is present in almost all cases of major outbreaks. This relation comes from the omega equation from the Quasi Geostrophic (QG) theory (Holton, 1973). In an analysis of three cases of severe storm, with the occurrence of hail and tornadoes, in the USA during the year of 1980, Maddox and Doswell (1982) showed that the three events were related to weak values of vorticity advection. Instead, it was demonstrated the importance of low-level warm advection, to which they concluded that thermal advection fields probably dominate vorticity advection in generating vertical motion.

Another important feature is jet streaks, which are features observed in jet streams with varying along-flow wind speed (Doswell and Bosart, 2001). According to Palmen and Newton (1969) they are defined as regions of isotach maxima. Several authors have studied the role of jet streaks in severe convective weather, such as Palmen and Newton (1969), Ludlam (1963), Newton (1967), among others.

The regions where the jet streak decelerates is called the exit region, located downstream, upstream, where it accelerates, is called entrance region. A direct and indirect circulation is found in the entrance and exit region, respectively. The vertical motion field generated by the jet streaks can be explained with the Q-vector, derived from the QG theory.

Synoptic-scale vertical motions are usually too weak to provide enough lifting to initiate convection, but it can modify the environment to make it favorable for severe storms, by adding moisture and changing the lapse rate (Doswell, 1987). Rockwood and Maddox (1988) studied an event on June, 1992 that was observed in northeast Kansas and northern

Missouri, which occurred due to an interaction between large scale and mesoscale. According to them, the large scale features acted to change the environment into a favorable one for supporting convection, but the initiation was related to mesoscale lifting.

One example is the most common known large scale system, the extratropical cyclone, it provides an environment that favors processes on smaller scales that generate vertical motions larger than the synoptic scale motions, like fronts (Doswell and Bosart, 2001).

2.3 Bibliographic Revision for São Paulo

In this section, relevant features associated with severe storms in São Paulo will be discussed. As it was already mentioned previously (section 1) the southeast of South America presents the most severe storms in the world (Zipser et al, 2006).

According to Romatschke and Houze (2010) the climatological pattern seen for South America at the level of 200 hPa during summer shows the presence of the Bolivian High, centered east of the Andes. In the 500 hPa easterly winds and westerly winds are seen northern and southern South America, evidencing the presence of a tropical climate and a subtropical/midlatitude climate, respectively. Still according to them, in the 700 hPa level the presence of the Andes is noticeable leading to the northwest flow. In the southeast region, the flow from northwest merges with the westerlies to form the South Atlantic Convergence Zone (SACZ).

“The SACZ is subjectively defined as a zone of enhanced convective activity that is most pronounced during South Hemisphere summer (...)” (Carvalho et al, 2002). The rainfall distribution in the southeast region of South America is, during summer, strongly influenced by the SACZ (Nogués-Paegle and Mo, 1997; Carvalho et al 2002; Lenters and Cook 1999). Carvalho et al (2002) studied the relationship between extreme precipitation events (20 % or more of the seasonal climatological total observed in one day) in the State of São Paulo and

the intensity and extension of the SACZ. A total of 1576 events were selected between 1979-1996 (DJF), extreme precipitation events occurred in 146 days. They concluded that around 65 % of the extreme precipitation events were related to strong and extensive convective activity in the SACZ, and also that regional distribution of the events were affected by the spatial characteristics of the SACZ.

Romatschke and Houze, 2010 divided radar echo structures in different categories according to their properties, and they identified that deep and wide convective cores (reflectivity ≥ 40 dBZ, extending ≥ 10 km in height and extending over an area of ≥ 1000 km²) have a peak in the afternoon in the Brazilian High Lands (eastern part of the continent). They also identified that this strongly diurnally forced convection occurs mainly along the coastal region of the southern Brazilian High Lands, in region of surface wind convergence. This indicates that the heating during the day is important to the development of storms in the region. Similar results were found by other authors regarding the importance of the diurnal heating in precipitation events in the region, more specific in the State of Paulo, such as Gandu and Silva Dias (1984), and Vicent et al (2002).

The State of São Paulo has complicated surface distributions that make the analysis of storms complicated. Near to the coast, the Serra do Mar extends along the coast with its higher elevations seen between São Paulo and Rio de Janeiro. Serra da Mantiqueira is present in the region between the State of São Paulo and Minas Gerais, and the highest altitudes are seen in northeastern São Paulo and southeastern Minas Gerais. In the northeast region of the State, a valley forms between Serra do Mar and Serra da Mantiqueira, known as Vale do Paraíba. Advancing inland topographic heights decrease. Another important factor is the coast, which lead to the formation of the land-sea breeze. Some authors have identified the importance of the surface characteristics in convective precipitation events (Gandu and Silva Dias, 1984, Vicente et al 2002). The regional circulations that develop due to the complexity

of the region also play an important role in the pollution dispersion in the region (e.g., Freitas, 2003; Silva Dias e Machado, 1997).

Gandu and Silva Dias (1984) analyzed radar echoes from the São Roque radar during January of 1979 and March of 1980, and used surface synoptic charts to group them in similar observed conditions. According to the authors the highest daily average and the second highest contribution to the total observed occurred in conditions in the absence of fronts and when the area was under the influence of a high pressure system, which means they are probably related to the sea breeze and/or valley-mountains circulations. Another important result from their work is that the high frequency (around 60 %) of occurrence in the north-northeast and east directions from the region of radar, in the location of the highest altitudes of Serra do Mar and Mantiqueira. This shows the importance of the topography in the region. Vicente et al (2002) analyzed events in the period of September to March of 1990 to 1995 using the radar of São Paulo. The events selected had initial precipitation rates above 20 mm h⁻¹. In their results 40 % of the cases started in the region of Serra da Mantiqueira, and 36 % reached their maximum intensity in the region of São Paulo, 23 % in the region of Vale do Paraíba, which indicates the presence of sea breeze and of another important factor seen in the region of São Paulo, the urban heat island.

One of the most important studies of the sea breeze penetration in the city of São Paulo is Oliveira and Silva Dias (1982). The sea breeze circulation forms in response to the differential heating between the continent and the ocean. This circulation is influenced by a number of aspects, like topography, curvature of the coast, latitude, and synoptic conditions. It can reach 150 km into the continent. They also analyzed and classified sea-breezes into three categories considering different features of its penetration in the city of São Paulo during the year of 1978. The three categories were: standard sea breeze, sea breeze with northwest flux and sea breeze with intensification of the southeast winds. According to

Oliveira and Silva Dias (1982), the sea breeze penetration is seen through abrupt changes in wind, moisture and temperature. The first category was observed during days with no pre-frontal or post-frontal conditions, with the pressure gradient pointed to the ocean. Winds are from northeast through the day before turning to southeast. In the second category winds are from northeast and change to northwest early in the morning, it intensifies until the afternoon, when it turns to southeast. The third case occurs in the presence of southeast winds usually related to post-frontal conditions.

Still according to the authors the sea breeze in most cases penetrated between 13:00 and 14:00 local time. The sea breeze with northwest flux and intensification of southeast winds propagate later and earlier than that interval, respectively.

Some authors have studied the coupling of the sea breeze with the mountain-valley circulation (e.g., Silva Dias et al, 1995; Silva, 1986), and several have studied the impact of the heat island in the sea breeze circulation, some of it already mentioned in section 1 (Silva Dias et al, 2013; Silva, 1986; Pereira Filho et al, 2004; Pereira Filho, 2000; Freitas et al, 2009; Vemado and Pereira Filho, 2016). Silva Dias et al, (2013) analyzed changes in extreme daily rainfall in São Paulo using data from 1933 to 2010 from a climatological station located in Parque do Estado das Fontes do Ipiranga. They also examined the probable relation between these changes and climatic indices. According to the authors, during the wet season, the analysis points to the fact that urban effects can be relevant in the explanation of the daily rainfall extremes. Freitas et al (2009) used numerical simulations to verify the effects of the urban heat island and sea surface temperature (SST) in the formation and development of the thunderstorm of February, 1, 2003. In their results, the urban heat island contributed to increase in precipitation. An increase in SST (2°C) also had a positive contribution for precipitation. According to Silva (1986) the urban heat island acts to retard the sea breeze penetration and that the topography intensifies the circulation. Similar results were found by

Silva Dias et al (1995), in which the sea breeze intensifies by coupling with the circulation over Serra do Mar and coupling again with the circulation over Serra da Mantiqueira. However, there other studies showing that the urban heat island can accelerate the sea breeze propagation due to the increase in the thermal gradient already existent between the urban area and the ocean (Freitas et al, 2007). Therefore, the cities can act in both ways, i. e., accelerating or preventing the sea breeze cell propagation.

Pereira Filho et al (2004) analyzed 18 events of floods in the Metropolitan Area of São Paulo (MASP) related to the sea breeze and the urban heat island. According to their results more than half of the events were related to air temperature above 30 °C and dew point temperatures above 20 °C. Another important fact is that the frequency of rain rate above 10 mm h⁻¹ is up to three times higher in the MASP than the surrounding regions. Still according to the authors, most of the high wind gusts which lead to fall of trees were related to flood events due to the sea breeze and the heat island. Similar results were obtained by Pereira Filho et al. (2002), analyzing 14 convective events during February, 1998, the authors also showed a core of high precipitation (normalized precipitation) in the region of the MASP. The probability of precipitation above 5 mm is also higher in the region. The study of Vemado and Pereira Filho (2016) also presented similar effects, analyzing events between 2005 and 2008, in which a core of 600 mm of total rainfall estimated by the São Paulo Weather Radar is seen over MASP, slightly shifted northeastward. Pereira Filho et al (2004) also analyzed a case that occurred on February, 04, 2004, in which heavy rain was observed. The hodograph showed a weak vertical wind shear at the 12:00 UTC sounding at Campo de Marte. Vemado and Pereira Filho (2016) obtained another important result that 74 % of the analyzed cases (125) occurred when winds turned from northwest to southeast, a case that in general, occurs when a frontal system is observed in the south region of Brazil. Averages of dew point temperature at the

IAG weather station showed that when the parameter was below 15 °C before the sea breeze penetration, only weak and ordinary cells developed, according to the authors.

Machado and Silva Dias (1982) analyzed a severe weather occurrence on February, 15th, 1980, heavy rain and hailstorms were reported. In the synoptic scale scenario, a low pressure system was seen at the 200 hPa level near the region, which is a condition that favors the development of deep convective cells, according to the authors. The sounding was typical of severe storm, with high moisture content near the surface, a subsidence inversion at 500 hPa, and dry air above. A humidity convergence field was developed by the authors using interpolation of surface data, and a convergence is seen at 12:00 UTC parallel to the coast, indicating the sea breeze front.

Frontal systems have also been responsible or related to severe weather occurrences on the region, as studied by Silva Dias and Grammelsbacher (1991), Massambani (1992) and Held et al (2006). The three events were related to tornadoes or possible tornadoes. Silva Dias and Grammelsbacher (1991) analyzed a case on April, 26th, 1991, in the day, as mentioned a frontal system was observed in southern Goiás, central part of São Paulo and Paraná. Another important feature seen that day was a low pressure system observed in the 850, 500 and 250 hPa levels, centered in western Paraná. Massambani (1992) case analyzed occurred on September, 30th, 1991. The frontal system was between Cabo de São Tomé and Vitória, extending southeast. Associated to it, a low pressure system is seen affecting the State of São Paulo. Soundings for both of this mentioned cases showed the atmosphere was wet throughout the troposphere, according to Silva Dias and Grammelsbacher (1991), due to the frontal system. The CAPE parameter for the case of April was 986 J kg^{-1} , and the bulk Richardson number was 38. The vertical shear of the module of the wind between the surface and 500 hPa was $3.2 \cdot 10^{-3} \text{ s}^{-1}$, and according to the author, comparing with midlatitude values, both CAPE and wind shear would be too low for tornado occurrence. This is due to the

baroclinic forcing being stronger at midlatitudes than at subtropical regions. Another important feature about this event is the anticlockwise turn with height of the wind, between the surface and the level of 700 hPa, indicating warm advection.

Held et al (2006) analyzed tornadoes occurrences on May, 24th and 25th of 2005. A radar analysis was shown and the authors also evaluated model forecasting for the event of May, 24. They showed that a trough at the level of 500 hPa was producing upward motion on the region, wind divergence at 300 hPa was also observed.

3 METHODOLOGY

In this project, data from selected events of severe storms in the State of São Paulo will be analyzed; the events are from the summer 2016-2017. Brazil does not have an official database for severe weather occurrences, therefore, the events were chosen based on news published by the local media or selected by the research group.

The data available for analysis are:

- Outputs from GFS and BRAMS models;
- Satellite images (GOES-13, from CPTEC);
- Radar images (São Roque radar and Campinas radar, from CPTEC and IPMET radar);
- Surface data from INMET;
- METAR from airports around the State of São Paulo;
- Synop;
- Atmospheric Soundings.

The outputs of the GFS model were used to analyze the synoptic fields related to each event. We analyzed streamlines, isotachs and mass divergence at 200 hPa, geopotential height, vorticity and vorticity advection at 500 hPa, streamlines, relative humidity and temperature advection at 850 hPa, sea level pressure and winds at 1000 hPa, and surface temperature. Also, from the GFS model, analysis of the 700-500 hPa lapse rate and LI were made. The fields analyzed using the output of the BRAMS model were: CAPE, CIN, surface wind, sea level pressure, water vapor mixing ratio.

The satellite images were obtained from GOES-13 satellite provided by CPTEC. Infrared, enhanced infrared, visible and water vapor channels will be used.

Radar images from the São Roque and Campinas (X-band) radar were obtained from CPTEC. The analyzed fields were: 3 km CAPPI (São Roque radar) and precipitation

(Campinas). Images from the IPMET radars were also used. They are located at Presidente Prudente and Bauru and the analyzed image is a composition for both locations.

The surface data from automatic stations of INMET, covering the State of São Paulo, were time series of temperature, dewpoint temperature, precipitation, wind speed and direction, wind gust, and pressure. To improve surface analyses, METAR data from airports in the State of São Paulo and Synop data were also used.

Lastly, soundings from the Campo de Marte airport in the city of São Paulo were obtained for the day of each event, in which several important parameters were analyzed, like the presence of instability, vertical wind shear, lapse rate in mid-levels and several thermodynamic indices.

A comparison between the sounding parameters and those obtained by the GFS and BRAMS outputs were made in order to evaluate if the analysis from the models can be useful to make conclusions about those parameters for each event, when soundings were not available. However, only a few number of events were compared, a more complete analysis using a greater number of events would be more appropriate to make a final conclusion about the reliability of the parameters derived from the models used here.

In order to better understand the events, they were classified and separated according to the phenomena that led to their occurrence.

3.1 EVENTS

Table 3-1 presents a description of the all events that were analyzed in this project. Data from floods in the city of São Paulo were obtained from CGE (from the Portuguese “Centro de Gerenciamentos de Emergências”, meaning Emergency Management Center). All of them produced rain and most of them had occurrences of hail and wind gusts.

Table 3-1: Description of the selected events.

Date	Occurrences	Damages	Category
December, 3, 2016	Rain, floods, wind gusts	Flood in São Paulo (1 point)	(1a)
December, 18, 2016	Rain, hail, wind gusts	Flood in São Paulo (7 points)	(2)
December, 25, 2016	Rain, hail, wind gusts (In Campinas and São Carlos).		(2)
December, 28, 2016	Rain. Wind gusts in Campinas, São José dos Campos and hail in Vila Pirituba.	Flood in São Paulo (7 points). Loss of crops in Salesópolis.	(2)
January, 7, 2017	Rain	Flood in São Paulo (26 points).	(1b)
January 15-17, 2017	Rain, 64.6 mm accumulated in the station Mirante de Santana in São Paulo	Flood in São Paulo (11 points on the 15 th and 31 on the 16 th). One death in Guarulhos	(1a)
January, 30, 2017	Rain, wind gusts. Hail in Jundiaí.	Flood in Campinas and fall of trees in Jundiaí	(1b)
February, 6, 2017	Rain, wind gusts	Flood in São Paulo (36 points). Fall of trees in São Paulo and Campinas	(1b)
February, 22, 2017	Rain. Hail	Flood in São Paulo (27 points).	(2)
February, 24, 2017	Rain, hail	Flood in São Paulo (57 points).	(1a)

The events were characterized in two categories: related to strong synoptic scale forcing (1a,b) and weak synoptic forcing (2). The first category will be divided into two, one related to the northwest flow, the Low-Level Jet, which leads to the formation of SACZ (South Atlantic Convergence Zone) and humidity convergence zones (1a). The other one is related to

other large-scale features that could destabilize the environment, such as Upper Level Cyclonic Vortex, trough or fronts (1b). The second category is related to storms that developed during weak synoptic forcing, which means that no large-scale processes or features that could contribute in their formation were present. The categories of each event are seen on Table 3-1.

4 RESULTS

4.1 STRONG SYNOPTIC FORCING

4.1.1 Category 1a

As described in the section above, this category has events related to the northwest flow that adds moisture from the Amazon region to the southeast region of South America.

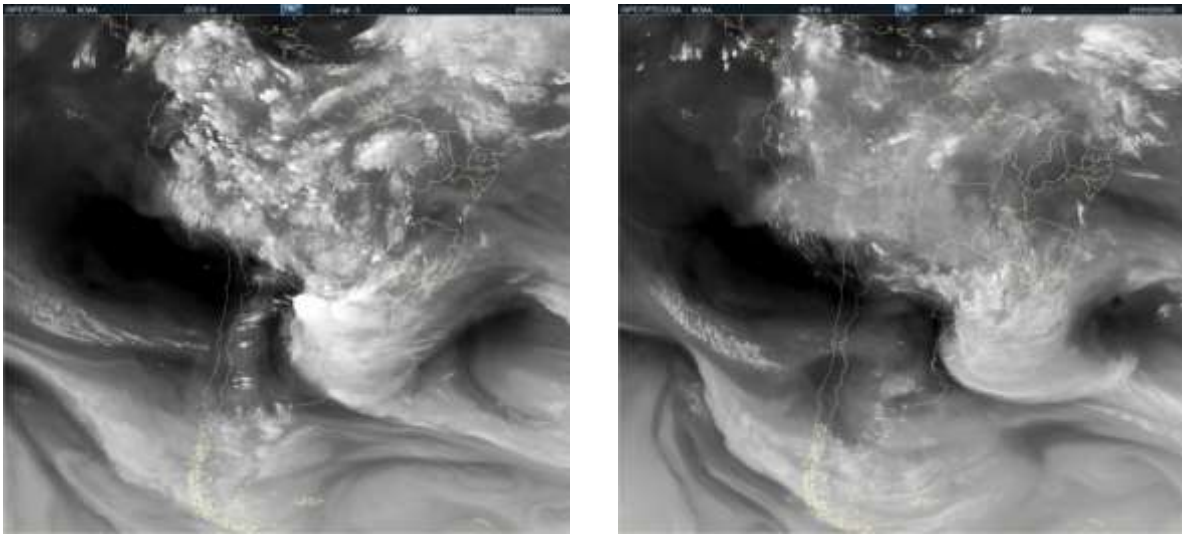
4.1.1.1 December, 3rd, 2016

This event led to severe weather occurrences, reported by the news, in Campinas, fall of trees was observed (8 trees), and winds of 70 km h^{-1} (19.7 ms^{-1}) were registered. Rain was also reported, although it did not lead to the occurrence of floods. In São Paulo, rain led to the occurrence of 1 point of flood in the city (CGE), strong winds were also reported. Fall of trees were also reported in Mogi das Cruzes, Suzano and Itaquaquecetuba.

Other details will be given in the surface stations analysis section.

a. Satellite

In the images of the water vapor channel from South America it is possible to see that the event was related to a larger scale system. Moisture coming from the Amazon region is seen connecting to a low pressure system in the south region of Brazil (Figure 4-1 a,b). Further details of the synoptic environment will be given in section c.

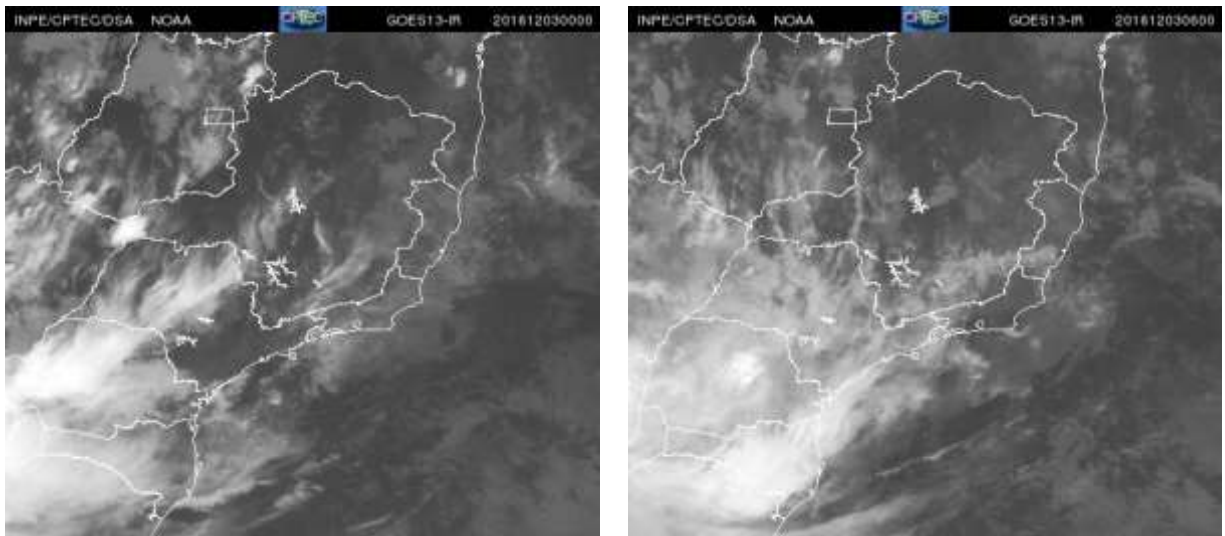


(a)

(b)

Figure 4-1: Water vapor channel images at 00:00 UTC (a), and 12:00 UTC (b) for December, 3rd, 2016.

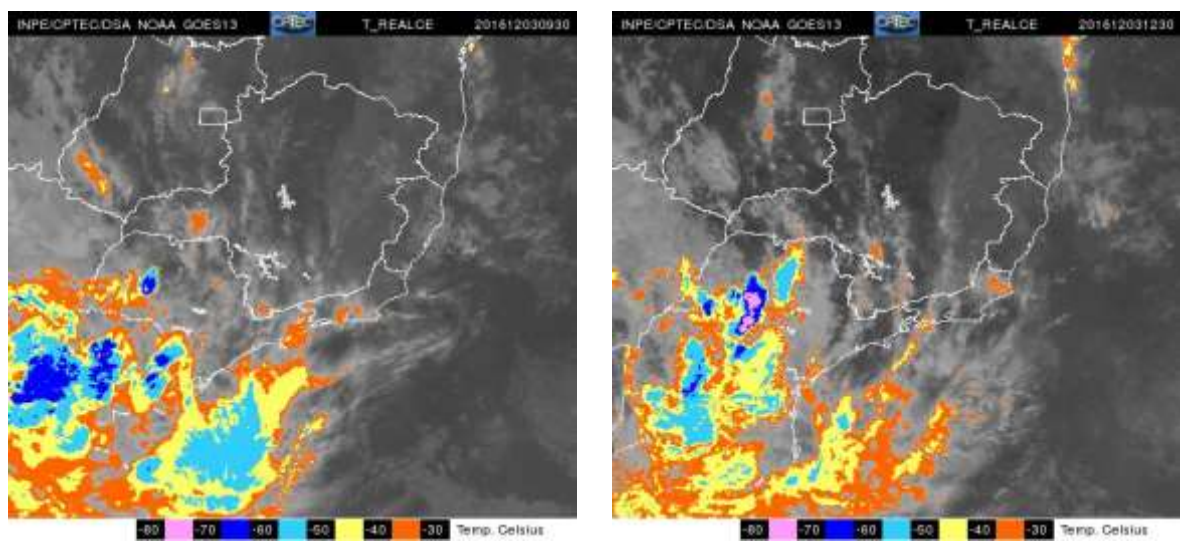
Using the infrared images showing only the southeast region of Brazil, lower clouds are seen in the analyses since 00:00 UTC in the State of São Paulo, and at 6 UTC they cover most of the State (Figure 4-2). At 09:00 UTC, a convective cloud starts to form in the southwest section, at 9:30 UTC it reaches its lower value of temperature ($-70\text{ }^{\circ}\text{C}$), which is an indicative of high convective clouds, as can be seen in Figure 4-3 a. That system loses its strength, and another one becomes stronger, and reaches values as lower as $-70\text{ }^{\circ}\text{C}$ as can be seen at 12:30 UTC (Figure 4-3). As it moves along the State in a northeast direction, it appears to contribute in the development of new cells (seen at 14:30 and 15:00 UTC in Figure 4-3). These new cells get stronger, and as can be seen at 16:30 UTC, temperature values are lower than $-80\text{ }^{\circ}\text{C}$. This system continues to move across the State, in the same northwest direction, and it covers all the north section and most of the west part of the State at 19:30 UTC (Figure 4-3). It continued to advance and lost its strength as can be seen at 23:30 UTC. At 2:00 UTC on December 4th, the system is in the State of Minas Gerais and Rio de Janeiro, is not as strong as shown before, but temperatures are still lower than $-70\text{ }^{\circ}\text{C}$ in some regions.



(a)

(b)

Figure 4-2: Infrared satellite images at 00:00 UTC (a), and 06:00 UTC (b) for December, 03rd, 2016.



(a)

(b)

Figure 4-3: Infrared enhanced temperature satellite images at 09:30 UTC (a), 12:30 UTC (b), 14:30 UTC (c), 15:00 UTC (d), 16:30 UTC (e), 19:30 UTC (f), 23:30 UTC (g), 2:00 UTC (h.) for December, 03rd, 2016.

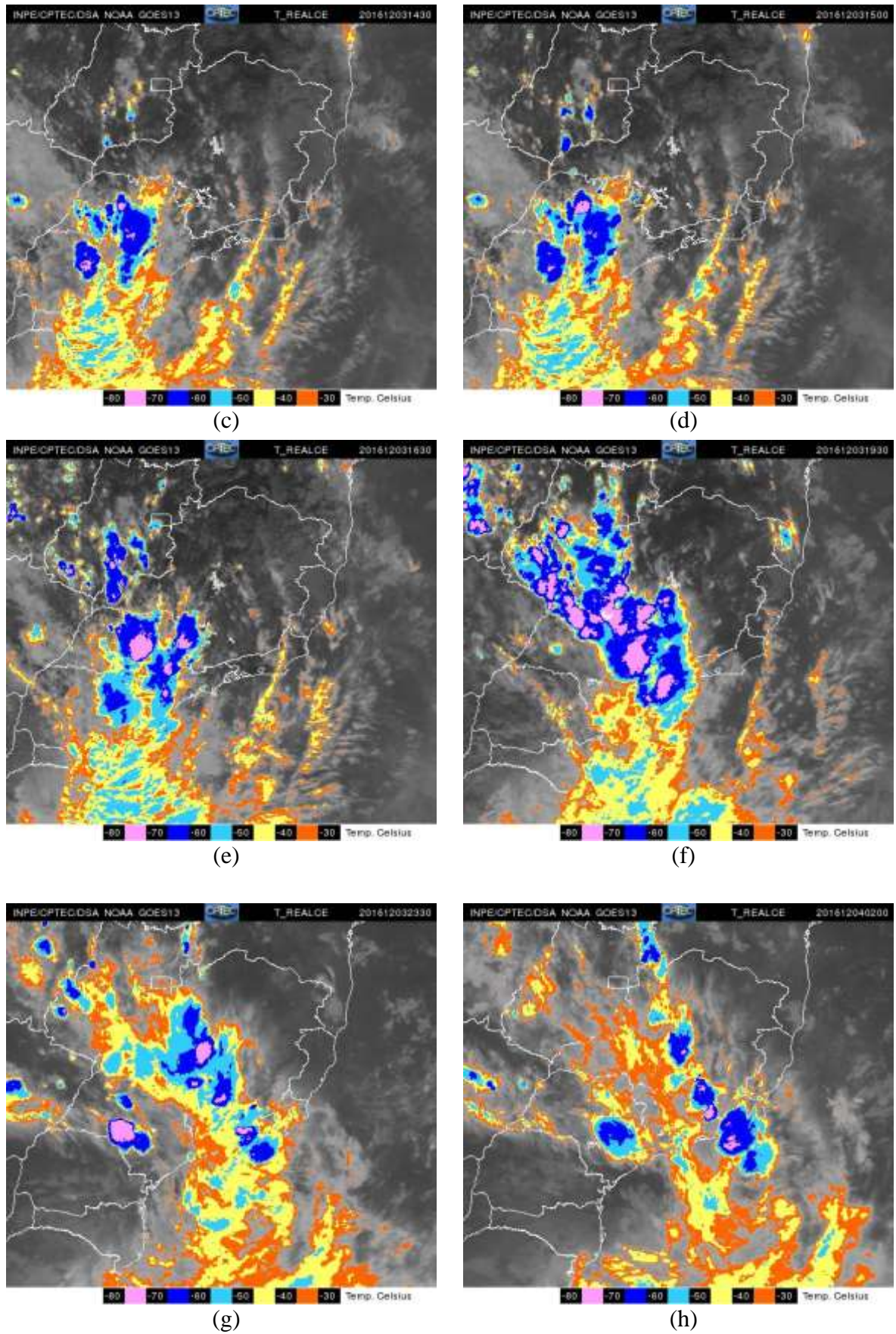


Figure 4-3: Continuation.

b. Radar

At 09:00 UTC in the IPMET radar, as also observed in the satellite images, a convective cell started to develop in the southwest of the State, with reflectivity values around 40 dBZ. Other cells are seen at this time, but with lower reflectivity values (Figure 4-4). More cells develop in the region as can be seen at 10:30 UTC (8:30 LT) in Figure 4-4. At this time, clouds are observed in the region of Presidente Prudente and are seen until 14:00 UTC with reflectivity values on the order of 30 dBZ, during this period, rain was recorded by the two automatic surface stations in the region. As the cells move in a northeast direction, new cells develop from them, as it was mentioned in the previous section (Figure 4-4 c,d).

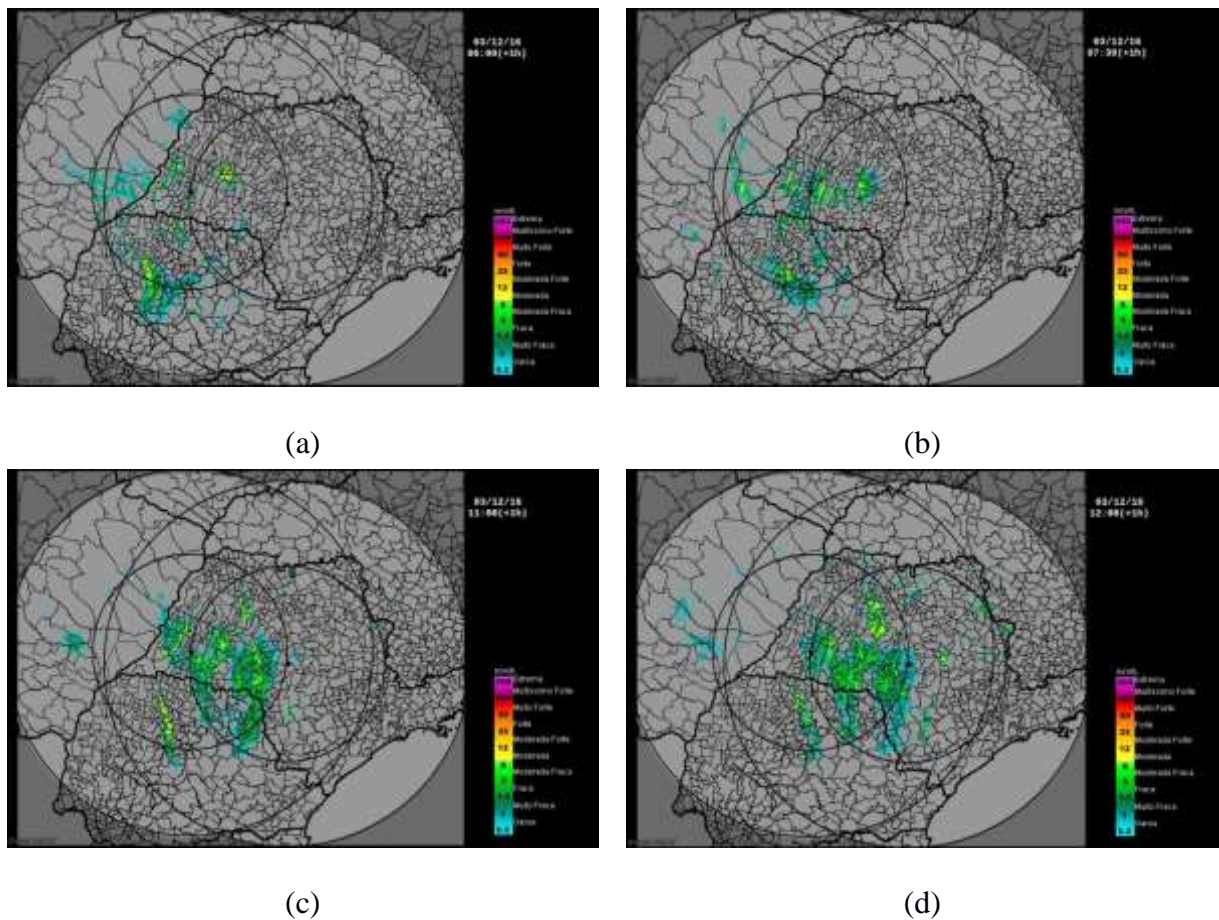
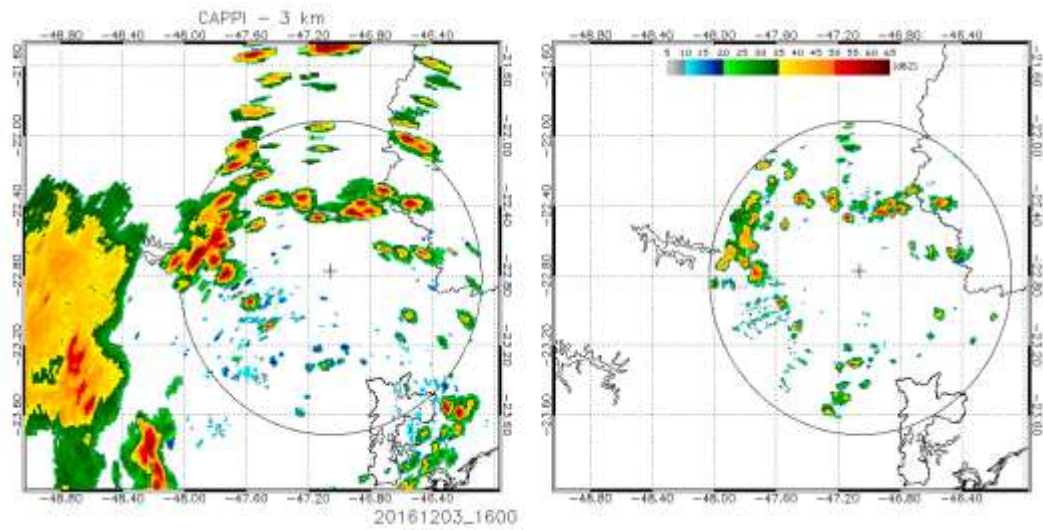


Figure 4-4: IPMET radar reflectivity at 09:00 UTC (a), 10:30 UTC (b), 14:00 UTC (c), and 15:00 UTC (d) for December, 03rd, 2016.).

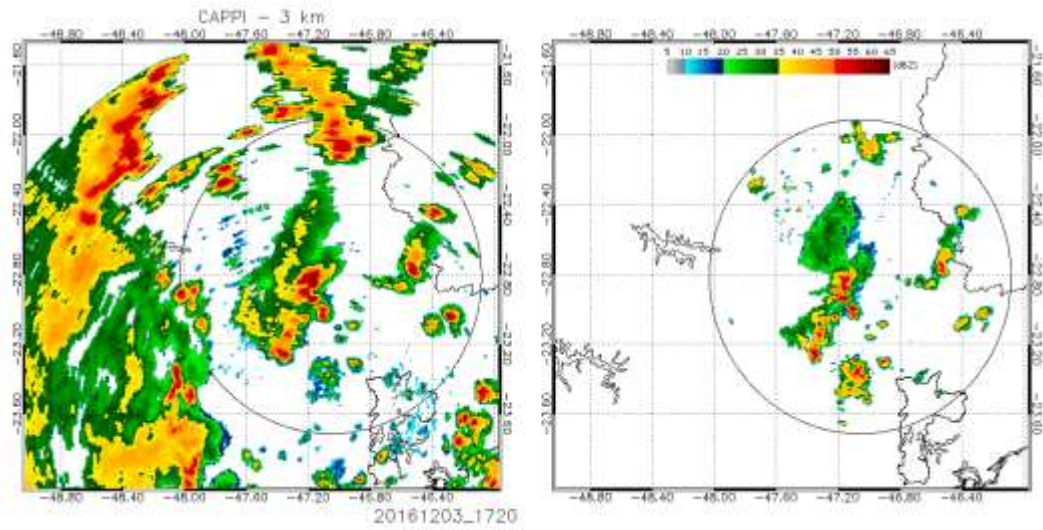
Analyzing the reflectivity images of the radar at São Roque and Campinas in Figure 4-5, at 16:00 UTC, a few cells around the region of Campinas are seen, and they move in to the direction of Campinas and merge. At 17:20 UTC strong convective cells are seen in the region of Campinas with high reflectivity values around 60-65 dBZ. At 18:30 UTC (Figure 4-5 c), reflectivity values are around 40 dBZ with higher values around 60 dBZ, indicating that the storm in this region was more severe than in the southwest region that occurred previously in the day. In the radar images, it is also possible to see the system moving northeast, as it was noted in the satellite images (section a), but it also seems to move southeast in Figure 4-5, which could be because storms move related to the wind and also to the most favorable environment.

c. Synoptic and mesoscale

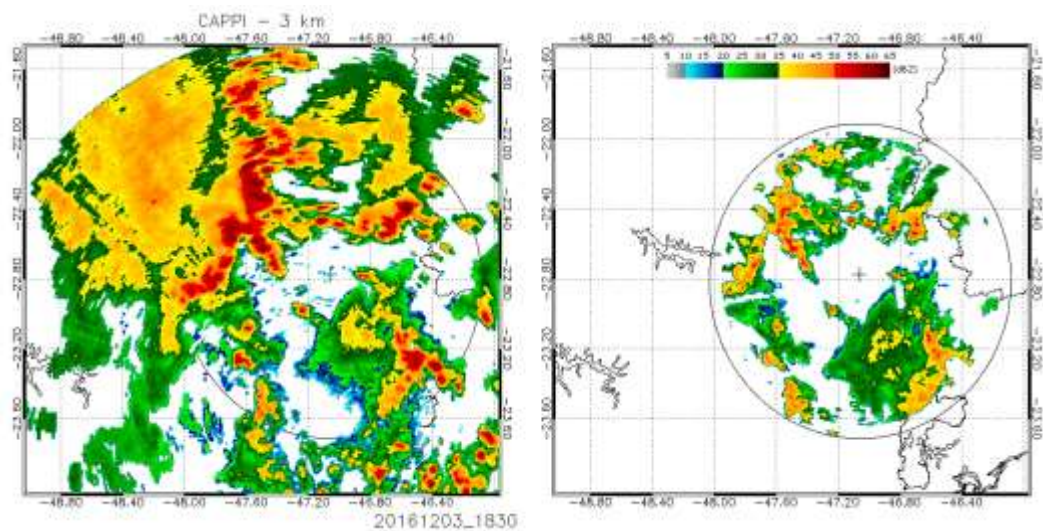
The synoptic scale environment was characterized by a trough at higher levels (200 hPa), it can be seen at 00:00 UTC in the day of the event the trough is located at north of Argentina. It reaches the south region of Brazil, as can be seen at 12:00 UTC (Figure 4-6). Mass divergence is seen around the State during the day, but it is only seen near the region of Campinas at 06:00 UTC, ranging from 0.2 to 0.6 10^{-3} s^{-1} .



(a)



(b)



(c)

Figure 4-5: São Roque (left) and Campinas (right) radar reflectivity at 16:00 UTC (a), 17:20 UTC (b), and 18:30 UTC for December, 03rd, 2016.

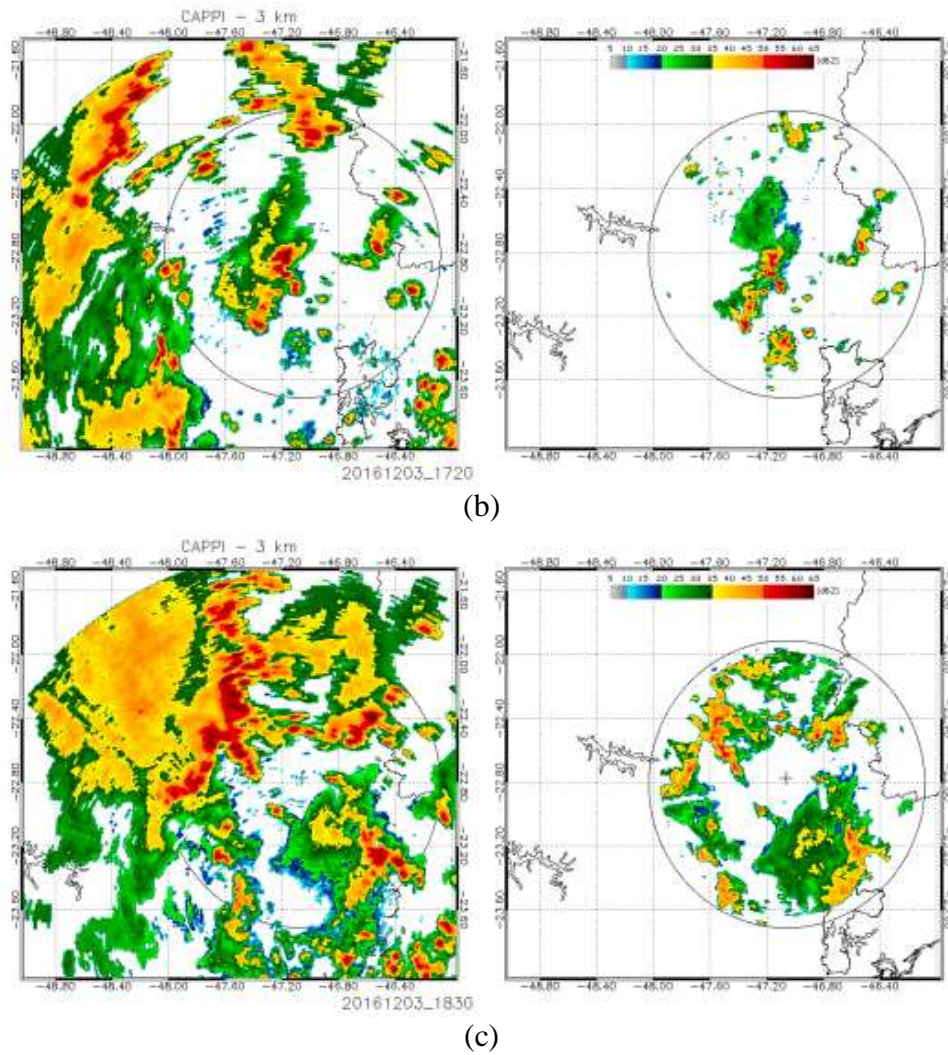


Figure 4-5: Continuation.

In the 500 hPa analysis, shown in Figure 4-7, the trough is also seen in the south region of Brazil at 12:00 UTC, reaching the States of Mato Grosso do Sul and São Paulo with negative vorticity associated to it. The vorticity advection by the geostrophic wind was also analyzed for the level of 500 hPa due to its relation to vertical velocity in the omega equation (as explained in section 2.2.2). Near neutral values of vorticity and vorticity advection are seen in the State of the São Paulo throughout the analysis (Figure 4-7). One important feature associated with this event is the northwest flow that developed in the 850 hPa analysis, which carries moisture from the Amazon region into the southeast of South America. The low-level jet is seen at 12:00 UTC in Figure 4-8 directed to the State of Parana and to the south of the State of São Paulo. At 15:00 UTC the low-level jet is directed to the State of São Paulo, and it

is possible to see the increase in the relative humidity values between 12:00 and 15:00 UTC analysis, from around 75 and 80% to above 90% (Figure 4-8). In the temperature advection analysis, it can be seen warm advection throughout most of the State, shown in Figure 4-9. The largest values are seen at 12:00 UTC, in the east and west regions, above $1 \times 10^{-4} \text{ K s}^{-1}$ (Figure 4-9 b).

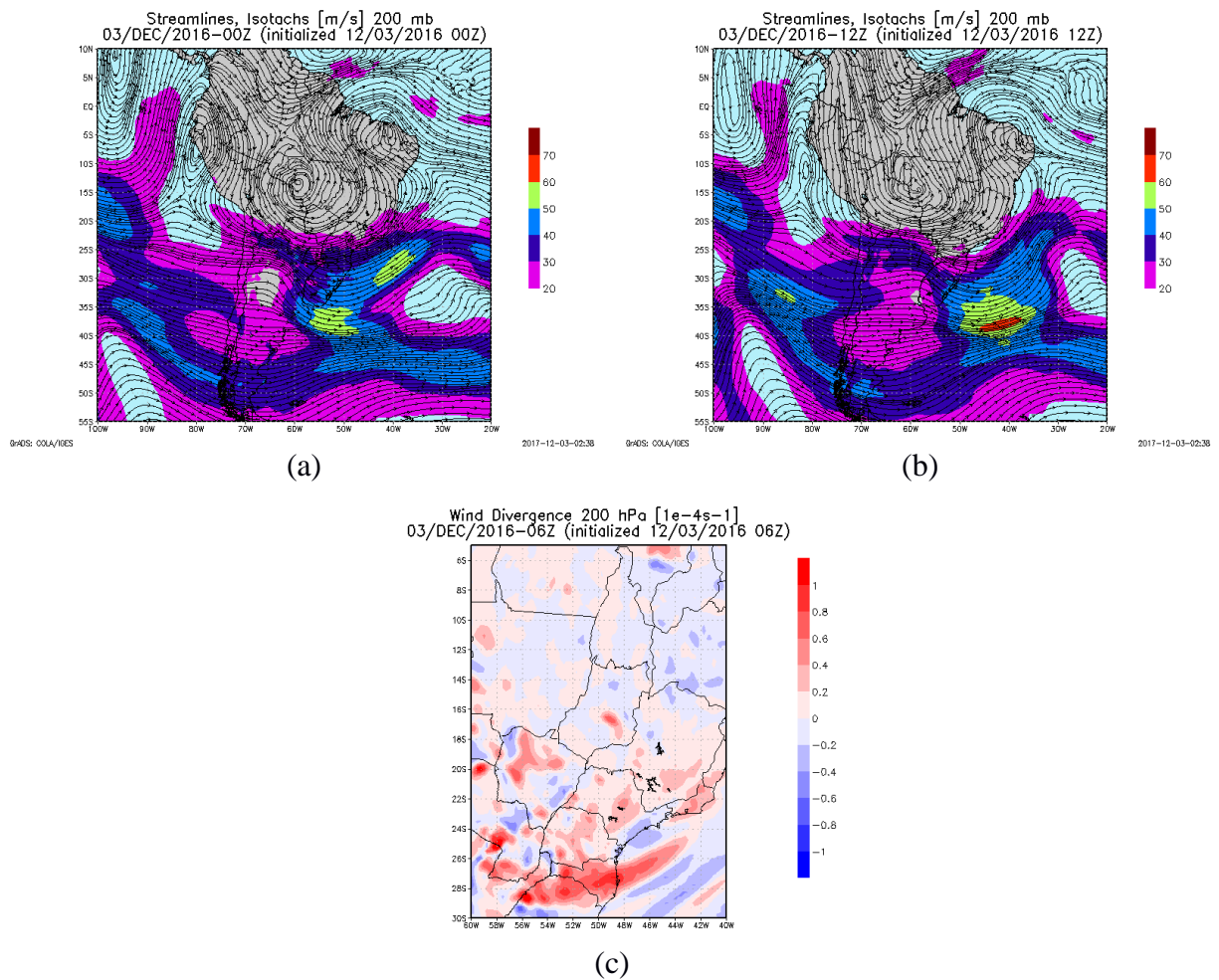


Figure 4-6: Streamline and isotachs (m s^{-1}) at 200 hPa at 00:00 UTC (a) and 12:00 UTC (b), mass divergence (10^{-4} s^{-1}) at 06:00 UTC (c), for December, 03, 2016).

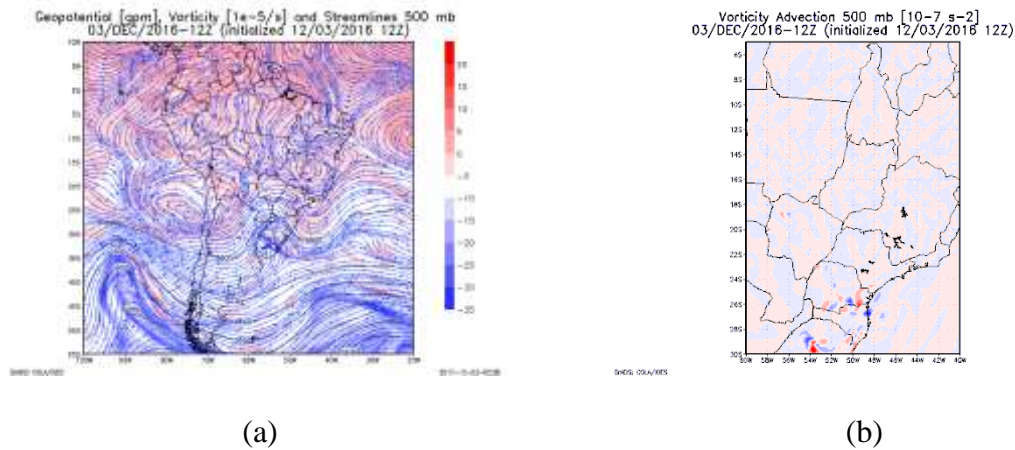


Figure 4-7: Geopotential height and vorticity at 500 hPa, 12:00 UTC (a), and vorticity advection at 500 hPa, 12:00 UTC (b).

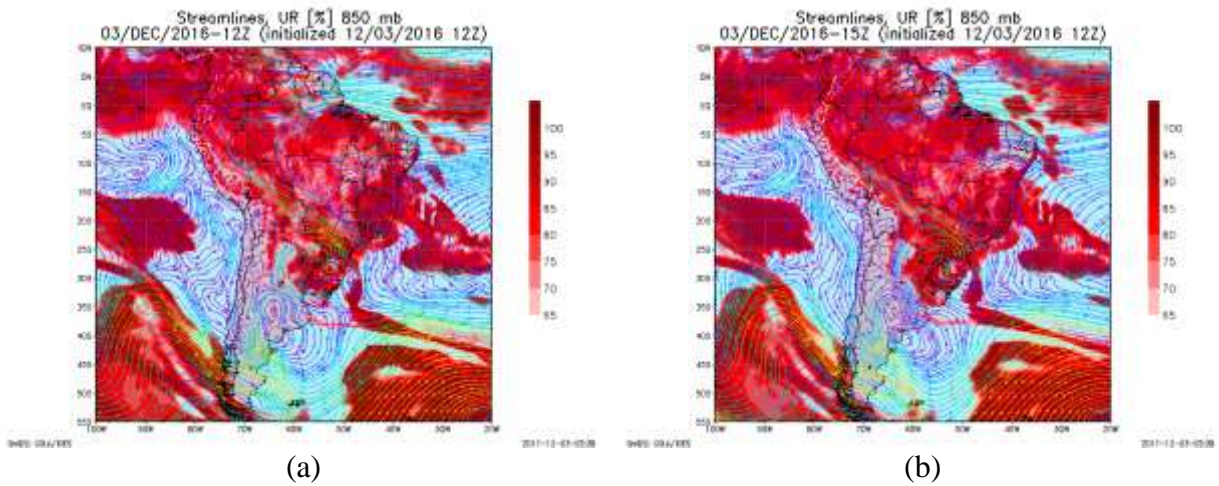


Figure 4-8: Streamlines and relative humidity at 850 hPa at 12:00 UTC (a) and 15:00 UTC (b).

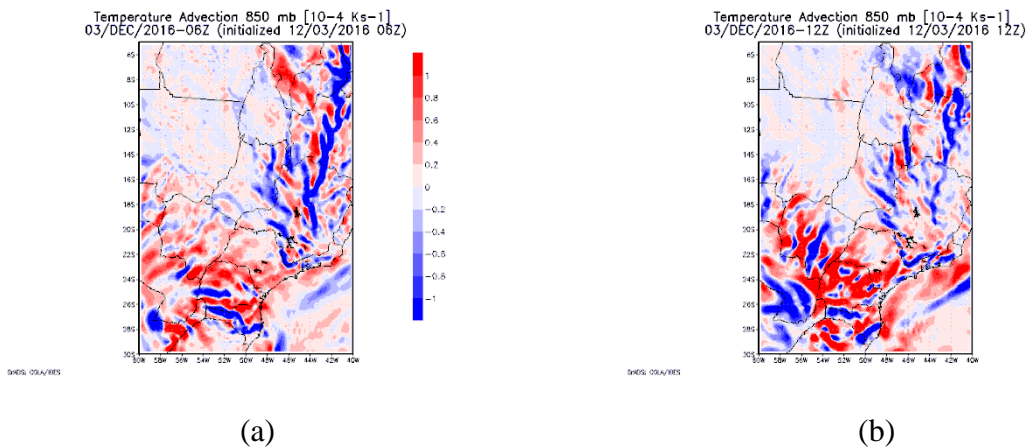


Figure 4-9: Temperature advection at 850 hPa at 06:00 UTC (a), and 12:00 UTC (b) for December, 03rd, 2016.).

In surface analysis, a high-pressure system is located at the Atlantic with a center of 1020 hPa near to the coast of São Paulo. This high-pressure system moves away from the continent in the analyses. A cyclonic circulation develops in the south region of Brazil associated with the trough in higher levels, as can be seen at 18:00 UTC (Figure 4-10).

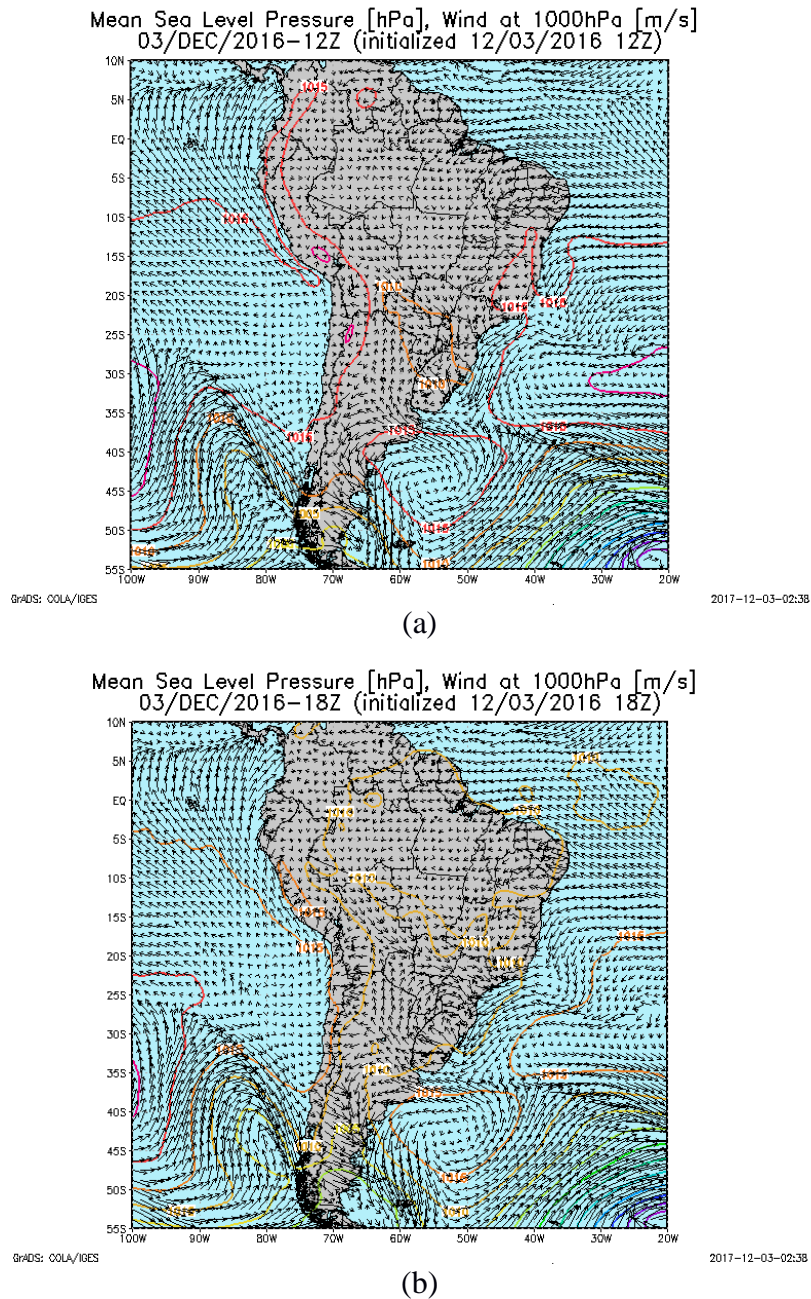
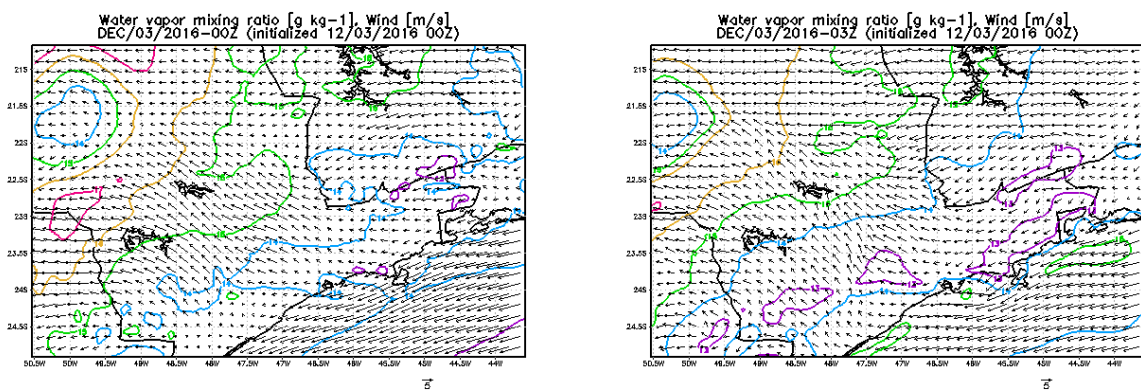


Figure 4-10: Mean sea level pressure (hPa) and wind (m s^{-1}) at 12:00 UTC (a), and 18:00 UTC (b) for December, 3rd, 2016.

This low pressure system is the one previously mentioned in the satellite image (section 4.1.1.1, Figure 4-1).

Using the BRAMS model output, winds are observed in Figure 4-11. At 00:00 UTC winds in the east and central parts of the State are from southeast related to the sea breeze penetration that occurred in the previous day. Wind changes its direction throughout the day; at 15:00 UTC, winds are from northwest. In the east coast of State, at this hour, winds from southeast are observed, in this region high moisture convergence is observed at the same time (Figure 4-12). This is probably the formation of the sea-breeze near the coast, but it does not move into the continent due to the winds from Northwest seen in the State. Analysis of water vapor mixing ratio shown is an output from the BRAMS model. Values around 14 g kg^{-1} in the east region and around 16 g kg^{-1} in the west region, are seen at 00:00 UTC (Figure 4-11). An increase in these values is observed, which could be related to the low-level jet directed to the State of São Paulo in the 850 hPa analysis. At 12:00 UTC the east part has mixing ratio of 16 g kg^{-1} and the west region 18 g kg^{-1} .



(a)

(b)

Figure 4-11: Water vapor mixing ratio (g kg^{-1}) and wind (m s^{-1}) at 00:00 UTC (a), 03:00 UTC (b), 06:00 UTC (c), 09:00 UTC (d), 12:00 UTC (e), 15:00 UTC (f), 18:00 UTC (g), and 21:00 UTC (h) for December, 03rd, 2016.

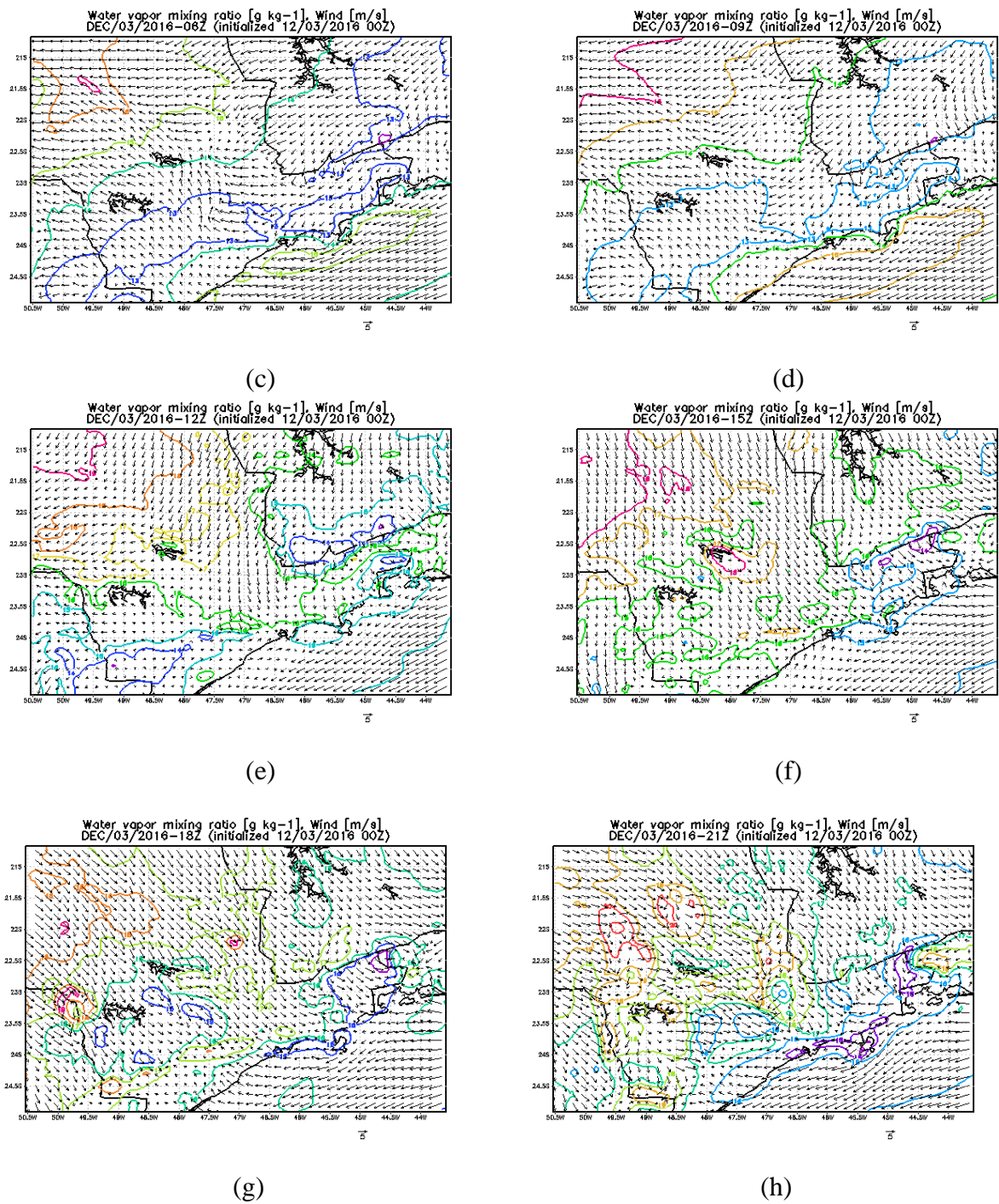


Figure 4-11: Continuation.

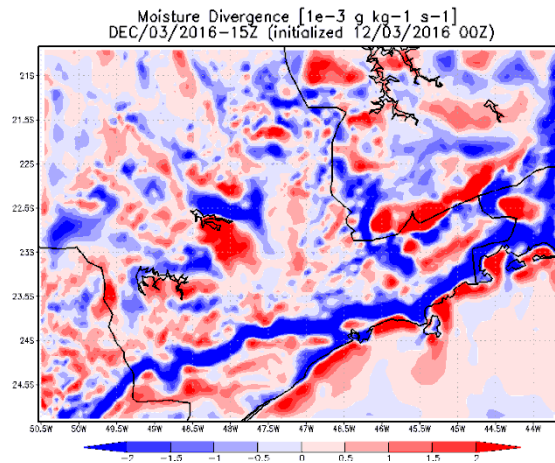


Figure 4-12: Moisture divergence ($\text{g kg}^{-1} \text{s}^{-1}$) at 12:00 UTC for December, 03, 2016.

Convective available potential energy and convective inhibition were analyzed using the BRAMS model outputs and are shown in Figure 4-13 and Figure 4-14, respectively. CAPE starts to increase in the east region after 11 UTC. At 12:00 UTC the region of Campinas already has values above 1000 J kg^{-1} (between 1500 and 1800 J kg^{-1}). At 15:00 UTC, smaller values were seen near the coast (below 600 J kg^{-1}), but most of the region has CAPE between 2100 and 2400 J kg^{-1} . Higher values are seen in the central and west region of the State (above 2700 J kg^{-1}). At 18:00 UTC, the north and west region have values above 2700 J kg^{-1} , including the region of Campinas, and near the city of São Paulo.

These high values are related to the high moisture values observed during this day, and show the high potential for severe weather occurrence.

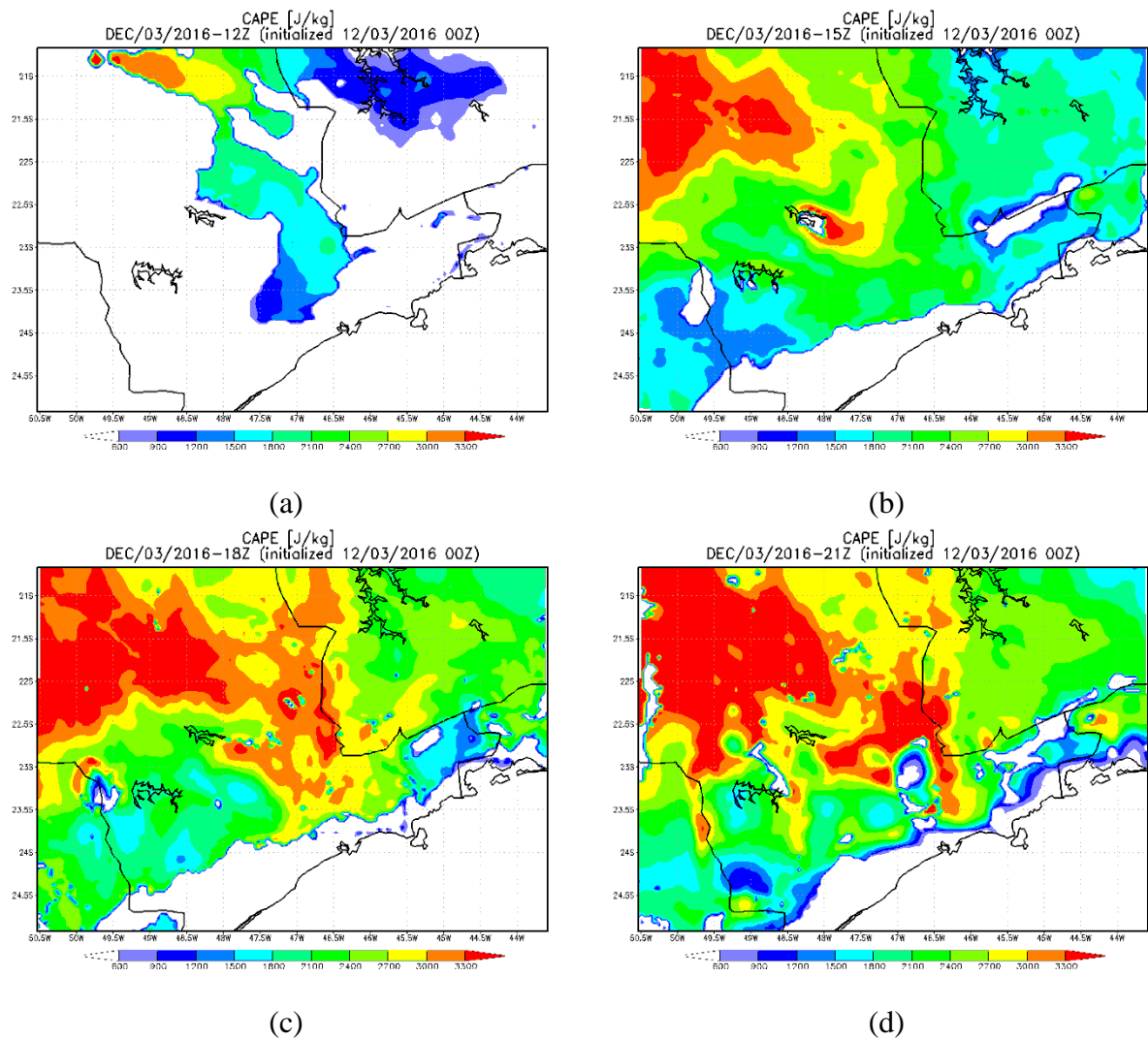


Figure 4-13: CAPE (J kg^{-1}) at 12:00 UTC (a), 15:00 UTC (b), 18:00 UTC (c), and 21:00 UTC (d) for December, 03rd, 2016.

CIN values increase from the beginning of the analyses. At 09:00 UTC the highest values in the day are observed, increasing to the east, from $100\text{--}150 \text{ J kg}^{-1}$ in the west to $200\text{--}350 \text{ J kg}^{-1}$ in the central section. In this region values above 400 J kg^{-1} can be seen in a small region. In the northeast and southeast regions CIN increases after 09:00 UTC, while it decreases elsewhere. CIN is around $250\text{--}300 \text{ J kg}^{-1}$ in the northeast at 10:00 UTC and at 11:00 UTC is seen through most of the east region, with values, at some region between 200 and 250 J kg^{-1} . After 12:00 UTC, CIN is only observed near the coast, with small values (between $0\text{--}50 \text{ J kg}^{-1}$).

Lifted index was analyzed from the GFS output (Figure 4-15). Using a surface parcel it ranges from -4 to -6 K through most regions at 12:00 UTC, and at 12:00 UTC it is between -5 and -6 K, with smaller values (lower than -6 K) seen in the north region. This parameter, indicates an unstable condition, with the probable formation of storms. At 12:00 UTC, values below -6 K are seen in northern São Paulo, this indicates a strong unstable condition. From the satellite analyses it was seen that strong convection occurred in the north region of the State.

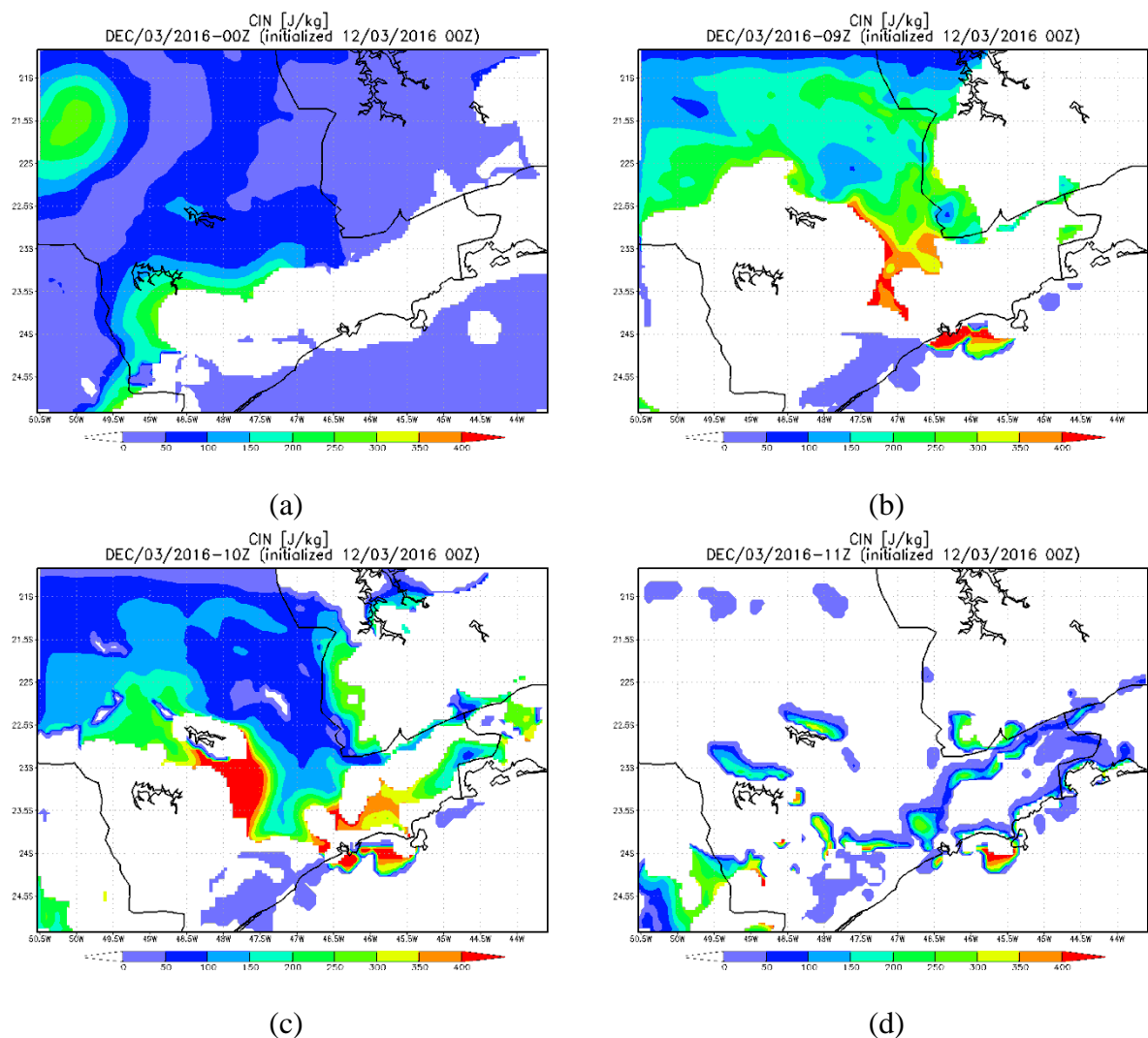
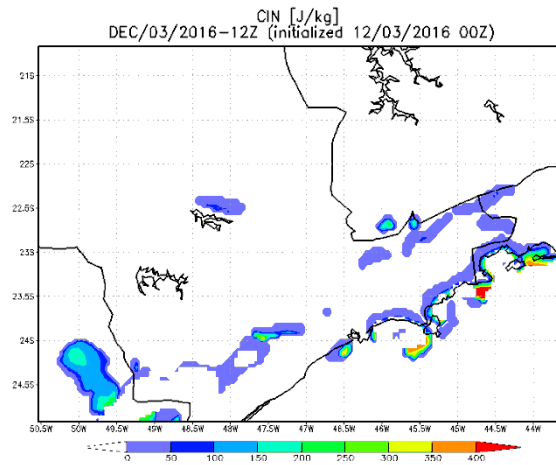
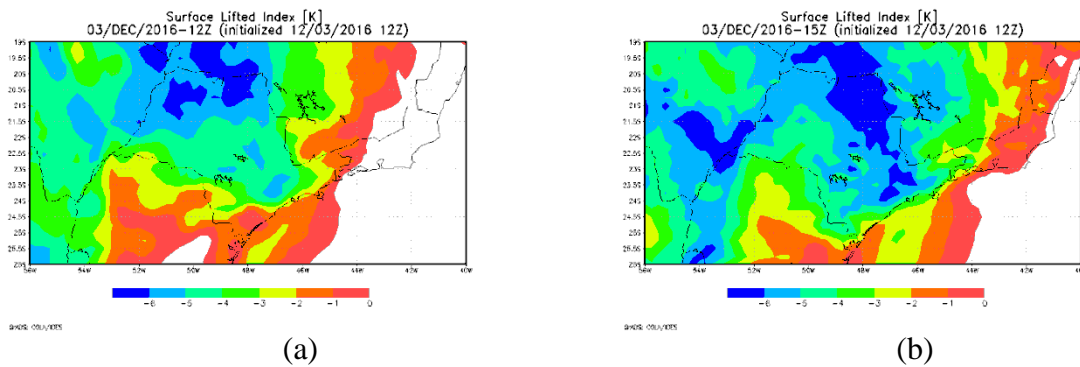


Figure 4-14: CIN at 00:00 UTC (a), 09:00 UTC (b), 10 UTC (c), 11 UTC (d), 12:00 UTC (e) for December, 03rd, 2016.



(e)

Figure 4-14: Continuation



(a)

(b)

Figure 4-15: LI from GFS(K) at 12:00 UTC (a), 12:00 UTC (b) for December, 03rd, 2016.

The 700-500 hPa lapse rate is seen in Figure 4-16. Lapse rate increases in the east and northeast region, at 00), 15:00 UTC it is raging from 5-5.5 K km⁻¹, and reaches the interval of 6-6.5 K km⁻¹ at 12:00 UTC

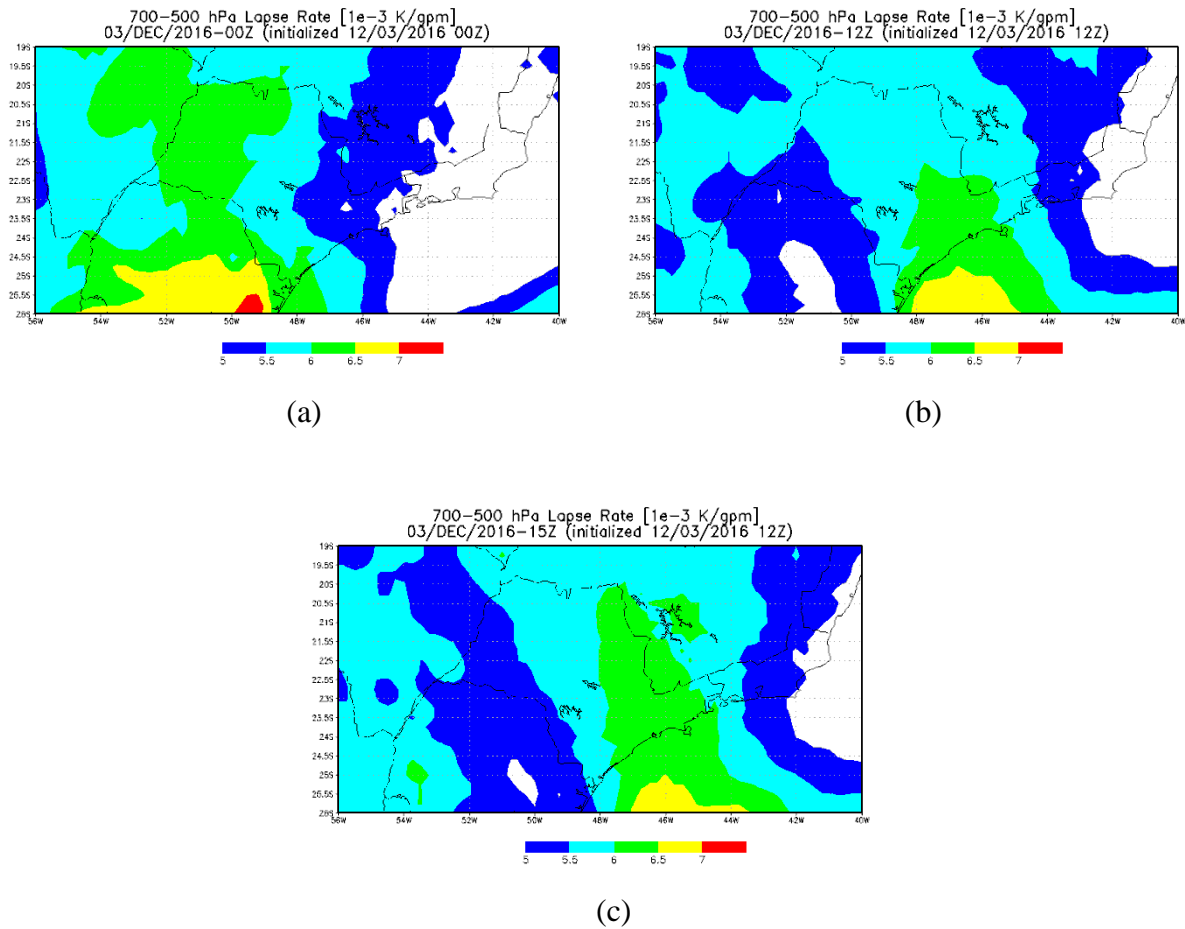


Figure 4-16: 700-500 hPa lapse rate at 00:00 UTC (a), 12:00 UTC (b), and 12:00 UTC (c), for December, 03, 2016.

CAPE from GFS is, at 12:00 UTC ranging from 600-1200 $J\ kg^{-1}$, with higher values in the northwest region, and lower values (between 300-600 $J\ kg^{-1}$) in the northeast and southeast regions. At 12:00 UTC, it has increased and is between 1500 and 1800 $J\ kg^{-1}$, through most of the State, with higher values, between 1800 and 2400 $J\ kg^{-1}$ in the north region, and between 2400-2700 $J\ kg^{-1}$ in a region in the central-north portion.

CIN is above $-20\ J\ kg^{-1}$ at 12:00 UTC everywhere in the State using a surface parcel.

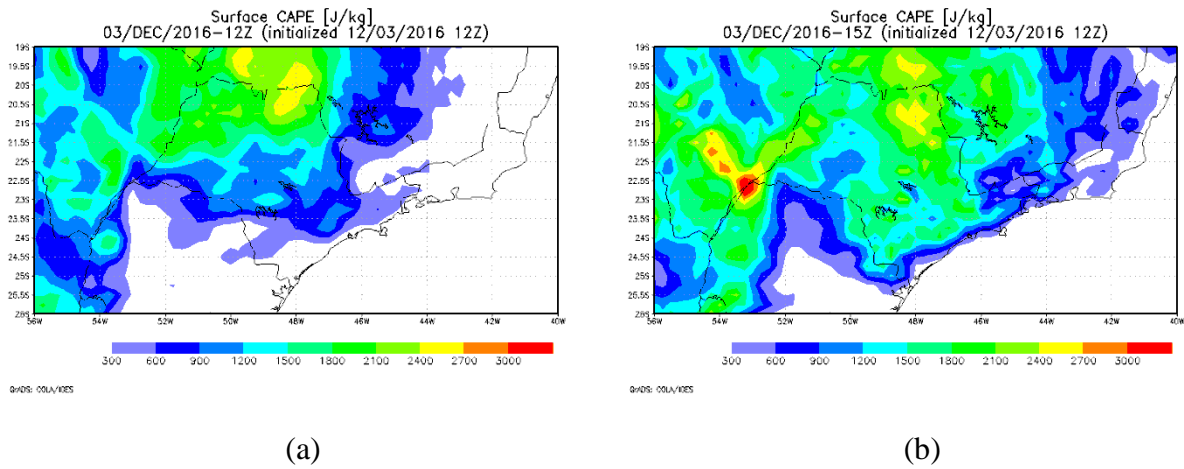


Figure 4-17: CAPE from a surface parcel at 12:00 UTC (a), and at 12:00 UTC, for December, 03, 2016.

CAPE derived from the BRAMS indicates a moderately unstable atmosphere at 12:00 UTC in the region of Campinas. At 12:00 UTC, it was at highly unstable condition. From the GFS, the parameter indicated a marginally unstable condition, and at 12:00 UTC, a moderately unstable condition.

The vertical cross section of relative humidity for the region of Campinas (23.0° latitude) is shown in Figure 4-18.

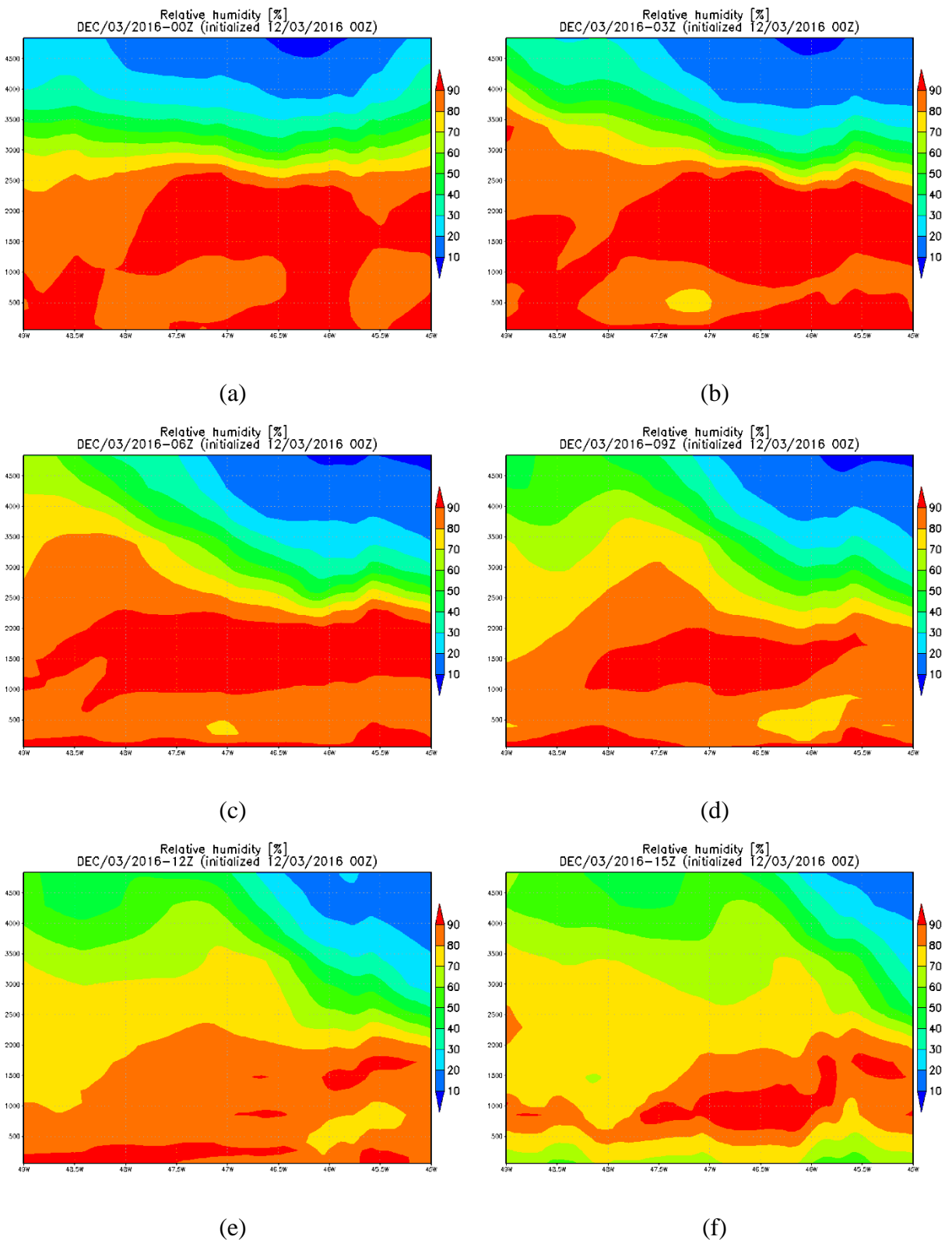


Figure 4-18: Vertical cross section of relative humidity at 23.0° , at 00:00 UTC (a), 03:00 UTC (b), 06:00 UTC (c), 09:00 UTC (d), 12:00 UTC (e), 12:00 UTC (f), for December, 03, 2016.

Low relative humidity is seen at 00:00 UTC and until 06:00 UTC, in the region of Campinas and east of it, values are around 10-20 %, and even lower than 10 % near the top. It increases after 06:00 UTC from west to east, at 12 and 12:00 UTC around 40-50 %, but lower values of the same order as earlier are still seen east of Campinas. This analysis is important to verify the presence of dry air in mid-levels, which could increase evaporation and lead to strong downdrafts. Although, values were low early in the day, it increased, and when convection started values were around 40-50 %, a comparison with other events will be made to better evaluate these values regarding the occurrence of downdrafts. This event is related to high wind gusts observed in the surface analysis, as will be shown in the next section.

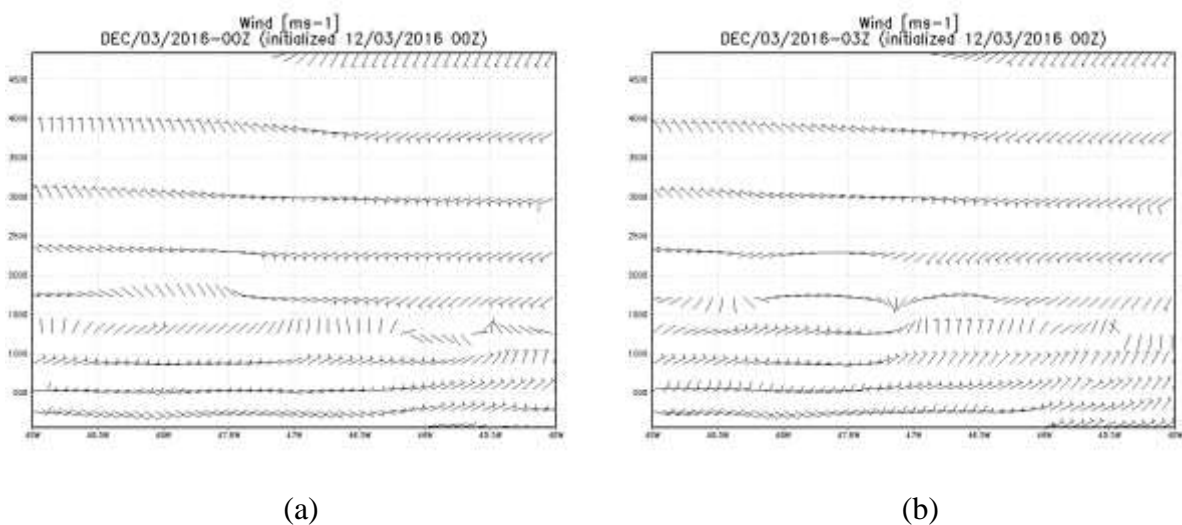
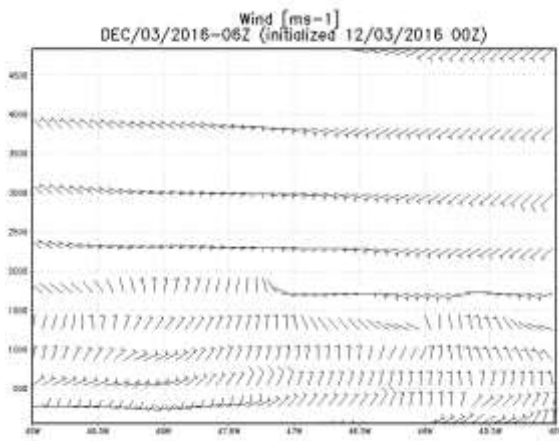
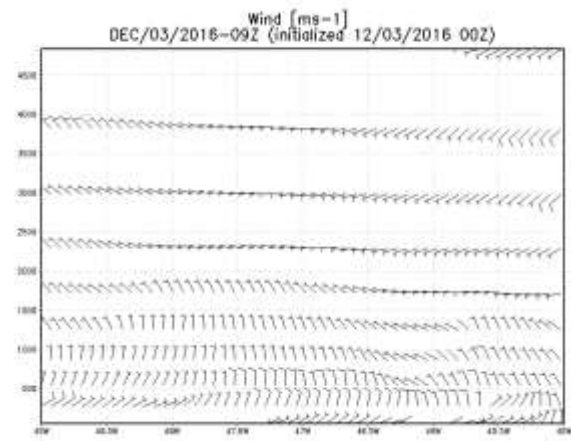


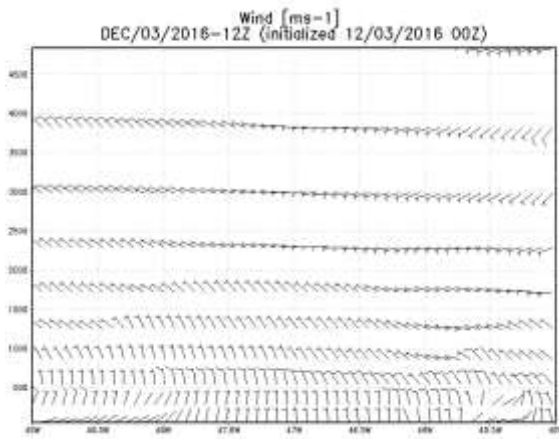
Figure 4-19: Vertical cross section of wind at 23.0° from BRAMS, at 00:00 UTC (a), 03:00 UTC (b), 06:00 UTC (c), 09:00 UTC (d), 12:00 UTC (e), 12:00 UTC (f) 18:00 UTC (g), and 21:00 UTC (h), for December, 03, 2016.



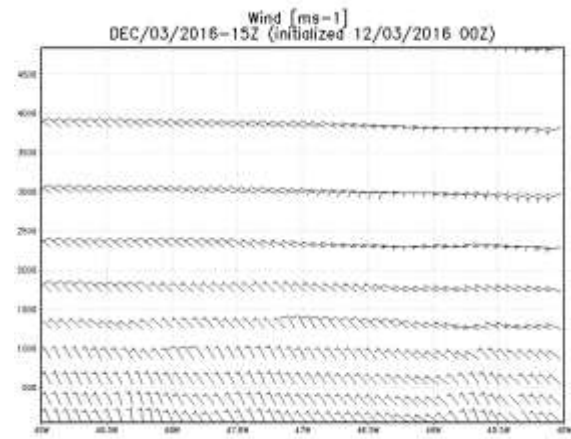
(c)



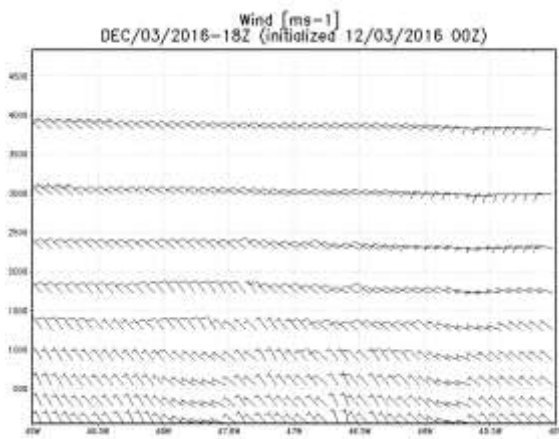
(d)



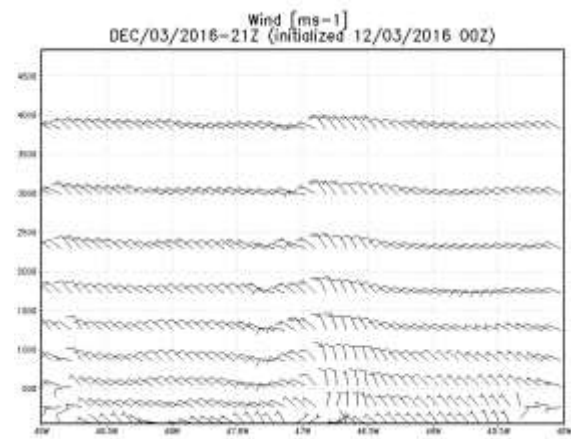
(e)



(f)



(g)



(h)

Figure 4-19: Continuation.

In the vertical cross section of the wind (Figure 4-20), it is possible to see it turning to northeast throughout the whole layer analyzed. At 09:00 and 12:00 UTC the wind turns anticlockwise with height, indicating, through the thermal wind relation, that a warm advection is occurring in the region. At 15:00 UTC and 18:00 UTC the wind is from northeast, increasing with height, and turning anticlockwise, but it is not significant.

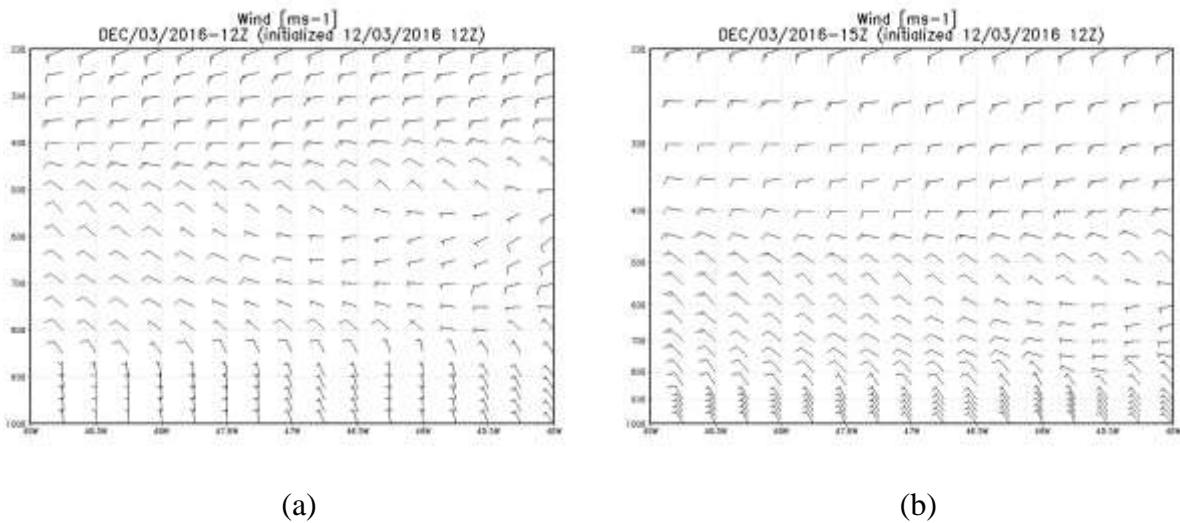


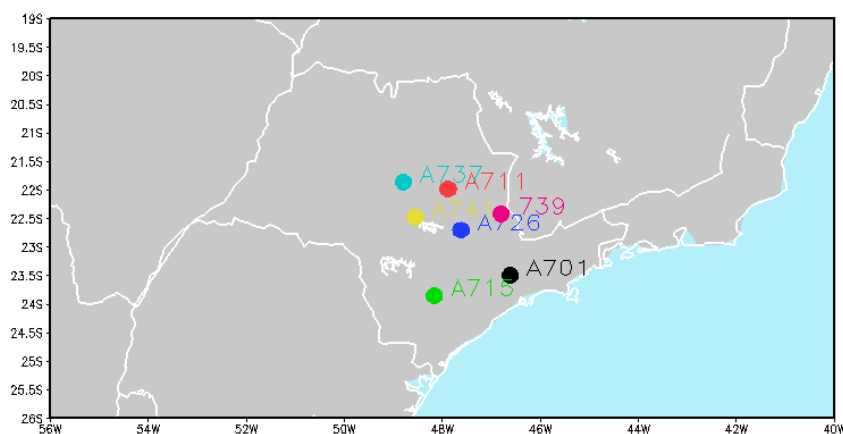
Figure 4-20: Vertical cross section of wind at 23.0° from GFS, at 12:00 UTC (a), 15:00 UTC (b), for December 03, 2016.

d. Surface stations

A total of 21 automatic surface stations from INMET spread around the State of São Paulo were analyzed. Only two of them did not record any precipitation, station A738, located at Casa Branca in the north central part of the State, and A712, located at Iguape, in the southeast coast. Seven stations recorded wind gusts above 15 m s^{-1} (Figure 4-21) and two of them recorded wind gust above 20 m s^{-1} . The highest wind gust registered was 21.3 m s^{-1} at A737 station, which also registered the highest precipitation value observed (30.6 mm between 2-3 pm local time). At station A726 the second highest wind gust occurred (20.9 m s^{-1}). At station A711 wind gusts of 18.2 m s^{-1} were observed two hours straight (2 and 3 pm). The city of São Paulo had 1 point of floods in the city during this event, at the station A701

located in the city, the accumulated precipitation was 15 mm and it rained for 5 hours. The maximum registered was 12 mm at 19:00 UTC (5 pm local time). In the city of Campinas it was reported fall of trees due to severe wind gusts. The city is in the region of stations which registered wind gusts above 15 m s^{-1} . It rained for around 4-6 hours in each station. The time of the precipitation varied among the stations due to their location, it is possible to compare the time of precipitation in each station and the satellite and radar images (Figure 4-3, Figure 4-4, and Figure 4-5). Maximum rain observed above 10 mm occurred in seven stations. Only three stations recorded rain in one hour of observation higher than 15 mm (A725, A737, A739, Figure 4-22).

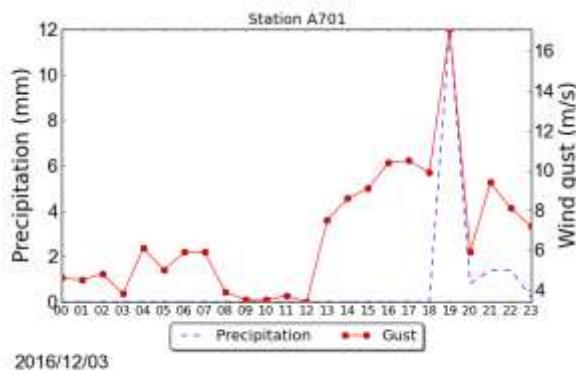
One important thing to notice is the falling of temperature related to wind gusts, in the seven stations with wind gusts exceeding 15 m s^{-1} . Temperature dropped 6-9 °C because the downdrafts carry cold air from above, leading to the formation of the cold pool (section 2.1).



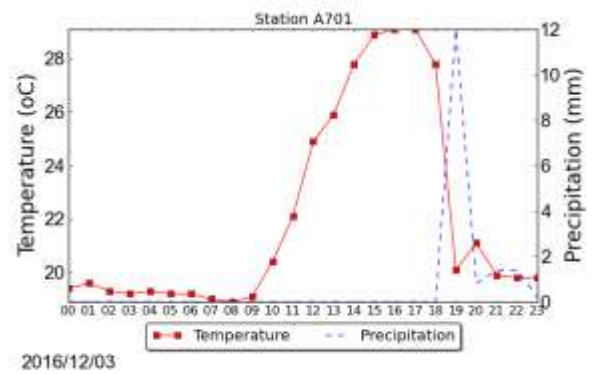
GrADS: COLA/IGES

2017-11-01-22:22

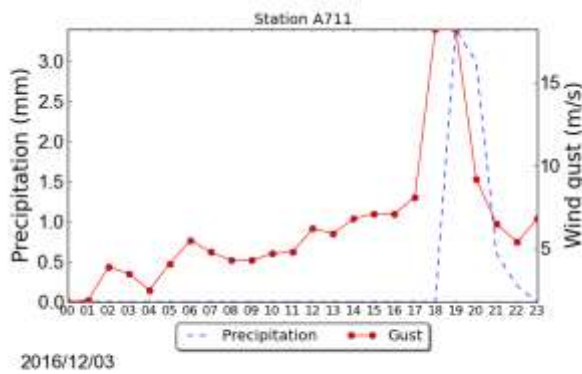
Figure 4-21: Automatic surface station which recorded wind gust above 15 ms^{-1} , for December, 03, 2016.



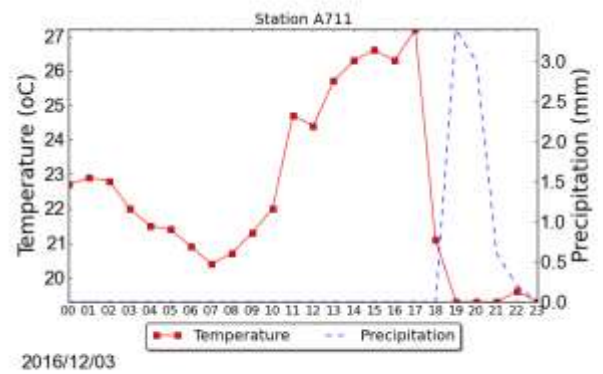
(a)



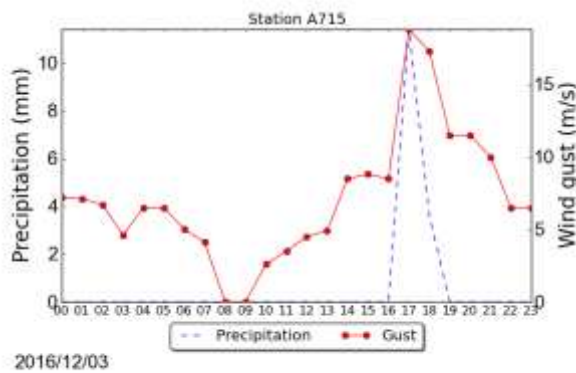
(b)



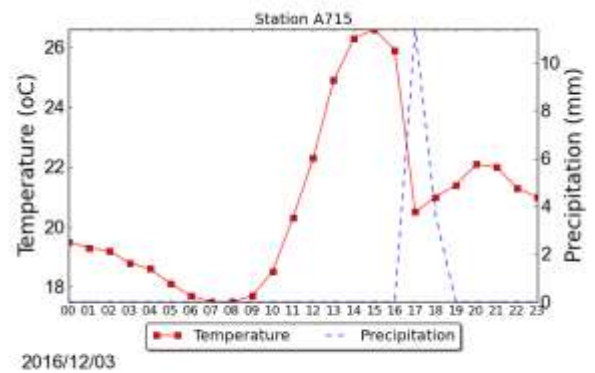
(c)



(d)

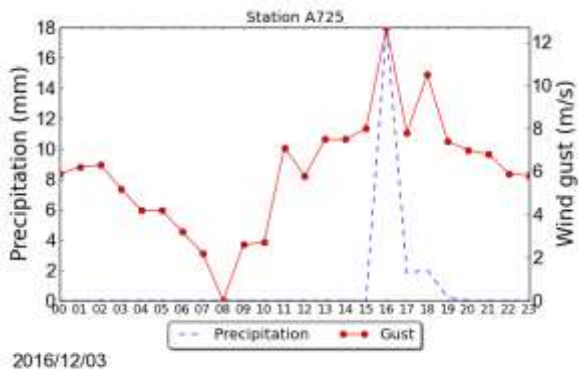


(e)

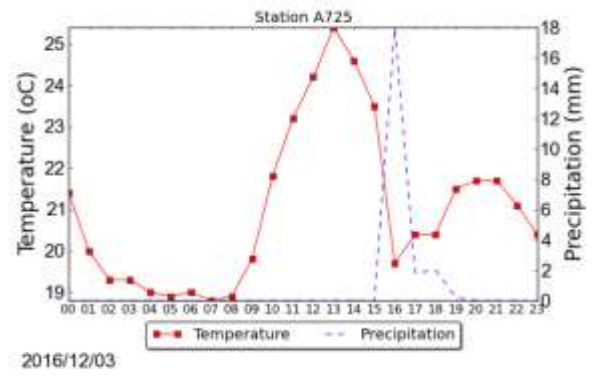


(f)

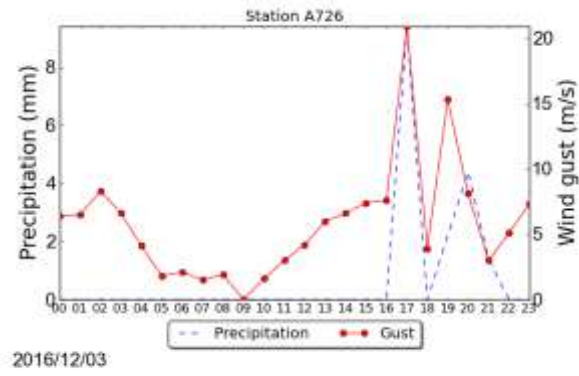
Figure 4-22: Precipitation (mm), wind gust (ms^{-1}), and temperature ($^{\circ}\text{C}$) at stations A701 (a) and (b), A711 (c) and (d), A715 (e) and (f), A725 (g) and (h), A726 (i) and (j), A737 (k) and (l), A739 (m) and (n), A741 (o) and (p).



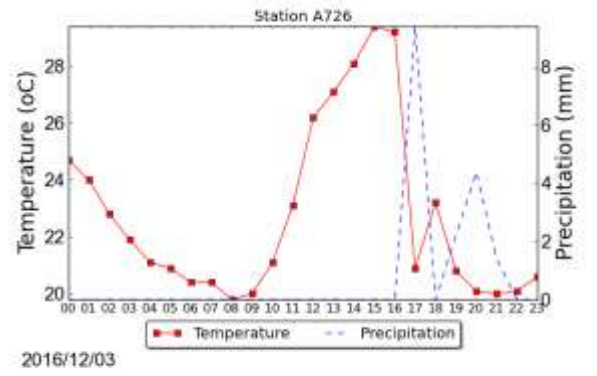
(g)



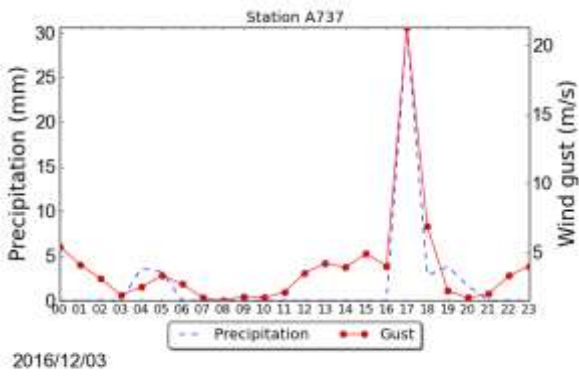
(h)



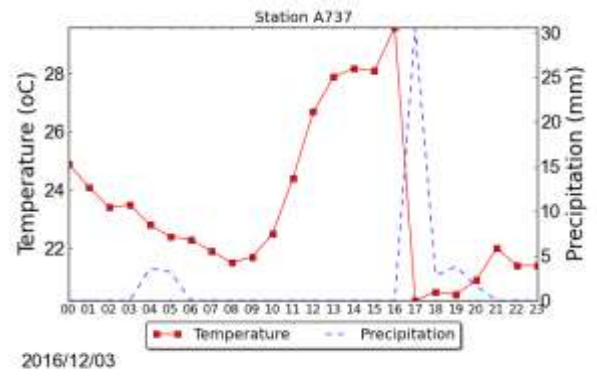
(i)



(j)

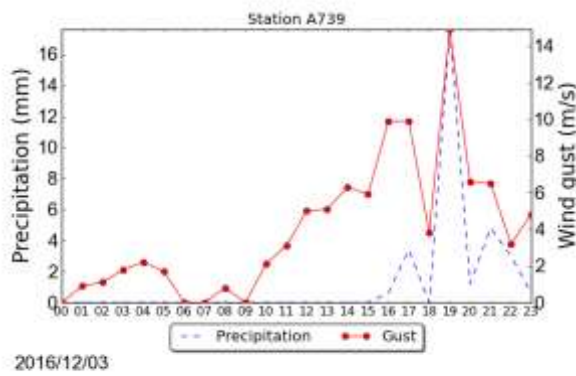


(k)

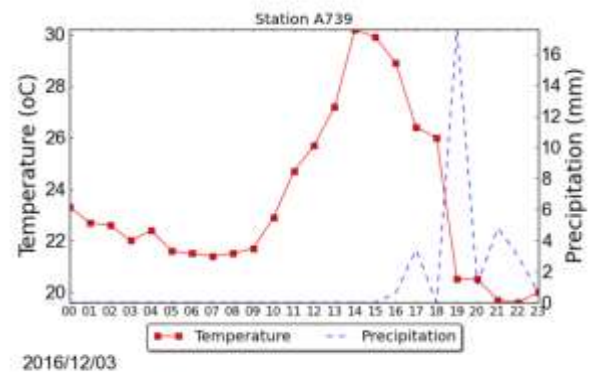


(l)

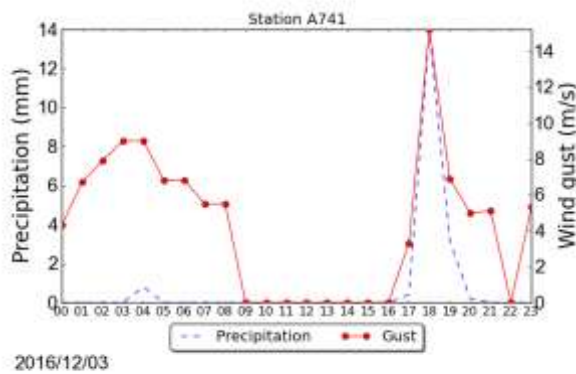
Figure 4-22: Continuation.



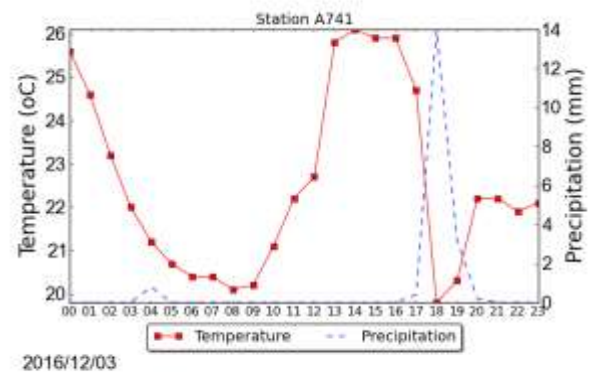
(m)



(n)



(o)



(p)

Figure 4-22: Conclusion.

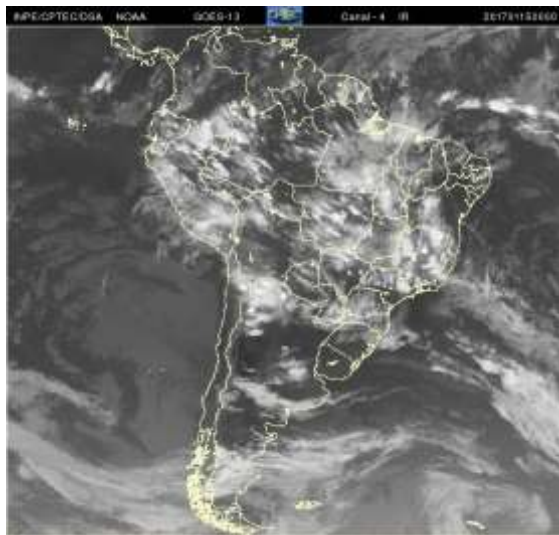
4.1.1.2 January, 15-17th, 2017

The highest accumulated rainfall among the events, and according to the news, the highest observed during 24 hours in 68 years at the Mirante do Santana station was observed between the night of January, 15 and the dawn of January, 16. Floods were registered in the city of São Paulo, Guarulhos, Osasco, Carapicuíba, Barueri, Francisco Morato, Franco da Rocha e Caieras. On January, 16, floods were reported at Campinas, Jundiaí and Santos.

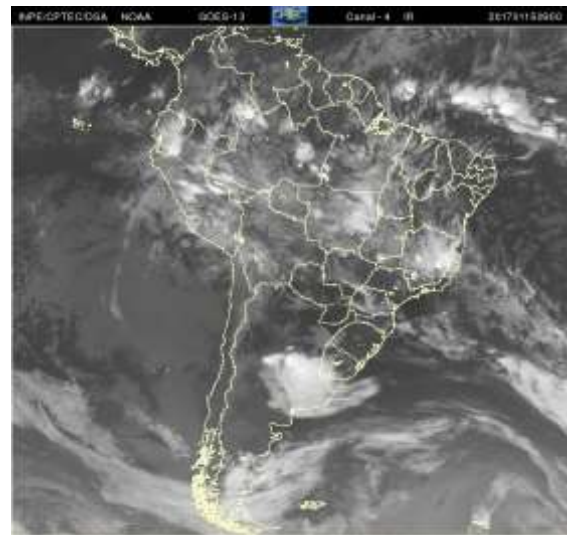
a. Satellite

Infrared images for South America and enhance infrared images for the southeast region will be analyzed in this section.

At 00:00 UTC on January, 15 clouds are seen in the State of São Paulo, probably related to some event that occurred on the previous day. At 09:00 UTC no clouds are present in the State of São Paulo, but it possible to see clouds extending from the Amazon region to the State of Minas Gerais, indicating the presence of the northwest flow, which will be shown in the synoptic scale analysis section. It also possible to see, in the State of Paraná, clouds extending from a frontal system, observed in the Atlantic Ocean. It is moving to the State of São Paulo. Several clouds develop between Amazon region, the center-west region of Brazil, and on Minas Gerais after 17:30 UTC. After 21:30 UTC they move to the region of São Paulo. It is possible that the advance of those clouds related to the frontal system, may have aided in the development of this event.

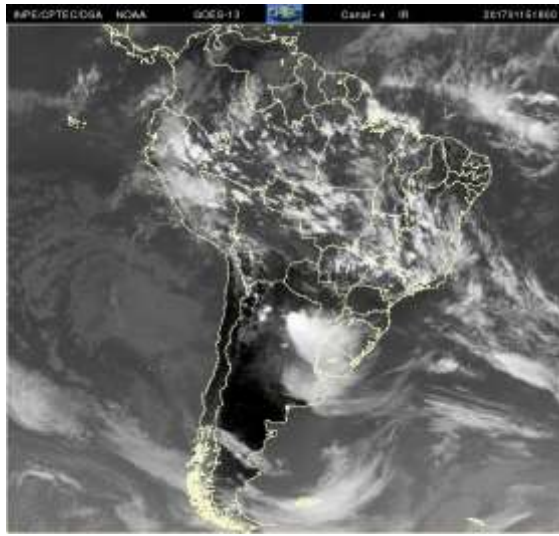


(a)

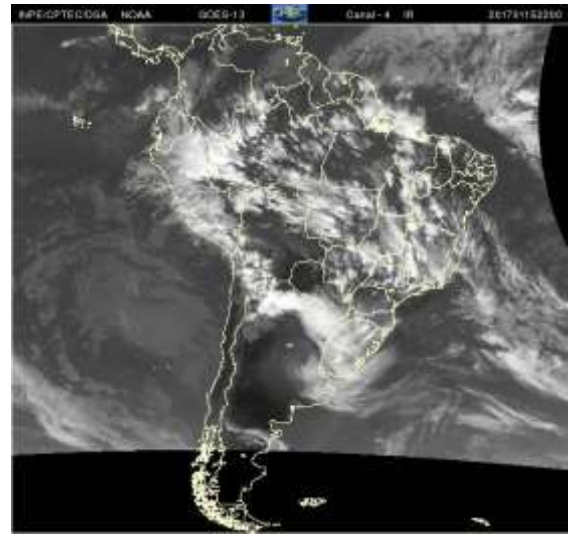


(b)

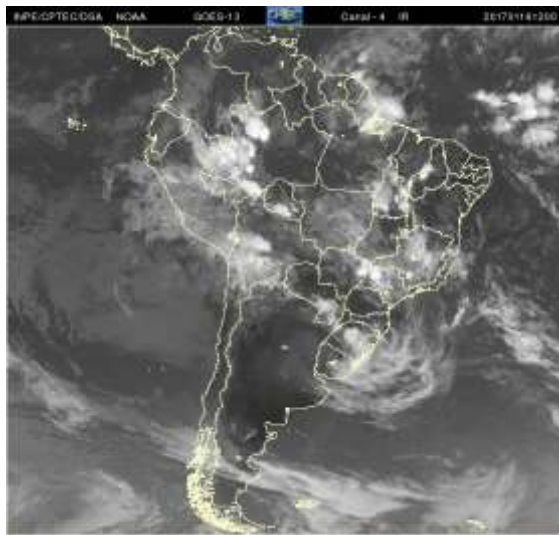
Figure 4-23: Infrared satellite images for January 15 at 00:00 UTC (a), 09:00 UTC (b), 18:00 UTC (c), and 22 UTC (d); January, 16 at 12:00 UTC (e), and 18:00 UTC (f); January, 17 at 12:00 UTC (g), and 18:00 UTC (h).



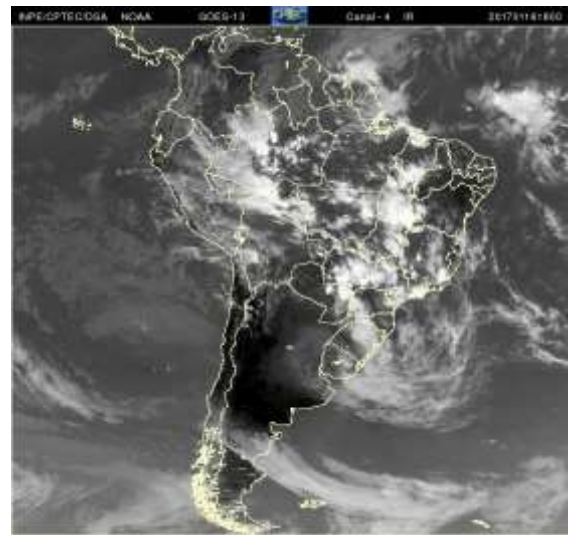
(c)



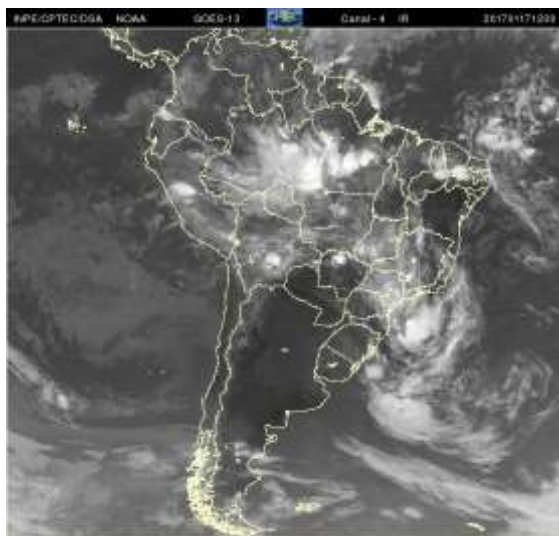
(d)



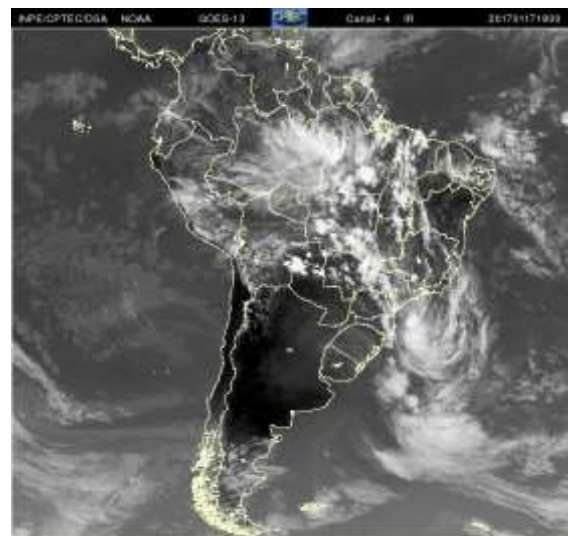
(e)



(f)



(g)



(h)

Figure 4-23: Continuation.

On January, 16, at 12:00 UTC, it is possible to see clouds forming in the northwest region of the State related to the low pressure system seen in the 850 hPa analysis (section c). Clouds are also observed in the low pressure system in the south region of Brazil. After 17:00 UTC, clouds are extending from the Amazon through the center-west region to the southeast and south regions of the country.

Through the next day (January, 17), clouds are extending through those regions along the day, indicating the formation of the humidity convergence zone.

In the enhanced infrared images, on January, 15, those clouds, mentioned extending from the frontal system, are seen reaching the State of São Paulo at 15:00 UTC. After 16 UTC, cells forming are in southern of Minas Gerais, and northwestern São Paulo. At 17:00 UTC, in the northeast region, cells are seen in the region of Serra da Mantiqueira. At 1730 UTC, cells are still in the region and are beginning to form in the region of Vale do Paraíba, probably due to the sea breeze or to the local topography. At 18:30 UTC, clouds are seen with temperature values around -50 and -60°C in the region, they move northeastward. After 20:30 UTC, seen more clearly at 22:00 UTC, clouds are forming in the State of São Paulo, extending from the southwest region to the northeast region.

At 00:00 UTC on January, 16, in the region of São Paulo, temperature is around -60°C . Clouds are seen in the region until 09:00 UTC. At 11:00 UTC clouds with temperature around -70°C are present in the northwest region related to the low pressure system in the 850 hPa level. At 18:00 UTC several cells are present in the State of São Paulo reaching temperature values of -70°C near the coast in the northeast region. At 19:00 UTC the entire east coast has clouds with temperature of that order, and at 20:30 UTC values reach -80°C in the southeast region. At 23:30 UTC clouds are still seen in eastern São Paulo, with values around -60°C .

On January, 17, those clouds in the east region move southeastward and at 05:00 UTC clouds reaching temperature values of the order of -60°C and even -70°C are present in the

central region, extending southeastward. They also move southeastward. At 17:00 UTC, cells are forming in a northwest-southeast direction related to the presence of the low-level jet. This is seen through the rest of the day.

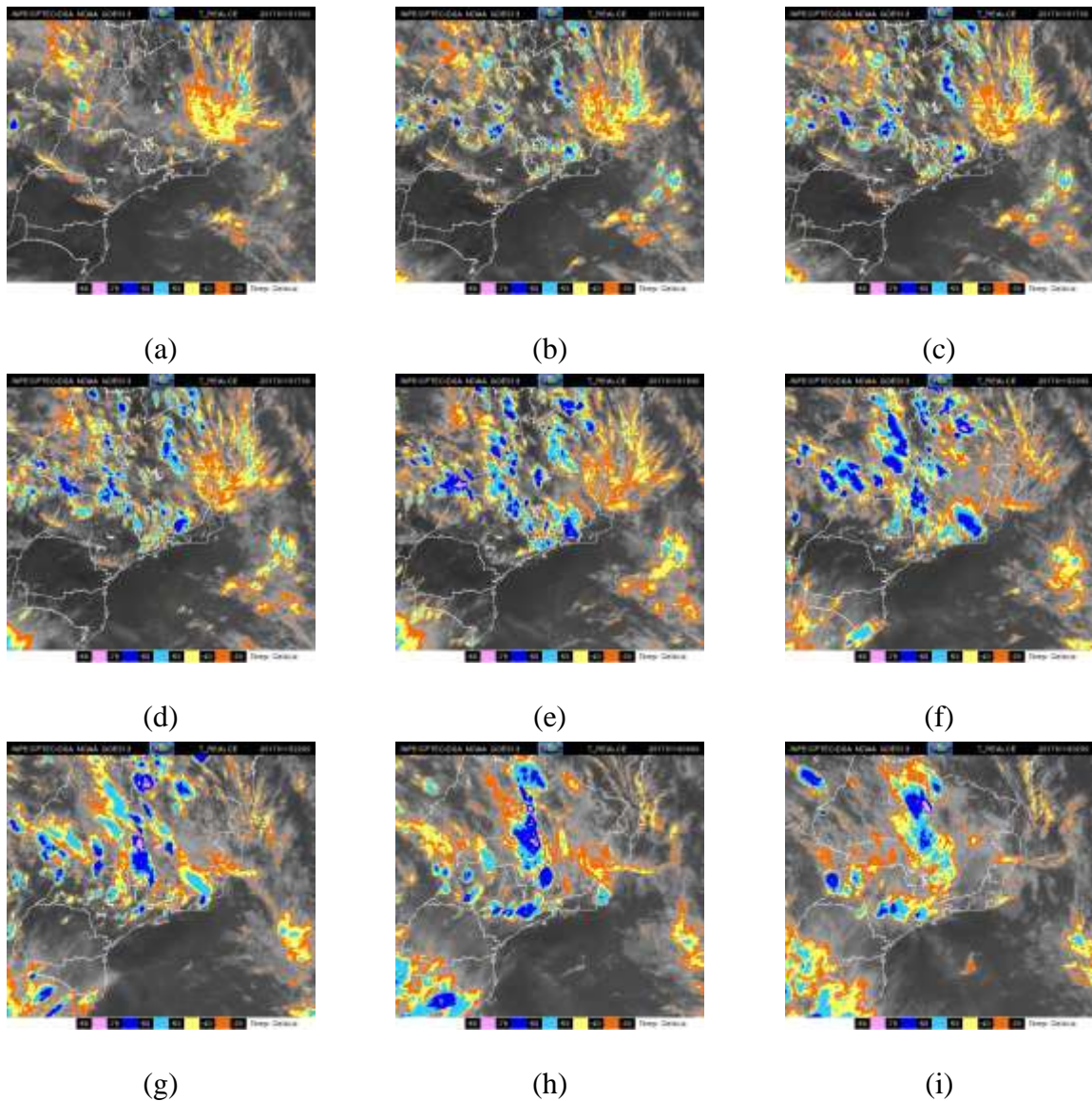


Figure 4-24: Enhanced infrared satellite images for January, 15 at 15:00 UTC (a), 16:30 UTC (b), 17:00 UTC (c), 17:30 UTC (d), 18:30 UTC (e), 20:30 UTC (f), 22:00 UTC (g); January, 16 at 00:00 UTC (h), 02:30 UTC (i), 09:00 UTC (j), 11:00 UTC (l), 18:00 UTC (m), 19:00 UTC (n), 20:30 UTC (o), 23:30 UTC (p); January, 17 at 05:00 UTC (r), 17:00 UTC (s).

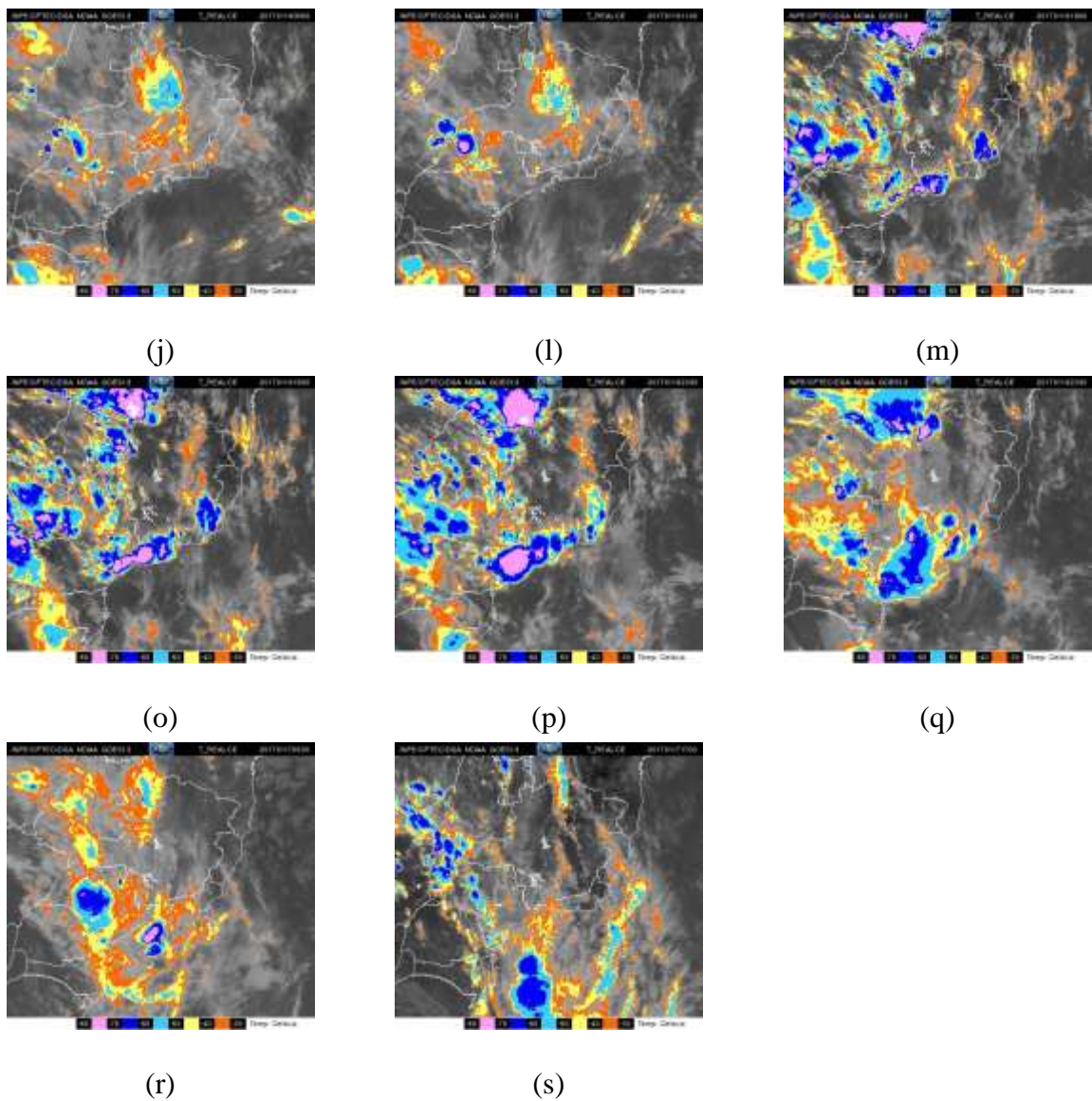


Figure 4-24: Continuation.

b. Radar

On January, 15 cells started to form in the region of Serra da Mantiqueira at 15:00 UTC. They move southeastward and at 16:20 UTC they are seen in the region of Guarulhos and Vale do Paraíba. Between 16:50 and 17:10 UTC, reflectivity is around 55 dBZ in the east region of São Paulo. At 17:10 UTC it is possible to see that clouds are parallel to the coast, which may be related to the sea breeze. Between 17:40 and 1750 UTC reflectivity is around 45 dBZ in the region of São Paulo (central). It loses its strength and moves away; at 19:00 UTC no cells are seen in the region. Cells from Minas Gerais continued to propagate in a

southeastward direction, seen at 21:30 UTC in the northeast region of the State of São Paulo, with reflectivity around 40-45 dBZ. They approach the region of the city of São Paulo after 23:00 UTC. Until 23:50 reflectivity values around 45 dBZ are observed in the north region of São Paulo, Franco da Rocha and Francisco Morato.

At 04:50 UTC on January, 16, cells with reflectivity around 30-45 dBZ are seen close to São Paulo and in the east region of the city. These cells remain in the region until after 08:00 UTC, and at 10:30 UTC clouds are no longer seen. After 15:00 UTC, still on January, 16, cells are observed again propagating in a southeastward direction. After 16:00 UTC are seen in the region of the city of São Paulo, and intensifying near the coast. At 17:40 UTC reflectivity is reaching 55 dBZ near the coast and in the south region of São Paulo. Cells even more intense are observed at 18:50 UTC with reflectivity of 60-65 dBZ near the coast (around the height of São Paulo), and around 55 dBZ in the southeast region. At 20:20 UTC reflectivity is around 55-60 dBZ in the southeast region, these intense convective cells were observed in the satellite analysis. They move in a southeastward direction. At 21:10 UTC, cells with reflectivity around 55 dBZ are seen in the region of Campinas, moving southeastward. Cells with the same order of reflectivity are seen again after 23:00 UTC. These cells move through the region of Jundiaí. Both cities reported floods during this day.

During the last day of analysis, January, 17, cells are seen moving through the region of the radar southeastward, this is related to the northwest flow, which led to the formation of the humidity convergence zone, as already mention in the previous analysis, and will be shown in the next section. Reflectivity above 50 dBZ is not seen during this day.

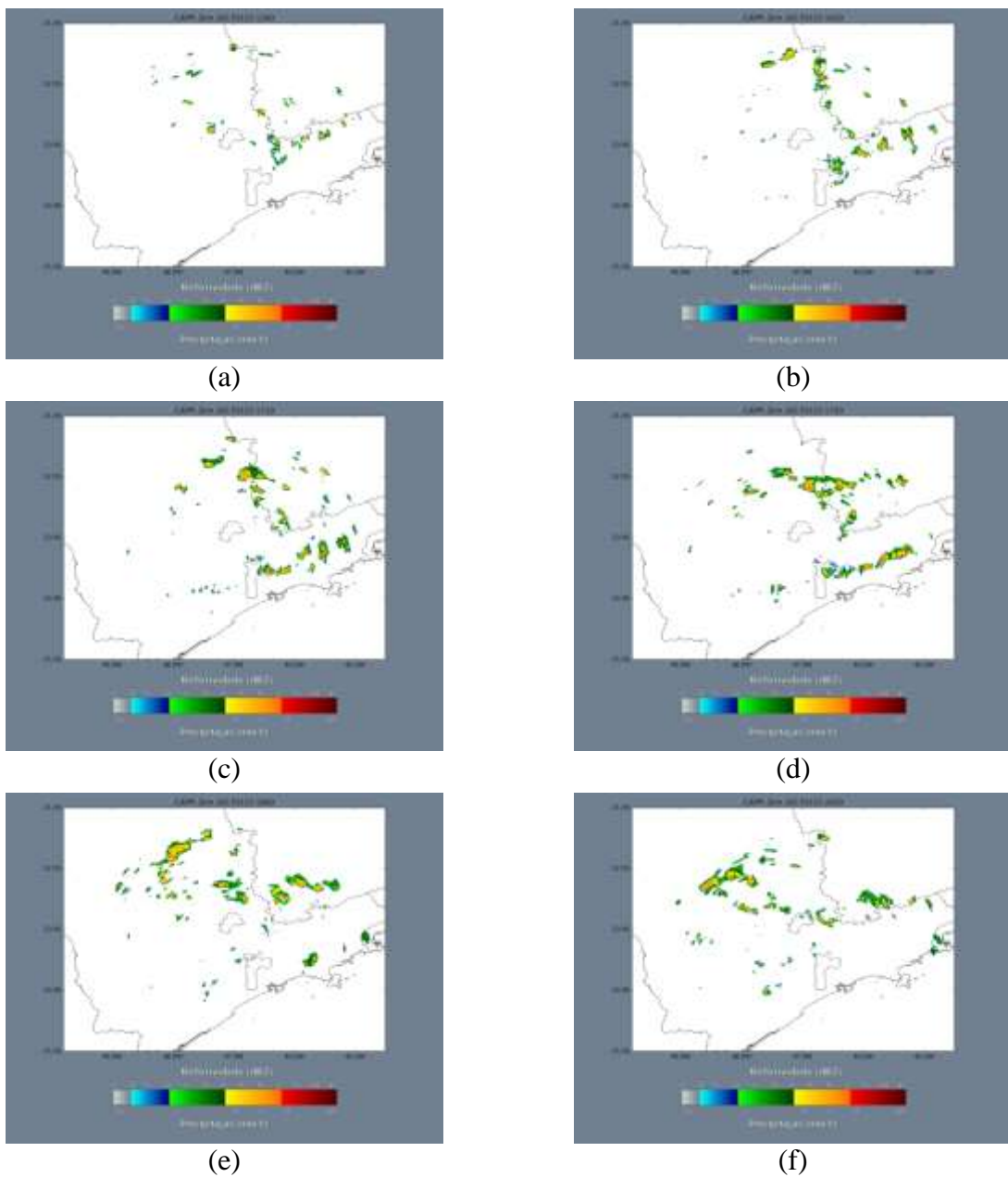


Figure 4-25: Radar images from the São Roque radar at January, 15 at 15:00 UTC (a), 16:20 UTC (b), 17:10 UTC (c), 17:50 UTC (d), 19:00 (e), 20:20 UTC (f), 21:30 UTC (g), 23:50 UTC (h); January, 16, at 04:50 UTC (i), 08:00 UTC (j), 10:30 UTC (l), 15:00 UTC (m), 16:20 UTC (n), 17:40 UTC (o), 20:20 UTC (p), 21:10 UTC (q), 23:30 UTC (r), 23:50 UTC (s); January, 17 at 06:10 UTC (t), 12:10 UTC (u).



(g)



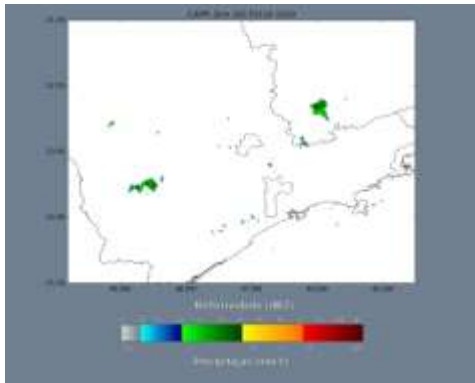
(h)



(i)



(j)



(l)

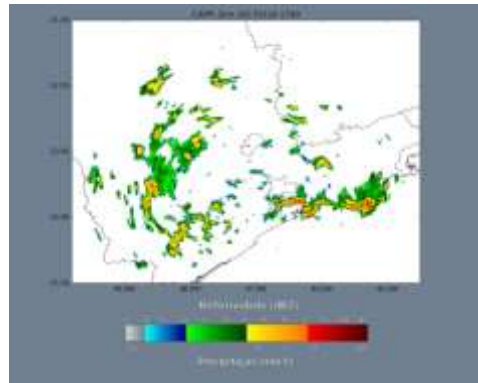


(m)

Figure 4-25: Continuation.



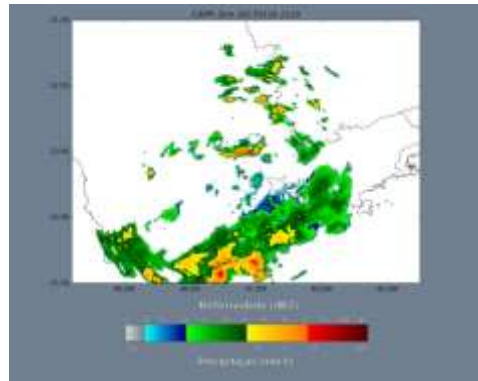
(n)



(o)



(p)



(q)

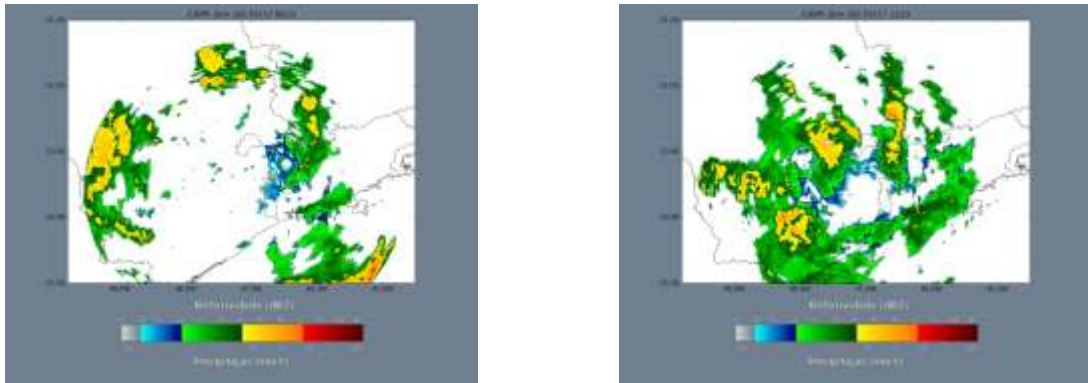


(r)



(s)

Figure 4-25: Continuation.



(t)

(u)

Figure 4-25: Conclusion.

c. Synoptic scale analysis

At the 200 hPa analysis, an upper level cyclonic vortex is seen in the Atlantic near the coast of the northeast region of Brazil, and a trough is observed in the Atlantic Ocean away from the coast of the south region of the country associated with a front at the surface. Also present in the analysis is the Bolivian High, at northern Chile. The only synoptic pattern observed at this level is a diffluence at the State of São Paulo at 18:00 UTC. This diffluence pattern is related to the Bolivian High and it is also seen through the next two days (January, 16 and 17).

Wind divergence is only seen at 21:00 UTC, on January 15, around $0.2-0.4 \cdot 10^{-4} \text{ s}^{-1}$ in the northeast region. Through the next day, wind divergence is observed at different regions in the State, seen in Figure 4-27. It is seen in the region of Campinas and Jundiaí, until 06:00 UTC.

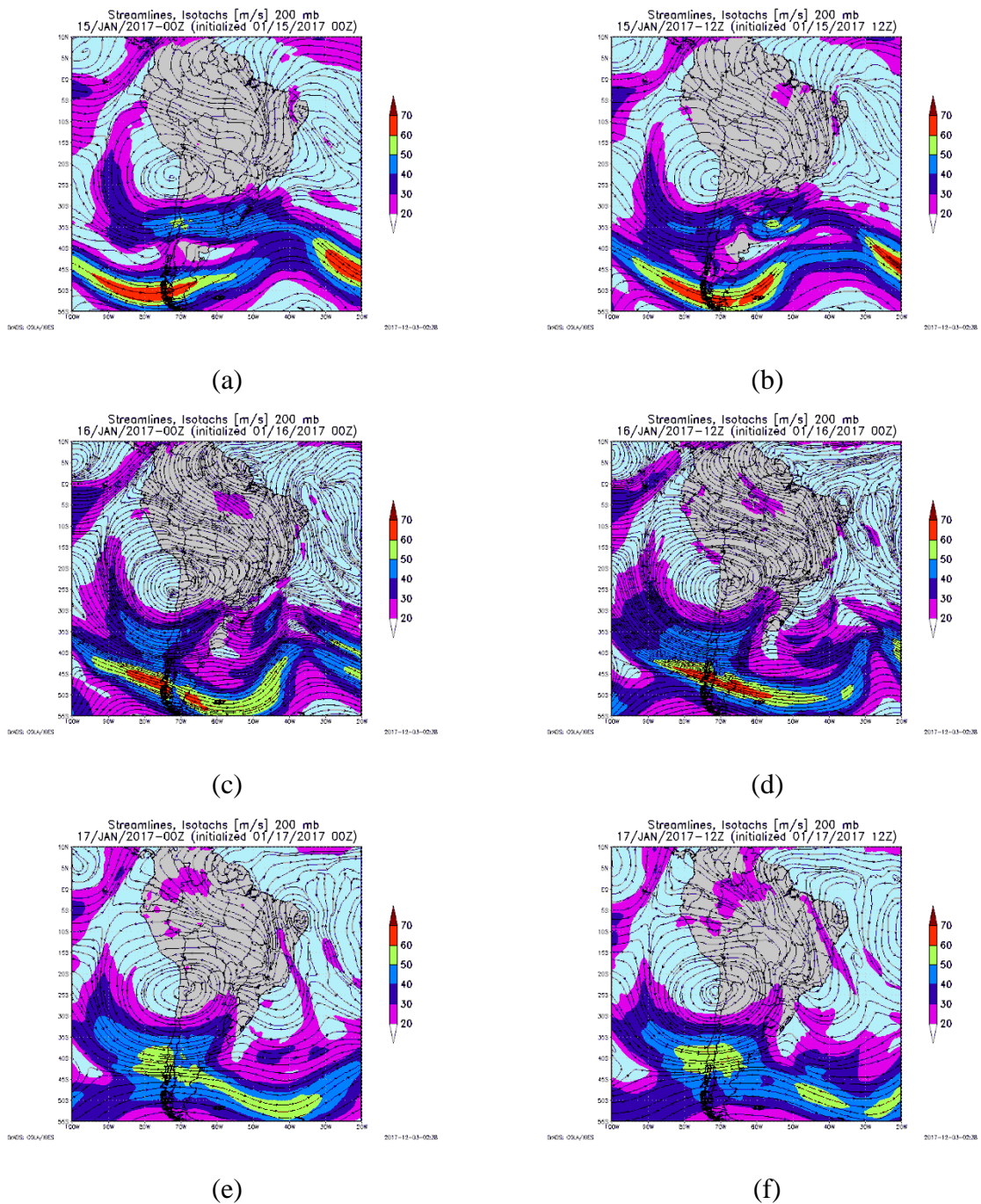


Figure 4-26: Streamlines and isotachs (m s^{-1}) at 200 hPa at 00 and 12:00 UTC for January, 15 (a), (b), January, 16, (c), (d), January, 17 (e), (f).

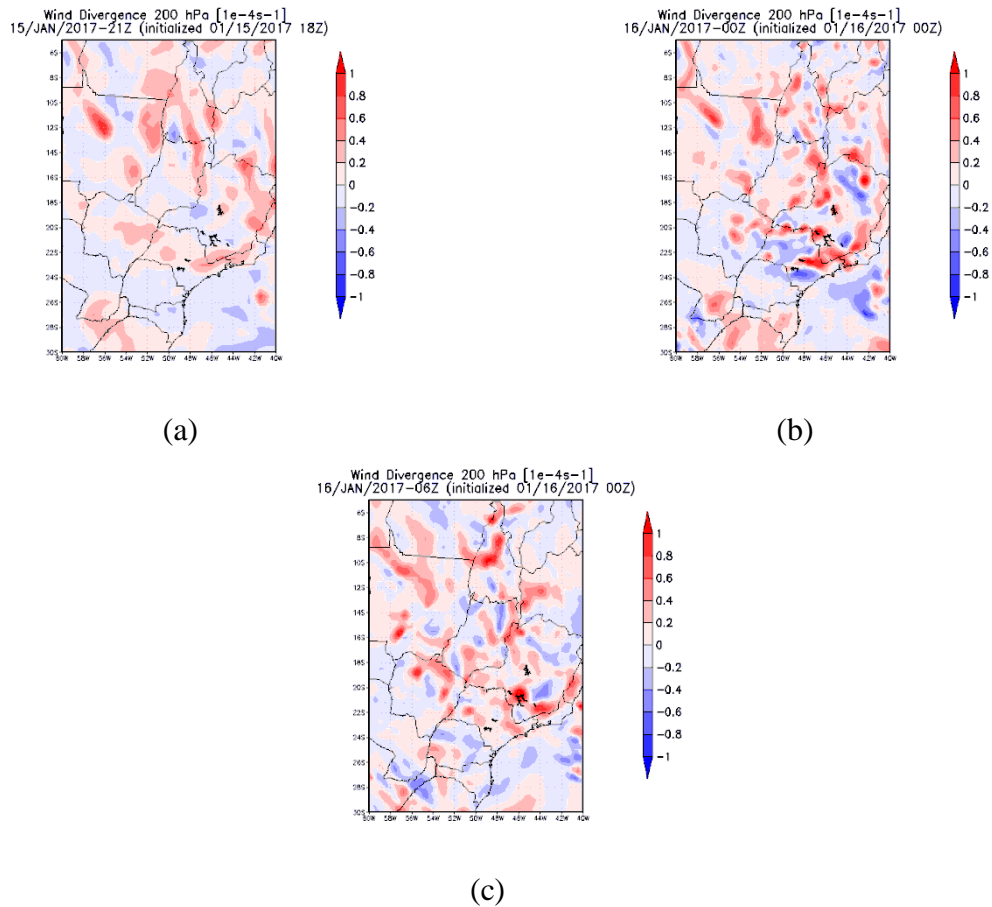


Figure 4-27: Mass divergence at 200 hPa for January, 15 at 21:00 UTC (a), January, 16 at 00:00 UTC (b), and 06:00 UTC (c).

At the 500 hPa level, a low pressure system with negative vorticity associated is seen in the northwest region of the State of São Paulo, through the day on January, 15. On January, 16 negative vorticity is seen extending from southeastern Minas Gerais through the central region of the State of São Paulo.

At January, 15th, two low pressure systems in the region of São Paulo are seen in the 850 hPa analysis; one is located in the northwest region, between São Paulo and Minas Gerais, the other one is in the northeast part of the State, between São Paulo and Rio de Janeiro. They are seen as a trough until 18:00 UTC. This may have generated instability in the State. Low relative humidity is observed at the east part of the State. Values are around 65-70% at 00:00 UTC, but decrease below 65 % after. After 15:00 UTC it increases again, and at

18:00 UTC values are, with the exception of a small region southeastern, above 85 % and above 95% in the northwest region. One important feature about this event is the northwest flow from the Amazon region. The flow entering the continent moving westward is deflected by the Andes to the southeast region of the country. At 00:00 UTC, it is seen directed to the State of Minas Gerais. At 12:00 UTC it is more intense and directed to the south region of Minas Gerais, this is seen until 21:00 UTC. Relative humidity at this region, at 12:00 UTC, is above 90 %. At this hour, in the region of Vale do Paraiba, relative humidity has already increased and is between 75-90 %.

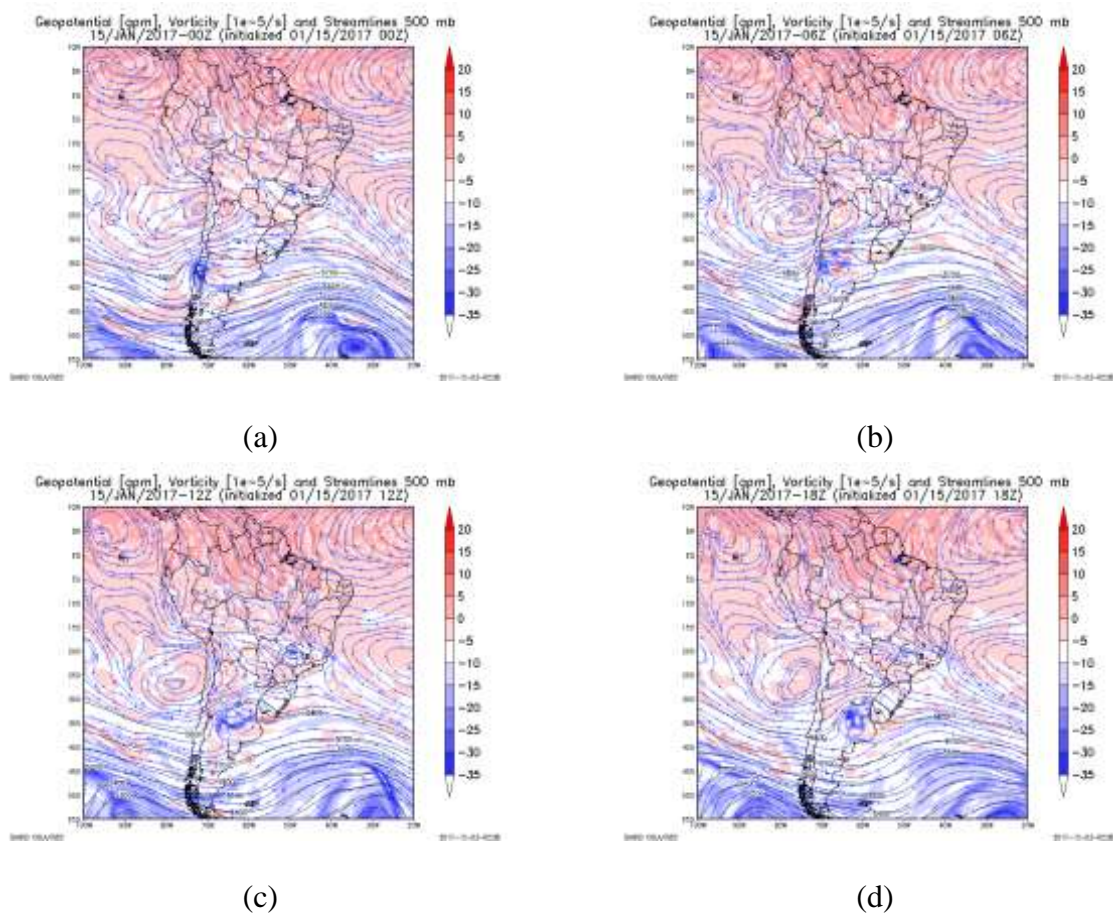


Figure 4-28: Streamlines, geopotential height (gpm) and vorticity ($1 \times 10^{-5} \text{ s}^{-1}$) at 500 hPa for January, 15th, at 00:00 UTC (a), 06:00 UTC (b), 12:00 UTC (c), 18:00 UTC (d).

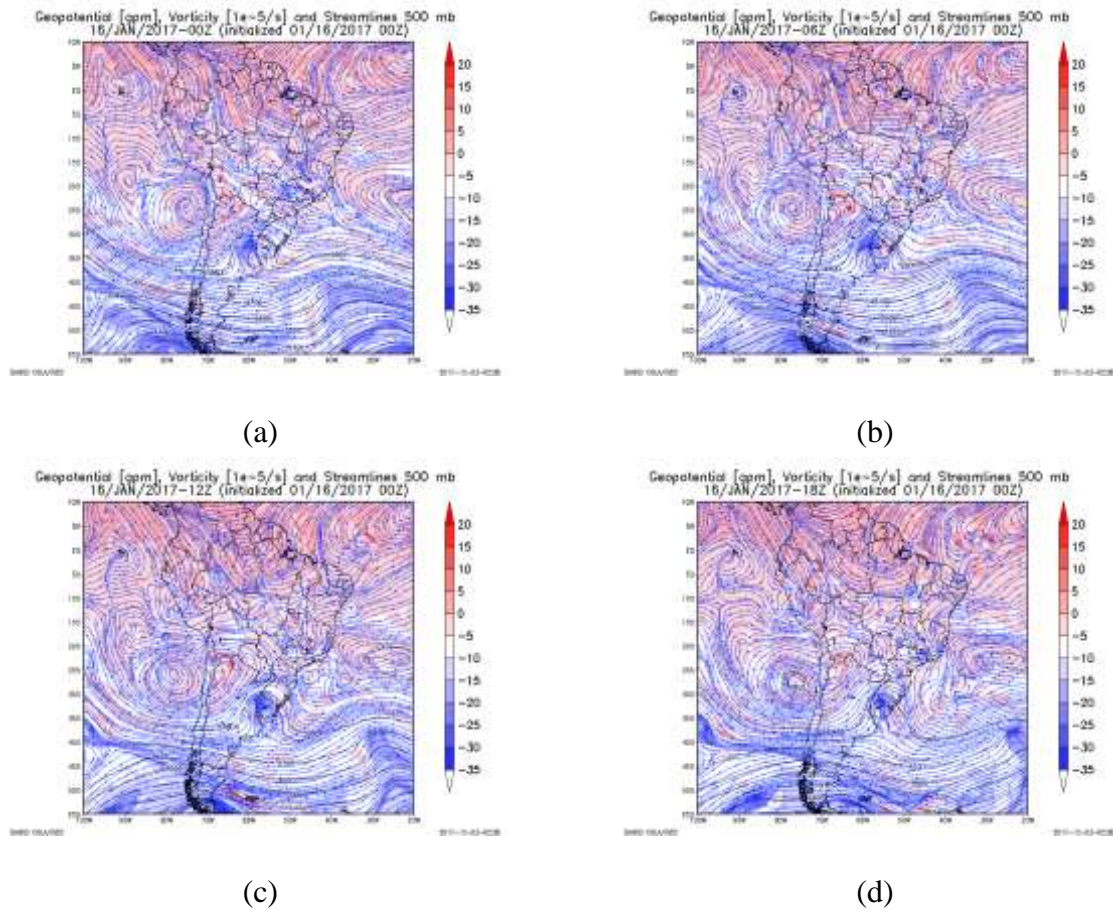


Figure 4-29: Streamlines, geopotential height (gpm) and vorticity ($1 \times 10^{-5} \text{ s}^{-1}$) at 500 hPa for January, 16th, at 00:00 UTC (a), 06:00 UTC (b), 12:00 UTC (c), 18:00 UTC (d).

At 00:00 UTC, on the next day, the low pressure system on the northwestern part of the State is present, this system moves to the southwest region of São Paulo through the day. After 21:00 UTC from the previous day, the northwest flow moved to be directed to the State of São Paulo, seen at 00:00 UTC (January, 16) and throughout the entire day. Relative humidity increases during the day, at 00:00 UTC it is above 75 %, but values above 95 % are observed near the low pressure system (northwest region) and in the east region. After 06:00 UTC values are above 85 % in the entire State. After 12:00 UTC, regions with values higher than 95 % also increased. This change observed in the northwest flow direction seen at 00:00 UTC of this day is the most important feature related to this event. As showed in the previous satellite and radar analysis, convection started to form between northern São Paulo and

southern Minas Gerais, these convective cells moved following the northwest flow, to São Paulo, and caused the rain observed at the city of São Paulo and others close to it. At 06:00 UTC January 17, the low pressure system vanished. This northwest flow persists through the next day (January, 17) directed to the State of São Paulo.

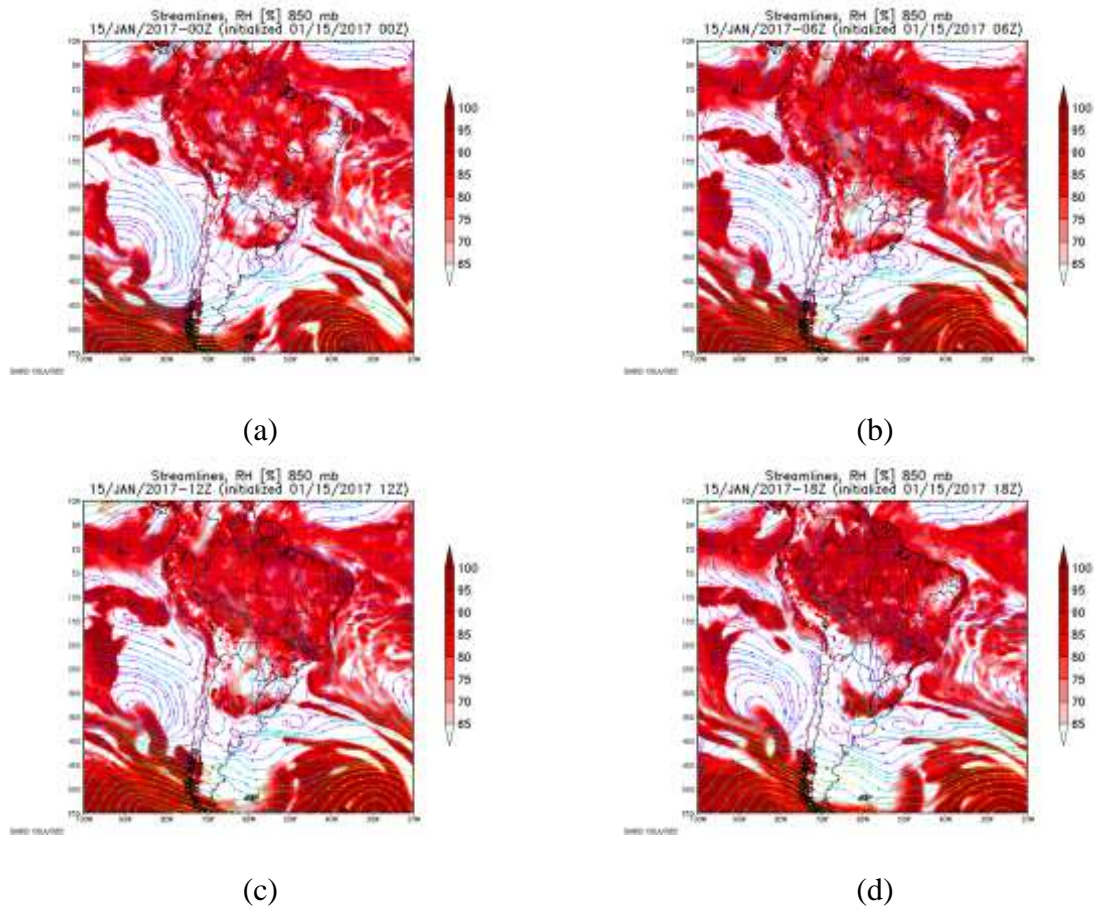


Figure 4-30: Streamlines and relative humidity (%) at 850 hPa at January, 15 at 00:00 UTC (a), 06:00 UTC (b), 12:00 UTC (c), 18:00 UTC (d).

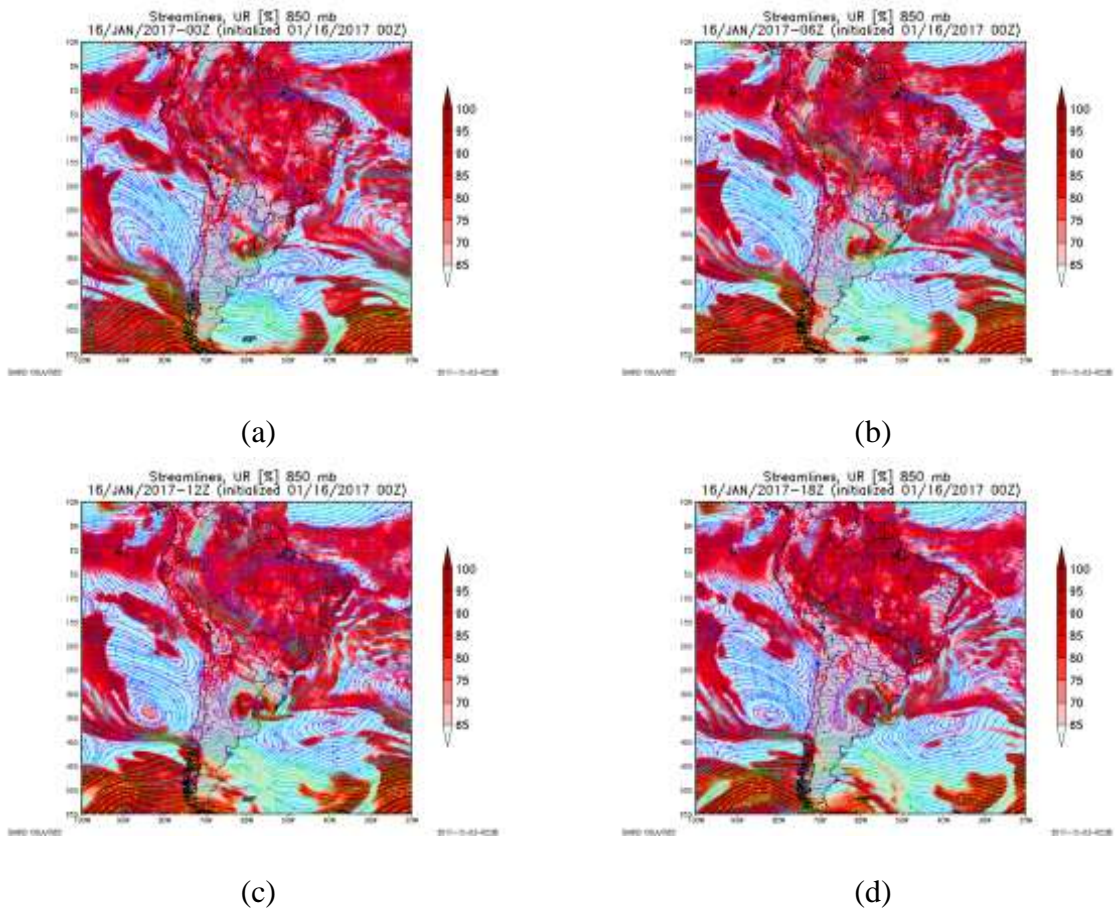


Figure 4-31: Streamlines and relative humidity (%) at 850 hPa at January, 16th at 00:00 UTC (a), 06:00 UTC (b), 12:00 UTC (c), 18:00 UTC (d).

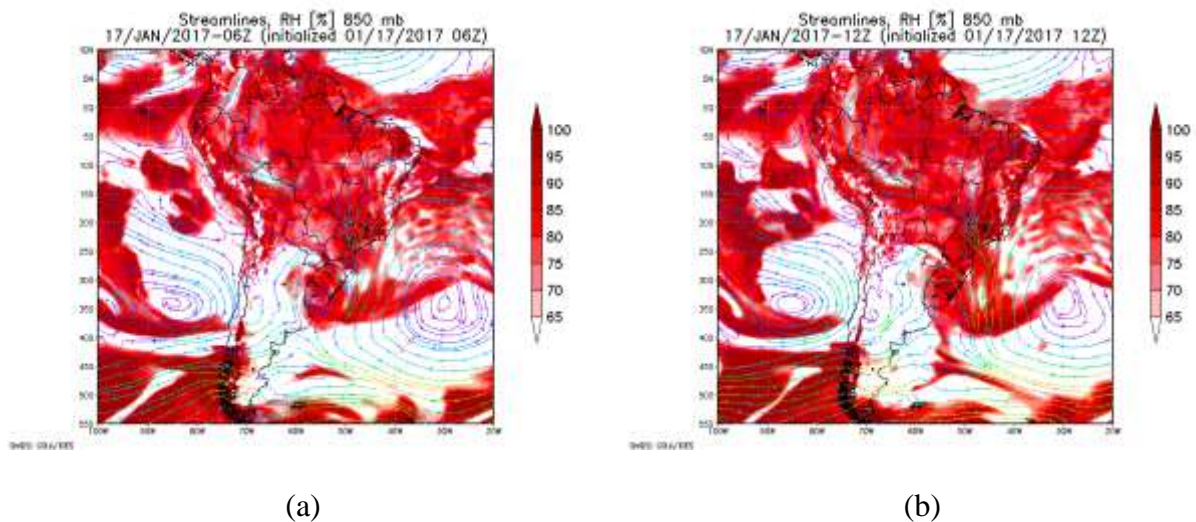


Figure 4-32: Streamlines and relative humidity at 850 hPa at January, 17th at 006:00 UTC (a), 12:00 UTC (b).

Warm advection at 850 hPa level is seen in the northwest region of São Paulo on January, 15. At 12:00 UTC on January, 16, intense warm advection (above $1 \times 10^{-4} \text{ K s}^{-1}$) is present in the east region of the State. Warm advection, persists during the day in the northwest region; this is related to the low pressure system observed in the region.

At surface analysis, on January 15, a cold front is seen away from the coast of Rio Grande do Sul. This system moves eastward through the day, clouds extending from this system have aided the development of storms in the State of São Paulo on January, 15. After 12:00 UTC of this day, winds are more intense from northwest directed to northern São Paulo and southern Minas Gerais, this is seen until 18:00 UTC. This is also observed on the next days (January, 16 and 17).

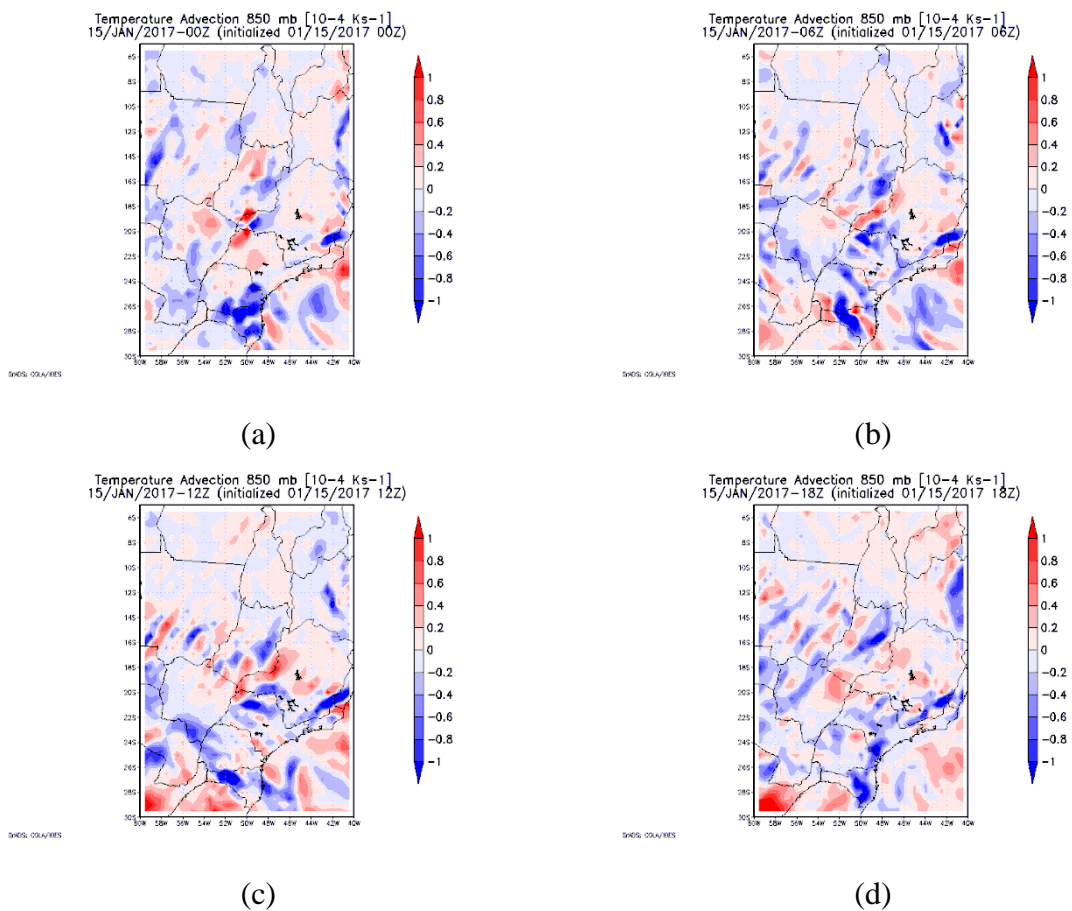


Figure 4-33: Temperature advection at 850 hPa on January, 15 at 00:00 UTC (a), 06:00 UTC (b), 12:00 UTC (c), 18:00 UTC (d).

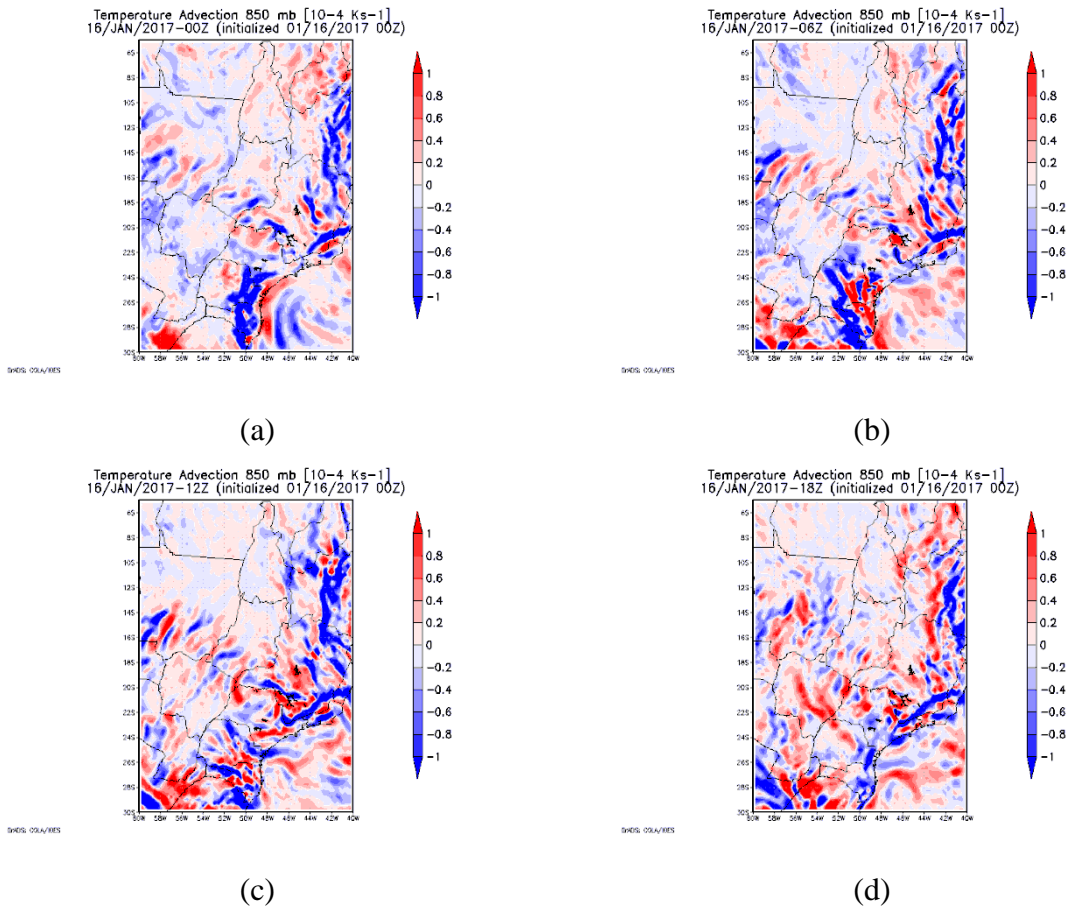


Figure 4-34: Temperature advection at 850 hPa on January, 16 at 00:00 UTC (a), 06:00 UTC (b), 12:00 UTC (c), 18:00 UTC (d).

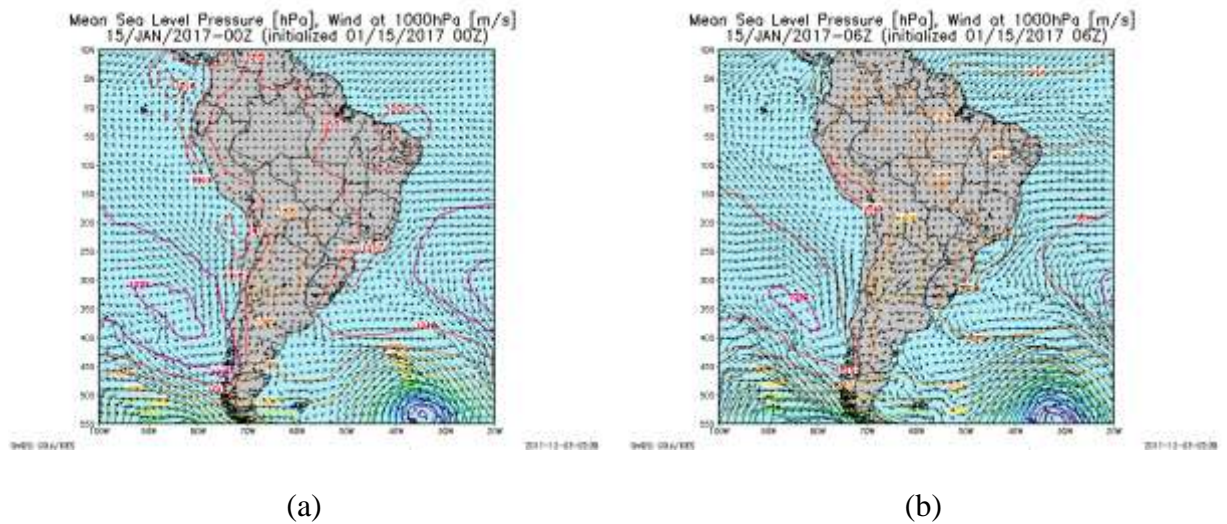
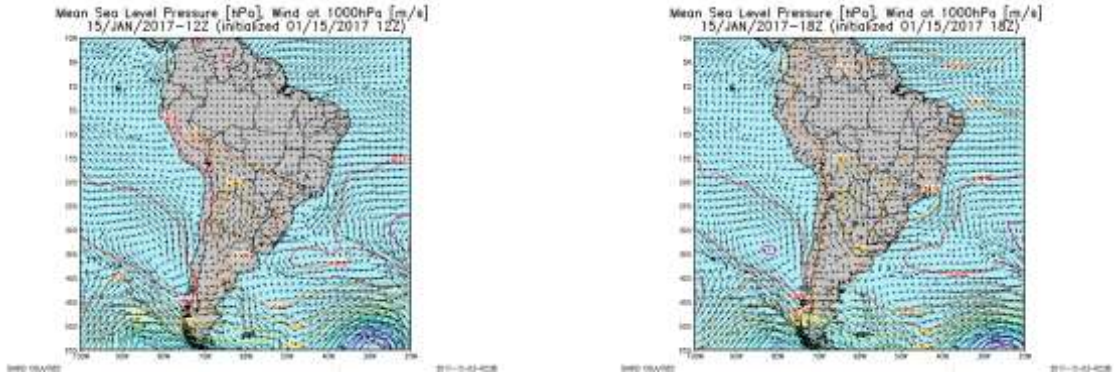


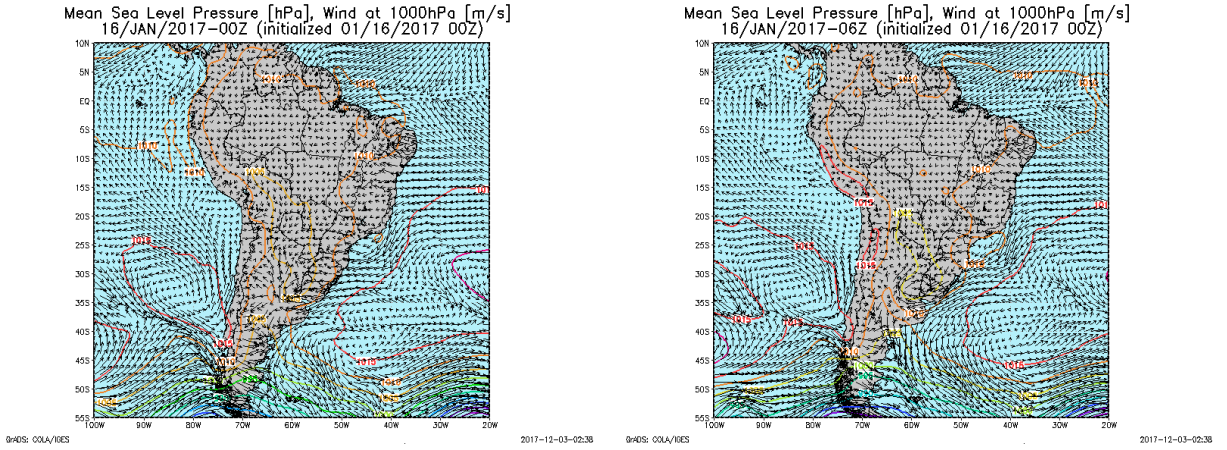
Figure 4-35: Mean sea level pressure and wind on January, 15th at 00:00 UTC (a), 06:00 UTC (b), 12:00 UTC (c), 18:00 UTC (d).



(c)

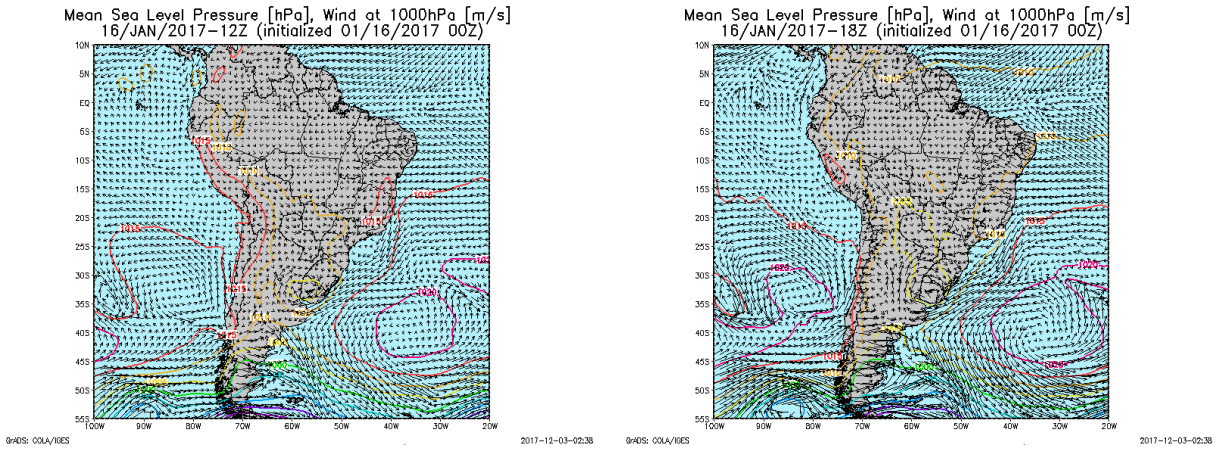
(d)

Figure 4-35: Continuation.



(a)

(b)



(c)

(d)

Figure 4-36: Mean sea level pressure and wind on January, 16th at 00:00 UTC (a), 06:00 UTC (b), 12:00 UTC (c), 18:00 UTC (d).

For this event the BRAMS model output and soundings were not available, therefore, the GFS model will be used for the analysis of CAPE, CIN and LI. Vertical cross sections of wind and relative humidity will be also be analyzed.

At 12:00 UTC on January 15, CAPE in the region of São Paulo shows values between 400 and 800 J kg⁻¹. At 15:00 UTC it is around 800-1200 J kg⁻¹ near São Paulo, and at 18:00 UTC most of the regions on the eastern side has values between 1200-1800 J kg⁻¹. A small area close to São Paulo has values around 1800-2400 J kg⁻¹. At 12:00 and 15:00 UTC these values indicate a condition between marginally and moderately unstable. At 18:00 UTC it indicates a moderately unstable condition. CIN is only seen in a region in the southeast part, close to São Paulo, values are below -50 J kg⁻¹. LI is between -2 and -4 K near São Paulo at 12:00 UTC, at 15:00 UTC it is between -3 and -4 K, and at 18:00 UTC it is ranging from -3 to -5 K. All these values indicate an unstable condition with probable storm, even severe. The 700-500 lapse rate is between 5.5 and 6 K km⁻¹ at 12:00 UTC and 15:00 UTC. At 18:00 UTC the same range is seen in the east part.

On January, 16, at 12:00 UTC it is between 600 and 1200 J kg⁻¹ through the east part of the State. At 15:00 UTC most of this region has values between 1400 and 1800 J kg⁻¹. At 12:00 UTC the condition is between marginally and moderately unstable, and at 15:00 it is moderately unstable. CIN is above -20 J kg⁻¹ everywhere in the State at 12:00 UTC. The LI parameter, at 12:00 UTC is through most of the east region, between -3 and -4 K, smaller values are seen in the northeast region, between -2 and -3 K. At 15:00 UTC values are between -4 and -6 K through most of the State. The 700-500 hPa lapse rate is between 5.0 and 6.0 K km⁻¹, near São Paulo, at 12:00 UTC and 15:00 UTC.

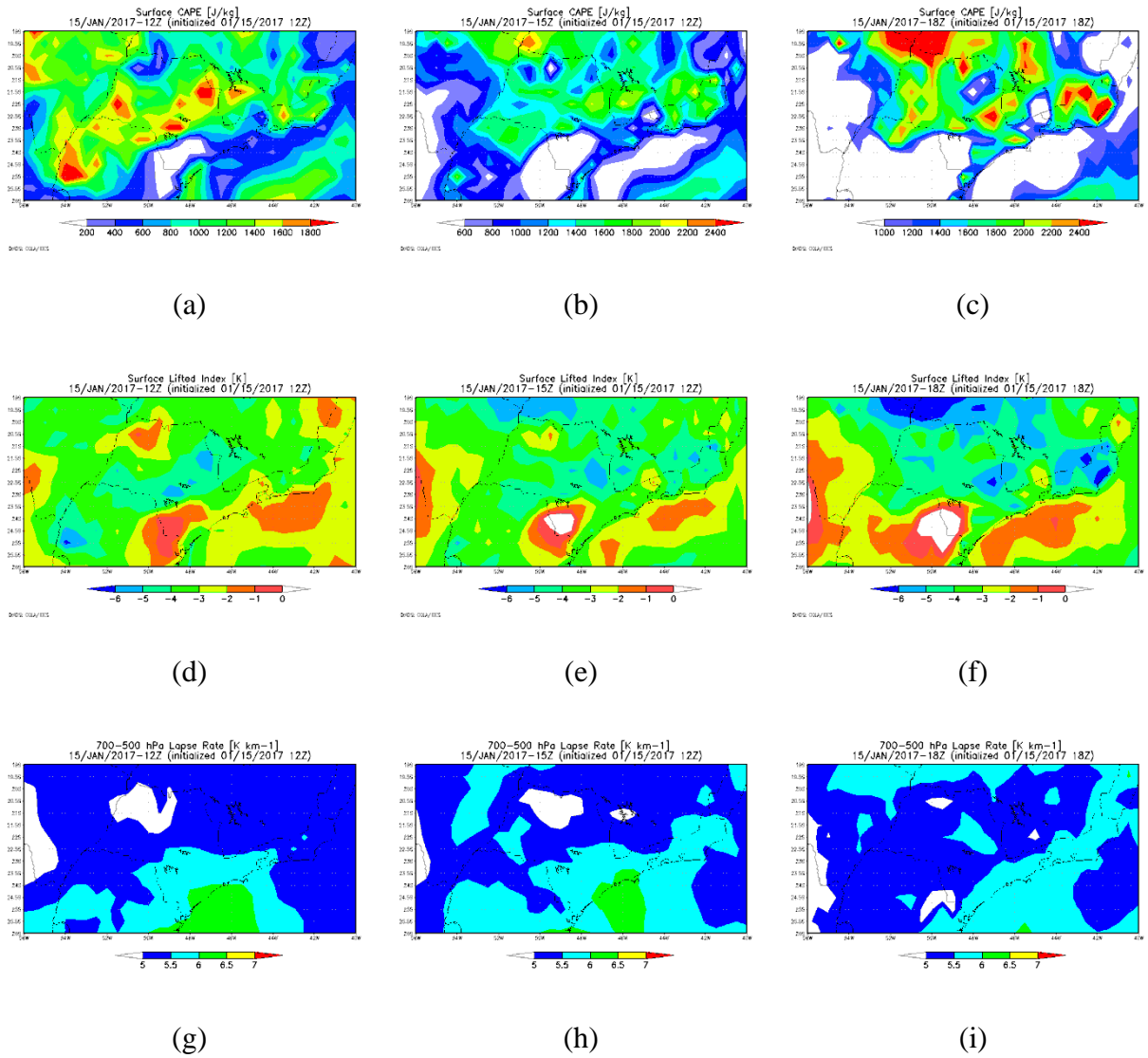
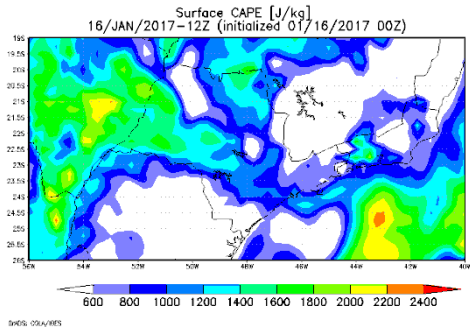
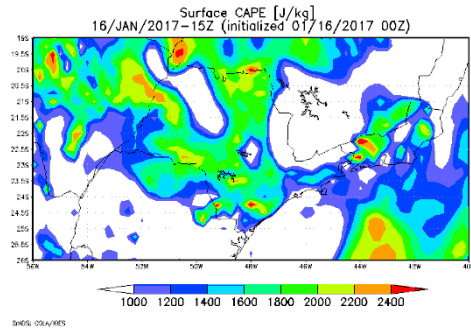


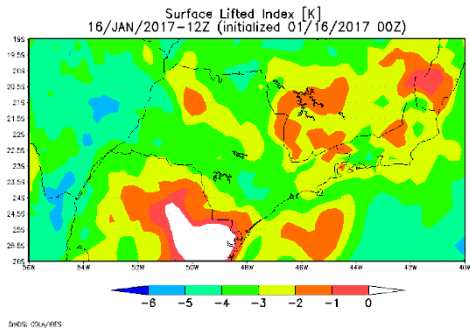
Figure 4-37: CAPE at 12:00 UTC (a), 15:00 UTC (b), 18:00 (c); LI at 12:00 (d), 15:00 (e), 18:00 (f); 700-500 hPa lapse rate at 12:00 UTC (g), 15:00 UTC (h), 18:00 UTC (i) from GFS for January, 15th, 2017.



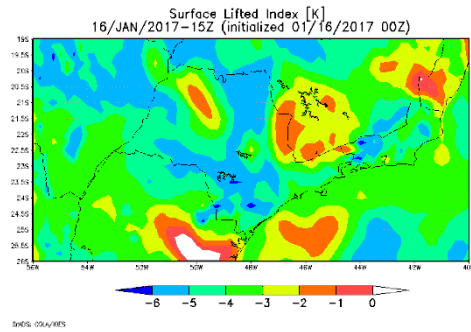
(a)



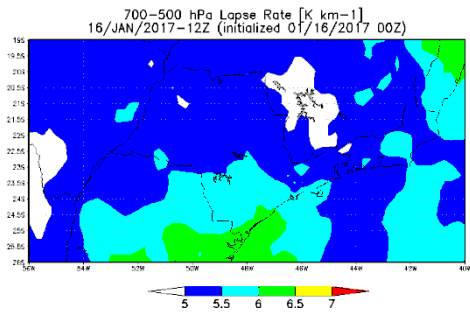
(b)



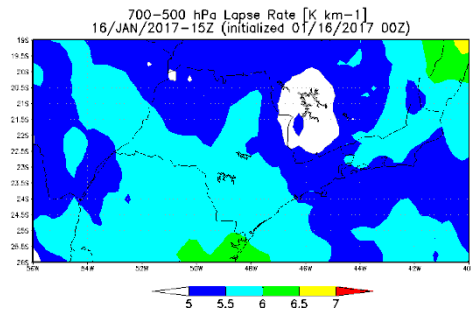
(c)



(d)



(e)



(f)

Figure 4-38: CAPE at 12:00 UTC (a), 15:00 UTC (b), LI at 12:00 (c), 15:00 (d); 700-500 hPa lapse rate at 12:00 UTC (e), 15:00 UTC (f) from GFS for January, 16th, 2017.

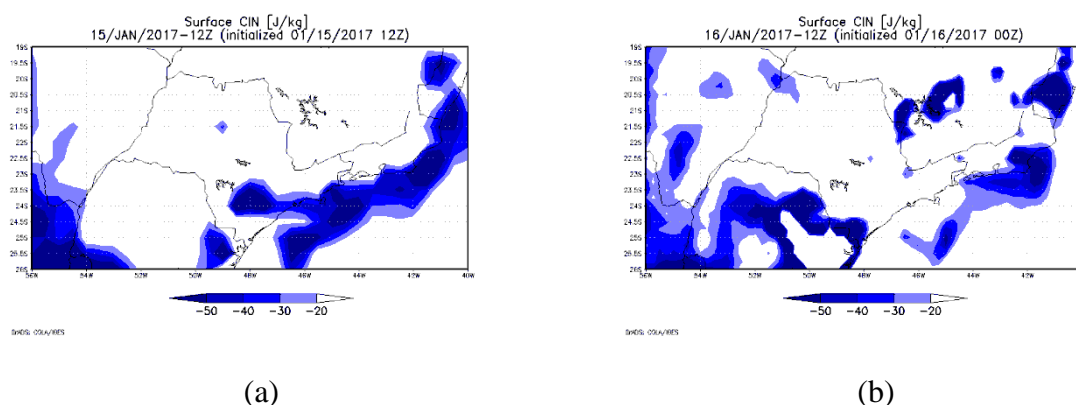


Figure 4-39: CIN from GFS at January, 15th (a), and January, 16th (b), at 12:00 UTC.

d. Surface stations

For this event 19 INMET surface stations were analyzed and METAR from airports in the city of São Paulo, Guarulhos and Taubaté were used.

On January, 15, the first day of the analysis, it was possible to see the sea breeze penetration into the State of São Paulo on stations localized in the city São Paulo (METAR and INMET), Guarulhos (METAR) in the southeast coast (INMET), in the city of Santos (METAR), and at the Vale do Paraíba (METAR and INMET).

In the southeast coast, station A712, registered southeast wind with increase in dew point temperature is seen after 10:00 UTC. At station A746, still in the southeast region, but inland, registered these changes at 10:00 UTC, but southeast winds are seen after 11:00 UTC.

At station A701, in the city of São Paulo, winds turned to southeast at 17:00 UTC, increase in dew point temperature, relative humidity, wind speed, and decrease in temperature are seen at 18:00 UTC. The turn to southeast in the airport of Campo de Marte occurred at the same hour with associated changes also at 17:00 UTC. In the METAR analysis for the Congonhas airport southeast winds are observed at 16:00 UTC with the associated changes seen at 17:00 UTC. At Guarulhos, increase in dew point temperature and relative humidity is seen at 17:00 UTC, but southeast are only observed at 19:00 UTC. On January, 15 no rain

was recorded at the A701 station. Some stations, according to the CGE, registered rain, until 17:35 local time, the highest observed was 19.8 mm at Jabaquara.

During the night of January, 15 the northwest flow on the 850 hPa analysis changed to be directed to the State of São Paulo (seen at January, 16 at 00:00 UTC), this caused the occurrence of heavy rainfall leading to floods and landslides in the city of São Paulo, Osasco, Carapicuíba, Barueri, Franco da Rocha e Francisco Morato. In one hour, 64.6 mm were registered at the city São Paulo (Mirante de Santana). One hour before, 26.2 mm were recorded, and rain was registered for 4 hours. It stopped for one hour, and rain was registered again for three hours with a maximum of 10.8 mm.

Station A755, Barueri, registered increase in dew point temperature and relative humidity at 16 UTC. Less than 3.0 mm were registered between 18:00-19:00 UTC and 19:00-20:00 UTC. Rainfall was more intense later that night and during dawn, as mentioned, leading to damages. It started between 22:00 and 23:00 UTC and lasted 4 hours, with a peak of 33.0 mm between 23:00 and 00:00 UTC.

Later, it rained for another 4 hours, starting between 05:00 and 06:00 UTC with a peak of 18.0 mm.

Station A740 registered increase in dew point temperature and relative humidity at 17:00 UTC with northeast winds. Rain was registered for 7 hours; it started between 17:00 and 18:00 UTC, but the peak was only 2.6 mm. Only 0.2 mm was registered isolated during dawn three times. Also at Vale do Paraiba, station A728 registered southeast with increase in dew point temperature and relative humidity at 18:00 UTC, this was also observed at the METAR analysis for the airport in the city.

At Sorocaba, station A713 registered southeast winds at 21:00 UTC with increase in dew point temperature, relative humidity, and decrease in temperature. It rained for two hours,

starting between 21 and 22 UTC with a peak of 10.4 mm. Rain started again around 01:00-02:00 UTC on January, 16, and lasted 4 hours with a peak of 9.8 mm.

On January, 16 at station A701 winds were from north-northeast and northwest after 08:00 UTC. Southeast winds with increase in dew point temperature and relative humidity, and decrease in temperature were observed at 21:00 UTC at station A701, and also at the METAR analysis for Campo de Marte and Congonhas. At station A701, 6.6 mm were registered between 17:00 and 18:00 UTC. Later that night, between 22:00 and 23:00 UTC rain was observed and lasted for 8 hours with a peak of 14.4 mm and an accumulated of 23 mm. During January, 17th, winds were from north-northeast and northwest, during this day, the sea breeze did not penetrate into the continent. It rained for several hours at the station, including the 8 hours already mentioned, but other than those 14.4 mm registered, the one-hour accumulated rain was less than 7.0 mm.

Related to the development of the humidity convergence zone, rain was registered all over the State. Only stations A738 and A712 did not record rain during this period. Station A740 recorded several peaks of 0.2 m during January, 16th, but no rain was registered on the next day, it is complicated to affirm that these values are correct.

Through this event it is possible to see the importance of the northwest to bring moisture to the State of São Paulo.

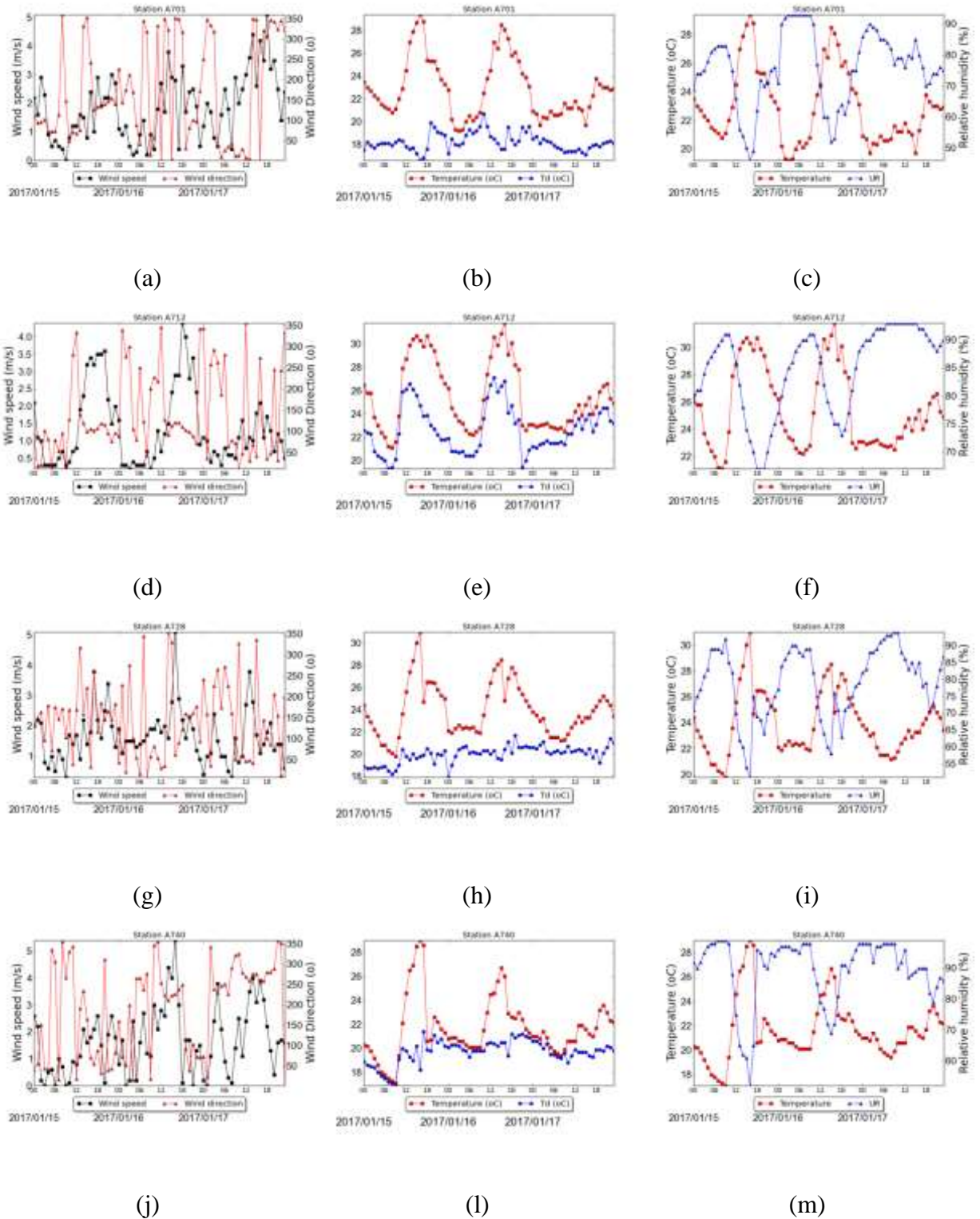
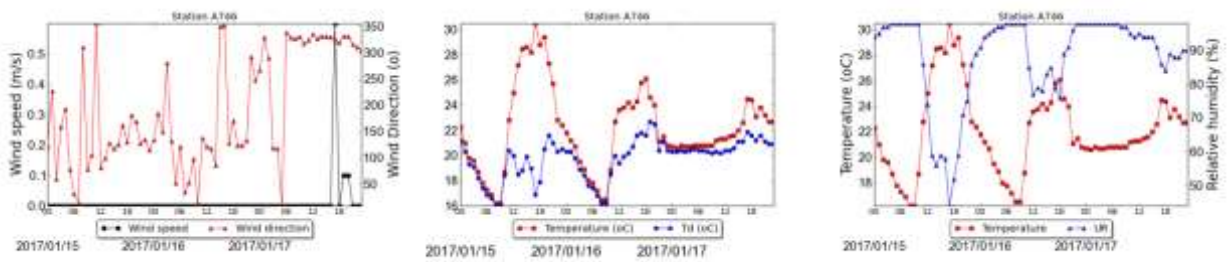


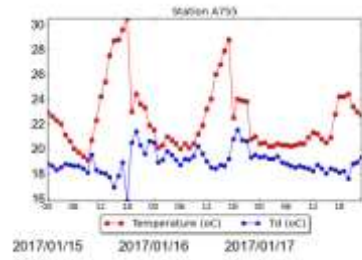
Figure 4-40: Wind speed and direction, temperature and dew point temperature, temperature and relative humidity at stations A701 (a), (b), (c), A712 (d), (e), (f), A728 (g), (h), (i), A740 (j), (l), (m), A746 (n), (o), (p), A755 (q), (r).



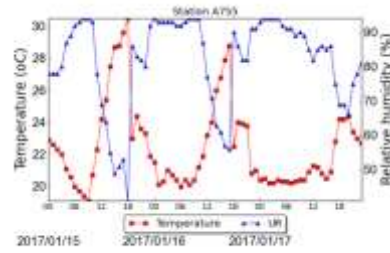
(n)

(o)

(p)

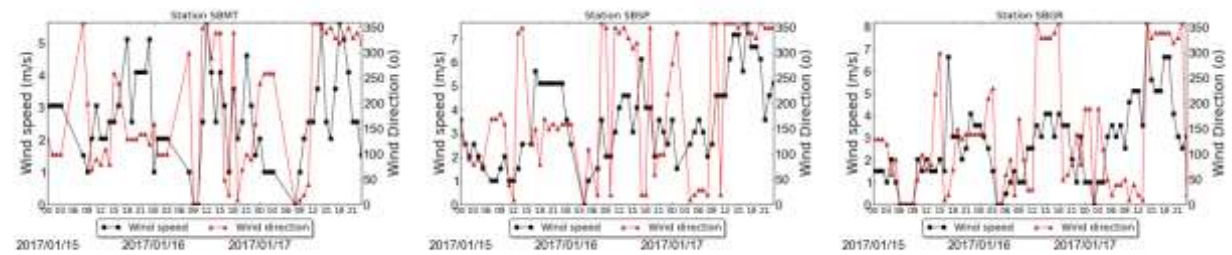


(q)



(r)

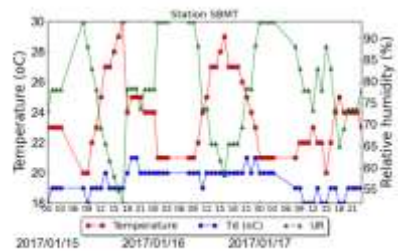
Figure 4-40: Continuation.



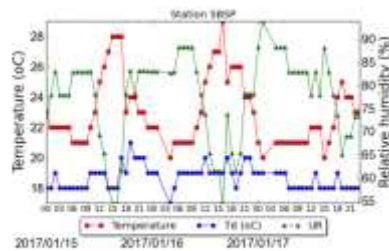
(a)

(b)

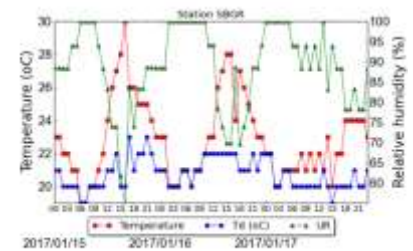
(c)



(d)



(e)



(f)

Figure 4-41: Wind speed and direction and temperature, dew point temperature and relative humidity from METAR at stations SBMT (a), (d), SBSP (b), (e), SBGR (c), (f).

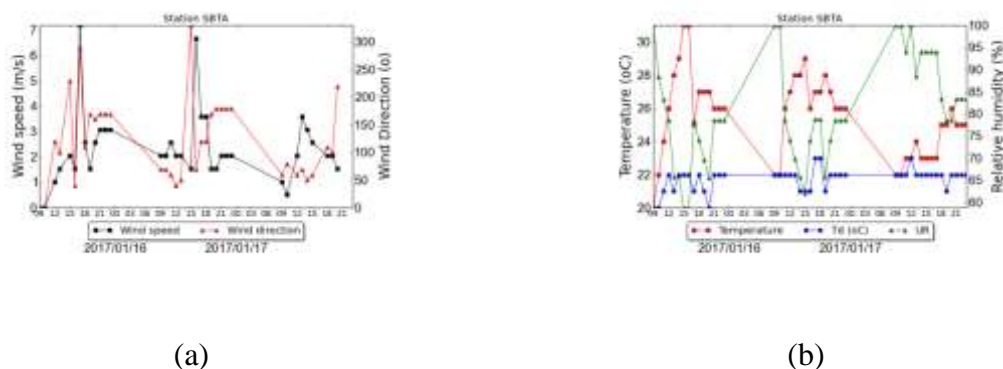


Figure 4-42: Wind speed and direction (a) and temperature, dew point temperature and relative humidity (b) from METAR at station SBTA.

4.1.1.3 February, 24, 2017

During this event heavy rain was reported in the city of São Paulo, which led to the occurrence of floods. Strong wind gusts were also reported at the airport of Guarulhos. Hailstorm was observed in the city of São Paulo. Further details will be given in the surface station analysis section.

a. Satellite

Clouds are seen in the State of São Paulo, throughout the day, in the infrared images for South America. This is related to the instability generated by the synoptic scale pattern, as will be shown in a future section. Images in Figure 4-43 are shown at 00:00 UTC, 06:00 UTC, 12:00 UTC and 18:00 UTC.

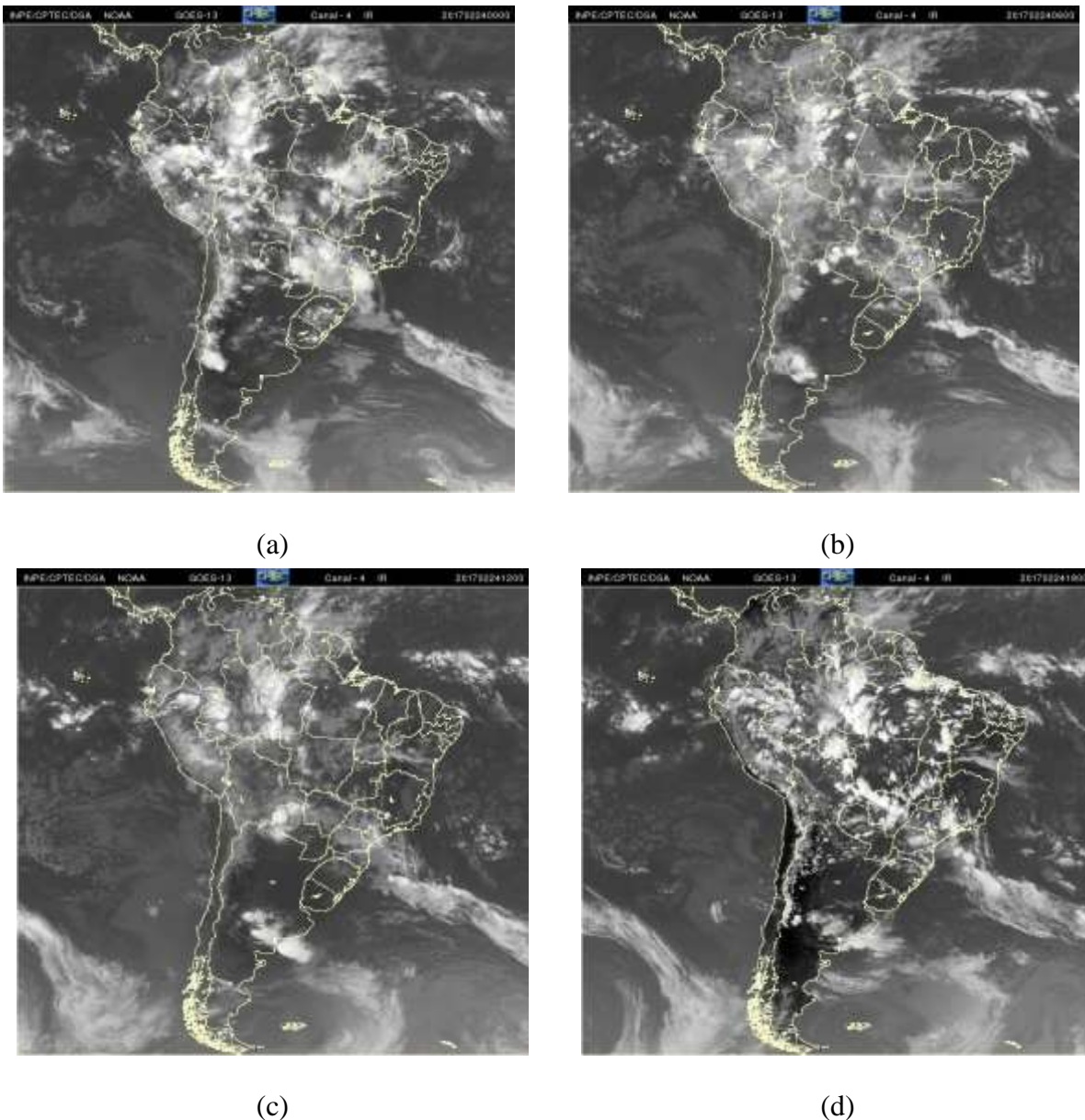
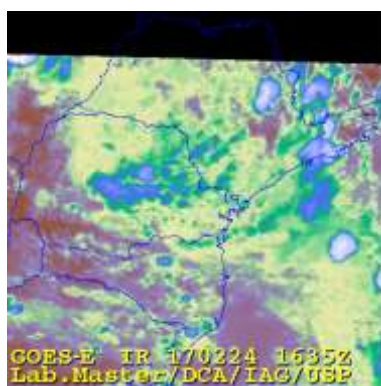


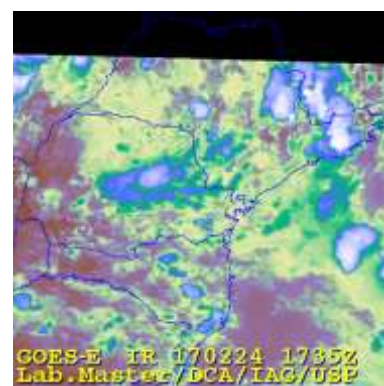
Figure 4-43: Infrared images for South America at 00:00 UTC (a), 06:00 UTC (b), 12:00 UTC (c), 18:00 UTC (d) on February 24.

Figure 4-44 shows the evolution of the event through the infrared images for the State of Paulo. The enhanced infrared images also analyzed here are seen in Figure 4-45. At 16:35 UTC, in infrared image for the State of São Paulo, clouds are forming in the region of topography, northeast of the State and near to the coast. As the hours advance, these cells intensified. At 19:00 UTC, in the enhanced infrared image, clouds have temperature values around $-60\text{ }^{\circ}\text{C}$, in the northeast region, and in the central part of the State. Clouds located at

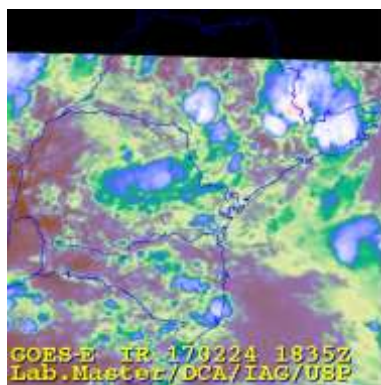
Vale do Paraíba, moved northeast, but some other cells, from the region of Serra da Mantiqueira, moved to the region of São Paulo and intensified, as seen at 20:35 UTC in the infrared and at 21:00 UTC with values around $-60\text{ }^{\circ}\text{C}$ in the enhanced infrared images. These cells lost strength, as can be seen at 21:35 UTC, and another intensified next to them. At 22:35 UTC, it had also lost its strength, and it possible to see clouds moving in a northeast direction.



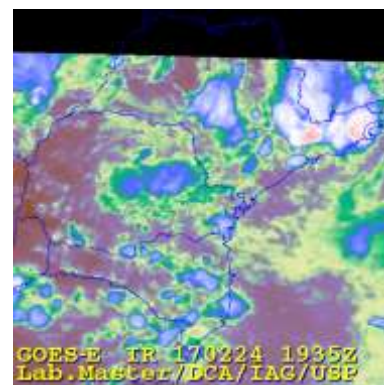
(a)



(b)

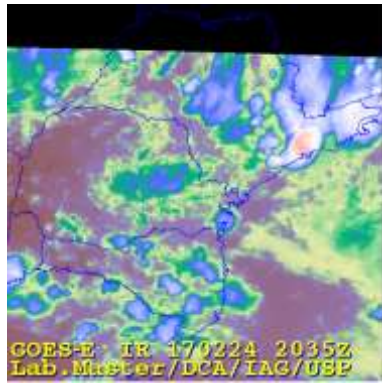


(c)

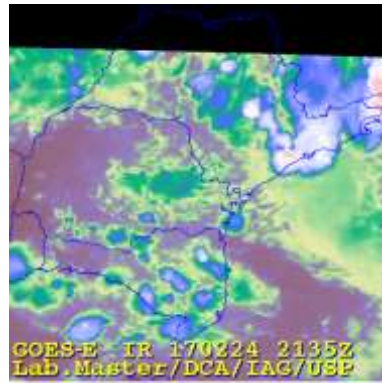


(d)

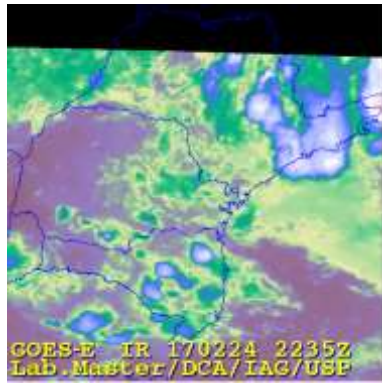
Figure 4-44: Infrared satellite images for February, 24 at 16:35 UTC (a), 17:35 UTC (b), 18:35 UTC (c), 19:35 UTC (d), 20:35 UTC (e), 21:35 UTC (f), 22:35 UTC (g), and 23:35 UTC (h).



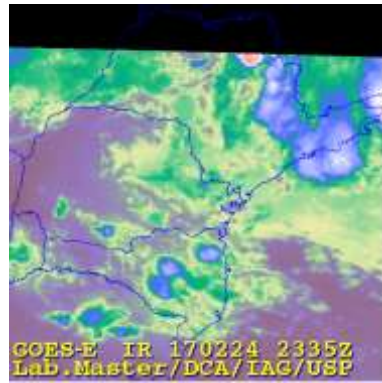
(e)



(f)

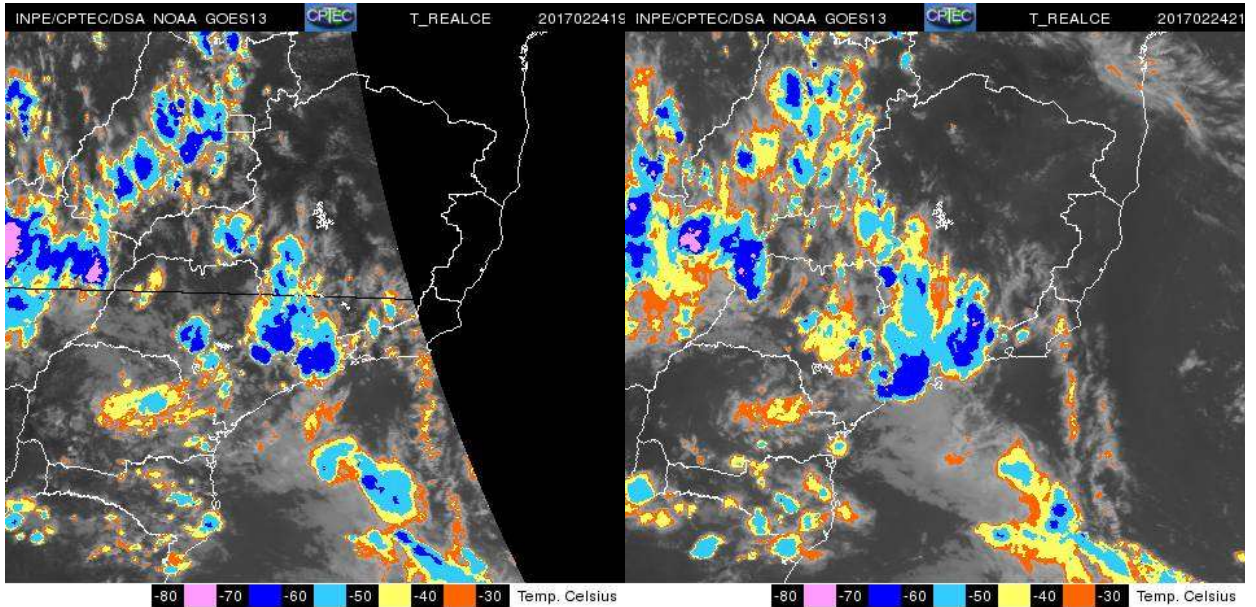


(g)



(h)

Figure 4-44: Continuation.



(a)

(b)

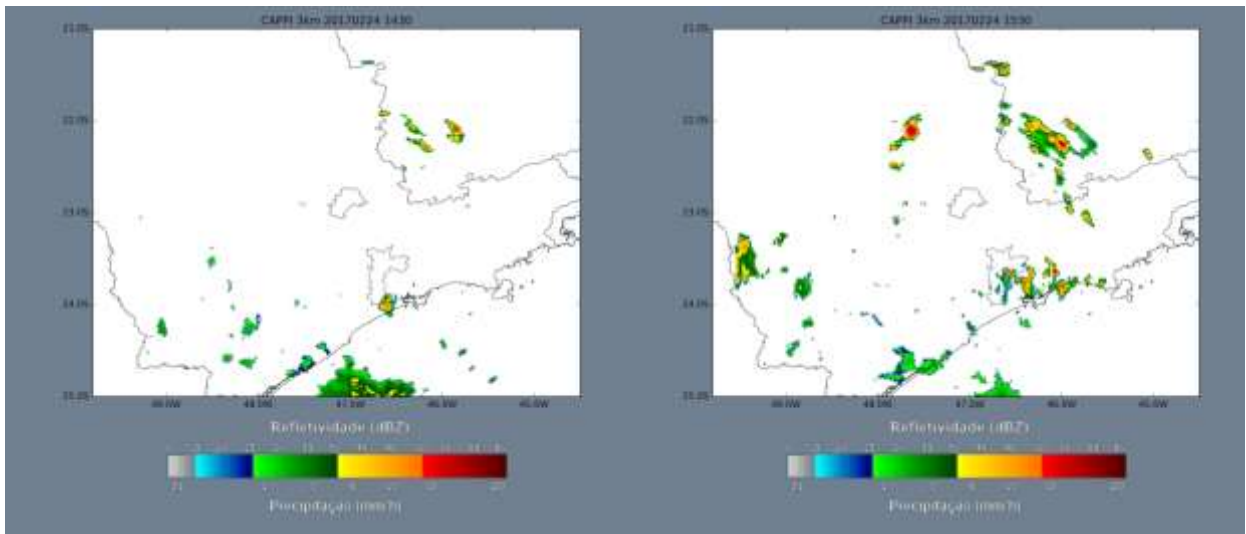
Figure 4-45: Enhanced infrared satellite images for February, 24 at 19:00 UTC (a), and 21:00 UTC (b).

b. Radar

The radar images for this event are seen in Figure 4-46.

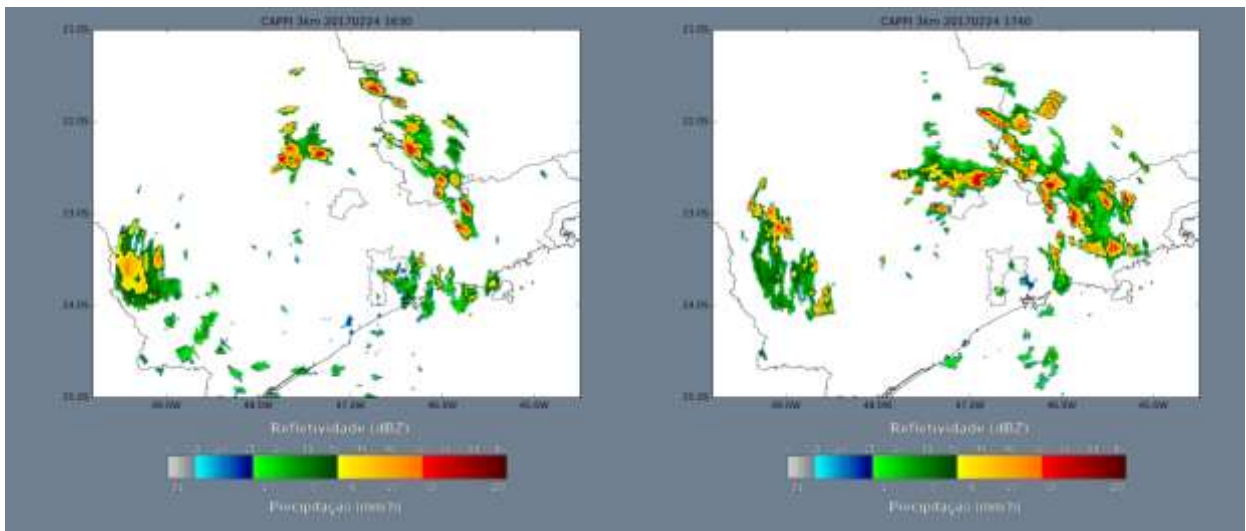
After 14:30 UTC cells are developing in the region of São Carlos, southeastern Minas Gerais, and near to the coast. At 15:00 UTC, high reflectivity values are already seen in those regions, around 50 dBZ, and even higher near the coast (around 55-60 dBZ). Close to the coast, clouds could be related to the sea breeze. Cells move in a southeast direction, including the clouds near to the coast, showing that the sea breeze could not penetrate into the continent, due to the dominance of the synoptic scale pattern over the regional scale circulation. Further details of the synoptic scale pattern and regarding the sea breeze will be given in future sections. It is interesting to notice that high reflectivity values are seen as these cells move (around 55-60 dBZ), and a merge between cells from Minas Gerais and originated at the region of São Carlos is observed between 17:40 and 18:00 UTC. These clouds continued to propagate southeast. At 19:10 UTC high reflectivity values, around 60 dBZ are present in the region of Atibaia, although there is no record of severe weather occurrences in the region. As they continue to propagate they advance towards São Paulo, and at 19:50 UTC reflectivity is around 60-65 dBZ in the region of São Paulo. At 20:10 UTC, again high reflectivity is observed, around 60 dBZ, in the region between São Paulo and São Bernardo, and at 20:20 UTC reflectivity is around 55-60 dBZ. The system continues to move in a southeast direction.

After 21:20 UTC a few cells with reflectivity values around 30-35 dBZ intensified to around 40-45 dBZ near the coast and in the region of São Paulo and Guarulhos. Reflectivity values of this order are still observed in these regions at 23:00 UTC.



(a)

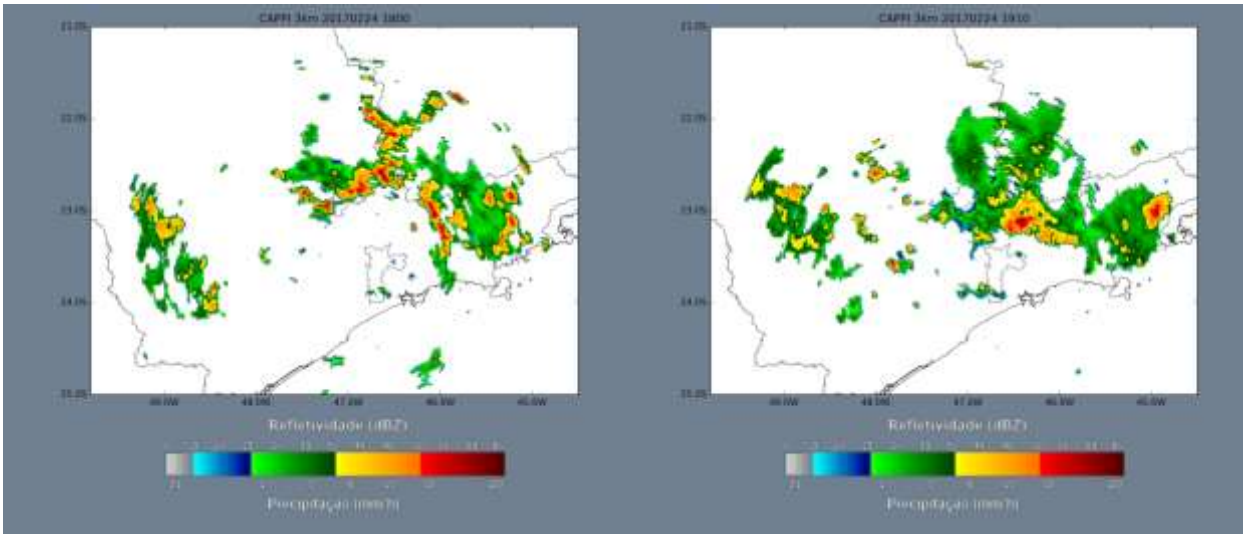
(b)



(c)

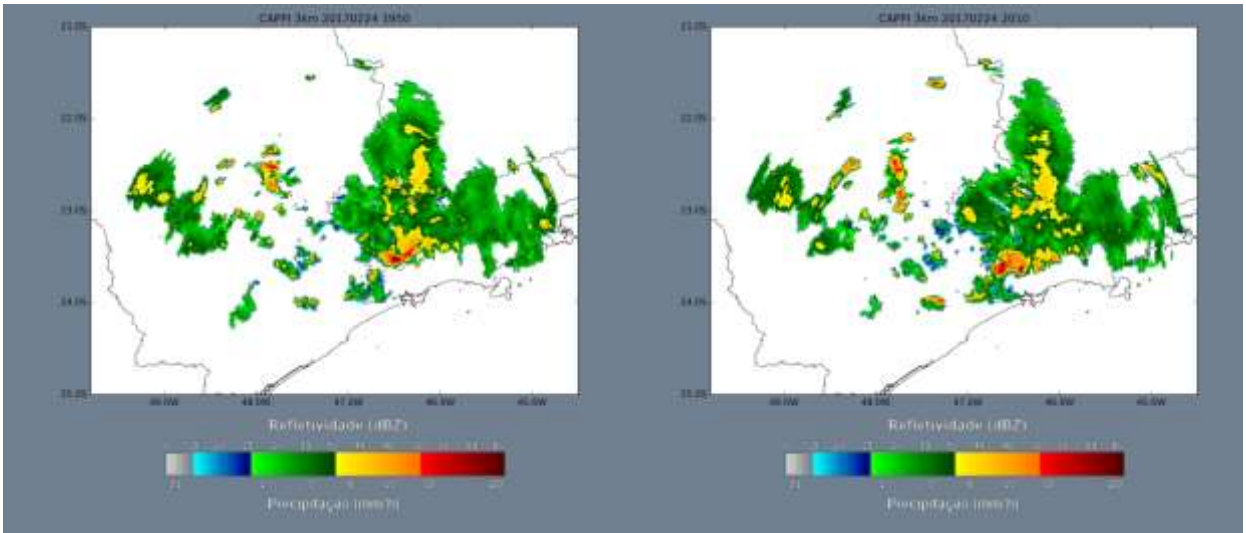
(d)

Figure 4-46: São Roque radar images from February, 24th at 14:30 UTC (a), 15:30 UTC (b), 16:30 UTC (c), 17:40 UTC (d), 18:00 UTC (e), 19:10 UTC (f), 19:50 UTC (g), 20:10 UTC (h), 20:20 UTC (i), 21:20 UTC (j), 22:20 UTC (k), and 23:00 UTC (l).



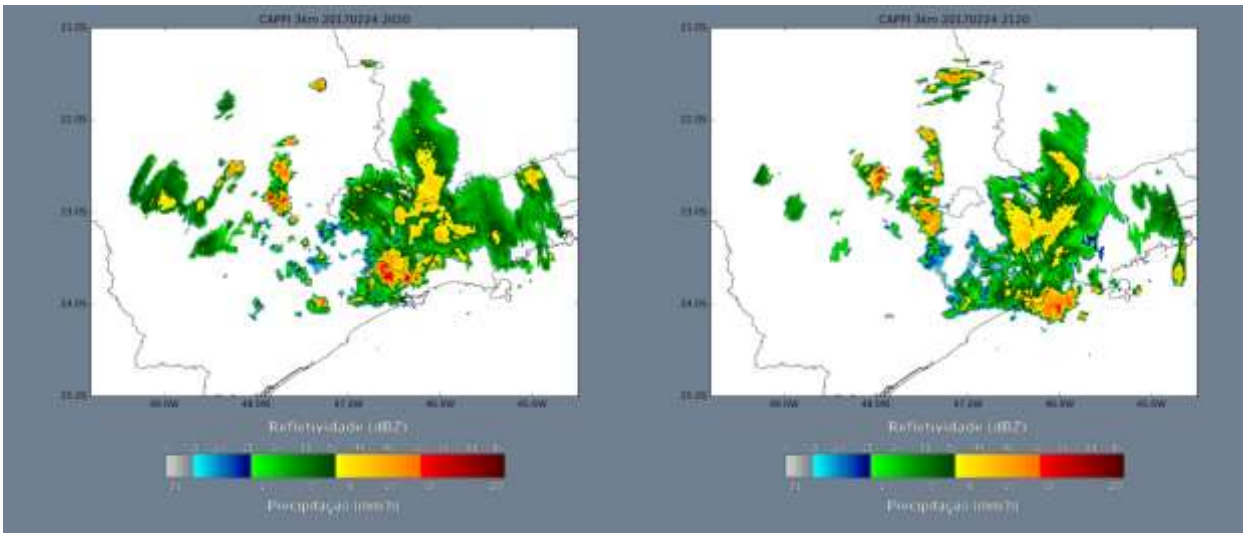
(e)

(f)



(g)

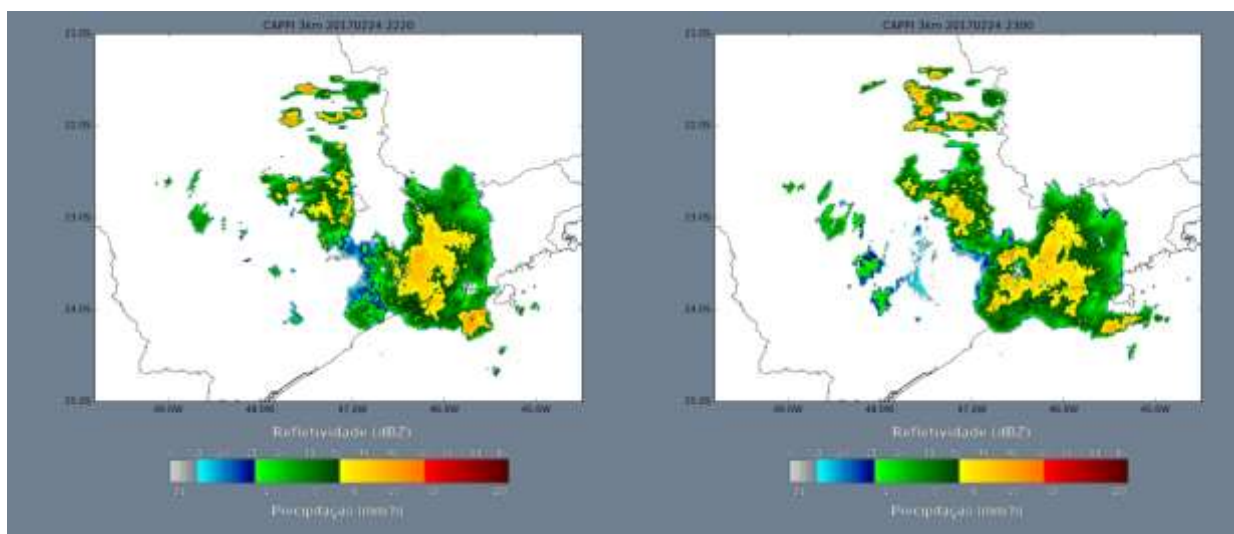
(h)



(i)

(j)

Figure 4-46: Continuation.



(k)

(l)

Figure 4-46: Conclusion.

c. Synoptic scale analysis

At 00:00 UTC in the upper air analysis, at 200 hPa, an Upper level cyclonic vortex is seen in the region of Espírito Santo, causing instabilities in the southeast region of the country. There is a trough in the Atlantic Ocean associated with a frontal system at the surface. Both systems move eastward throughout the day (Figure 4-47). The trough is seen at the 500 hPa analysis with negative vorticity associated to it, seen in Figure 4-49. The Upper Level Cyclonic Vortex is not seen at this level. Mass divergence at 200 hPa is seen at 00:00 UTC, shown in Figure 4-48, except in the northern part of the State, with values between $0.2-0.4 \cdot 10^{-4} \text{ s}^{-1}$, and higher values in the southeast part, between $0.4-0.8 \cdot 10^{-4} \text{ s}^{-1}$. At 06:00 UTC it is seen in the northwest region with values around $0.4-0.6 \cdot 10^{-4} \text{ s}^{-1}$, and in the northeast region, with values of the same order. Wind divergence is not seen at 12:00 UTC, but at 18:00 UTC values around $0.2-0.4 \cdot 10^{-4} \text{ s}^{-1}$ are observed in the east part of the State. Values between $0.2-0.6 \cdot 10^{-4} \text{ s}^{-1}$ are also present in the southwest region.

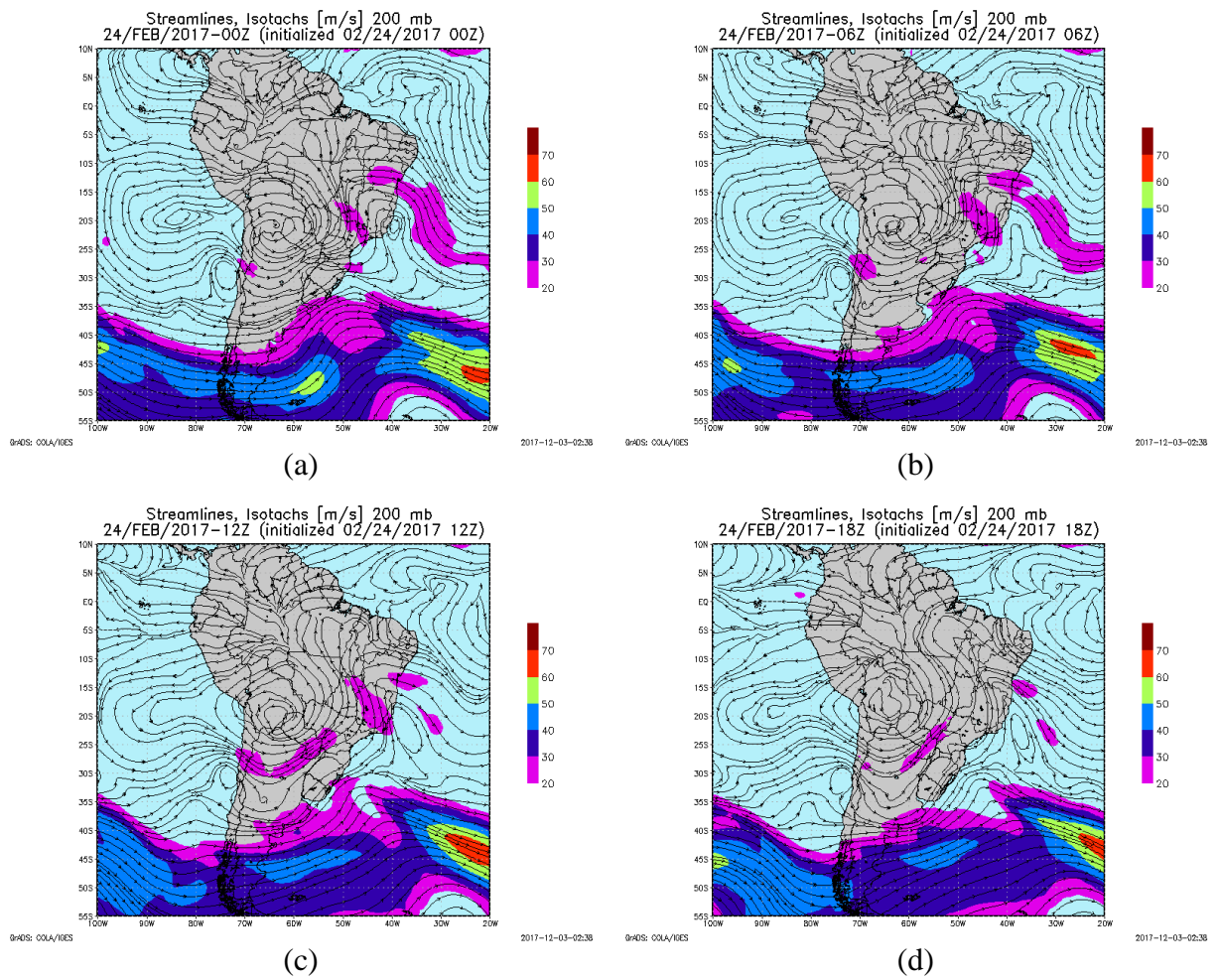


Figure 4-47: Streamlines and isotach (m s^{-1}) for February, 24 at 00:00 UTC (a), 06:00 UTC (b), 12:00 UTC (c), and 18:00 UTC (d).

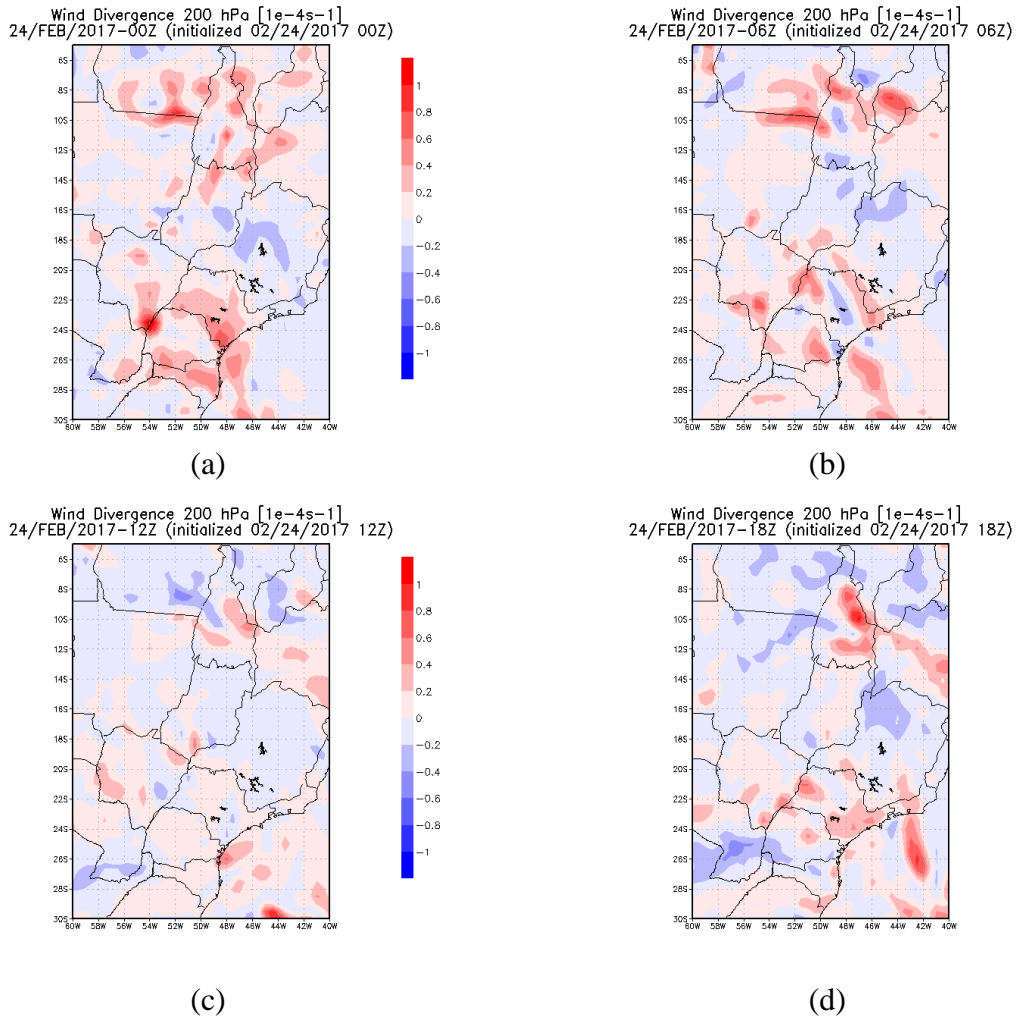


Figure 4-48: Mass divergence for February, 24th at 00:00 UTC (a), 06:00 UTC (b), 12:00 UTC (c), and 18:00 UTC (d).

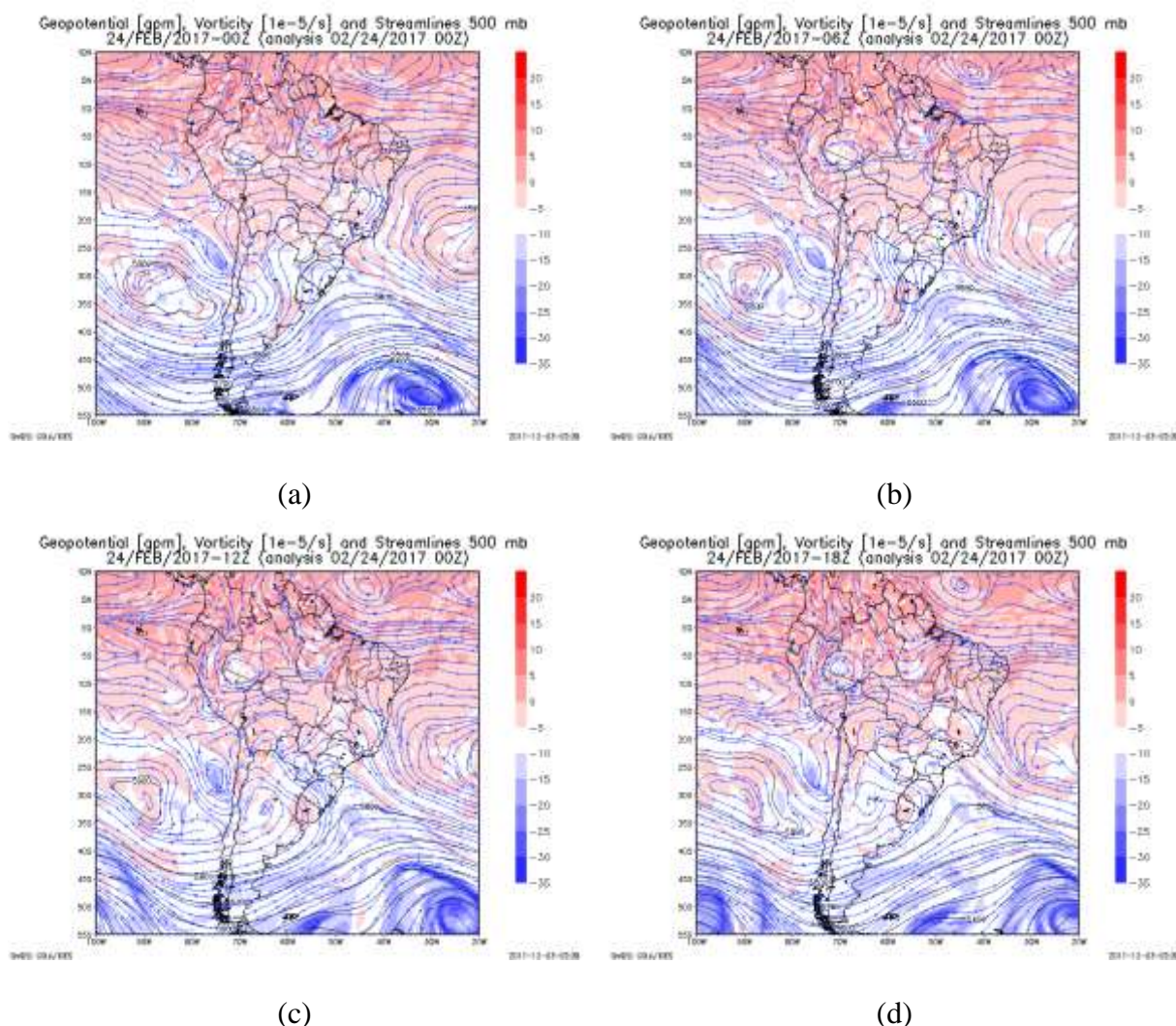


Figure 4-49: Geopotential height (gpm), vorticity ($1 \times 10^{-5} \text{ s}^{-1}$) and streamlines at 500 hPa from February, 24th at 00:00 UTC (a), 06:00 UTC (b), 12:00 UTC (c), and 18:00 UTC (d).

After 12:00 UTC, at 500 hPa, a trough is seen in the region of the State of São Paulo, causing instability (Figure 4-49).

In the 850 hPa analysis, shown in Figure 4-50, the region of frontal system presents intense temperature gradient and high relative humidity. Low relative humidity is present in the eastern region of the State of São Paulo (65-70 %) at 00:00 UTC. On February, 22th, a high-pressure system was present at the 500 hPa, as will be shown in the discussion of that event, it is still seen at February, 23th, at 00:00 UTC (not shown), but it was getting weaker. It is not present anymore, but this caused the dryness seen at this level, as mentioned before.

After 12:00 UTC the South Atlantic subtropical high is adding moisture in the coast of the northeast region of Brazil, as it was from the beginning of the day, but it is deflected by the Andes to the southeast region. Relative humidity is still low, between 65-75 % at this hour. At 18:00 UTC moisture has increased in the State.

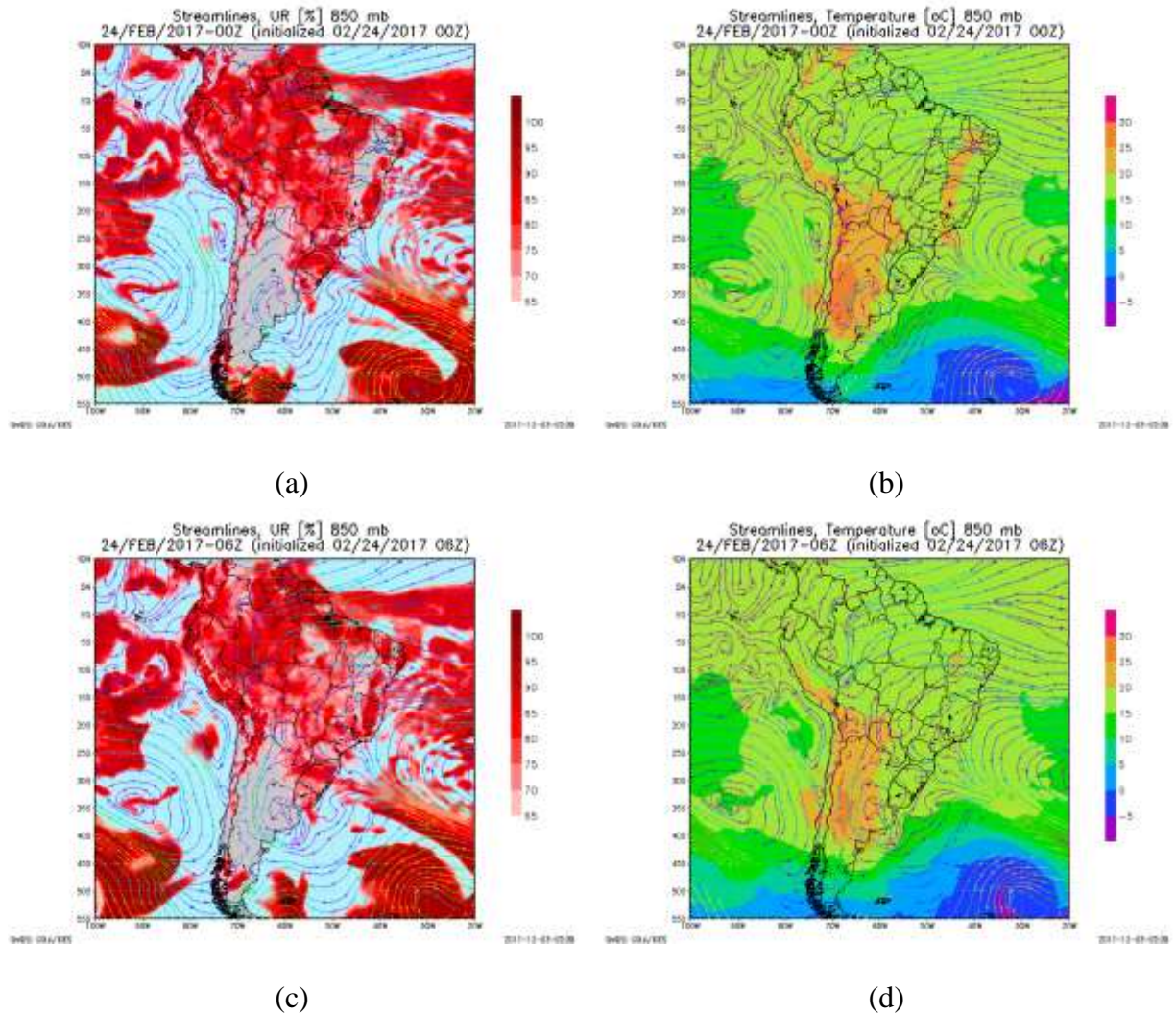


Figure 4-50: Streamlines and relative humidity, streamlines and temperature at 850 hPa for February, 24 at 00:00 UTC (a) and (b), 06:00 UTC (c) and (d), 12:00 UTC (e) and (f), and 18:00 UTC (g) and (h).

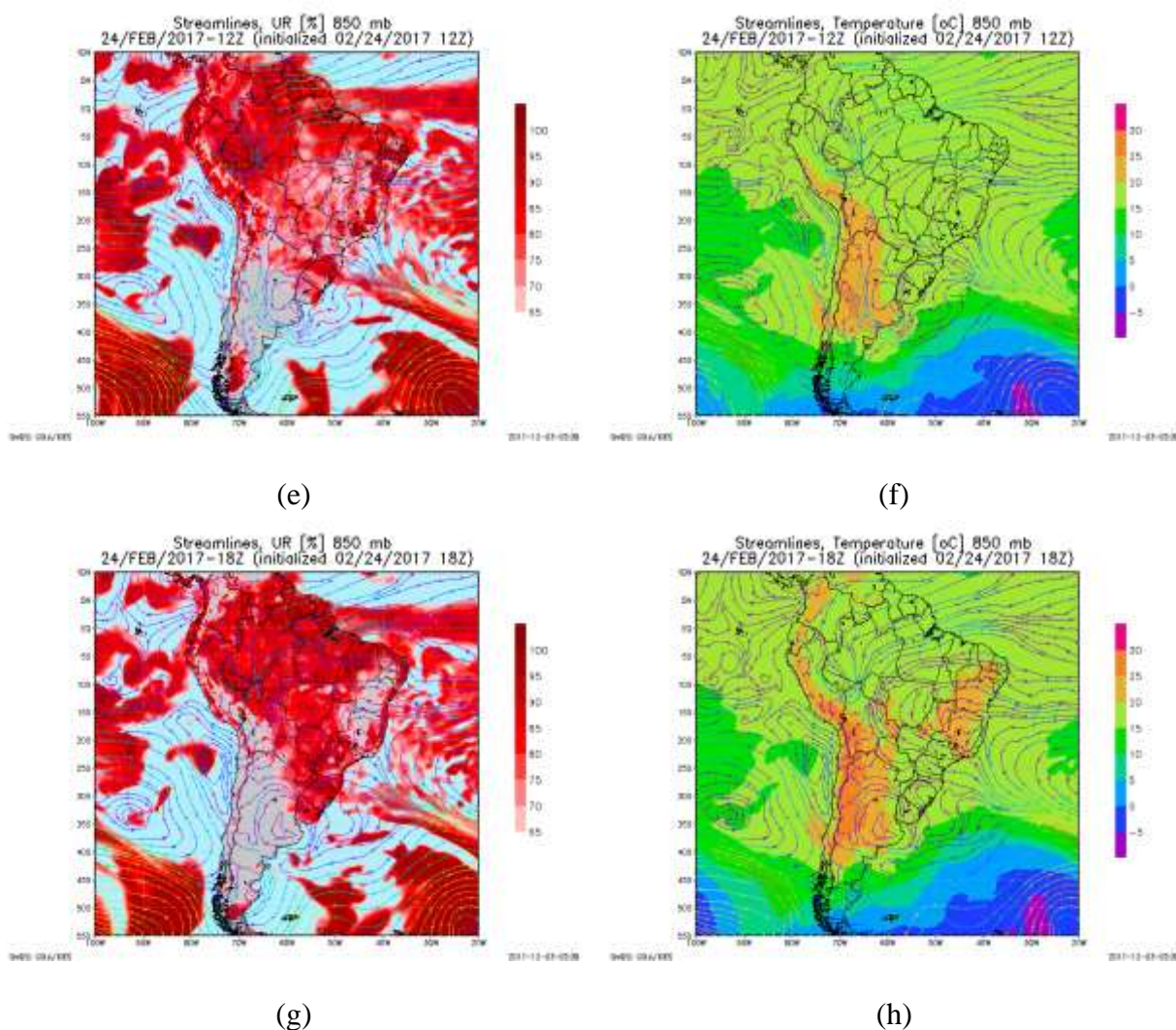


Figure 4-50: Continuation.

Warm advection (Figure 4-51) is only seen at 18:00 UTC, in the eastern part of the State, with low values, between 0.2 and $0.4 \cdot 10^{-4} \text{ K s}^{-1}$.

At the surface the analysis shows the frontal system in the Atlantic Ocean (Figure 4-52), and the Atlantic Ocean subtropical high, with a 1020 hPa center, outside the domain of the figure. The frontal system moves eastward throughout the analysis, and it is localized at around the height of the coast of Paraná at 18:00 UTC. It is possible to see winds from northwest in the State of São Paulo at 18:00 UTC.

Temperature Advection 850 mb [10^{-4} K s^{-1}]
 24/FEB/2017-18Z (initialized 02/24/2017 18Z)

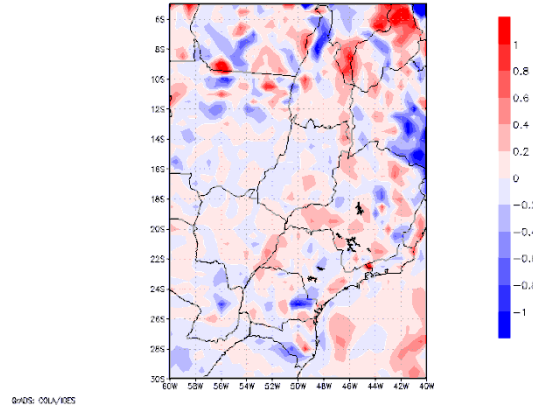
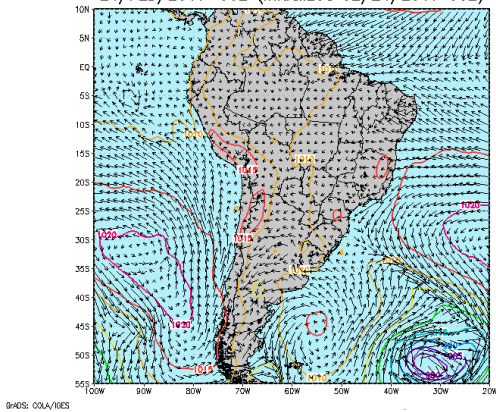


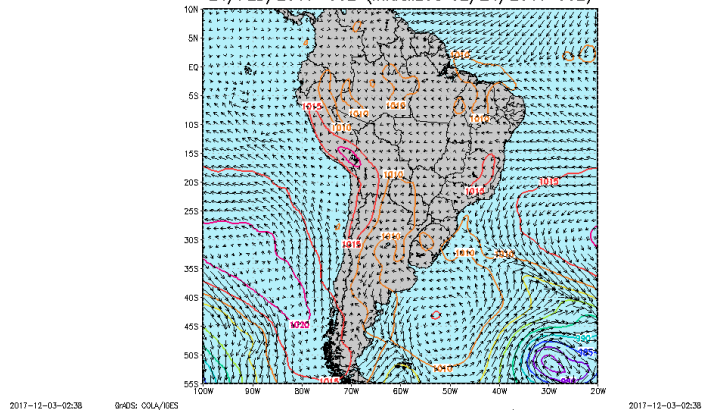
Figure 4-51: Temperature advection ($1 \times 10^{-4} \text{ K s}^{-1}$) at 850 hPa for February, 24th at 18:00 UTC.

Mean Sea Level Pressure [hPa], Wind at 1000hPa [m/s]
 24/FEB/2017-00Z (initialized 02/24/2017 00Z)



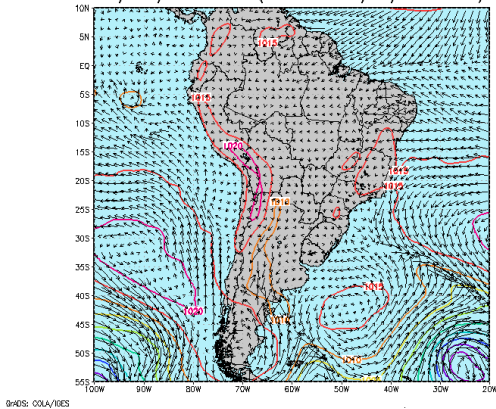
(a)

Mean Sea Level Pressure [hPa], Wind at 1000hPa [m/s]
 24/FEB/2017-06Z (initialized 02/24/2017 06Z)



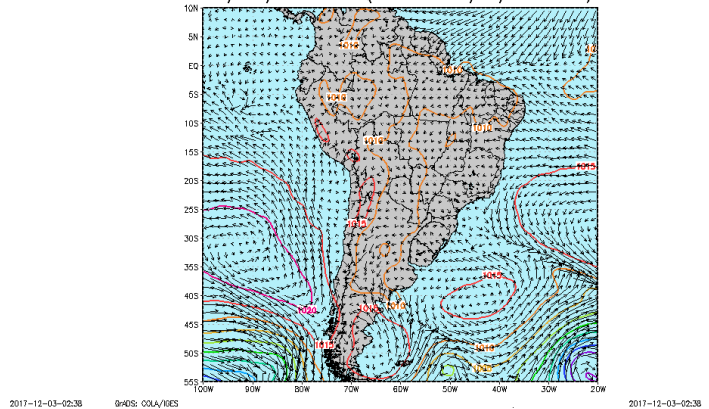
(b)

Mean Sea Level Pressure [hPa], Wind at 1000hPa [m/s]
 24/FEB/2017-12Z (initialized 02/24/2017 12Z)



(c)

Mean Sea Level Pressure [hPa], Wind at 1000hPa [m/s]
 24/FEB/2017-18Z (initialized 02/24/2017 18Z)



(d)

Figure 4-52: Mean sea level pressure (hPa) and winds (m s^{-1}) for February, 24th at 00:00 UTC (a), 06:00 UTC (b), 12:00 UTC (c), and 18:00 UTC (d).

d. Thermodynamic and mesoscale analysis

In the sounding obtained at 12:00 UTC, seen in Figure 4-53, it is possible to see that air is moister on low levels and gets dry with height, specially above 750 hPa. However, the amount of moisture is still low, as it was mentioned on the previous event, and a small moisture inversion is seen in the first few levels (between 933 and 883 hPa). The subsidence inversion is not present in this sounding.

The vertical structure of the relative humidity, water vapor mixing ratio, and equivalent potential temperature derived from the sounding was analyzed (Figure 4-54). The water vapor mixing ratio increases with height in first levels, starting at 13.07 g kg^{-1} , and reaching 14 g kg^{-1} . It, then, decays, reaching 2.30 g kg^{-1} at 605 hPa, increasing again until around 550 hPa. Decreased below 2 g kg^{-1} after. The relative humidity at the first level is 58 %, and it varies between this value and 79 % until 850 hPa. Between 500-600 hPa it drops below 20 %, and the water vapor mixing ratio is below 1 g kg^{-1} . The equivalent potential temperature also increased in the first few levels, starting from 344.2 K. This variable could be important, considering that storms are usually associated with high values of it, for the reason that high values indicate warm and moist regions.

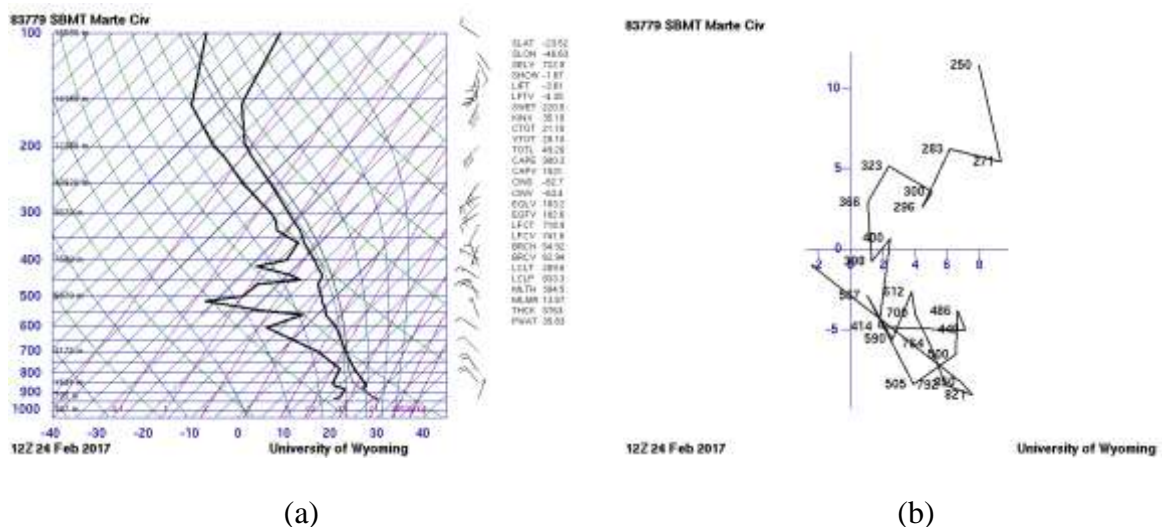


Figure 4-53: Sounding (a) and hodograph (b) for February, 24th at 12:00 UTC. (source: <http://weather.uwyo.edu/upperair/sounding.html>).

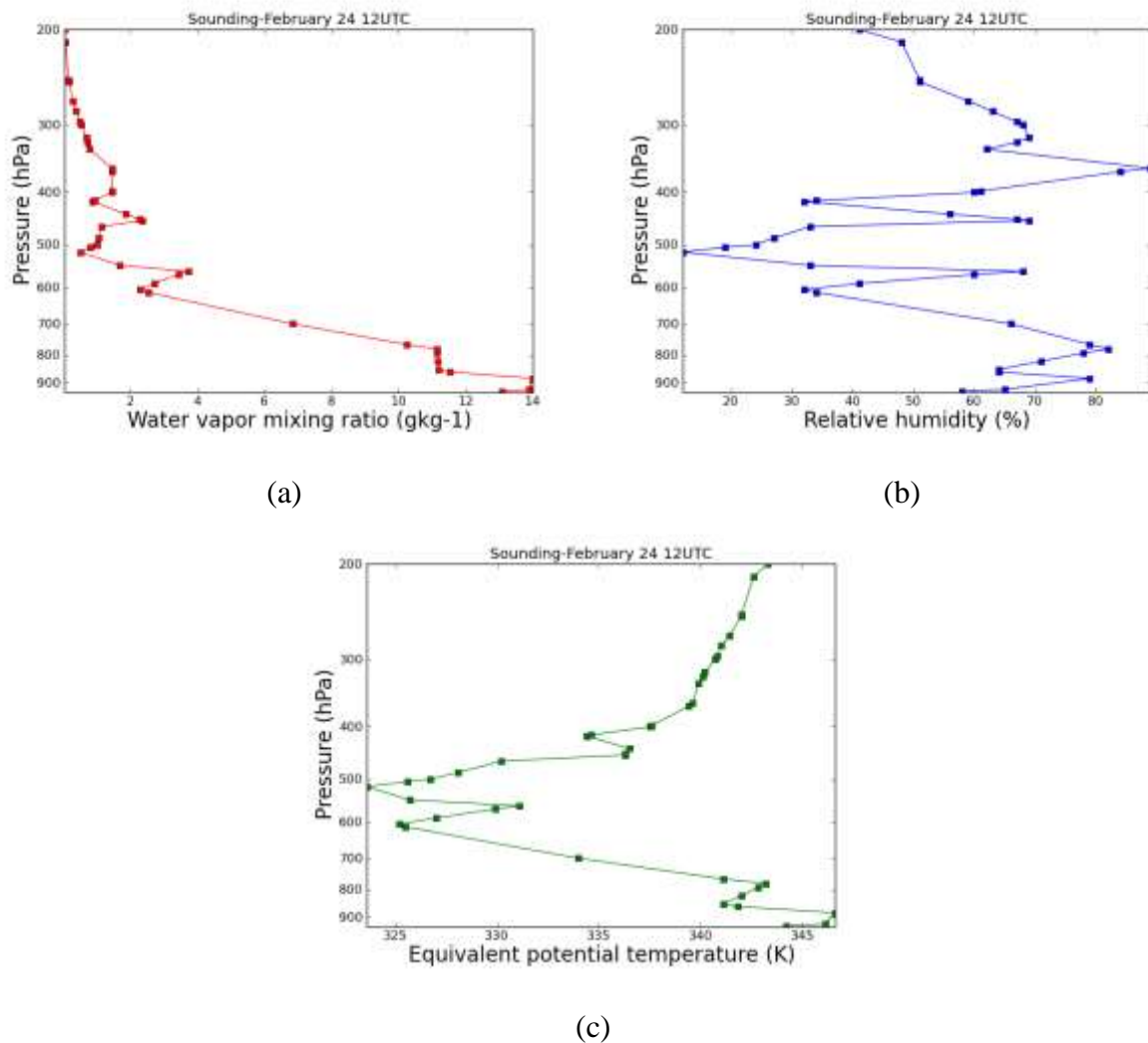


Figure 4-54: Vertical variation of water vapor mixing ratio (g kg^{-1}) (a), relative humidity (%) (b), and equivalent potential temperature (K) (c) for February, 24th at 12:00 UTC.

In the hodograph (Figure 4-53), winds near the surface are from northeast, and they change to north-northwest, and intensify. However, it remains from this direction until 400 hPa, and then turns to southwest. The wind intensified around 850 hPa, which is due to the circulation of the high-pressure system deflected to this region, shown in the synoptic scale analysis, leading to the formation of a humidity convergence zone.

CAPE derived from the sounding using temperature is 900.3 J kg^{-1} . Using the virtual temperature correction, the value is 1031 J kg^{-1} . Considering the hour of the sounding, 09 AM

local time, these values indicate potential for storm development. Using the Table 2-1 these values indicated a marginally unstable condition, and a moderately unstable condition.

CIN is -82.7 J kg^{-1} and using the correction is -63.4 J kg^{-1} . The 700-500 lapse rate is 6.3 K km^{-1} . LI is -3.61 K , and using the virtual temperature correction is -4.35 K , indicating an unstable condition with probable storm development. The level of free convection is 718.97 hPa , and using the virtual temperature correction is 741.60 hPa .

Comparing these values with the BRAMS analysis, it is possible to see that CAPE decreases until 10:00 UTC, increase at 11:00 UTC, but decrease again at 12:00 UTC. At 11:00 UTC CAPE in a small region near São Paulo was varying between $800\text{-}1400 \text{ J kg}^{-1}$, higher values are seen around it (between $1400\text{-}2000 \text{ J kg}^{-1}$), with values between $600\text{-}1000 \text{ J kg}^{-1}$ in the southeast and northeast region. The northeast and southeast values indicate a marginally unstable condition, but the higher values indicate a moderate unstable condition. At this time CAPE was higher than the value derived from the sounding close to the region of São Paulo, indicating a higher potential for storm development.

At 12:00 UTC, a small region near São Paulo has CAPE values around $2700\text{-}3000 \text{ J kg}^{-1}$, which is much higher than the value derived from the sounding. Everywhere else has values between $0\text{-}200 \text{ J kg}^{-1}$, much lower than from the sounding. After this hour, CAPE increased everywhere, and at 15:00 and 16:00 UTC the region of the city of São Paulo is between $2100\text{-}2700 \text{ J kg}^{-1}$. Values above 3300 J kg^{-1} are shown in the western part of the State. It is not possible to affirm that CAPE derived from the BRAMS is accurate for this day, but this increase could also be related to the increase in moisture after 12:00 UTC shown in the 850 hPa analysis. CIN from the BRAMS analysis increase until 09:00 UTC, and then starts to decrease, and at 12:00 UTC no CIN is shown in the region of São Paulo. At 11:00 UTC it was between $20\text{-}60 \text{ J kg}^{-1}$. A small region close to São Paulo has values between $60\text{-}80 \text{ J kg}^{-1}$ at

this hour. Values of CIN are also, as CAPE values, closer to the sounding derived value at 11 UTC than at 12:00 UTC.

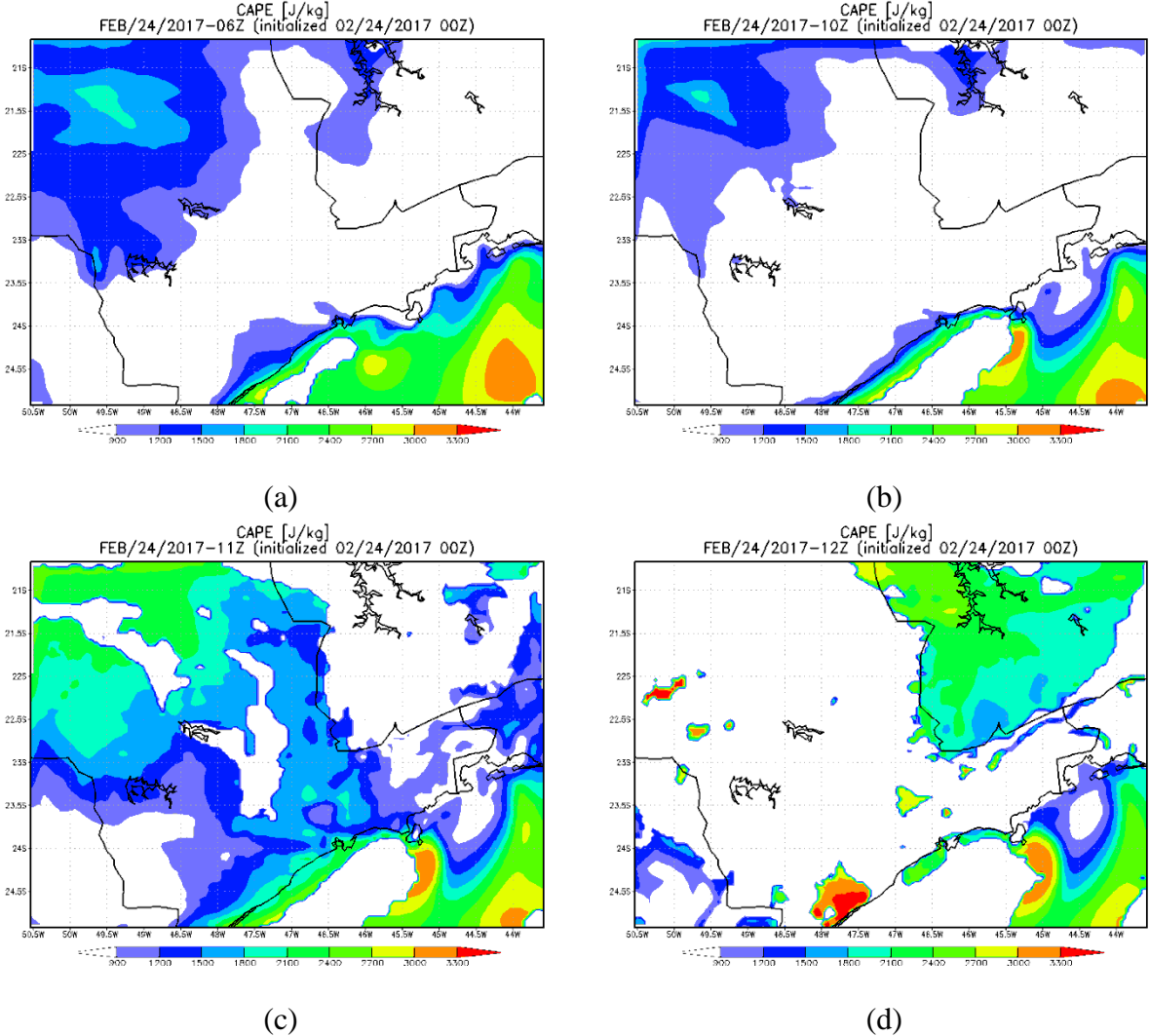


Figure 4-55: CAPE from BRAMS for February, 24th at 06:00 UTC (a), 10:00 UTC (b), 11:00 UTC (c), 12:00 UTC (d), 15:00 UTC (e), and 16:00 UTC (f).

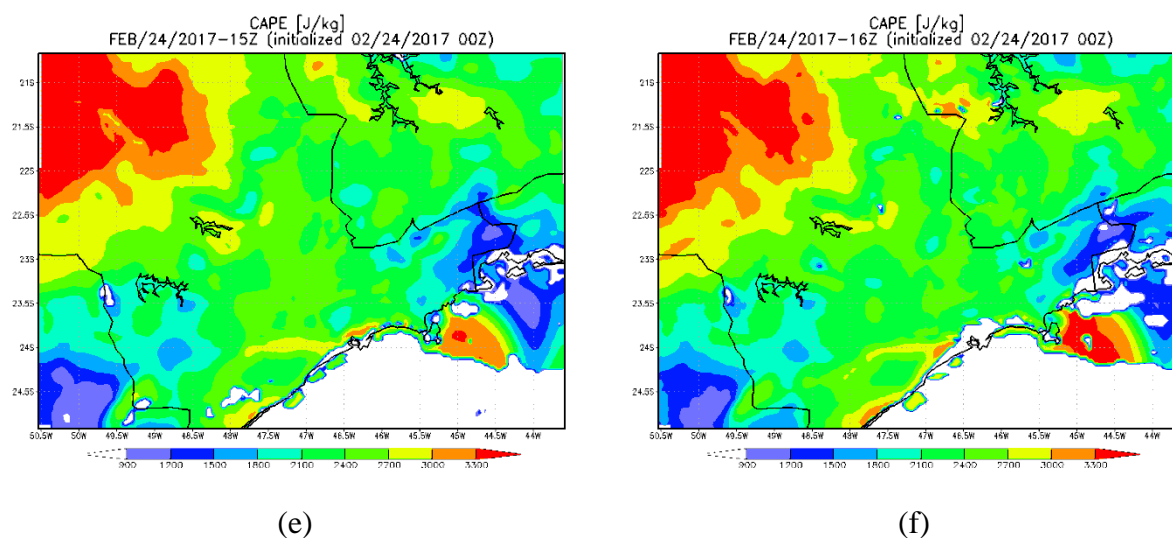


Figure 4-55: Continuation.

CAPE, CIN, LI and 700-500 lapse rate for the GFS model are shown in Figure 4-56 at 12:00 UTC. The LI parameter has to be compared with the GFS output, at 12:00 UTC in the eastern part of the State, values are between -4 and -6 K, and lower values are seen in the southeast and northeast regions (around -1 and -2 K). These values indicate an unstable condition with probable storm development, just as seen in the sounding.

Analyzing CAPE from the GFS using a surface parcel, values at 12:00 UTC are around 1200-1500 J kg^{-1} through most of the eastern part, with some regions between 1100-1200 J kg^{-1} . At 12:00 UTC, CAPE is still around the same range of values, still indicating a moderately unstable condition.

CIN, at 12:00 UTC, also from the GFS, is above -20 J kg^{-1} everywhere in the State. LI is between -4 and -6 K at 12:00 UTC. Although these values are higher than derived from the sounding, it still indicates the same condition. At 12:00 UTC it is still in the same range.

Using the GFS analysis, values are close to the derived from the sounding and the range points to the same instability condition. Values of CIN, on the other hand, are not well presented, which makes a comparison complicated.

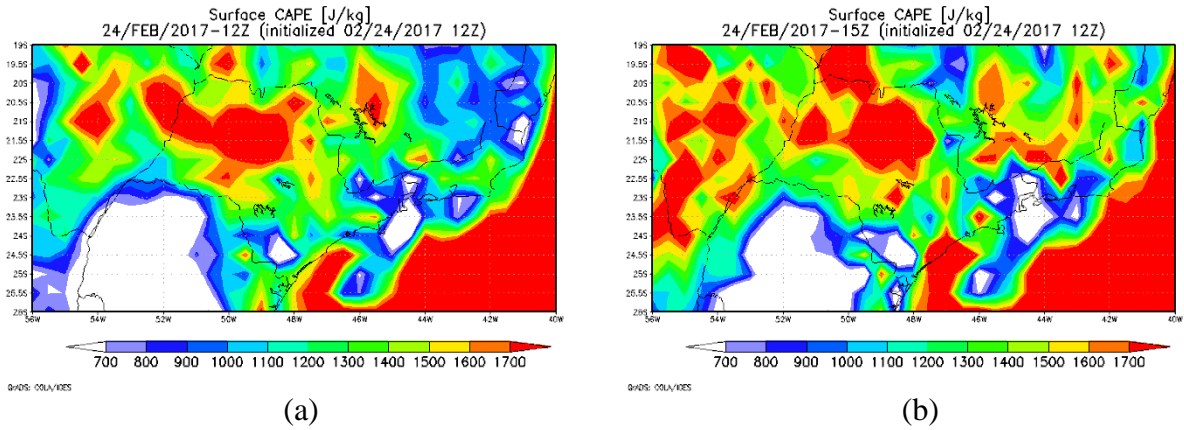


Figure 4-56: CAPE from GFS at 12:00 UTC (a), and 15:00 UTC (b) for February, 24, 2017.

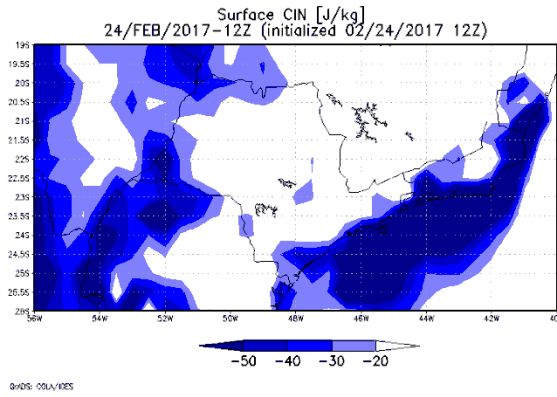


Figure 4-57: CIN for a surface parcel at 12:00 UTC, for February, 24, 2017.

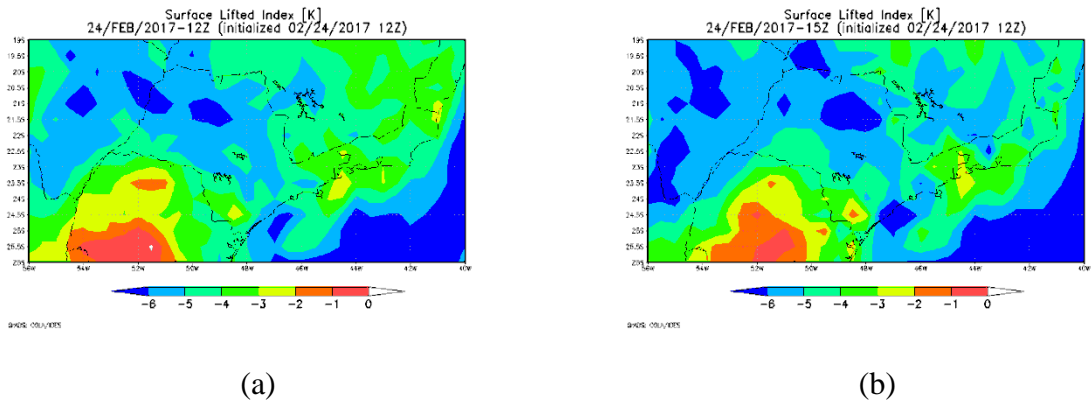


Figure 4-58: LI from GFS at 12:00 UTC (a), and at 12:00 UTC (b) for February, 24, 2017.

The 700-500 lapse rate from the GFS this parameter is between 6 and 6.5 K km^{-1} , in most of the northeast region of the State at 12:00 UTC, the same range observed in the sounding. At 15:00 UTC the parameter is still in this range.

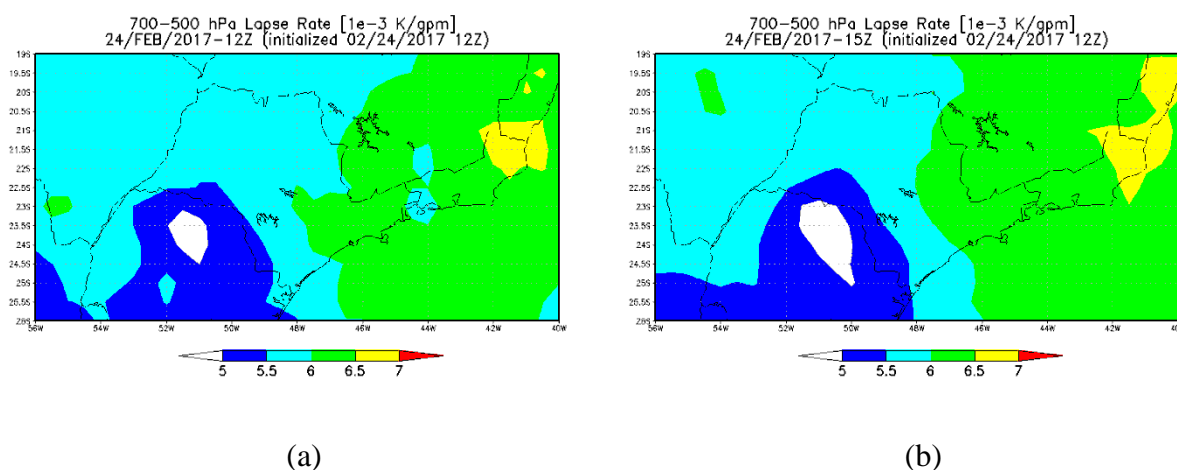


Figure 4-59: 700-500 hPa lapse rate from GFS at 12:00 UTC (a), and 15:00 (b), for February, 24, 2017.

Comparing the vertical analysis of relative humidity and water vapor mixing ratio derived from the sounding with the BRAMS output, it is seen that near the surface moisture is much higher in the model output than it is in the sounding. Near to the surface the water vapor mixing ratio is between 16-18 g kg^{-1} and the relative humidity is between 85-90%. At the top of the domain the magnitude is much closer the sounding. Near the top, relative humidity is around 30-40% close to the values obtained in the sounding. This could be useful for other events to analyze moisture content on middle levels in the absence of atmospheric soundings. However, the air can be drier above this last level seen in the model, just as it is seen here; therefore it is not possible to make comparisons quantitatively.

The vertical cross section of wind does not represent the change close to the surface, from northeast to northwest, seen in the hodograph from the sounding, but the direction shown from the BRAMS is from northwest throughout the vertical extension, which is seen in

the hodograph. The increase in speed seen at around 850 hPa is also not present in the BRAMS output, but it is seen in the GFS analysis.

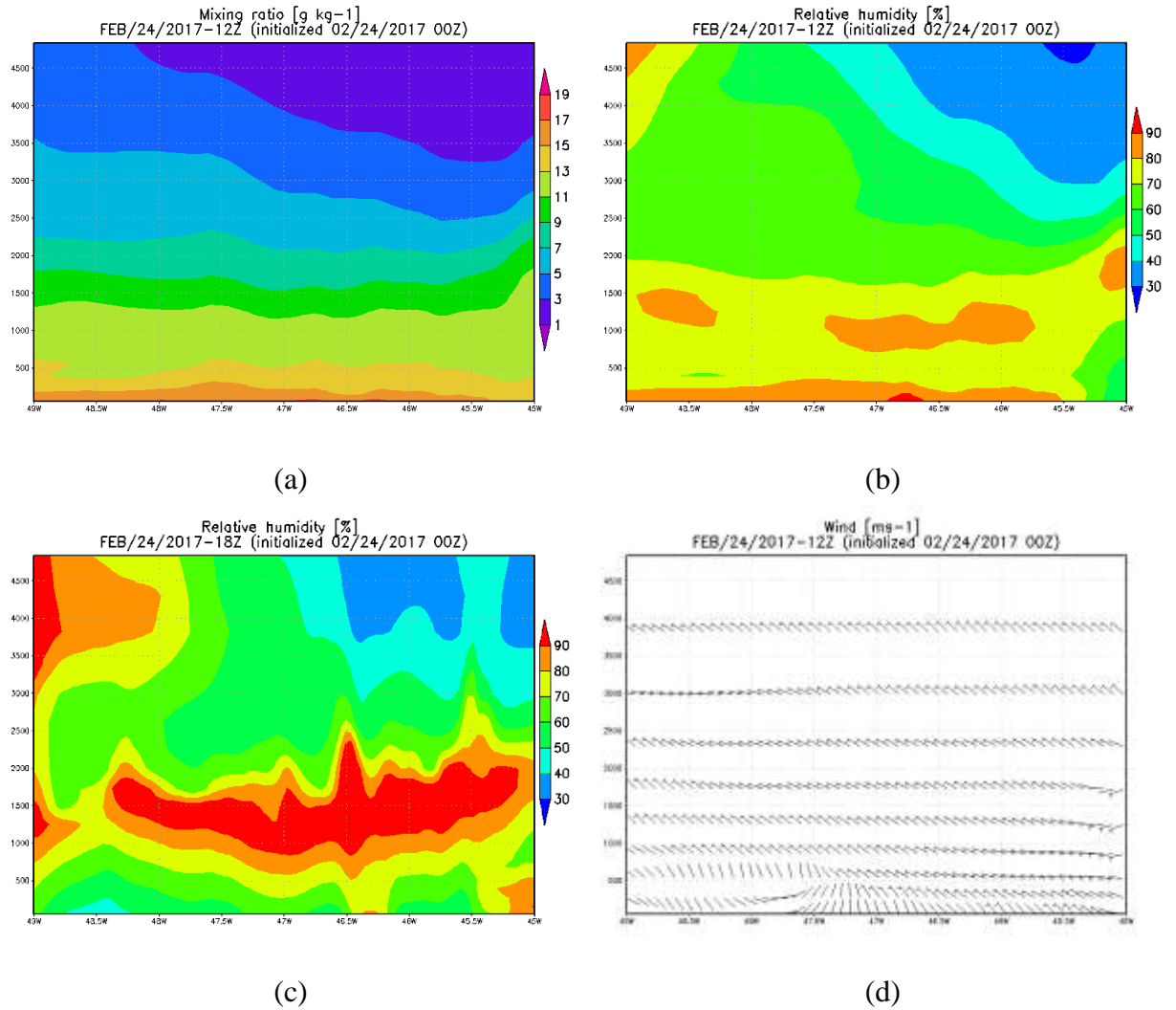


Figure 4-60: Vertical cross section of water vapor mixing ratio at 12:00 UTC (g kg^{-1}) (a), relative humidity at 12:00 UTC (%) (b), and 18:00 UTC (c), and wind at 12:00 UTC (ms^{-1}) (d) from BRAMS for February, 24th

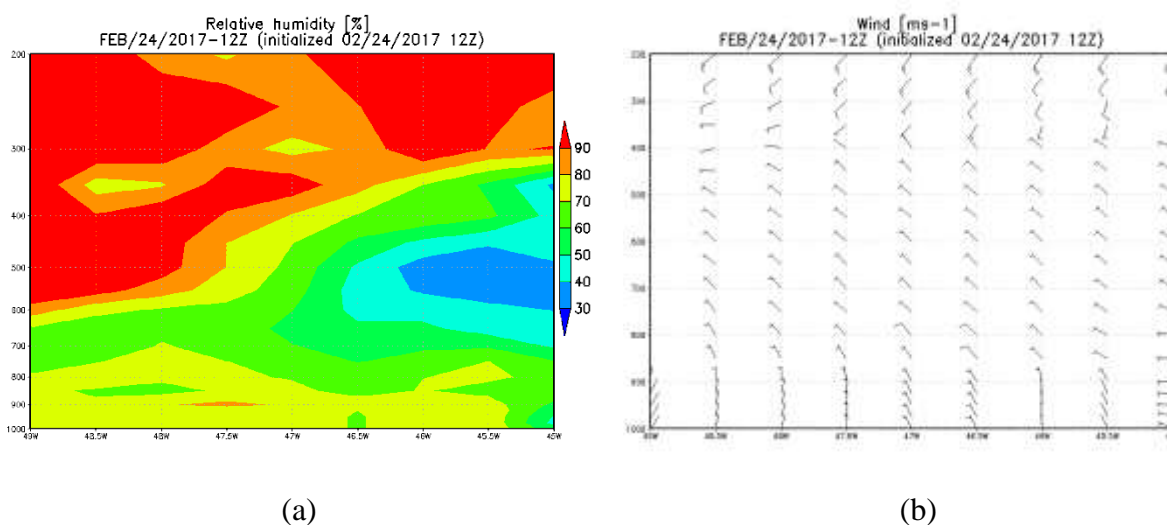


Figure 4-61: Vertical cross section of relative humidity (a) and winds (b) from GFS at 12:00 UTC for February, 24, 2017.

Analyzing moisture divergence using the BRAMS output (Figure 4-62), it is seen that a line of moisture convergence with values below $-4 \cdot 10^{-3} \text{ g kg}^{-1} \text{ s}^{-1}$ is present, denoting the sea breeze. It is possible to see its propagation into the continent. Moisture convergence is also seen in the region of Serra da Mantiqueira, in the northeastern region of the State.

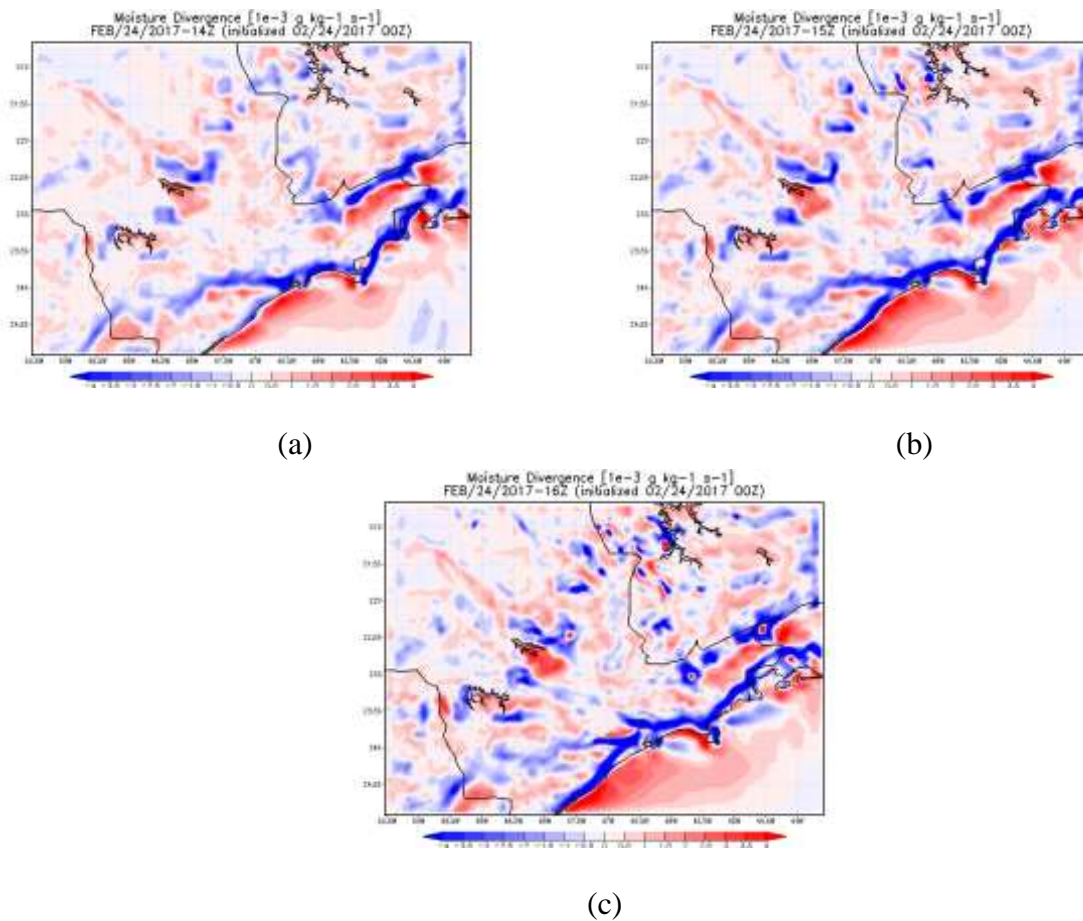


Figure 4-62: Moisture divergence for February, 24th at 14:00 UTC (a), 15:00 UTC (b), and 16:00 UTC (c).

Wind is from northeast in the north and northeast regions and from southeast in the southwest region at the beginning of the analysis. After 03:00 UTC, winds intensified and, are now from northwest and northeast in the northeast region, including in the region of São Paulo, and are still from southeast in the south and southwest regions. After 10:00 UTC the wind weakens.

At 15:00 UTC southeast winds are seen near to the coast, where a moisture gradient is observed. It is possible to see, after this hour, the sea breeze propagation into the continent, and it reaches the region of the city of São Paulo around 17:00 UTC, as will be shown in the surface data analysis. However, the sea breeze does not propagate further than this, due to the

northwest winds in the continent, related to the northwest flow seen in the synoptic scale analysis.

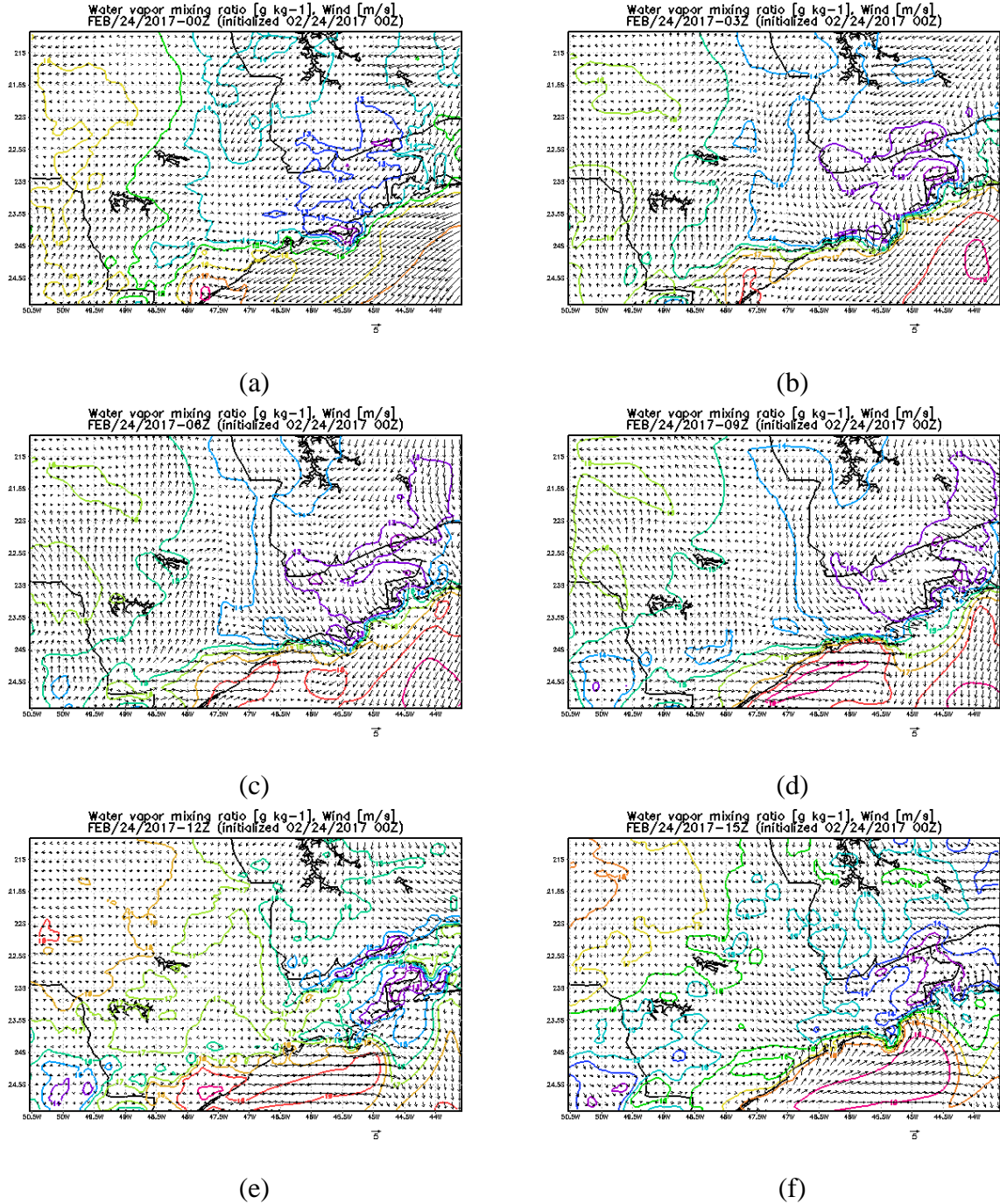


Figure 4-63: Water vapor mixing ratio and wind for February, 24 at 00:00 UTC (a), 03 UT (b), 06:00 UTC (c), 09:00 UTC (d), 12:00 UTC (e), 15:00 UTC (f), 18:00 UTC (g), and 21:00 UTC (h).

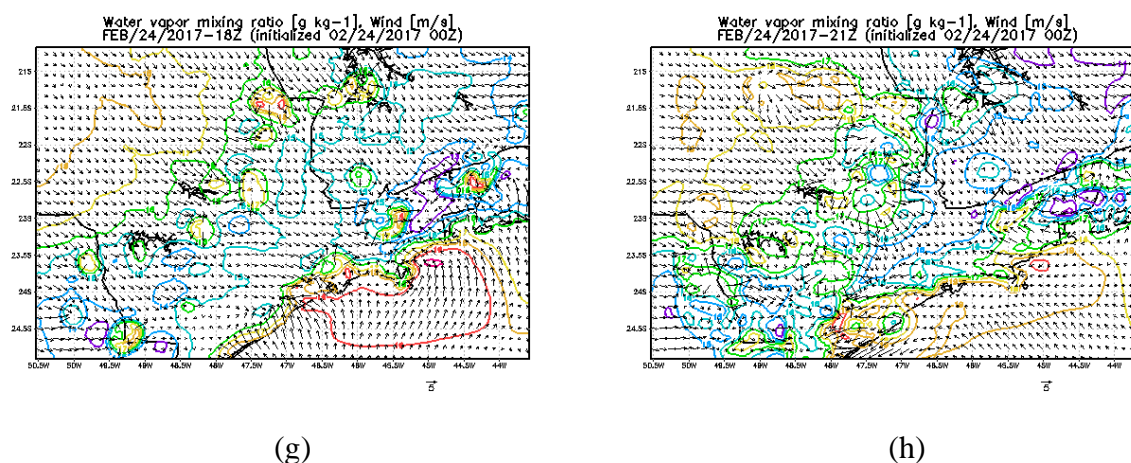


Figure 4-63: Continuation.

This “convergence”, allied with instability generated by the large scale and appropriate thermodynamic conditions, led to the severe weather occurrence, details will be shown in the next section.

d. Surface stations

For this event, 17 INMET surface stations were analyzed, METAR from airports in the city of São Paulo and Guarulhos were also used.. As it was mentioned in the previous section, the sea breeze penetration was observed in the region of the city São Paulo.

Figure 4-64 shows wind speed and direction, dew point temperature, relative humidity and temperature at station A701 and A755 (except wind records) for this day. At station A701 southeast winds were observed until 07:00 UTC, turning to northeast, after 12:00 UTC it turned to northwest. At 17:00 UTC the turn to southeast related to the sea breeze was registered. In the Campo de Marte and Congonhas METAR analysis wind turned to southeast at 17:00 and 16:00 UTC, respectively. The turn to southeast occurred, also, at 17:00 UTC in the Guarulhos airport. At all of these stations southeast winds were accompanied by increase in dew point temperature, relative humidity, and decrease in temperature. Station A701 recorded rain from 19:00-20:00 UTC to 23:00-00:00 UTC. The peak was 14.4 mm between 19:00 and 20:00 UTC. In the previous period a wind gust of 17.6 m s^{-1} was recorded at the station. The total accumulated precipitation was 34.6 mm.

According to the CGE, a total of 36 point of floods was considered insurmountable in the city during this day. Until 7:50 pm local time, all zones (north, southeast and west) registered an average above 15 mm, in the east zone, the average was above 30 mm. Wind gusts of 20 m s^{-1} were observed in the Guarulhos airport and from their automatic stations. Until 7:40 PM local time, 14 out of 31 stations recorded rain above 25 mm. Two of them recorded values above 70 mm (Ipiranga and Vila Prudente). From the Alto Tietê network, 27 stations recorded rain indices above 25 mm, 10 recorded above 50 mm, and one recorded above 70 mm. Still according to the CGE, three locations registered hail, two in the east zone, and one in the south zone.

Stations A755 (Barueri) recorded an increase in dew point temperature and relative humidity after 15:00 UTC, but this is probably not related to the sea breeze, for the fact that this city is close to São Paulo. These parameters decreased at 18:00 and increased again at 19:00 UTC. In the city of São Paulo, station A701 also registered an increase in dew point temperature and relative humidity after 14:00 UTC, smaller than the increases after 17:00 UTC, which were related to the sea breeze. These changes earlier in the day occurred with winds from northwest, which were already related to the synoptic pattern. This is probably also what happened at station A755, but there is no record of wind direction to confirm it.

A total of 14 stations recorded rain (Figure 4-66), but only three of them, including São Paulo (A701) recorded more than 10 mm in one hour. The other two are also close to the city of São Paulo, Sorocaba and Barueri, which recorded a maximum of 15.2 mm and 14.6 mm, respectively.

The highest wind gust was registered at station A701 of 17.6 m s^{-1} , as already mentioned.

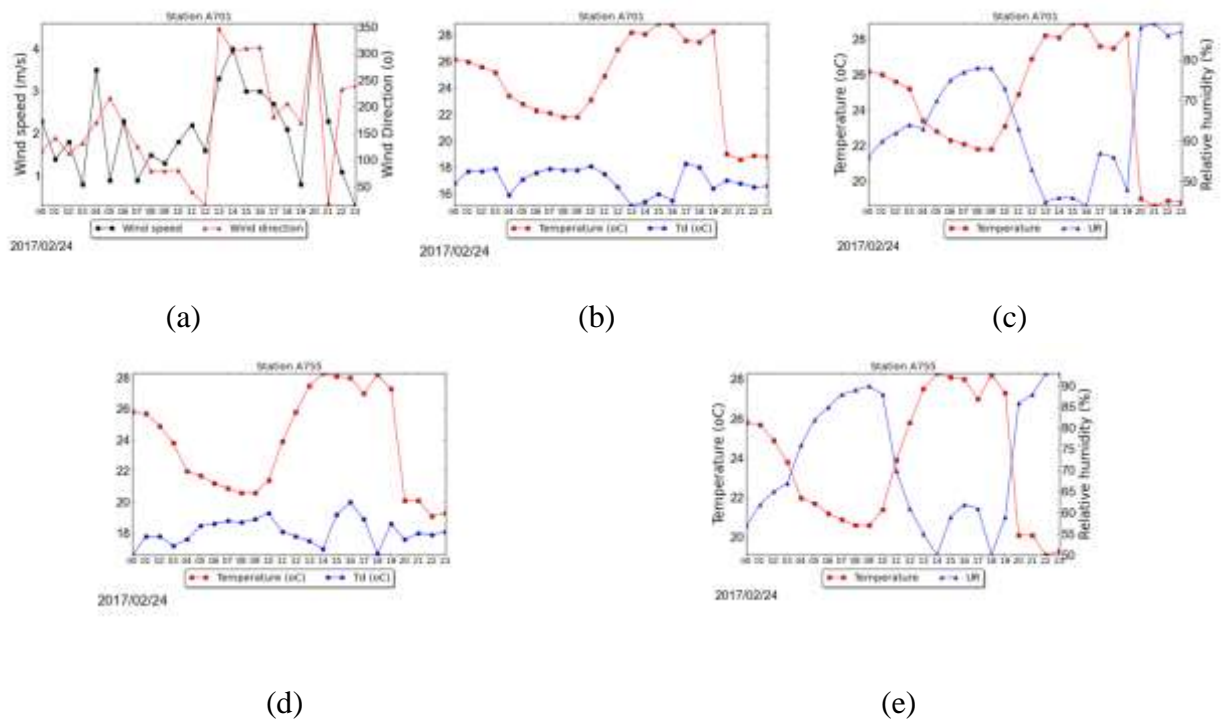


Figure 4-64: Wind speed and direction (a), temperature and dew point temperature (b), temperature and relative humidity (c) for station A701, temperature and dew point temperature (d), and temperature and relative humidity (e) for station A755 for February, 24, 2017.

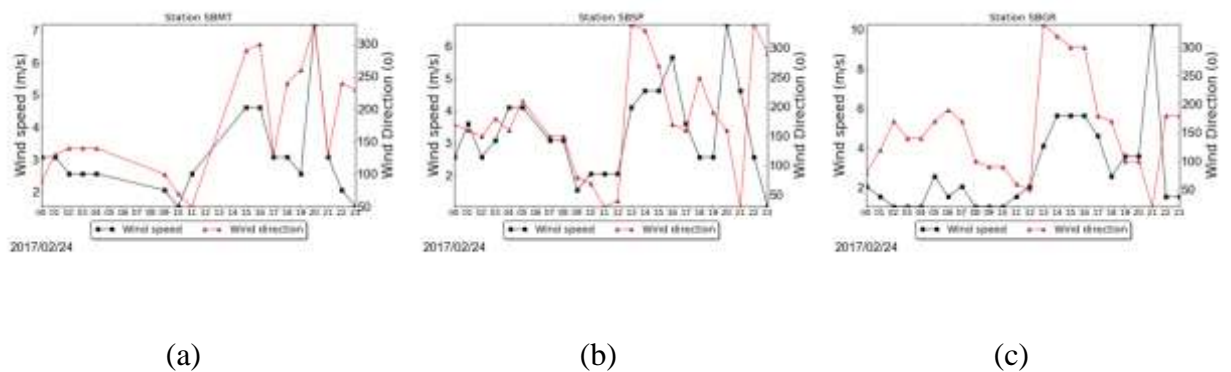
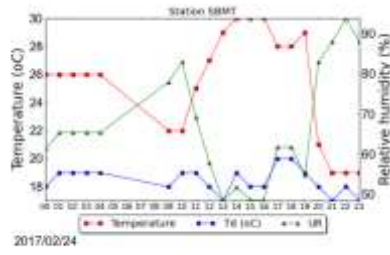
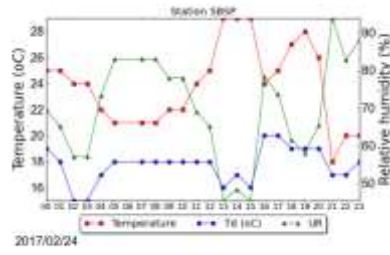


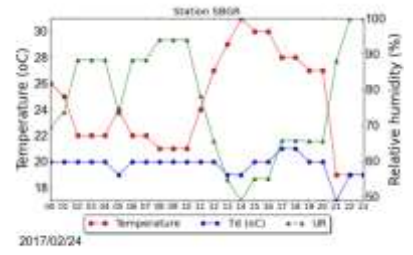
Figure 4-65: Wind speed ($m s^{-1}$) and direction (degrees), temperature, dew point temperature and relative humidity from METAR for stations SBMT (a), (d), SBSP (b), SBGR (c), (f), for February, 24th.



(d)

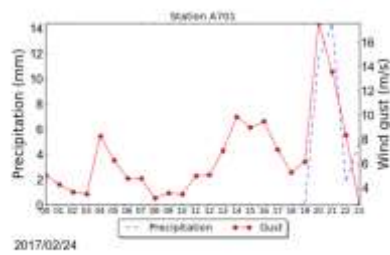


(e)

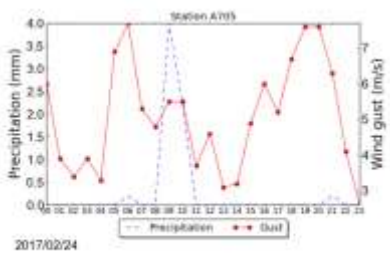


(f)

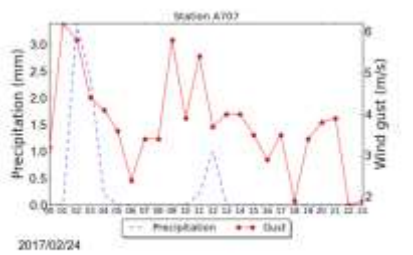
Figure 4-65: Continuation.



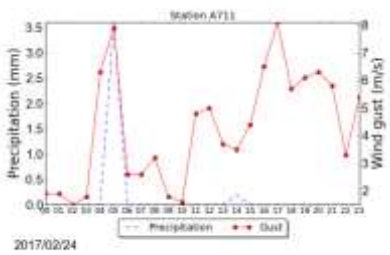
(a)



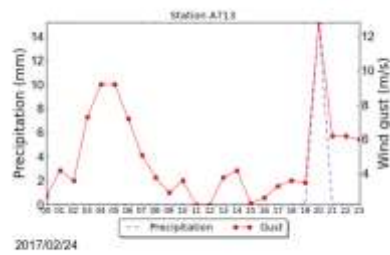
(b)



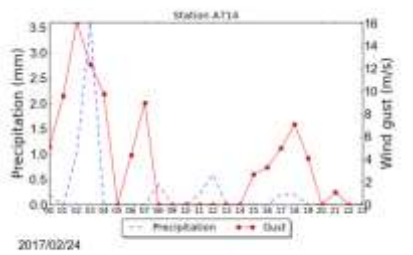
(c)



(d)



(e)



(f)

Figure 4-66: Precipitation (mm) and wind gust (ms^{-1}) for February, 24th at stations A701 (a), A705 (b), A707 (c), A711 (d), A713 (e), A714 (f), A716 (g), A718 (h), A725 (i), A726 (j), A728 (l), A741 (m), A746 (n), and precipitation (mm) at station A755 (o).

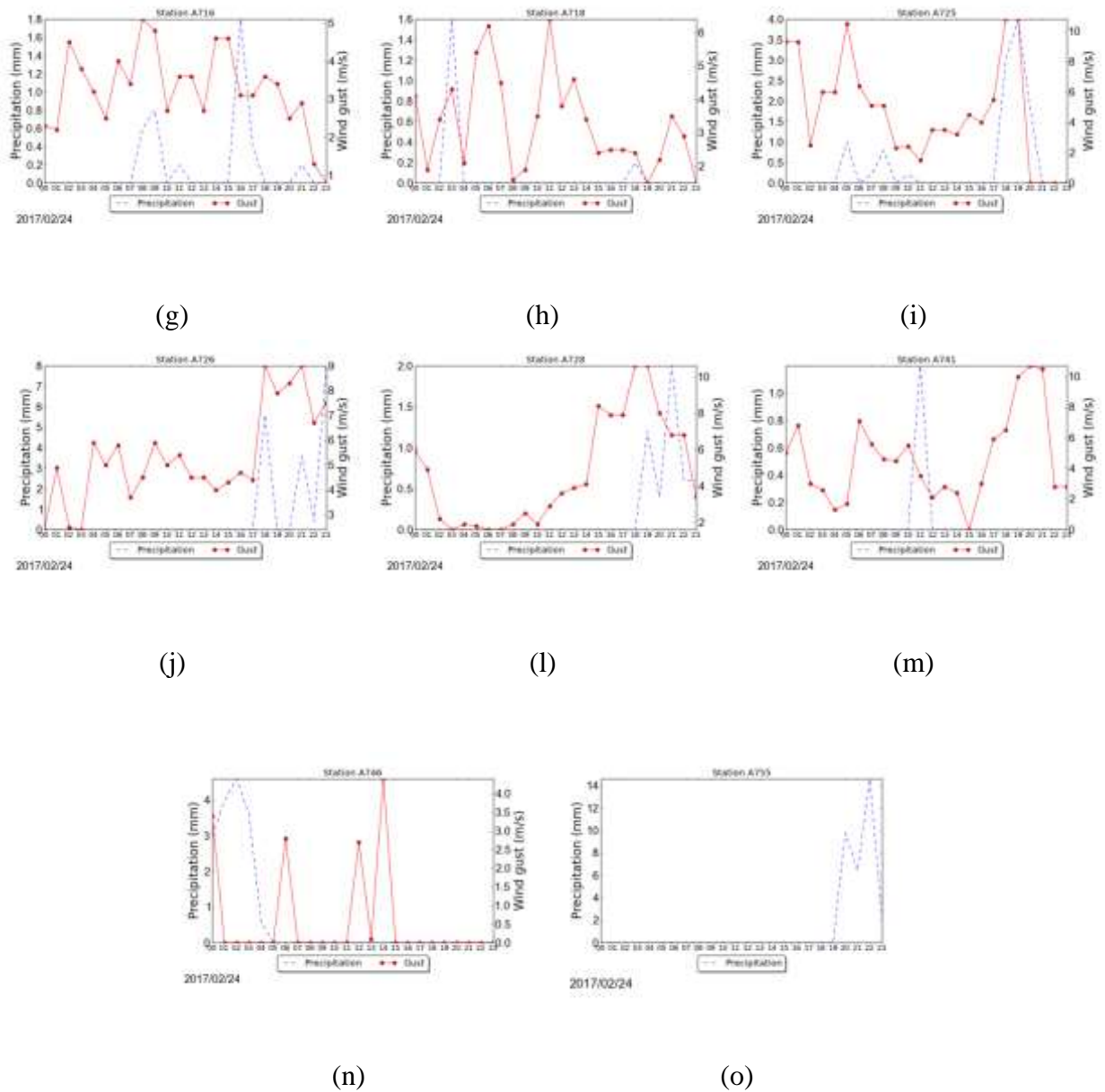


Figure 4-66: Continuation.

4.1.2 Partial conclusions for category 1a

This category was related to the northwest flow adding moisture to the southeast region of the country from the Amazon region. Three events were classified for this category.

On December, 03th, strong wind gusts were reported; however, rain was not as significant as it was seen in other events of this category. Only 1 point was registered in the city of São Paulo. On January, 15-16 and February, 24 heavy rain was reported leading to 57

point of the 24th. The highest accumulated precipitation for a period of 24 hour in 68 years at the station Mirante de Santana was observed between January, 15th and 16th. During one hour, 64.6 mm was recorded, between 01:00 and 02:00 UTC on January, 16th, at Mirante de Santana. Several cities, including the city of São Paulo, reported flash floods during this event, such as Guarulhos, Francisco Morato, Osasco, Barueri, Franco da Rocha.

During all the events it was possible to identify the presence of a large scale system affecting the State of São Paulo. On December, 03th, it is not possible to identify the importance of the topography in storm initiation. On February, 24th, in the satellite images it is possible to see storms developing in the northeast region, however convective forms in other regions of the State. On January, 15-16, convection starts to form between the State of Minas Gerais and São Paulo, region in which the northwest flow was directed. One important feature observed during this event was a band of clouds advancing through the continent, reaching the State of São Paulo. This seemed to be important in storm initiation.

In the synoptic scale analysis it was confirmed the presence of the northwest flow at 850 hPa. On December, 03th, a low pressure system was also observed in the south region of Brazil. The flow is directed to the State of São Paulo after 12:00 UTC. The same is seen on February, 24th, during this day, this flow was following a frontal system at the surface. It was seen after 21:00 UTC on January, 15th. Warm advection above $1.0 \cdot 10^{-4} \text{ K s}^{-1}$ was seen in the east region of the State at 12:00 UTC on December, 03 and January, 16th.

A moisture convergence was seen near the coast on all events, and sea breeze penetration was observed on February, 24th and January, 15th. On December, 03th, the northwest winds prevented it to penetrate. On February, 24th, it reached the city of São Paulo, but did not propagate further, again due to the northwest flow. The hour of penetration was around 16:00-17:00 UTC on both days.

CAPE was between a marginally and moderately unstable condition for all events, and LI indicated an unstable condition, with probable storm, even severe, in the presence of some lifting mechanism. A region in the north part of the State, on December 03, had CAPE and LI values indicating a very unstable and strong unstable condition, respectively, interestingly, strong convection was seen in the region in the satellite analysis. The 700-500 hPa lapse rate was between 6.0 and 6.5 K km⁻¹ on December 03, between 6.0 and 6.5 K km⁻¹ on February, 24th, and 5.5 and 6.0 on January, 15th, and 5.0 and 6.0 K km⁻¹ on January, 16th.

On December, 03th, dry air, between 10 and 20 % was seen near the top of the BRAMS output in the beginning of the analysis, it increased during the day, and at 12:00 UTC it was around 40-50 %. However, dry air could still be present above; therefore, it is not possible to conclude that strong winds gusts observed were related to dry air in the atmosphere. On February 24th, less than 20 % was observed around the level of 500 hPa, strong wind gusts were reported in the city. Regarding the day of January, 15th, it is complicated to make a conclusion, the severe event occurred after the sea breeze penetration and after precipitation had already been observed in the city earlier, which, probably, emphasize the relevance of that band of clouds propagating and the northwest flow.

Northwest winds extending through the atmosphere were seen on December 03th and February, 24. Winds from north are seen on January, 16th, during the day of January, 15th, winds were weak near, especially near the surface.

Heavy rain was expected during these events, considering the moisture supply on low levels given by the northwest flow. However, as mentioned, the event on December, 03, did not registered high accumulated values; further analysis of this event could be useful to better understand this.

4.1.3 Category 1b

This category is also related to strong synoptic scale features, but they are related to different processes than the low-level jet, that lead to favorable environments.

4.1.3.1 January, 07, 2017

Heavy rain which led to flash flood occurrence during this day was reported in the city of São Paulo, according to CGE, 26 points of floods were registered in the city. Winds gusts of around 21 ms⁻¹ were registered on Campo de Marte and Mirante de Santana. Hail was reported in the north region of the city. Flash floods were also observed in cities at Vale do Paraíba, like São José dos Campos, Jacareí, Taubaté and Guaratinguetá, this last city also reported fall of trees.

a. Satellite

In this section we analyzed infrared satellite images for South America, seen in Figure 4-67 and enhanced infrared image for the southeast region of Brazil, shown in Figure 4-68.

Analyzing the infrared images for South America, it is possible to see the frontal system and clouds across the State of São Paulo, at 00:00 UTC. It is seen that this system moves away, with the advance of hours, even further, from the continent. It still influences the State, as clouds can still be seen at 12:00 UTC.

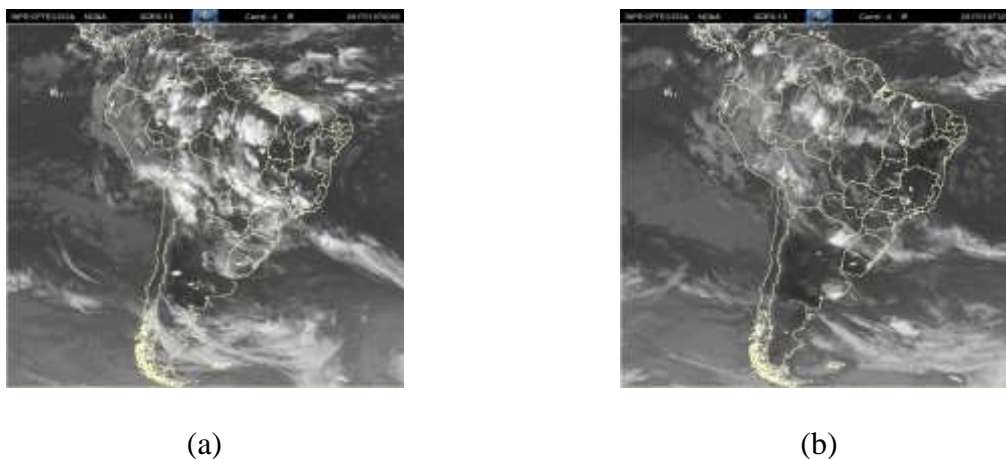


Figure 4-67: Infrared satellite image for January, 07 at 00:00 UTC (a), and 12:00 UTC (b).

Analyzing the enhanced infrared images for the southeast region of Brazil, at 16:30 UTC, cells have started to form in the region of Serra da Mantiqueira, and at the coast, in the southeast region of the State. These cells, related to topography, intensify as more clouds develop parallel to the coast, after 17:00 UTC, indicating the presence of the sea breeze in the continent, as will be further discussed in future sections. These cells intensify, and in the region of São Paulo and Vale do Paraíba, at 19:30 UTC, values are around $-70\text{ }^{\circ}\text{C}$. Northeast of the State of São Paulo, and southeast of Minas Gerais, convective cells with low values of the same order are still seen at 22:30 UTC.

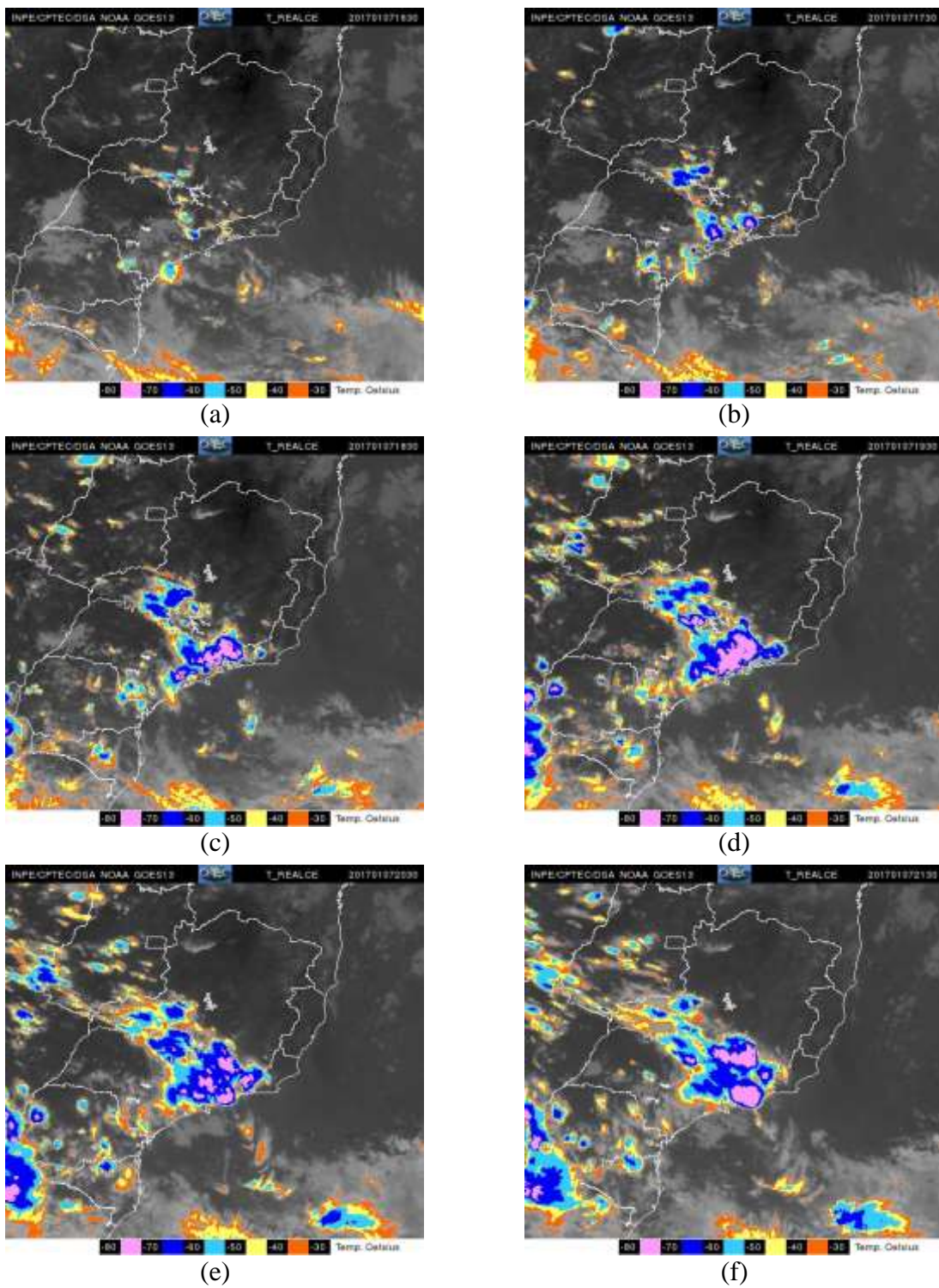


Figure 4-68: Enhanced infrared satellite image for January, 07 at 16:30 UTC (a), 17:30 UTC (b), 18:30 UTC (c), 19:30 UTC (d), 20:30 UTC (e), 21:30 UTC (f), 22:30 UTC (g), 23:30 UTC (h).

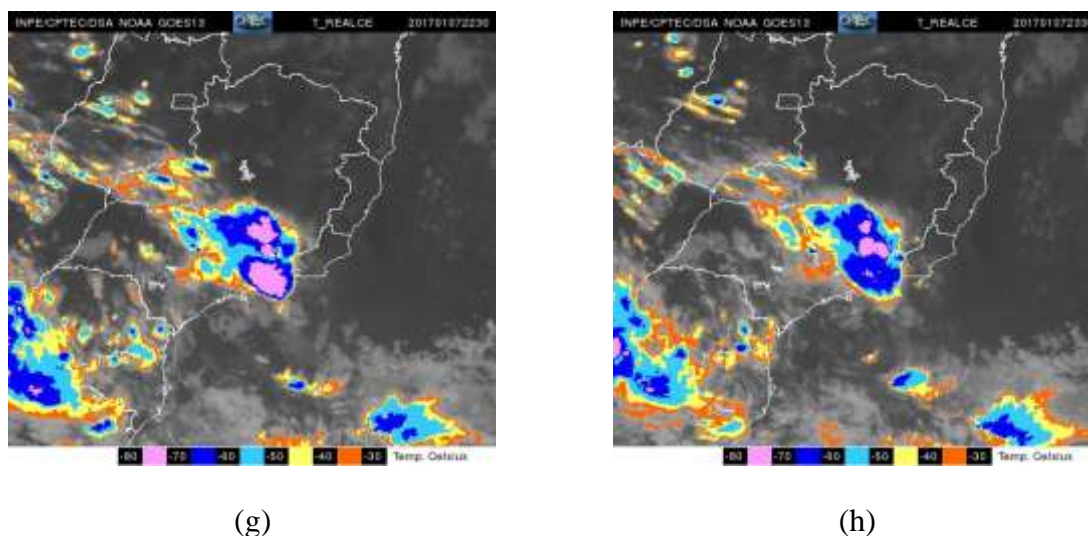


Figure 4-68: Continuation.

b. Radar

The evolution of the event is seen in Figure 4-69. At 17:00 UTC cells are forming parallel to the coast due to the sea breeze propagation and in the region of Serra da Mantiqueira. At 17:40 UTC, more cells are seen parallel to the coast with reflectivity values around 40 dBZ. Intense cells are present in the Serra da Mantiqueira and Vale do Paraíba, with reflectivity values around 60-65 dBZ. High reflectivity values are observed in the region of São Paulo, around 60-65 dBZ, between 17:50-18:00 UTC. At this interval (between 17:00-18:00 and 18:00-19:00 UTC) heavy rain was observed at the surface station, as will be shown in a future section. At 18:40 UTC new cells intensified in the region of Vale do Paraíba, with reflectivity values around the same order as before. In the region of São José dos Campos reflectivity values are as high as 60-65 dBZ at 18:50 UTC.

There was an apparent problem with the radar, and images are not available between 19 and 19:50 UTC. At 20:00 UTC clouds are seen covering the Vale do Paraíba region until São Paulo, with reflectivity around 45-50 dBZ in the Vale and 30-35 dBZ in São Paulo. Clouds with reflectivity around 60-65 dBZ are seen northeast of Campinas between 20:20 and 20:30 UTC, but no severe weather occurrences in the region were recorded.

Cells in the Vale do Paraíba remained with values around 40 dBZ until 22 UTC, but it lost its strength after 2230 UTC.

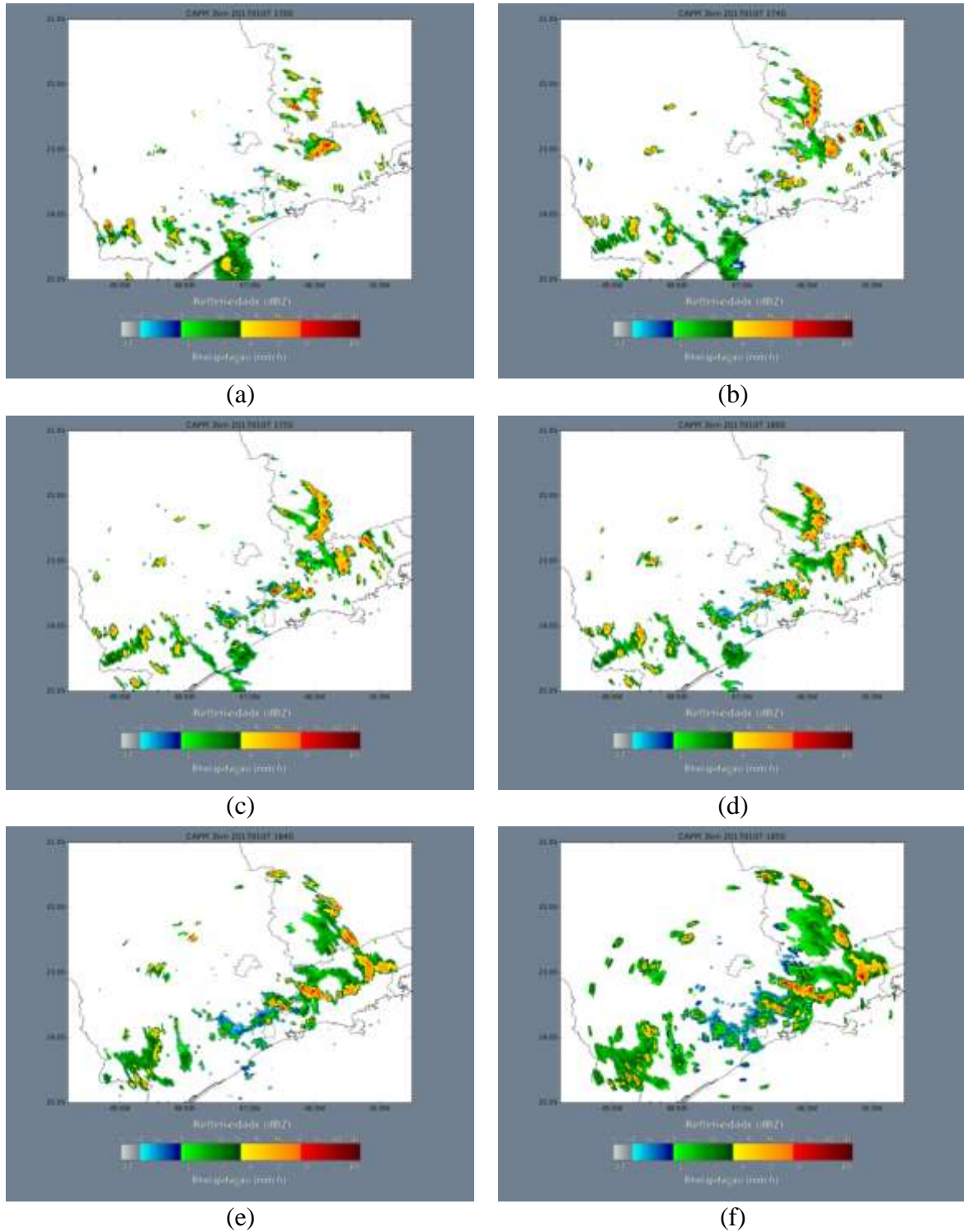


Figure 4-69: São Roque radar images for January, 07th at 17:00 UTC (a), 17:40 (b), 17:50 UTC (c), 18:00 UTC (d), 18:40 UTC (e), 18:50 UTC (f), 20:00 UTC (g), 20:20 UTC (h), 20:30 UTC (i), 22:00 UTC (j).

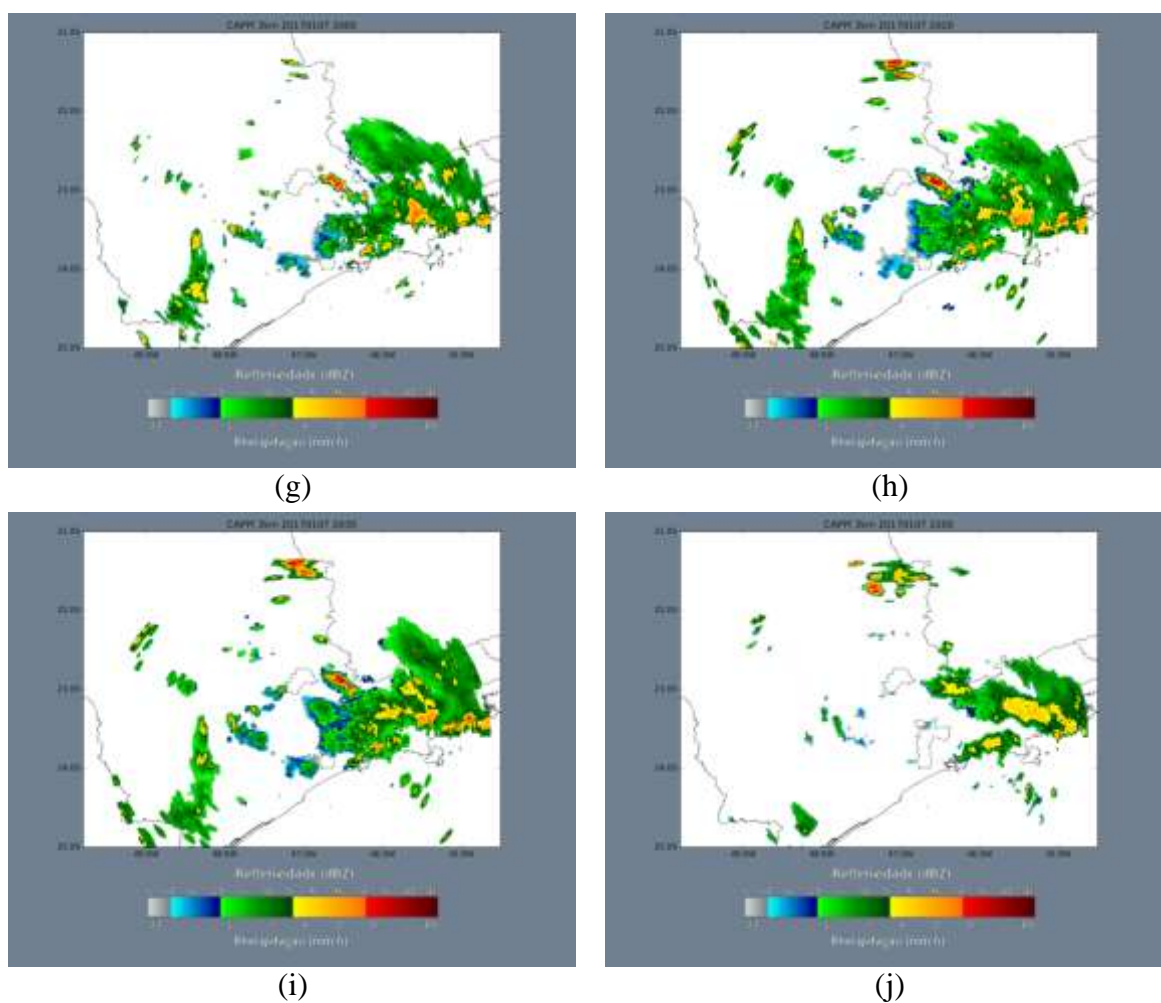


Figure 4-69: Continuation.

c. Synoptic scale analysis

The Bolivian high is located between southwest Bolívia and northern Chile, generating a ridge on top of the southeast region of Brazil. An upper level cyclonic vortex is present between the States of Pará and Mato Grosso. A diffluence forms in the southeast region of Brazil between the ridge and this upper level cyclonic vortex, causing confluence in low levels. This pattern is seen throughout the analysis (Figure 4-70).

A trough is seen in southern Argentina and another at around 30° - 20° W in the Atlantic Ocean. They are both associated to a frontal system at the surface and move eastward throughout the day. These troughs are also seen in the 500 hPa analysis with negative vorticity associated. The 500 hPa analysis is seen in Figure 4-72.

Mass divergence, at 200 hPa' shown in Figure 4-71, is seen at 00:00 UTC extending from the west, northwest and central-north region of São Paulo, with values around $0.2-0.8 \cdot 10^{-4} \text{ s}^{-1}$. Values between $0.2-0.6 \cdot 10^{-4} \text{ s}^{-1}$ are seen in the southeast region, and lower values (between $0.2-0.4 \cdot 10^{-4} \text{ s}^{-1}$) are observed in the central-south part of the State. This pattern disappears after this hour. At 12:00 UTC divergence is only shown in the region of the city of São Paulo, with values around $0.2-0.6 \cdot 10^{-4} \text{ s}^{-1}$, and it is still seen at 18:00 UTC, but is weaker ($0.2-0.4 \cdot 10^{-4} \text{ s}^{-1}$).

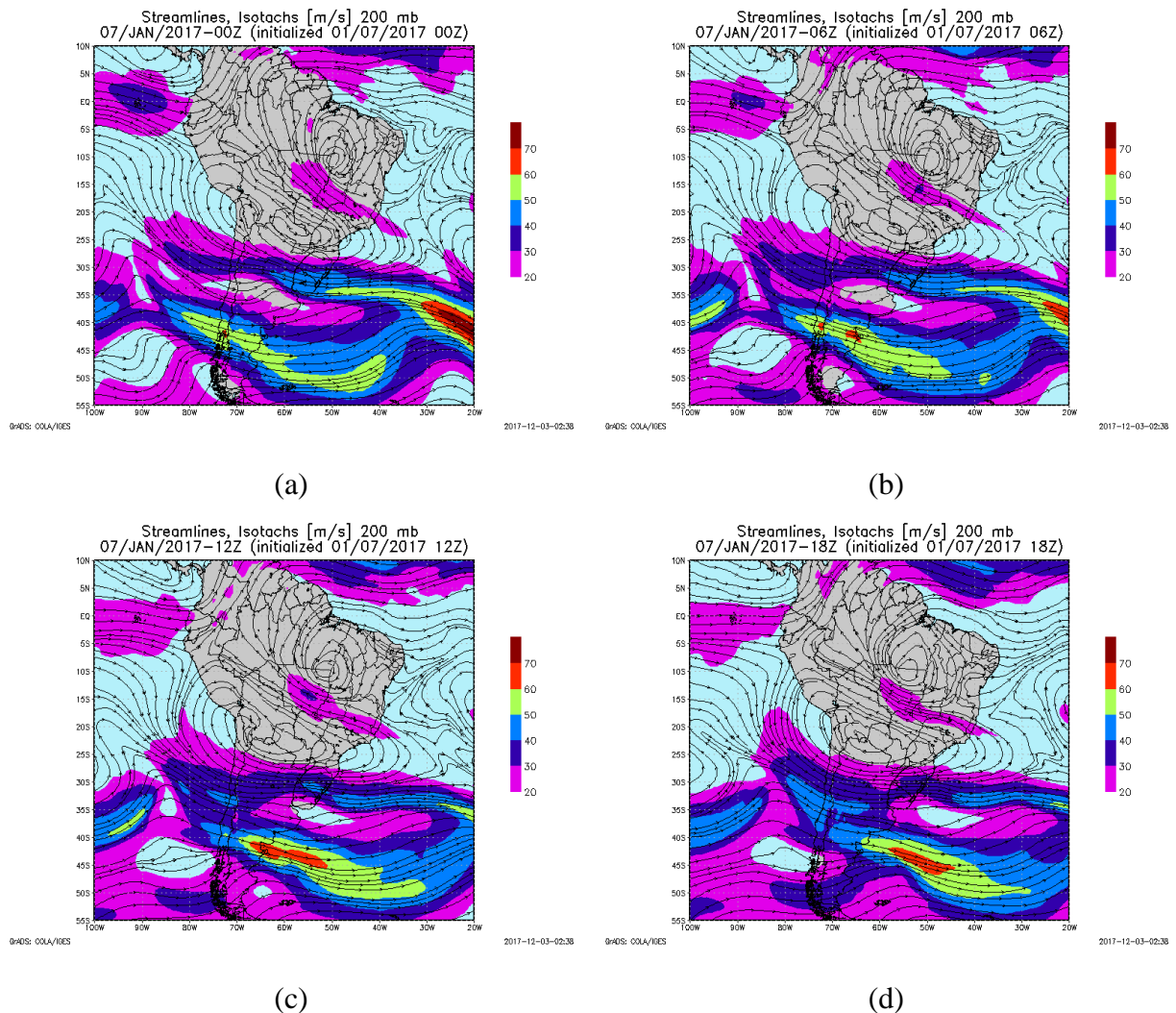


Figure 4-70: Streamlines and isotach (m s^{-1}) at 200 hPa for January, 07th at 00:00 UTC (a), 06:00 UTC (b), 12:00 UTC (c), and 18:00 UTC (d).

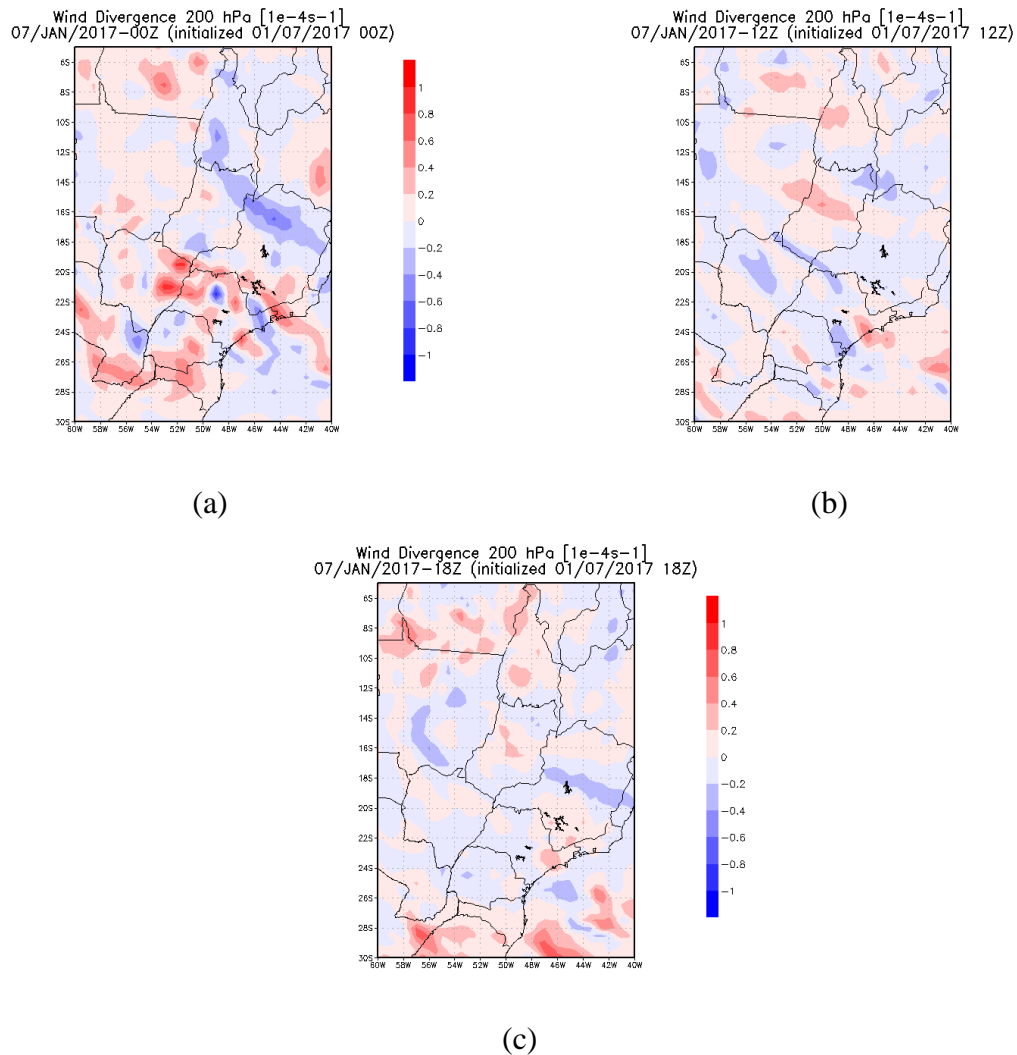


Figure 4-71: Wind divergence at 200 hPa for January, 07 at 00:00 UTC (a), 12:00 UTC (b), and 18:00 UTC (c).

Besides the troughs mentioned in the 500 hPa analysis, a high pressure system is present near to the coast of Espírito Santo, and a trough is seen in the east region of the State of São Paulo. This is seen throughout the analysis. A region of intense temperature gradient associated with the frontal systems in the surface is seen in the Atlantic at the 850 hPa level (Figure 4-73). A postfrontal high pressure system is seen in the Atlantic Ocean around the height of the coast of Rio Grande do Sul. Also seen in the surface analysis (Figure 4-74), these systems move eastward as the day advances. One of the frontal systems is around the height of the coast of Argentina, the other one is further from the continent, away from the

coast of Paraná and São Paulo. It is possible to identify them using the temperature and moisture at 850 hPa.

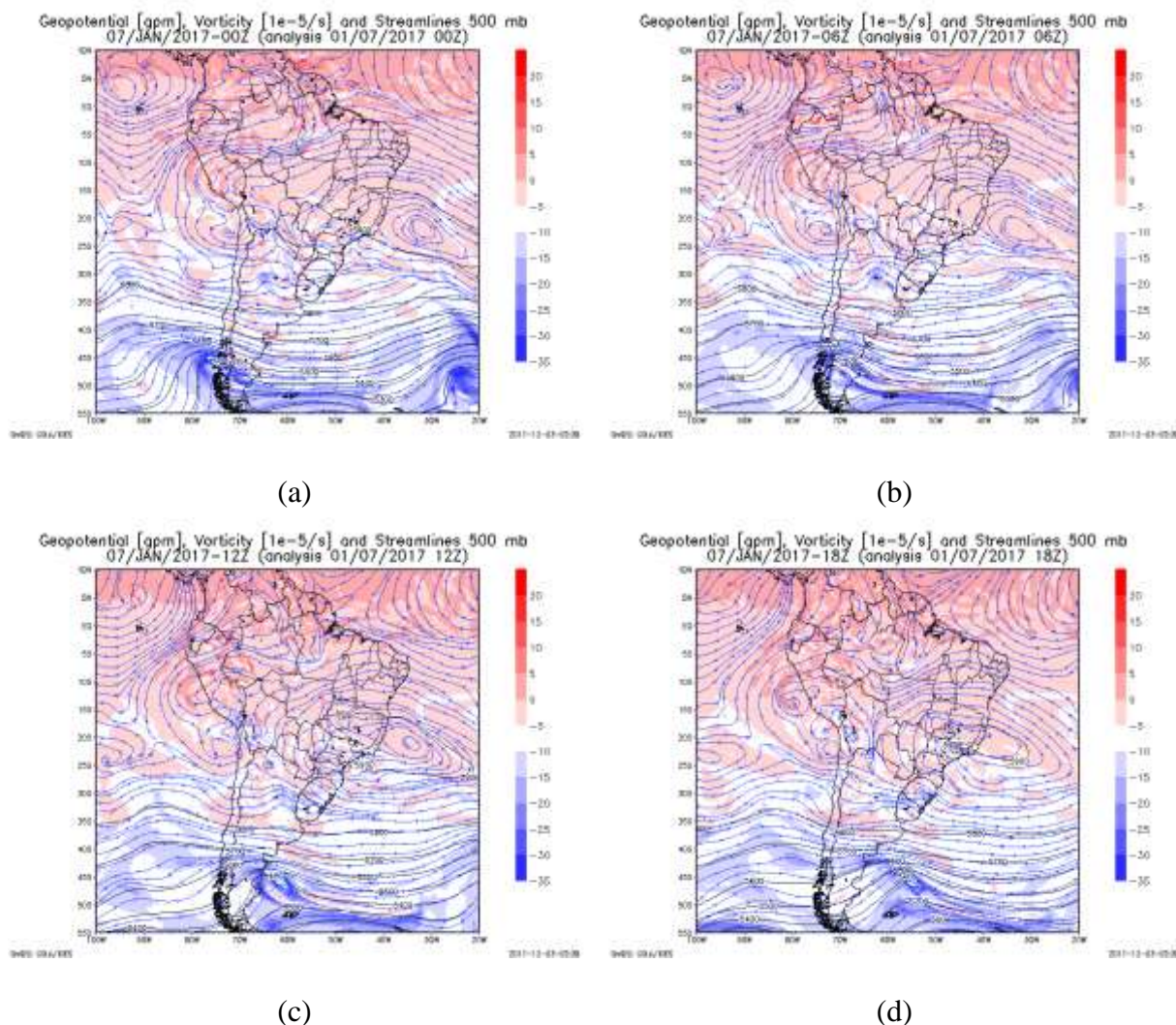


Figure 4-72: Geopotential, vorticity and streamlines at 500 hPa for January, 07 at 00:00 UTC (a), 06:00 UTC (b), 12:00 UTC (c), and 18:00 UTC (d).

A trough is seen near to the coast of São Paulo in the 850 hPa and surface analysis, and it is possible to observe high relative humidity extending from the front through this trough reaching the eastern part of the State of São Paulo. This is seen throughout the analysis, in which values are above 90 %. This high moisture content on low levels may have been important in this event. This is the reason for this event to be in this category. It is believed

that the synoptic scale pattern adding moisture to the east coast of the State may have been a relevant feature for the storm development.

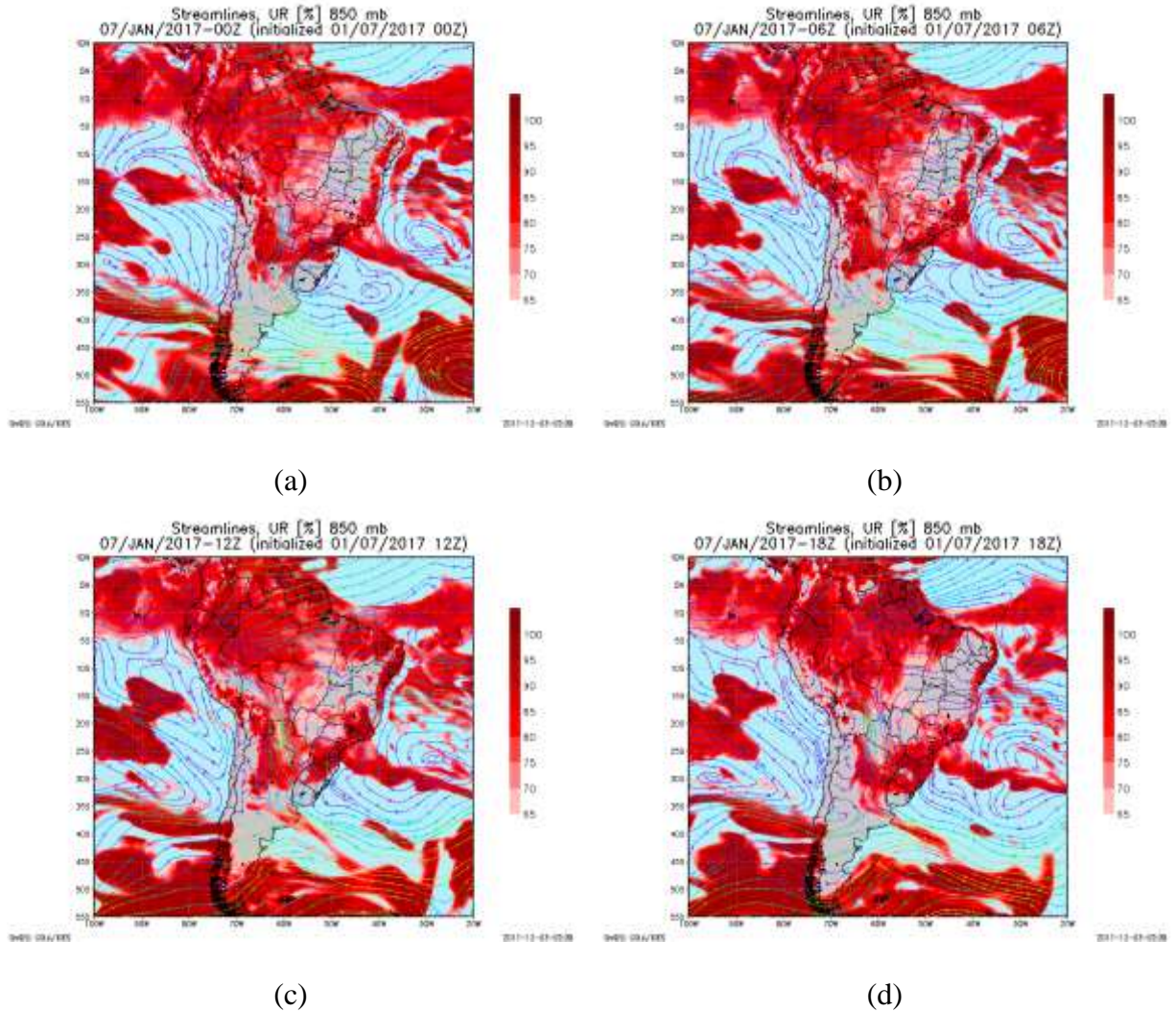


Figure 4-73: Streamlines and relative humidity (%) at 850 hPa for January, 07th at 00:00 UTC (a), 06:00 UTC (b), 12:00 UTC (c), and 18:00 UTC (d).

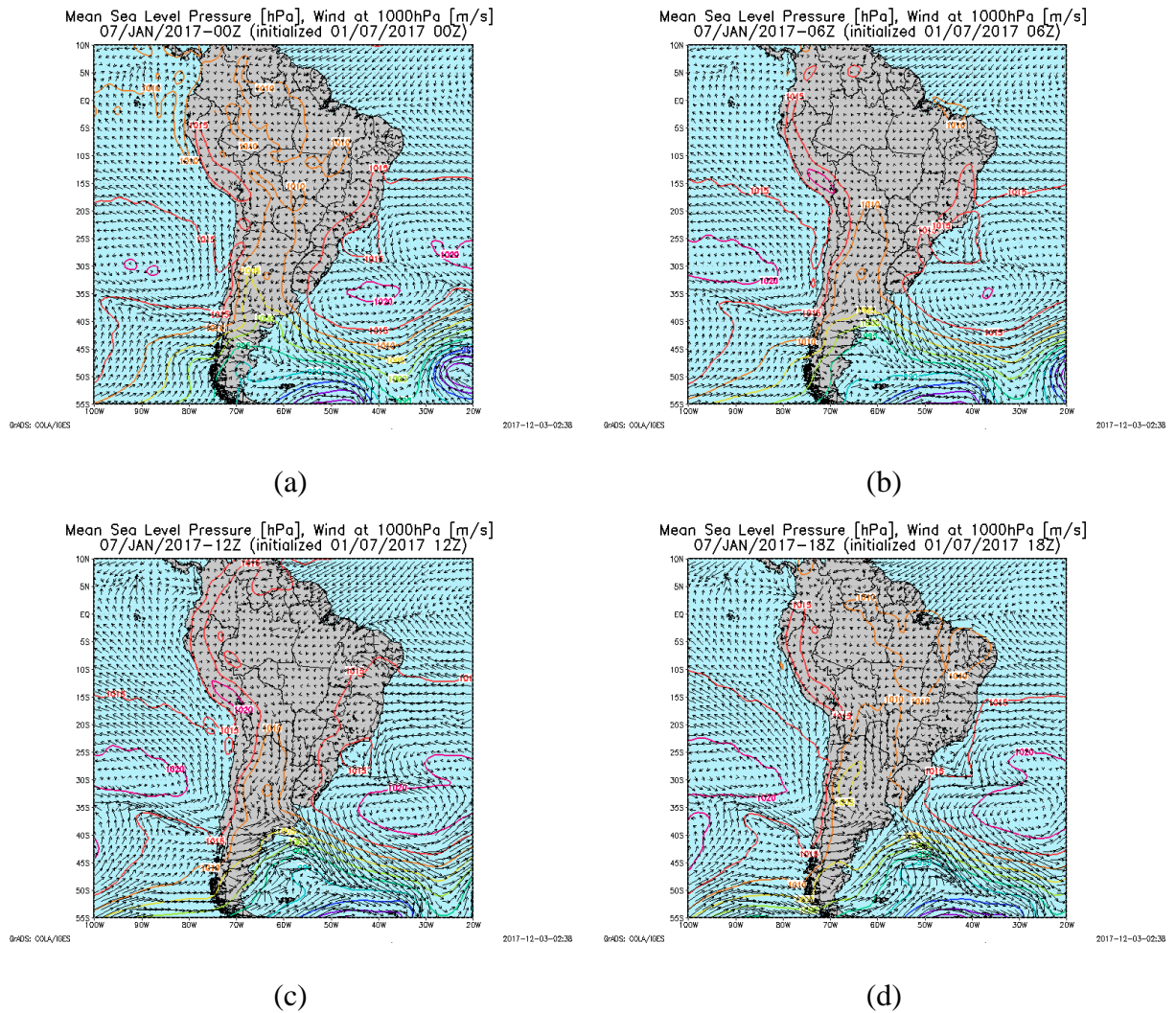


Figure 4-74: Mean sea level pressure (hPa) and wind (m s^{-1}) for January, 07th at 00:00 UTC (a), 06:00 UTC (b), 12:00 UTC (c), and 18:00 UTC (d).

d. Thermodynamic analysis

Soundings are not available for this event, and neither is the output from the BRAMS model, therefore, analysis of CAPE, CIN, LI and 700-500 hPa lapse rate will be carried out using the GFS model. These parameters are seen in Figure 4-76.

The CAPE parameter decreases after 00:00 UTC and increases again at 12:00 UTC. From a surface parcel, CAPE is ranging from 900 to 1200 J kg^{-1} in the region of São Paulo and Vale do Paraíba, except in the extreme northeast region. This indicates a condition

between marginally and moderately unstable. At 15:00 UTC, from a surface parcel, it is between 1300 and 1600 J kg⁻¹ near São Paulo, higher values are seen in the southeast coast and at the south region of Vale do Paraíba. It indicates a moderately unstable condition.

CIN is only seen below -20 J kg⁻¹ in the west region and in the extreme northeast regions of the State.

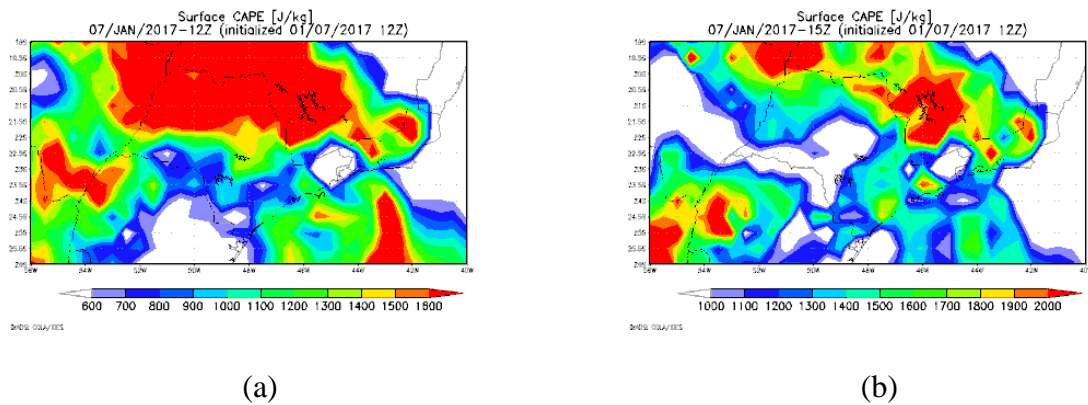


Figure 4-75: CAPE (J kg⁻¹) from GFS for January, 07th at 12:00 (a), and 15:00 UTC (b).

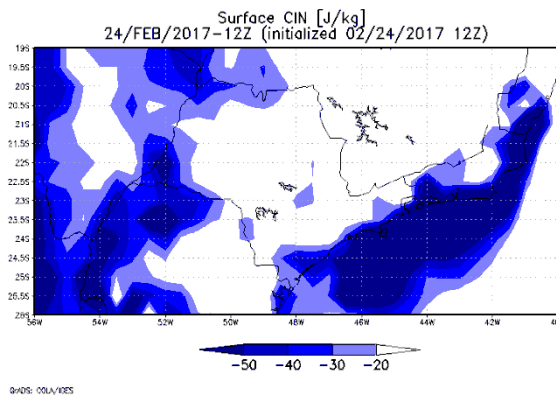


Figure 4-76: CIN (J kg⁻¹) from GFS for January, 07th at 12:00 (a).

LI from a surface parcel is between -3 and -4 K through most of the east region, smaller values, between -2 and -3 K are seen in the northeast and southeast regions. These values indicate an unstable condition, with probable storm, with the exception of the extreme northeast region, in the second method, which is in the slightly unstable condition. At 12:00

UTC, it is between -4 and -5 K through most of the east region, with higher values between -5 and -6 K in some small regions, and lower, around -3 and -4 K in the northeast region. These mentioned values indicate an unstable condition, with probable storm formation.

The 700-500 hPa lapse rate is between 5-5.5 K km⁻¹ at 00:00 UTC in eastern São Paulo, after 12:00 UTC it changes, and it is around 5.5-6 K km⁻¹ at 12:00 UTC.

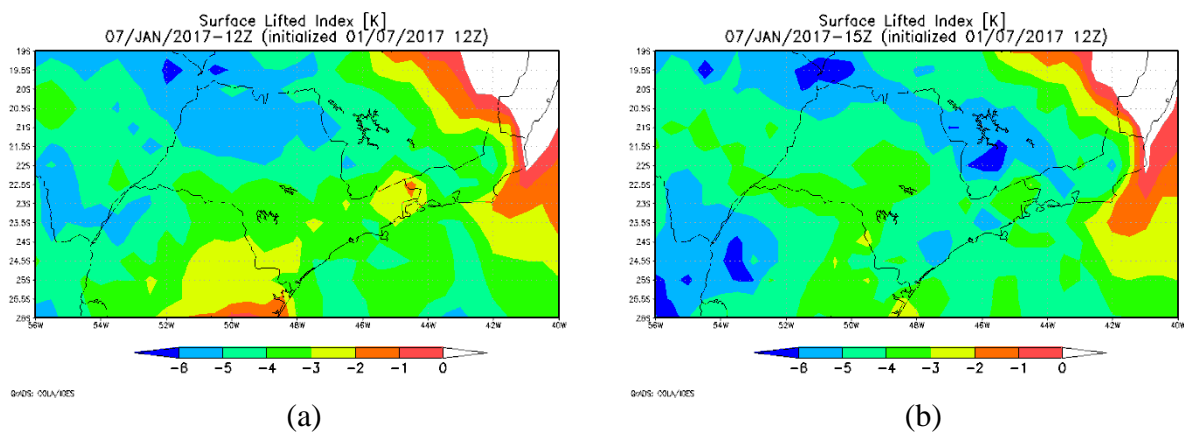


Figure 4-77: LI (K) from GFS for January, 07th at 12:00 (a), and 15:00 UTC (b).

From the analysis of these three parameters it is possible to see that CAPE and LI indicated the potential for storm development, and CIN was apparently not high enough to contribute to severe thunderstorm conditions.

However, it is complicated to assure that these values are reliable to make that conclusion. In events where a sounding is available it is possible to compare them with the GFS output to make a better statement on the matter.

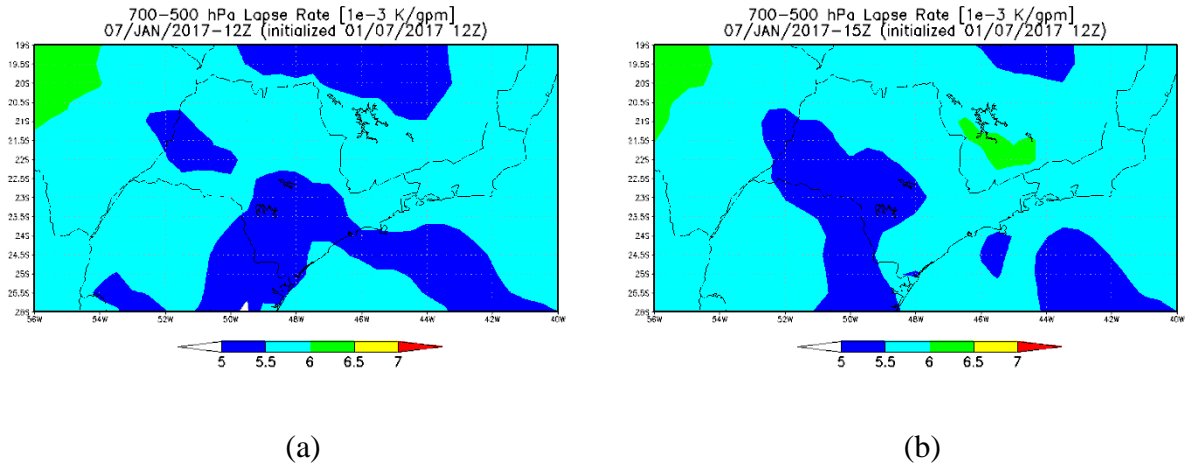


Figure 4-78: 700-500 hPa lapse rate ($1 \times 10^{-3} \text{ K gpm}^{-1}$) from GFS at 12:00 UTC (a), and 15:00 UTC (b), for January, 07.

Analyzing the vertical cross section of relative humidity, it is observed that, according to the model, the atmosphere was wet through its vertical extension at 12 and 12:00 UTC. Values are always above 70 % and even above 90 %. In the winds vertical cross section, it is seen that winds were weak throughout the atmosphere at 12 and 12:00 UTC, no significant shear is present, although a small increase is seen around 850 hPa.

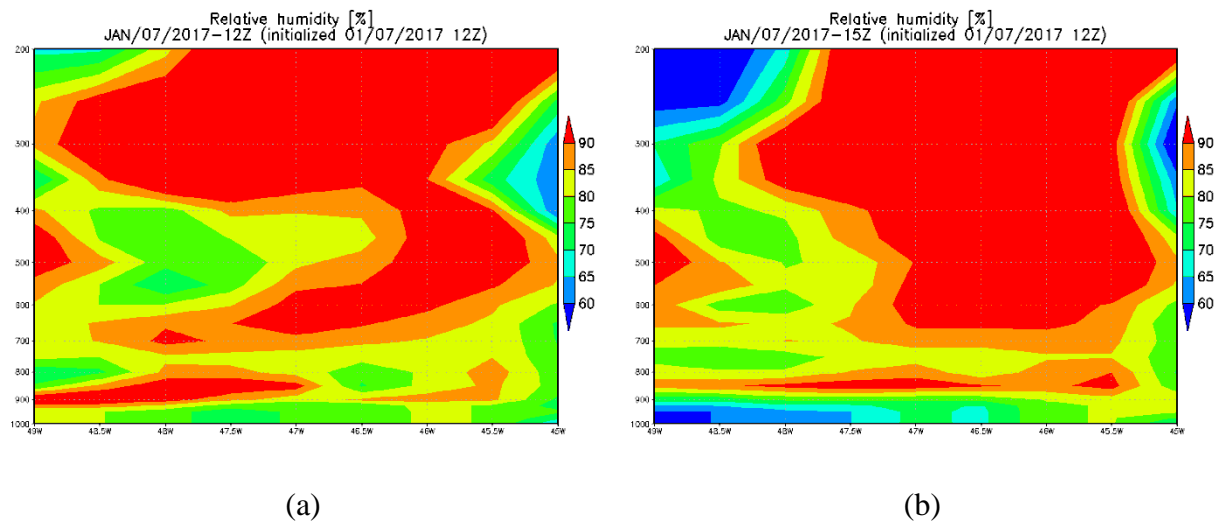


Figure 4-79: Vertical cross section at 23.5°S of latitude from GFS of relative humidity at 12:00 UTC (a), and 15:00 UTC (b), and of winds at 12:00 UTC (c), and 12:00 UTC (d), for January, 07, 2017

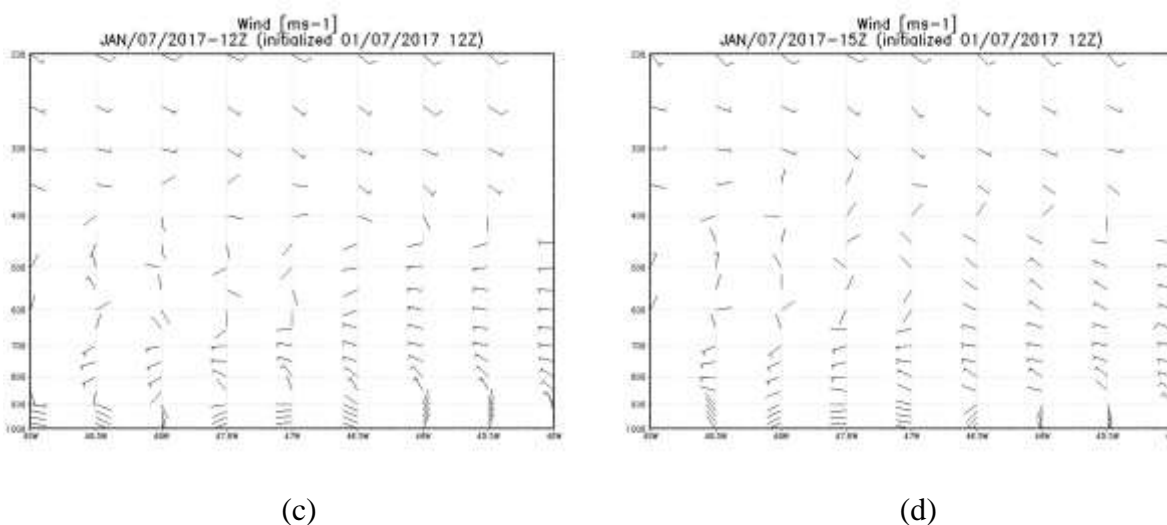


Figure 4-79: Continuation.

e. Surface stations

For this day, 19 INMET automatic surface stations were available. In the city of São Paulo, station A701, recorded southeast winds until 08:00 UTC. Afterwards, winds were from northeast. Southwest winds were observed after 13:00 UTC, and at 16:00 UTC winds turned to southeast. This was followed by an increase in dew point temperature, relative humidity, and decrease in temperature (Figure 4-80). It rained for 5 hours at the station an amount of 77.4 mm. Between 17:00 and 18:00 UTC 33.8 mm were recorded and another 42.0 mm in the next hour. Winds gusts of 21.9 m s⁻¹ were observed during these periods. Convective clouds are seen in the region during these hours, as it was mentioned in the radar analysis section. The maximum temperature registered was 30.7 °C.

In the METAR analysis from Congonhas and Campo de Marte, southeast winds with increase in dew point, relative humidity and decrease in temperature were observed at 15:00 and 16:00 UTC, respectively. In the airport of Guarulhos, southeast winds were observed at 17:00 UTC, but increase in dew point and relative humidity was not observed. Station A755 recorded increase in dew point temperature and relative humidity after 17:00 UTC, but this station has no record of wind speed and direction.

Station A712, localized at the coast, wind is from southeast at 10:00 UTC, with changes in variables related to the sea breeze after 11:00 UTC. Close to this station, southwest from it, station A746 recorded southeast winds with increase in dew point temperature after 11:00 UTC. Both of them are seen in Figure 4-80.

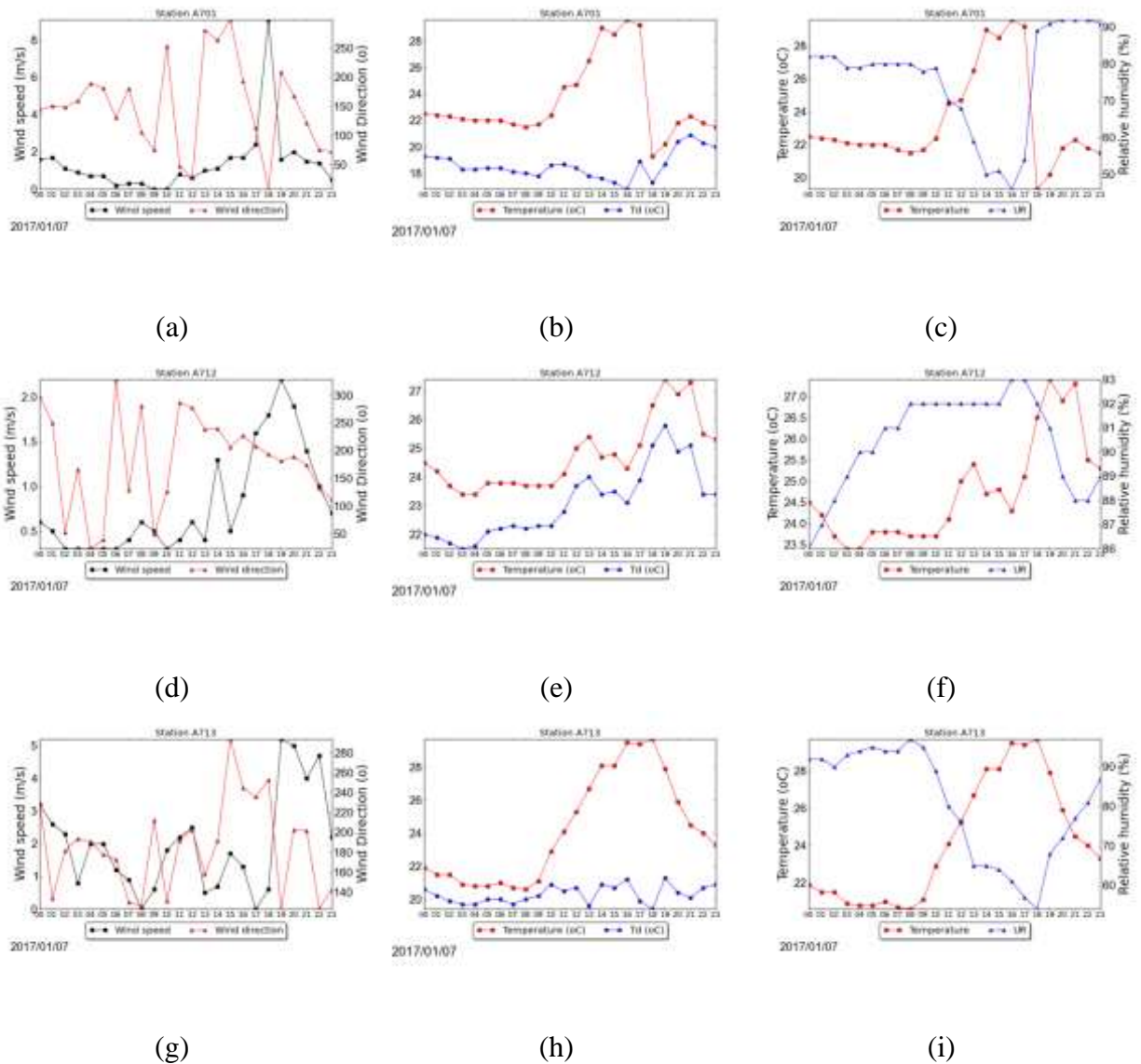


Figure 4-80: Wind speed and direction, temperature and dewpoint temperature, temperature and relative humidity for January, 07 at station A701 (a), (b), (c); A712 (d), (e), (f); A713 (g), (h), (i); A746 (j), (k), (l).

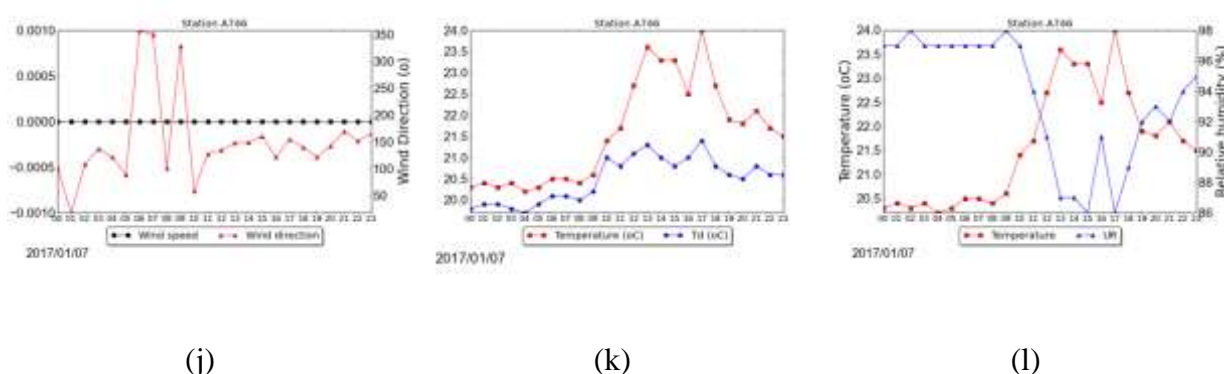
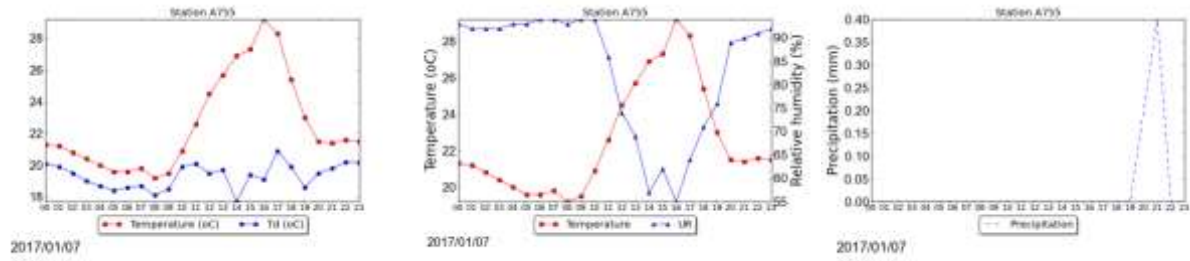


Figure 4-80: Continuation.

Analyzing stations A728 and A740, localized at the Vale do Paraíba, it is not possible to determine the hour of the sea breeze penetration in the region. Station A740 recorded a southeast wind at 17:00 UTC, but increase in dew point and relative humidity occurred in the next hour, in which rain was recorded. Station A728 recorded southeast wind at 19:00 UTC, but it was already raining at the station. At both stations, it rained for 6 hours, started between 17:00-18:00 UTC. At station A740 a total of 44.6 mm was recorded with a peak between 18:00-19:00 UTC of 32.0 mm. During this same period, a wind gust of 25.1 m s^{-1} was registered. Only an accumulated of 10.8 mm was recorded at Taubaté (station A728), with a peak of 4.6 mm between 18:00-19:00 UTC. A wind gust of 16.1 m s^{-1} was observed for two hours straight at this station (between 17:00-18:00 and 18:00-19:00 UTC). In the region of Vale do Paraíba convective cells were observed during 18:00-19:00 UTC, but clouds with lower reflectivity values (around 40 dBZ) are present until 22:20 UTC. Both stations recorded maximum temperature above 30°C , 30.3°C at 17:00 UTC at A740, and 33.3°C at 18:00 UTC at A728.

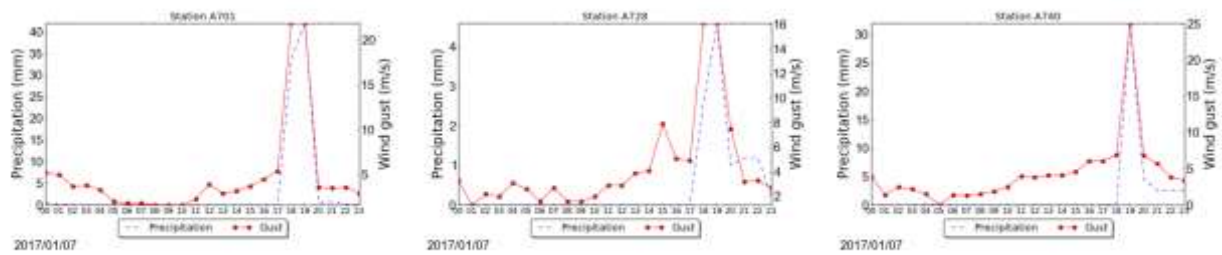
At Sorocaba, station A713 seen in Figure 4-80, recorded southeast wind at 19:00 UTC followed by increase in dew point temperature, relative humidity, wind speed, and decrease in temperature.

It is possible to conclude that the sea breeze penetration occurred between 15:00-17:00 UTC.



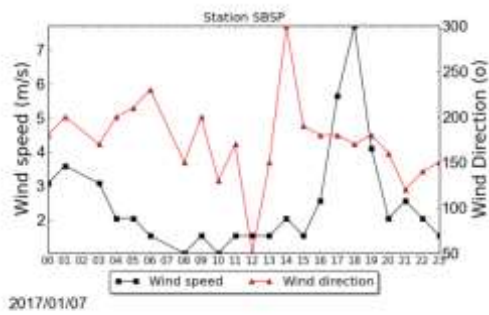
(a) (b) (c)

Figure 4-81: Temperature (°C) and dewpoint temperature (°C) (a), temperature (°C) and relative humidity (%) (b), precipitation (mm) (c) at station A755 for January, 07th.

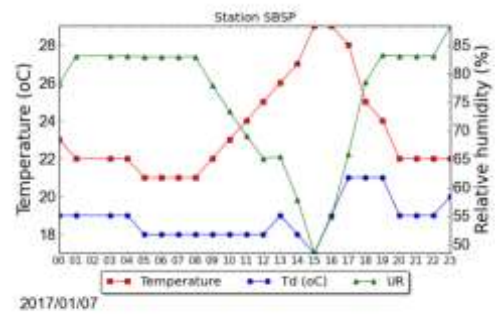


(a) (b) (c)

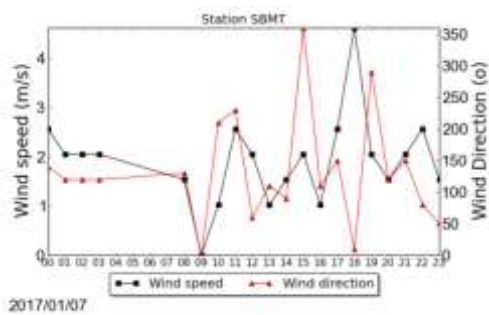
Figure 4-82: Wind gust ($m s^{-1}$) and precipitation (mm) for January, 07th at station A701 (a), A728 (b), and A740 (c).



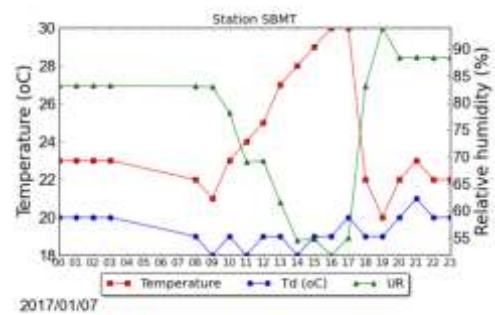
(a)



(b)



(c)



(d)

Figure 4-83: Wind speed and direction (a), relative humidity, temperature and dew point temperature from METAR at station SBSP (a), (b), and SBMT (c), (d), for January, 07th, 2017.

4.1.3.2 January, 30, 2017

During this day, occurrences and damages related to severe weather were reported in the region of Jundiaí, Campinas and Itatiba. In the region of Jundiaí, heavy rain, strong wind gusts of around 23 ms^{-1} and hail were registered. This led to flash floods and fall of trees. Campinas also registered strong wind gusts of around 23.6 ms^{-1} , and heavy rain, which also led to flash floods and fall of trees. Flash floods and fall of trees were also reported in Itatiba.

a. Satellite

In the satellite images, shown for South America in Figure 4-84, for January 30th at 12:00 and 15:00 UTC, it is possible to see clouds forming in the center-west, southeast and

south regions of Brazil related to a large-scale system (Figure 4-84). Further details of the characterization of the synoptic scale environment will be given in the next section.

In the images showing the State of São Paulo, it is seen that clouds are present in most parts of the State, shown in the figure from the infrared channel (Figure 4-86), from early hours. In the visible channel, at 14:45 UTC, clouds are covering most of the State, but it is possible to see the development of clouds near and parallel to the coast (due to the sea breeze) and in the region of Serra da Mantiqueira (Figure 4-85).

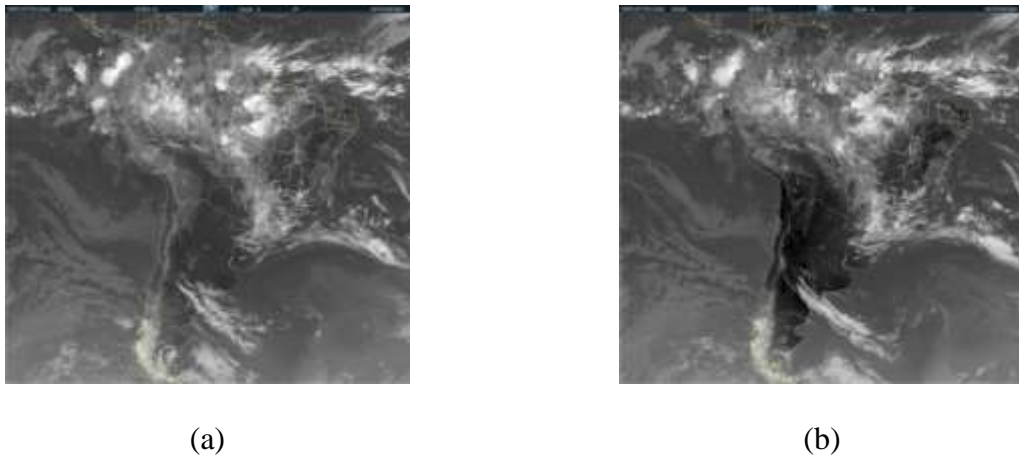


Figure 4-84: Infrared images for South America for January, 30th at 12:00 UTC (a), and 15:00 UTC (b).

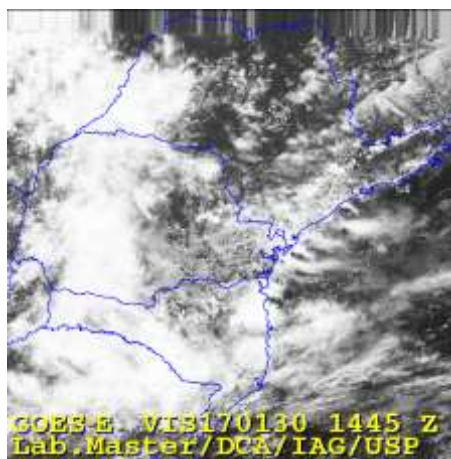


Figure 4-85: Visible channel satellite image for January, 30th at 14:45 UTC.

At 16:08 UTC more clouds have formed in the region of Serra da Mantiqueira, northeast portion, and close to the coast. From 17:08 to 17:45 UTC it is possible to see the

development of convective clouds in the region of Jundiaí. It also possible to notice that clouds formed due to the topography of the Serra da Mantiqueira merged with a cell in this region. From it, cells form and move to the region of Campinas, and southeast, to the region of Guarulhos, seen at 18:38 UTC. From 18:38 to 19:45 UTC, the cells in the region of Guarulhos intensified, but no record of severe weather was reported. After that hour the system lost its strength.

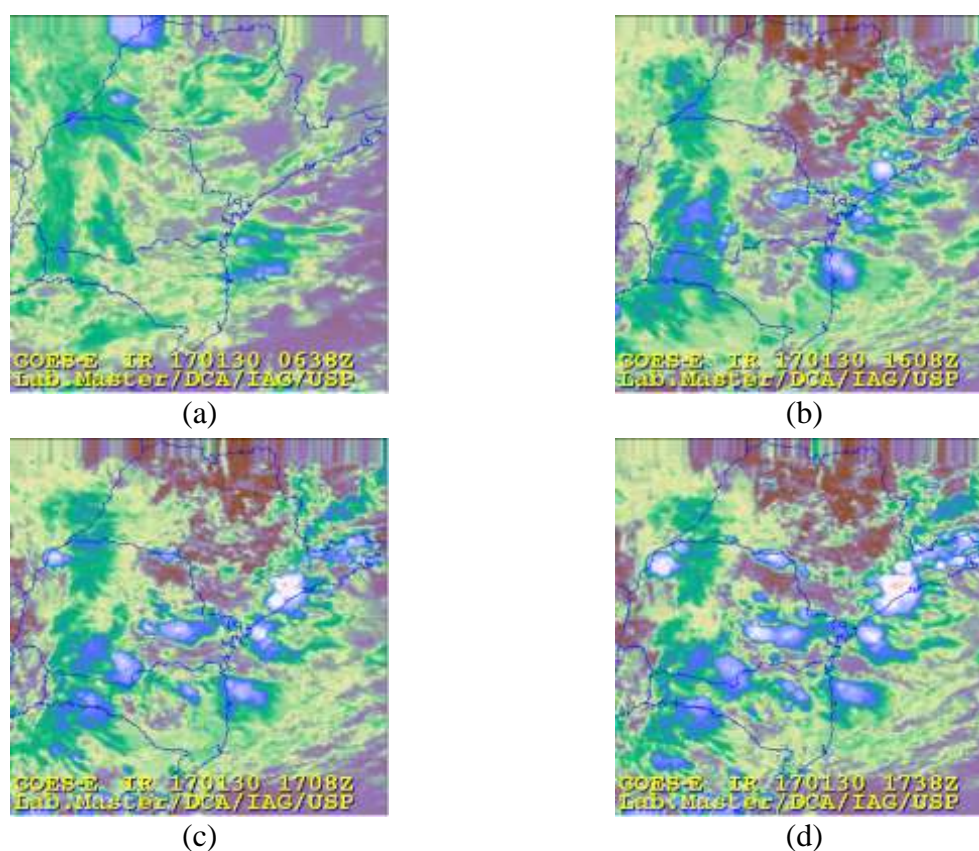


Figure 4-86: Infrared satellite images for January, 30th, at 06:38 UTC (a), 16:08 UTC (b), 17:08 UTC (c), 17:38 UTC (d), 17:45 UTC (e), 18:38 UTC (f), 19:08 UTC (g), 19:38 UTC (h).

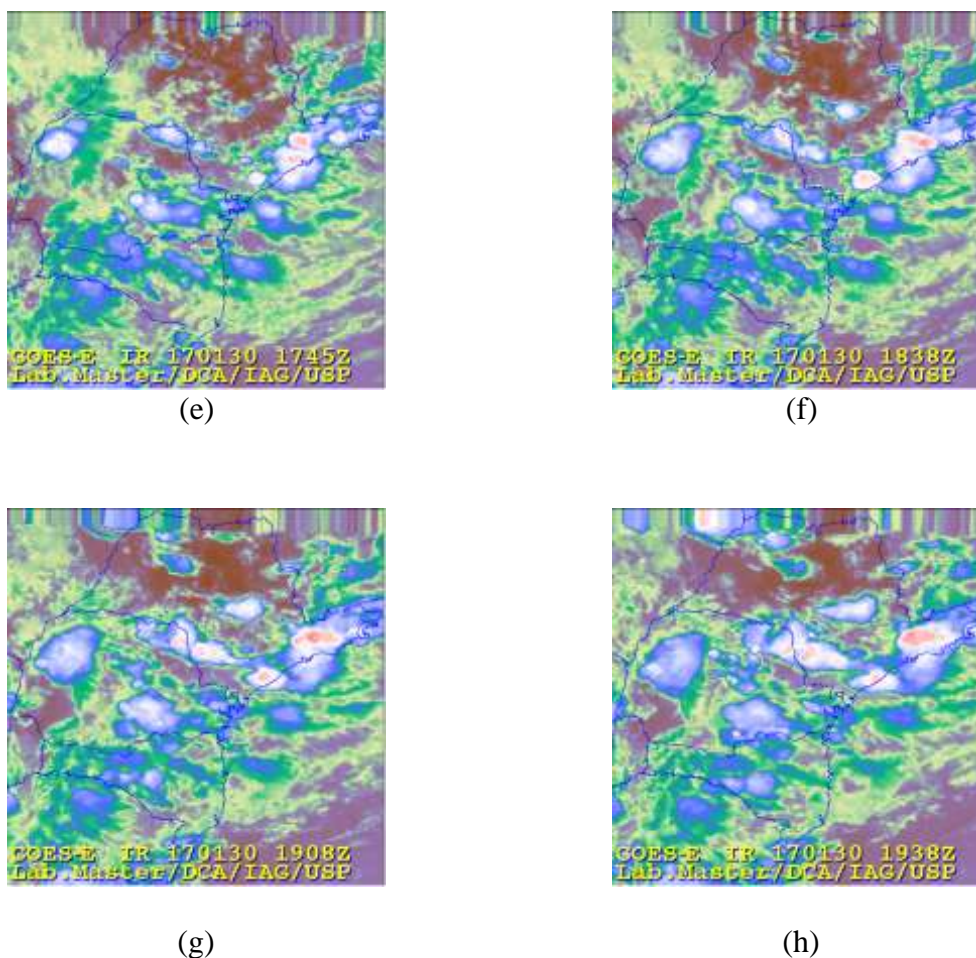


Figure 4-86: Continuation.

b. Radar

At 15:00 UTC clouds started to form in the region of Serra da Mantiqueira. As the hour advances, the cells intensified, and at 16:00 UTC there are seen extending in the region passing the Vale do Paraíba, and in the region of Bragança Paulista. At 16:30 UTC it is noticeable that new cells originated in the region of Bragança Paulista. From that hour on, these cells move, as they give origin to new ones, to the region of Jundiaí, and they merge with a local cell, that is possible to see at 17:00 UTC. This merge is seen between 17:20-17:30 UTC. Between 17:30 and 17:40 UTC high reflectivity values are shown in the region of Jundiaí, around 60-65 dBZ. After 18:00 UTC this cell divides, seen at 18:20 UTC, and a part moves to Campinas, where local cells are also seen at 18:00 UTC. It intensifies and

merge with the propagating cell, and at 18:40 UTC reflectivity values between 60-65 dBZ are present in Campinas. After that, it lost its strength.

The other part moves southeast to the region of Guarulhos, where it merges with another cell moving from Vale do Paraiba. This is also mentioned in the satellite analysis, but as already stated, no severe weather occurrence was reported in this region.

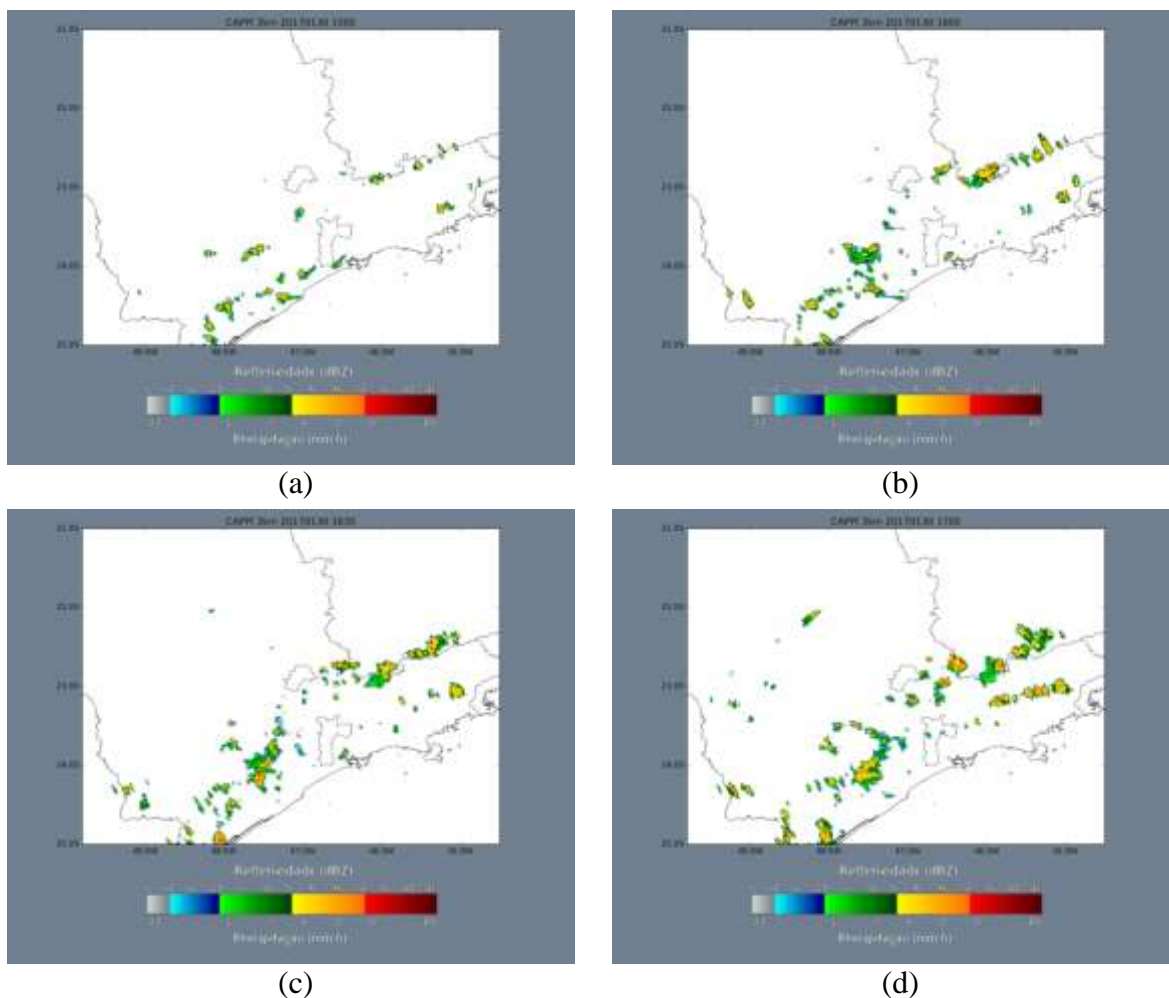
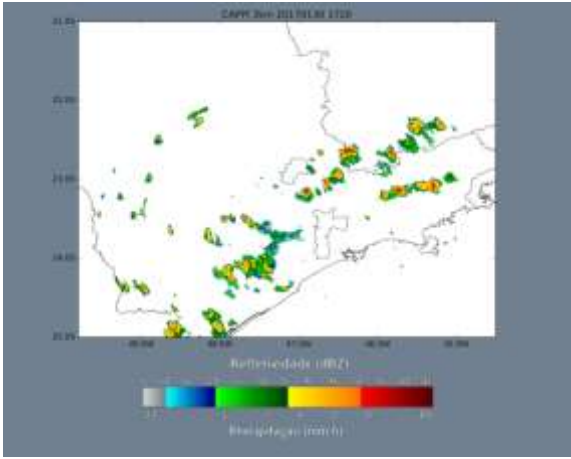
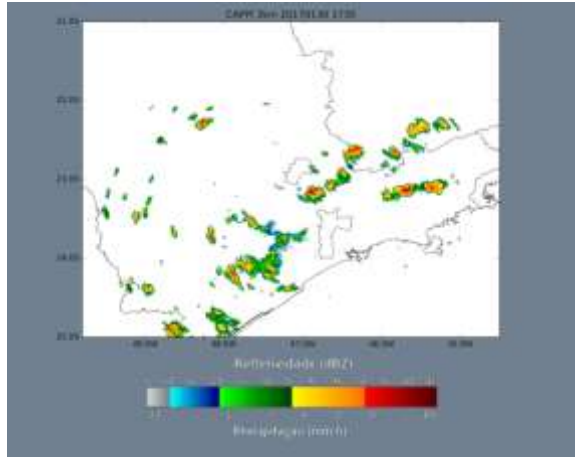


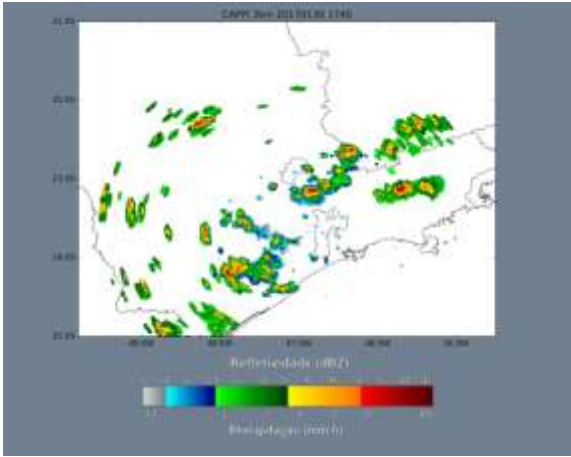
Figure 4-87: São Roque radar images for January, 30th at 15:00 UTC (a), 16:00 UTC (b), 16:30 UTC (c), 17:00 UTC (d), 17:20 UTC (e), 17:30 UTC (f), 17:40 UTC (g), 18:00 UTC (h), 18:20 UTC (i), 18:40 UTC (j), 19:30 UTC (l), 19:40 UTC (m).



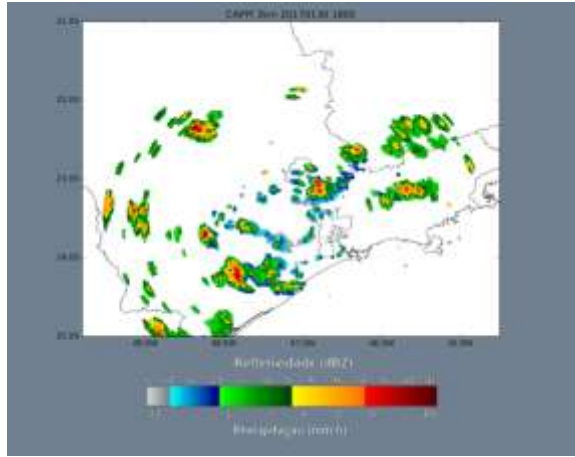
(e)



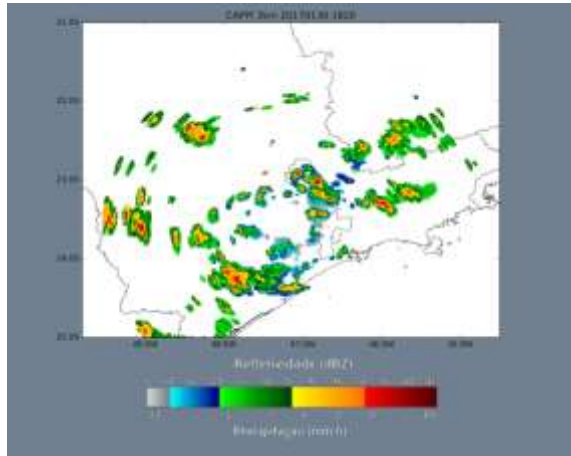
(f)



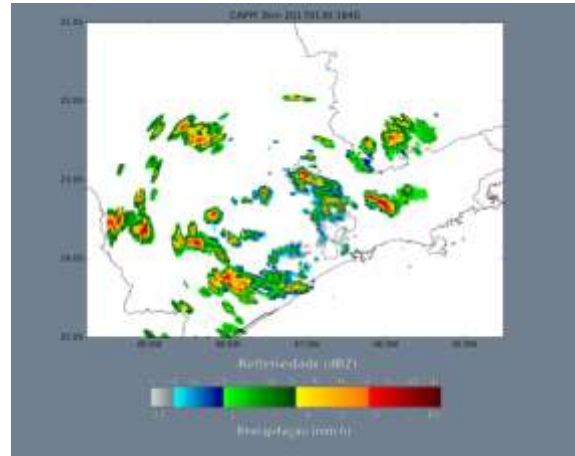
(g)



(h)

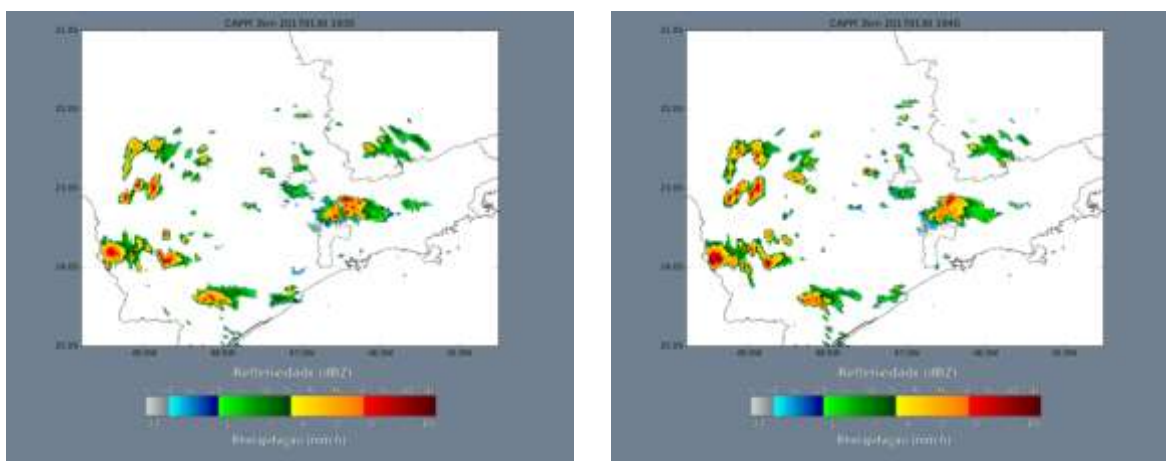


(i)



(j)

Figure 4-87: Continuation.



(l)

(m)

Figure 4-87: Conclusion.

c. Synoptic scale analysis

The most important feature associated with this event is the low pressure system located at Paraguay in the 200 hPa analysis, seen in Figure 4-88. It is an upper tropospheric cyclonic vortex, and it generates instability around its borders on lower levels. The vortex moves southeast, throughout the analysis. A trough is seen in the Atlantic near the coast of Rio Grande do Sul, and it moves eastward and amplifies during the day. Wind divergence at 200 hPa is seen at 06:00 and 09:00 UTC in the region of Campinas and Jundiaí, ranging from 0.2 to $0.4 \cdot 10^{-4} \text{ s}^{-1}$. It is seen again at 15:00 and 18:00 UTC between $0.2\text{-}0.4 \cdot 10^{-4} \text{ s}^{-1}$ and $0.2\text{-}0.6 \cdot 10^{-4} \text{ s}^{-1}$, respectively (Figure 4-89).

The upper tropospheric cyclonic vortex is observed in the 500 hPa analysis, shown in Figure 4-90, with negative vorticity associated. Silva Dias and Grammelsbacher (1991) analyzed the conditions that led to a possible tornado in São Paulo in 1991. An upper tropospheric cyclonic vortex was observed in their analysis in a similar position to the one seen in the present study.

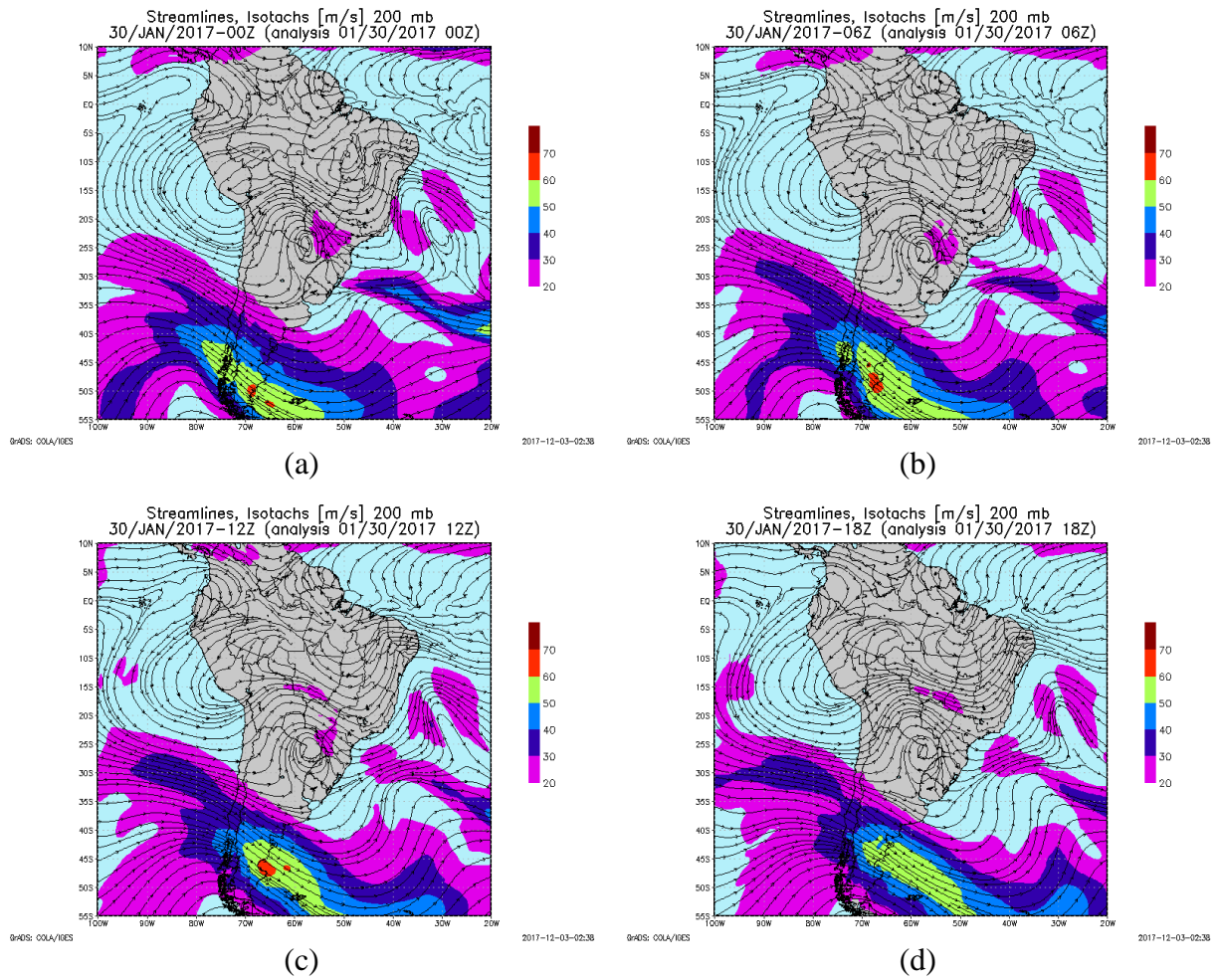


Figure 4-88: Streamlines and isotachs (m s^{-1}) at 200 hPa for January, 30th at 00:00 UTC (a), 06:00 UTC (b), 12:00 UTC (c), and 18:00 UTC (d).

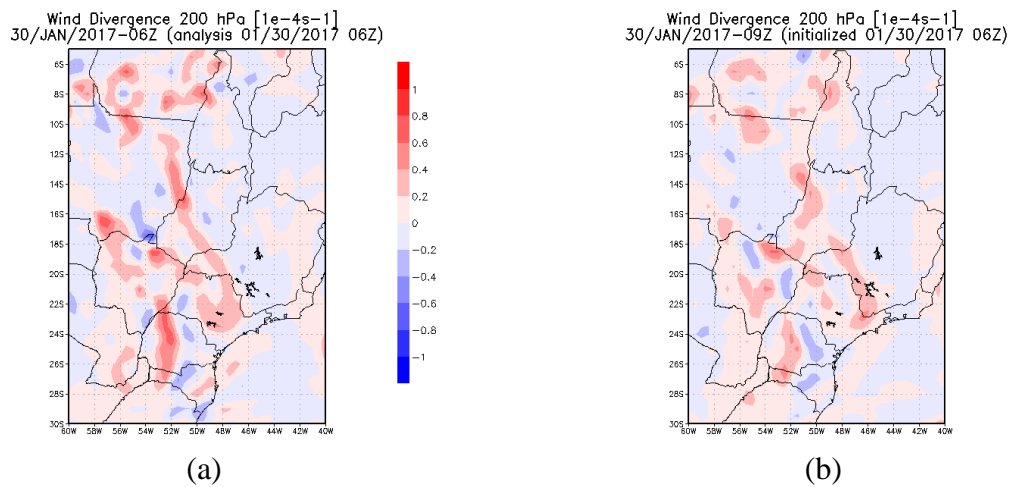


Figure 4-89: Wind divergence ($1 \times 10^{-4} \text{ s}^{-1}$) at 200 hPa for January, 30th at 06:00 UTC (a), 09:00 UTC (b), 15:00 UTC (c), and 18:00 UTC (d).

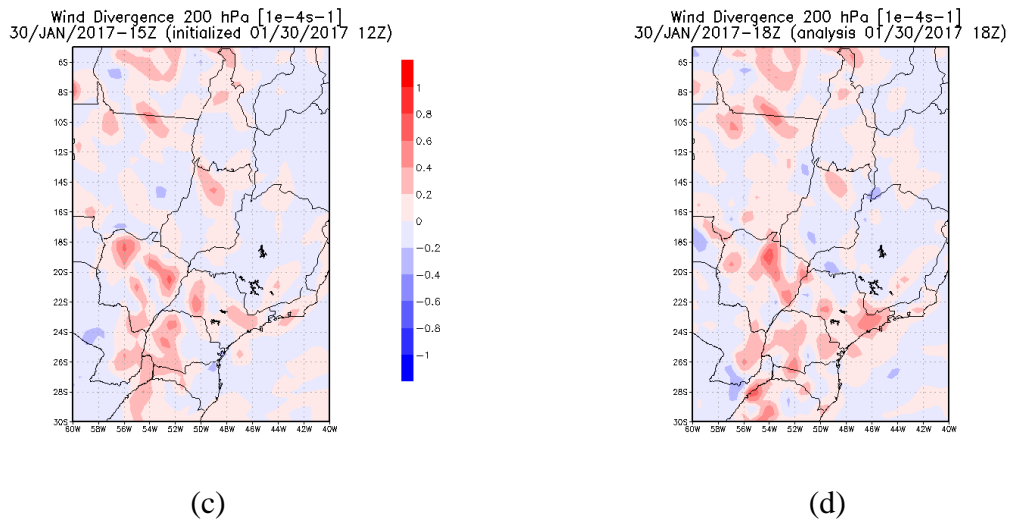


Figure 4-89: Continuation.

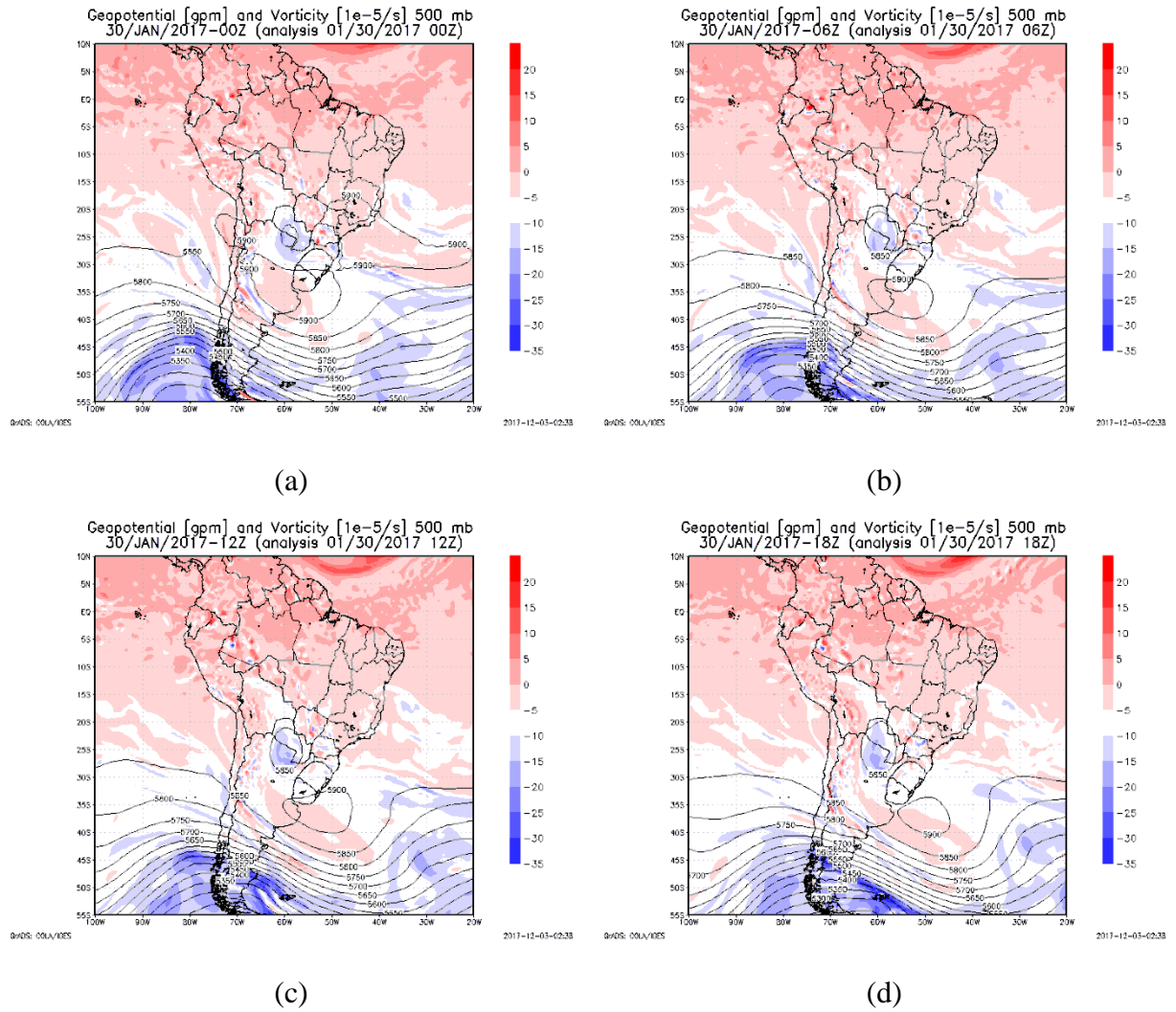


Figure 4-90: Geopotential (gpm) and vorticity ($1 \times 10^{-5} \text{ s}^{-1}$) at 500 hPa for January, 30th at 00:00 UTC (a), 06:00 UTC (b), 12:00 UTC (c), 18:00 UTC (d).

In the 850 hPa level high relative humidity is seen extending from the Amazon region through the center-west, south and southeast regions of Brazil, although the low level jet and northwest flow associated are not seen. Highest values are observed at 18:00 UTC, and it is above 95% in the State of São Paulo. Streamlines and relative humidity at 850 hPa are shown in Figure 4-91.

Still in the 850 hPa analysis, the temperature advection (Figure 4-92) shows warm advection in the State of São Paulo. At 09:00, 12:00 and 15:00 UTC, warm advection is seen in the region of Campinas and Jundiaí, values are around $0.2-0.4 \cdot 10^{-4} \text{ K s}^{-1}$ at 09:00 UTC and 15:00 UTC, higher values are seen at 12:00 UTC, between 0.2 and $0.8 \cdot 10^{-4} \text{ K s}^{-1}$.

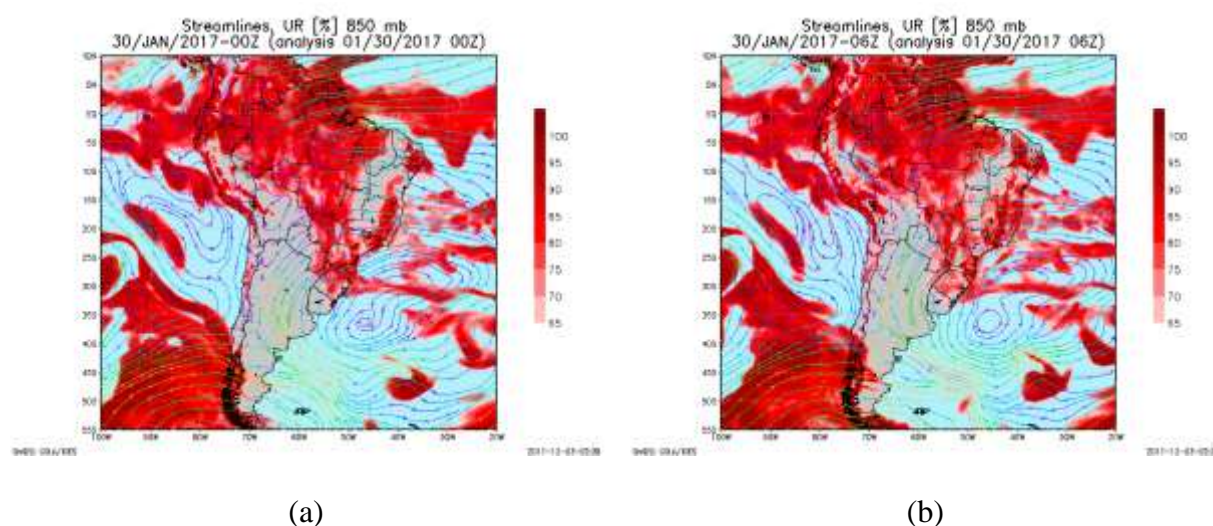


Figure 4-91: Streamlines and relative humidity (%) at 850 hPa for January, 30th at 00:00 UTC (a), 06:00 UTC (b), 12:00 UTC (c), and 18:00 UTC (d).

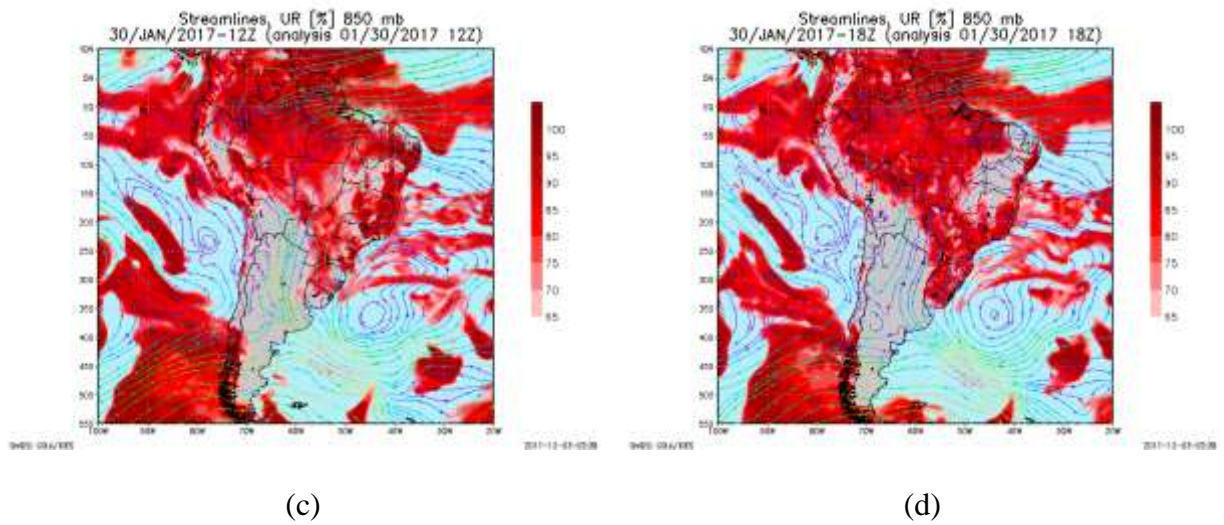
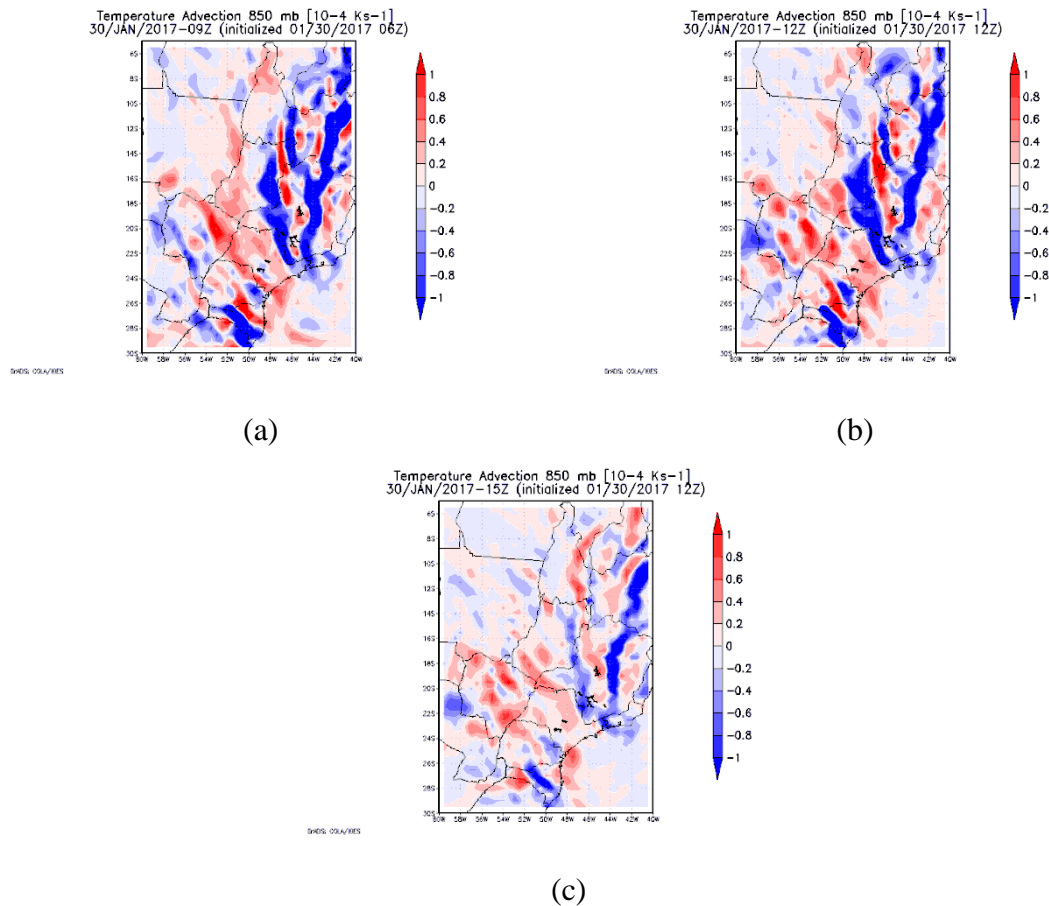


Figure 4-91: Continuation.

Figure 4-92: Temperature advection (K s^{-1}) at 850 hPa for January, 30th at 09:00 UTC (a), 12:00 UTC (b), 15:00 UTC (c).

The southeast region seems to be influenced by the high-pressure system in the Atlantic (South Atlantic Subtropical High). This system is seen in the surface analysis near to the coast

of the State of São Paulo. Throughout the day, winds appear to change from southeast to northeast in the State.

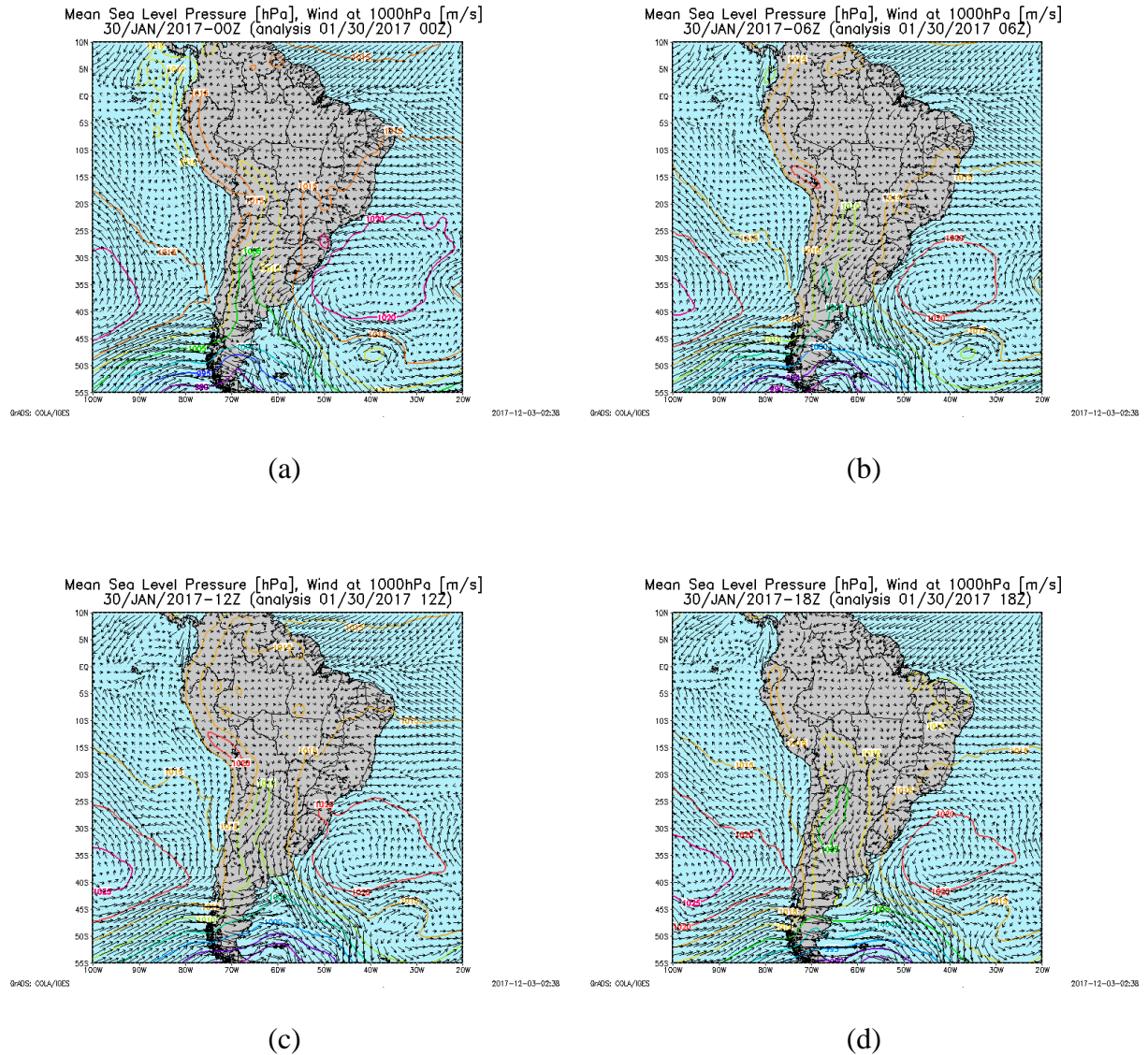


Figure 4-93: Mean sea level pressure and wind for January, 30 at 00:00 UTC (a), 06:00 UTC (b), 12:00 UTC (c), and 18:00 UTC (d).

d. Thermodynamic analysis

In the sounding obtained at 12:00 UTC (Figure 4-94) it shows that the atmosphere is moist in low levels, the inversion layer is around 900 hPa. It presents a subsidence inversion layer around 600 hPa and above that height the atmosphere becomes very dry. This

combination of moisture at low levels and dry air above is an important element to severe convective storms.

The value of CAPE from this sounding is 1042 J kg^{-1} , a high value indicating, especially considering that this sounding is from 10 AM local time. Using the virtual temperature correction, CAPE is 1192 J kg^{-1} . CIN is -90.5 J kg^{-1} , which means that some forcing must occur in order to overcome this value. This parameter using the virtual temperature is equal to -67.7 J kg^{-1} . The 700-500 lapse rate is $5.5 \text{ }^\circ\text{C km}^{-1}$. The level of free convection is at 747.45 hPa, and using the virtual temperature is at 762.17 hPa.

LI is -2.69 K , and LI using the virtual temperature is -3.60 K which represents an unstable condition, with probable storm formation, and even severe. The hodograph shows wind shear, but the wind is not significantly strong. It has a counterclockwise turn with height, indicating warm advection in the region, which is an important factor for the occurrence of severe storms (Figure 4-94).

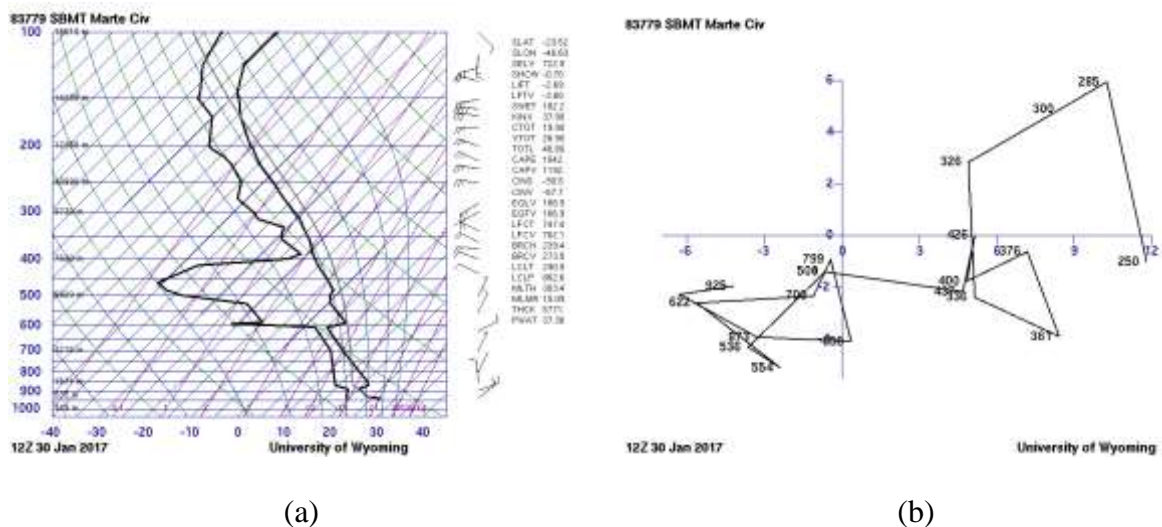


Figure 4-94: Sounding and hodograph for January, 30th at 12:00 UTC (source: <http://weather.uwyo.edu/upperair/sounding.html>).

Analyzing the water vapor mixing ratio derived from the sounding, shown in Figure 4-95, it is seen that it decays below 2 g kg^{-1} at 600 hPa, but even smaller values are observed between 500-400 hPa, in which it drops below 1 g kg^{-1} . Relative humidity, also seen in Figure

4-95, is between 10 and 20 % at 600-500 hPa, and smaller values are also seen between 500-400 hPa (below 10%), indicating, as mentioned, the atmosphere is very dry in these levels.

A rapid decrease with height, until 600 hPa (around 5900 m) is also observed in equivalent potential temperature profile. Decrease with height of this parameter indicates convective instability.

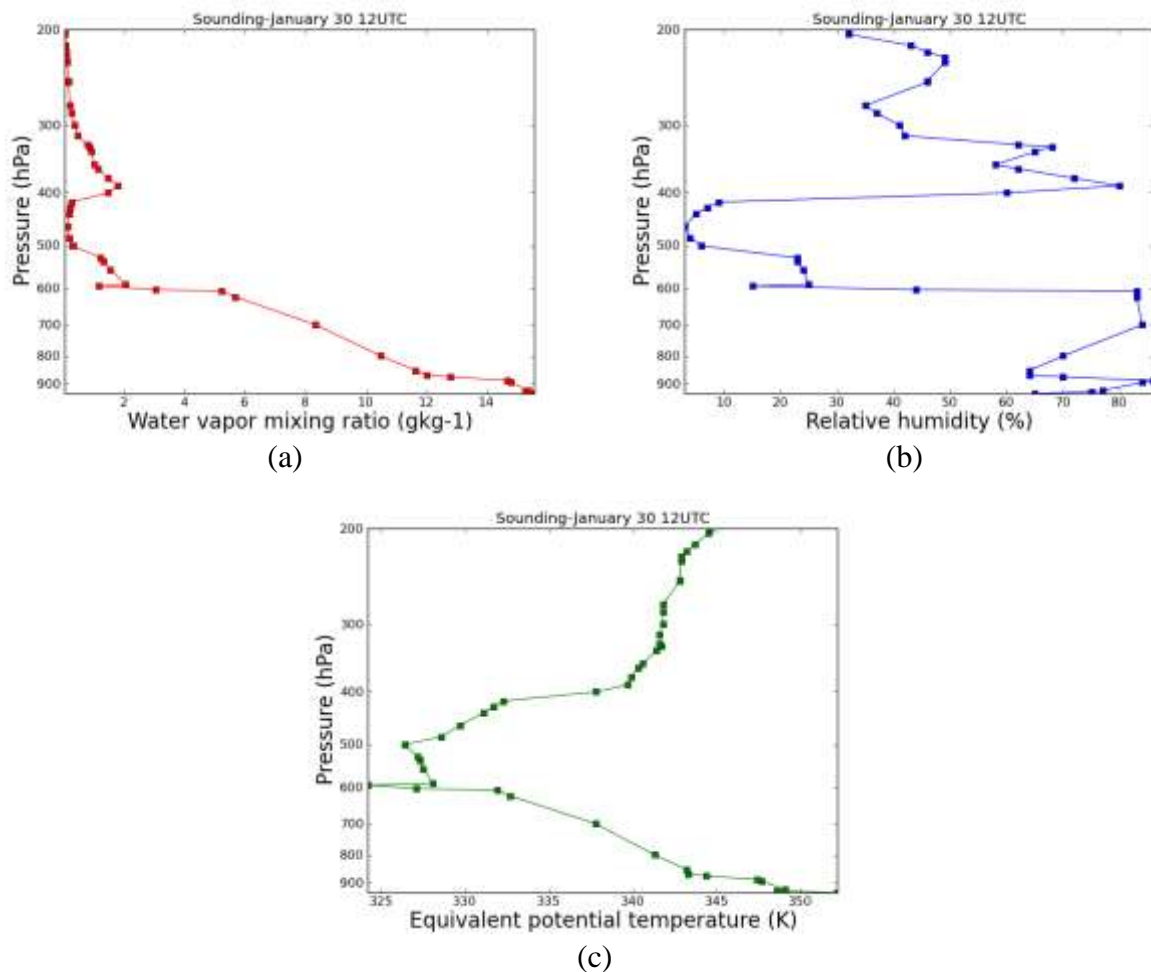


Figure 4-95: Vertical variation of water vapor mixing ratio (g kg^{-1}) (a), relative humidity (%) (b), and equivalent potential temperature (K) (c).

It is possible to compare CAPE, CIN, LI and 700-500 lapse rate from the GFS output with the sounding derived parameters, at 12:00 UTC. These parameters are shown in Figure 4-96. CAPE from the GFS, is, through most of the east region between 1000-1200 J kg^{-1} , although, close to São Paulo, values between 800-1000 J kg^{-1} are seen, and a small region has

CAPE around $600\text{-}800\text{ J kg}^{-1}$. These values indicate a moderately and a marginally unstable condition, respectively. In the region of Campinas and Jundiaí, it is between 1000 and 1400 J kg^{-1} , which also indicates a moderately unstable condition. At $15:00$ UTC, it is around $1200\text{-}1600\text{ J kg}^{-1}$ in the region, indicating the same condition as before.

CIN is between -20 and -30 J kg^{-1} on most of the northeast region of the State, which is much lower than derived from the sounding. LI is between -2 and -4 K in the east part of the State, near São Paulo, values are around -2 and -3 K , the value derived from the sounding is in this range. The same range is seen in the region of Campinas and Jundiaí. At $15:00$ UTC it has increased and it is between -4 and -6 K , however, it still indicates the same condition.

The $700\text{-}500\text{ hPa}$ lapse rate is around $5\text{-}5.5\text{ }^{\circ}\text{C km}^{-1}$ from the GFS at $12:00$ UTC, which again is in the range of the value obtained from the sounding. This parameter increases and at $15:00$ UTC it is between 5.5 and $6\text{ }^{\circ}\text{C km}^{-1}$.

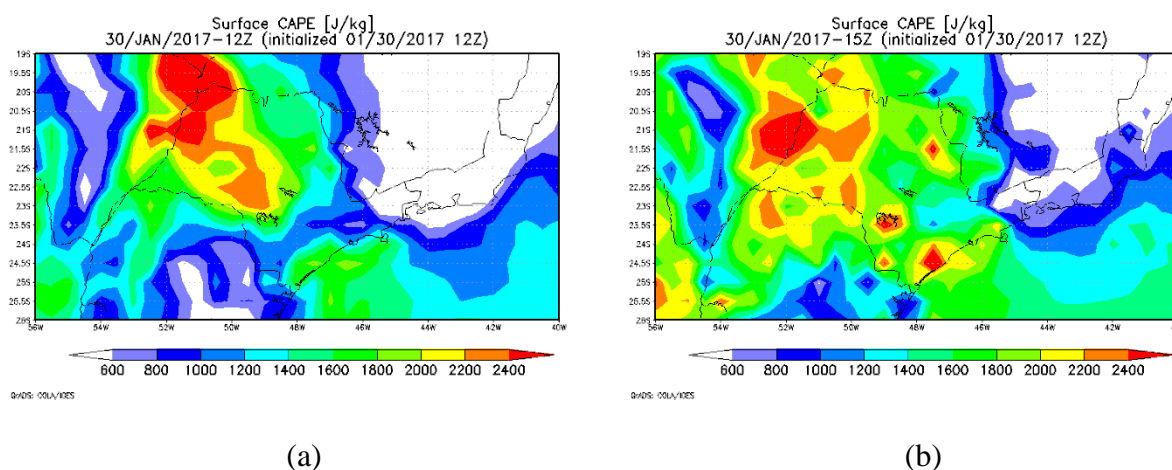


Figure 4-96: CAPE from GFS at $12:00$ UTC (J kg^{-1}) (a) and $15:00$ UTC (b) for January, 30th, 2017.

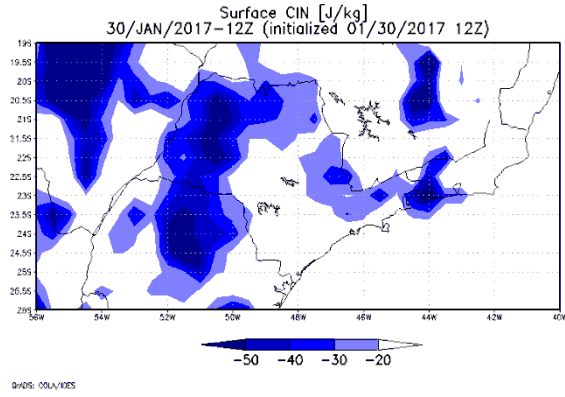


Figure 4-97: CIN from GFS at 12:00 UTC for January, 30th, 2017.

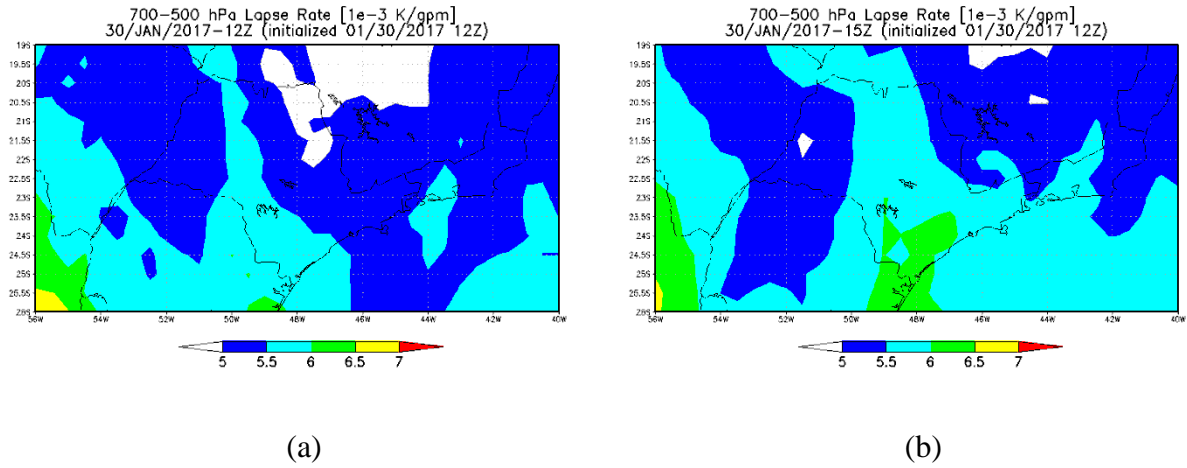


Figure 4-98: 700-500 hPa lapse rate from GFS at 12:00 UTC (a), and 15:00 UTC (b), for January, 30th.

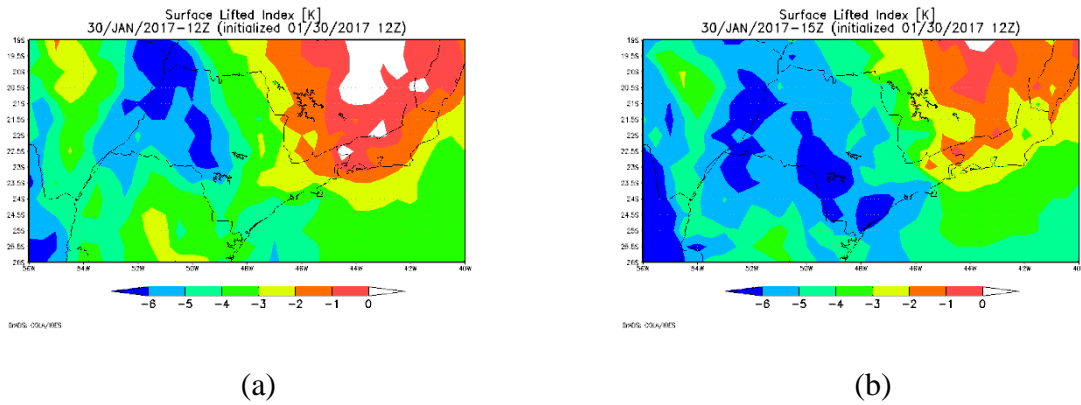


Figure 4-99: LI from GFS at 12:00 UTC (J kg⁻¹) (a) and 15:00 UTC (b) for January, 30th, 2017.

Analyzing the vertical cross section from GFS for relative humidity at the latitude of 23.5° S (Figure 4-100), it is seen that near the surface values are around 70-80 %, the increase seen at 700 hPa is present in this analysis, and the decrease to values below 10 % between 500 and 400 hPa, although lower values are seen in the sounding around 600-500 hPa. The same is seen in the region of Campinas, fixing the latitude at 23.0° S. The vertical cross section of winds is also similar to the one obtained from the sounding, for both latitudes. Winds are from northeast near the surface, and turn anticlockwise; a small increase around 900-850 hPa is seen near São Paulo and Campinas. Winds are weak through the atmosphere, just as it was seen in the hodograph. At 15:00 UTC, according to GFS, the relative humidity increased for the region of Campinas, and it is around 40-50 %, the wind is similar to the previous hour.

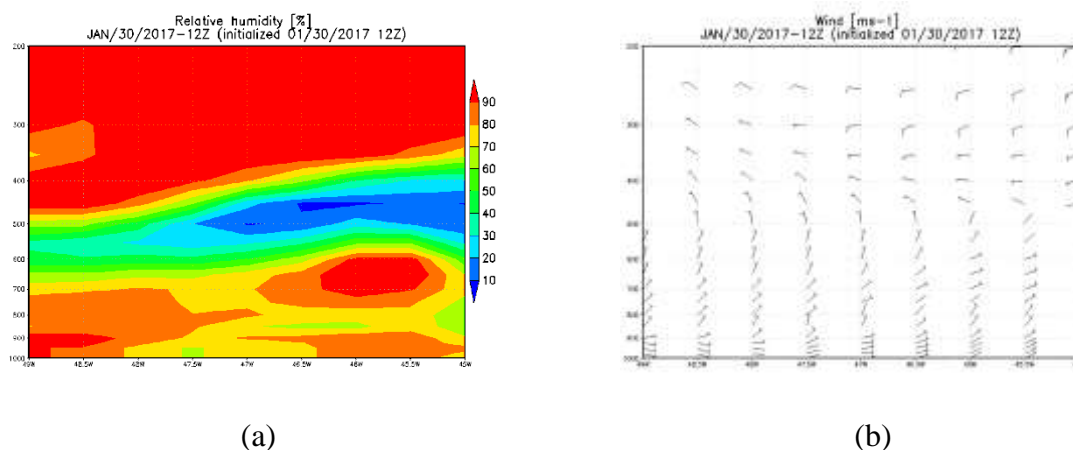


Figure 4-100: Vertical cross section of relative humidity (a), and wind (b), at the latitude of 23.5° S, at 12:00 UTC, for January, 30th, 2017.

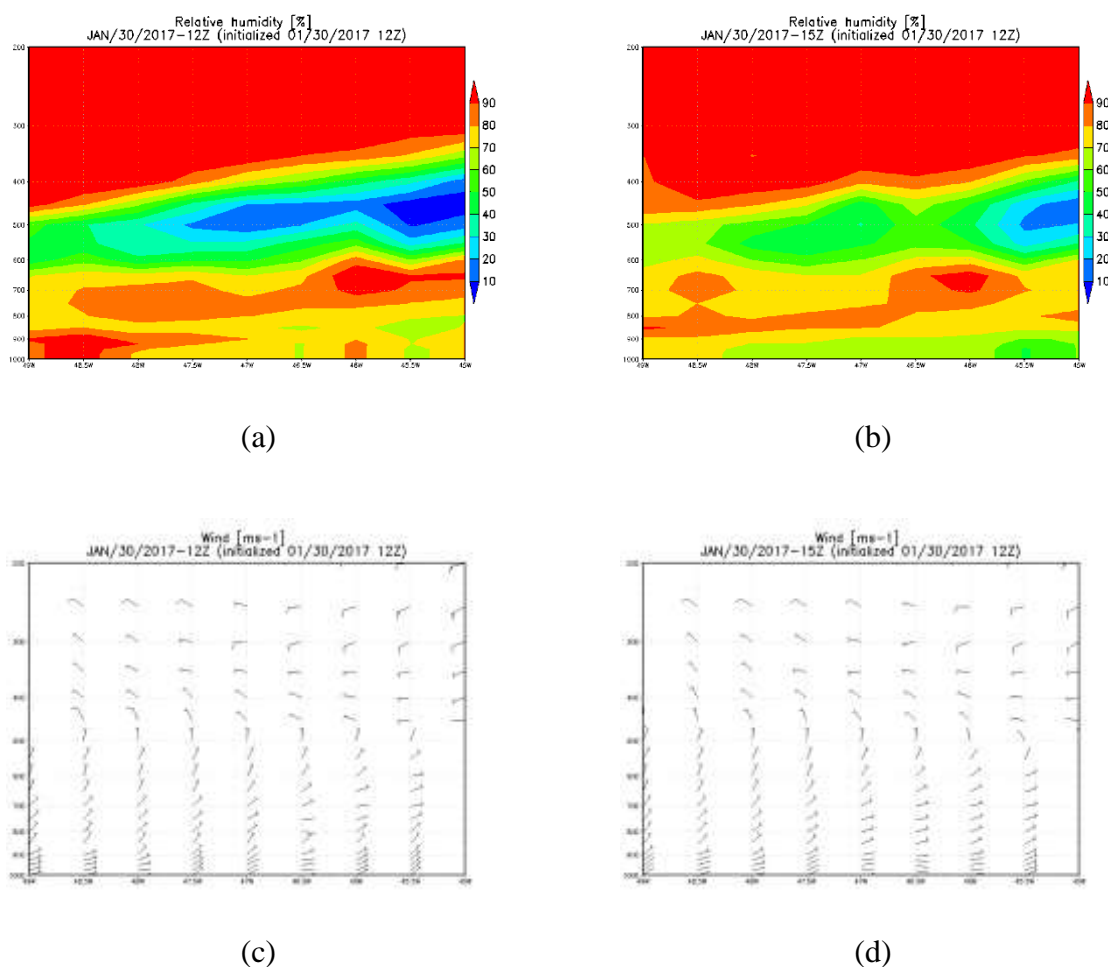


Figure 4-101: Vertical cross section of relative humidity (%) at 12:00 UTC (a), and 15:00 UTC (b), vertical cross section of wind (m s^{-1}) at 12:00 UTC (c), and 15:00 UTC (d) for the latitude of 23.0°S , from GFS for January, 30th.

e. Surface stations

For this event 17 INMET surface stations were analyzed. From their analysis it was possible to consider that even with the presence of clouds in the State, due to the upper level cyclonic vortex mentioned in the synoptic scale analysis, the sea breeze penetration occurred. In the city of São Paulo, the INMET station recorded southeast wind with increase in dew point temperature after 14:00 UTC, but after that the wind varied to east and a decrease in dew point temperature was observed. It increased again after 17:00 UTC when the wind turned back to southeast. Increase in relative humidity was also observed after 17:00 UTC. The same wind pattern was registered in the METAR observed at the Campo de Marte

airport, with winds turning back to southeast at 18:00 UTC. In the METAR analysis from the Congonhas airport winds turn from northeast to southeast at 15:00 UTC with increase in dew point temperature and relative humidity, both at 16:00 UTC. Guarulhos airport reported wind change from northeast to southeast at 17:00 UTC with increase in dew point temperature, relative humidity, wind speed, and decrease of temperature. Less than 3 mm were observed at the INMET station in São Paulo, between 20:00-21:00 UTC and 21:00-22:00 UTC. The closest station to the city of São Paulo (Barueri) shows an increase in dew point temperature and relative humidity after 16:00 UTC, but this station has no record of wind speed and direction. Only 4.0 mm were observed between 18:00-19:00 UTC. It seems that the sea breeze reached the region of São Paulo between 16:00-17:00 UTC.

Station A713, at Sorocaba, has south-southwest winds at 17:00 and 18:00 UTC, south-southeast at 19:00 UTC and southeast winds from 20 to 22 UTC. An increase in dew point temperature is seen at 19:00 UTC, and it may be caused by the sea breeze.

Located in the Vale do Paraíba, stations A740 and A728 (São Luiz do Paraitinga and Taubaté, respectively) also showed evidences of the sea breeze penetration. Increase in dew point temperature and relative humidity was observed at 16:00 UTC at station A740, although winds were from northeast. A wind gust of 15.4 m s^{-1} were registered between 15 and 16:00 UTC. In Taubaté, located further from the sea than São Luiz do Paraitinga, winds turned from northeast to southeast at 18:00 UTC with an increase in dew point temperature, relative humidity, and decrease in temperature. A wind gust of 10.9 m s^{-1} and 0.2 mm of rain was registered between 17:00-18:00 UTC, which could also explain the increase in relative humidity. Station A746 located southwest from São Paulo, registered southeast winds after 14:00 UTC with increase in dew point temperature, relative humidity and decrease in temperature. This station is located closer to the ocean than São Paulo, but the difference in the hour of penetration of the sea breeze could also be related to the topography in the region.

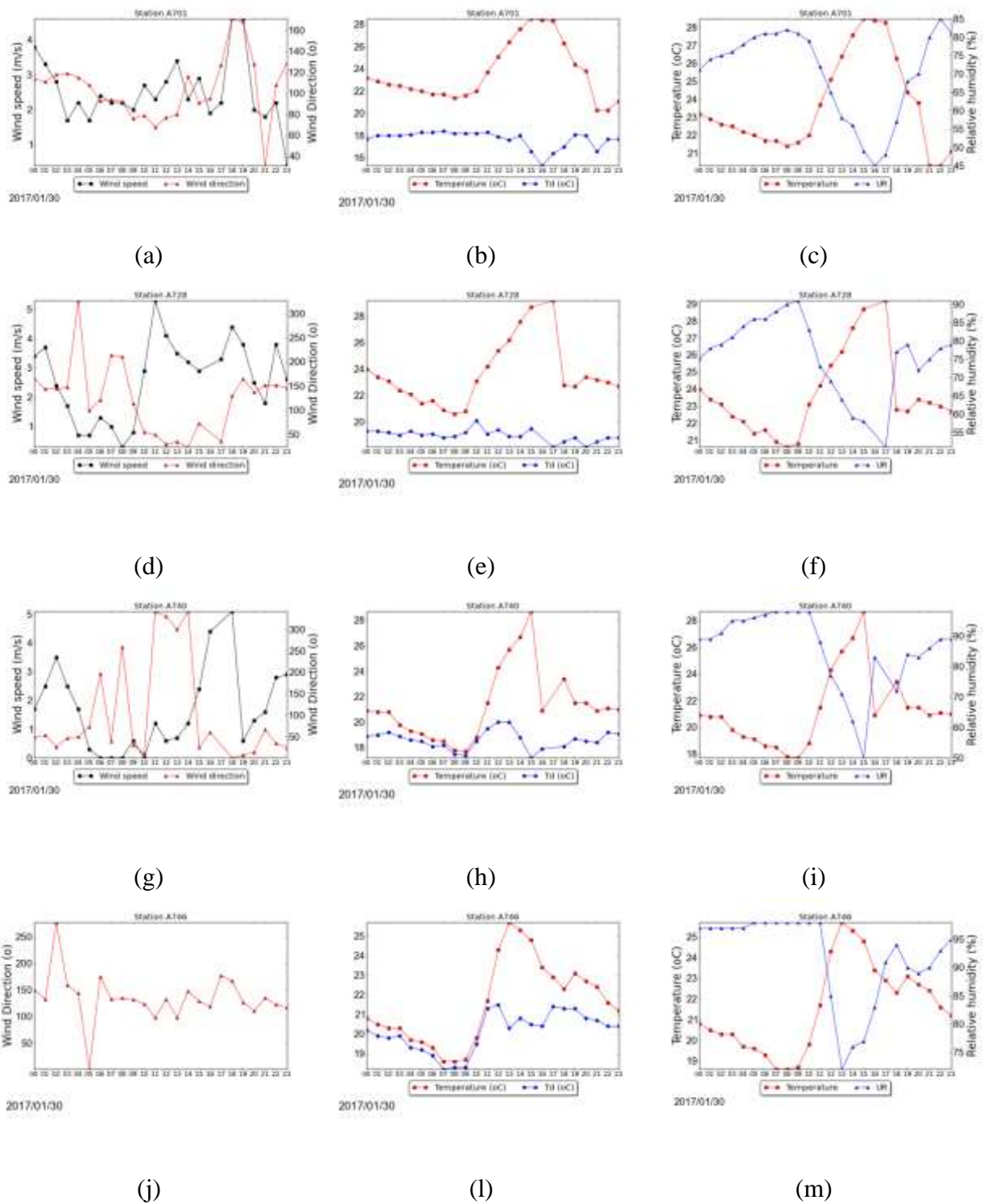


Figure 4-102: Wind speed and direction, temperature and dew point temperature, temperature and relative humidity for January, 30 at station A701 (a), (b), (c); A728 (d), (e), (f); A740 (g), (h), (i); A746 (j), (l), (m); A755 (n), (o), for January, 30th, 2017.

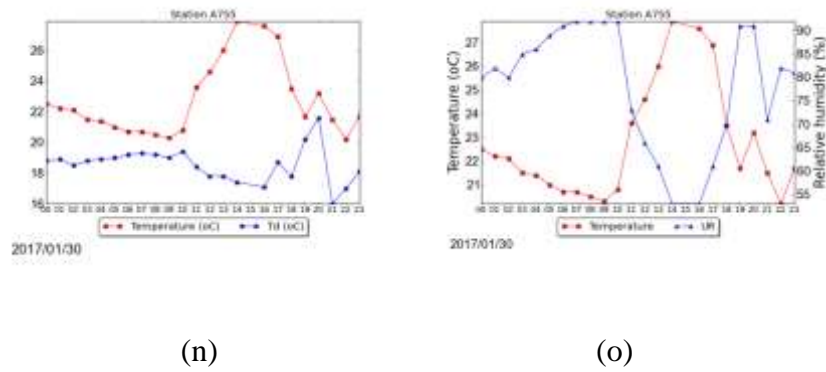


Figure 4-102: Continuation.

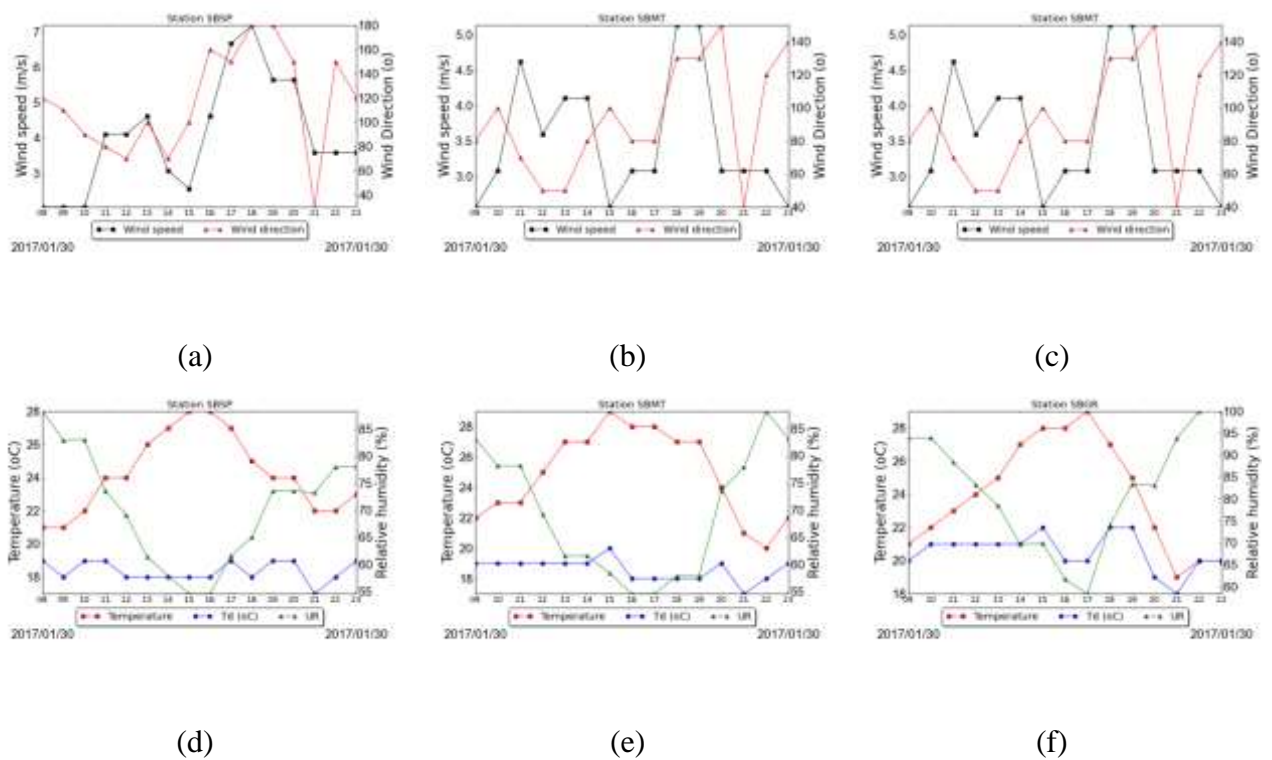


Figure 4-103: Wind speed, temperature, relative humidity and dew point temperature from METAR at station SBSP (a), (d), SBMT (b), (e), and SBGR (c), (f), for January, 30th, 2017.

4.1.3.3 February, 06, 2017

Severe weather occurrences were reported at São Paulo and Campinas, rain led to floods in the city of São Paulo, 36 points were registered (CGE). Both cities recorded strong wind gusts, 20 m s⁻¹ at São Paul, and 21.1 m s⁻¹ at Campinas. Fall of trees was also reported in both cities.

a. Satellite

Analysis in this section will be carried out using infrared images for the South American Continent, and enhanced infrared, infrared and visible images for the southeast region of Brazil.

At 00:00 UTC in the infrared images for South America, shown in Figure 4-104, clouds are covering most of the State. With the advance of hours, these clouds vanish, which was important to the sea breeze development. It is possible to see the frontal system in the Atlantic Ocean at 00:00 UTC east of Argentina, and moving eastward through the day. Clouds extending from the frontal system may have aided in the development of the severe convection, which is the reason this event is on this category. Convection in the State started after 16:30UTC, and moves in a northeast direction, following the large scale pattern.

In the infrared images for the State of São Paulo, it is possible to see clouds at the beginning of the analysis, and that, as mentioned, they vanish with through the day. A line of clouds ahead of frontal system forms in the continent, and propagates in a northeast direction, seen clearly after 14:08 UTC. At this hour, in the visible channel images, it is possible to see a line forming near the coast in the State of São Paulo, indicating the sea breeze. At 14:45 UTC these clouds reach the State of São Paulo, and at 16:08 UTC cells strengthened near the coast, in the southeast region of the State. In the central region, near the coast a cell is developing. At 16:38 UTC, these cells are more intense, and others have started to develop in the State with the advance of those clouds initially mentioned. All those clouds intensified, but the cell in the southeast region, close to the coast, became stronger, seen at 18:38 UTC. In the enhanced infrared images, temperature is around -70°C , but reaches values below -80°C , this is seen between 18:00 and 19:00 UTC. In the northwest region, clouds also reached values around -70°C . It is possible to see these clouds moving in a northeast direction. They move to the region of São Paulo, Campinas and Vale do Paraíba. At 21:00 UTC, most of it has values

around -60°C , but values of the order of -70°C are still seen, especially in the central region of the State.

These clouds lost their strength after that hour, and at 23:00 UTC, most regions have values around -50°C and -60°C , but temperatures of the order of -70°C are still seen in the central-north region.

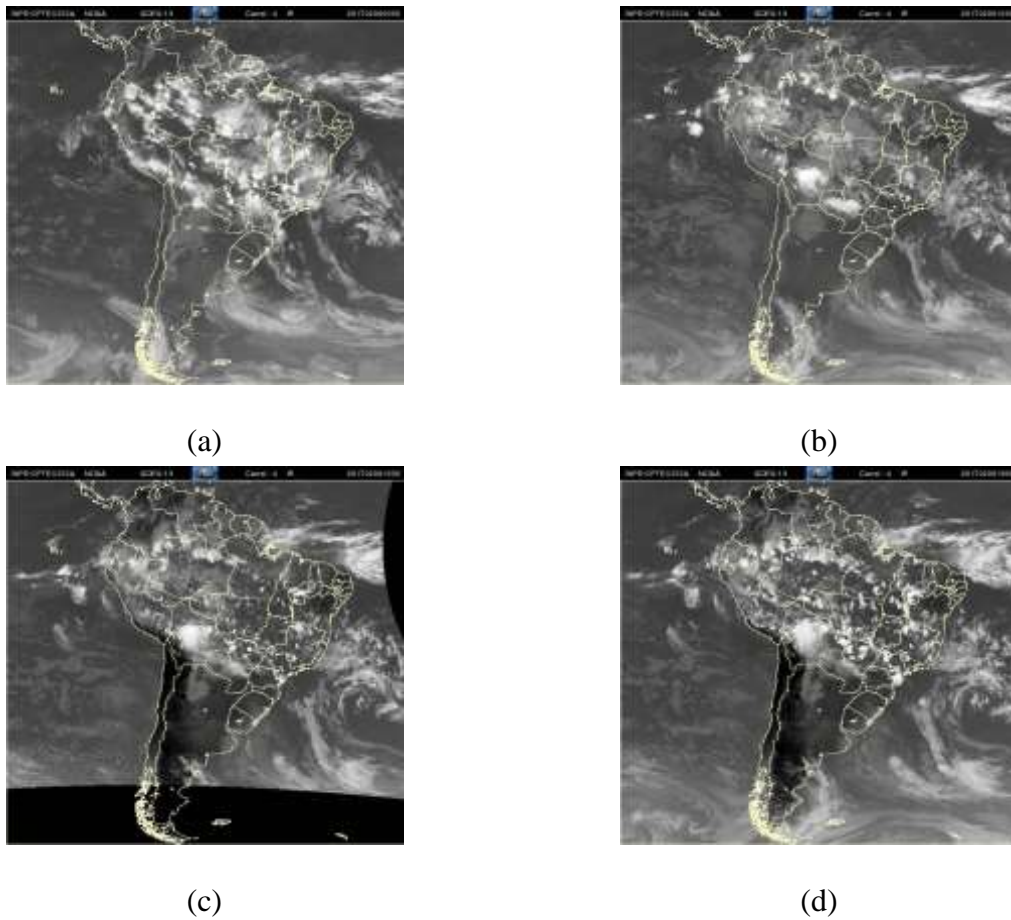


Figure 4-104: Infrared satellite image for South America at 00:00 UTC (a), 12:00 UTC (b), 16:30 UTC (c), 18:00 UTC (d), for February, 06th.

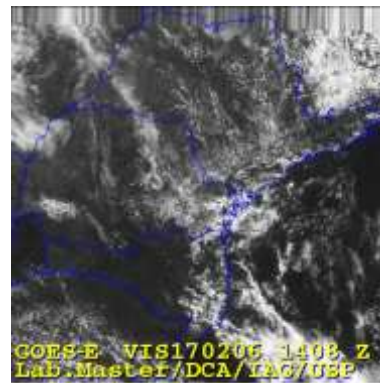
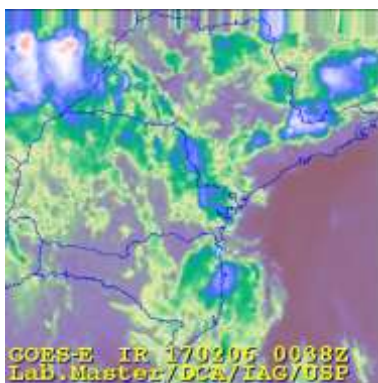
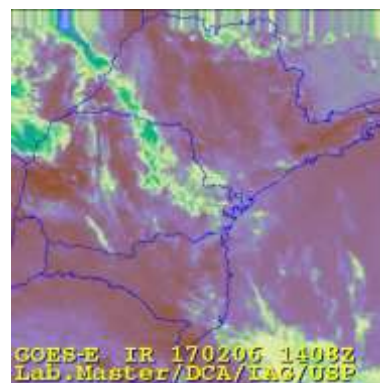


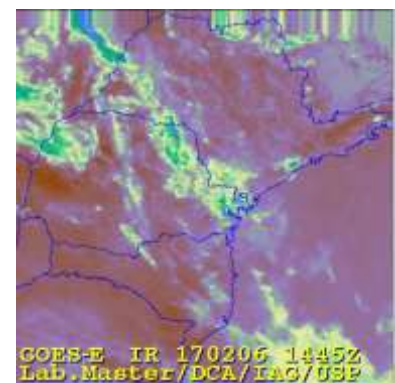
Figure 4-105: Visible channel satellite image for the State of São Paulo at 14:08 UTC for February, 06th.



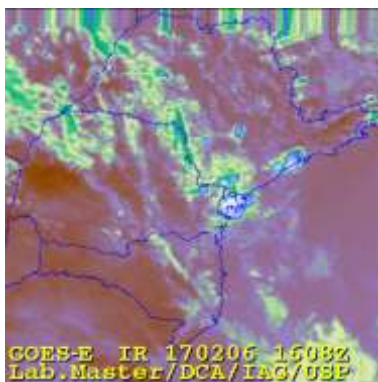
(a)



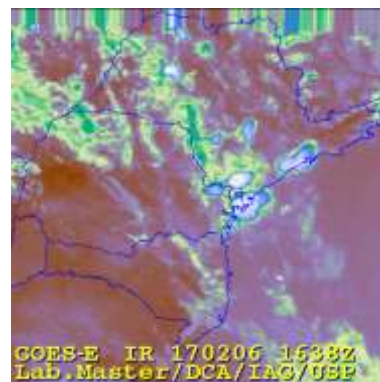
(b)



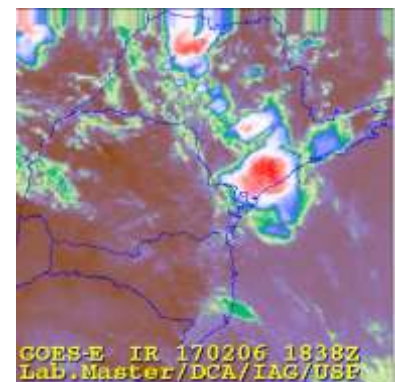
(c)



(d)



(e)



(f)

Figure 4-106: Infrared satellite images for the State of São Paulo at 00:38 UTC (a), 14:08 UTC (b), 14:45 UTC (c), 16:08 UTC (d), 16:35 UTC (e), 18:38 UTC (f), for February, 06th, 2017.

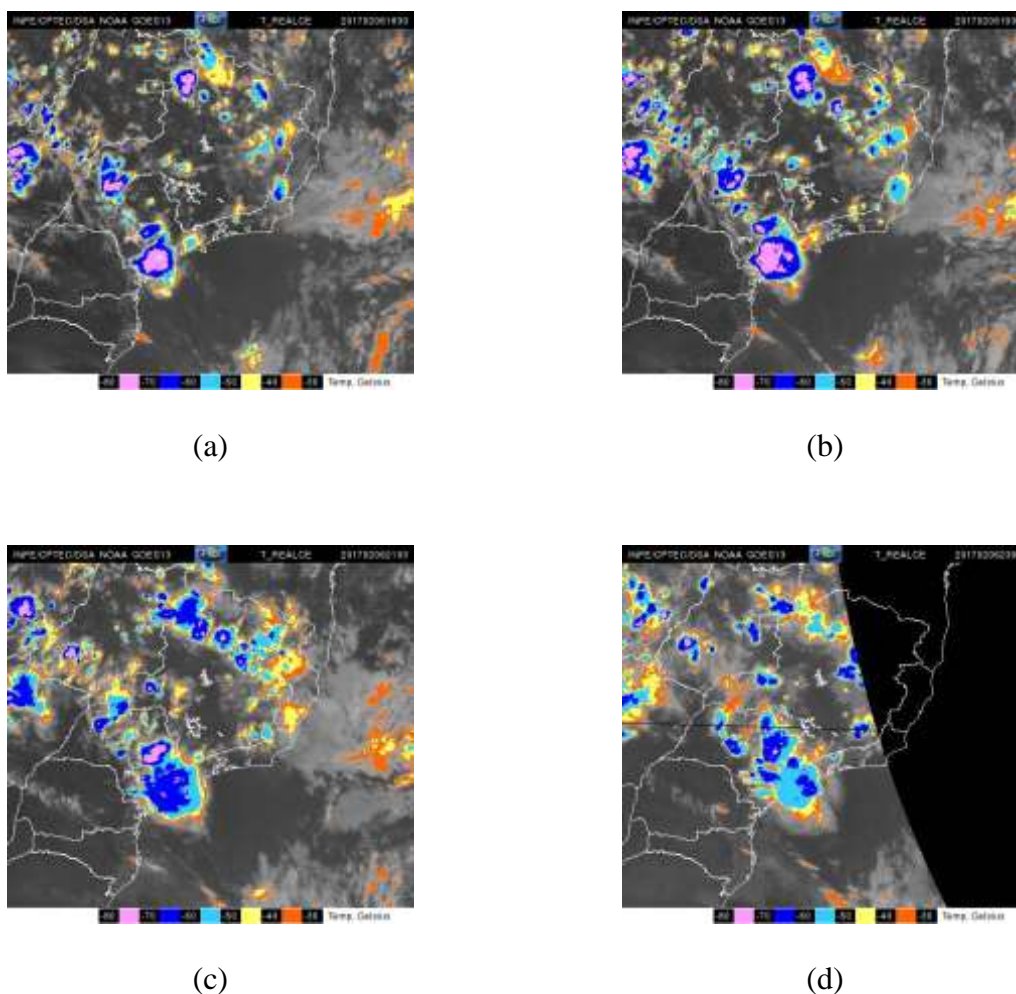


Figure 4-107: Enhanced infrared satellite images for the southeast region at 18:30 UTC (a), 19:30 UTC (b), 21:00 UTC (c), 23:00 UTC (d), for February, 06th, 2017.

b. Radar

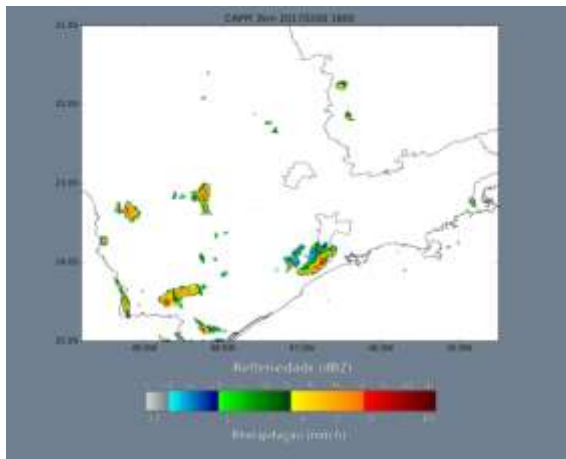
After 16:00 UTC convective cells, with reflectivity values are seen in the southeast region of the State, moving in a northeast direction, as mentioned in the satellite images. Clouds are also seen near the coast ahead of those. At 19:30 UTC cells started to form in the region of São Paulo, which may be related to the sea breeze penetration (further details of the sea breeze during this event will be given in future sections). At 19:40 UTC, reflectivity around 55 dBZ is seen near the north region of the city of São Paulo, around this hour strong downdrafts and rain was registered at stations at this region. At 20:00 UTC reflectivity of the same order is seen in the northeast region of São Paulo and Guarulhos.

Those cells originally propagating from southeast, reach the region of São Paulo, and a merge between the clouds is seen after 20:30 UTC. After this hour, clouds cover most of the city of São Paulo, but higher reflectivity is seen in the east and northeast region. At 21:10 UTC values are ranging from 60-65 dBZ. At 21:40 UTC cells have lost their strength, but the reflectivity of the order of 55 dBZ is still seen. Clouds continue to propagate in a northeast direction, reaching the region of Vale do Paraíba after 22:00 UTC. Clouds with reflectivity of the order of 40-45 dBZ is seen in the east region of São Paulo until 23:00 UTC.

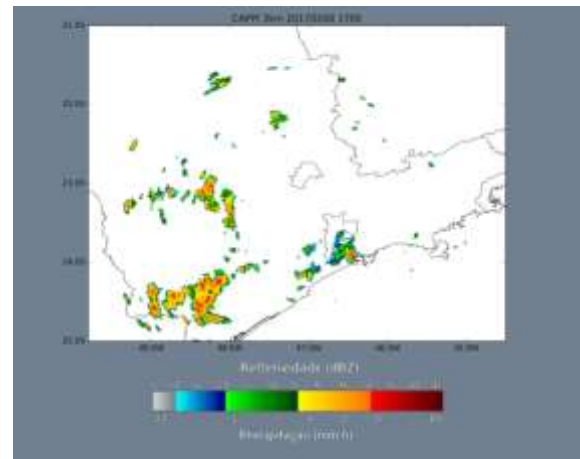
In the region of Campinas, cells start to develop after 20:30 UTC. Between 21:30 and 21:40 UTC reflectivity is higher, around 60-65 dBZ, in the northwest and north regions of the city. Between 21:50 and 22:00 UTC reflectivity is on the order of 55-60 dBZ in the north and northeast region of Campinas. At 21:50 UTC (7:50 PM local time), a wind gust of 21 ms^{-1} was recorded in the north region of the city. It is possible to see that these cells also propagate in a northeast direction, and a merge with the system propagating through the east part of the State is observed after 22:00 UTC.

At 22:40 UTC high reflectivity values are observed in the region of Bragança Paulista and São José dos Campos (Vale do Paraíba), values are around 60-65 dBZ. According to the news, between 7:00 and 9:00 PM local time, 600 lightings were observed at São José dos Campos. At Taubaté (Vale do Paraíba) and Bragança Paulista, between 8:00 and 11:59 PM local time, 250 and 260 lightings were observed, respectively.

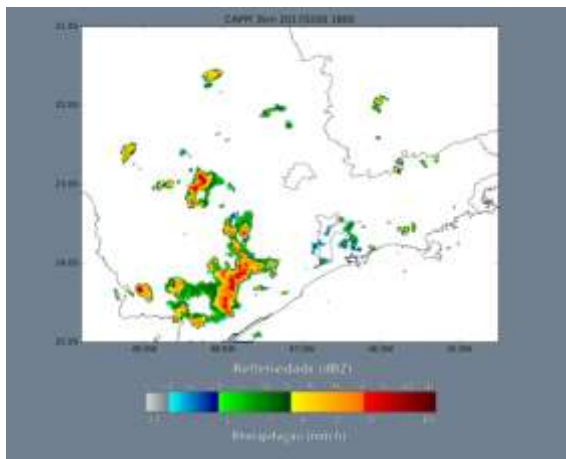
Reflectivity of the same order is observed at Vale do Paraíba until 23:40 UTC as the clouds propagated northeastward.



(a)



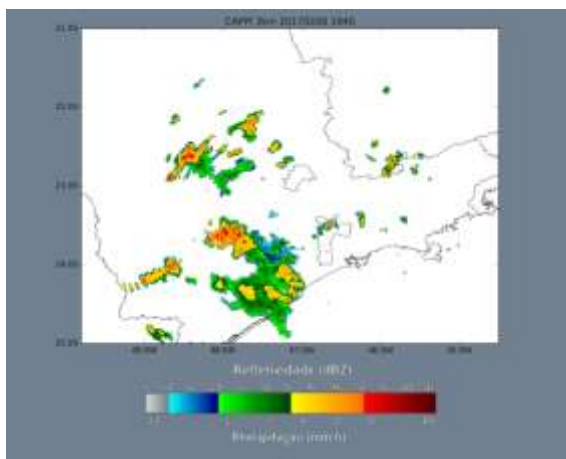
(b)



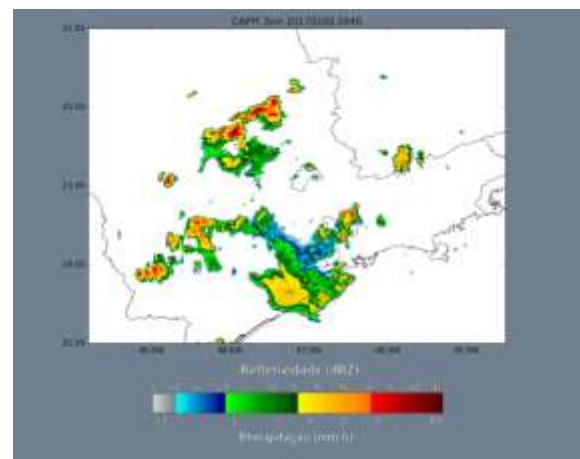
(c)



(d)

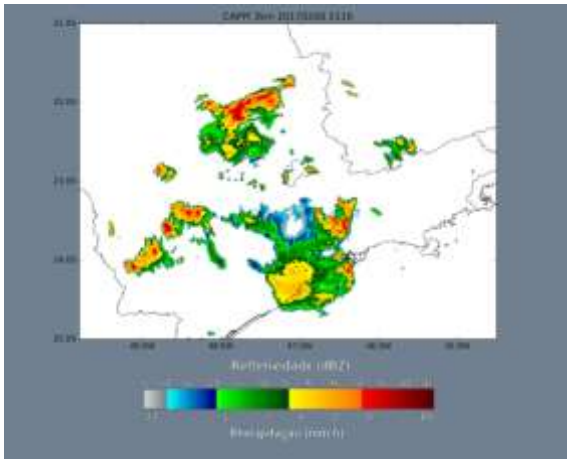


(e)

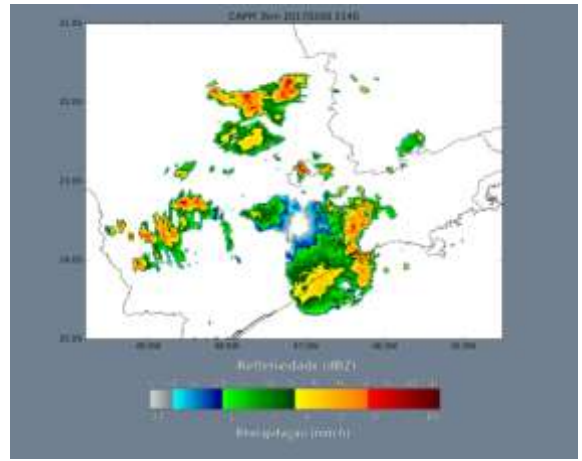


(f)

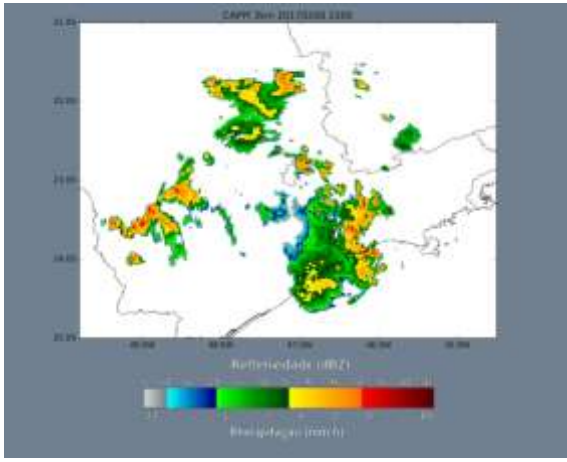
Figure 4-108: Radar images from the São Roque radar at 16:00 UTC (a), 17:00 UTC (b), 18:00 UTC (c), 19:30 TC (d), 19:40 UTC (e), 20:40 UTC (f), 21:10 UTC (g), 21:40 UTC (h), 22:00 UTC (i), 22:40 UTC (j), 23:00 UTC (l), 23:40 UTC (m).



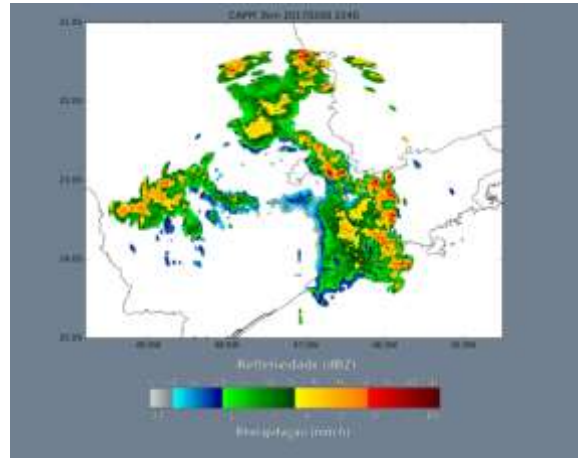
(g)



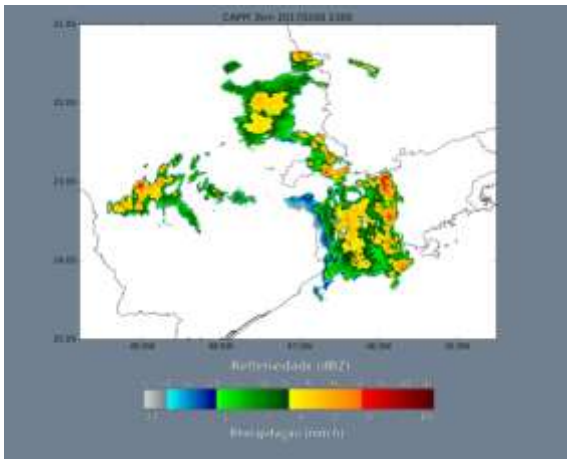
(h)



(i)



(j)



(l)



(m)

Figure 4-108: Continuation.

c. Synoptic scale analysis

In the 200 hPa analysis it is possible to see the Bolivian high, an upper level cyclonic vortex in the Atlantic Ocean, but the most important feature for this event is the trough extending from east to north Argentina at 00:00 UTC, with the subtropical jet associated. This trough is related to a frontal system at the surface. This trough moves eastward during the day.

A trough with a cyclonic vortex and negative vorticity associated is present in eastern Argentina at 00:00 UTC in the 500 hPa analysis, this trough extends to Rio Grande do Sul. As mentioned in the 200 hPa analysis, this system moves eastward throughout the day. At 18:00 UTC a high pressure system is seen between Mato Grosso do Sul and the west region of São Paulo.

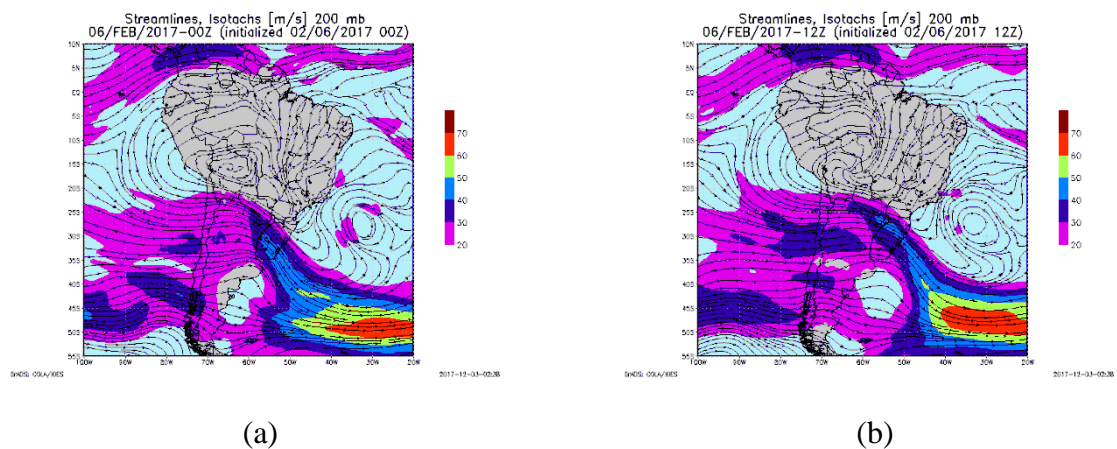


Figure 4-109: Streamlines and isotachs (m s^{-1}) at 200 hPa at 00:00 UTC (a), 12:00 UTC (b), for February, 06th, 2017.

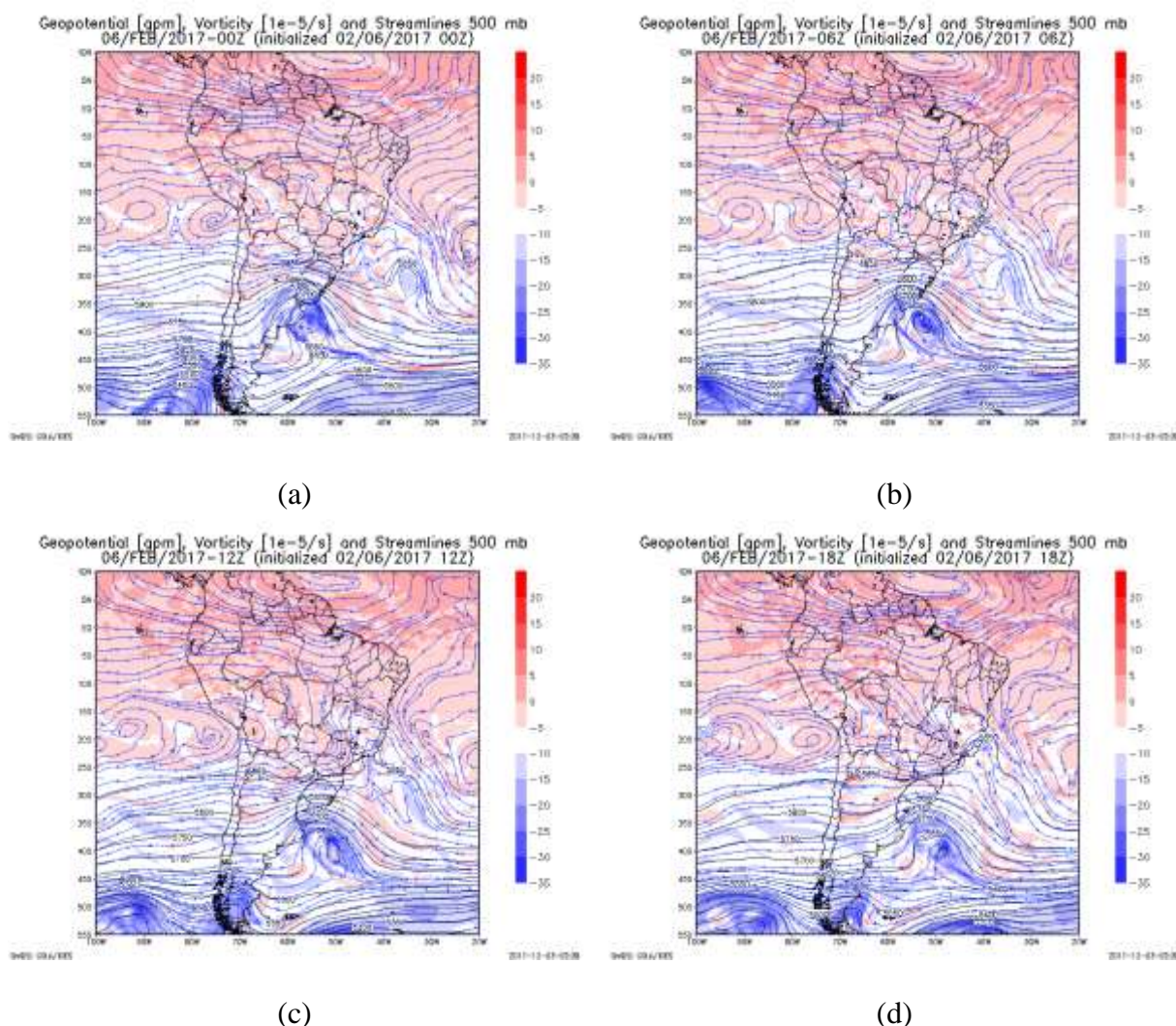


Figure 4-110: Geopotential height (gpm), vorticity (10^{-5} s^{-1}) and streamlines at 500 hPa at 00:00 UTC (a), 06:00 UTC (b), 12:00 UTC (c), 18:00 UTC (d) for February, 06th.

At the level of 850 hPa, the low pressure system associated with the frontal system is located in east of Argentina, in a region of temperature gradient and high moisture content. Between 00 and 06:00 UTC regions of relative humidity around 65-75% are seen in some regions of the State of São Paulo, but after 12:00 UTC this regions are no longer seen, and relative humidity is around 75-80 % in the State, with a few region where it is between 80-85%, which increased after 15:00 UTC. A trough is seen after 12:00 UTC extending from the low pressure system near the coast of São Paulo, the relative humidity was around 65-75% at 00:00 UTC at this region, but increased to 75-85% probably related to this trough

development. A trough is also seen after 12:00 UTC in the State of São Paulo, extending through Minas Gerais, this may have generated instability in the region.

At the surface, the low pressure system is seen east of Argentina, with the cold front in the State of Rio Grande do Sul. As this low pressure system moves eastward through the day, the cold front moves through the south region States of Rio Grande do Sul and Santa Catarina. A trough is seen near the coast of São Paulo at 00:00 UTC until 15:00 UTC, and is extending through the State at 06:00, 09:00 and 15:00 UTC.

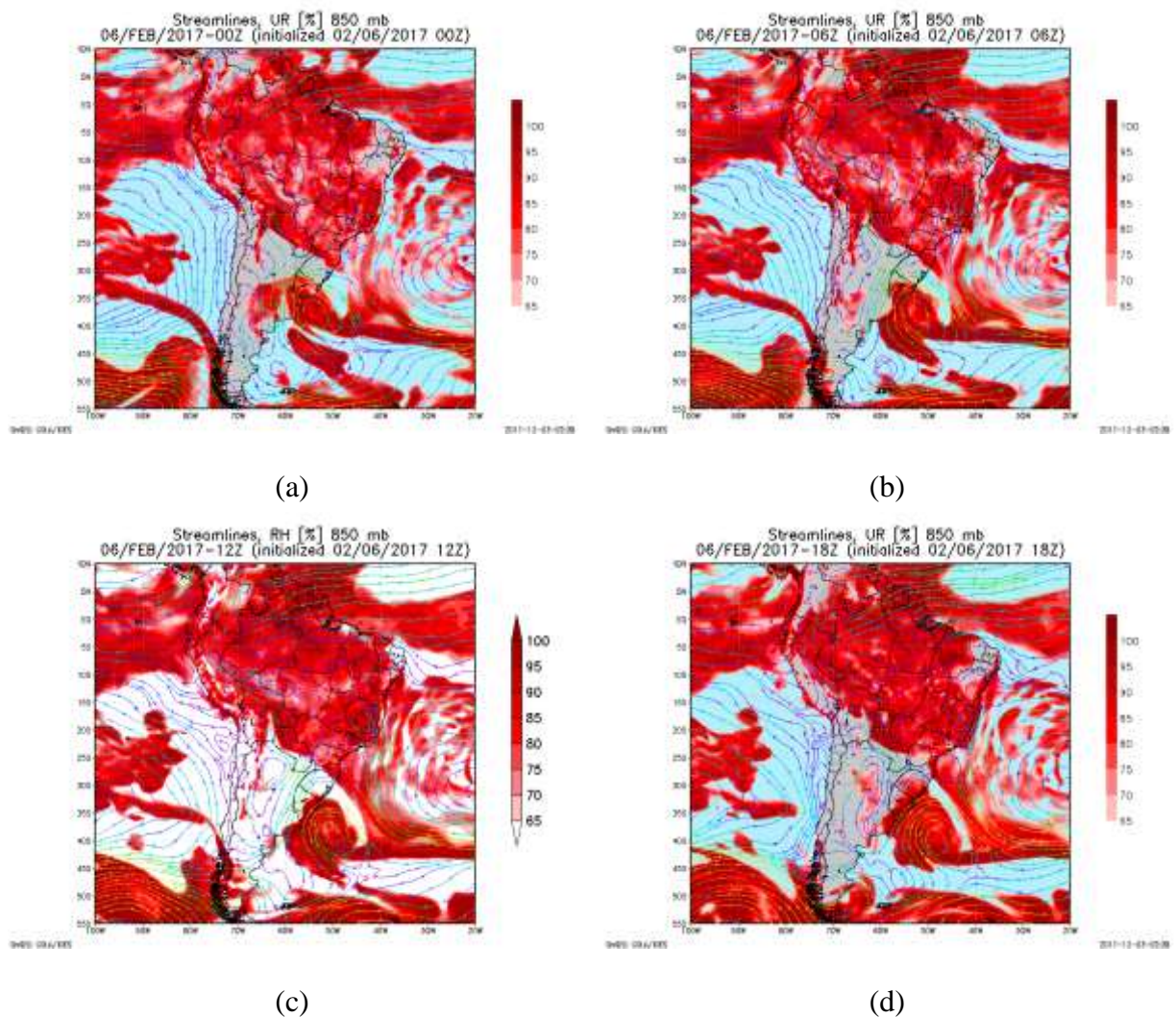


Figure 4-111: Streamlines and relative humidity (%) at 850 hPa at 00:00 UTC (a), 06:00 UTC (b), 12:00 UTC (c), 18:00 UTC (d) for February, 06th.

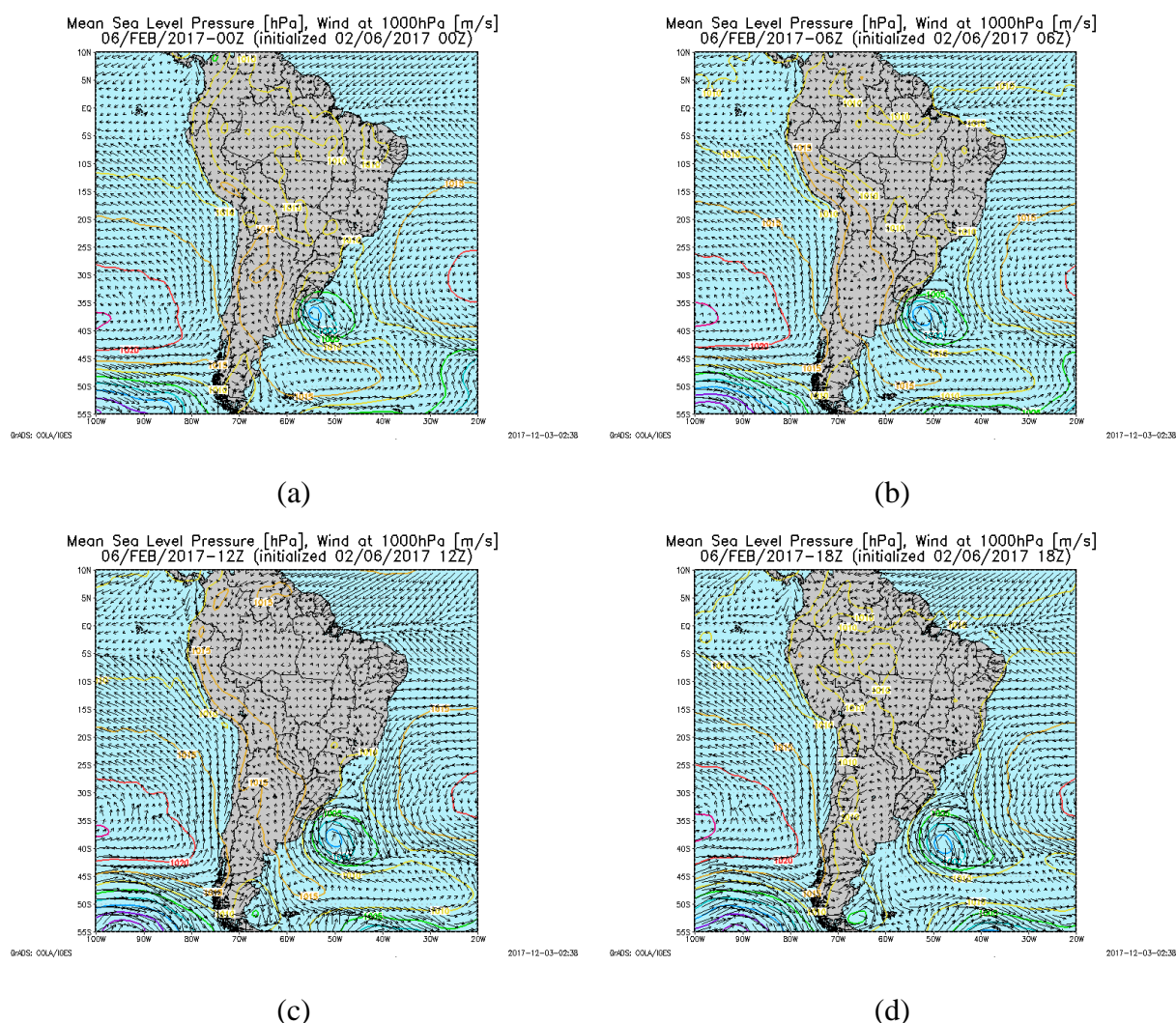


Figure 4-112: Mean sea level pressure (hPa), and wind (m s^{-1}) at 00:00 UTC (a), 06:00 UTC (b), 12:00 UTC (c), 18:00 UTC (d) for February, 06th, 2017.

d. Thermodynamic and mesoscale analysis

Sounding was not available for this day, therefore, CAPE and CIN will be analyzed from the BRAMS and GFS model, and LI will be analyzed only from the GFS model.

At 12:00 UTC in the GFS analysis CAPE is around $600\text{-}1200 \text{ J kg}^{-1}$ near São Paulo. Near Campinas the parameter shows a high variation in the region between $600\text{-}1800 \text{ J kg}^{-1}$. Also from the GFS at 12 UTC, in the south region of Vale do Paraíba, CAPE is around $600\text{-}800 \text{ J kg}^{-1}$. These values are in the same range at 15:00 UTC, indicating a condition between marginally and moderately unstable, and marginally unstable at Vale do Paraíba.

CAPE from the BRAMS analysis at 12:00 UTC, near São Paulo is around 1800-2100 J kg⁻¹. At 15 UTC most of the State has values above 2500 J kg⁻¹, including near Campinas. In the northeast region, CAPE is between 1700-2100 J kg⁻¹. These values indicate a moderately unstable condition for the northeast region of the State, including near São Paulo, and a very unstable condition in the rest of the State.

At 12:00 UTC CIN is below 20 J kg⁻¹ everywhere in the State from the BRAMS analysis. In GFS analysis, at 12:00 UTC, values are seen between -20 and -30 J kg⁻¹ in the region of Vale do Paraíba. Near São Paulo and Campinas, it is above -20 J kg⁻¹.

The LI parameter, at 12:00 UTC, is between -3 K and -5 K near São Paulo, and between -3 and -6 K near Campinas. The same range is seen at 15:00 UTC, these values indicate an unstable condition with probable storm, even severe. At the Vale do Paraíba, values are between 0 and -1 K in the extreme northeast region, and ranging from -1 K to -3 K. At 15:00 UTC, values are ranging from -2 to -4 K. At 12:00 UTC these values indicate a condition between slightly unstable with possible storm and unstable with probable storm, at 15:00 they are in the second category. The 700-500 hPa lapse rate is between 5.5 and 6 K km⁻¹ at 12:00 and 15:00 UTC.

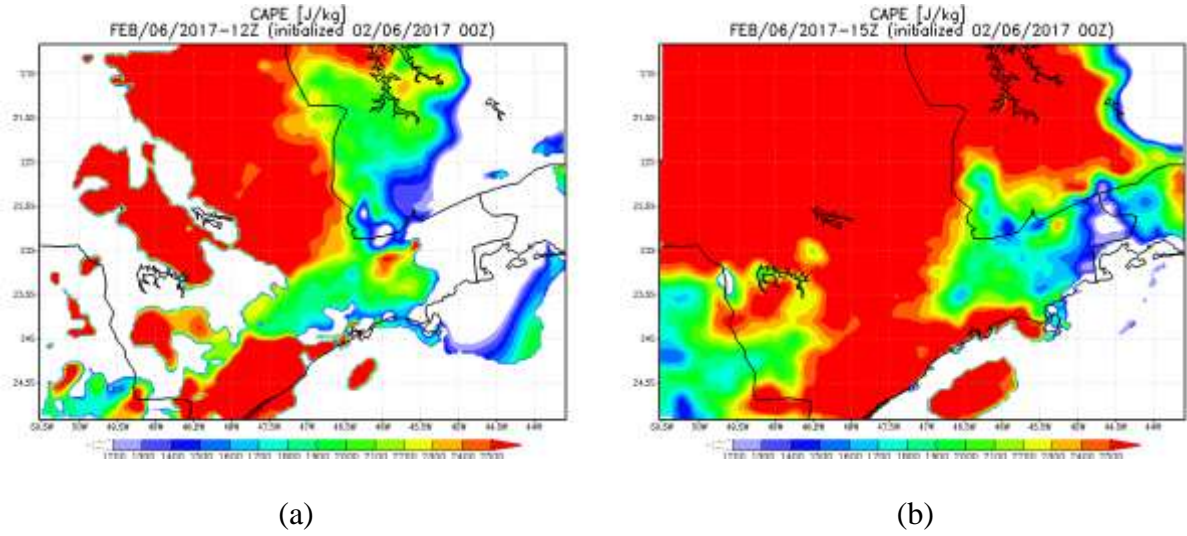


Figure 4-113: CAPE from BRAMS at 12:00 UTC (a), and 15:00 UTC (b) for February, 06th, 2017.

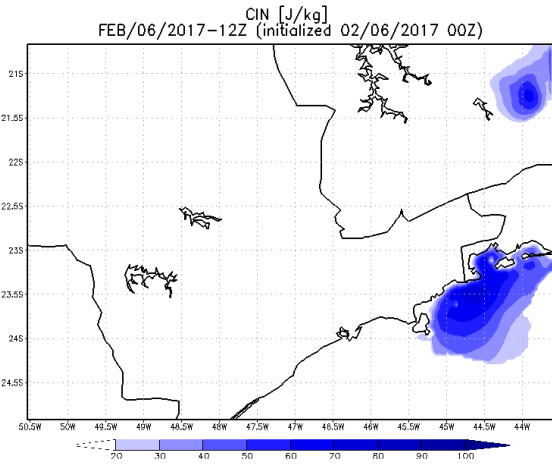


Figure 4-114: CIN from BRAMS at 12:00 UTC for February, 06th.

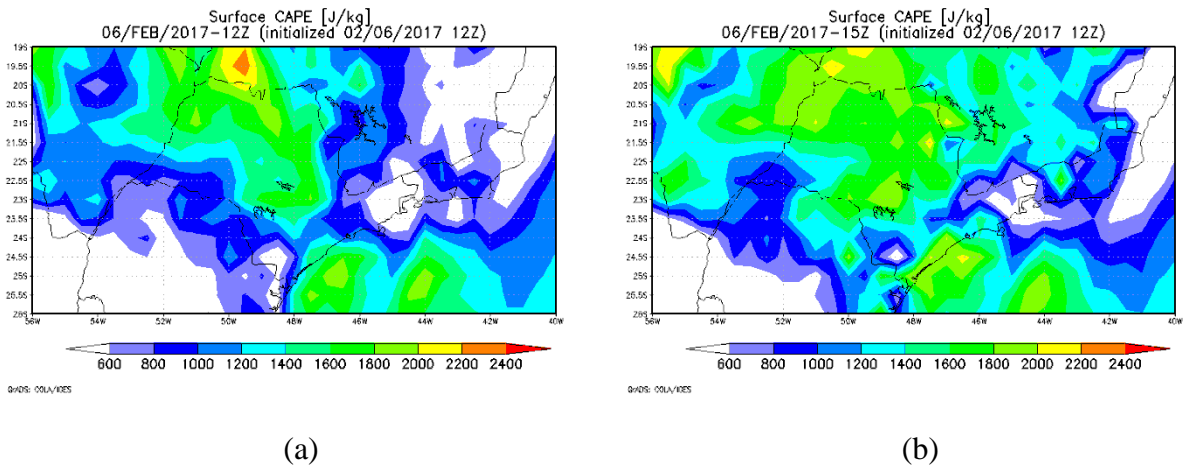


Figure 4-115: CAPE from GFS at 12:00 UTC (a), and 15:00 UTC (b) for February, 06th.

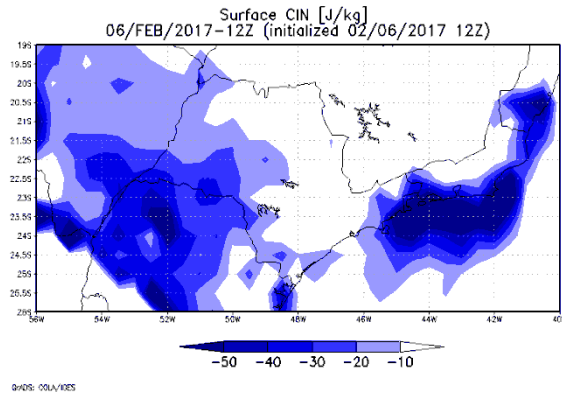


Figure 4-116: CIN from GFS at 12:00 UTC for February, 06th.

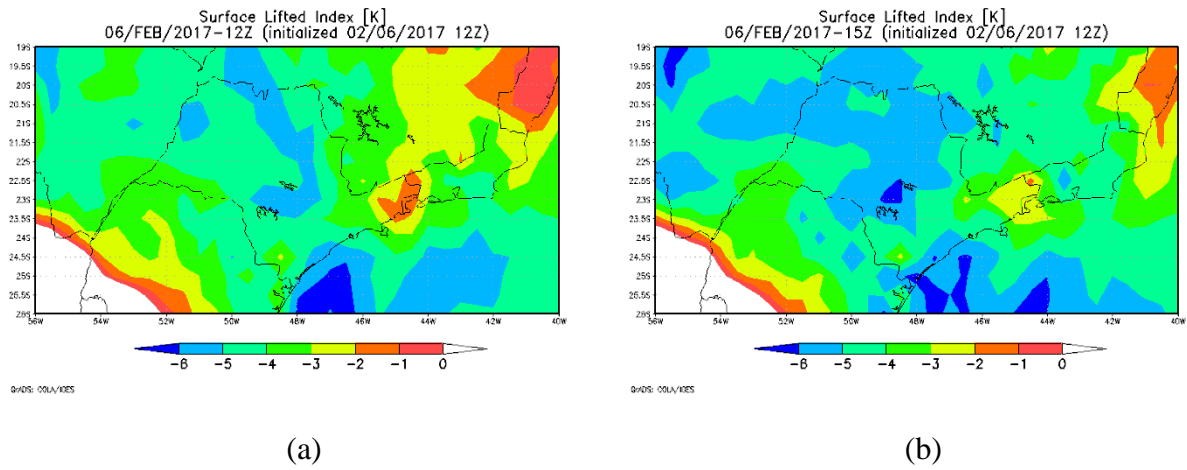


Figure 4-117: LI from GFS at 12:00 UTC (a), and 15:00 UTC (b) for February, 06th.

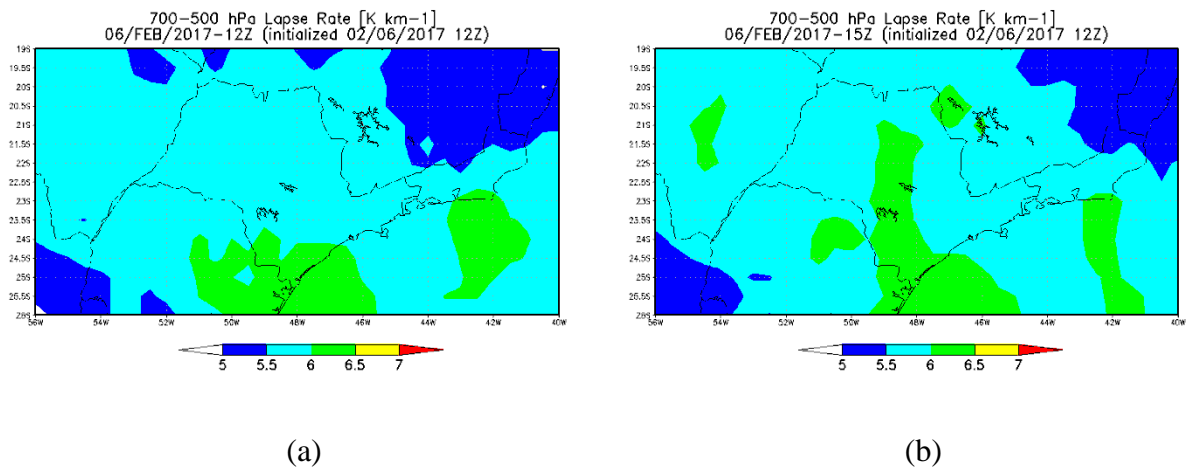


Figure 4-118: 700-500 hPa from GFS at 12:00 UTC (a), and 15:00 UTC (b) for February, 06th.

Analysis of moisture divergence shows convergence is present at the coast representing the sea breeze. At 15:00 UTC values are below $-4 \cdot 10^{-3} \text{ g kg}^{-1} \text{ s}^{-1}$. Figure 4-119 shows water vapor mixing ratio and wind, advancing through the day. Winds at 00:00 UTC are from southeast in most of the State, and from northeast in the northeast region. Close to São Paulo, winds are weak. A moisture gradient forms near the coast, and propagates with southeast winds, showing the sea breeze penetration, starting at 15:00 UTC. From this analysis it is possible to see that the sea breeze did not propagate far inland, as seen in other events, this is related to the synoptic scale patterns. In the satellite analysis clouds propagate in a southeast-northeast direction, following the large scale pattern; this may have inhibited the sea breeze to propagate further. It is important to emphasize that large scale system dominate over mesoscale systems.

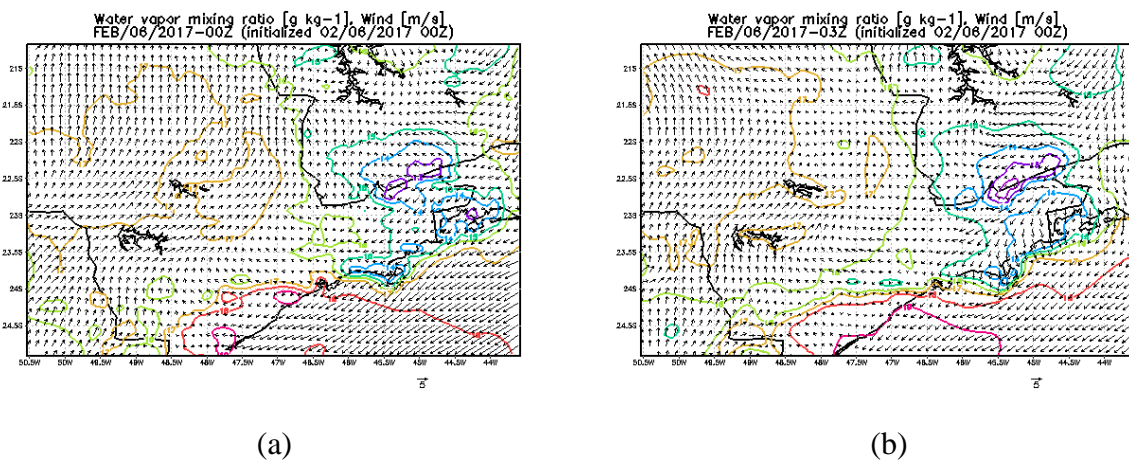


Figure 4-119: Water vapor mixing ratio and wind at 00:00 UTC (a), 03:00 UTC (b), 06:00 UTC (c), 09:00 UTC (d), 12:00 UTC (e), 15:00 UTC (f), 18:00 UTC (g), 21:00 UTC (h) for February, 06th.

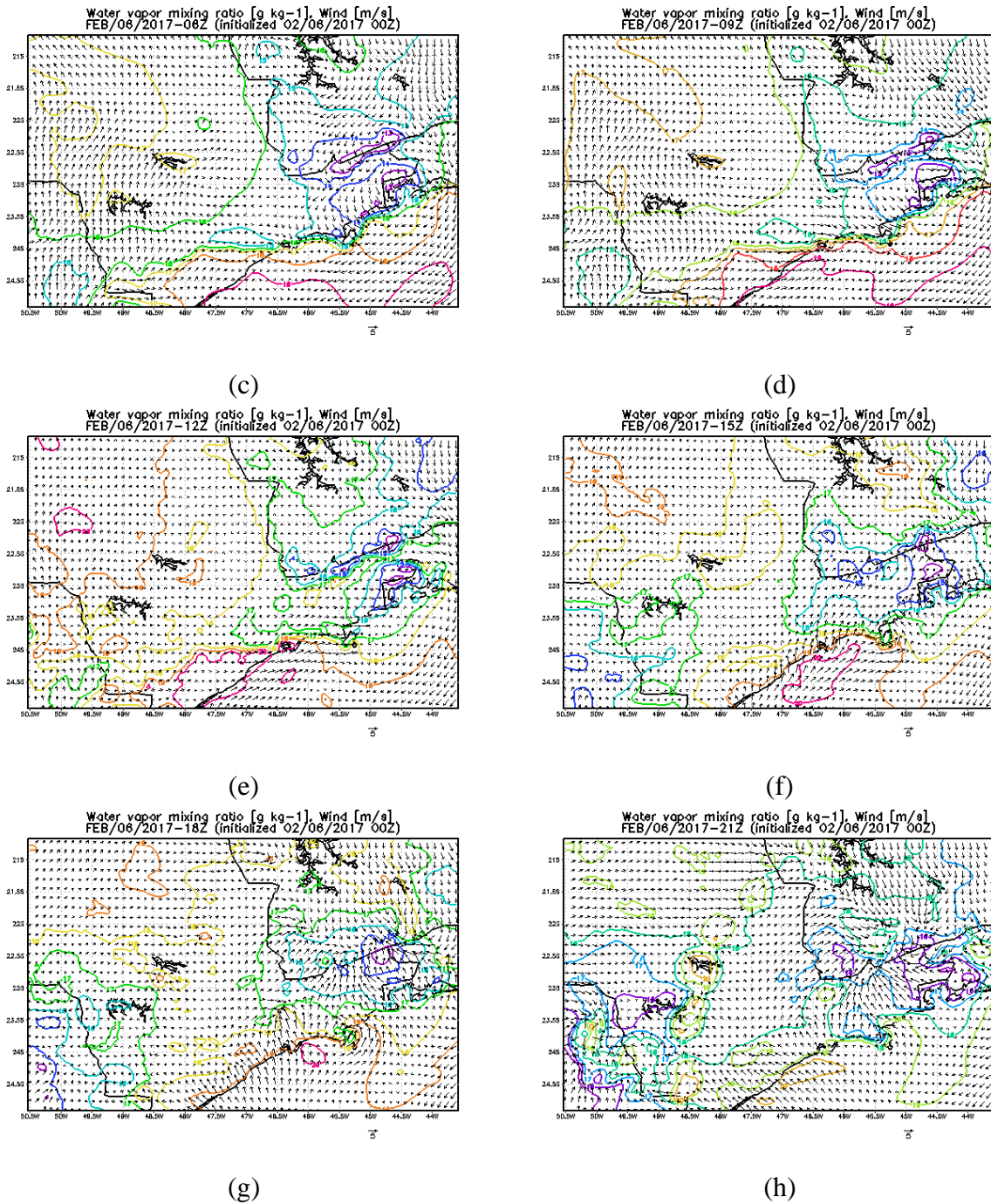


Figure 4-119: Continuation.

Vertical cross sections of wind, relative humidity and winds were analyzed using GFS and BRAMS. Both analysis shows that winds are weak through the day and through the vertical extension. At 12:00 UTC, winds are from southwest and south-southwest in the last vertical level, near São Paulo. Speed increased also in the last vertical level.

In the GFS analysis, near São Paulo, winds are from west, and northwest, a small increase in speed occurs after 800 hPa, but winds remained from west. After 700 hPa winds turned anticlockwise to south-southwest at 650 hPa, and again another small increase in speed is seen after this level.

In the vertical cross section of relative humidity at 12:00 UTC, on both analyses, moisture decrease with height. After 3000 m above the surface, from the BRAMS output, relative humidity is varying from 20-40 %, near São Paulo. The analysis from the GFS model show decrease with height in this region of the atmosphere, between 600-500 hPa values are around 50-60 %, lower values are seen east of São Paulo, ranging from 10 to 30 %. This is still seen at 15:00 UTC.

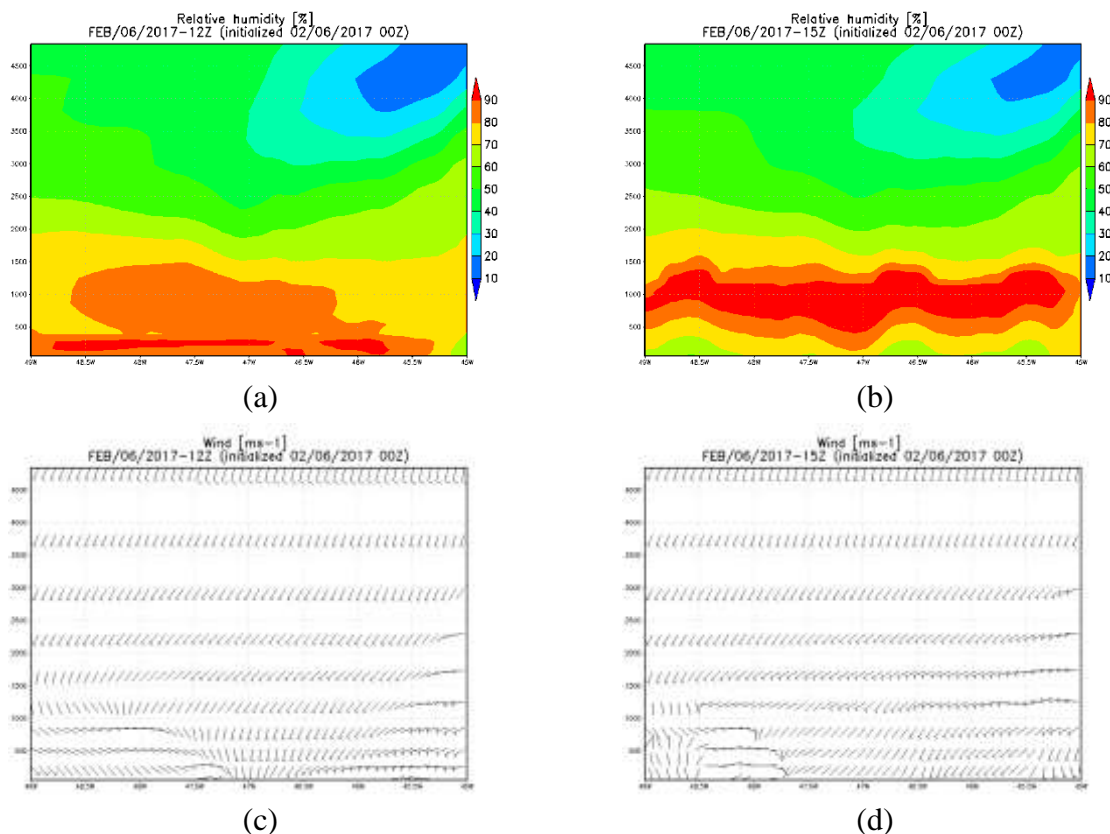


Figure 4-120: Vertical cross section from BRAMS of relative humidity at 12:00 UTC (a), 15 UTC (b), and of winds at 12:00 UTC (c), and 15:00 UTC (d) at 23.5 °S for February, 06th.

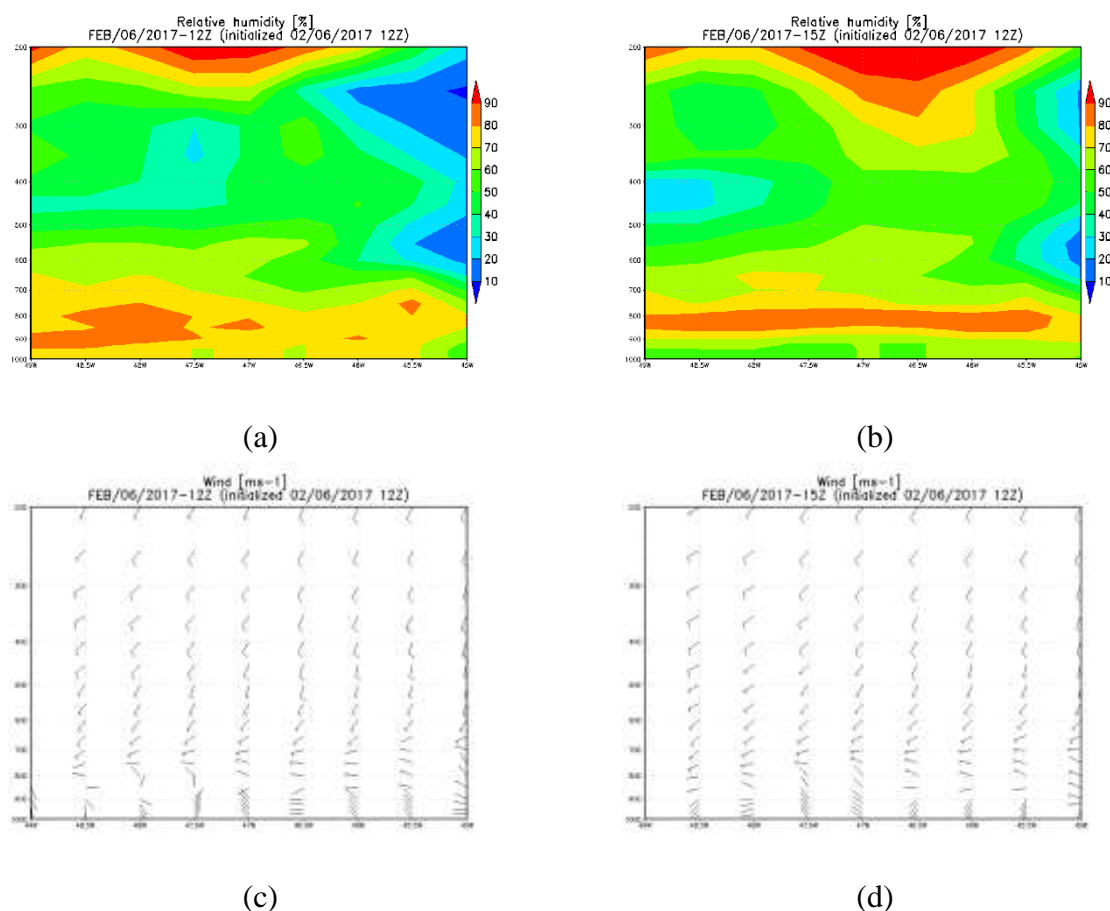


Figure 4-121: Vertical cross section from GFS of relative humidity at 12:00 UTC (a), 15 UTC (b), and of winds at 12:00 UTC (c), and 15:00 UTC (d) at 23.5 °S for February, 06th.

e. Surface stations

A total of 17 INMET surface automatic surface stations were analyzed. METAR from airports in the city of São Paulo, Guarulhos, Campinas and Taubaté are analyzed.

At station A701 wind was from southeast at 00:00 UTC, and northeast until 03:00 UTC. Winds were weak until 09:00 UTC, and then, they vary between northwest and west-northwest until 18:00 UTC. At 19:00 UTC winds turn to southeast followed by an increase in dew point temperature relative humidity, decrease in temperature. The maximum temperature registered was 31°C at 17:00 UTC, and dew point temperature remained above 15 °C during the day, and increased above 20 °C with the sea breeze. It rained for 5 hours, the accumulated was 38.8 mm. The peak was of 17.4 mm between 20:00 and 21:00 UTC, in the previous

interval, it rained 12.2 mm. A wind gust of 13.8 ms^{-1} was observed around 19:00 and 20:00 UTC. Wind gusts of 11.7 and 11.2 ms^{-1} were registered in the following hours. In the METAR analysis for Campo de Marte winds varied from southwest, west-northwest and northwest from 03:00 UTC until 18:00 UTC. Winds turned to southeast at 19:00 UTC, with increase in dew point temperature relative humidity, decrease in temperature. The turn to southeast followed by these changes occurred at 18:00 UTC, before, winds were from northwest from 09:00 to 16:00 UTC.

At the Guarulhos airport winds were from west and northwest from 11:00 UTC to 18:00 UTC, it then, turned to southeast at 19:00 UTC followed by the expected changes related to the sea breeze.

At station A755, Barueri, increase in dew point temperature is observed at 19:00 UTC, and increase in relative humidity and decrease in temperature is seen at 20:00 UTC.

From these analyses, it is possible to say that the sea breeze penetrated in the region of São Paulo around 18:00-19:00 UTC. According to the CGE, 9 out of the 31 stations recorded rain indices above 20 mm, 8 registered more than 30 mm and one, at Itaim Paulista more than 40 mm (42.8 mm). Stations from Alto do Tiete also recorded high rain indices, 10 of them recorded more than 30 mm, 4 recorded more than 40 mm and one more than 60 (60.8 mm). The Campo de Marte airport registered a wind gust of 19.5 ms^{-1} .

At station A740, São Luiz do Paraitinga, southeast winds are observed at 17:00 UTC, with increase in dew point temperature. It remained from southeast until 19:00 UTC, another sharp increase in dew point temperature, this time followed by increase in relative humidity and decrease in temperature is observed. Winds were from east and northeast in the following hours. Before turning to southeast, winds were varying from southwest, west-northwest and northwest.

Also localized at Vale do Paraiba, station A728, Taubat , had southwest and southeast winds between 13:00 and 19:00 UTC. At 20:00 UTC winds are from south-southwest, accompanied by the changes related to the sea breeze. Winds are from southeast at 21:00 UTC and remained until the end of the analysis. In the METAR analysis, southeast winds with the expected changes are seen at 20:00 UTC. bNo other station inland recorded the sea breeze penetration.

All of the analyzed stations recorded maximum temperature above 30  C, with the highest value of 34.1  C observed at station A707 (Presidente Prudente).

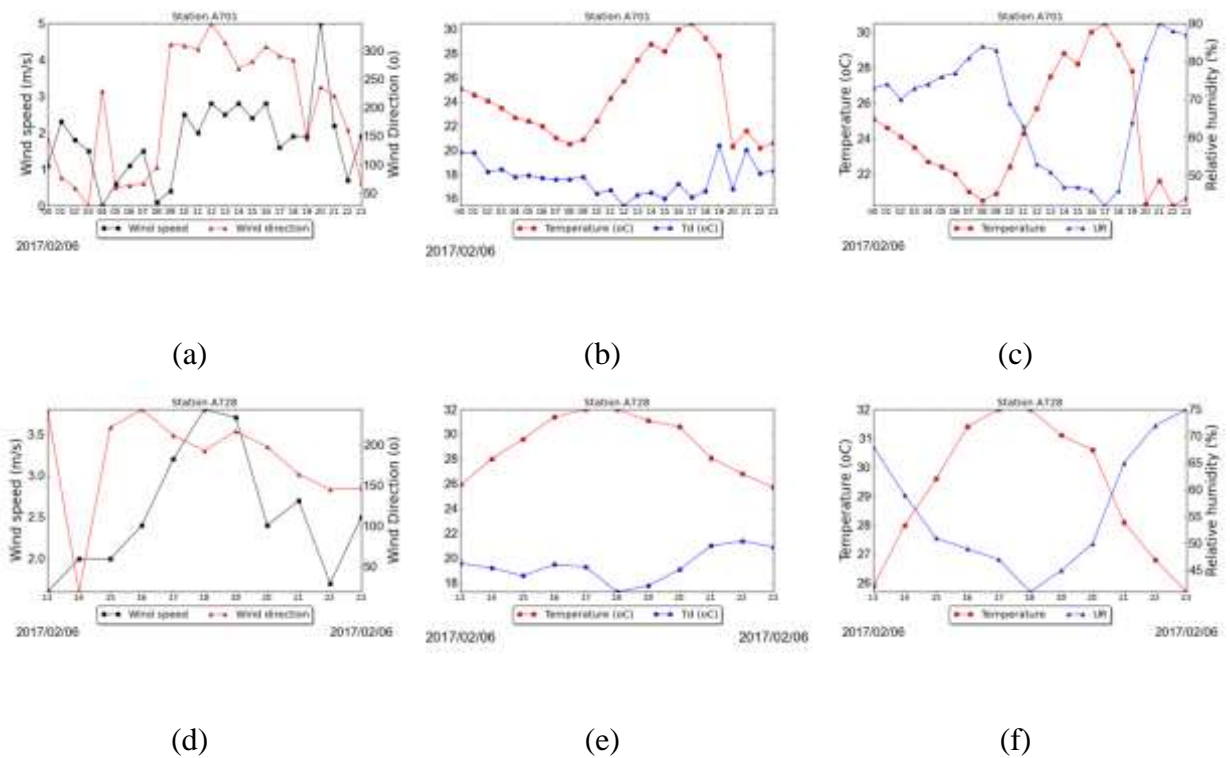


Figure 4-122: Wind speed and direction, temperature and dew point temperature, temperature and relative humidity at stations A701 (a), (b), (c), A728 (d), (e), (f), A740 (g), (h), (i) for February, 06th.

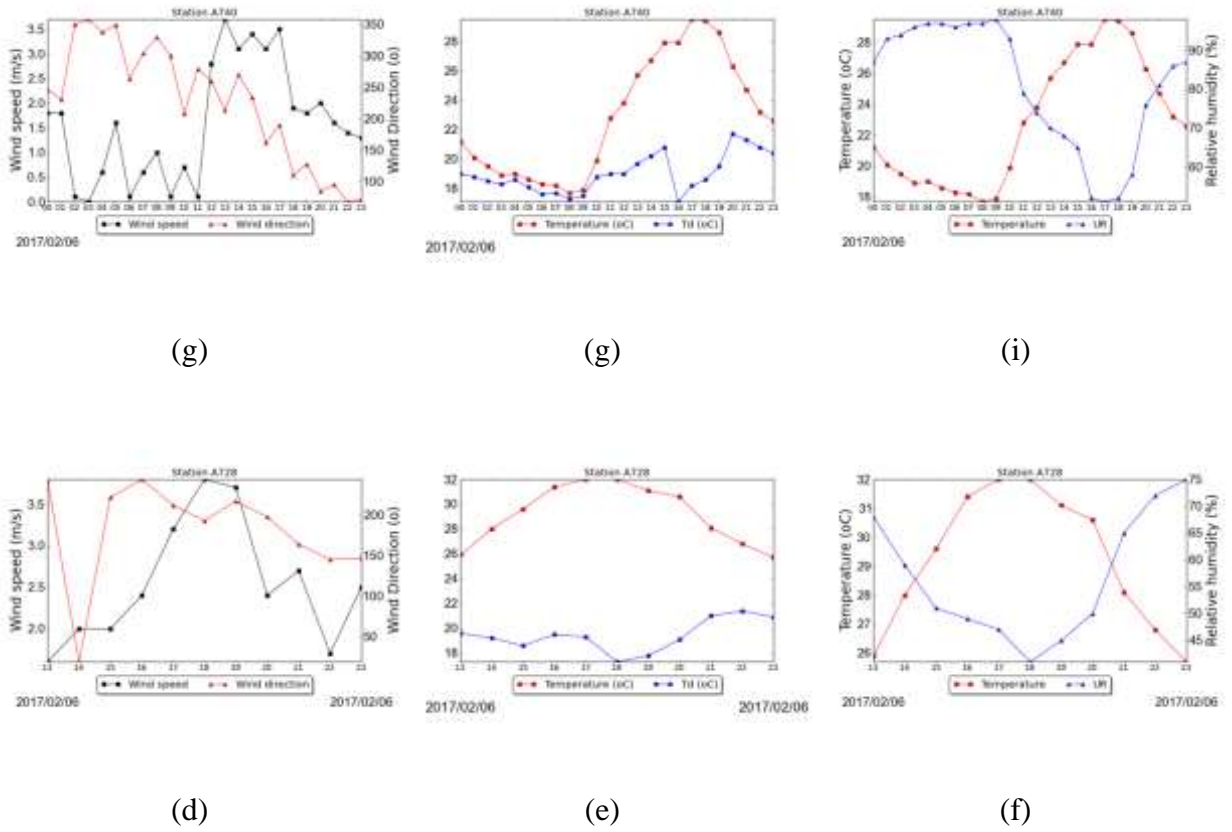
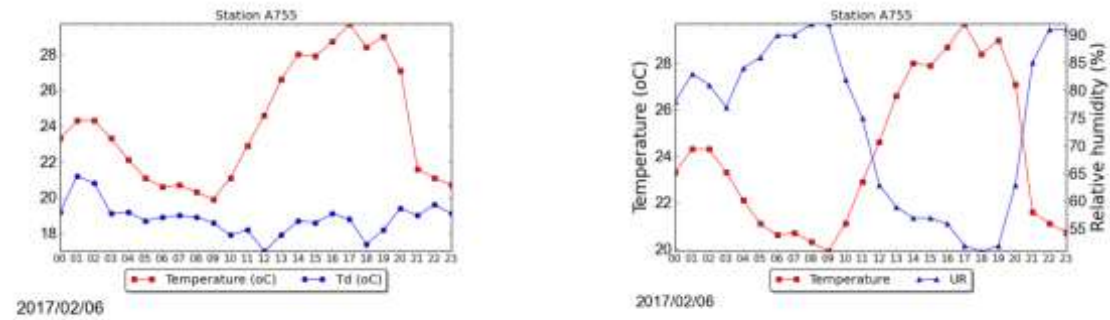


Figure 4-122: Continuation.



(a) (b)
 Figure 4-123: Temperature and dewpoint temperature (a), temperature and relative humidity (b) at station A755 for February, 06th.

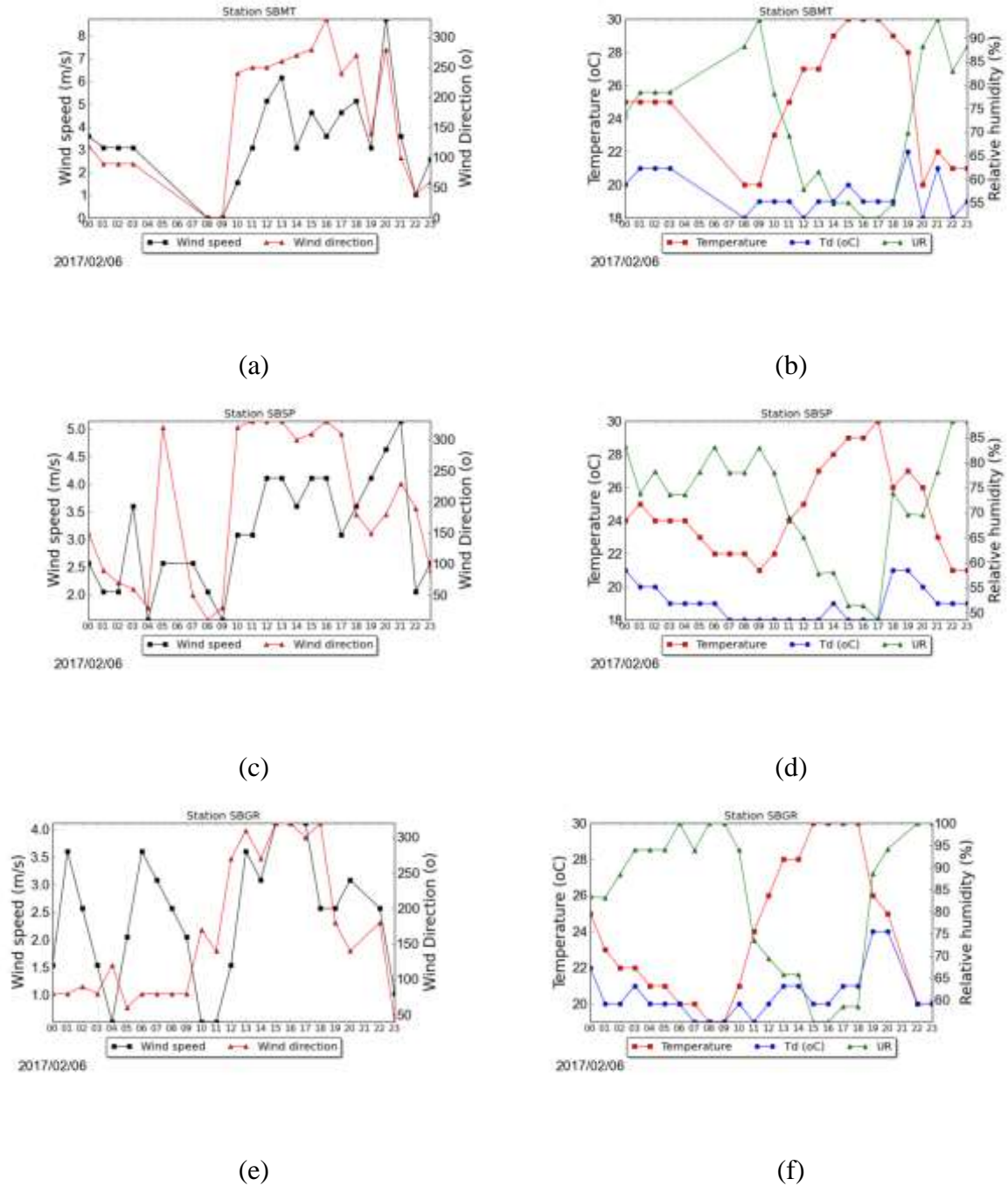
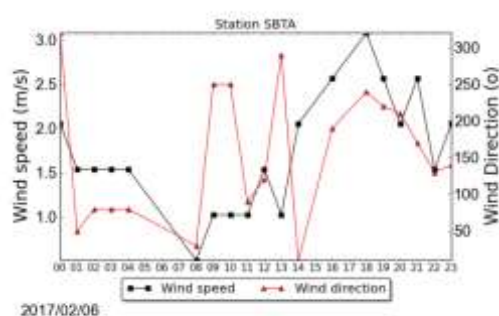
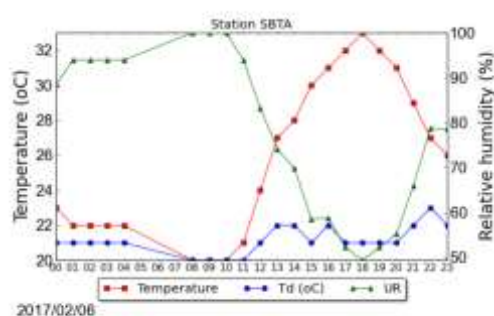


Figure 4-124: Wind speed and direction, temperature, dewpoint temperature and relative humidity from METAR at stations SBMT (a), (b), SBSP (c), (d), SBGR (e), (f), SBTA (g), (h) for February, 06th.

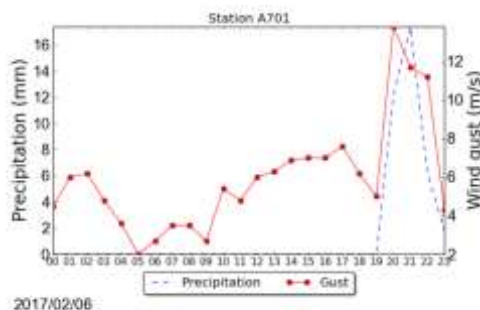


(g)



(h)

Figure 4-124: Continuation.

Figure 4-125: Precipitation (mm) and wind gust (m s^{-1}) at station A701 for February, 06th.

4.1.4 Partial conclusions for category 1 b

Three events were characterized according to this category. Heavy rain was observed during all the events, on January, 07th, 26 points of flash floods were reported in the city of São Paulo, on February, 06th, 36 points were registered (CGE). Floods were also reported on cities at Vale do Paraíba on January, 07th. Wind gusts were observed on January, 30th in the cities of Jundiaí and Campinas, in the city of São Paulo on January, 07th, and in Campinas and São Paulo on February, 06th. Hail was observed in Jundiaí on January, 30th.

The synoptic conditions for each of these events were different. On January, 30th an upper level cyclonic vortex was leading to instabilities in the region. On January, 07th a frontal system was seen near São Paulo, and moisture was extending from it through a trough near the coast, to the east part of the State. This event was put in this category, because it was

believed that this high moisture content on low levels was an important factor in the event. February 06th, is in this category because it seems that a band of clouds extending from a frontal system in the Atlantic Ocean was important in initiating convection. A trough at 850 hPa extending near São Paulo, also appeared to be responsible to increase in relative humidity near the coast.

Mass divergence was seen between $0.2-0.6 \cdot 10^{-4} \text{ s}^{-1}$ near the regions of severe weather occurrences on January, 07th at 12:00 UTC, and between $0.2-0.4 \cdot 10^{-4} \text{ s}^{-1}$ at 06:00, 09:00 and 15:00 UTC on January, 30th. Warm advection was only seen on January, 30th between 09:00 and 15:00 UTC, highest values are seen at 12:00 UTC ranging from 0.2 to $0.8 \cdot 10^{-4} \text{ K s}^{-1}$.

On January, 30th and 07th, the importance of the topography in storm initiation was observed in the satellite and radar images. On February, 06th, it is not clear, but convection developing near the coast could be related to the sea breeze. A moisture convergence and gradient was observed near the coast on February 06th, however the sea breeze appears to have not propagated far inland, probably due to the influence of the large scale system, convection is seen to move following this pattern. According to the stations, the sea breeze reached the city of São Paulo at around 19:00 UTC. On January, 07th it penetrated into the city around 16:00-17:00 UTC. The same hour observed on January, 30th.

Values of CAPE and LI indicated between a marginally and moderately unstable condition and an unstable condition, with probable storms, even severe, in the presence of some lifting mechanism, respectively, at 12:00 and 15:00 UTC. Atmospheric sounding was only available on January, 30th and CAPE was equal to 1042 J kg^{-1} and CIN was equal to -90.5 J kg^{-1} . The 700-500 hPa was between 5.5 and 6 K km^{-1} for all events.

Dry air was observed on January, 30th, values are between 20-30 % around 600-500 hPa, however, values below 20 % are seen between these levels. Relative humidity below 10 % is seen between 500-400 hPa in the atmospheric sounding. Relative humidity above 70 %

is observed on January, 07th, and values between 50 and 60 % are seen around 600-500 hPa on February, 06th, from GFS. The pattern of the vertical cross section of winds is similar between the days of January, 07th and February, 06th. Winds are weak near the surface and a small intensification is seen near 850-700 hPa. Winds near the surface on January, 30th are slightly stronger than seen on the other days and an anticlockwise turn is seen. No significant shear was observed in any of the days analyzed here.

On January, 30th, several occurrences of strong wind gusts were reported; dry air was observed during this day. A high number of analyses would be necessary to make a conclusion about this matter.

4.2 CATEGORY 2

In this category, events are associated with weak synoptic scale forcing, as explained in the methodology section (section 3), in these events the large-scale systems did not help to create a favorable environment for storms development, and they are related only to local circulations.

4.2.1 December, 18, 2016

During this event, severe weather occurrences were reported in São Paulo, Guarulhos, Campinas, and Campos do Jordão. Hail was observed at all these cities. Heavy rain led to flash floods in the city of São Paulo, 7 points according to CGE, Campinas and Guarulhos. A wind gust of more than 20 m s^{-1} was registered at the city of São Paulo; further details will be given in the surface stations analysis.

a. Satellite

From the infrared image at 12:00 UTC shown in (Figure 4-126) it is possible to see that this event was not related to any synoptic system.

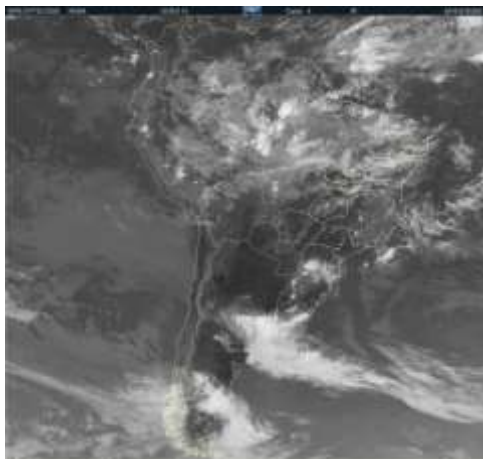


Figure 4-126: Infrared image at 12:00 UTC for December, 18th.

At 15:00 UTC, shown in Figure 4-127, in the 1km visible channel, it is possible to see the formation of the sea breeze in the coast of the State of São Paulo, in the region of Serra do Mar. Clouds began to form in the northeast part of the State, related to the topography in the region. At 16:00 UTC, cells are stronger near the coast and in the northeast region. At 17:00 UTC, the cells formed in relation to the topography and moved southwest to the region of Campinas. In the region of São Paulo, clouds are seen related to sea breeze. In the region of Campos do Jordão, cells develop related to the topography. At 18:00 UTC these clouds seems to merge, and at 19:00 UTC they lost their strength.

Using infrared enhance temperature analysis, shown in Figure 4-128, at 18:00 UTC values around -50 and -60 °C are seen.

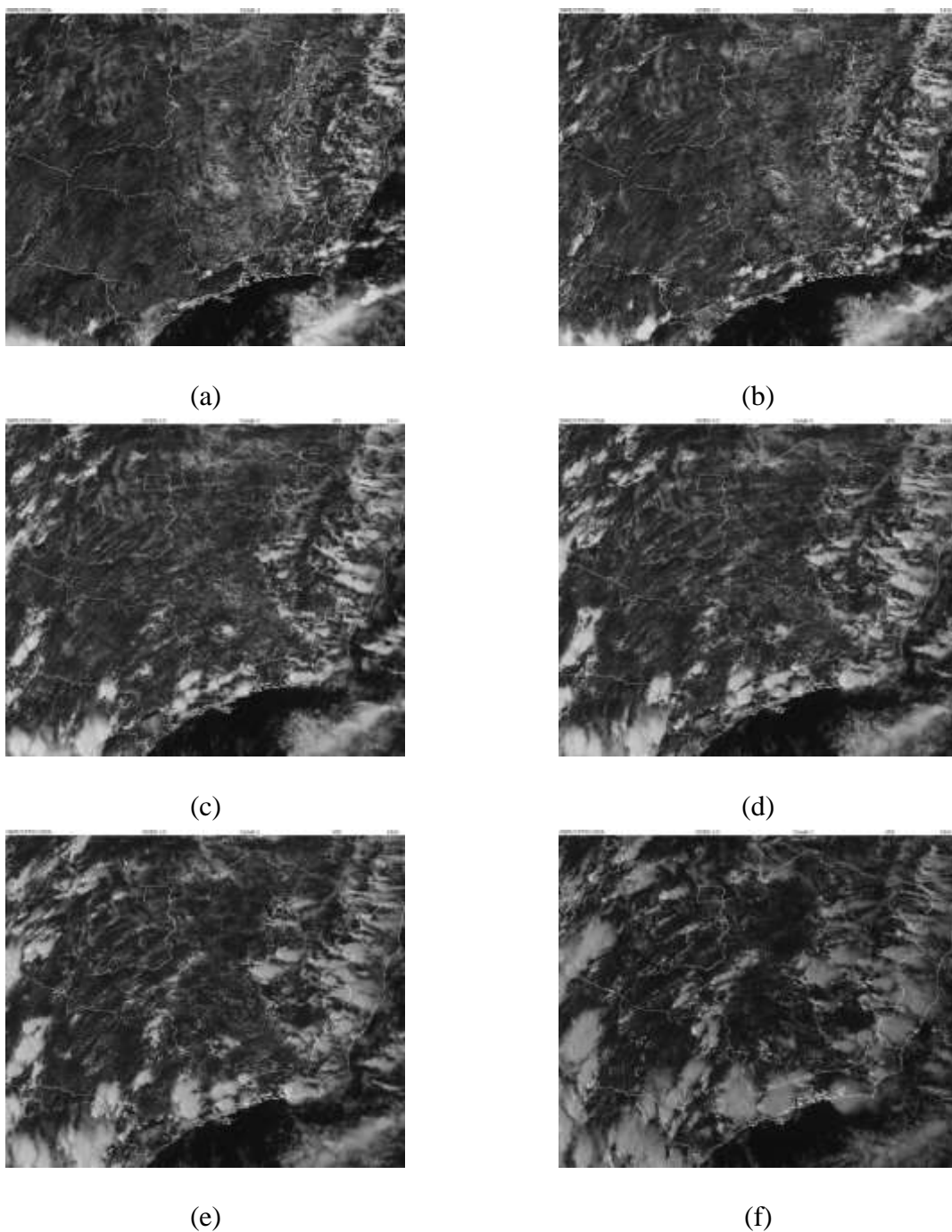


Figure 4-127: Satellite 1 km visible images, at 15:00 UTC (a), 16:00 UTC (b), 17:00 UTC (c), 17:30 UTC (d), 18:00 UTC (e), and 19:00 UTC (f).

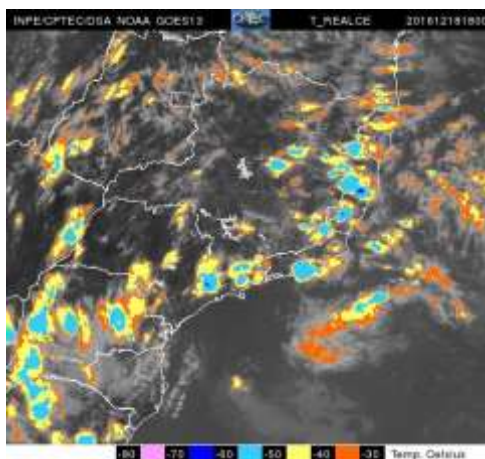


Figure 4-128: Infrared enhanced temperature satellite images at 18:00 UTC.

b. Radar

The development of the cells related to this event is shown in Figure 4-129

Cells started to develop in the region of Serra da Mantiqueira. At 16:00 UTC, it is possible to see that the cells formed in the region of Bragança Paulista are propagating to the region of Campinas. In the region of Francisco Morato and Franco da Rocha clouds are observed. At 17:00 UTC, a cell started to develop in the region of São Paulo, related to the sea breeze penetration. Several clouds are seen between São Paulo and Campinas at 17:20 UTC, and between 1720 and 17:40 UTC they seemed to merge in the region of São Paulo. At 17:30 UTC the highest reflectivity values is observed in the region of Campinas, around 55-60 dBZ. In São Paulo, the highest values are around 50-55 dBZ, at 17:40 UTC. Then, it moves to the region of Guarulhos, between 1820 and 18:40 UTC reflectivity values, in the region, are around 60-65 dBZ. It continued to move northeast, and eventually lost it strength.

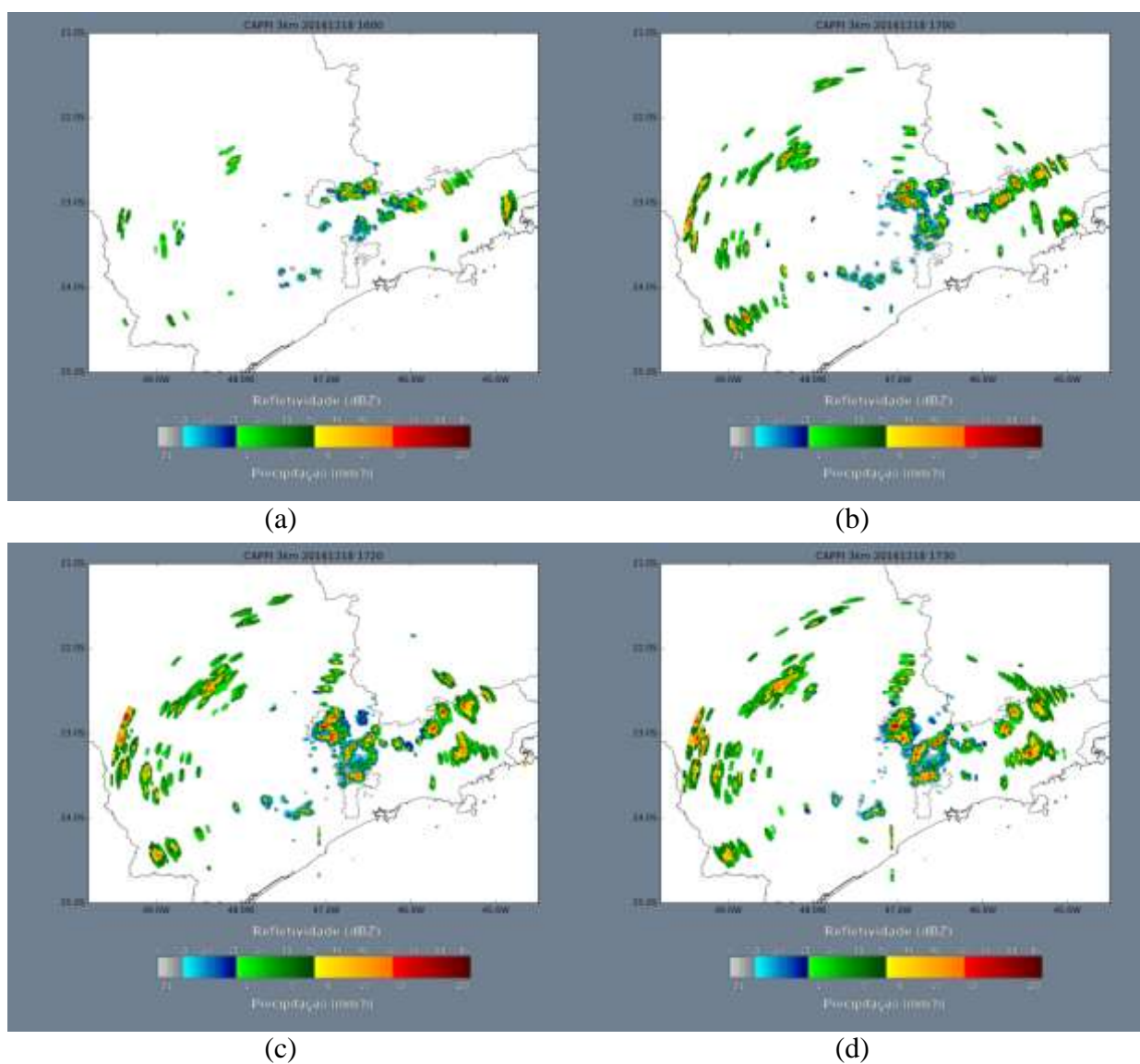


Figure 4-129: Images from the São Roque radar at 16:00 UTC (a), 17:00 UTC (b), 17:20 UTC (c), 1730 (d), 1740 (e), 18:00 UTC (f), 18:20 UTC (g), 18:40 UTC (h), 19:10 UTC (i), and 2030 UTC (j).

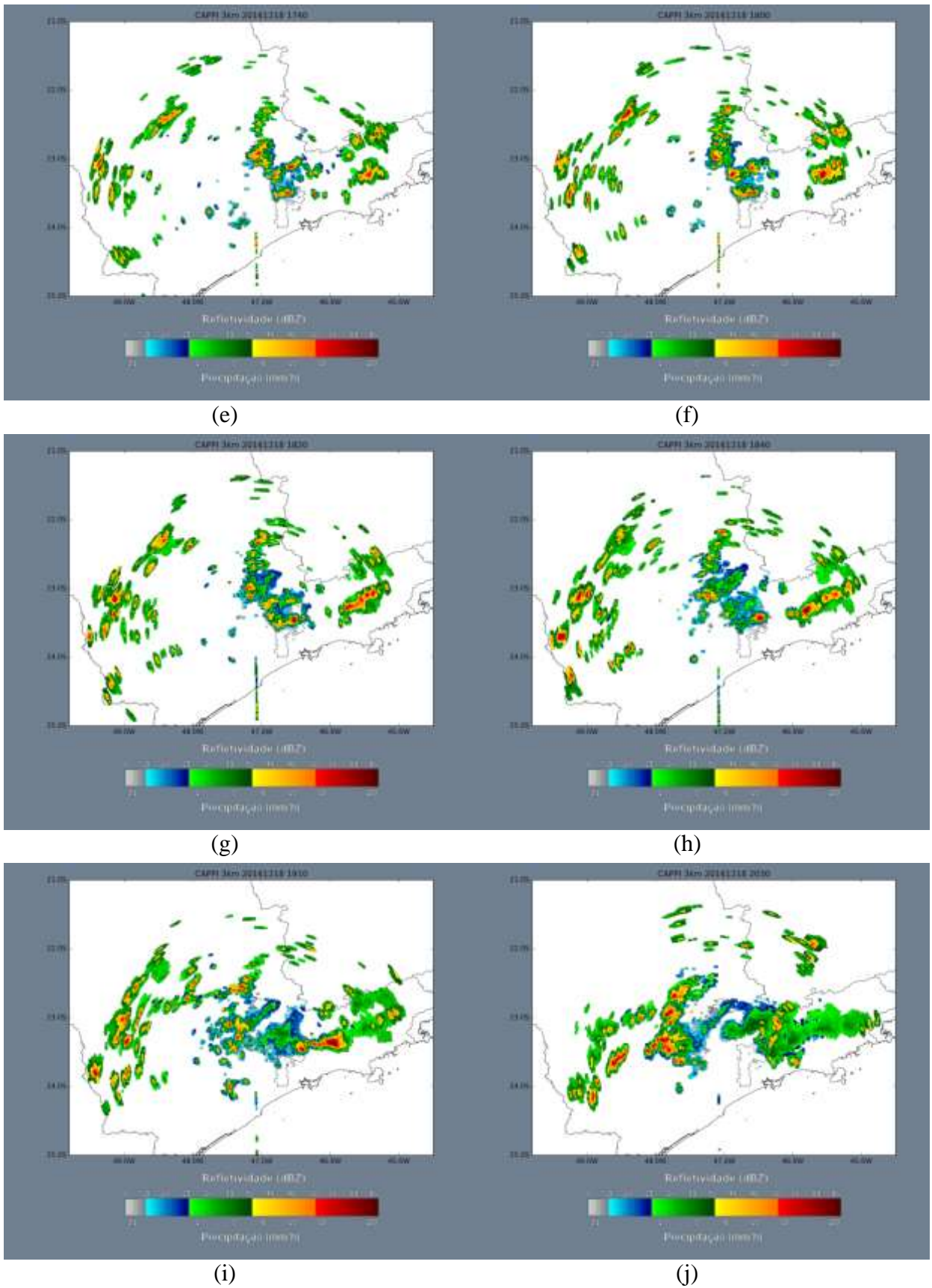


Figure 4-129: Continuation.

The city of Campos do Jordão registered hail on this day. In the region, cells formed due to the local topography, at 17:20 UTC, reflectivity values are between 55-60 dBZ.

c. Synoptic scale and mesoscale

There was a trough located at higher levels (200 hPa) southeast of the State of São Paulo at 00:00 UTC, it intensified throughout the analysis and at 12:00 UTC, a low circulation was seen in the State of Rio de Janeiro (Figure 4-130). At 18:00 UTC it was seen as trough again. At 18:00 UTC it is the only time a mass divergence is seen in this day, small values are observed in the east region and southwest, and a little more (between $0.4-0.6 \times 10^{-4} \text{ s}^{-1}$) intense values at center-north. A small negative vorticity is observed in the 500 hPa analysis in the region of the trough, seen in Figure 4-131. A high pressure system is seen at this level in southwest Minas Gerais and northern São Paulo after 12:00 UTC. Nearly neutral vorticity advection is seen on this day (Figure 4-131).

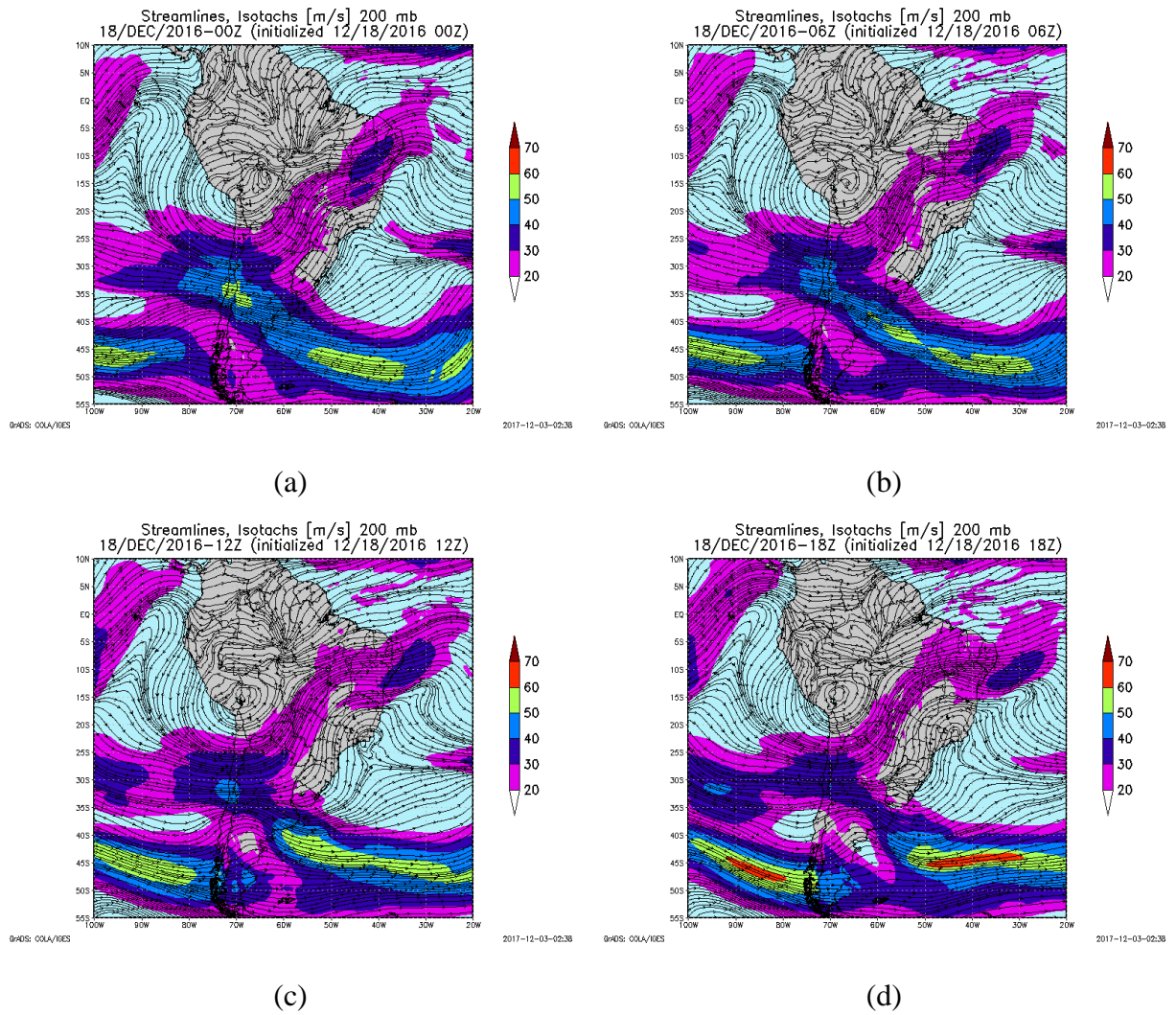


Figure 4-130: Streamlines and isotach (m s^{-1}) at 200 hPa at 00:00 UTC (a), 06:00 (b), 12:00 UTC (c), and 18:00 UTC (d) for December, 18th.

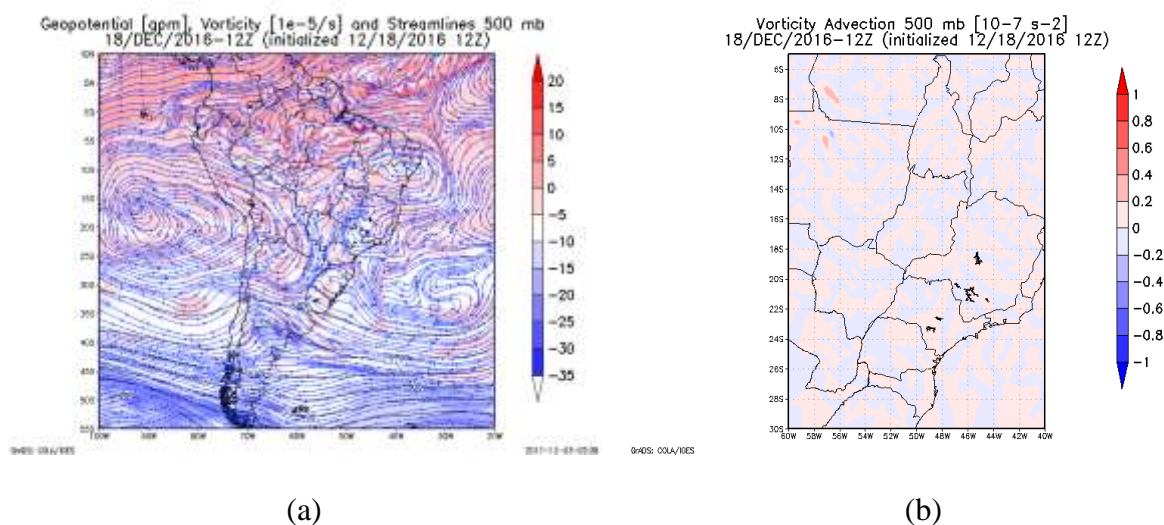


Figure 4-131: Geopotential (gpm) and vorticity ($1 \times 10^{-5} \text{ s}^{-1}$) (a), vorticity advection ($1 \times 10^{-7} \text{ s}^{-2}$) (b) at 500 hPa at 12:00 UTC, for December, 18th.

Figure 4-132 shows streamlines and relative humidity at 850 hPa and mean sea level pressure and winds at 12:00 UTC. A northwest flow is seen at 850 hPa directed to Uruguai and the south region of Brazil, which means that, this one was not related to the low-level jet. In the surface analysis a high pressure system is seen in the Atlantic throughout the day. Warm advection is seen near the region of Campinas at 12:00 UTC, between 0.4 and $0.6 \times 10^{-4} \text{ K s}^{-1}$ and above $1.0 \times 10^{-4} \text{ K s}^{-1}$ in the central region of the State.

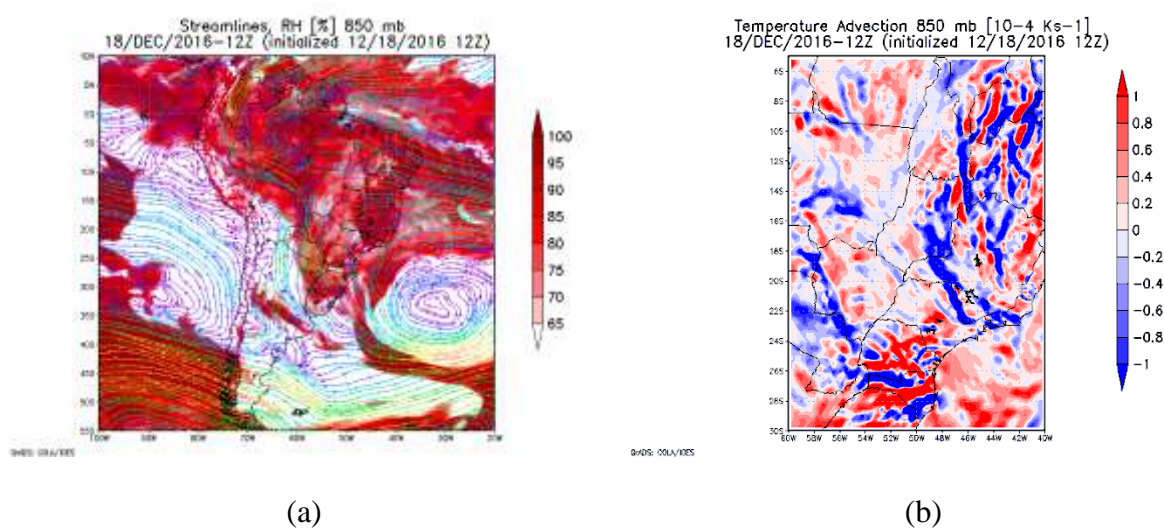


Figure 4-132: Streamlines and relative humidity (%) (a), temperature advection ($1 \times 10^{-4} \text{ K s}^{-1}$) (b) at 850 (b) , for December, 18th.

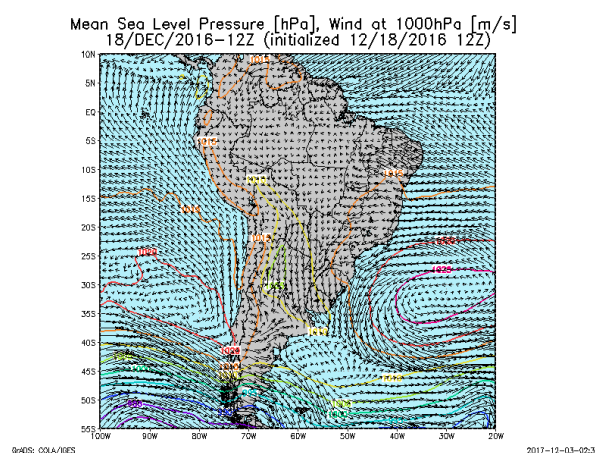


Figure 4-133: Mean sea level pressure (hPa) and wind (m s^{-1}) at 12:00 UTC for December, 18th.

d. Thermodynamic and mesoscale analysis

Using the BRAMS output fields, CIN, shown in Figure 4-134, at 12:00 UTC, is above -20 J kg^{-1} . In the CAPE analysis from the BRAMS, shown in Figure 4-135, at 12:00 UTC, is only seen in small regions between 1200 and 1600 J kg^{-1} . At 15 and 16 UTC, CAPE values in the regions of the event are around 1400 - 2200 J kg^{-1} , indicating a moderately unstable condition.

From the GFS, at 12:00 UTC, CAPE was around 800 - 1200 J kg^{-1} , near São Paulo and Campinas. This indicates a condition between marginally and moderately unstable. At 15:00 UTC it is between 1200 and 1600 J kg^{-1} , indicating a moderately unstable condition.

In the LI analysis from GFS, seen in Figure 4-136, is between -3 and -5 K through most of the State at 12:00 UTC, and between -5 and -6 K in the region of São Paulo and Campinas at 15:00 UTC, these values, both at 12:00 and 15:00 UTC indicates an unstable condition with probable storm, even severe. CIN, from the GFS at 12:00 UTC, is below -50 J kg^{-1} in the southeast region of the State, values between -20 and -30 J kg^{-1} are seen in the north and central regions. Near Campinas, values between -30 and -40 J kg^{-1} are also seen at this hour.

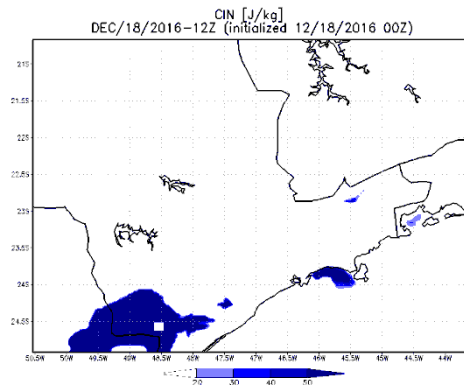
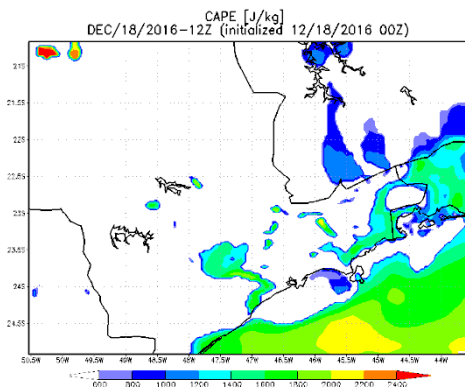
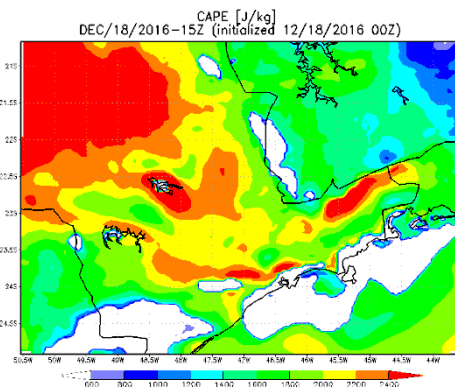


Figure 4-134: CIN from BRAMS at 12:00 UTC, for December, 18th.

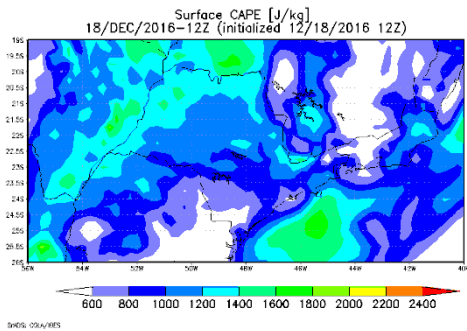


(a)

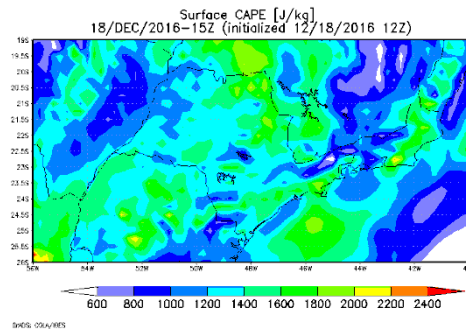


(b)

Figure 4-135: CAPE from BRAMS at 12:00 UTC (a), and 15:00 UTC (b), for December, 18th.

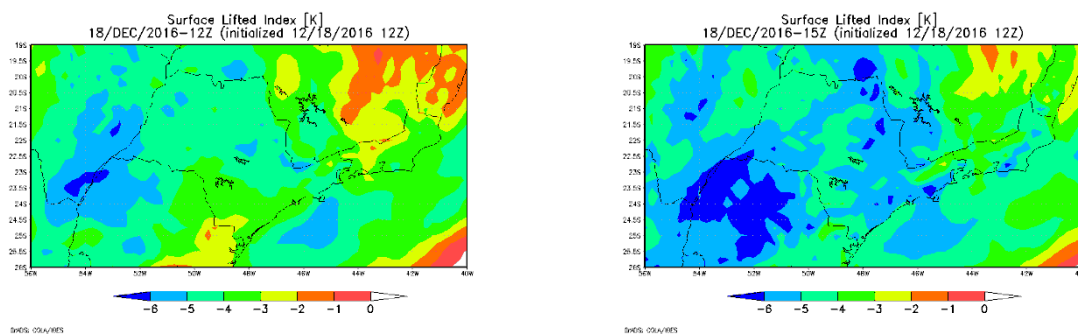


(a)



(b)

Figure 4-136: CAPE from GFS at 12:00 UTC (a), and 15:00 UTC (b), for December, 18th.



(a)

(b)

Figure 4-137: LI from GFS at 12:00 UTC (a), and 15:00 UTC (b), for December, 18th.

The 700-500 hPa lapse rate from GFS, seen in Figure 4-139, increased from the beginning of the analysis, from 6-6.5 K km⁻¹ to 6.5-7.0 K km⁻¹ at 12:00 UTC.

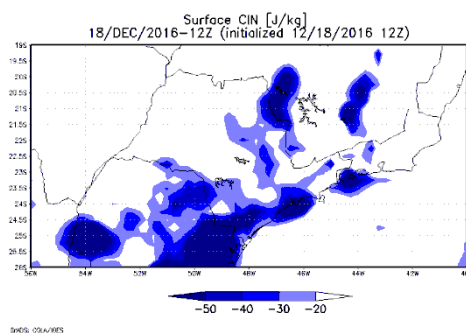
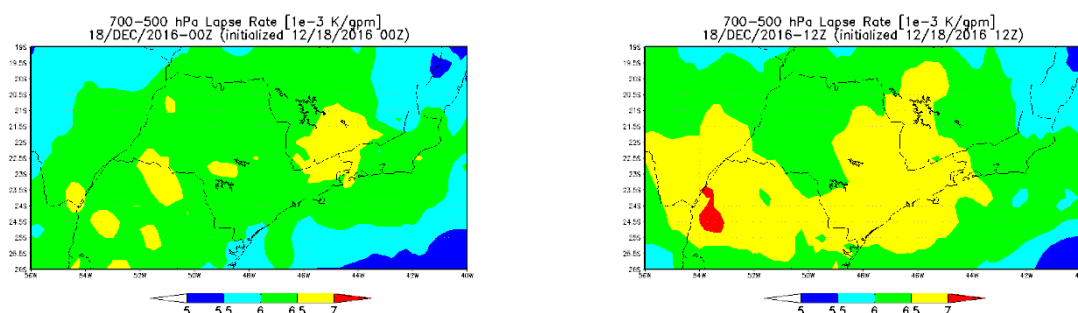


Figure 4-138: CIN from GFS at 12:00 UTC, for December, 18th.



(a)

(b)

Figure 4-139: 700-500 hPa lapse rate from GFS at 00:00 UTC (a), and 12:00 UTC (b), from December, 18th.

At 15:00 UTC and 16:00 UTC, gradient of moisture is observed related to the sea breeze. Moisture divergence is shown in Figure 4-140. At 13:00 UTC it is possible to see the formation of a line of moisture convergence along the coast with values around -3.5 to $-4 \times 10^{-3} \text{ g kg}^{-1} \text{ s}^{-1}$. Between 13:00 and 16:00 UTC it is possible to see this convergence moving into the continent.

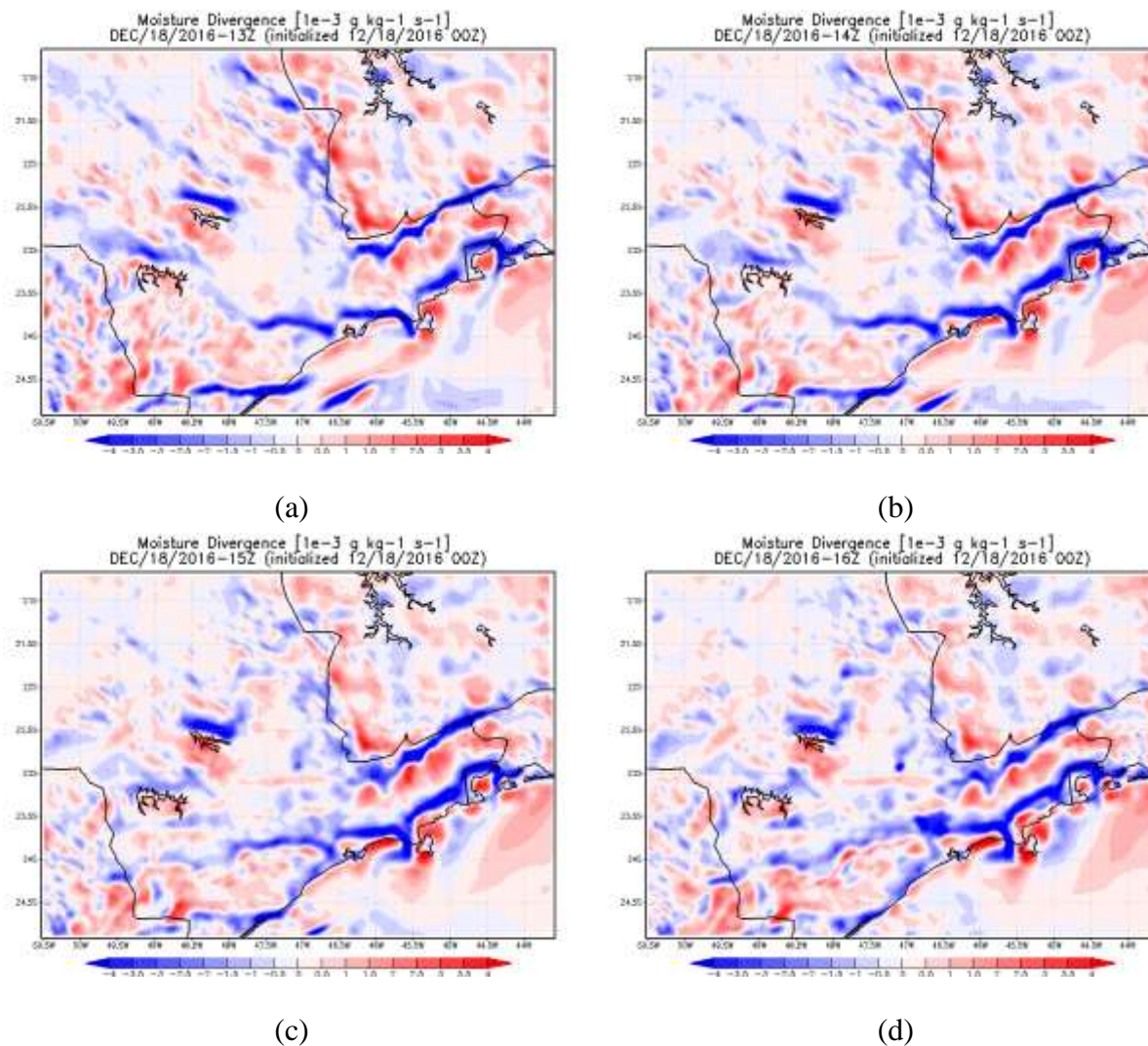


Figure 4-140: Moisture divergence at 13 UTC (a), 14:00 UTC (b), 15:00 UTC (c), and 16:00 UTC (d).

The wind throughout the day is shown in Figure 4-141.

At 00:00 UTC winds were in the southeast-east quadrant. Throughout the day it changed to northeast, as can be seen at 12:00 UTC. At 13:00 UTC the wind near the coast is

starting to change its direction, from that hour it is possible to see the wind changing to southeast and getting stronger as the sea breeze advances into the continent. After 23:00 UTC the wind starts to change its direction northeast, as can be seen at 04:00 UTC, December, 19th.

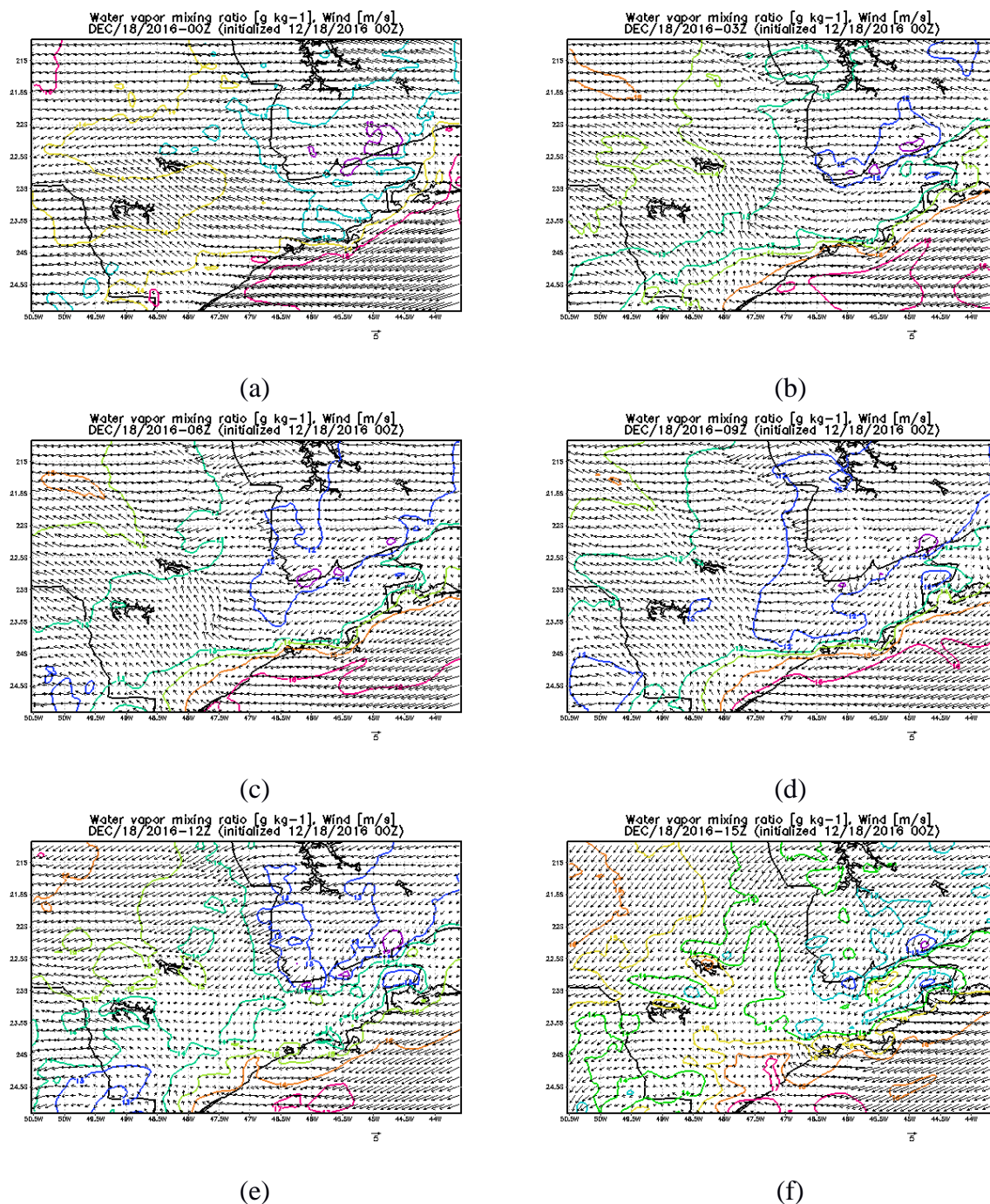


Figure 4-141: Water vapor mixing ratio and wind at 00:00 UTC (a), 03 UTC (b), 06:00 UTC (c), 09:00 UTC (d), 12:00 UTC (e), 15:00 UTC (f), 18:00 UTC (g), 21:00 UTC (h).

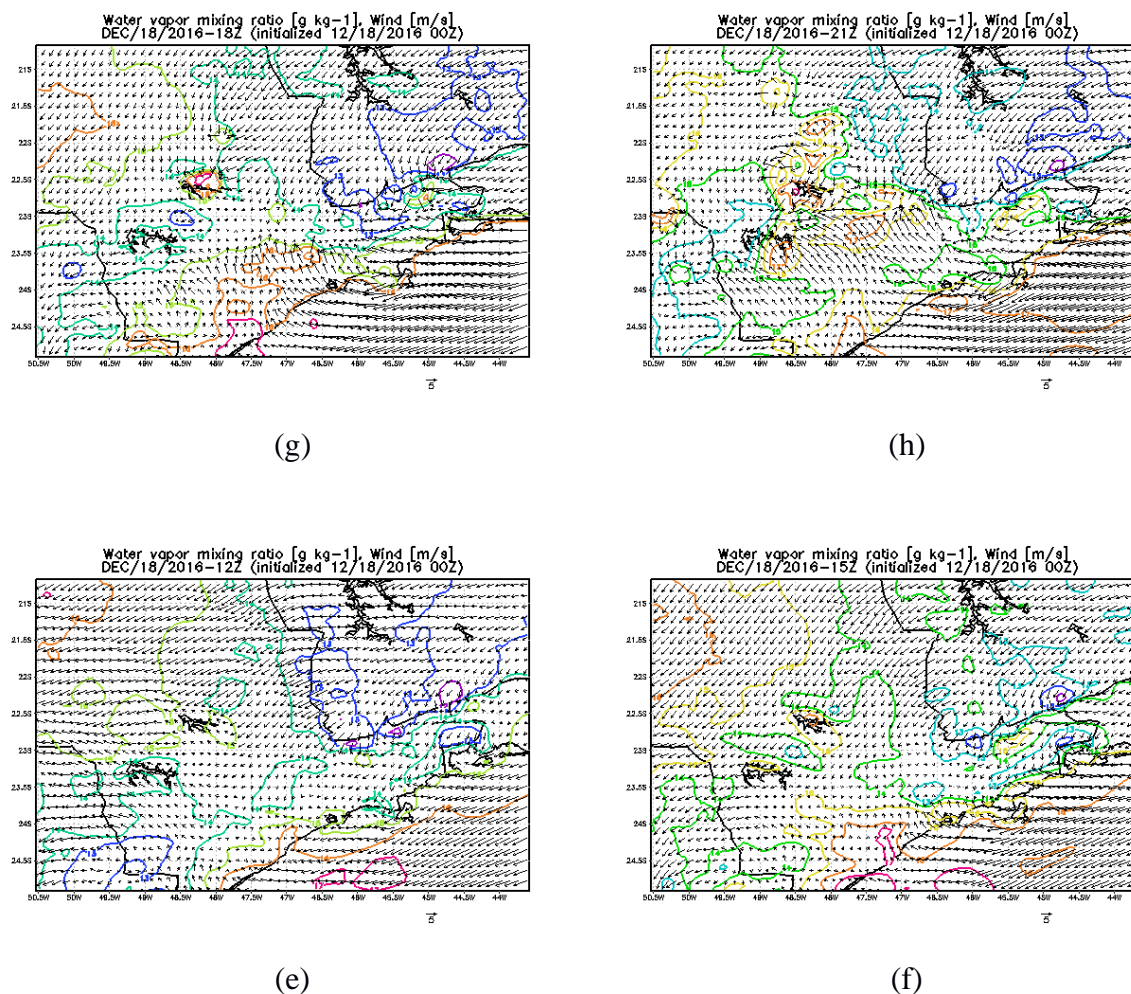


Figure 4-141: Continuation.

To analyze the vertical structure of the atmosphere in this event, the latitude of the city of São Paulo was fixed to show vertical cross sections of variables in this region. The relative humidity cross sections show how dry was the atmosphere that day, and it reached values around 40-50 % in mid-levels, near the top of the model, at 12:00 UTC (Figure 4-142), indicating instability and the potential for severe storms. When the atmosphere is dry, there is a potential for the development of wind gust, due to the evaporation at mid-levels. West from 47° W, values are between 30 and 40 %. The same is seen at 15:00 UTC.

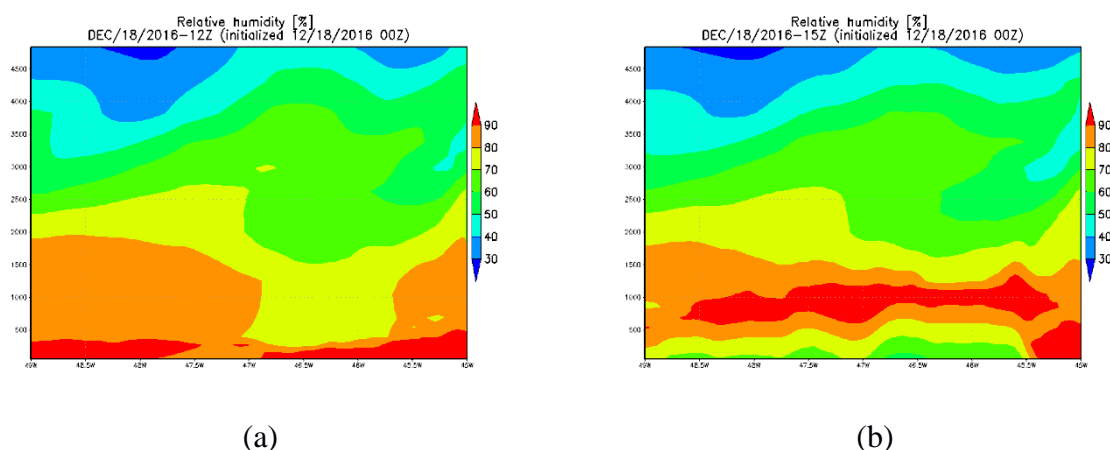


Figure 4-142: Vertical cross section of relative humidity from BRAMS at 23.5° at 12:00 UTC (a), and 15:00 UTC (b), for December, 18th.

Winds, from the BRAMS analysis, (Figure 4-143), are weak through the atmosphere, at 12:00 UTC. Near 46.5°W a small increase with height is seen near the surface, but winds get weak again. Winds are still weak at 15:00 UTC, with no predominantly direction.

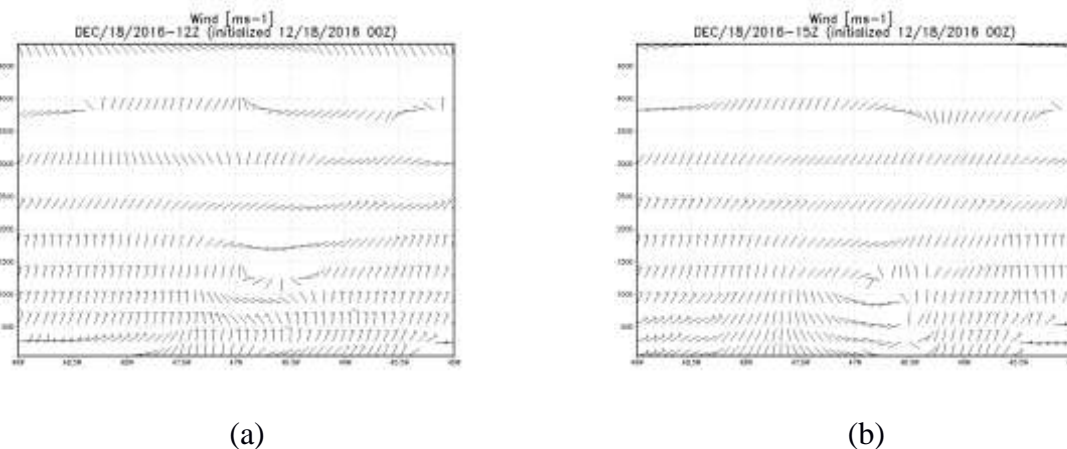


Figure 4-143: Vertical cross section of wind from BRAMS at 23.5° at 12:00 UTC (a), 15:00 UTC (b), for December, 18th.

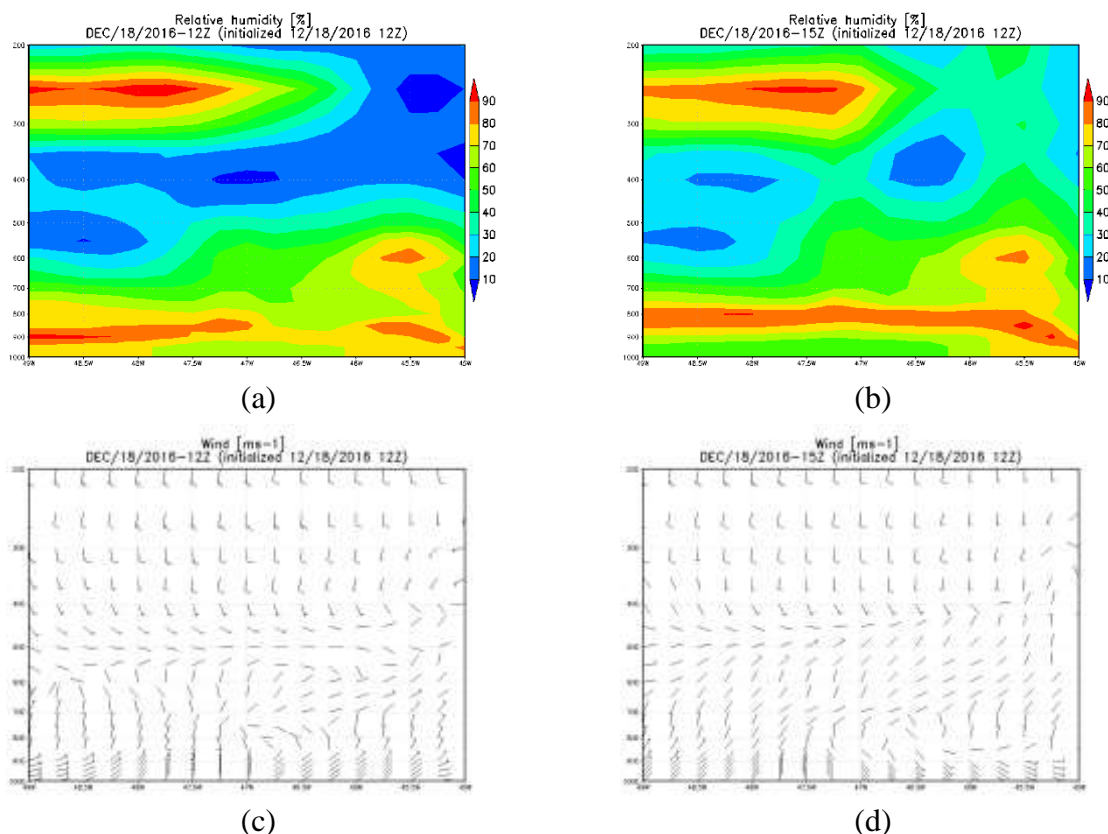


Figure 4-144: Vertical cross section from GFS at 23.5°S of relative humidity at 12:00 UTC (a), 15:00 UTC (b); winds at 12:00 UTC (c), and 15:00 UTC (d), for December, 18th, 2016.

From GFS, the vertical cross section for the latitude of 23.5°S, at 12:00 UTC, shows that, between 600-500 hPa, it is around 40-60 %, lower values, between 10 and 30 % are seen in this layer, west of 47°W. This same range is seen everywhere, between 450-300 hPa. This values increase at 15:00 UTC, and, between 600-500 hPa, it is around 50-70 %. Values of the same range are still seen between 450 and 300 hPa. The vertical cross section of winds also shows that winds were weak through the atmosphere and only increased above 450 hPa, this is seen at 12:00 and 15:00 UTC.

e. Surface stations

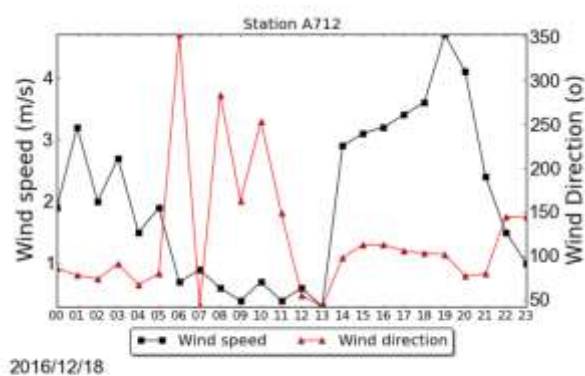
For this event 19 stations were analyzed. As it was already noted, this event was related to the sea breeze penetration in the State. Station A712 is located at the coast of the State shows an increase in dew point temperature starting at 11 UTC, with wind change to

southeast (Figure 4-145). The maximum temperature registered that day was of 29.3 °C at 16:00 UTC. The wind turns to southeast at 16:00 UTC at A701, seen in Figure 4-145, this was also noted in the METAR analysis from Congonhas airport, and at 17:00 UTC southeast winds are seen at Campo de Marte, these are all related to increase in dew point temperature and relative humidity.

Precipitation and wind gust observed are shown in Figure 4-147. The most severe phenomena happened in the station localized in the city of São Paulo, Mirante de Santana, where it rained 53.6 mm in two hours (peak between 17:00 and 18:00 UTC of 39.6 mm) with a gust of 21.5 ms⁻¹ between 17:00 and 18:00 UTC. Less than 1 mm was registered at between 19:00 and 20:00 UTC. According to CGE, until 17h10 local time, six stations recorded more than 30 mm, three stations registered rain indices above 60 mm, station localized at Lapa, recorded 73.4 mm. From the Alto do Tiete network, four registered more than 60 mm, and one also recorded more than 70 mm. A wind gust of 14.3 ms⁻¹ was registered at the airport of Guarulhos.

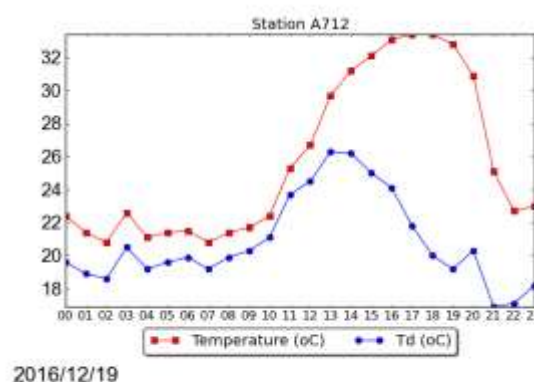
Station A713 (Sorocaba) registered a total of 30.8 mm in two hours (started between 19:00 and 20:00 UTC), wind gust of 18 ms⁻¹ was registered between 19:00 and 20:00 UTC and 14.7 ms⁻¹ was observed in the following hour. Analyzing this station is not possible to determine if the sea breeze reached it and at the time it occurred. The wind changed to southeast at 19:00 UTC, but dew point temperature increased at 20:00 UTC, the same hour which rain was registered. In the radar analysis, convection that formed in the topographic region of Serra da Mantiqueira, moved to the region of Campinas and continued to move and reached the region of Sorocaba. It is possible, considering the time of the sea breeze penetration in the city of São Paulo, that the sea breeze did help convection to get strong, adding moisture in the region. In the BRAMS analysis, it is possible to see the sea breeze reaching this region around 18:00-19:00 UTC.

Station A755, located at Barueri, the closest to the city of São Paulo, registered an increase in dew point temperature and relative humidity at 17:00 UTC, which is indicative of the sea breeze, but this station does not have a record of wind direction. It was registered 13.6 mm at 19:00 UTC, less than 1 mm was observed at 20:00 UTC. Station A740, located at the city of São Luiz do Paraitinga, in the Vale do Paraíba, also registered, wind change with increase in dew point temperature, at 17:00 UTC, shown in Figure 4-145. Rain was registered in the station, between 17:00 and 18:00 UTC.



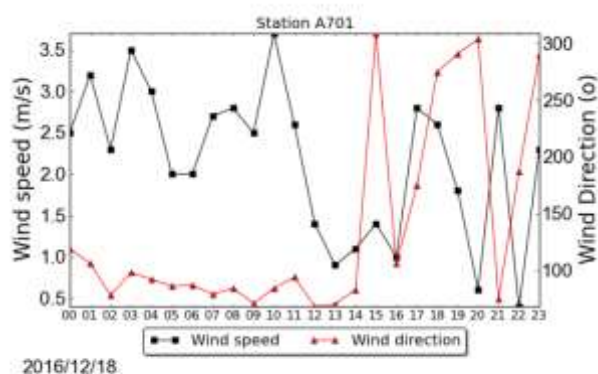
2016/12/18

(a)



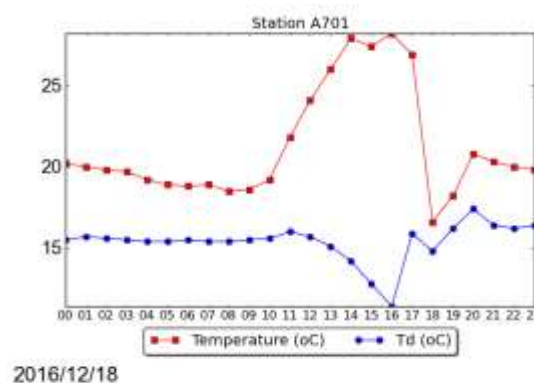
2016/12/19

(b)



2016/12/18

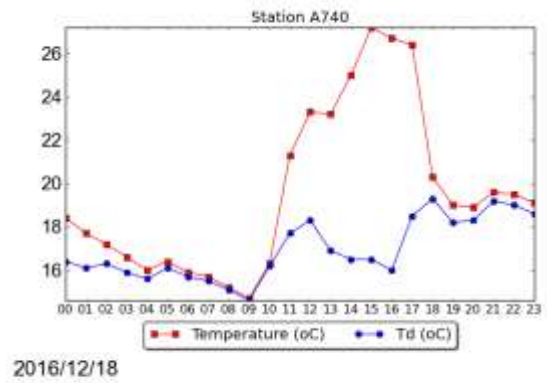
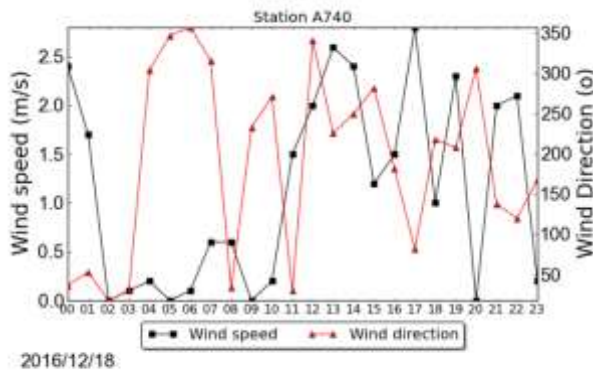
(c)



2016/12/18

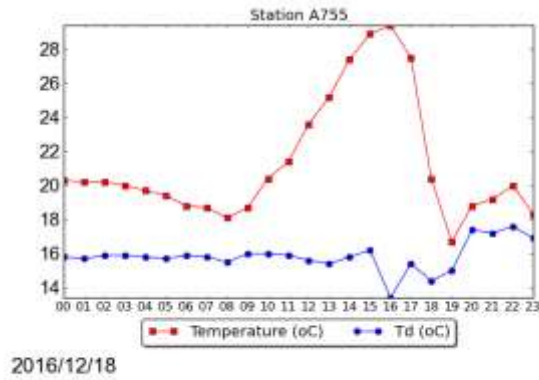
(d)

Figure 4-145: Wind speed and direction, temperature and dew point temperature at stations A712 (a) and (b), A701 (c) and (d), A740 (e) and (f), A755 (g), , for December, 18th.



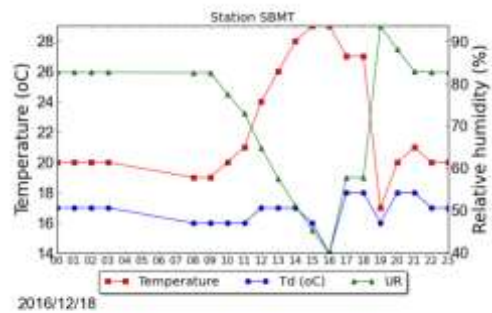
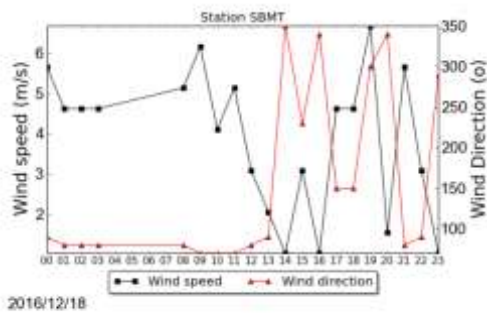
(e)

(f)



(g)

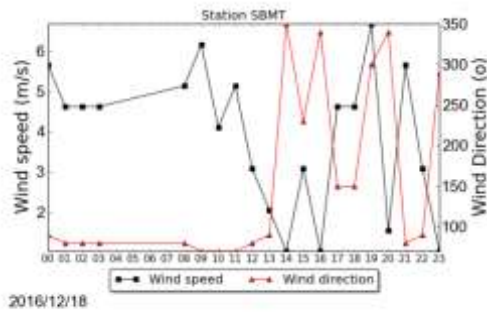
Figure 4-145: Continuation.



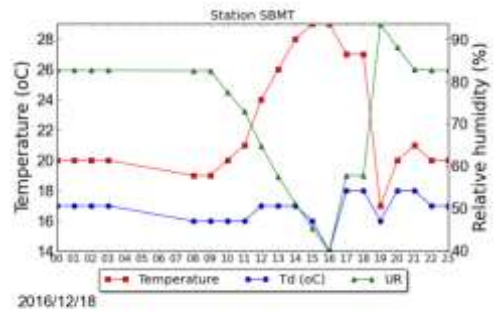
(a)

(b)

Figure 4-146: Wind speed and direction from METAR at SBSP (a), SBMT (c); temperature, relative humidity, and dew point temperature at SBSP (b), and SBMT (d).

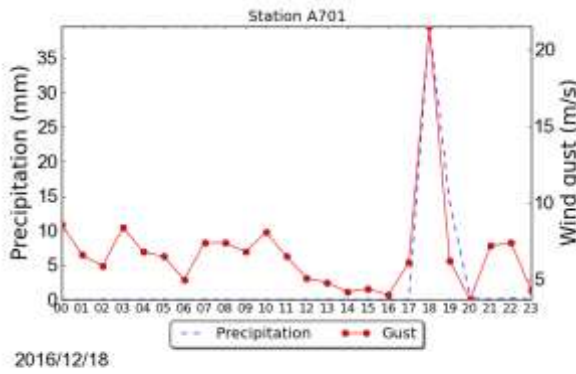


(c)

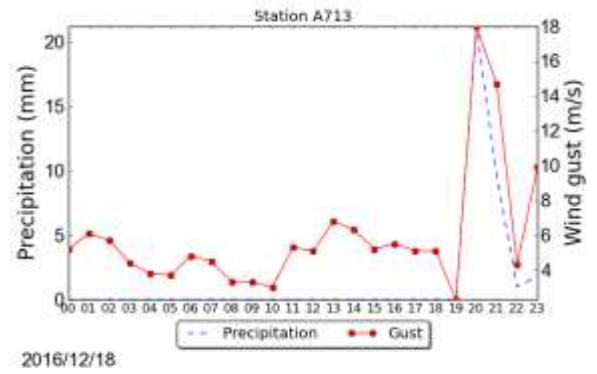


(d)

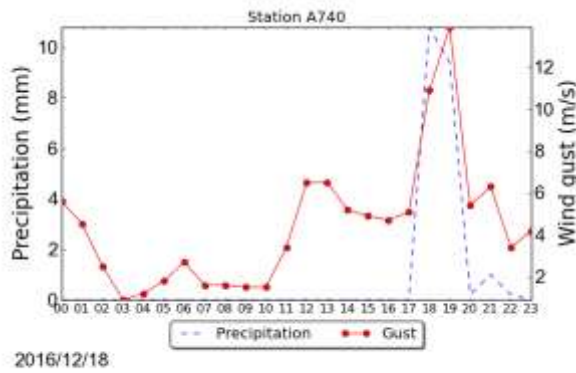
Figure 4-146: Continuation.



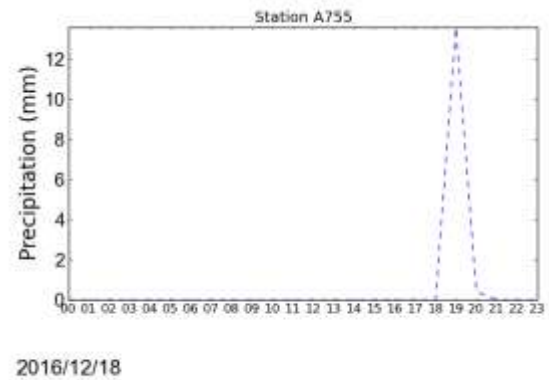
(a)



(b)



(c)



(d)

Figure 4-147: Precipitation and wind gust at station A701 (a), A713 (b), A740 (c), and precipitations at station A755 (d), for December, 18th.

4.2.2 December, 25, 2016

Severe weather occurrences were only reported for Campinas during this event. Hail and strong wind gusts, of 26.8 ms^{-1} , were observed in the city. This led to fall of trees, no floods were reported.

a. Satellite

In Figure 4-148 is seen the infrared satellite image for South America, and it is possible to see that this event was not related to a synoptic scale system.



Figure 4-148: Infrared satellite image at 12:00 UTC.

The satellite images seen in Figure 4-149 show the evolution of the cells in this event. At 13:00 and 14:00 UTC it is possible to see the formation of the sea breeze in the coast of the State. At 15:00 UTC cells start to develop in the region of Serra da Mantiqueira, in the northeast region of the State, the sea breeze is also seen in the coast. Cells related to the sea breeze penetration are already developing in the continent at 16:00 UTC (Vale do Paraíba) and at 17:00 UTC. At 18:00 UTC, these cells are stronger in the southeast of Minas Gerais

and northeast of São Paulo, it is possible that, in the northeast region of São Paulo, the sea breeze penetration aided in their development. It moves to the region of Campinas.

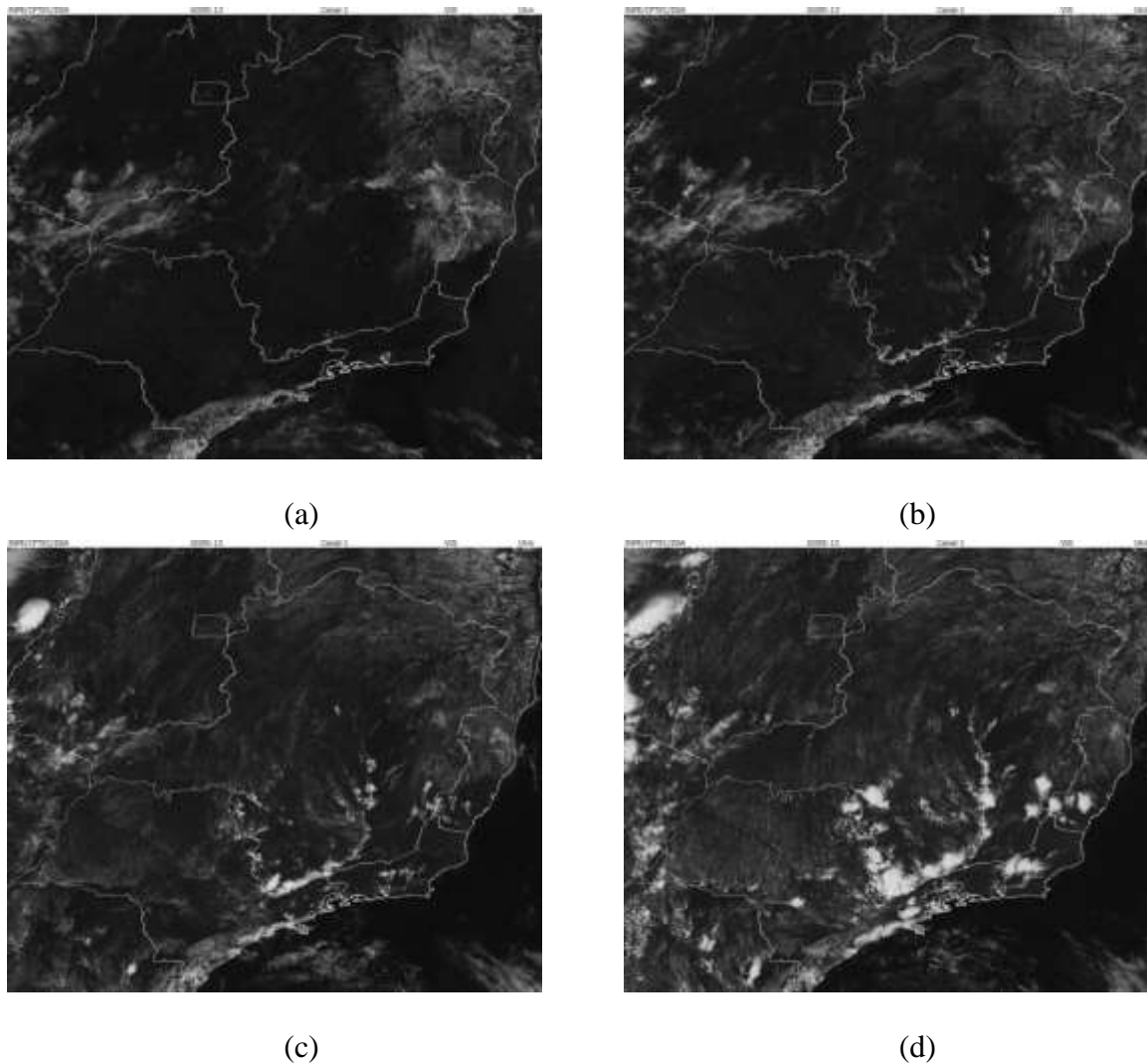


Figure 4-149: Satellite 1 km visible images, at 13 UTC (a), 14:00 UTC (b), 15 UT (c), 16:00 UTC (d), 17:00 UTC (e), 18:00 UTC (f), 1830 UTC (g), and 19:00 UTC (h), for December, 25th.

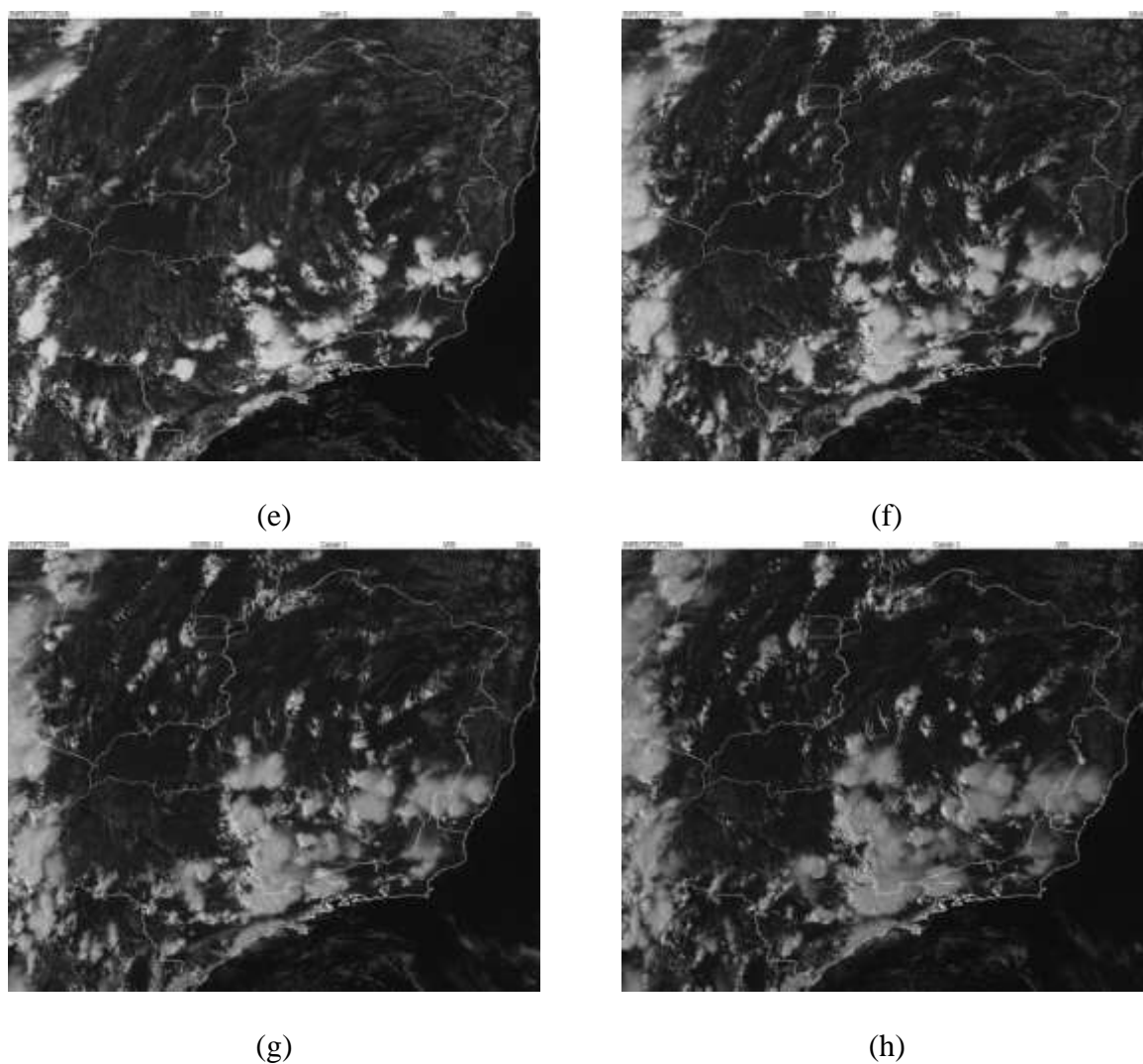


Figure 4-149: Continuation.

b. Radar

The development of the storm that occurred on December, 25 is seen in the radar images from São Roque in Figure 4-150. At 14:00 UTC a few clouds formed in the northeast region of the State of São Paulo and southeast region of Minas Gerais, probably due to the local topography. At 16:50 UTC reflectivity values are between 60-65 dBZ in the region of Extrema, Minas Gerais. Some cells are observed, at this hour, in the region of Campinas, probably local, related to the high temperatures observed during the day. These cells are not very intense (around 40 dBZ).

At 17:20 UTC, northeast of Guarulhos, cells with reflectivity values around 55 dBZ are observed, probably related to the sea breeze circulation and topography (in the city of Nazaré Paulista). Between 17:20 and 18:00 UTC new cells developed from these cells and the cells in the southeast region of Minas Gerais, and merged, while local convection is still seen in Campinas with reflectivity values around 40 dBZ. It continued to propagate, and at 18:50 UTC and intense convective clouds are seen in the region of Jarinu, Itatiba, Valinhos and Campinas, with reflectivity values around 60 dBZ, in Itatiba is between 60-65 dBZ. In the region of Campinas it intensifies and values around 60-65 dBZ are observed at 19:40 UTC. In Campinas, strong wind gusts and hailstorm were reported.

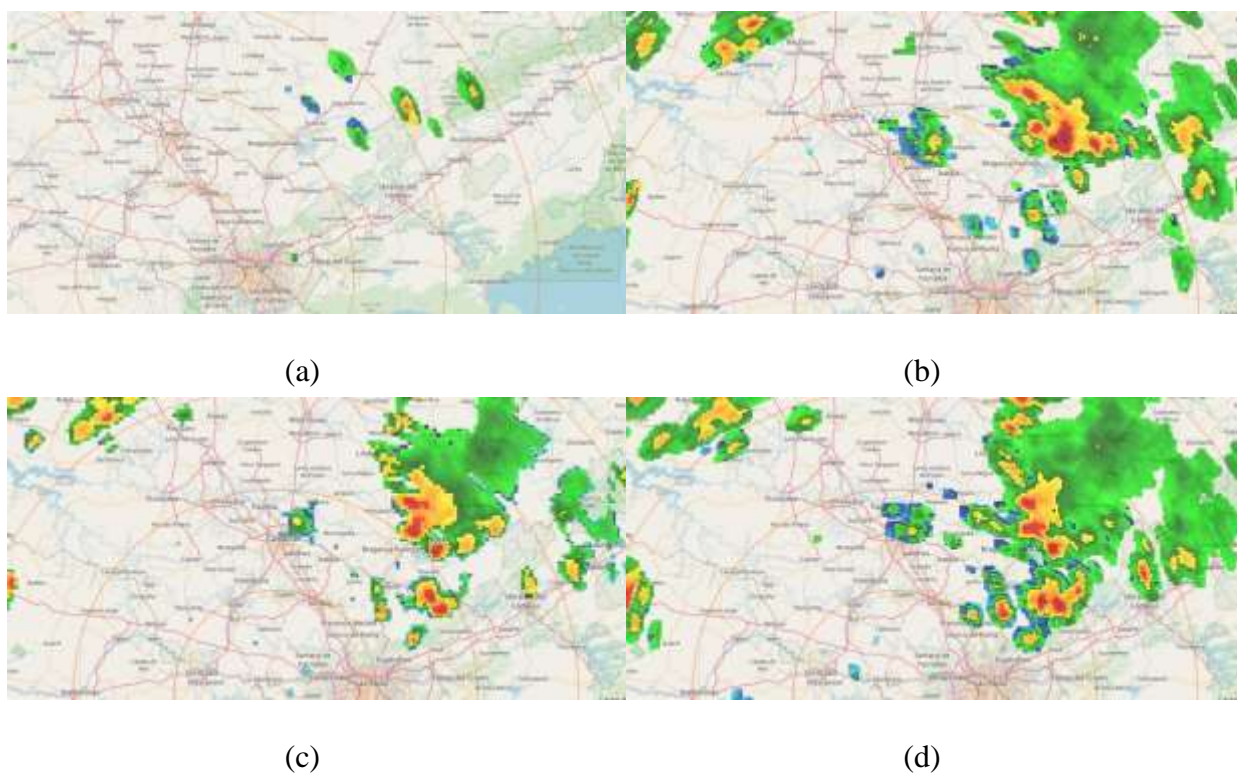


Figure 4-150: Images from the São Roque radar at 14:00 UTC (a), 1650 UTC (b), 17:20 UTC (c), 1730 (d), 1740 (e), 18:00 UTC (f), 1850 UTC (g), 19:10 UTC (h), 19:40 UTC (i), and 20:00 UTC (j).



(e)

(f)



(g)

(h)



(i)

(j)

Figure 4-150: Continuation.

In this event, several factors contributed to the occurrence of severe weather. The sea breeze was a factor that helped add moisture to the State. The local topography also had an important role.

c. Synoptic scale and mesoscale

In the 200 hPa analysis, the Bolivian high is seen, but is not well characterized. The most relevant parameter is a trough in the Atlantic, east of the south region of Brazil, which moves eastward throughout the day, seen in Figure 4-151 at 12:00 UTC. In the 500 hPa

geopotential and vorticity analysis, the trough is seen associated with negative vorticity (Figure 4-151). After 12:00 UTC a high pressure system is seen between northeastern Paraná and southeastern São Paulo, this system causes subsidence.

There is a frontal system associated with this trough, from the 850 hPa temperature field is possible to determine its position located in the region of high temperature gradient and confluent winds, it is also possible to locate it in the surface analysis in the region of confluent winds. The front is located far from the coast of the State of São Paulo, and it moves even further away throughout the day, as the system moves eastward. Another important feature is the high pressure system associated with this front moving behind it, seen in the east of Uruguai and the State of Rio Grande do Sul at 00:00 UTC, and also moving further away from the continent in the day. Low relative humidity is seen in the State at 12:00 UTC, it is below 65 %.

In the wind divergence at 200 hPa, vorticity advection at 500 hPa and temperature advection at 850 hPa fields no significant pattern is seen (shown for the 12:00 UTC analysis in Figure 4-152) which means, vorticity advection, wind divergence at 200 hPa and warm advection were not important in this event.

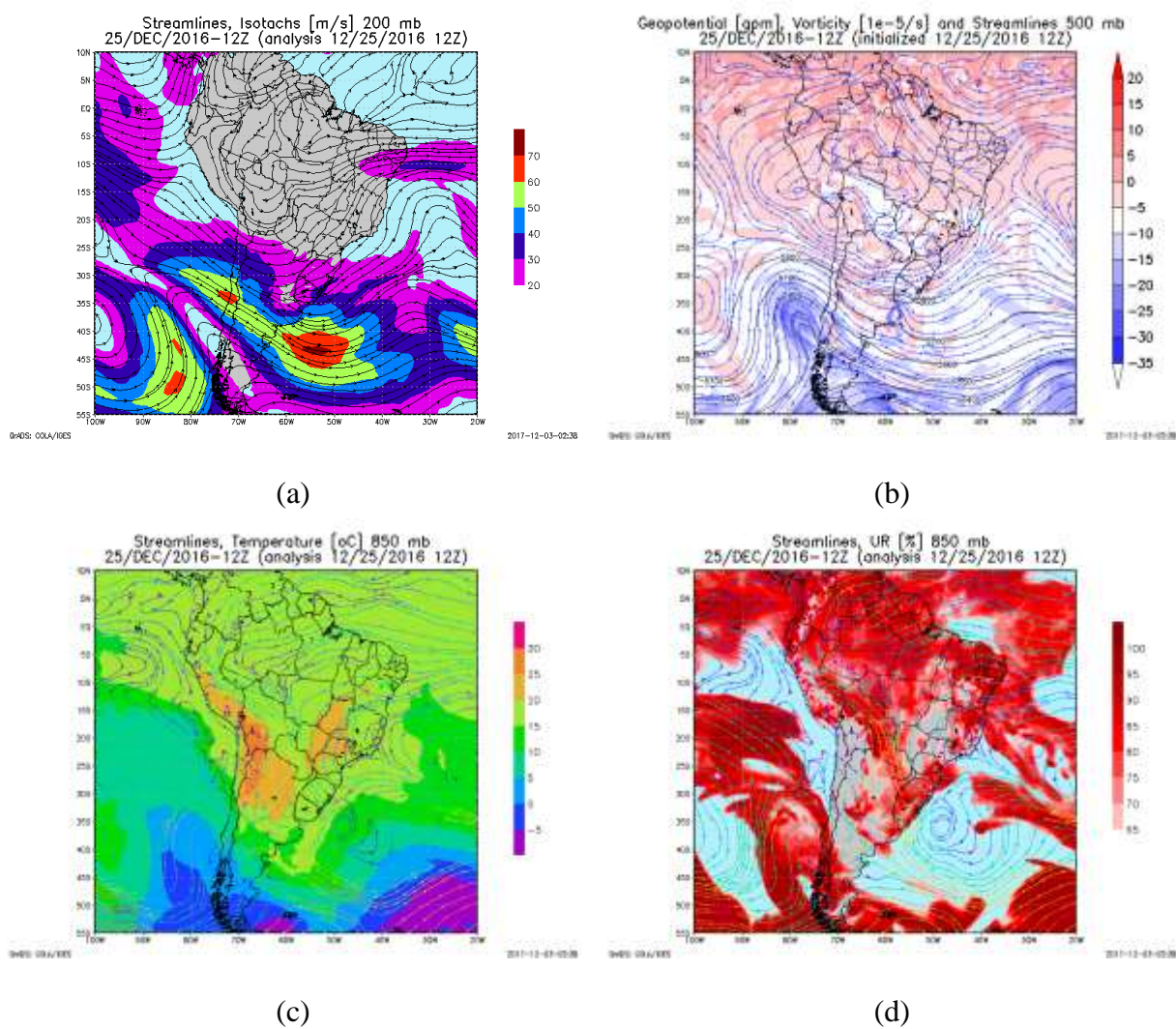


Figure 4-151: Streamlines and isotachs ($m s^{-1}$) at 200 hPa (a), geopotential height (gpm) and vorticity at 500 hPa (b), streamlines and temperature ($^{\circ}C$) at 850 hPa (c), and streamlines and relative humidity (%) at 850 hPa (d) at 12:00 UTC.

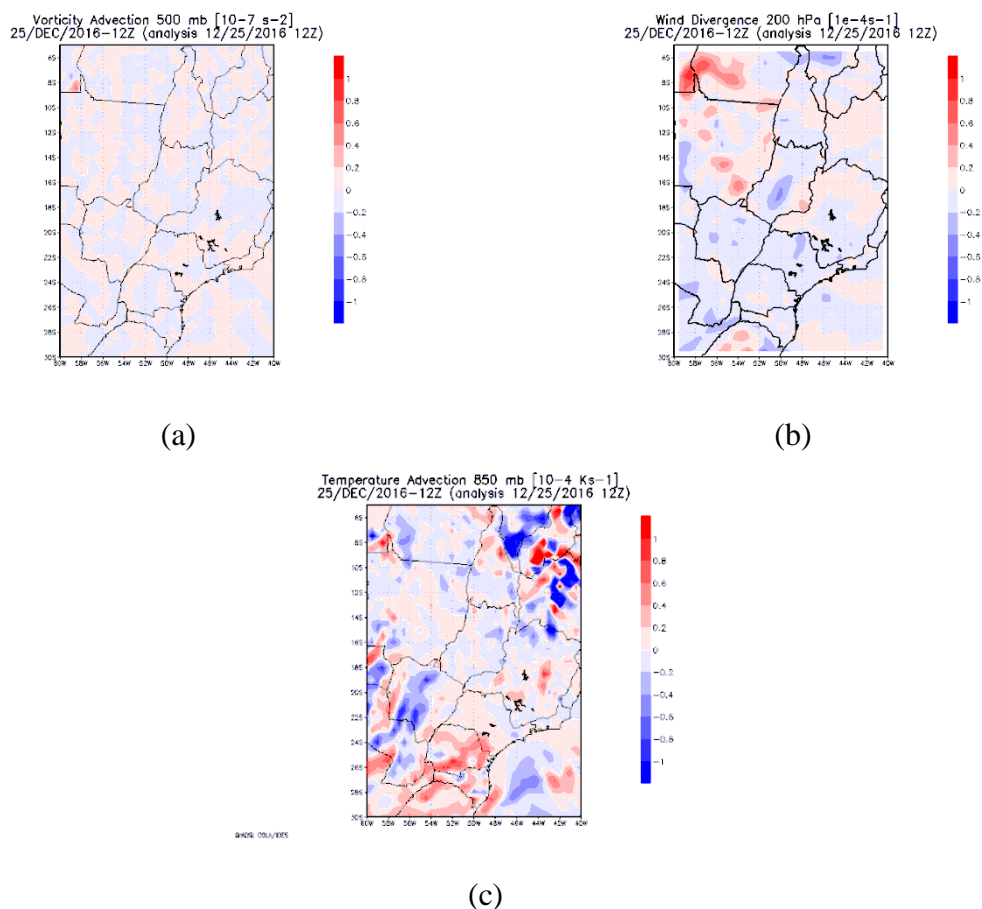


Figure 4-152: Vorticity advection at 500 hPa (a), wind divergence at 200 hPa (b), temperature advection at 850 hPa (c) at 12:00 UTC.

In the surface analysis, as already mentioned, the cold front is seen in the region of confluent winds. One interesting thing is the post-frontal high pressure system, as it moves eastward, after 12:00 UTC, it seems to be leading to southeast winds near the coast of São Paulo.

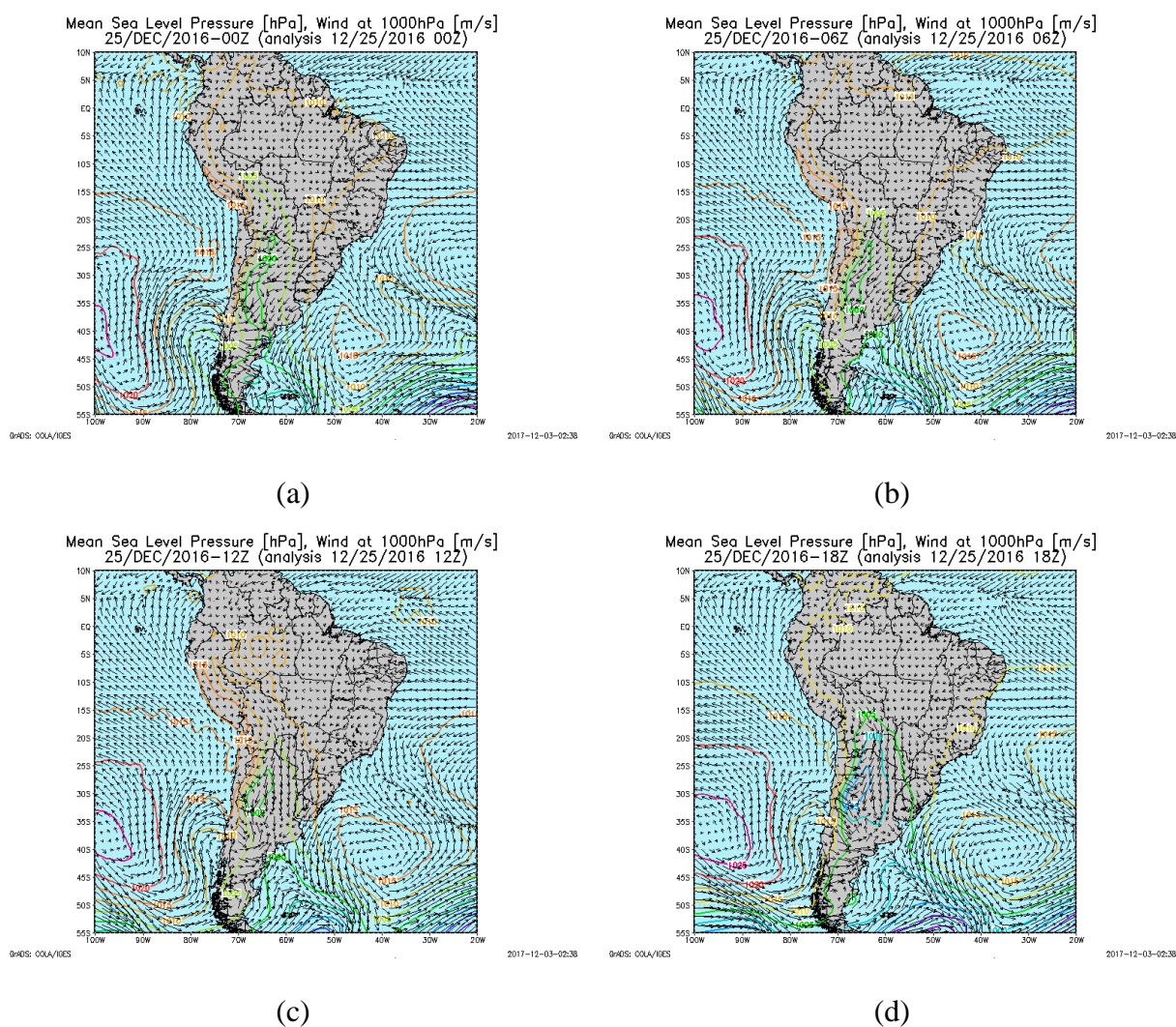


Figure 4-153: Mean sea level pressure and winds at 00:00 UTC (a), 06:00 UTC (b), 12:00 UTC (c), 18:00 UTC (d).

d. Thermodynamic and mesoscale analysis

Convective inhibition (Figure 4-155) is below 20 J kg^{-1} at 12:00 UTC.

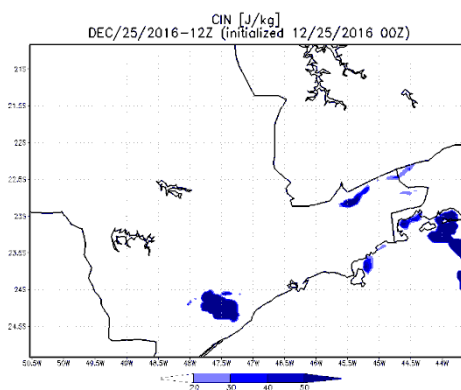


Figure 4-154: CIN (J kg^{-1}) from the BRAMS model at 12:00 UTC.

Values of CAPE from BRAMS are seen in Figure 4-156, at 15:00 UTC the region of Campinas has CAPE between 1400-1800 J kg^{-1} . It increases, and at 17 UTC, in the region of Campinas it is around 1800- 2200 J kg^{-1} . CAPE is not seen in the State at 12:00 UTC. These values indicate a moderately unstable condition.

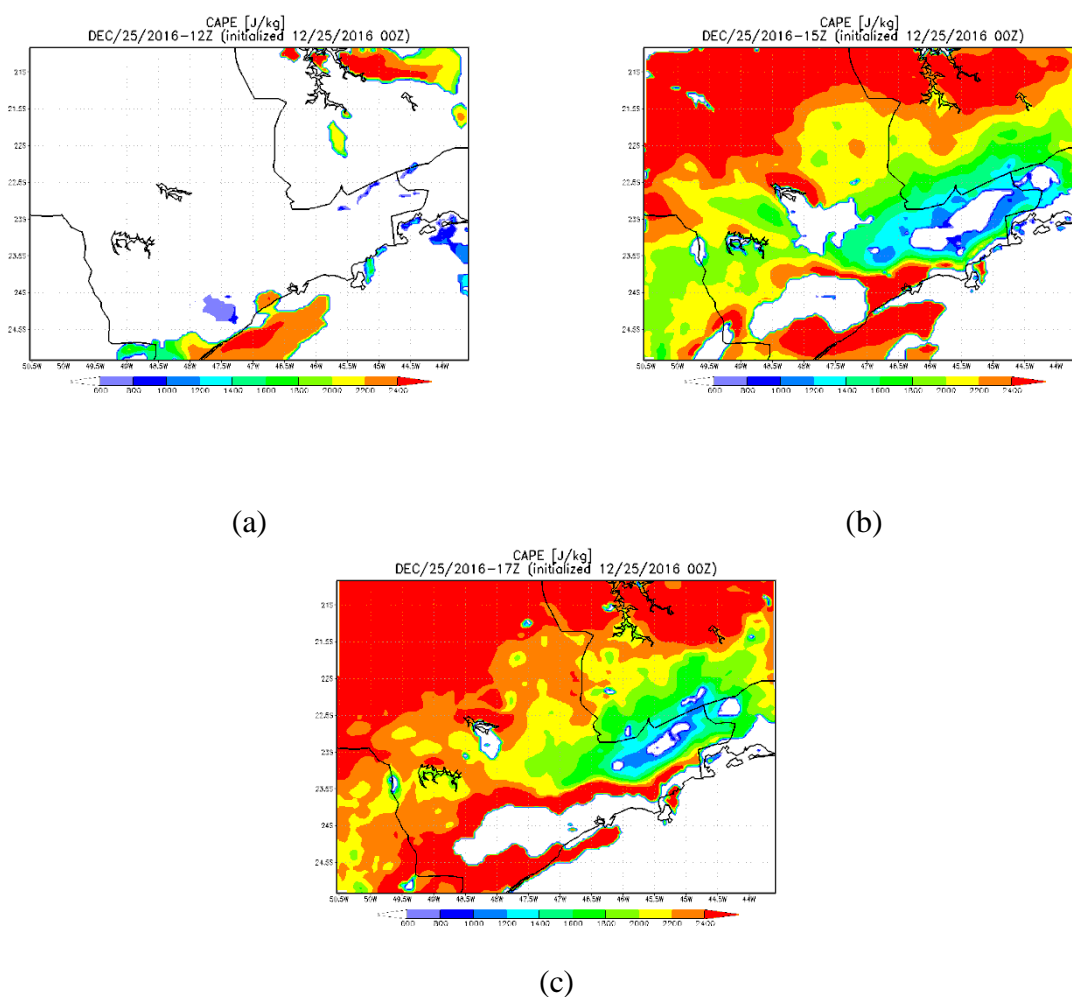
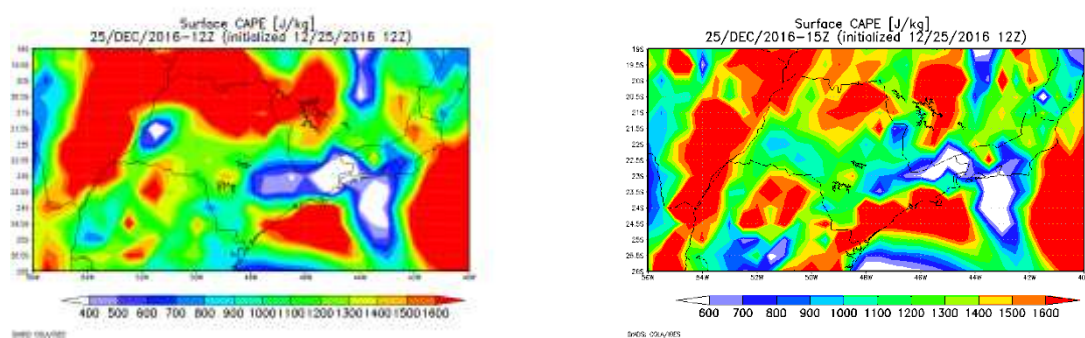


Figure 4-155: CAPE (J kg^{-1}) from BRAMS at 12:00 UTC (a), 15:00 UTC (b), and 17 UTC (c), for December, 25th.

From GFS, CAPE is between 400 and 500 J kg^{-1} near Campinas at 12:00 UTC. At 15:00 UTC, in the same region it is ranging from 800 to 1100 J kg^{-1} . These values indicate a marginally unstable condition at 12:00 UTC, and it is between a marginally and a moderately unstable condition at 15:00 UTC. LI is between -2 and -3 K at 12:00 UTC, and -3 and -4 K at 15:00 UTC. These ranges indicate an unstable condition with probable storm, even severe in

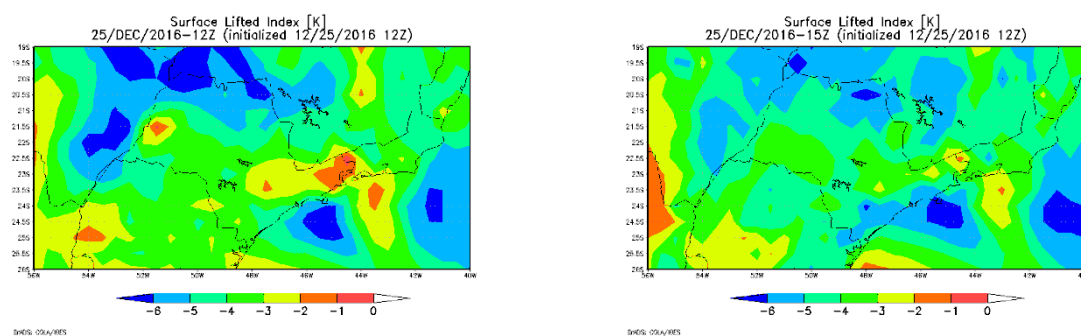
the presence of some lifting mechanism. High values of CIN are seen in the region at 12:00 UTC, it is between -40 and -60 J kg^{-1} . However, other events were compared with the GFS output, and it was noted that, at 12:00 UTC, it is usually lower than expected, which makes it possible for this parameter to be even higher in reality. Considering this argument and the values of CAPE observed, also considering that the range is correctly, is possible to say that it does not seem likely that a storm would develop in the region. The 700-500 hPa lapse rate also from GFS, at 12:00 and 15:00 UTC is between 5.5 and 6.0 K km^{-1} , although values ranging from 6 to 6.5 K km^{-1} are seen nearby.



(a)

(b)

Figure 4-156: CAPE (J kg^{-1}) from GFS at 12:00 UTC (a), and 15:00 UTC (b), for December, 25th.



(a)

(b)

Figure 4-157: LI (K) from GFS at 12:00 (a), and 15:00 UTC (b), for December, 25th.

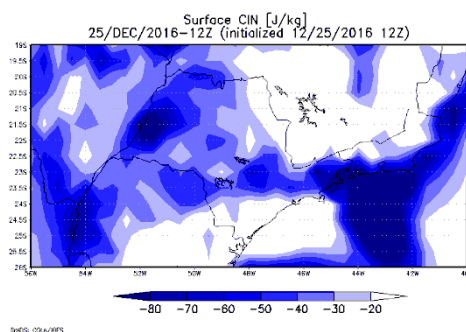
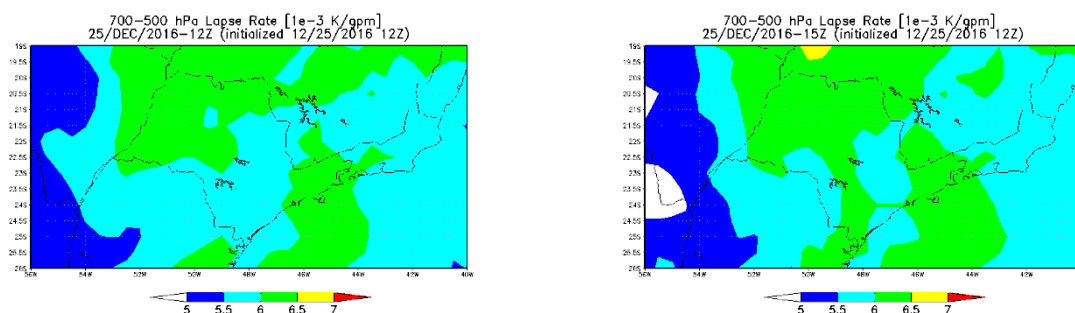


Figure 4-158: CIN (J kg^{-1}) from GFS at 12:00 UTC for December, 25th.



(a)

(b)

Figure 4-159: 700-500 hPa lapse rate from GFS at 12:00 UTC (a), and 15:00 UTC (b), for December, 25th.

Vertical cross section of relative humidity and wind from BRAMS and GFS were also analyzed fixed at 23.0°S and are shown in Figure 4-160. At 12:00 UTC, from the BRAMS output, an inversion is seen around the level of 500 m, values are between 50-55 %. Above that values are between 65 and 85 %, near the top it is ranging from 65 to 75 %. At 15:00 UTC, values near the top remain in the same range. From GFS, values between 600-500 hPa are ranging from 50 to 70 %. East of 46°W and west of 47.5°W values between 40-50 % are seen between 500 and 400 hPa. These values are still observed at 15:00 UTC. Winds near the surface are weak, and a small intensification is only seen above 1500 m from the BRAMS analysis at 12:00 UTC. This is still seen at 15:00 UTC. Weak winds are also seen in the GFS analysis, at 12:00 and 15:00 UTC, a small intensification is seen around 700 hPa.

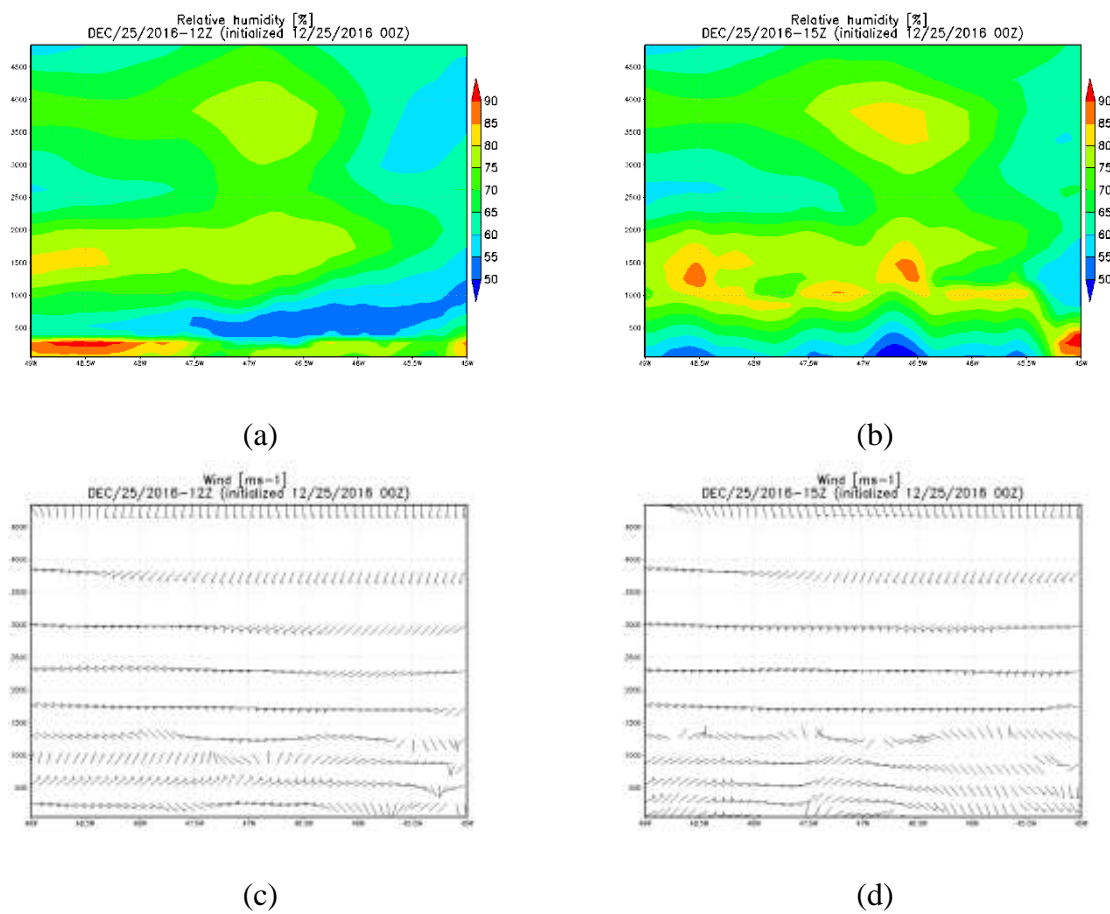


Figure 4-160: Vertical cross section from BRAMS at 23°S of relative humidity at 12:00 UTC (a), and 15:00 UTC, of wind at 12:00 UTC (c), and 15:00 UTC (d).

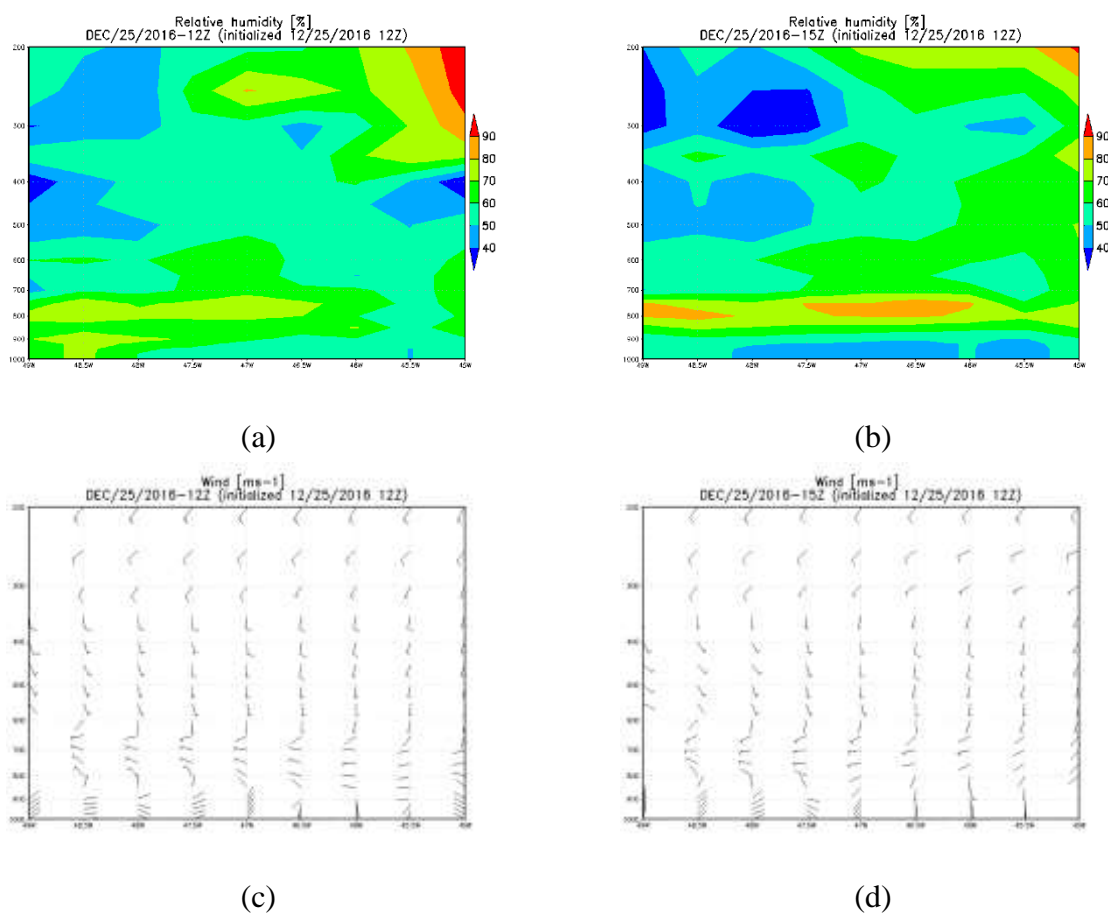


Figure 4-161: Vertical cross section from GFS at 23°S of relative humidity at 12:00 UTC (a), and 15:00 UTC, of wind at 12:00 UTC (c), and 15:00 UTC (d).

Moisture convergence form in the coast line of the State related to the formation of the sea breeze, at 15:00 UTC it follows the line of topography in the coast and it has started to advance into the continent (Figure 4-162). Values are below $-4 \times 10^{-3} \text{ g kg}^{-1} \text{ s}^{-1}$. It is possible to see the moisture gradient at this time in the coast related to the sea breeze. Moisture convergence is also seen in the regions of Serra da Mantiqueira.

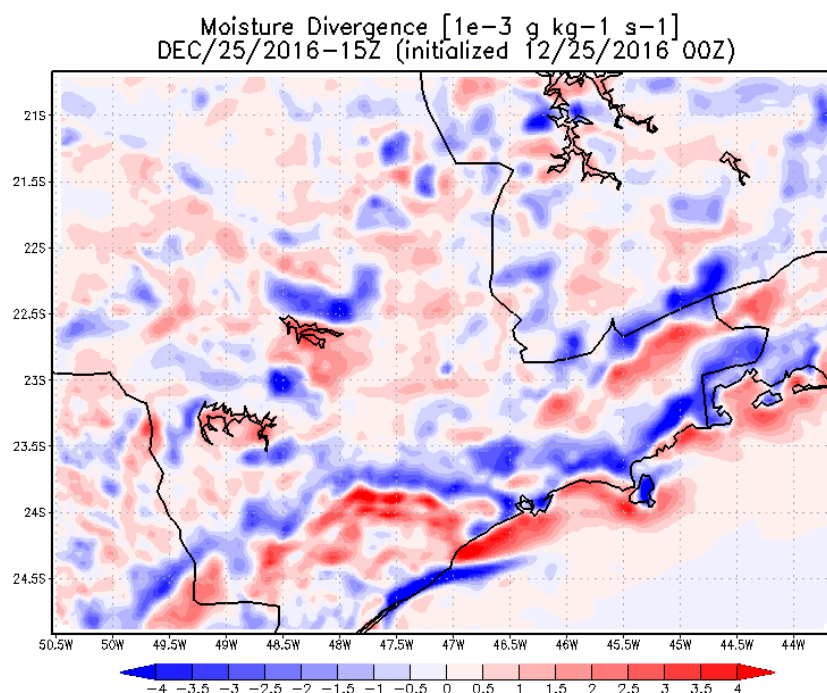


Figure 4-162: Moisture divergence at 15:00 UTC.

The change in wind during the day is shown in Figure 4-163. Winds were from southeast in the east and central part of the State at 00:00 UTC. This is related to the high pressure system mentioned in the synoptic scale analysis. At 09:00 UTC, the south part showed southeast winds, while in the north region winds were from northeast. After 09:00 UTC wind weakened in the east part, which is also observed in the surface station analysis, in the west section winds are from northeast and east and remains strong. At 15:00 UTC it is already possible, as mentioned in the moisture analysis, to see the southeast winds near the coast, related to the sea breeze. In the northeast part of the State, at this hour, winds get stronger and are from southeast, related to the topography in the region.

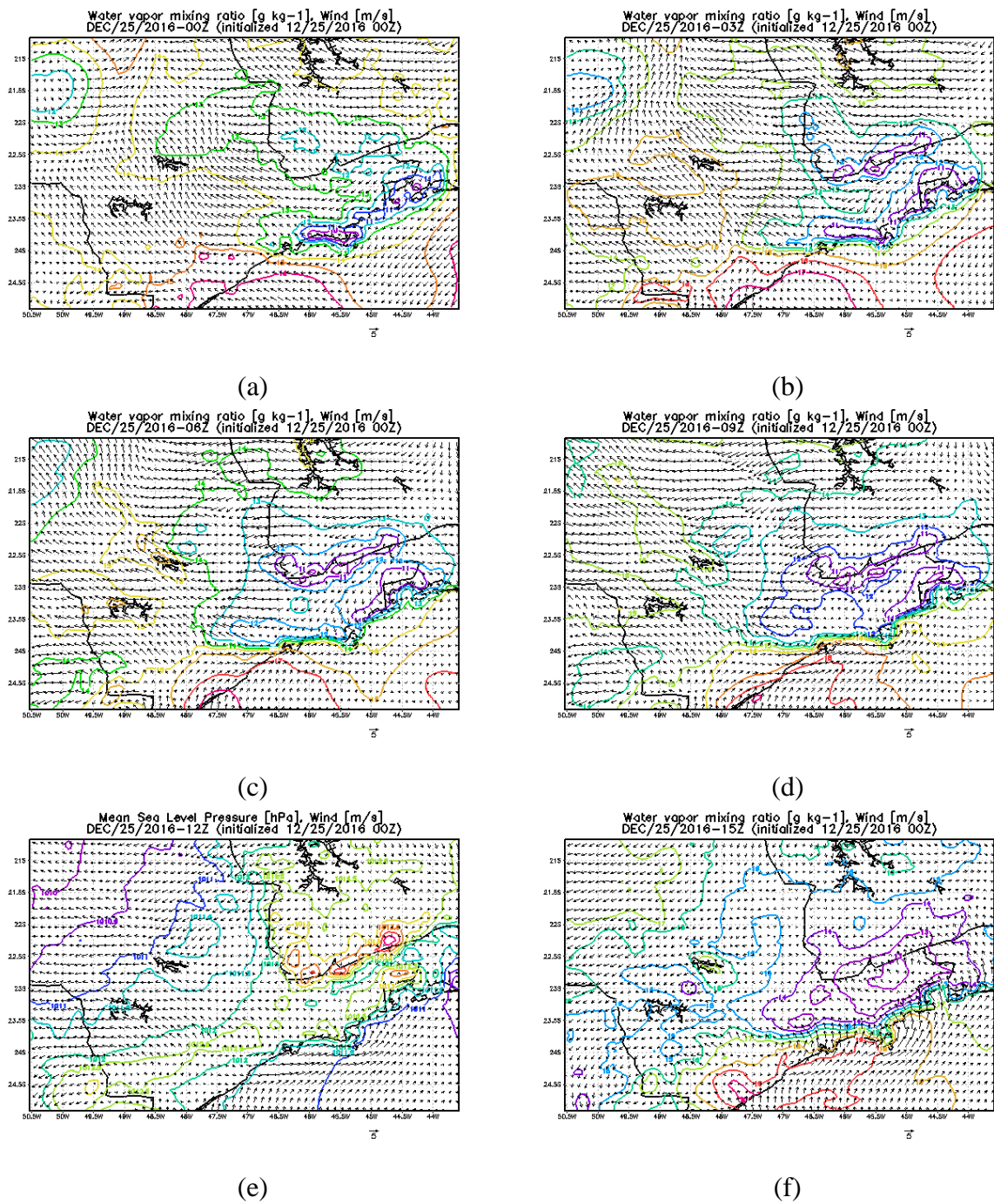


Figure 4-163: Water vapor mixing ratio and wind at 00:00 UTC (a), 03:00 UTC (b), 06:00 UTC (c), 09:00 UTC (d), 12:00 UTC (e), 15:00 UTC (f), 18:00 UTC (g), 21:00 UTC (h).

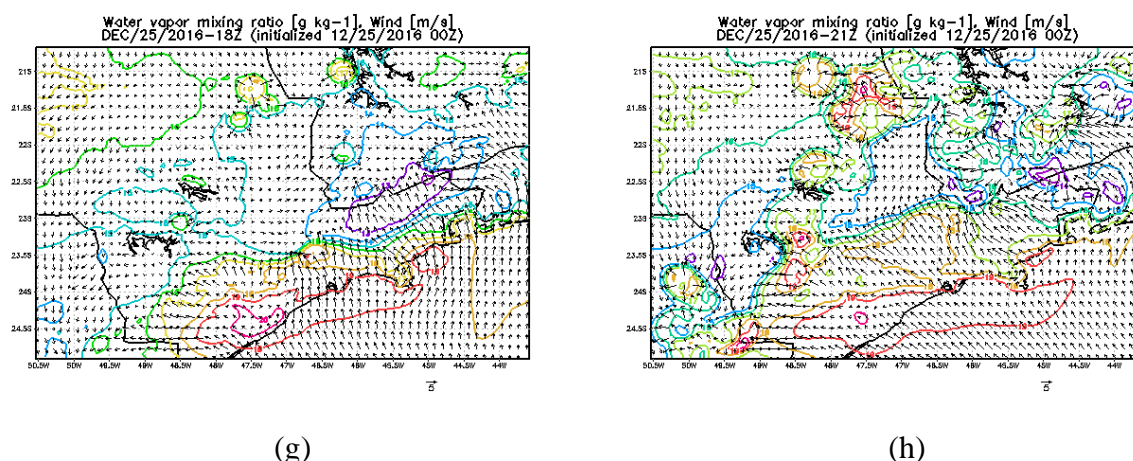


Figure 4-163: Continuation

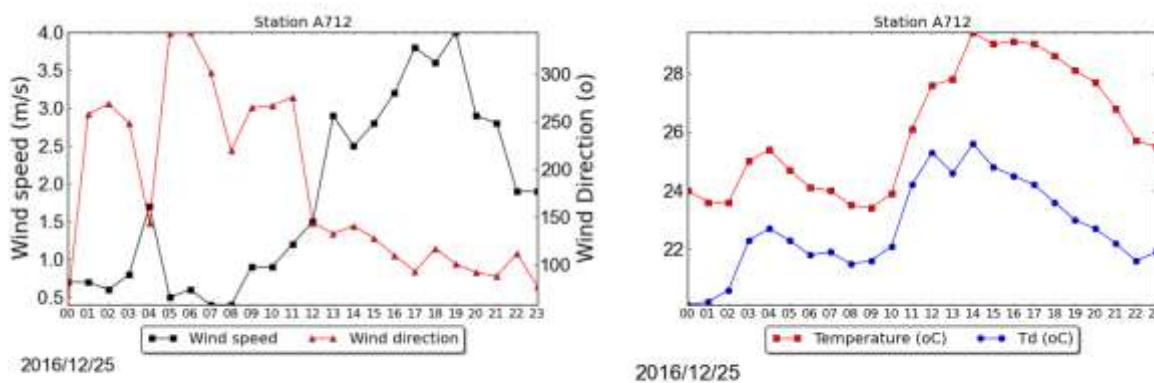
It is possible to see the moisture gradient advancing with the wind into the continent, representing the sea breeze front in Figure 4-163. At 22:00 UTC it appears to have lost its characteristics.

e. Surface station

Nineteen stations were analyzed for this event. In total, 5 stations registered rain during December, 25. This event was classified as related to the sea breeze penetration into the State. Analyzing the winds for the stations close to the coast it is possible to see the turn to southeast with increase in dew point temperature. The station A712 (Iguape) is located at the southeast coast of the State, during the day southwest winds were observed until it turned to southeast at 12:00 UTC with an increase of the dew point temperature (Figure 4-167). In the city of São Paulo, seen in Figure 4-167, the winds were from southeast during the day, it then turned to southwest at 12:00 UTC, and then back to southeast at 15:00 UTC. Increase in the dew point temperature and wind speed was observed in the station since 13:00 UTC. At the Campo de Marte airport, also located in the city of São Paulo, southeast winds were also observed during the day, with a few changes at 13:00 UTC, and then back to southeast at 16:00 UTC, increase in the dew point temperature also seen starting at 13:00 UTC with increase in wind speed. In the Congonhas airport, southeast winds were observed during the day, and increase in the dew point temperature and wind speed observed at 12:00 UTC. In the METAR analysis

cloud cover increased at 13:00 (Congonhas) and 14:00 UTC (Campo de Marte), but none of the stations analyzed registered rain in the city of São Paulo. It is possible that the fact that no severe event was observed in São Paulo is related to the fact that the sea breeze penetrated into the State earlier. The closest station to the city of São Paulo, is station A755 (Barueri), seen in Figure 4-166. At this station increase in the dew point temperature is seen at 14:00 UTC, but it has no record of wind direction. No rain was registered at this station either.

The sea breeze probably penetrated in the city of São Paulo around 15:00-16:00 UTC.

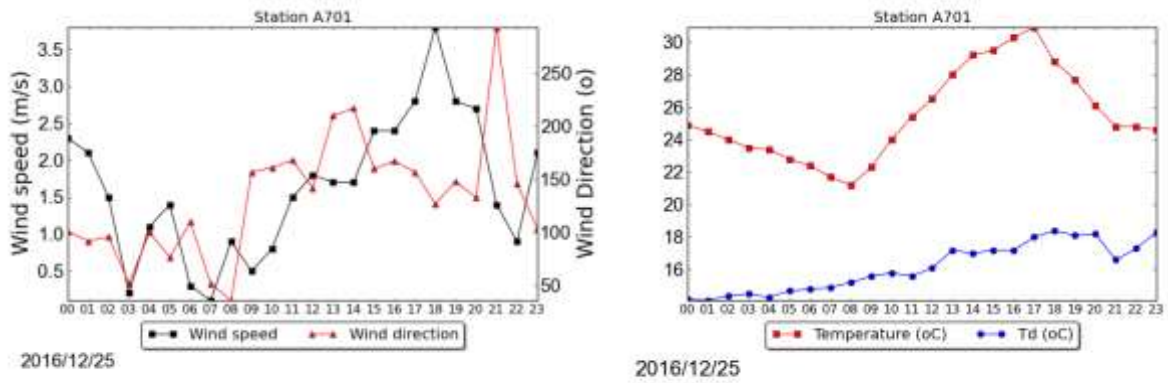


(a)

(b)

Figure 4-164: Wind speed and direction (a), temperature and dew point temperature (b) at station A712.

Stations A739 (Itapira) and A26 (Piracicaba) registered rain, which is related to the event observed in Campinas (Figure 4-167). In Itapira it rained from 19:00 to 23:00 UTC, the peak was between 19:00 and 20:00 UTC of only 5.6 mm, wind gusts of 10.6 m s^{-1} were observed at 19:00 UTC. In Piracicaba it only rained for one hour, between 21:00 and 22:00 UTC, in which 16.2 mm was registered, convective cells can be seen in the region in the radar images, related to the cells propagating into the State, which formed due to the sea breeze propagation and the merge with cells propagating from the north, as explained in the radar analysis.



(a)

(b)

Figure 4-165: Wind speed and direction (a), temperature and dew point temperature (b) at station A701.

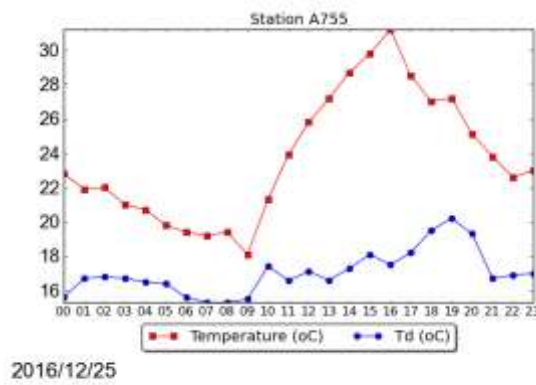
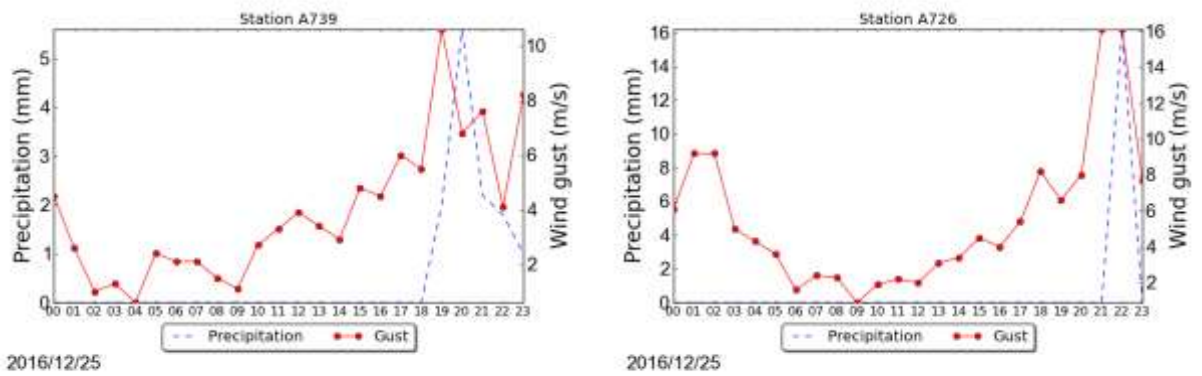


Figure 4-166: Temperature and dew point temperature at station A755, for December, 25th.



(a)

(b)

Figure 4-167: Precipitation and wind gust at Station A739 (a), and A726 (b), for December, 25th.

4.2.3 February, 22

Severe weather occurrences were reported in the city of São Paulo during this day. Rain led to flash floods in the city, 27 points were registered (CGE), hail was also reported.

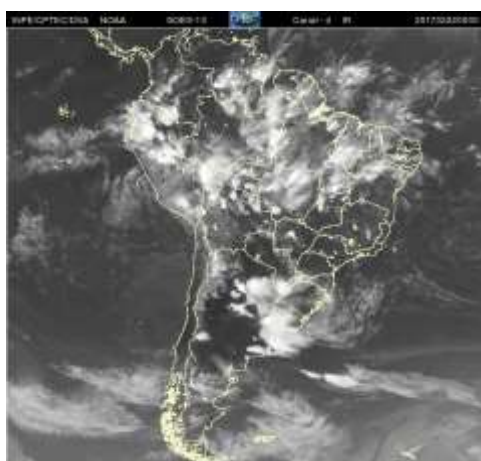
a. Satellite

Analyzing the infrared satellite image for the South American continent at 00:00 UTC clouds are seen in the south region of Brazil due to a low-pressure system. This system moves eastward and at 12:00 UTC is in the Atlantic Ocean and a few clouds are near the coast of São Paulo. However, it is possible to conclude that no synoptic system is influencing the State of São Paulo and leading to convective storms (Figure 4-168). This event was only related to regional aspects.

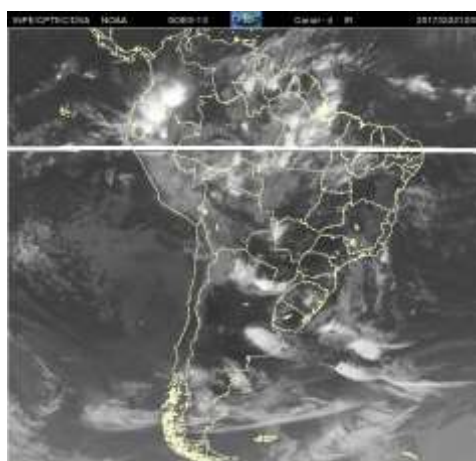
In the visible channel images for the southeast region of Brazil, seen in Figure 4-169, it is possible to see a few clouds developing parallel to the coast and near the region of Serra da Mantiqueira at 16:00 UTC. After 17:00 UTC cells are forming in the continent, still close to the coast, due to the propagation of the sea breeze. It moved to the region of São Paulo, and intensified, as can be seen in the enhanced infrared images after 19:30 UTC (Figure 4-170)

Between 20:20 and 20:30 UTC values around $-60\text{ }^{\circ}\text{C}$ are present in the region of São Paulo. After that, it lost its strength.

During this day, it is not possible to see the formation of various cells around the State, as it is usually seen, even in the region of topography (Serra da Mantiqueira), in which the development of clouds is usually seen, only a few developed, but did not intensify. This is probably due to the high-pressure system observed at 500 hPa, which will be explained in the synoptic scale analysis section.

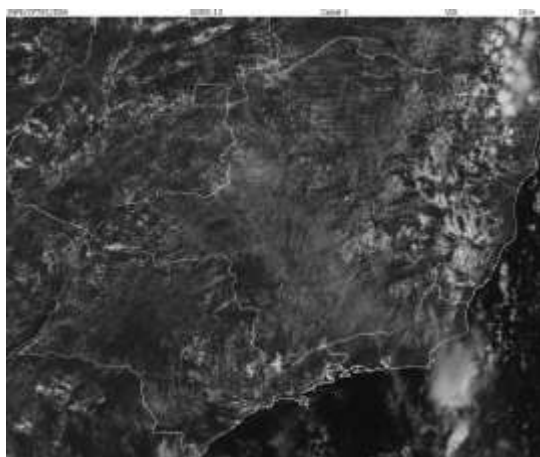


(a)

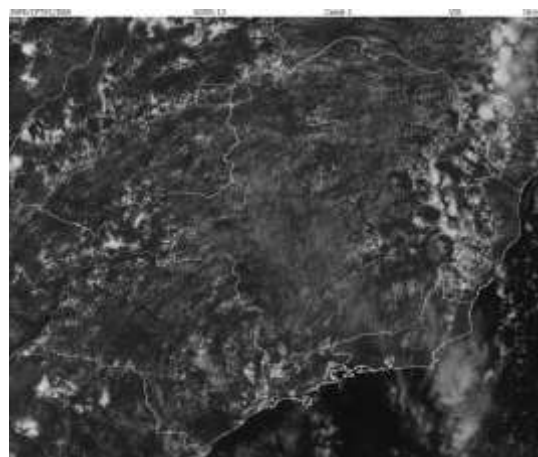


(b)

Figure 4-168: Infrared images for South America for February, 22 at 00:00 UTC (a), and 12:00 UTC (b).



(a)

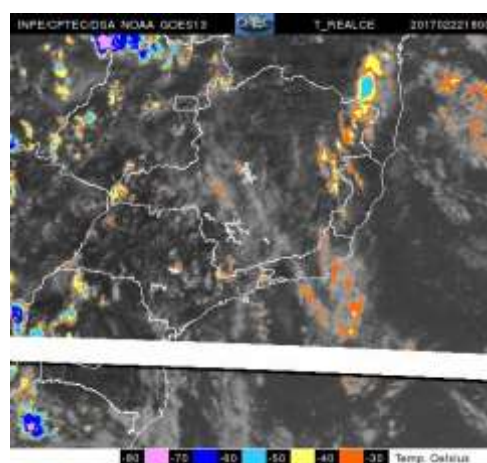


(b)

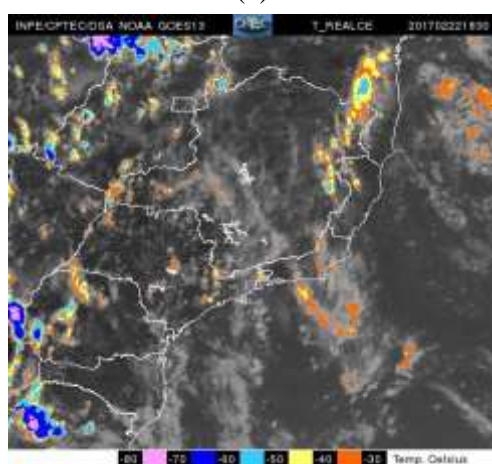
Figure 4-169: Visible channel satellite images at 16:00 UTC (a) and 177 UTC (b).



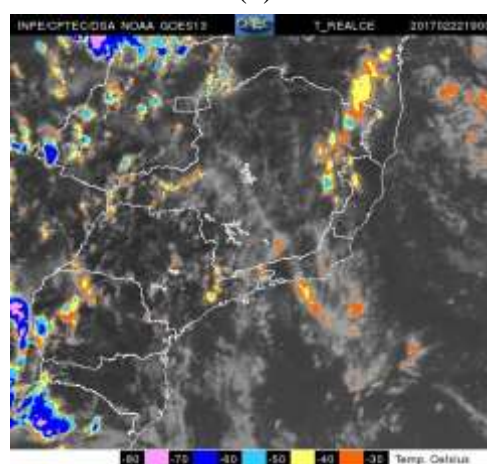
(a)



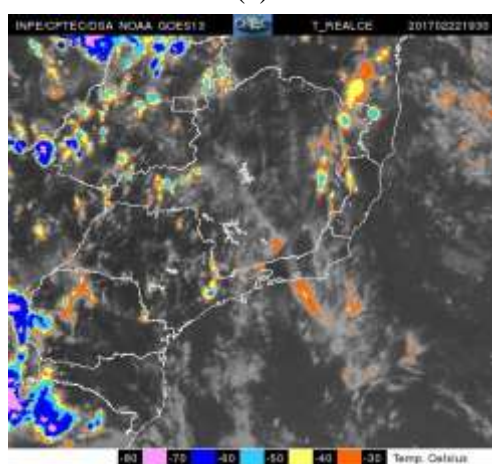
(b)



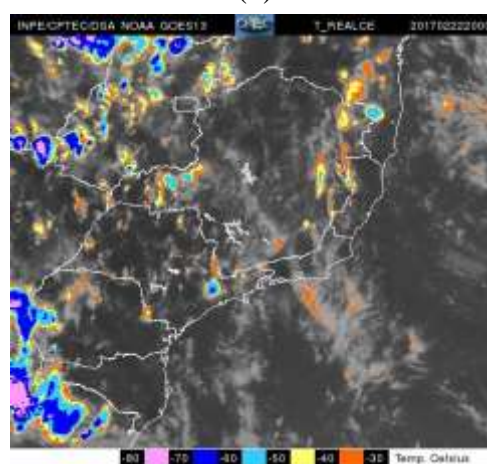
(c)



(d)



(e)



(f)

Figure 4-170: Enhanced infrared satellite image for February, 22 at 17:30 UTC (a), 18:00 UTC (b), 18:30 UTC (c), 19:00 UTC (d), 19:30 UTC (e), 20:00 UTC (f), 20:30 UTC (g), 21:30 UTC (h).

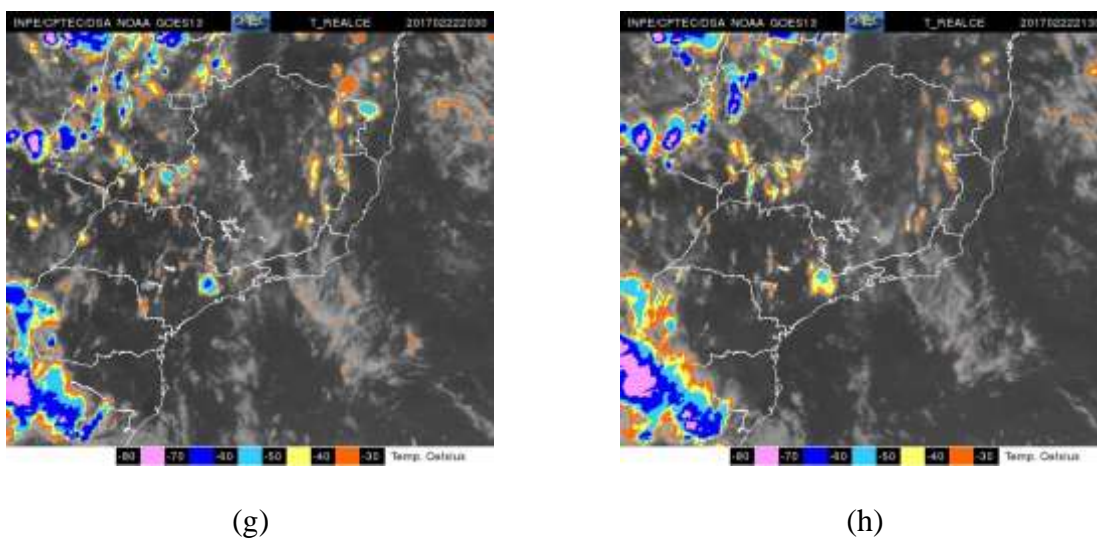


Figure 4-170: Continuation.

b. Radar

After 17:00 UTC, a few cells started to form in the continent. At 18:00 UTC, several cells are seen near São Paulo, in the region of Bragança Paulista, close to the coast in the northeast region (near Vale do Paraíba), and in the region between Jundiaí and Campinas.

Between 19:20 and 19:30 UTC, high reflectivity values are shown, around 60 dBZ. After 19:30 UTC it lost its strength, and another intensified still in the region of São Paulo, and at 20:10 UTC reflectivity values are around 60 dBZ. According to the CGE, between 4:00 and 6:00 pm local time hailstorm and heavy rain was reported in the city of São Paulo.

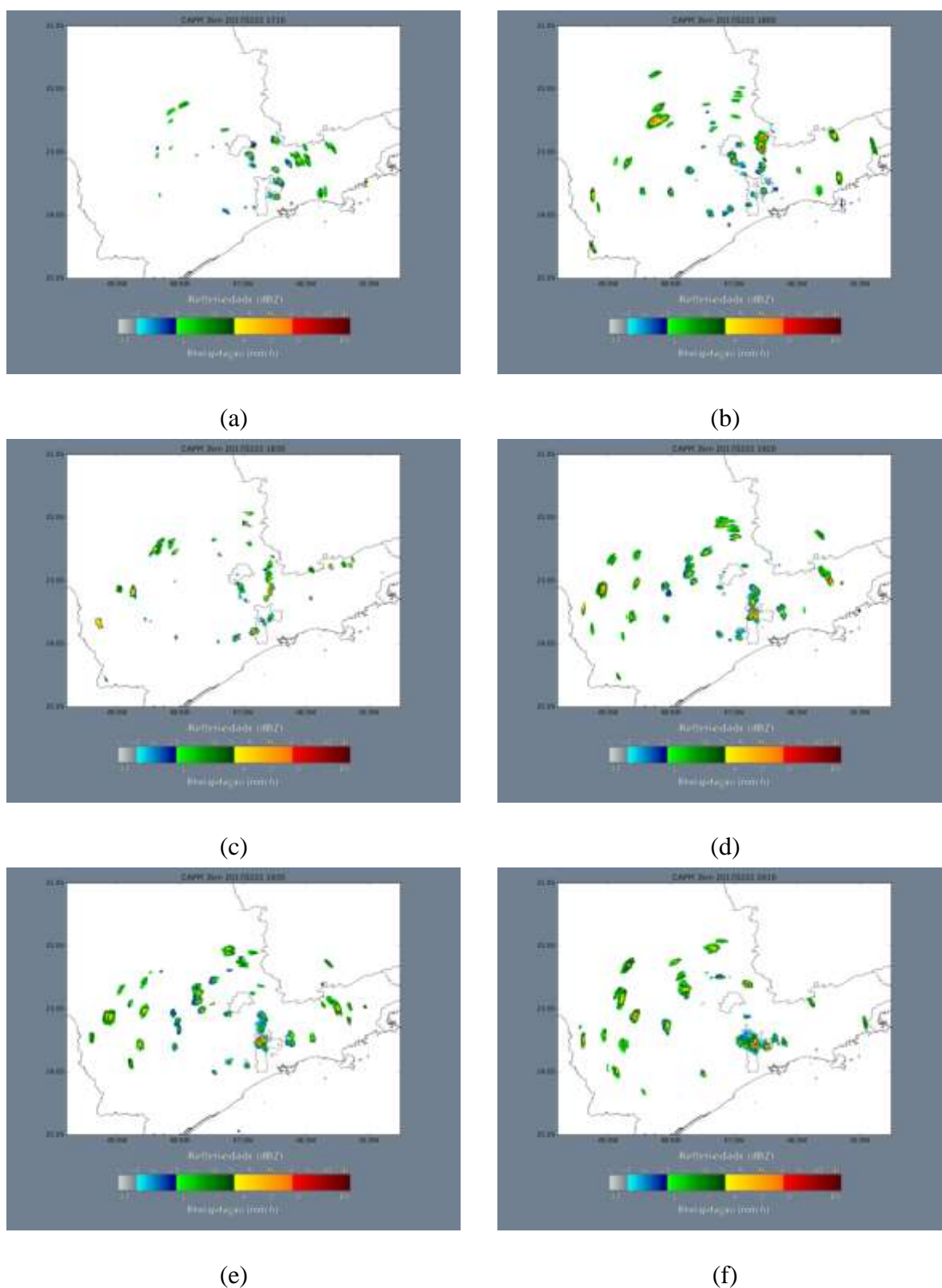


Figure 4-171: São Roque radar images for February, 22 at 1710 UTC (a), 18:00 UTC (b), 1830 UTC (c), 1920 UTC (d), 1930 (e), 20:10 UTC (f).

c. Synoptic scale analysis

At 00:00 UTC in the 200 hPa analysis a high-pressure system is located in the north of Chile. Two different upper level cyclonic vortex are seen, one between Mato Grosso and Rondônia, and the other in the coast region of Bahia. Neither of them is influencing the State of São Paulo. A trough is present in the Atlantic Ocean around the height of the coast of Rio Grande do Sul. This trough intensified throughout the day. Another trough is seen, initially in the eastern region of Argentina, and at 18:00 UTC is between Argentina and Rio Grande do Sul. The 200 hPa analysis is shown in Figure 4-172, wind divergence at this level is on Figure 4-173. Small wind divergence ($0.2-0.4 \cdot 10^{-4} \text{ s}^{-1}$) is shown at 12:00, 15:00 and 18:00 UTC in the northeastern part of the State of São Paulo.

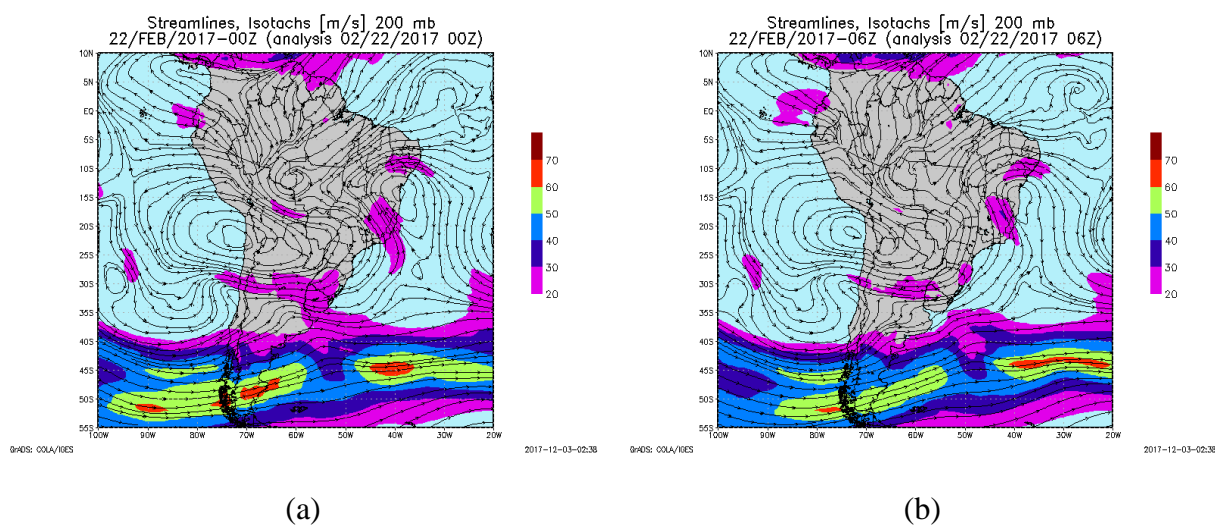


Figure 4-172: Streamlines and isotachs (m s^{-1}) at 200 hPa at 00:00 UTC (a), 06:00 UTC (b), 12:00 UTC (c), 18:00 UTC (d), for February, 22th.

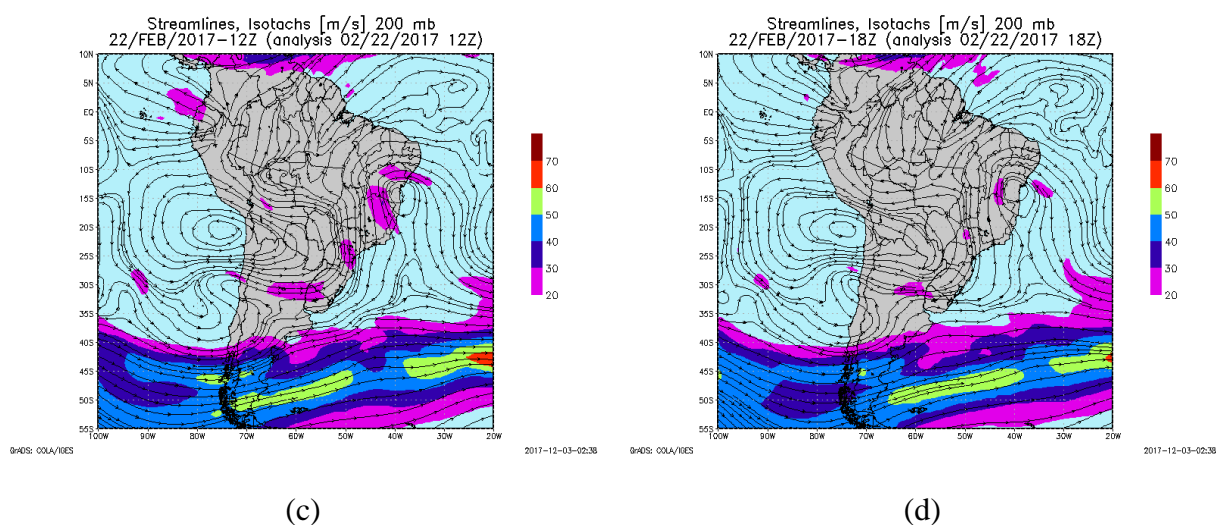


Figure 4-172: Continuation.

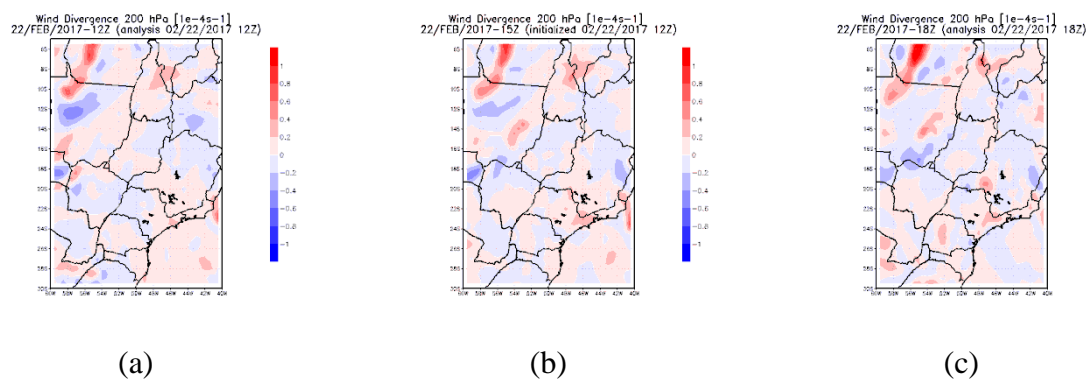


Figure 4-173: Mass divergence ($1 \times 10^{-4} s^{-1}$) at 200 hPa at 12:00 UTC (a), 15:00 UTC (b), and 18:00 UTC (c), for February, 22th.

In the 500 hPa analysis (Figure 4-174) the trough located in the south region of Brazil is seen with negative vorticity associated. There is a high-pressure system on the State of Paraná and south of São Paulo. This system appears to lose its strength throughout the day. It is affecting the State of São Paulo, causing stability, dry air, and high temperatures. This system is also seen in the previous day (02/21/2017, not analyzed here), and low relative humidity values are seen in the 850 hPa and on the sounding. CIN derived from the sounding at 12:00 UTC for February, 21 is $-272.77 J kg^{-1}$, indicating atmospheric stability (not shown).

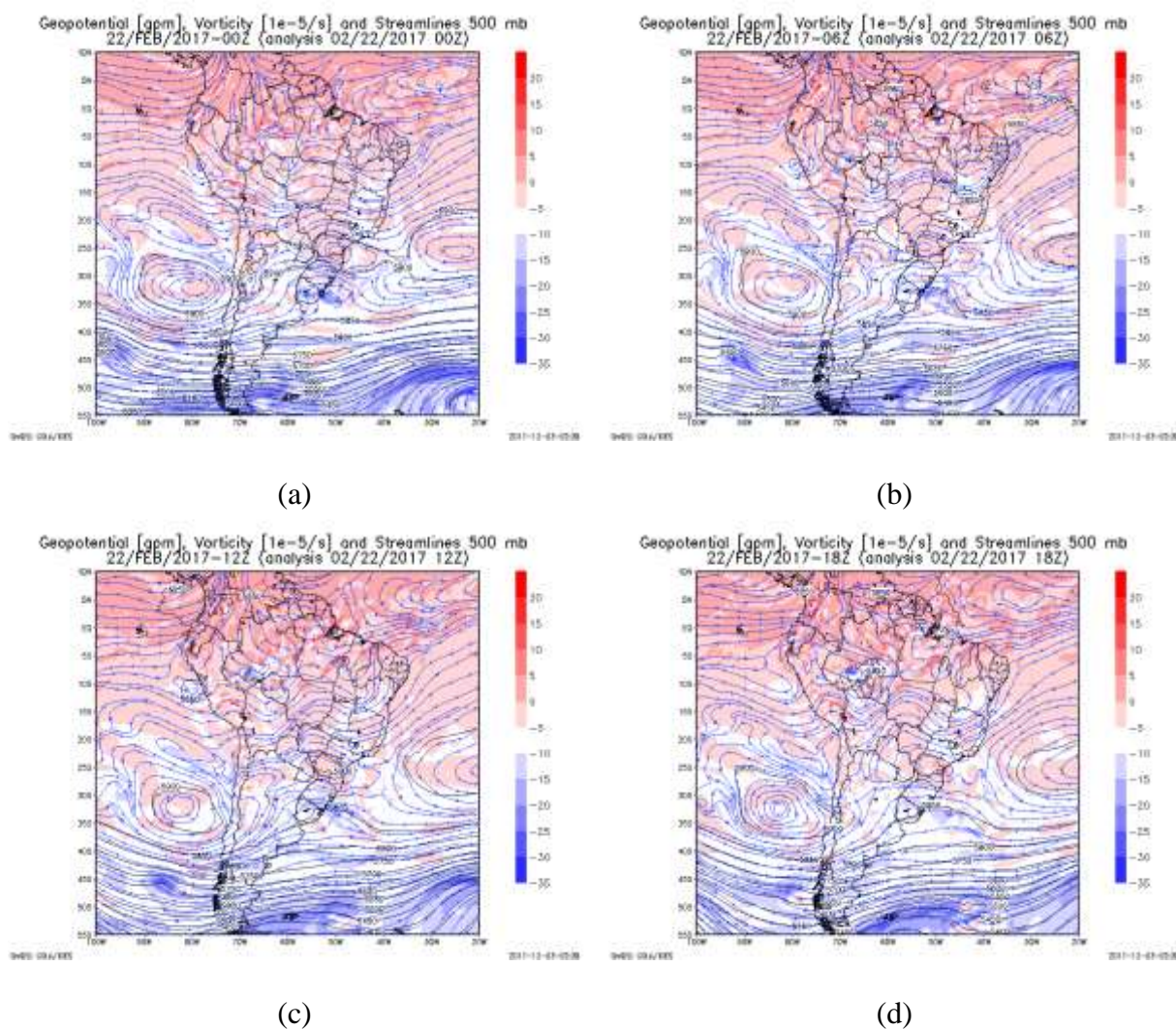


Figure 4-174: Geopotential height (gpm), vorticity ($1 \times 10^{-5} \text{ s}^{-1}$) and streamlines at 500 hPa at 00:00 UTC (a), 06:00 UTC (b), 12:00 UTC (c), and 18:00 UTC (d), for February, 22th.

Figure 4-175 shows streamlines and relative humidity at 850 mb. Low relative humidity, below 65%, is shown in the east part of the State of São Paulo, but it increased and at 12:00 UTC is around 70-75% in the northeast region. This low humidity is caused by the high pressure at 500 hPa.

After 12:00 UTC a trough is seen near the coast of Uruguay. The only system influencing the State of São Paulo is the Atlantic high-pressure system. At 00:00 UTC a strong warm advection is present in the southeast region of the State with values above 1.0×10^{-5}

4 K s^{-1} . It vanishes throughout the analysis, and warm advection is no longer seen in São Paulo.

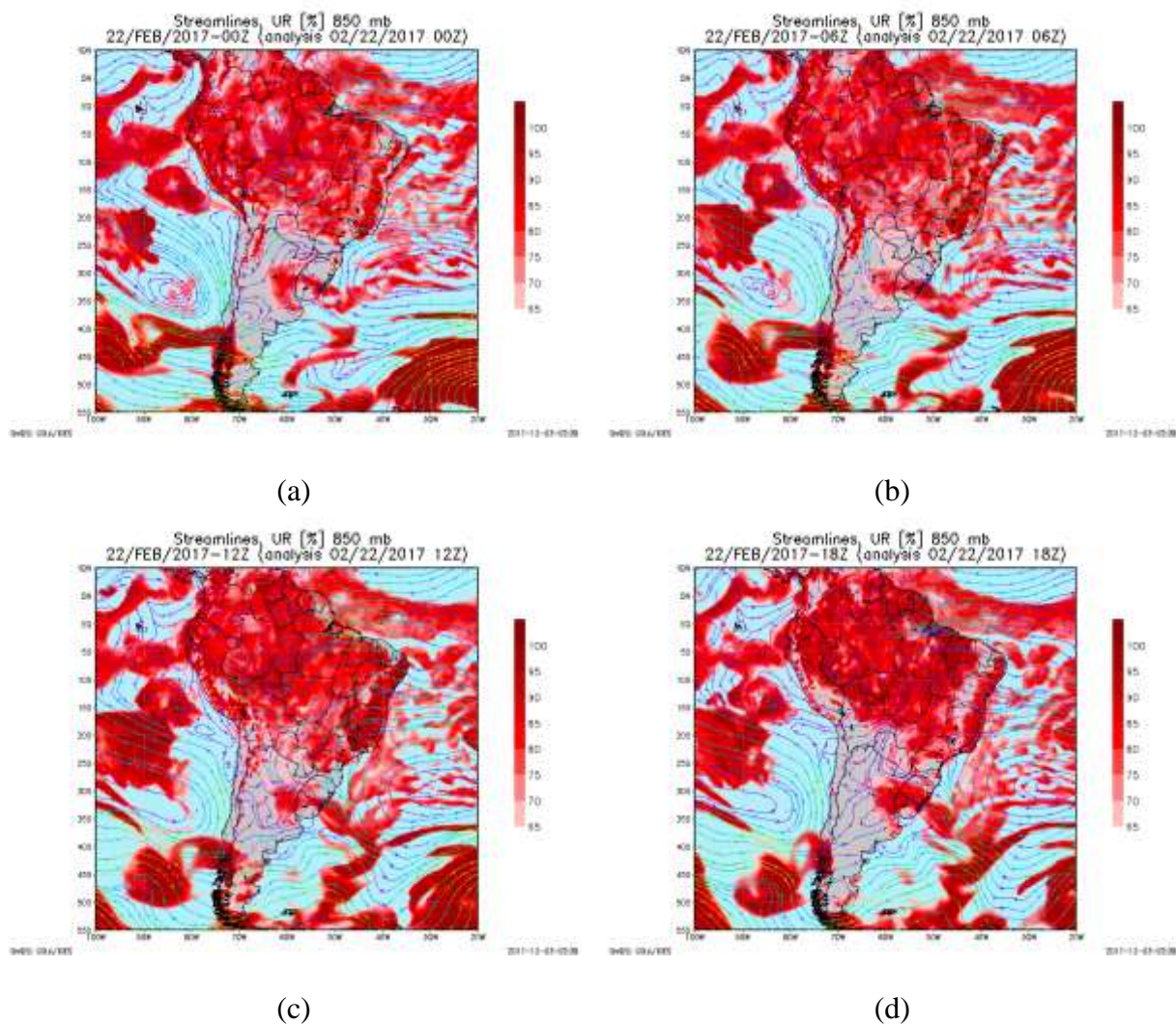


Figure 4-175: Streamlines and relative humidity (%) at 850 hPa at 00:00 UTC (a), 06:00 UTC (b), 12:00 UTC (c), and 18:00 UTC (d) for February, 22th.

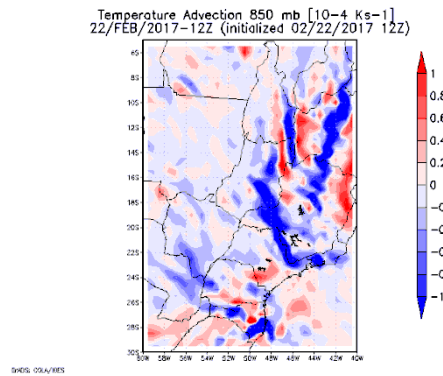


Figure 4-176: Warm advection ($1 \times 10^{-4} \text{ K s}^{-1}$) at 850 hPa at 12:00 UTC, for February, 22, 2017.

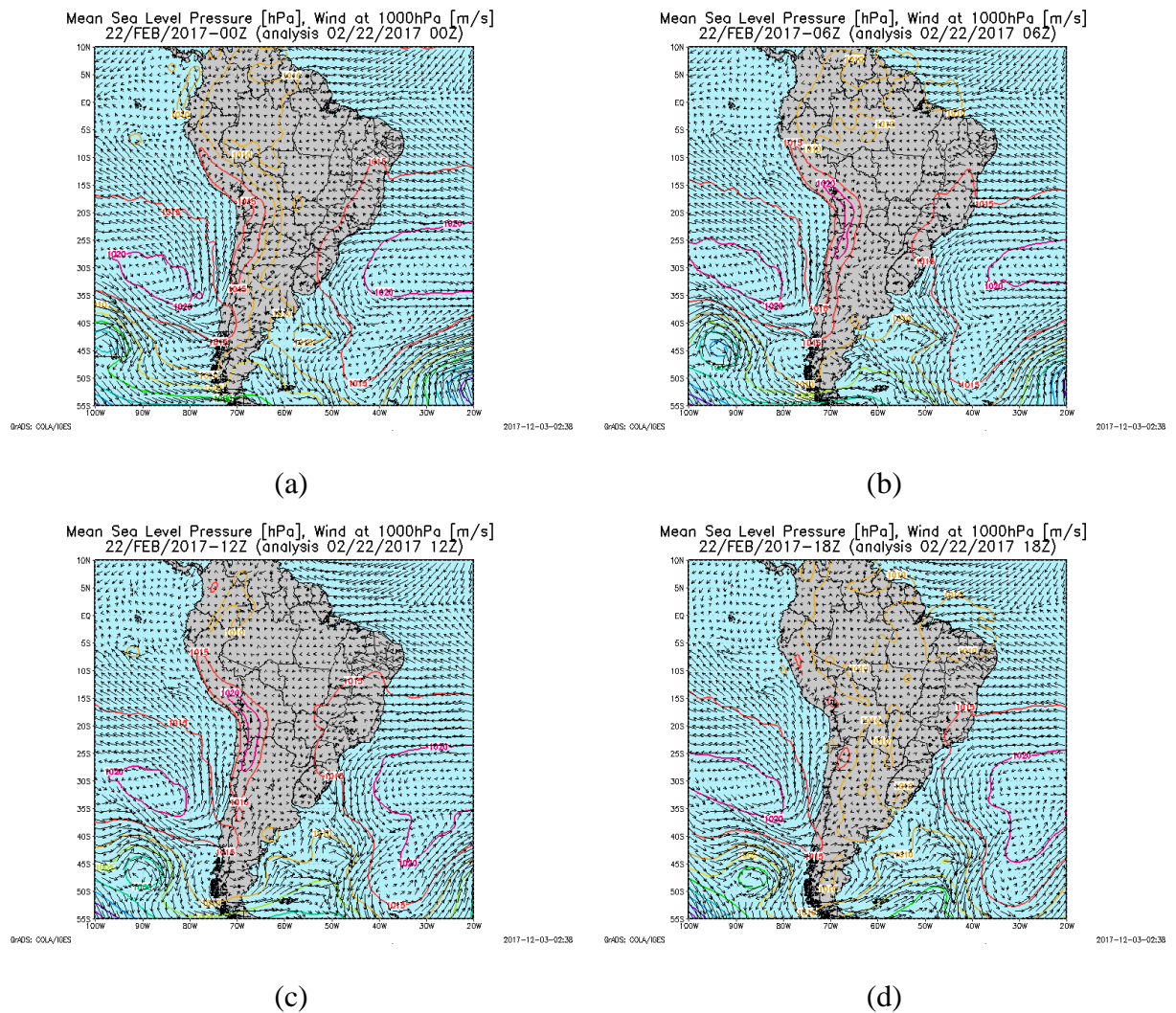


Figure 4-177: Mean sea level pressure (hPa) and wind (m s^{-1}) for February, 22 at 00:00 UTC (a), 06:00 UTC (b), 12:00 UTC (c), and 18:00 UTC (d).

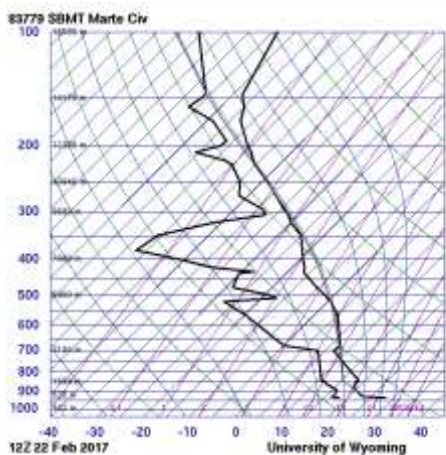
The Subtropical South Atlantic High is around 30 °S and 35 °W, in the surface analysis (Figure 4-176), and it is the only synoptic system influencing the southeast region of Brazil, in the surface analysis, on this day.

d. Thermodynamic and mesoscale analysis

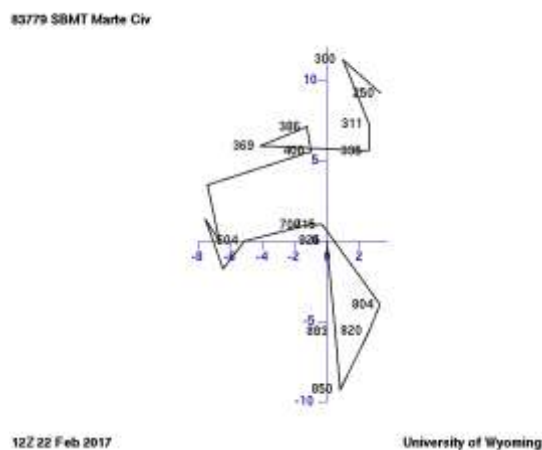
The sounding and hodograph obtained for this day is shown in Figure 4-178. The vertical variation of water vapor mixing ratio, relative humidity and equivalent potential temperature derived from the sounding is seen in Figure 4-179.

The pattern of dry air above moist air is seen in the sounding obtained at 12:00 UTC. However, the moisture content on low levels is not very high. This can be seen analyzing the relative humidity and water vapor mixing ratio vertical profiles. In the first few levels water vapor mixing ratio is between 12-14 g kg⁻¹ and relative humidity is between 50-70 %.

A subsidence inversion is shown in this sounding at 700 hPa, above that, the atmosphere becomes dry. Between 500-600 hPa the relative humidity reaches 15 % and between 400-300 it reaches 2 %. Equivalent potential temperature is around 340-350 K near the surface. CAPE derived from the sounding is 278.1 J kg⁻¹, which indicates a low potential for the development of storms, but it indicates a marginally unstable condition. CIN is -88.0 J kg⁻¹, lifting must be enough to break this lid. LI is -0.83 K, which indicates a slightly unstable condition, with possible storm. The level of free convection is 738.06 hPa and the equilibrium level is 262.04 hPa. Using the virtual temperature correction these parameter are equal to 381.58 J kg⁻¹, -64.35 J kg⁻¹, -1.34 K, 752.28 hPa, and 260.38 hPa. The 700-500 lapse rate is -5.0 K km⁻¹. The hodograph shows wind turning anticlockwise with height until around 600 hPa, and then it starts to turn clockwise. However, an increase is seen only between the surface and the level of 850 hPa.

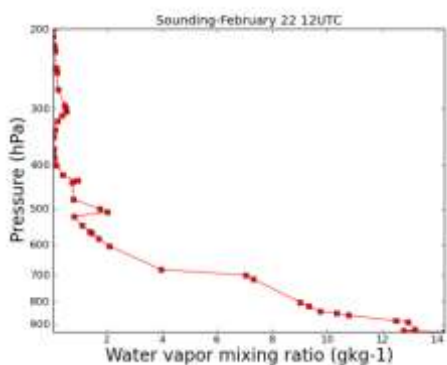


(a)

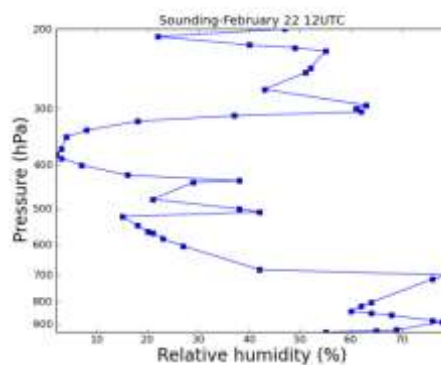


(b)

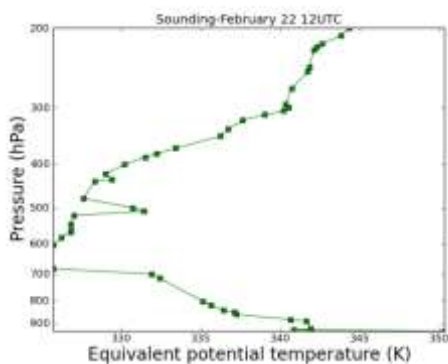
Figure 4-178: Sounding and hodograph for February, 22 at 12:00 UTC. (source: <http://weather.uwyo.edu/upperair/sounding.html>).



(a)



(b)



(c)

Figure 4-179: Vertical variation of water vapor mixing ratio (a), relative humidity (b), and equivalent potential temperature (c) derived from the sounding for February, 22 at 12:00 UTC.

Considering the analysis of the sounding at 12:00 UTC, it is possible to conclude that the potential for storm development on this day was low.

Comparing the sounding to the BRAMS model output (Figure 4-180), it is seen that CAPE is no observed at 12:00 UTC. This parameter only starts to increase after 14:00 UTC. At 15:00 UTC, near São Paulo, a region is between 800 and 1200 J kg^{-1} , but CAPE on most of the northeast region is ranging from 1200 to 1600 J kg^{-1} . The first range, close to São Paulo, indicates a condition between marginally and moderately unstable. The second range indicates a moderately unstable condition.

CIN at 12:00 UTC is below 20 J kg^{-1} , which means the BRAMS underestimated the convective inhibition parameter. At 11 UTC most of the State has CIN between 60-80 J kg^{-1} , but a few region, including close to São Paulo, this parameter is above 100 J kg^{-1} . This value is closer to the sounding value.

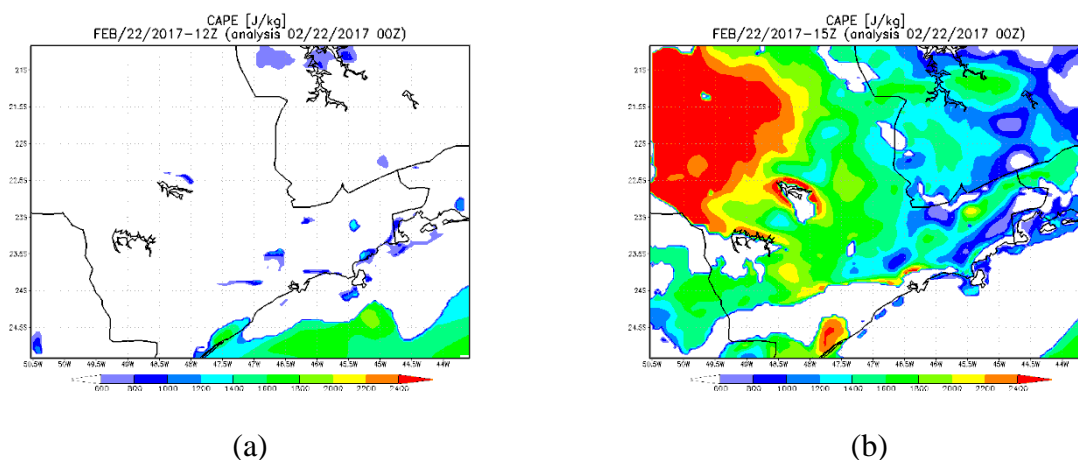
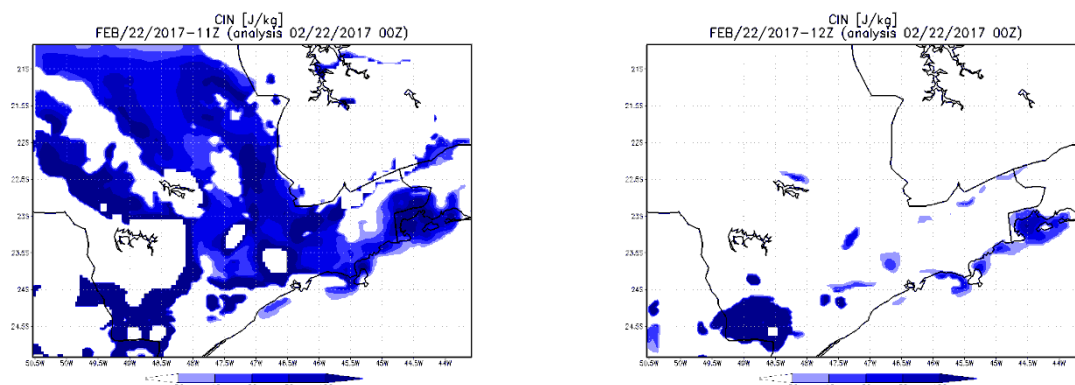


Figure 4-180: CAPE (J kg^{-1}) from BRAMS at 12:00 UTC (a) and 15:00 UTC (b) for February, 22th.



(a)

Figure 4-181: CIN (J kg^{-1}) from BRAMS at 11:00 UTC (a) and 12:00 UTC (b) for February, 22th.

CAPE from the GFS is around $600\text{-}800 \text{ J kg}^{-1}$ through the east region, at 12:00 UTC. At 15:00 UTC, it is between 1000 and 1200 J kg^{-1} . This indicates a marginally unstable and a moderately unstable condition, respectively. CIN is above -20 J kg^{-1} through most of the State at 12:00 UTC, but close to São Paulo, values between -20 and -30 J kg^{-1} are seen. The LI parameter is compared with GFS output, and from the model at 12:00 UTC, the parameter is between -2 and -4 K , which indicates a different condition than derived from the sounding, it indicates an unstable condition, with probable storm, even severe. At 15:00 UTC, it has increased and is between -4 and -5 K , however, it still indicates the same condition. The 700-500 hPa lapse rate, at 12:00 UTC is between 5.5 and 6.0 K km^{-1} , which is higher than seen in the sounding. At 15:00, it is between 6.0 and 6.5 K km^{-1} .

These parameters from the GFS model are seen in Figure 4-182.

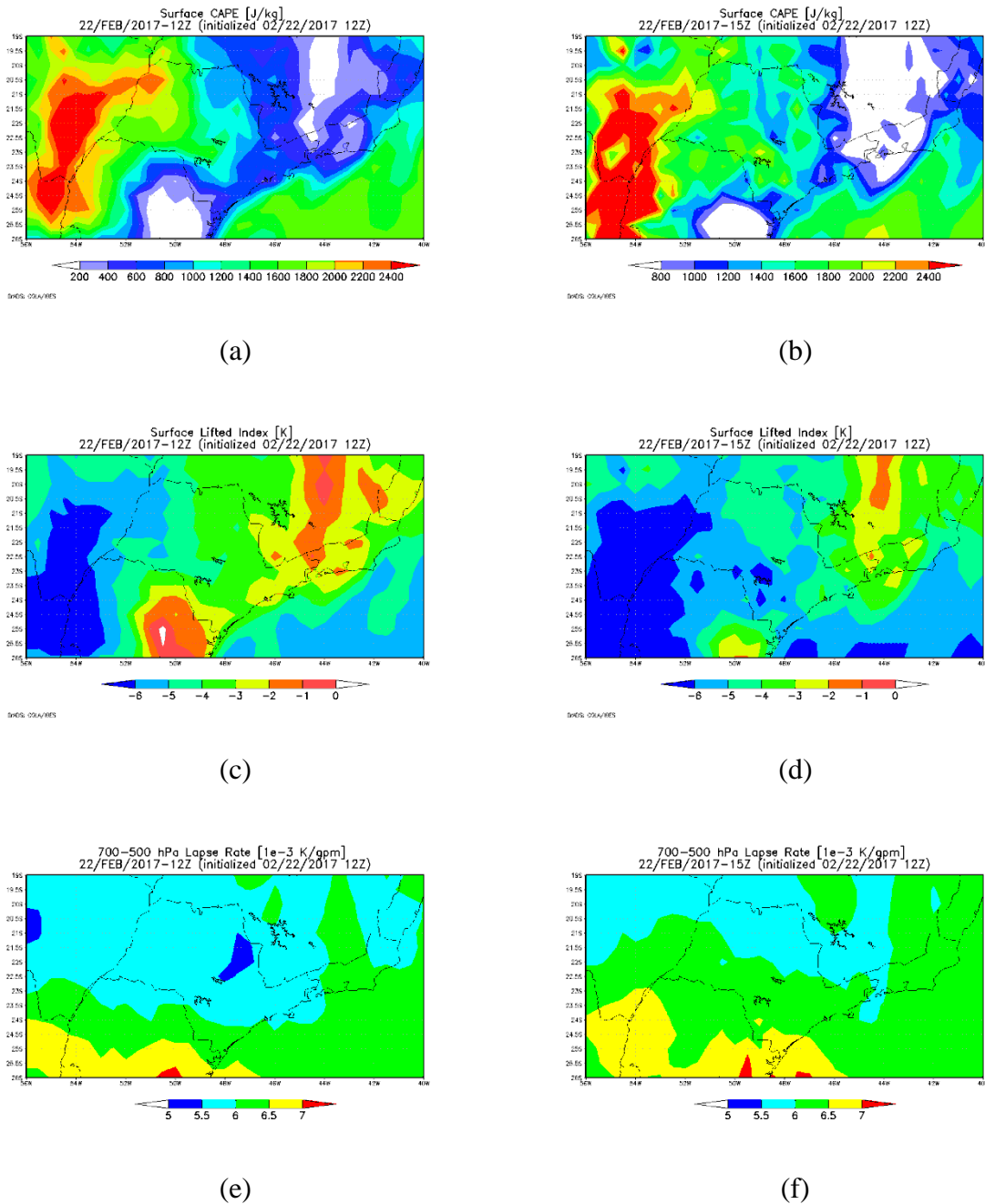


Figure 4-182: CAPE at 12:00 UTC (a), 15:00 UTC (b); LI at 12:00 UTC (c), and 15:00 UTC (d); 700-500 hPa lapse rate at 12:00 UTC (e), and 15:00 UTC (f), from GFS for February, 22th.

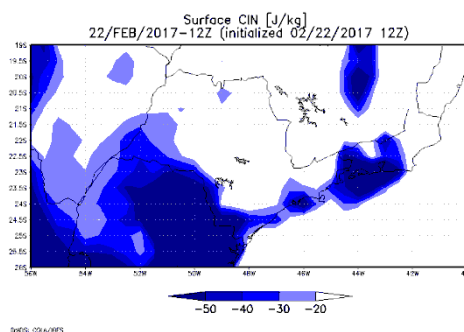


Figure 4-183: CIN from GFS at 12:00 UTC, for February, 22th.

The vertical cross section of relative humidity from BRAMS shows that, at 12:00 UTC, near the top, it is between 20 and 40 %. It is similar to the values seen in the sounding, however, lower relative humidity is seen above. The water vapor mixing ratio is between 1 and 3 g kg⁻¹ at this hour near the top, also similar to the sounding. These values are also seen at 15:00 UTC, but near the surface the relative humidity is closer to the derived from the sounding at 15:00 UTC, it is between 40 and 60 %. The water vapor mixing ratio is around 11 and 15 g kg⁻¹, at 15:00 UTC. In the vertical cross section of winds, at 12:00 UTC, winds are weak near the surface, a small intensification is seen, but winds get weak again around the level of 1000 m. West of 48°W winds intensify and turn anticlockwise with height until around the level of 1000 m. At 15:00 UTC winds are still weak near the surface, they are slightly stronger west of 47°W. The pattern seen at 12:00 UTC is very similar to the one seen in the hodograph. From GFS, winds are also similar to the hodograph; near the winds are from north and turn anticlockwise to northwest and intensify around 850 hPa. This is also seen west of 47°W; warm advection is seen in the region at this level. The anticlockwise turn is no longer seen at 15:00 UTC.

In the vertical cross section of relative humidity from GFS, smaller values are seen between 600 and 400 hPa at 12:00 UTC. Between 600 and 500 hPa, values are between 30 and 50 % near São Paulo, west from 47°W values are between 20 and 40 %, which is closer to

the sounding. Values are between 10 and 20 % around 400 hPa, values are below 10 % in the sounding. At 15:00 UTC it has increased and it around 40-60 % near São Paulo, between 600 and 500 hPa, west from 47°W values are between 30 and 40%. Near São Paulo, values are higher than expected from the sounding at 12:00 UTC, especially between 500 and 600 hPa, similar values are seen around 400 hPa, indicating the difficulty in quantifying the dry air present in the atmosphere.

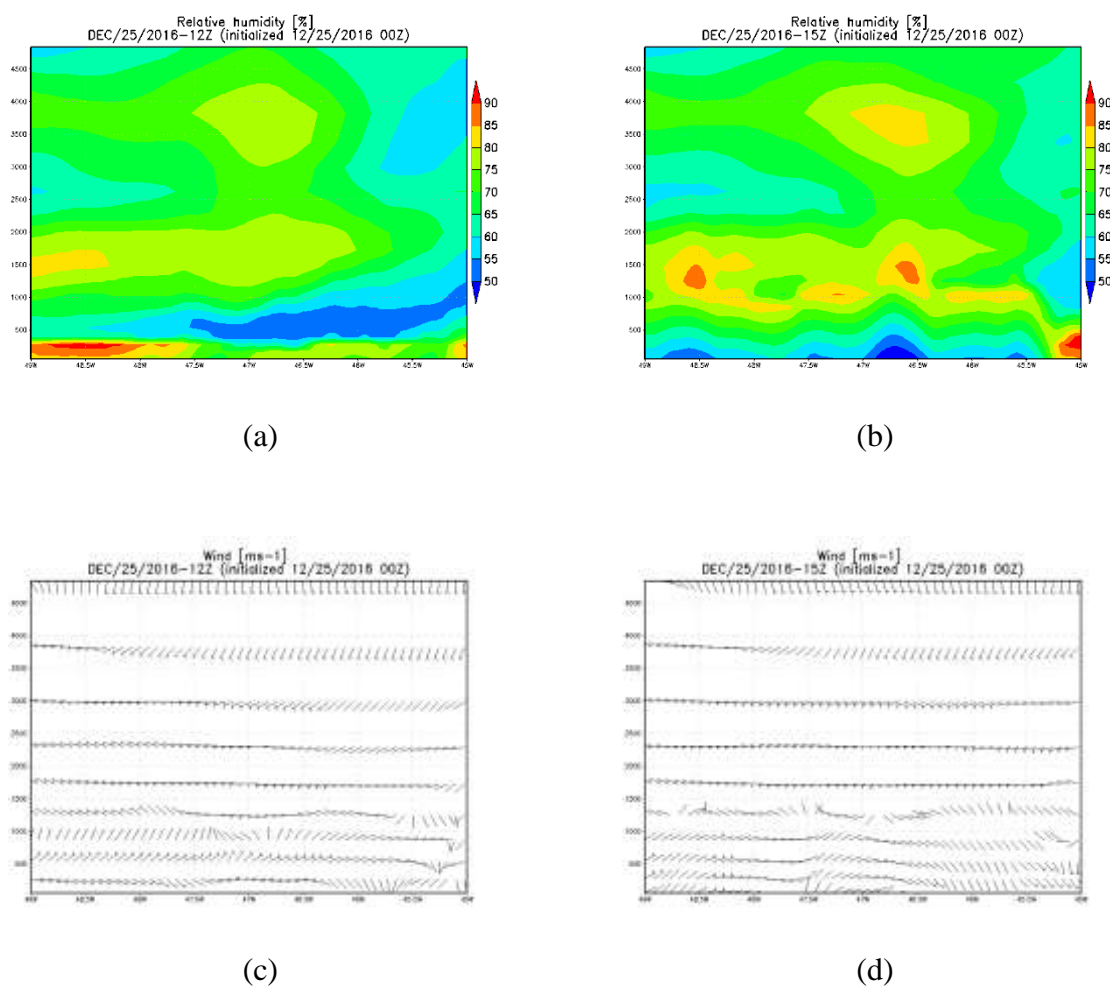


Figure 4-184: Vertical cross section from BRAMS at 23.0°S of relative humidity at 12:00 UTC (a), and 15:00 UTC (b), and winds at 12:00 UTC (c), and 15:00 UTC (d) for February, 22th.

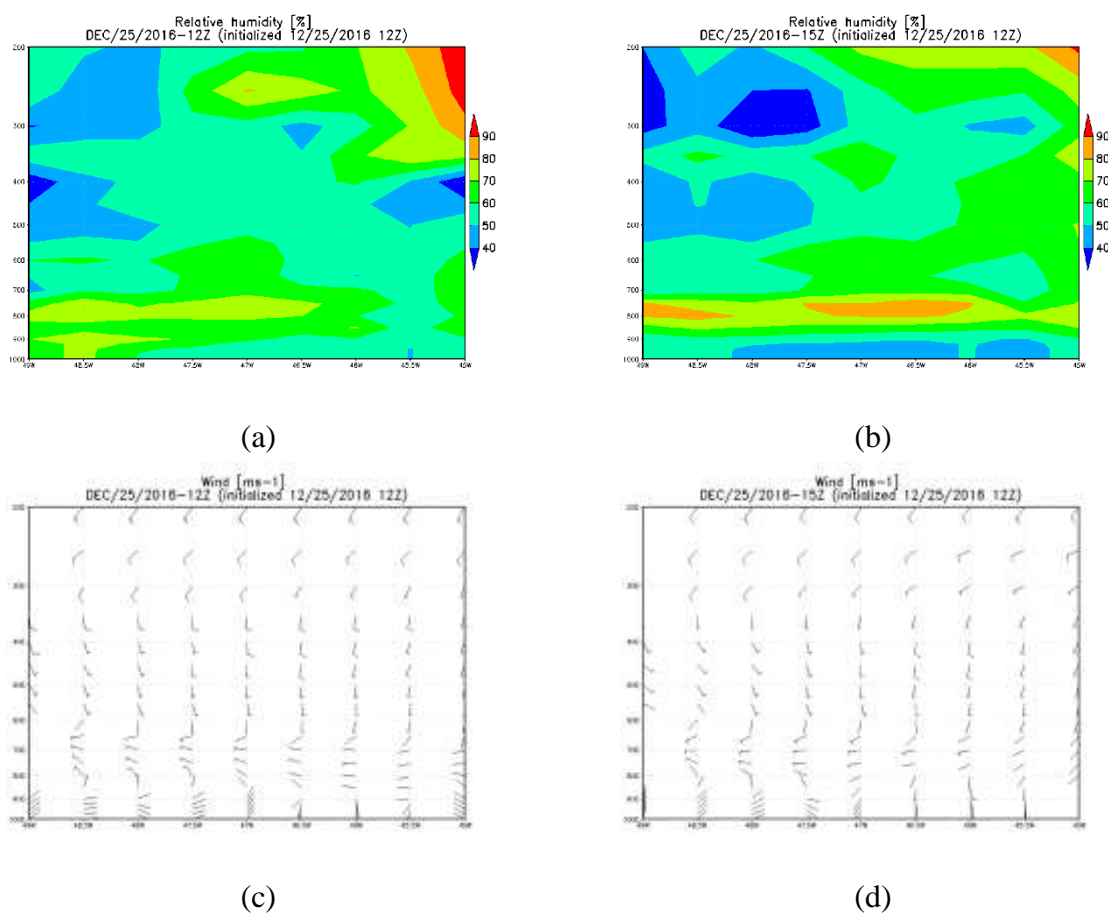


Figure 4-185: Vertical cross section from GFS at 23.0°S of relative humidity at 12:00 UTC (a), and 15:00 UTC (b), and winds at 12:00 UTC (c), and 15:00 UTC (d) for February, 22th.

Divergence of moisture and wind patterns were also analyzed using the BRAMS model, as it was done for the other events. Convergence of moisture is shown in the analysis, and can be seen in the coast, with values lower than $-4 \cdot 10^{-3} \text{ g kg}^{-1} \text{ s}^{-1}$, at 14 UTC, and at 15:00 UTC it has started to advance into the continent. The wind starts the day from southeast, turns to northeast, and as the sea breeze advances, it turns to southeast. Another fact about the event, also mentioned in previous analysis of the sea breeze penetration, is the gradient of moisture that forms near the coast, and propagates with the wind, representing the sea breeze front. The wind and water vapor mixing ratio changes through the day are shown in Figure 4-187.

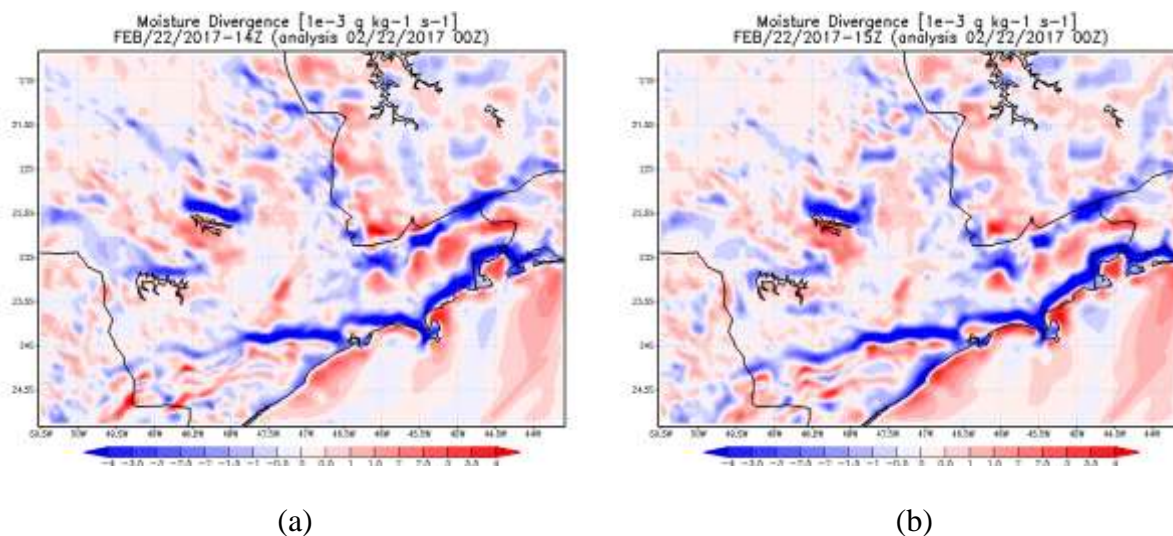


Figure 4-186: Moisture divergence for February, 22 at 14:00 UTC (a), and at 15:00 UTC (b).

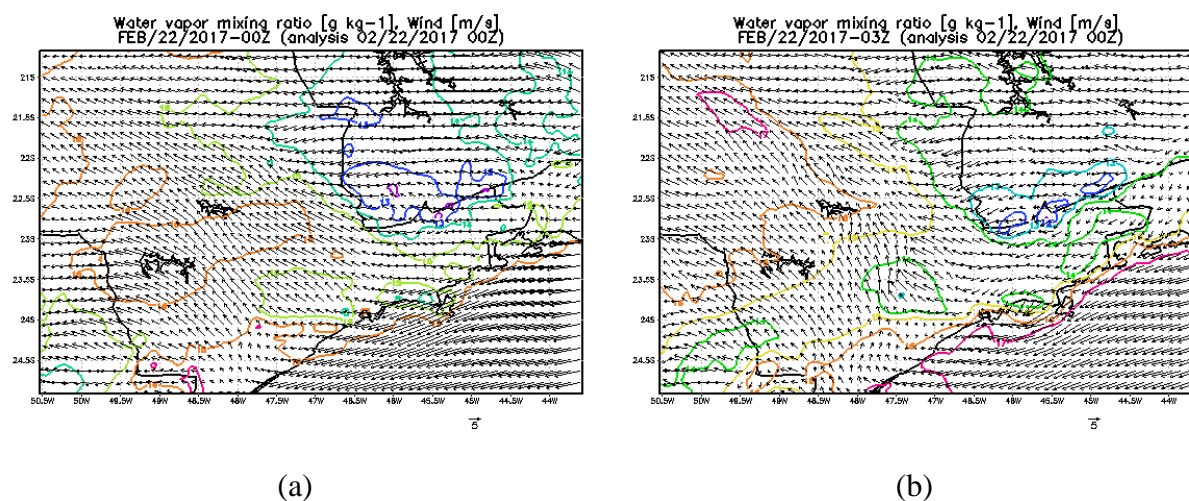


Figure 4-187: Water vapor mixing ratio and wind for February, 22 at 00:00 UTC (a), 03 UTC (b), 06:00 UTC (c), 09:00 UTC (d), 12:00 UTC (e), 15:00 UTC (f), 18:00 UTC (g), and 21:00 UTC (h).

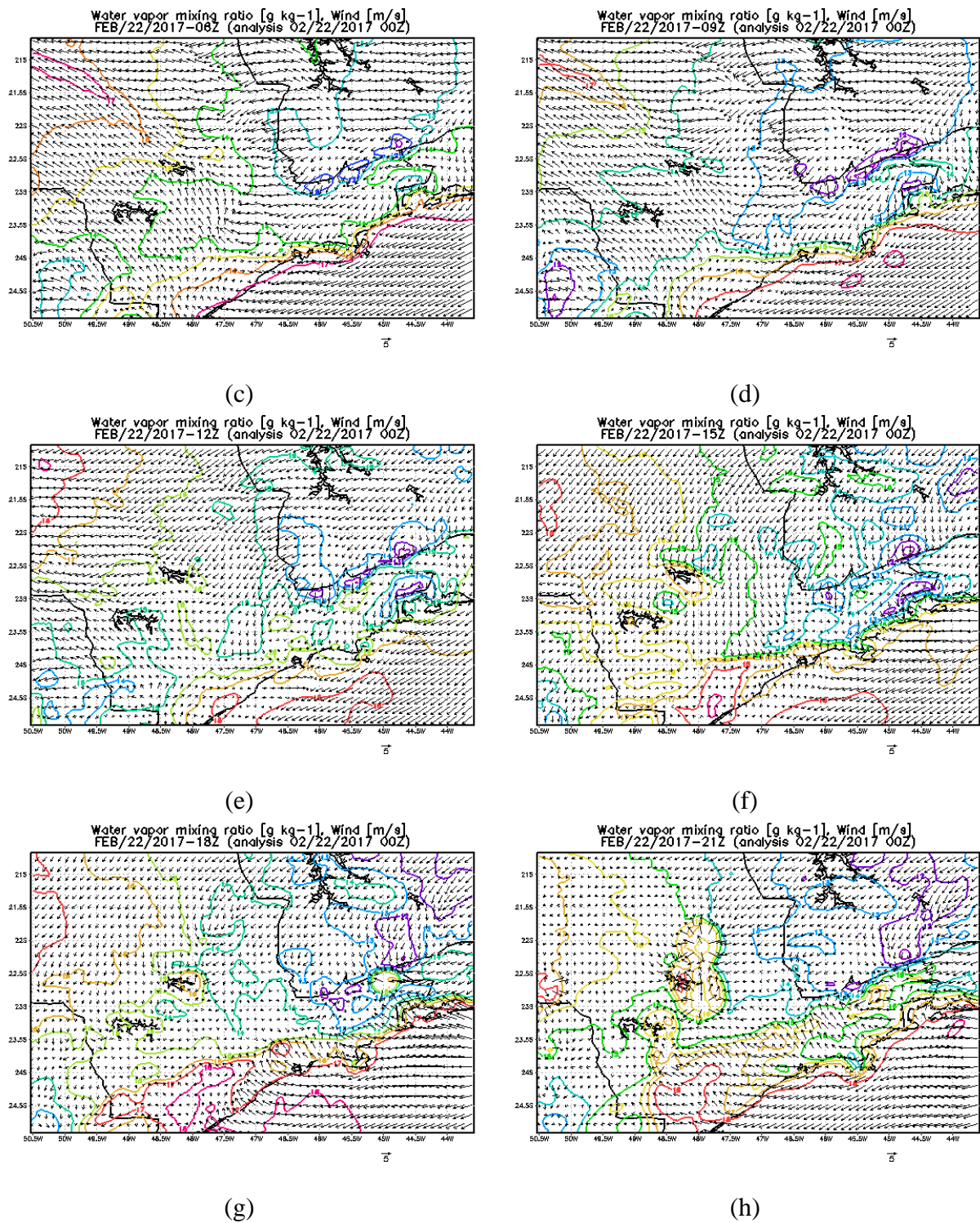


Figure 4-187: Continuation.

e. Surface stations

For this event 17 stations were analyzed. All of the stations mentioned that recorded the sea breeze penetration are seen in Figure 4-188.

Station A701 (Mirante de Santana) had southeast winds at the beginning of the day, turning to northeast at 05:00 UTC, and after 14:00 UTC varying between northwest, southwest and northeast. At 18:00 UTC wind turns to east-southeast followed by an increase in dew point temperature, relative humidity and decrease of temperature. In the Congonhas airport and Campo de Marte airport a similar wind pattern through the day is seen, but expected changes in variables related to the sea breeze are observed after 19:00 UTC, on both METAR analysis, however southeast winds were only registered on the Congonhas airport, on the Campo de Marte data, winds were varying from northeast to southwest, and a southeast wind is only recorded at 00:00 UTC on February, 23.

Only 0.6 mm of rain was registered in Mirante de Santana between 20:00-21:00 UTC, shown in Figure 4-190. According to the CGE, in the north region of the city of São Paulo, where the station is located, it rained an average of 3.7 mm. In the central and west regions the average was above 20 mm. Still according to them, a few stations recorded as much as 40 mm. Only data until 6:22 PM local time was considered, as stated by them.

The highest registered temperature on station A701 was 33.1°C, so the storm in the city is also probably related to the heat observed during this day.

Analyzing METAR from Guarulhos airport, it is seen that southeast winds are observed followed by increase in dew point temperature, relative humidity, and decrease in temperature, at 17:00 UTC.

In Barueri (station A755), dew point temperature and relative humidity increased on the same hour in which rain was registered, therefore it is complicated to assess the hour of the sea breeze penetration in the region. It rained for two hours on the station, but only an accumulated of 5 mm was recorded, 0.6 mm between 19-20 UTC and 4.2 mm between 20-21 UTC (Figure 4-190).

Station A713 recorded increase in dew point temperature and relative humidity after 21:00 UTC, but winds were from southwest.

Localized on Vale do Paraíba, stations A740 and A728 both registered variations related to sea breeze penetration. On station A740 southeast wind was observed at 17:00 UTC, but the variables variations were only observed after 19:00 UTC. Varying winds are seen after 17:00 UTC on this station. Further from the ocean than station A740, station A728 registered increase in dew point temperature, relative humidity and decrease of temperature, associated with a turn to southeast wind, after 19:00 UTC. Winds were also varying on this station after this hour. No rain was recorded in either of the stations.

Located in the southeast part of the State, station A746 registered southeast wind with changes related to the sea breeze after 10 UTC.

Further inland, stations A739 and A726 both registered southeast wind followed by increase in dew point temperature and relative humidity at 22 UTC. It is possible to see the advance of the sea breeze reaching those regions on the wind and moisture figure obtained from the BRAMS model (Figure 4-187).

All of the stations analyzed recorded temperatures above 30 °C, station A741 registered the highest value of 36.1 °C. These high temperatures are related to the high pressure system localized on 500 hPa as was mentioned on the analysis of the synoptic scale scenario.

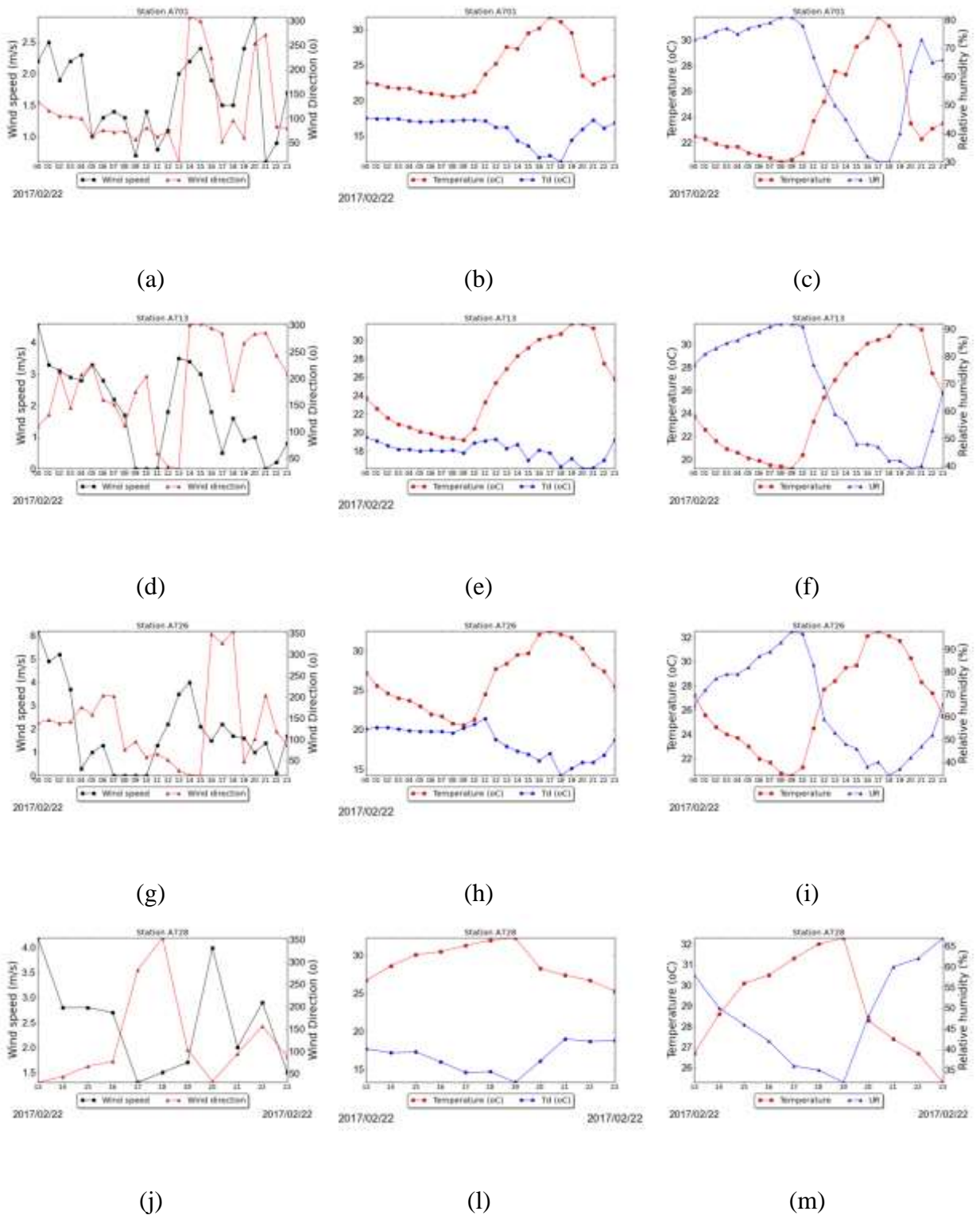
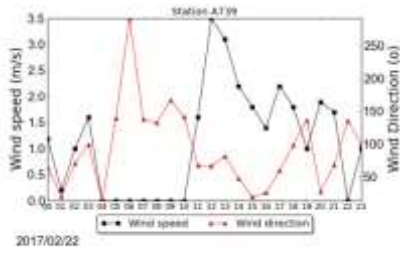
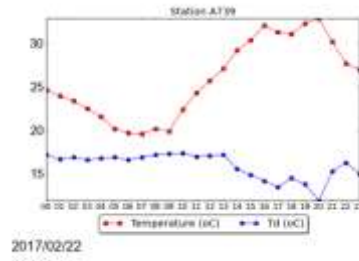


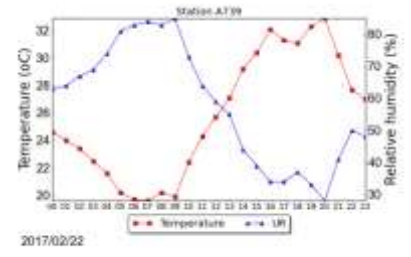
Figure 4-188: Wind speed and direction, temperature and dew point temperature, temperature and relative humidity for February, 22 at A701 (a), (b), (c); A713 (d), (e), (f); A726 (g), (h), (i); A728 (j), (l), (m); A739 (n), (o), (p); A740 (q), (r), (s); A746 (t), (u), (v).



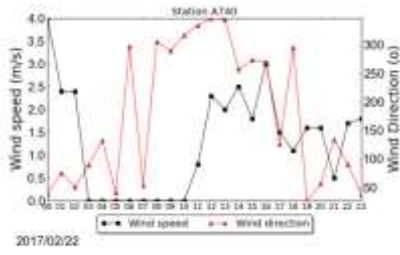
(n)



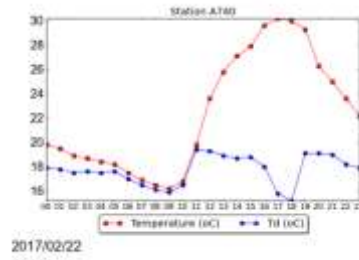
(o)



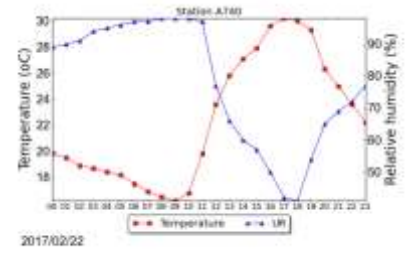
(p)



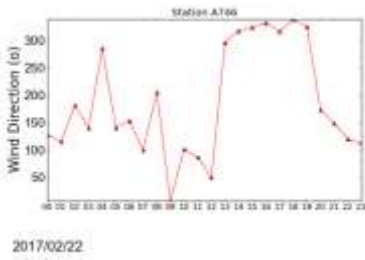
(q)



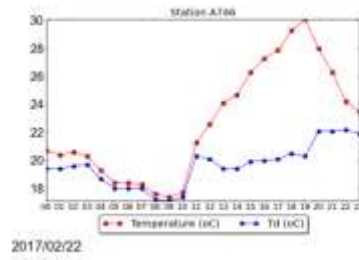
(r)



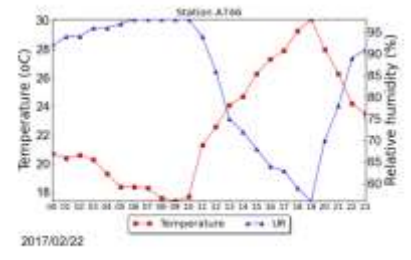
(s)



(t)



(u)



(v)

Figure 4-188: Continuation.

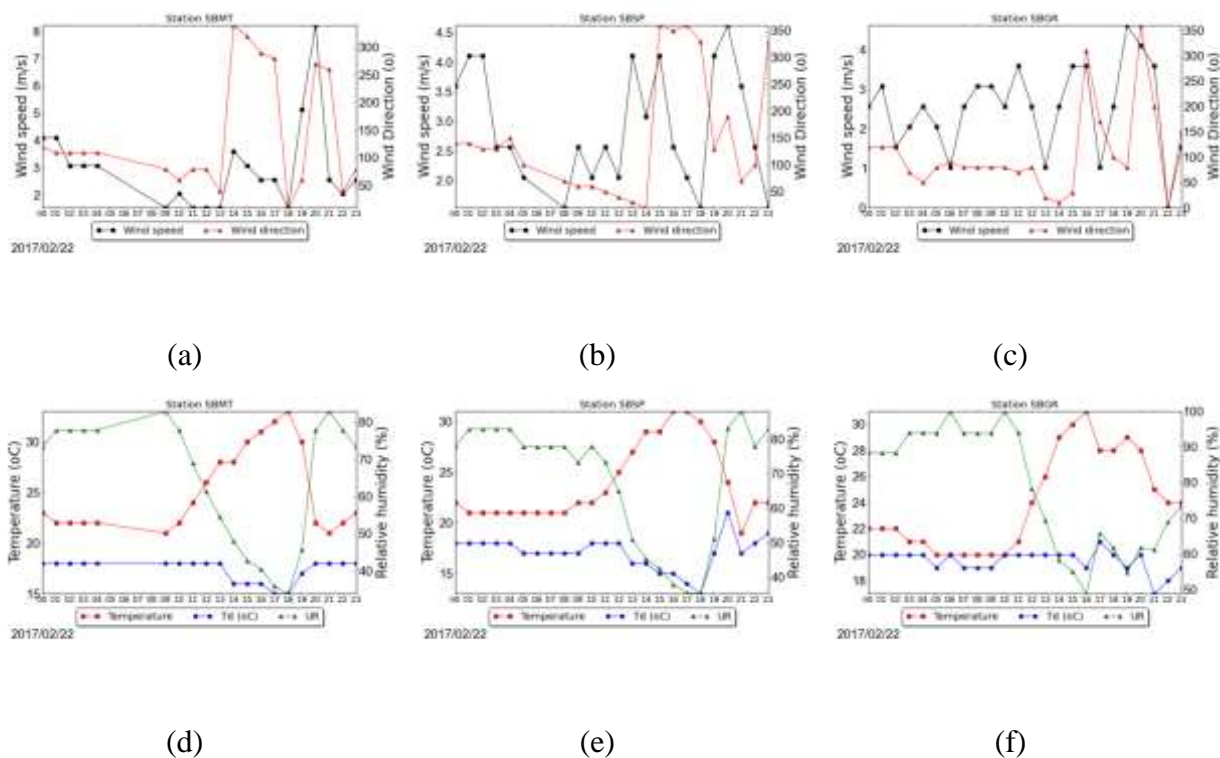


Figure 4-189: Wind speed and direction from METAR at station SBMT (a), SBSP (b), and SBGR (c); temperature, dew point temperature and relative humidity at stations SBMT (d), SBSP (e) and SBGR (f), for February, 22, 2017.

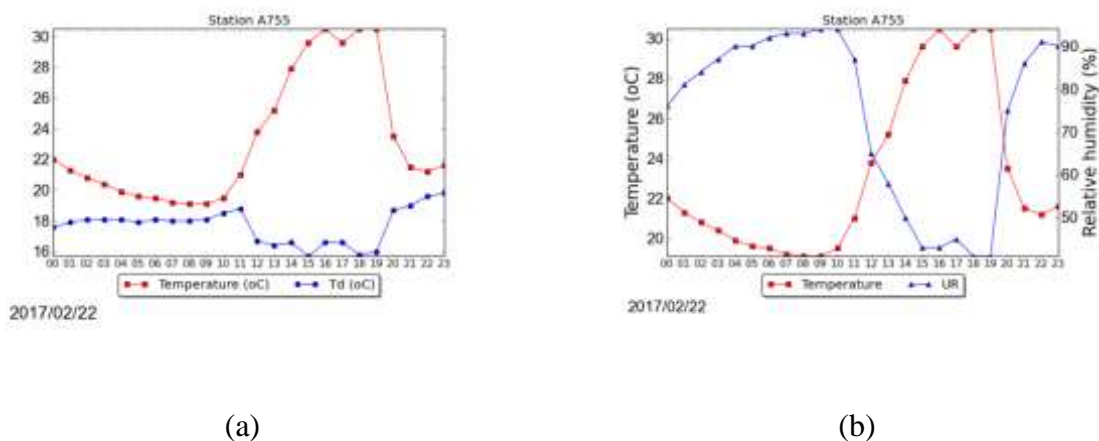
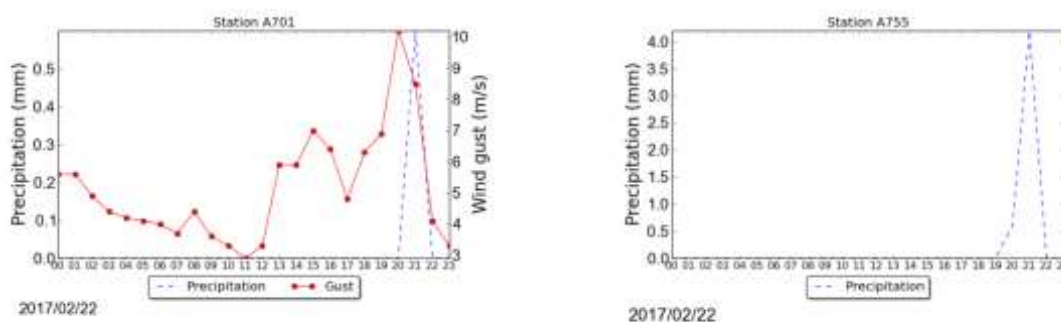


Figure 4-190: Temperature and dew point temperature (a), temperature and relative humidity (b) at station A755 for February, 22.



(a)

(b)

Figure 4-191: Precipitation (mm) and wind gust (m s^{-1}) at station A701 (a), and precipitation at station A755 (b) for February, 22th.

4.2.4 December, 28, 2016

During this event, rain was registered in the city of São Paulo, in which 7 points of flood were registered. At Campinas strong wind gusts were reported of 21.3 m s^{-1} , fall of trees, damages to roofs and to walls. Fall of trees were also reported in São José dos Campos and Guaratinguetá. Hail was reported at the cities of São Paulo, Campinas and Salesópolis, this last city reported damages on crops.

a. Satellite

In this section analysis of infrared images for South America and enhanced infrared images and visible images for the southeast region of Brazil will be carried out.

In the images for South America it is seen that after 00:00 UTC, only a few clouds are seen in the State of São Paulo in the west part of the State, while the east region remains cloud free. This is seen until convection starts to form in the west region after 11:00 UTC and after 16:00 UTC in the east region. These images are seen in Figure 4-192.

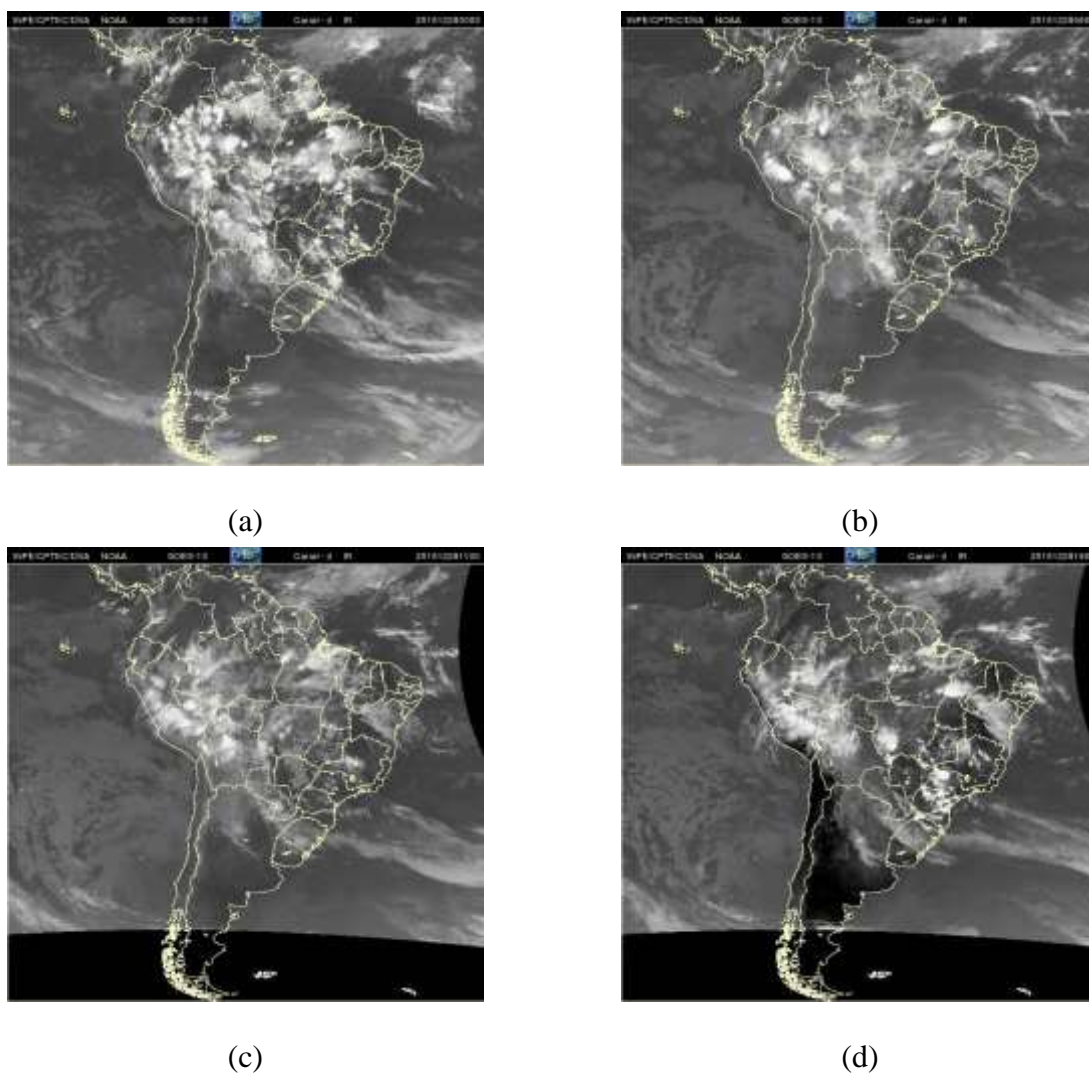


Figure 4-192: Infrared satellite images for South America for December, 28 at 00:00 UTC (a), 06:00 UTC (b), 11 UTC (c), 16:00 UTC (d).

In the visible channel images (Figure 4-193) convection is seen to form in the west region of the State after 10:38 UTC. Clouds form near the coast, indicating the presence of the sea breeze, seen at 13:38 UTC and more clearly at 14:45 UTC. It is possible to see the sea breeze advancing into the continent through the hours.

Enhanced infrared images are shown in Figure 4-194. At 16:00 UTC, cells are forming in the southeast region, while in the northwest region, in the enhanced infrared images, temperatures are around -60 to -70 °C. At 17:30 UTC cells are seen in the south region reaching values of -70 °C, cells are also observed close to the São Paulo (temperature around -

60°C) and forming at the Vale do Paraíba. These clouds move inland, and between 20:30 and 22:20 UTC temperature in the northeast region is reaching -70°C, which corresponds to the region of severe weather occurrences.

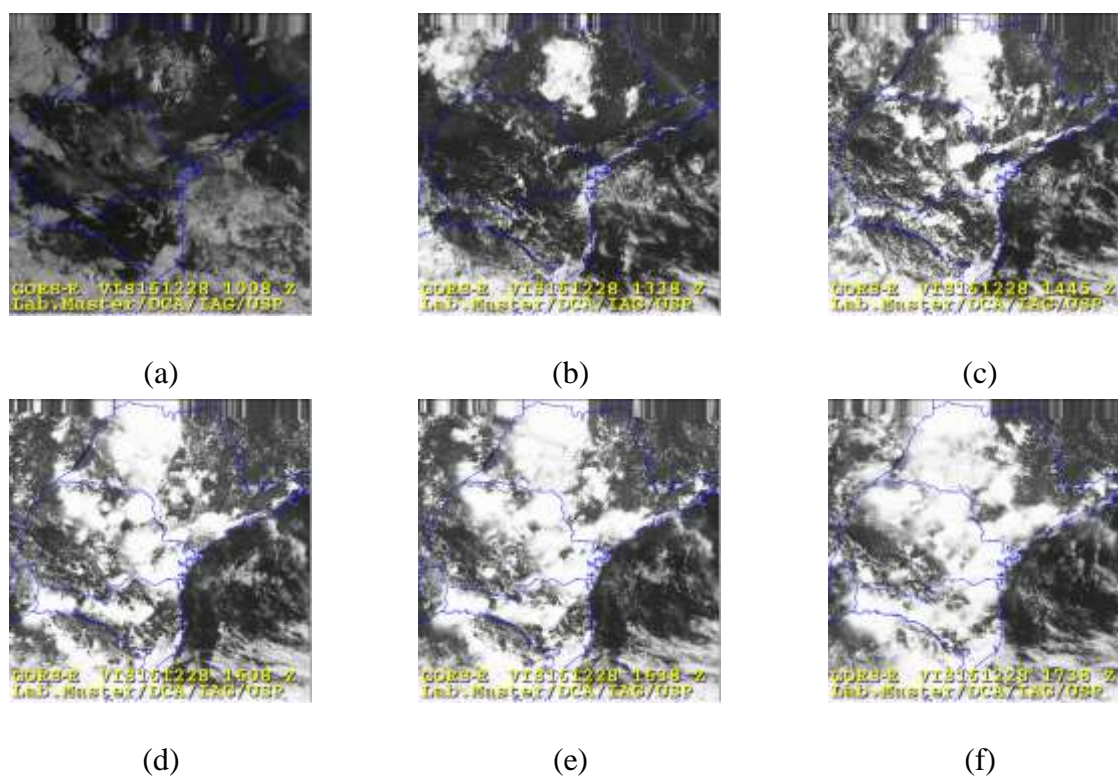


Figure 4-193: Visible channel satellite images for December, 28 at 10:08 UTC (a), 13:38 UTC (b), 14:45 UTC (c), 16:08 UTC (d), 16:38 UTC (e), and 17:38 UTC (f).

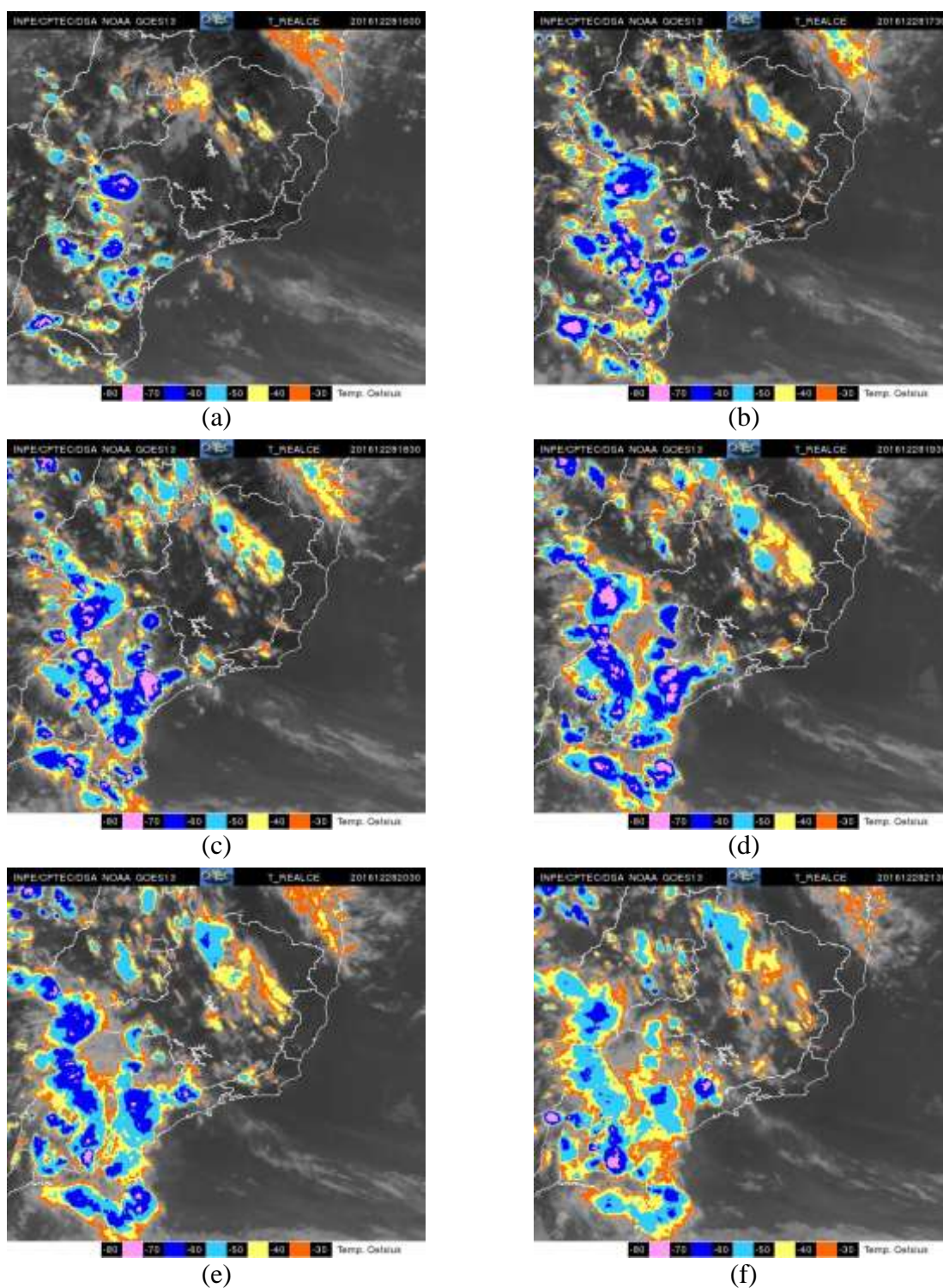


Figure 4-194: Enhanced infrared satellite images for December, 28 at 16:00 UTC (a), 17:30 UTC (b), 18:30 UTC (c), 19:30 UTC (d), 20:30 UTC (e), 21:30 UTC (f), 22 UTC (g), 23:00 UTC (h).

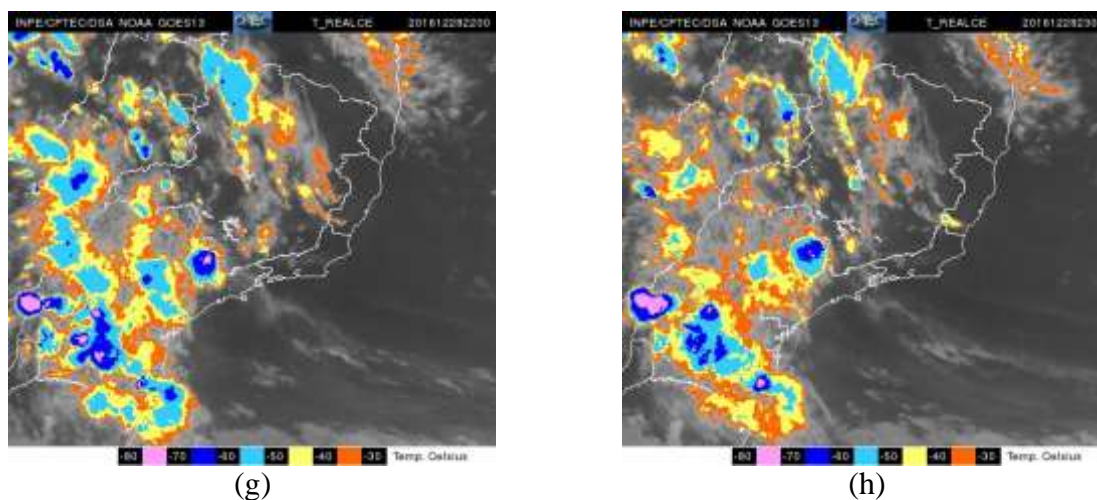


Figure 4-194: Continuation.

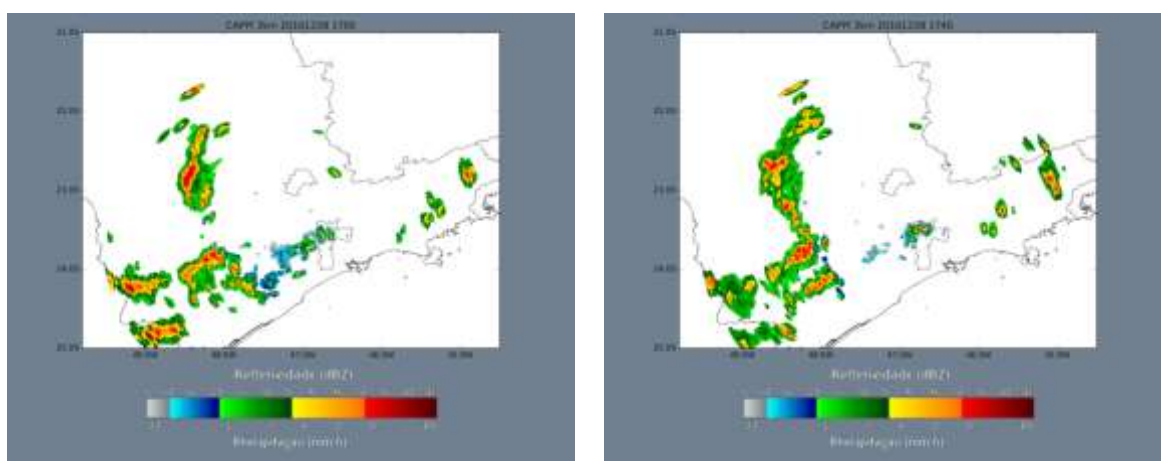
b. Radar

The advance of this event from the São Roque radar is seen in Figure 4-195.

At 17:00 UTC cells are seen parallel to the coast, and are present in the region of São Paulo and at the Vale do Paraíba. At 17:40 UTC reflectivity around 55 dBZ is seen in the region of Guaratinguetá, localized at the Vale do Paraíba. Some clouds have started to develop in the region of Serra da Mantiqueira, in the northeast region. Between 1740 and 1750 UTC reflectivity in the region of São Paulo is around 55 dBZ and at 18:00 UTC it reaches 60 dBZ. At this hour, cells with high reflectivity are in the north zone of the city of São Paulo, between 3h50 and 4h pm local time, hail was registered at the surface in this region. After 18:00 UTC, some clouds move to Guarulhos, still with reflectivity of the same order. Some clouds move inland to the region of Campinas. Between 1830 and 1850 UTC, reflectivity is ranging from 60 to 65 dBZ in the region of Guarulhos. After 18:00 UTC clouds are seen in the region of São José dos Campos, reaching high reflectivity values (around 65 dBZ) at 1850 UTC. Fall of trees were reported at this city.

As mentioned in the satellite analysis, it is possible to see the clouds moving inland with the advance of the hours, and at between 2010 and 2030 UTC cells moving from Vale do

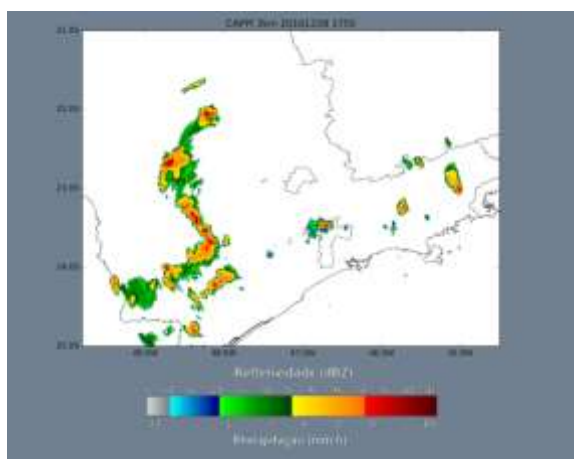
Paraíba merged with cells moving from Guarulhos, as they continue to advance toward Campinas. Clouds reached the region of Campinas at 1920 UTC, moving from São Paulo, as mentioned before, and at 20:00 UTC, reflectivity is around 55 dBZ in the south region of Campinas. At 2040 UTC high reflectivity, of the order of 60-65 dBZ is seen in the north region of Campinas, in the region of Bragança Paulista and Socorro (east-southeast of Campinas), and between São José dos Campos and Mogi das Cruzes. Campinas was the only that recorded severe weather according to the news. After 2040 UTC reflectivity decreased, but increased to the same order after 21:00 UTC, when cells from this region merged with clouds propagating from east-southeast. At 2150 UTC reflectivity is still high, around 55-60 dBZ in the east region of Campinas. Several damages were reported in the city during this event, including fall of trees, walls, and damages to houses roofs. At 8 pm local time, a wind gust of 21 ms⁻¹ was observed in the city, but only 14.2 mm were registered in one and a half hour, according to CEPAGRI (mentioned on the news).



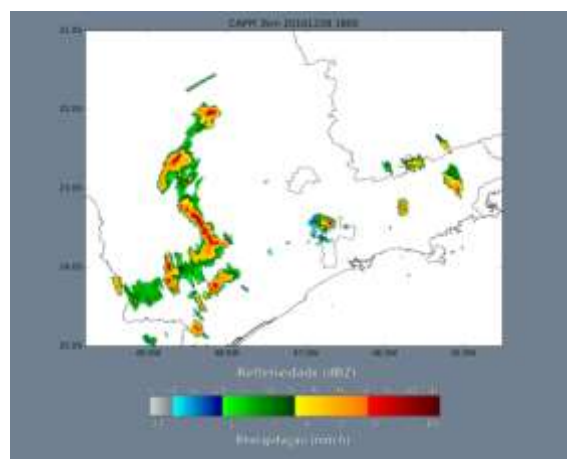
(a)

(b)

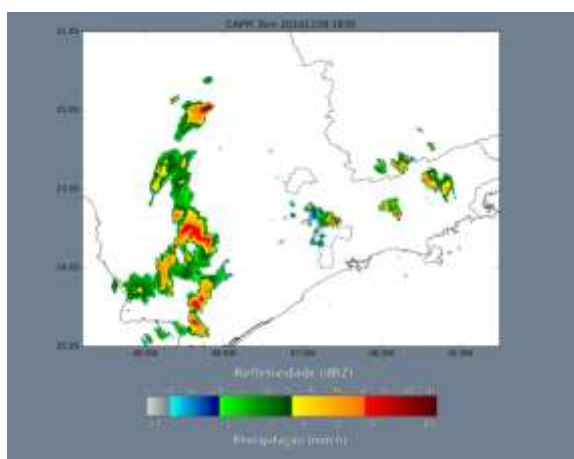
Figure 4-195: São Roque radar images for December, 28 at 17:00 UTC (a), 17:40 UTC (b), 1750 UTC (c), 18:00 UTC (d), 1830 UTC (e), 1850 UTC (f), 1920 UTC (g), 20:00 UTC (h), 20:10 UTC (i), 2030 UTC (j), 2040 UTC (l), 21:00 UTC (m), 2150 UTC (n), 2250 UTC (o).



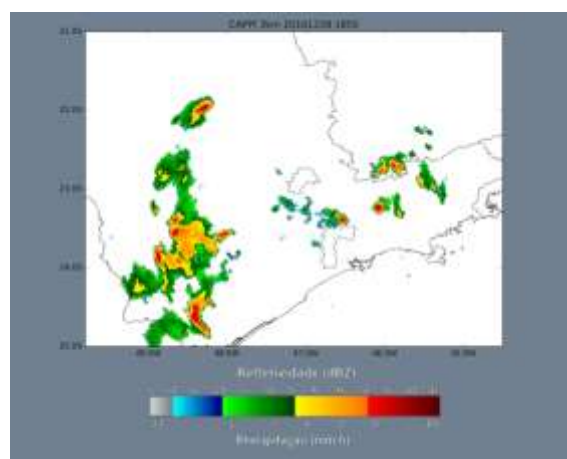
(c)



(d)



(e)



(f)



(g)

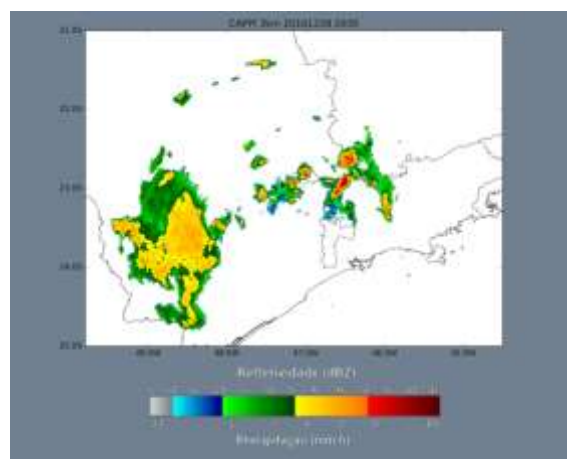


(h)

Figure 4-195: Continuation.



(i)



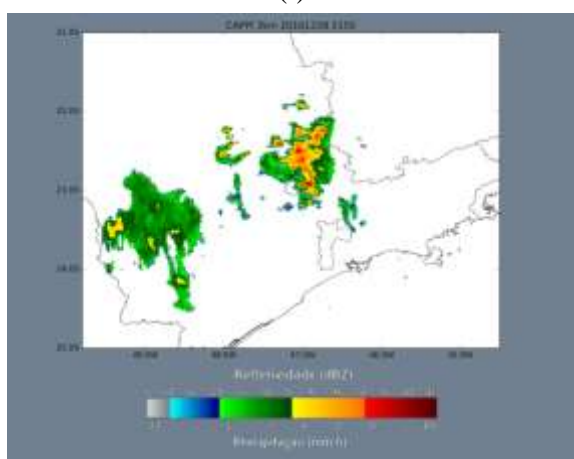
(j)



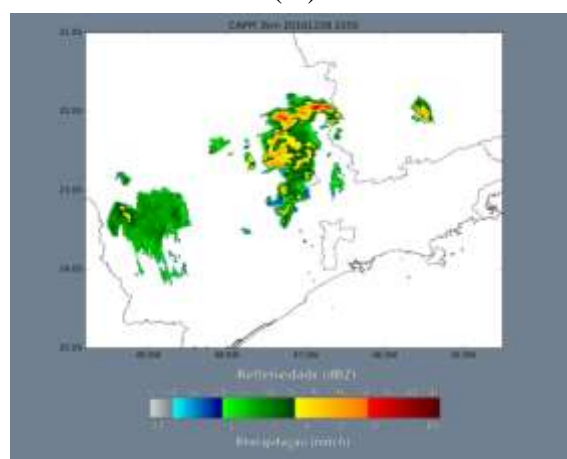
(l)



(m)



(n)



(o)

Figure 4-195: Conclusion.

c. Synoptic scale analysis

In the 200 hPa analysis, an upper level cyclonic vortex is present on top of the State of Bahia, but is not influencing region of the State of São Paulo. An anticyclone is seen in eastern Paraná, this system is causing a diffluence pattern on the region of Paraguay. This system loses strength during the day. In the 500 hPa after 06:00 UTC a high pressure system is on top of the State of São Paulo, this system causes subsidence, inhibiting convection. At 12:00 UTC the system is between Paraná and São Paulo. This pattern is still seen in the next day. Low values of wind divergence at 200 hPa (around $0.2-0.4 \cdot 10^{-4} \text{ s}^{-1}$) are seen throughout the day at different regions, at 00:00 UTC is located at central-north and west, at 06:00 UTC an area of divergence is present at northwest, at 12:00 UTC no divergence is seen, and at 18:00 UTC it is at southwest. This means that divergence was not relevant at this event. Neither is vorticity advection.

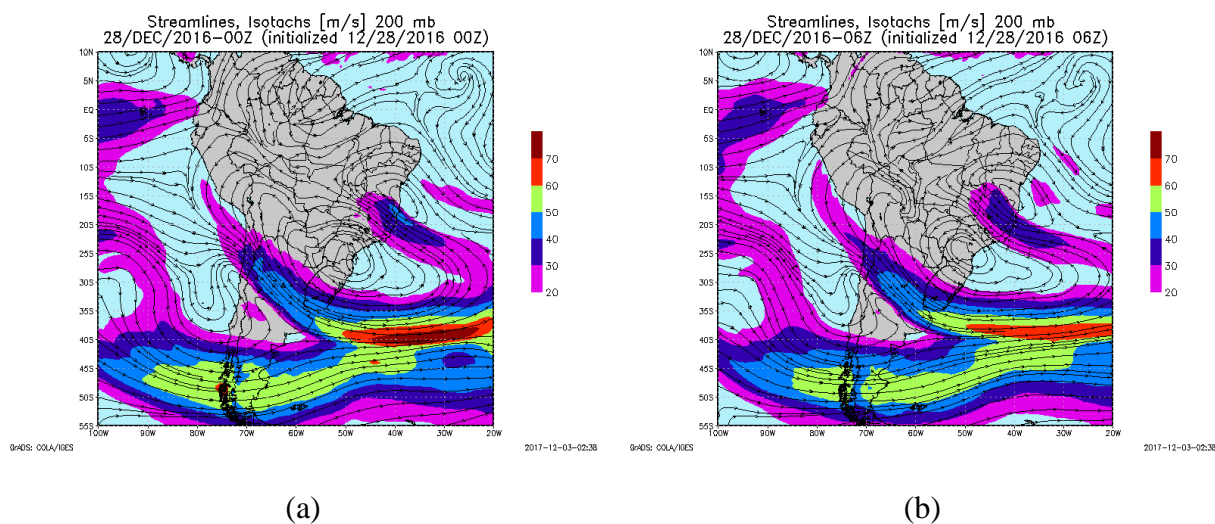


Figure 4-196: Streamlines and isotach (m s^{-1}) at 200 hPa at 00:00 UTC (a), 06:00 UTC (b), 12:00 UTC (c), and 18:00 UTC (d) for December, 28th.

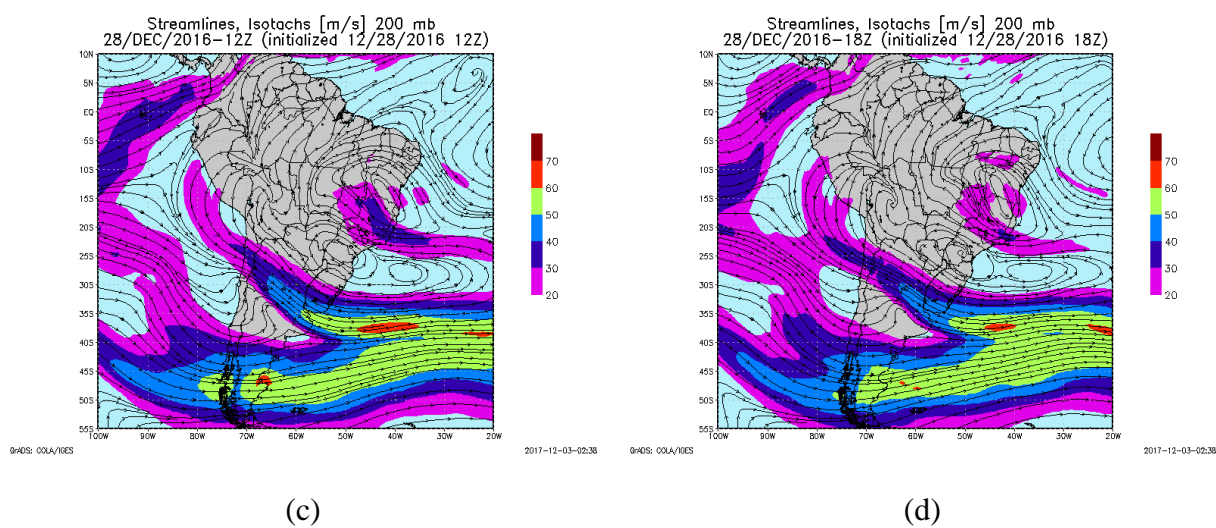
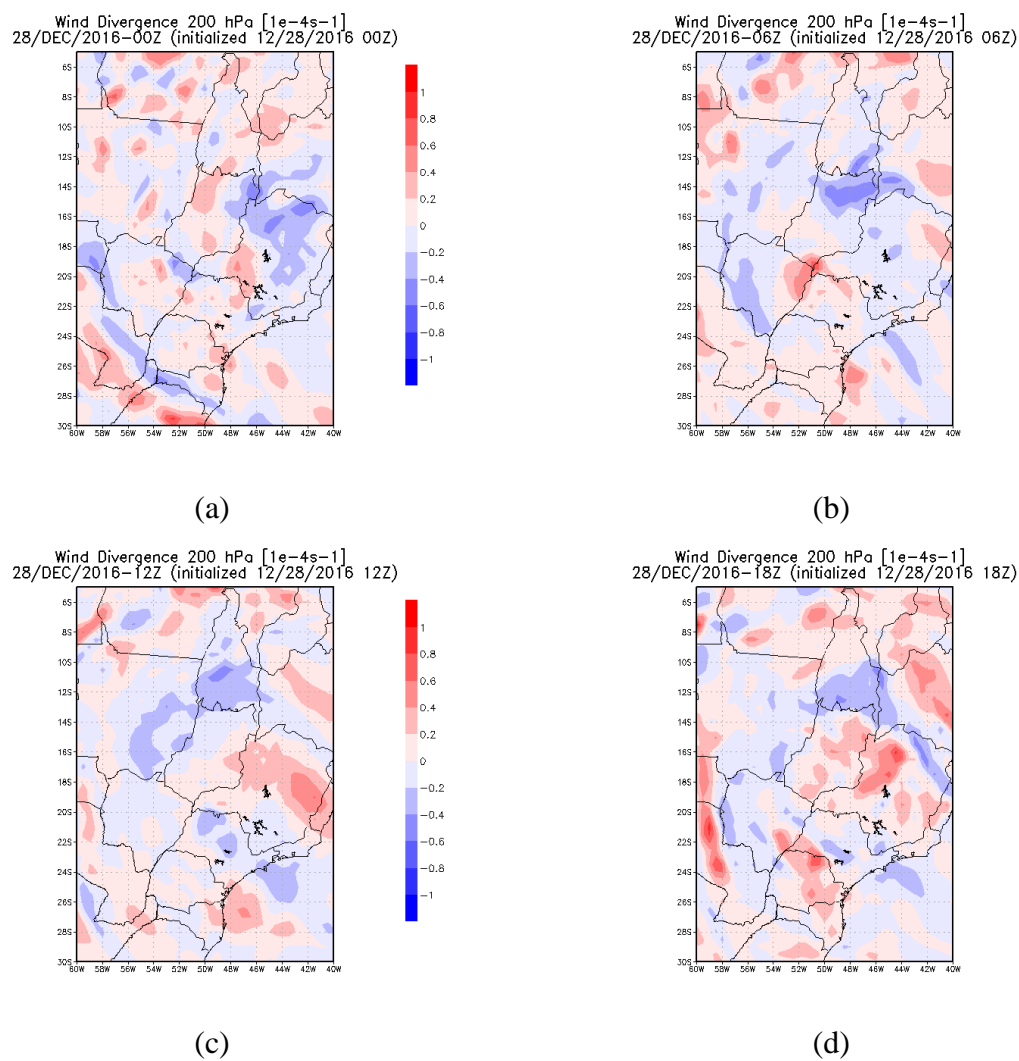


Figure 4-196: Continuation.

Figure 4-197: Wind divergence ($1 \times 10^{-4} s^{-1}$) at 200 hPa at 00:00 UTC (a), 06:00 UTC (b), 12:00 UTC (c), and 18:00 UTC (d), for December, 28th.

Temperature in the 850 hPa analysis is around 20-25 °C throughout the day (Figure 4-199). Relative humidity is low, at 00:00 UTC is below 65% in the eastern region and around 65-70% in the rest of the State. At 12:00 UTC is between 65-75%, and at 18:00 UTC it has regions, again, with values below 65 %, but most of the State has values between 65-75%, only a small region southeast has values around 75-80%. This dryness and high temperatures are related to the high pressure system at 500 hPa. Streamlines and relative humidity at 850 hPa is also seen in Figure 4-199.

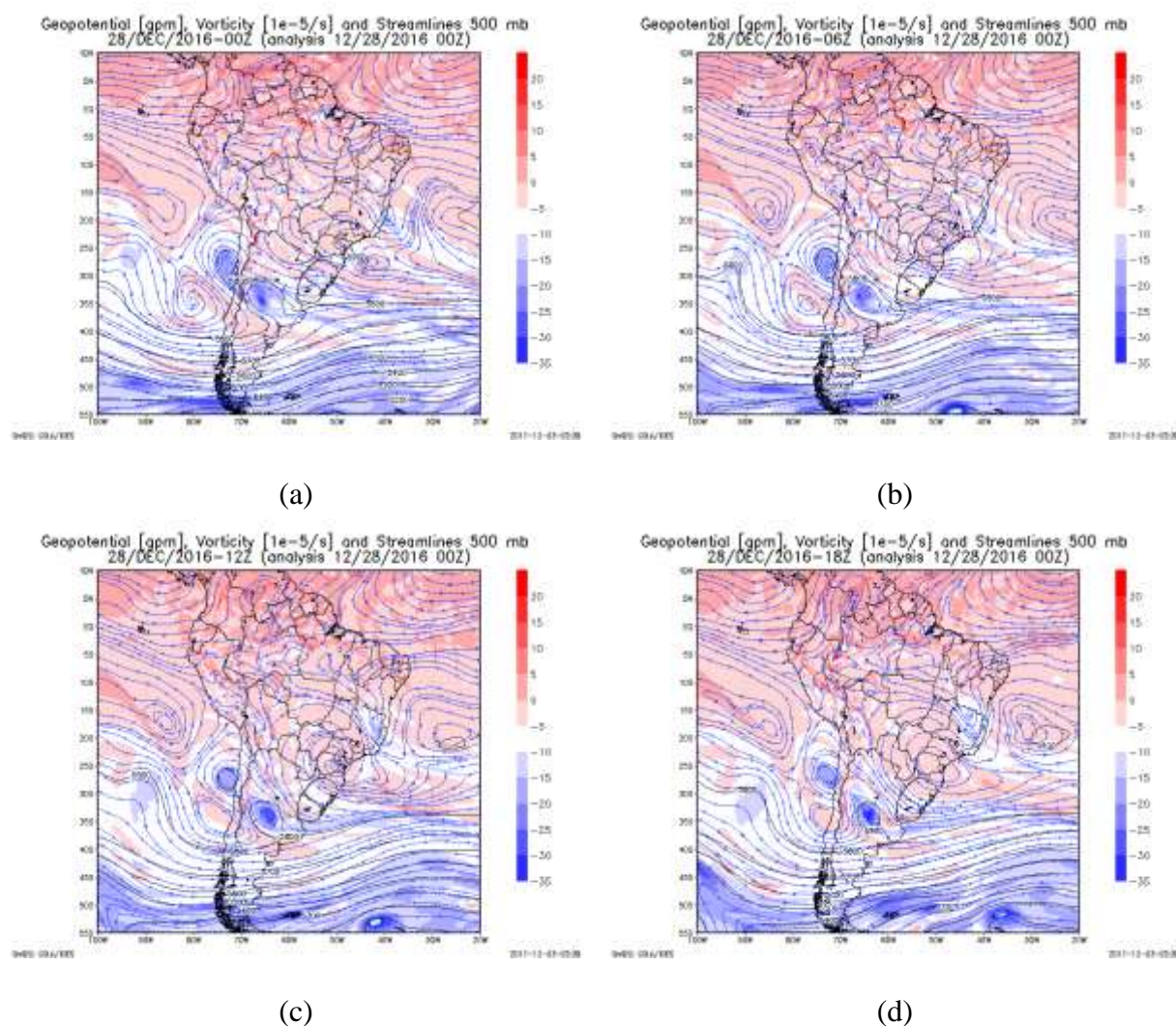


Figure 4-198: Geopotential height (gpm), vorticity ($1 \times 10^{-5} \text{ s}^{-1}$) and streamlines at 500 hPa at 00:00 UTC (a), 06:00 UTC (b), 12:00 UTC (c), and 18:00 UTC (d), for December, 28th.

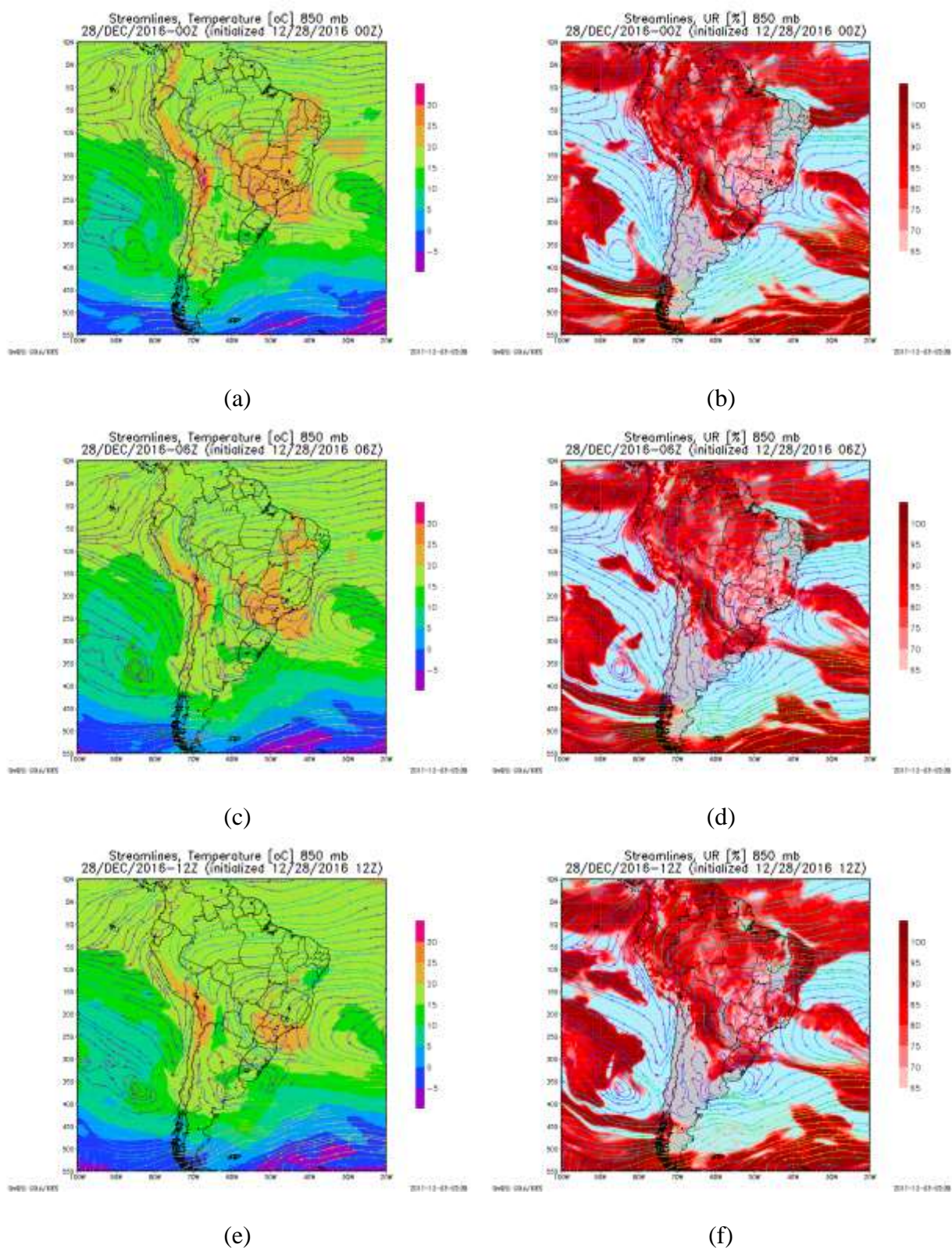


Figure 4-199: Streamlines and temperature ($^{\circ}\text{C}$), streamlines and relative humidity (%) at 850 hPa at 00:00 UTC (a), (b), 06:00 UTC (c), (d), 12:00 UTC (e), (f), and 18:00 UTC (g), (h) for December, 28th.

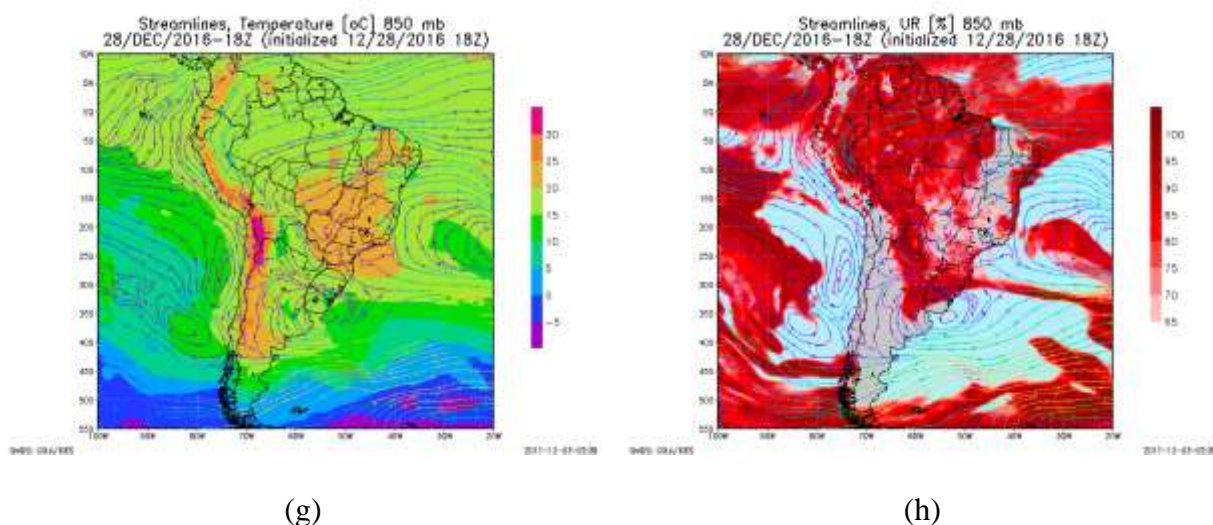


Figure 4-199: Continuation.

In the surface analysis, shown in Figure 4-200, a frontal system is in the Atlantic Ocean, east of Rio Grande do Sul, the Atlantic subtropical high is around 25°S with the center located east of 20°W, beyond the limits of the figure. It is the only system influencing the State of São Paulo in the surface analysis. The temperature in the surface analysis, at 12:00 UTC is above 27°C in the entire State, and values between 29-31 °C are observed, again, as already mentioned in the 850 hPa analysis this high temperatures are related to the high pressure system at the 500 hPa level

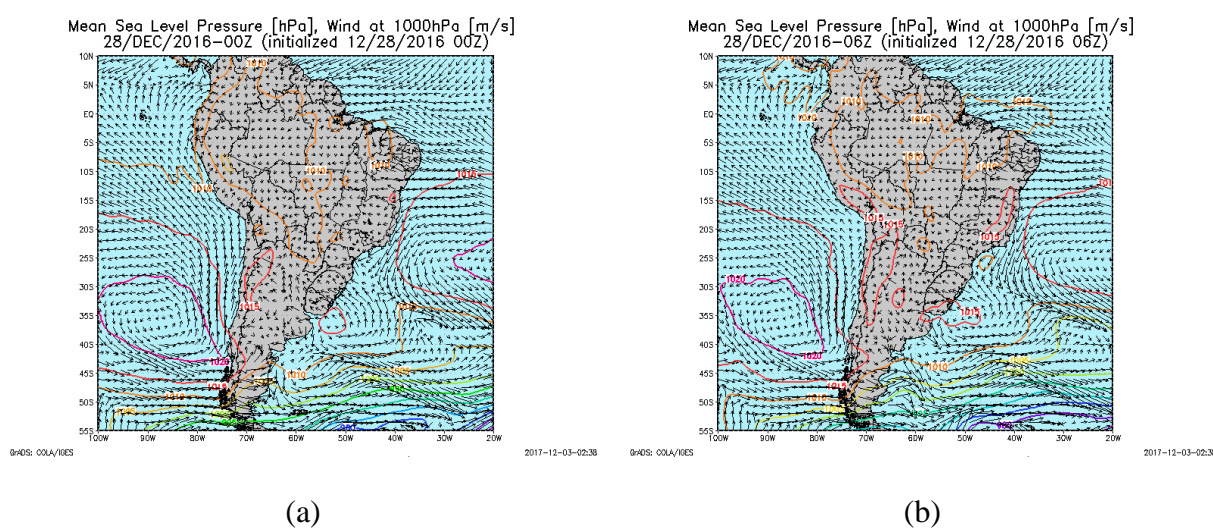


Figure 4-200: Mean sea level pressure (hPa) and wind (m s^{-1}) at 00:00 UTC (a), 06:00 UTC (b), 12:00 UTC (c), and 18:00 UTC (d), for December, 28th.

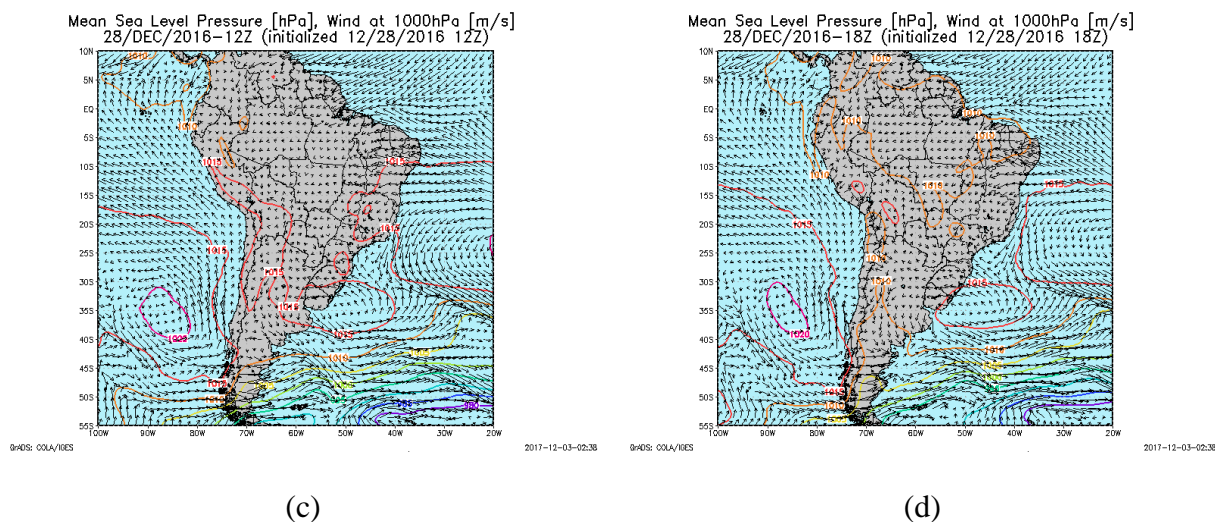


Figure 4-200: Continuation.

d. Thermodynamic analysis

Besides the LI parameter, which is always analyzed using the GFS output, CAPE, CIN and 700-500 hPa lapse rate analysis will also be carried out using the GFS model output, for the fact that, the BRAMS model output and sounding were not available for this day. These parameters at 12:00 UTC are shown in Figure 4-201.

CAPE values, at 12:00 UTC, are higher in the west region, in which values are between 2100-2400 J kg^{-1} . In the east region of the State, a high variability is seen; smaller values are seen in the northeast region, between 600-1000 J kg^{-1} , the rest of the east part varies from 1000 to 2000 J kg^{-1} . These ranges indicate a marginally unstable and a moderately unstable condition, respectively. At 15:00 UTC, CAPE still shows high variability in the east region, small values are still seen in the extreme northeast region, the rest of the east section is between 1400-2000 J kg^{-1} . This still indicates a moderately unstable condition.

At 12:00 UTC, CIN is higher in the west part, near the coast and in the southwest part, where values are around -20 to -40 J kg^{-1} in the first, and -20 to -50 J kg^{-1} , in the second and even below -50 J kg^{-1} in the third. The rest the State has values around -10 and -20 J kg^{-1} . This value is lower than obtained for other events with similar synoptic scale pattern; it is possible that CIN is underestimated at this hour.

The highest LI values at 12:00 UTC are seen in the central-south region and southeast near the coast, the parameter is around -6 K in those regions. In the northeast region lower values, around -2 to -4 K are observed, the rest of the State has values between -4 and -6 K. The same range is seen at 15:00 UTC (around -4 to -6 K). These values indicate an unstable condition, with probable storm, even severe.

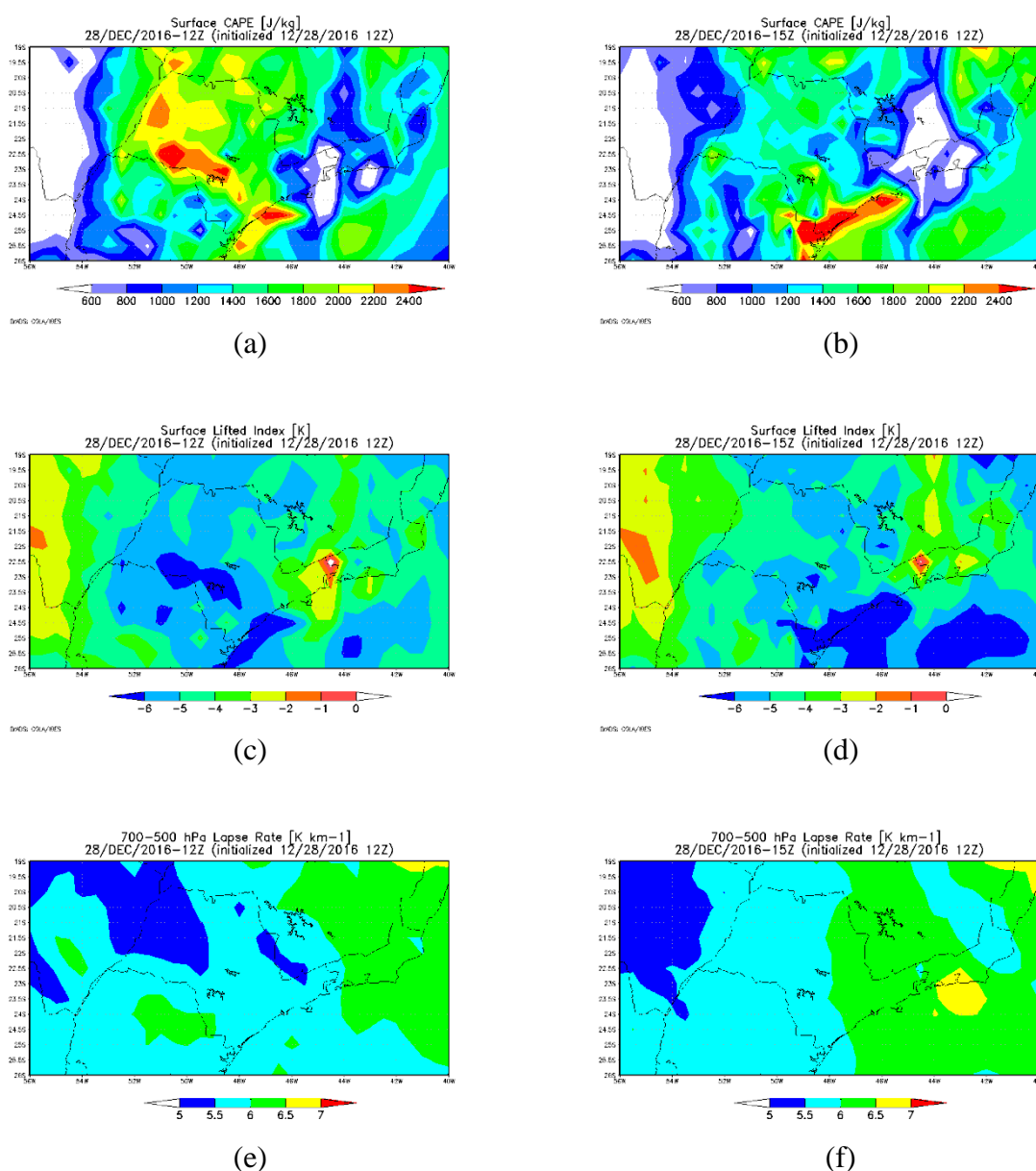


Figure 4-201: CAPE at 12:00 UTC (a), and 15:00 UTC (b); LI at 12:00 UTC (c), and 15:00 UTC (d); 700-500 hPa Lapse rate at 12:00 UTC (e), and 15:00 UTC (f), from GFS for December, 28, 2016.

The 700-500 hPa lapse rate is between 5.5-6 K km⁻¹ at 12:00 UTC, and it increases to around 6.0 and 6.5 K km⁻¹ at 15:00 UTC.

Vertical cross sections of relative humidity and wind were also analyzed (Figure 4-202). Winds are weak throughout the vertical; only a small intensification is seen after 400 hPa, which means no significant wind shear is present. At 12:00 UTC, the wind direction is the same until 800 hPa, above, the wind turns clockwise with height, and anticlockwise after 400 hPa, near São Paulo.

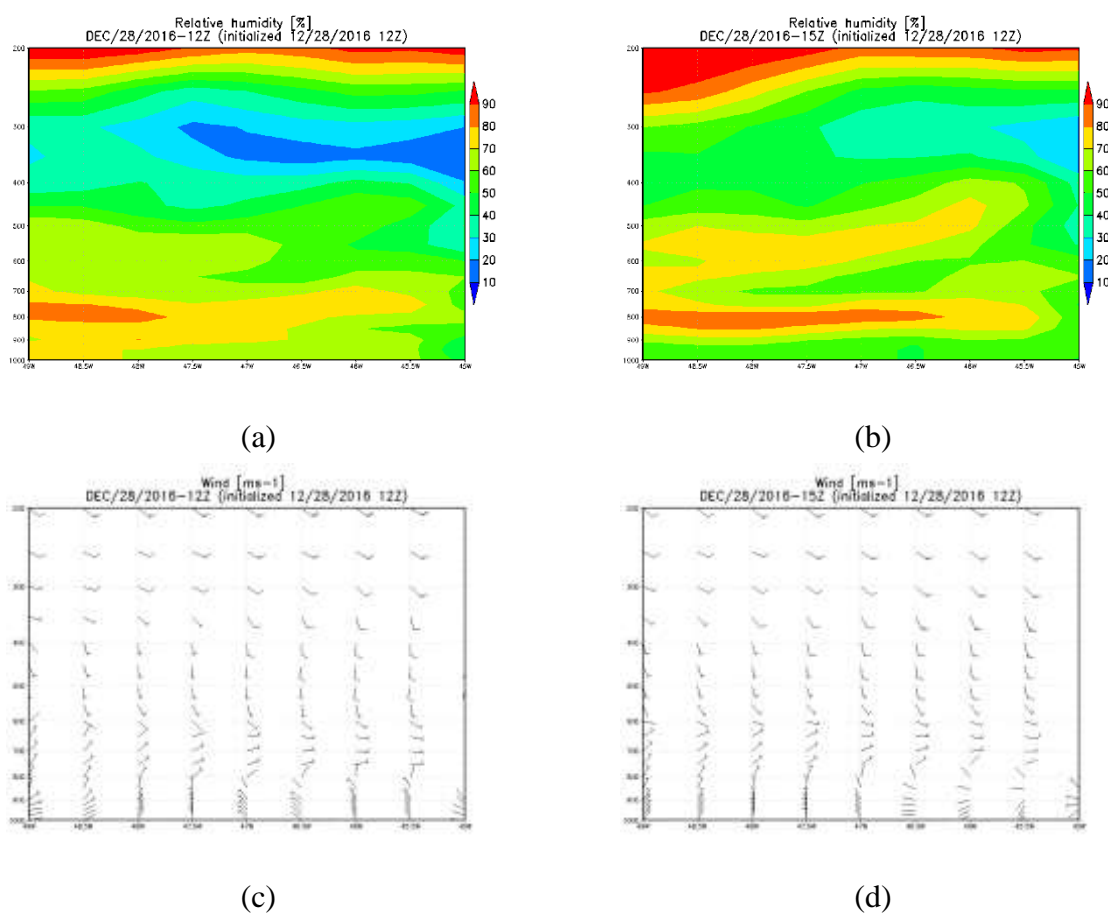


Figure 4-202: Vertical cross section of relative humidity from GFS at 23.5°S at 12:00 UTC (a), 15:00 UTC (b), of winds at 12:00 UTC (c), and 15:00 UTC, for December, 28, 2016.

As already mentioned in previous events, wind increasing in an anticlockwise direction indicates warm advection in a layer, through the thermal wind relation, but this does not seem to be occurring at this day. The analysis of the vertical cross section of relative humidity

shows that, between 400 and 300 hPa, the atmosphere has low levels of humidity, at 12:00 UTC, values around 10-20 % are seen. Between 600 and 500 hPa, it is ranging from 50 to 70 %. This is important to verify the presence of dry air in the atmosphere during the event, although it is not possible to affirm that this is the actual lowest values seen in the atmosphere. Analyzing other events in which soundings were available showed that, although it is possible to identify the presence of dry air in the atmosphere and the level of occurrence using the GFS model, the lowest value observed in the model output is sometimes, greater than the one observed in the sounding. At 15:00 UTC, it is between 60 and 80 % between 600 and 500 hPa, and around 30-50 % between 400 and 300 hPa. The same pattern is seen in the vertical cross section of relative humidity and winds for the region of Campinas, fixing the latitude at 23.0°S.

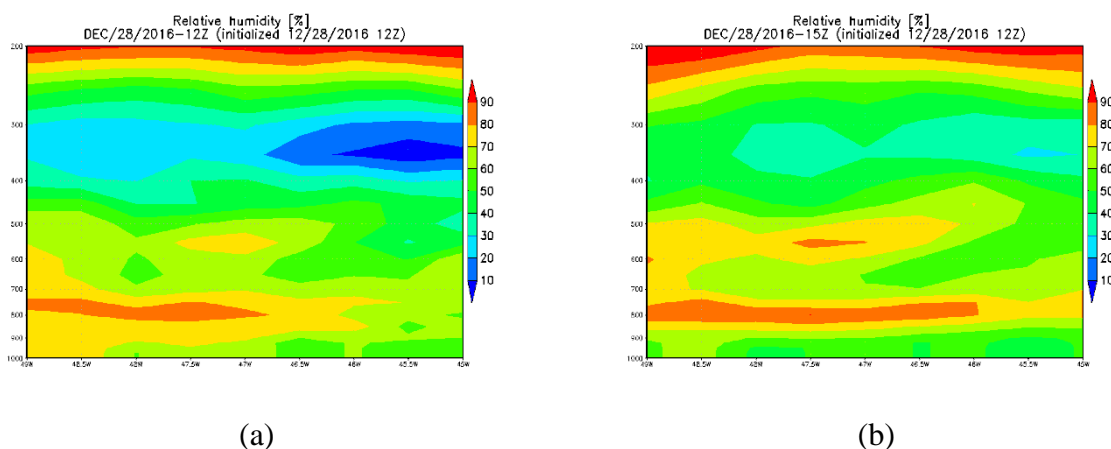


Figure 4-203: Vertical cross section of relative humidity from GFS at 23°S at 12:00 UTC (a), 15:00 UTC (b), of winds at 12:00 UTC (c), and 15:00 UTC, for December, 28, 2016.

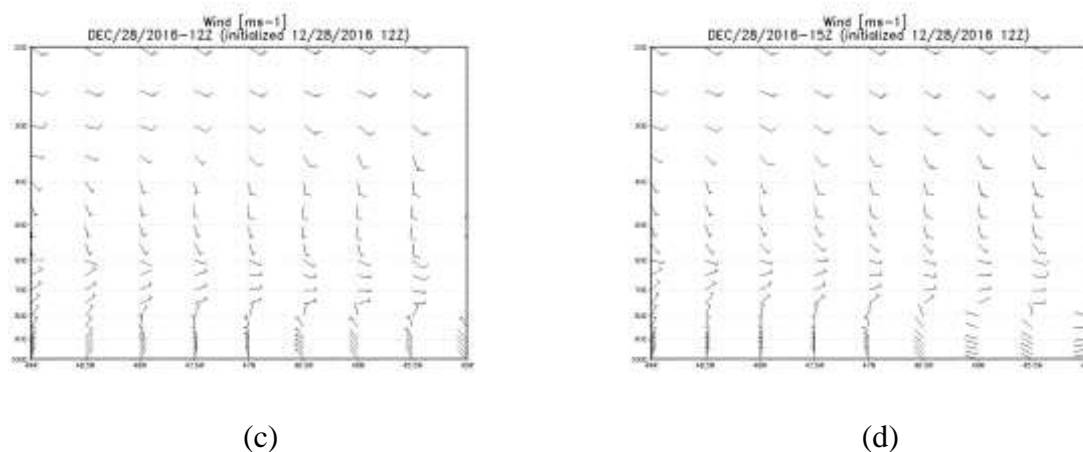


Figure 4-203: Continuation.

This event was not related to a synoptic forcing, meaning that no large scale system aided in the development of the storms. Actually, the presence of the high pressure system at 500 hPa inhibits the development of storms.

e. Surface stations

For this event 18 INMET surface stations were analyzed, plus METAR analysis from the airports at the city of São Paulo, Guarulhos and Taubaté.

At station A701, in São Paulo, wind is from east and northeast until 03:00 UTC, after that, winds are varying and are weak, with speed below 1.0 m s^{-1} . At 13:00 UTC it is from northwest and the speed increased, it then turned to northeast at 15:00 UTC. At 17:00 UTC winds turned to southeast followed by an increase in dew point temperature, relative humidity wind speed, and decrease in temperature, these changes are seen at 18:00 UTC. A wind gust was observed between 17:00 and 18:00 UTC of 13.9 m s^{-1} .

At the Campo de Marte airport, winds are from northeast until 08:00 UTC. Between 09:00 and 16:00 UTC it changes from southeast, southwest, north-northwest, and northeast. At 17:00 UTC winds turn to southeast. At the Congonhas airport the turn to southeast also occurred at 17:00 UTC. At the beginning of the day, at this airport, winds are also from northeast, until 05:00 UTC, it, then, varies between southeast, northeast and southwest until

12:00 UTC, after that it is from northeast and an hour before turning to southeast, it is from northwest.

At both stations, the turn to southeast were all accompanied by increase in dew point temperature, relative humidity, wind speed and decrease in temperature.

In the Guarulhos analysis, winds are from east and northeast until 10:00 UTC, a change to southeast and southwest occurred after, but at 14:00 UTC it was back from northeast. Southeast winds are observed only at 19:00 UTC, but the visibility dropped to 80 m at this hour. An hour before, an increase in relative humidity and decrease in temperature is observed, but the dew point temperature does not change. It is not possible, considering all that has been described from observations at this airport, to identify the sea breeze.

According to the CGE, the highest rain average observed was in the north zone of 10.2 mm. Two CGE stations recorded rain indices above 20 mm, Pirituba and Lapa, with 44.6 and 29.6 mm, respectively. Also, two stations from the Alt do Tietê network registered more than 20 mm (29.6 and 27.2 mm). Hailstorm was observed at Pirituba, in the north zone between 03:50 and 4:00 PM local time. Wind gusts around 11 and 12 m s^{-1} were observed at the Guarulhos and Congonhas airport.

Station A712 is located at the southeast coast of the State, and registered the sea breeze penetration at 11:00 UTC, with southeast winds and increase in all expected variables. Station A746 is probably the closest to the ocean after this one, and it registered southeast wind with increase in dew point temperature at 13:00 UTC. Between 14 and 15:00 UTC, 7.2 mm of rain and a wind gust of 9.3 m s^{-1} were observed.

The closest station to São Paulo, Barueri, recorded increase in dew point temperature, relative humidity and decrease in temperature at 17:00 UTC, around the same hour observed at the city of São Paulo. Between 17:00 and 18:00 UTC, 18 and 19:00 UTC, 3.2 and 1.2 mm were observed. At Sorocaba, southeast winds were observed at 19:00 UTC, with increase in

dew point temperature and relative humidity in the previous period. Decrease in temperature and increase in wind speed were also observed after 19:00 UTC. No rain was registered.

Station A740, at Vale do Paraíba, recorded all the expected changes related to the sea breeze at 17:00 UTC, the wind followed by those changes were from northeast. No rain was registered. Also at Vale do Paraíba, station A728, all those changes were observed related to southeast winds at 17:00 UTC, also observed at the METAR analysis from the airport at the city. Wind gusts of 17.4 and 15.6 m s⁻¹ were registered between 18:00-19:00 and 19:00-20:00 UTC, but only 0.2 mm of rain was observed.

At station A714, between 19:00-20:00, 20:00-21:00 and 21:00-22:00 UTC, 4.6, 5.4, and 1.2 mm were registered, respectively. A wind gust of 12.6 m s⁻¹ was observed for two hours (18:00-19:00 and 19:00-20:00 UTC). Station A718 registered wind gusts of 13.2 m s⁻¹ and 15.5 m s⁻¹ between 16:00-17:00 UTC and 17:00-18:00 UTC, but less than 4 mm was registered. Station A726 recorded a wind gust of 12 m s⁻¹ between 18:00-19:00 UTC, less than 2 mm of rain was observed. Station A738 registered 13 m s⁻¹ around 21:00-22:00 UTC, but no rain was recorded. At station A741 a wind gust of 14.1 m s⁻¹ was recorded between 17:00 and 18:00 UTC, only 4.0 mm of rain was recorded at this interval, although, 9.8 mm was recorded around 11-12 UTC. The highest wind gust was observed at station A739, between 21:00-22:00 UTC, 18.4 m s⁻¹ was observed, but only 2 mm of rain was registered.

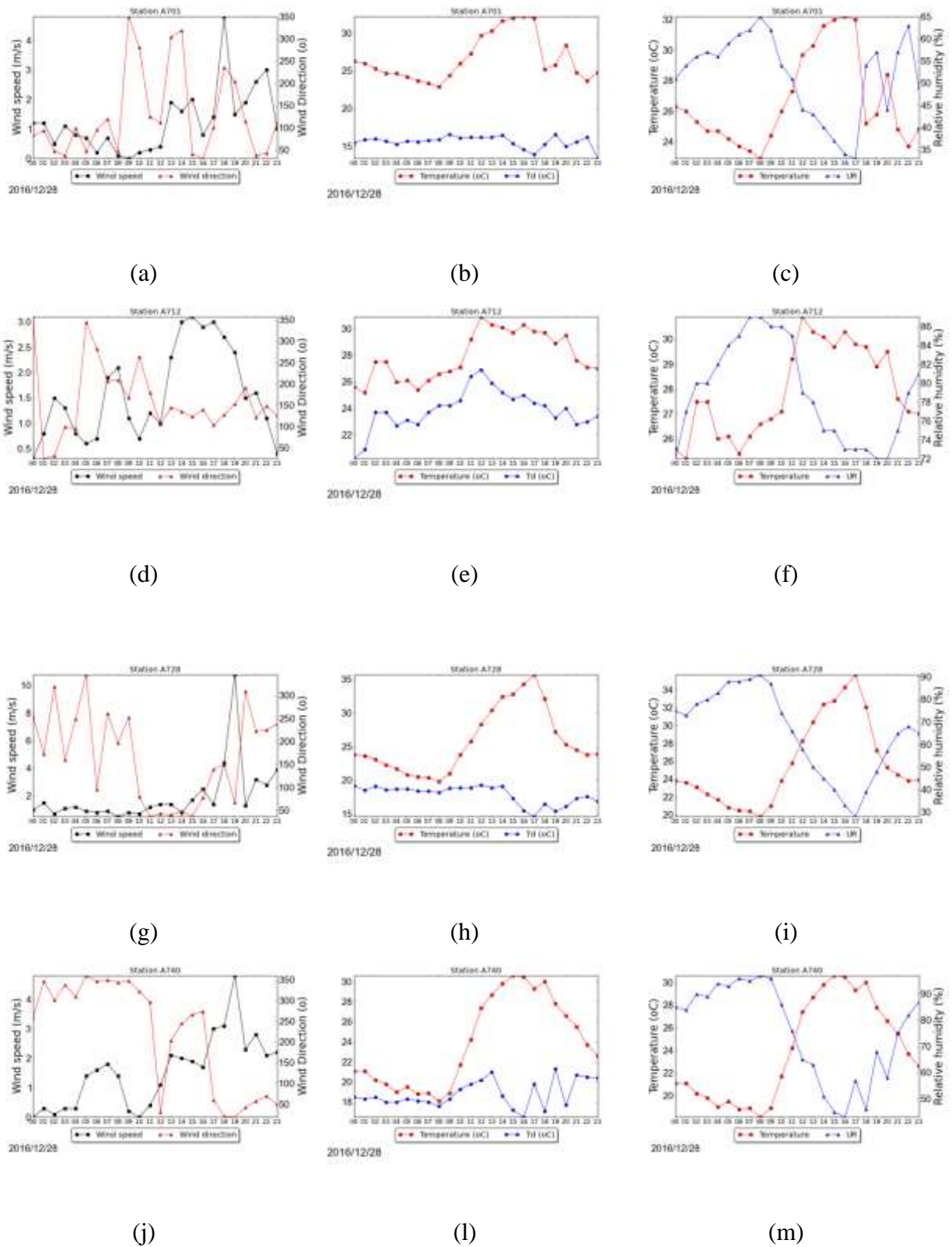


Figure 4-204: Wind speed and direction, temperature and dewpoint temperature, temperature and relative humidity for December, 28 at station A701 (a), (b), (c); A712 (d), (e), (f); A728 (g), (h), (i); A740 (j), (l), (m); A746 (n), (o), (p).

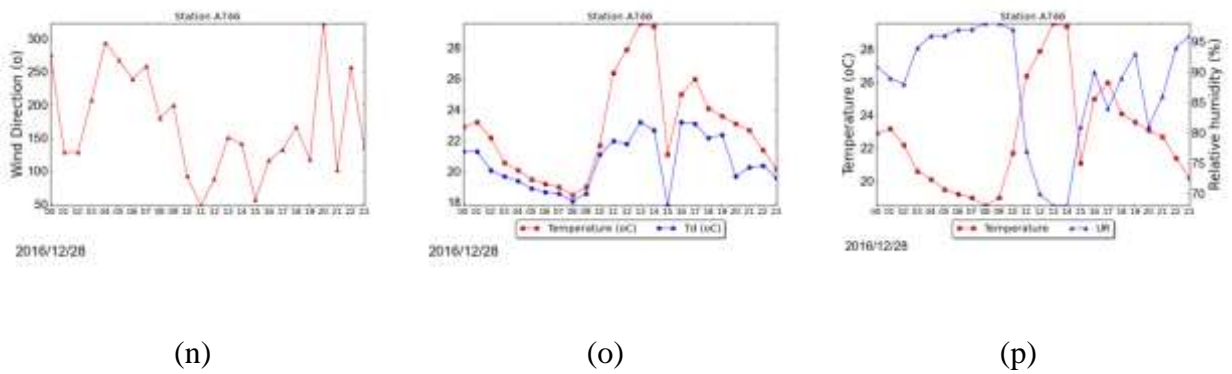


Figure 4-204: Continuation.

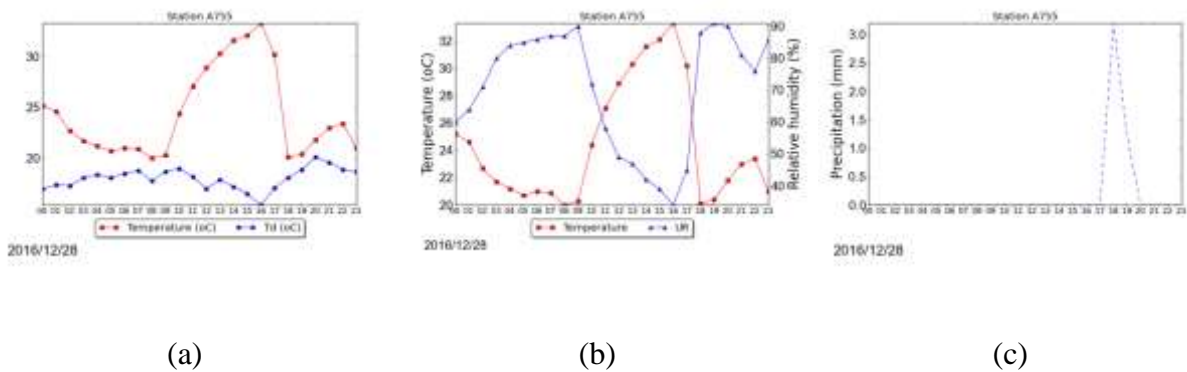


Figure 4-205: Temperature (°C) and dewpoint temperature (°C) (a), temperature (°C) and relative humidity (%) (b), and precipitation (mm) (c) at station A755 for December, 28th.

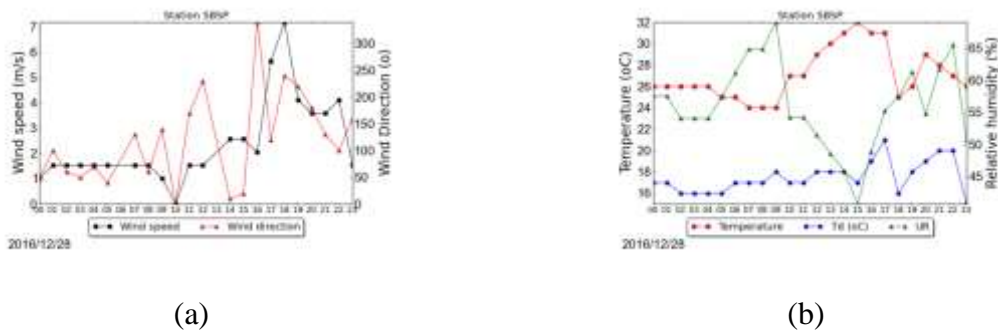
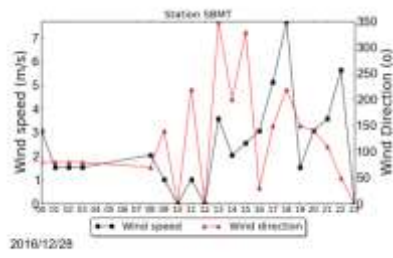
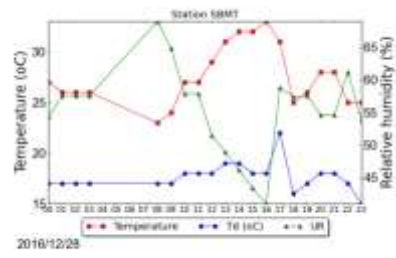


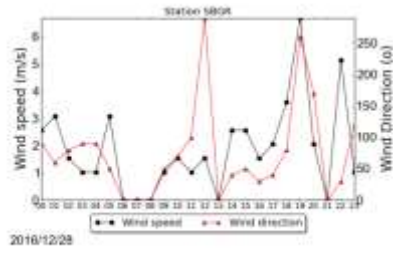
Figure 4-206: Wind speed ($m s^{-1}$) and direction, temperature, (°C) dew point temperature (°C), and relative humidity(%) for METAR at stations SBSP (a), (b), SBMT (c), (d), SBGR (e), (f), SBTA (g), (h), for December, 28, 2016.



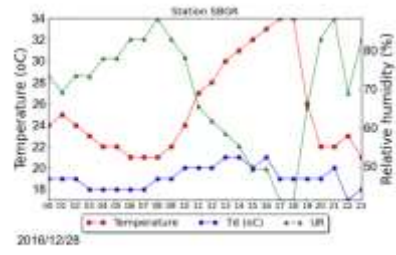
(c)



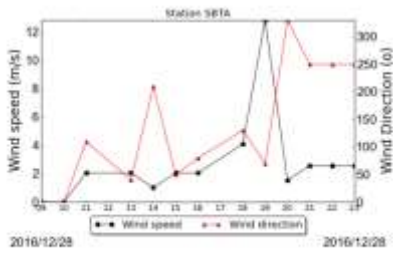
(d)



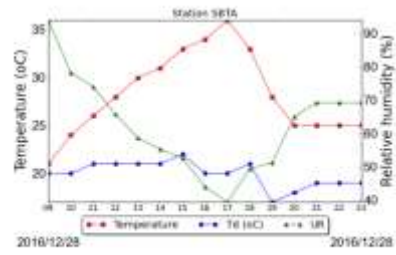
(e)



(f)

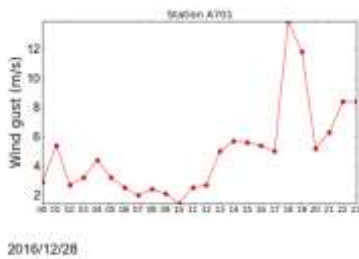


(g)

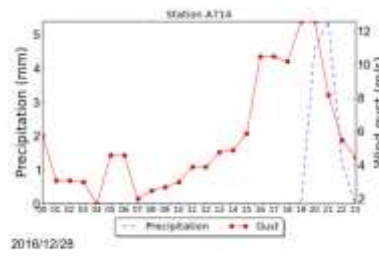


(h)

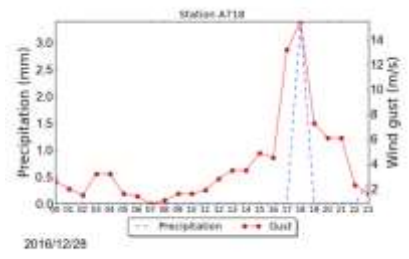
Figure 4-206: Continuation.



(a)



(b)



(c)

Figure 4-207: Precipitation (mm) and wind gust (m s^{-1}) at station A701 (a), A714 (b), A718 (c), A726 (d), A728 (e), A739 (f), A741 (g) for December, 28th.

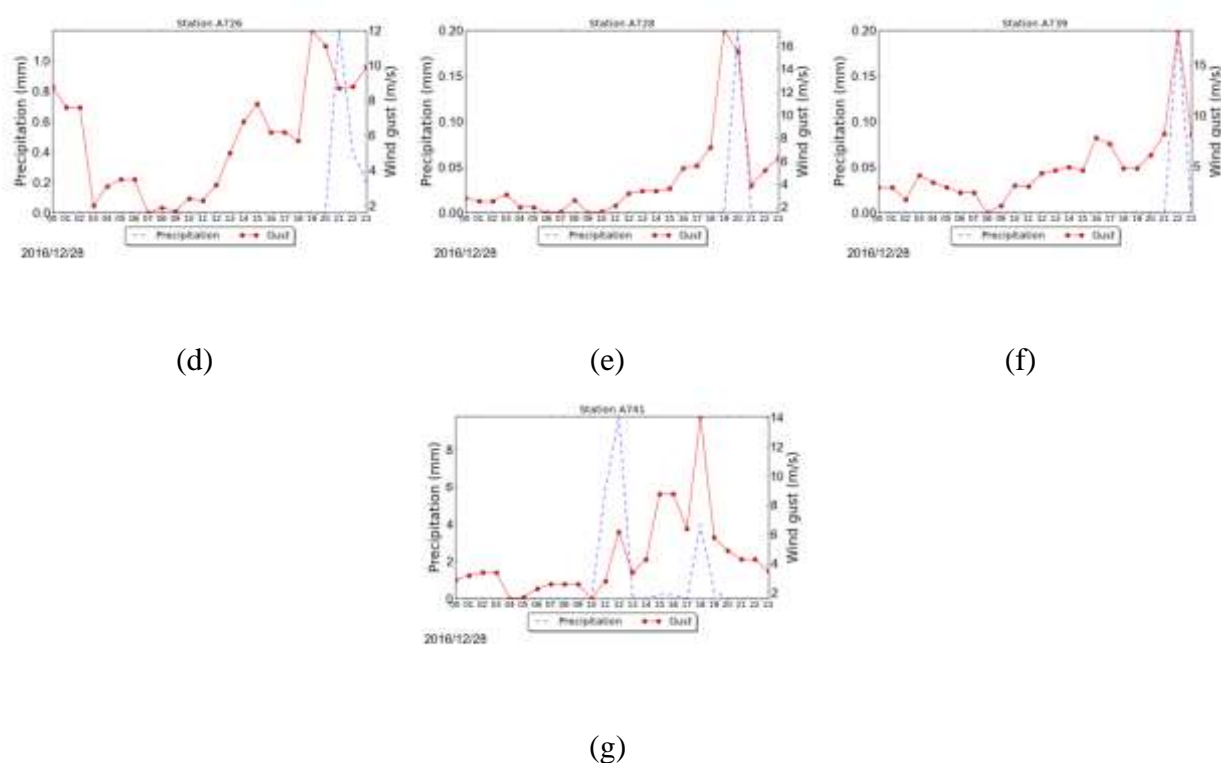


Figure 4-207: Continuation.

Only one station, A705, did not record maximum temperatures above 30 °C, although this station recorded 29.9 °C. The highest value observed was 34.9 °C at station A728, at the northeast region of the State. These high temperatures are related to the synoptic pattern observed at 500 hPa.

4.2.5 Partial conclusion for category 2

Four events were selected at this category; they were all related to occurrences of hail. On December, 28th, 2016 hail caused damage to crops. Only one event did not register the occurrence of flash floods, December, 25th, 2016. This event was only related to severe weather occurrence in Campinas. Strong wind gusts were reported on December, 28, 2016 in the region of Campinas, São José dos Campos e Garatinguetá, leading to fall of trees. Campinas, on December, 25th, 2016 also registered strong wind gusts of around 26.8 m s⁻¹ leading to fall of trees. In the city of São Paulo, 7 point of flash flood was registered on December, 18th and 28th, 2016. On February, 22th, 2017, 27 points were reported.

In the satellite analysis for South America, it is possible to see the absence of a large scale system affecting the State, in all events. The importance of the topography is also seen in the satellite analysis. Further evidence of the topography is seen in the radar analysis. Convection initiation was seen in the region of Serra do Mar and Serra da Mantiqueira. The presence of sea breeze was also important in the initiation for this category.

The synoptic scale analysis confirmed the absence of a large scale system affecting the State of São Paulo, which could lead to a favorable environment. During December, 28th, 2016 and January, 22th, 2017 a high pressure system is seen in the level of 500 hPa, which causes subsidence and inhibits convection. A high pressure system at this same level develops after 12:00 UTC on December, 25th, 2016, between São Paulo and Paraná. Mass divergence at 200 hPa, was only seen in the region on February, 22th, 2017, between 12:00 and 18:00 UTC, values were around $0.2-0.4 \cdot 10^{-4} \text{ s}^{-1}$. Warm advection at 850 hPa was observed at 12:00 UTC near the region of Campinas on December, 18th and near São Paulo on February, 22th.

In the BRAMS analysis it was possible to see, more clearly, around 14:00 and 15:00 UTC a moisture gradient and a moisture convergence near the coast identifying the sea breeze, except on December, 28th, due to the fact that BRAMS output was not available for this event. Winds turning to southeast and propagating into the continent was also seen in the BRAMS analysis. CAPE from the GFS output indicated conditions between marginally and moderately unstable conditions. LI, also from GFS, indicated an unstable condition with probable storm, even severe in the presence of some lifting mechanism. Atmospheric sounding was only available for one event, February, 22. CAPE indicated the same condition, and it was equal to 278.1 J kg^{-1} , LI was equal to -0.83 K and indicated a slightly unstable condition. CIN was -88 J kg^{-1} . These parameters do not point to a severe storm development, which makes this event interesting. Comparing CIN from the sounding with the GFS output, the second underestimated the parameter. The 700-500 hPa lapse rate was between $5.5 -6 \text{ K}$

km^{-1} at 12:00 UTC, except for December, 18th, which was around 6.5 -7 K km^{-1} . At 15:00 UTC it increased on February, 22th and December, 28th, to 6.0-6.5 K km^{-1} .

Dry air was observed in the sounding for February, 22th, between 10-20 % around the levels of 600-500 hPa. From the GFS, relative humidity was around 40-60 % between these levels for all events. Around the same range was seen near the top of the BRAMS output. Lower values were seen around the levels of 400-300 hPa, between 10-30 % for December, 18th and December, 28th. Strong wind gusts were observed on December, 25th and 28th, therefore it is not possible to make a conclusion regarding the presence of dry air in the atmosphere and strong wind gusts at the surface for this category.

Winds were weak through the atmosphere and no significant shear was observed, it is important to affirm that this analysis was only visual, no method was applied to calculate wind shear, due to the absence of atmospheric sounding on most events. Winds turning anticlockwise and intensifying with height were only seen on February, 22th, this indicates the presence of warm advection.

It was possible to see the importance of the afternoon in storms development during these events. All events occurred during days with high temperatures, above 29 °C. According to Johnson and Mapes (2001), the sea breeze does not, usually, trigger convection in its whole extension. This is seen in this category, in which the sea breeze was observed during all events, especially on February, 22th, convection only developed in the city of São Paulo, which could be related to the urban heat island effect.

5 CONCLUSION AND FUTURE STUDIES

During the present work ten cases of severe convective storms were selected during summer 2016/2017. They were separated into three different categories; the first two were related to strong synoptic condition (1a and 1b) and the third was related to weak synoptic condition (2). Events related to strong synoptic forcing were then divided into related to the northwest flow (SACZ or humidity convergence zone), and related to another feature (e.g., fronts, upper level cyclonic vortices).

The classification was done in order to try to verify the importance of the large scale on storms development in the region and differences between convection related only to regional features. Three events were identified as category 1a, also three as category 1b and four in the last category. During these events, several severe weather occurrences and damages were reported. The classification was made using satellite images to verify the presence of a large scale system, and synoptic fields from GFS were analyzed to understand the large scale environment.

Heavy rain leading to flash floods was observed in the events, with the exception of December, 25th. In the city of São Paulo, 26 points were observed on January, 07th, 36 on February, 06th, 57 on February, 24th and 22 on February, 22th. Also, on January 15th and 16th the highest accumulated precipitation in 24 hours in 68 years at Mirante de Santana was observed, with a total of 113.4 mm, and 64.6 mm in one hour. Only 7 points were seen on December 18th and 28th, and 1 on December, 03th. This indicates a connection between heavy rain and events related to strong synoptic forcing.

Hail was registered in all events of category 2 in different cities, even damages related to hailstorm was reported on December, 28th. Strong wind events were observed in several events, and it does not appear to be related to a category.

Important features were noticed in the satellite and radar images related to the surface characteristics, including the relevance of the topography in the region. This was particularly important in category 2, in which storm initiation was related to Serra da Mantiqueira, between southeast Minas Gerais and northeast São Paulo, and to the sea breeze. However, this was also observed on January, 30th and 07th (1b) and February, 24th (1a).

The northwest flow was identified on all events of category 1a on the 850 hPa level. An upper level cyclonic vortex was present on January, 30th, moisture was extending from a frontal system through a trough near the coast of the State of São Paulo, adding moisture to the east region on January, 07th, and finally on February, 06th, a band of clouds in the continent propagating with a frontal system appeared to have initiated convection. This was also seen on the night of January 15th, although the northwest flow moved, and was directed, at this period, to the State of São Paulo. This led to the most severe occurrence regarding accumulated precipitation. Interestingly, the sea breeze penetrated earlier in the continent and rain had already been observed on January, 15th in the city of São Paulo.

On February, 22th and December, 28th a high pressure system was seen in the region on the 500 hPa analysis, causing subsidence and inhibiting convection. A high pressure system also developed after 12:00 UTC on the other two events of the same category (December, 18th and 25th). The convective suppression is evident on February, 22th, only a few cells developed in the State, still heavy rain led to 27 points of floods in the city of São Paulo. This could be related to a coupling between the sea breeze circulation and the urban heat island.

On December, 03th a low pressure system is seen in the south region of the country on low levels, the northwest flow is seen directed to the State of São Paulo at 12:00 UTC, convective initiation was not clear during this event. On February, 24th the sea breeze penetrated into the continent, and it was seen at the surface analysis at the city of São Paulo, but it did not advance further due to the northwest flow.

Vorticity advection at 500 hPa was not seen in any of the events. Warm advection at 850 hPa appeared to be more relevant during the analysis; it was seen on December, 03th (at 12:00 UTC), 18th (at 12:00 UTC) February, 22th (at 06:00 UTC), January, 16th (at 12:00 UTC) and 30th (between 09:00 and 15:00 UTC). Values were around 0.2 to $0.8 \cdot 10^{-4} \text{ K s}^{-1}$, values above $1.0 \cdot 10^{-4} \text{ K s}^{-1}$ was seen on December 03th and January, 16th. Considering that severe weather occurrences were seen on January, 15th and 16th, less than half of the events occurred in a region with warm advection, considering this it is not possible to make a conclusion about this parameter.

Mass divergence at 200 hPa was observed on December 03th (at 06:00 UTC), January, 07th (at 12:00 UTC) and 30th (at 06:00, 09:00 and 15:00 UTC), February, 22th (12:00 UTC) and 24th (00:00 and 06:00 UTC), values were ranging from 0.2 to $0.6 \cdot 10^{-4} \text{ s}^{-1}$. Again, it is not possible to make a conclusion about this parameter.

Analysis of the thermodynamic indices, CAPE, LI and CIN, it was possible to see, from atmospheric sounding and the GFS output, values of CAPE indicated a condition between marginally and moderately unstable at 12:00 and 15:00 UTC. LI indicated an unstable condition with probable storm, even severe in the presence of some lifting mechanism. Values of LI indicating a slightly unstable condition were seen in the atmospheric sounding on February, 22th. CAPE derived from the sounding during this day was equal to only 278.15 J kg^{-1} and CIN was equal to -88 J kg^{-1} . CIN from atmospheric sounding for January, 30th and February 24th were equal to -90.56 J kg^{-1} and -82.79 J kg^{-1} . Analysis of CIN from GFS and BRAMS at 12:00 showed that the models did not represent this value well, comparing to the atmospheric sounding. However, it is important to notice that only three events were compared. Also, on February, 22th, values from the BRAMS at 11:00 UTC seemed to be closer to the sounding parameter. LI indicating a very unstable condition was seen on December, 03th, in a region of intense convection seen in the satellite analysis.

Regarding the occurrence of strong wind gusts, three events that recorded strong wind gusts had values of relative humidity below 10 % at some level, between 600 and 500 hPa. According to the new several damages were observed related to strong wind gusts on December, 28th. However, on December, 03th, in which several stations recorded wind gusts above 15 m s^{-1} and even above 20 m s^{-1} , these values are seen before 12:00 UTC near the top of the BRAMS model. After, values are around 40-50 %. This makes a conclusion about the relation of dry air and strong wind gusts difficulty.

Values of 700-500 hPa lapse rate were very similar during the events; most of them had values between 5.0 and 6.0 K km^{-1} . The highest range was observed on December, 18th, between 6.5 and 7.0 K km^{-1} . December, 03th and February, 24th had values between 6.0 and 6.5 K km^{-1} . A relation between this parameter and the categories of the events or to a particular severe weather occurrence was not seen.

Winds near the surface were weak on most events, and no significant shear was observed in any of the events.

5.1 SUGGESTIONS TO FUTURE STUDIES

As future work suggestion it would be necessary to include the rest of the interesting cases of severe weather occurred in the area of SOS-CHUVA project during the summer 2016-2017. Besides, a more comprehensive selection of cases for other years would allow us to characterize an average behavior of severe weather occurrence in the state. Our work was based only on observed data from different sources available over the interest area. Modeling studies could be carried on in order to clarify important features of the thermodynamic and microphysical processes. Also, in our study we only analyze the observed cases, but no evaluation of the weather forecast for such cases was performed. That would be something very important for the nowcasting community.

6 REFERENCES

- ALBRECHT, Rachel I. et al. Where are the lightning hotspots on Earth?. *Bulletin of the American Meteorological Society*, v. 97, n. 11, p. 2051-2068, 2016.
- ALTINGER DE SCHWARZKOPF, M. L.; ROSSO, L. C. Severe storms and tornadoes in Argentina. In: *Preprints, 12th Conf. on Severe Local Storms, San Antonio, TX, Amer. Meteor. Soc.* 1982. p. 59-62.
- BENDER, A. Eventos de tempo severo associados às linhas de instabilidade sobre o estado de São Paulo. 105 p. Dissertação – Instituto de Astronomia, Geofísica e Ciências Atmosféricas, Universidade de São Paulo, São Paulo, 2012.
- BROOKS, Harold E.; LEE, James W.; CRAVEN, Jeffrey P. The spatial distribution of severe thunderstorm and tornado environments from global reanalysis data. *Atmospheric Research*, v. 67, p. 73-94, 2003.
- BYERS, Horace Robert; BRAHAM, Roscoe R. The thunderstorm: report of the Thunderstorm Project. *US Government Printing Office*, 1949.
- CARVALHO, L. M. V.;; LIEBMANN, B. The South Atlantic Convergence Zone: Persistence, Form, Extreme Precipitation and Relationships with Intraseasonal Activity. *Journal of Climate*, v. 17, n.1, p. 88-108, 2004.
- CARVALHO, Leila MV; JONES, Charles; LIEBMANN, Brant. Extreme precipitation events in southeastern South America and large-scale convective patterns in the South Atlantic convergence zone. *Journal of Climate*, v. 15, n. 17, p. 2377-2394, 2002.
- CENSO, I. B. G. E. Disponível em:< <http://www.censo2010.ibge.gov.br/>>. **Acesso em**, v. 14, 2017.
- COLQUHOUN, J. R. A decision tree method of forecasting thunderstorms, severe thunderstorms and tornadoes. *Weather and forecasting*, v. 2, n. 4, p. 337-345, 1987.

- COTTON, W. R. & ANTHES, R. A. *Storm and Cloud Dynamics*. Academic Press, 883 pp., 1989.
- COTTON, W. R. & PIELKE, R. A. *Human Impacts on Weather and Climate*, Cambridge University Press. 288 pp., 1995.
- CEPED, UFSC. Atlas brasileiro de desastres naturais 1991 a 2012: volume Brasil. Florianópolis, CEPED UFSC, 2013a.
- CEPED, UFSC. Atlas brasileiro de desastres naturais 1991 a 2012: volume São Paulo. Florianópolis, CEPED UFSC, 2013b.
- DOSWELL III, Charles A. The distinction between large-scale and mesoscale contribution to severe convection: A case study example. *Weather and Forecasting*, v. 2, n. 1, p. 3-16, 1987.
- DOSWELL III, Charles A. Severe convective storms—An overview. In: *Severe convective storms*. American Meteorological Society, 2001. p. 1-26.
- DOSWELL, Charles A. Societal impacts of severe thunderstorms and tornadoes: lessons learned and implications for Europe. *Atmospheric Research*, v. 67, p. 135-152, 2003.
- DOSWELL III, Charles A.; BOSART, Lance F. Extratropical synoptic-scale processes and severe convection. In: *Severe Convective Storms*. American Meteorological Society, 2001. p. 27-69.
- DOSWELL III, C. A.; CARACENA, F.; MAGNANO, M. Temporal evolution of 700–500 mb lapse rate as a forecasting tool—A case study. In: *Preprints, 14th Conf. on Severe Local Storms, Indianapolis, IN, Amer. Meteor. Soc.* 1985. p. 398-401.
- EMANUEL, Kerry A. Overview and definition of mesoscale meteorology. In: *Mesoscale Meteorology and Forecasting*. American Meteorological Society, 1986. p. 1-17.
- FAWBUSH, Ernest J.; MILLER, Robert C. The types of airmasses in which North American tornadoes form. *Bulletin of the American Meteorological Society*, p. 154-165, 1954.

- FREITAS, Edmilson Dias de. Circulações locais em São Paulo e sua influência sobre a dispersão de poluentes. 2003. Tese de Doutorado. Universidade de São Paulo.
- FREITAS, E. D.; ROZOFF, C. M.; COTTON, W. R.; DIAS, P. L. S. Interactions of an urban heat island and sea-breeze circulations during winter over the metropolitan area of Sao Paulo, Brazil. *Boundary-Layer Meteorology*, v. 122, n. 1, p. 43-65, Jan 2007.
- FREITAS, E. D; SILVA DIAS, P. L.; CARVALHO, V. S. B.; MAZZOLI, C. R. R.; MARTINS, L. D.; MARTINS, J. A.; ANDRADE, M. F. Factors Involved in the Formation and Development of Severe Weather Conditions over the Megacity of São Paulo. In: *89th American Meteorological Society Meeting*, Phoenix, AZ, United States, 10-15 January 2009.
- FUELBERG, Henry E.; BIGGAR, David G. The preconvective environment of summer thunderstorms over the Florida panhandle. *Weather and Forecasting*, v. 9, n. 3, p. 316-326, 1994.
- GAN, Manoel Alonso; RAO, Vadlamudi Brahmananda. Surface cyclogenesis over South America. *Monthly Weather Review*, v. 119, n. 5, p. 1293-1302, 1991.
- GANDU, A. W.; SILVA, FAM. Características ambientes durante a observação de ecos de radar na região leste do estado de São Paulo. In: *Congresso Brasileiro de Meteorologia. 1984*. p. 381-388.
- HELD, Gerhard; GOMES, Jorge Luis; NASCIMENTO, E. Forecasting a severe weather occurrence in the State of São Paulo, Brazil, on 24 May 2005: The Indaiatuba Tornado. In: *8th International Conference on Southern Hemisphere Meteorology and Oceanography, Foz do Iguaçu*. 2006. p. 24-28.
- HOLTON, James R. *An introduction to dynamic meteorology*. American Journal of Physics, v. 41, n. 5, p. 752-754, 1973.

- IBGE, 2010. CENSO 2010. Available at: <<https://censo2010.ibge.gov.br/>>. **Last access: 01/03/2018.**
- IBGE, 2015. Áreas Urbanizadas do Brasil 2015. Available at: <https://biblioteca.ibge.gov.br/visualizacao/livros/liv100639.pdf>. Last access: 01/03/2018.
- JAMES, Richard P.; MARKOWSKI, Paul M. A numerical investigation of the effects of dry air aloft on deep convection. *Monthly Weather Review*, v. 138, n. 1, p. 140-161, 2010.
- JOHNS, R. H. & DOSWELL, C. A. III Severe Local Storm Forecasting. *Weather and Forecasting*, 7, 588-612, 1992.
- JOHNSON, Richard H.; MAPES, Brian E. Mesoscale processes and severe convective weather. In: Severe Convective Storms. *American Meteorological Society*, 2001. p. 71-122.
- JORGETTI, T. A Zona de Convergência do Atlântico Sul e os processos oceânicos do Atlântico e do Pacífico. 2009. 169 f. 2009. Tese de Doutorado. Tese (Doutorado em Meteorologia) - Instituto de Astronomia, Geofísica e Ciências Atmosféricas, Universidade de São Paulo, São Paulo.
- LENTERS, J. D.; COOK, K. H. Summertime precipitation variability over South America: Role of the large-scale circulation. *Monthly Weather Review*, v. 127, n. 3, p. 409-431, 1999.
- LIGDA, Myron GH. Radar storm observation. In: *Compendium of meteorology*. American Meteorological Society, 1951. p. 1265-1282.
- LUDLAM, F. H. Severe local storms: A review. In: *Severe Local Storms*. American Meteorological Society, Boston, MA, 1963. p. 1-32.
- MADDOX, Robert A.; DOSWELL III, Charles A. An examination of jet stream configurations, 500 hPa vorticity advection and low-level thermal advection patterns

- during extended periods of intense convection. *Monthly Weather Review*, v. 110, n. 3, p. 184-197, 1982.
- MACHADO, L. A. T.; SILVA DIAS, M. A. F. Análise de uma Tempestade severa sobre a cidade de São Paulo: Um exemplo de interações entre diferentes escalas de movimento. In: *Congresso Brasileiro de Meteorologia*. 1982.
- MARKOWSKI, P.; RICHARDSON, Y. *Mesoscale meteorology in midlatitudes*. John Wiley & Sons, 2011.
- MASSAMBANI, Oswaldo; CARVALHO, LMV de; VAZQUEZ, M. A. Tornado ou microexplosão? Um diagnóstico via radar do evento de Itú-São Paulo. In: *Congresso Brasileiro de Meteorologia*. 1992. p. 763-768.
- MILLER, Robert C. Notes on analysis and severe-storm forecasting procedures of the Air Force Global Weather Central. *AIR WEATHER SERVICE SCOTT AFB IL*, 1972.
- MILLS G. A. & COLQUHOUN J. R. Objective Prediction of Severe Thunderstorm Environments: Preliminary Results Linking a Decision Tree with an Operational Regional NWP Model. *Weather and Forecasting*, 13, 1078–1092, 1998.
- MOLLER, A. R. Severe local storms forecasting. In: *Severe Convective Storms*, C. A. Doswell III (Ed.), *American Meteorological Society Monographs* v. 28, n. 50, p. 433-480, 2001.
- NASCIMENTO, E. L. Identifying severe thunderstorm environments in southern Brazil: analysis of severe weather parameters. In: *Preprints, 22nd Conf. on Severe Local Storms*. 2004.
- NASCIMENTO, E. L.; MARCELINO, I. P. V. O. Preliminary analysis of the 3 January 2005 tornadoes in Criciúma/SC. *Bull. Braz. Meteor. Soc.*, v. 29, p. 33-44, 2005.

- NEWTON, Chester W. Severe convective storms. In: *Advances in Geophysics*. Elsevier, 1967. p. 257-308.
- NOGUÉS-PAEGLE, Julia; MO, Kingse C. Alternating wet and dry conditions over South America during summer. *Monthly Weather Review*, v. 125, n. 2, p. 279-291, 1997.
- OLIVEIRA, A. P.; SILVA DIAS, L. Aspectos observacionais da Brisa Marítima em São Paulo, *Anais II Congr. Bras. Meteor*, v. 2, p. 18-22, 1982.
- ORLANSKI, I. A rational subdivision of scales for atmospheric processes. *Bulletin of the American Meteorological Society*, 56(5), 527-530, 1975.
- PALMÉN, Erik Herbert; NEWTON, Chester W. Atmospheric circulation systems: their structure and physical interpretation. *Academic press*, 1969.
- PEREIRA FILHO, Augusto José. Chuvas de verão e as enchentes na Grande São Paulo: El Niño, Brisa marítima e ilha de calor. In: *XI Congresso Brasileiro de Meteorologia, Rio de Janeiro, RJ. Anais... Soc. Bras. Meteorologia*. 2000.
- PEREIRA FILHO, A. J.; HAAS, R.; AMBRIZZI, T. Caracterização de Eventos de Enchente na Bacia do Alto Tietê por meio do Radar Meteorológico e da Modelagem Numérica de Mesoescala. In: *Anais do XII Congresso Brasileiro de Meteorologia, Foz do Iguaçu - PR, (CDROM)*, 2002.
- PEREIRA FILHO, Augusto José et al. Enchentes na região metropolitana de São Paulo: aspectos de mesoescala e avaliação de impactos. In: *XIII Congresso Brasileiro de Meteorologia*. 2004
- REBOITA, M. S. Ciclones Extratropicais sobre o Atlântico Sul: Simulação Climática e Experimentos Numéricos de Sensibilidade. 294 p. Tese – Instituto de Astronomia, Geofísica e Ciências Atmosféricas, Universidade de São Paulo, São Paulo, 2008.

- ROCKWOOD, Anthony A.; MADDIX, Robert A. Mesoscale and synoptic scale interactions leading to intense convection: The case of 7 June 1982. *Weather and Forecasting*, v. 3, n. 1, p. 51-68, 1988.
- ROMATSCHKE, Ulrike; HOUZE JR, Robert A. Extreme summer convection in South America. *Journal of Climate*, v. 23, n. 14, p. 3761-3791, 2010.
- SALES, F. H.; PEREIRA FILHO, Augusto José. Comparações entre aspectos observacionais e simulação numérica de uma linha de instabilidade simétrica de longa duração sobre o Estado de São Paulo. In: *Anais do XI Congresso Brasileiro de Meteorologia, Rio de Janeiro, Rio de Janeiro*. 2000. p. 1626-1634.
- SANTOS, Eliane Teixeira dos. Impactos econômicos de desastres naturais em megacidades: o caso dos alagamentos em São Paulo. 2013. Dissertação de Mestrado. Universidade de São Paulo.
- SEADE, 2014. Fundação Sistema Estadual de Análise de Dados. PIB dos Municípios Paulistas 2002-2014. Available at: <http://www.seade.gov.br/produtos/pib-municipal/>. Last access: 01/03/2018.
- SEADE, 2016. Fundação Sistema Estadual de Análise de Dados. PIB anual. Available at: <http://www.seade.gov.br/produtos/pib-anual/>. Last access: 01/03/2018.
- SILVA, H. S. Estudo da circulação associada a uma ilha de calor urbana com um modelo de simulação da brisa marítima. São Paulo, v. 86, 1986.
- SILVA DIAS, M. A. F. Sistemas de mesoescala e previsão de tempo a curto prazo. *Revista Brasileira de Meteorologia*, v. 2, p. 133-150, 1987.
- SILVA DIAS, M. A. F. Storms in Brazil. *Hazards and Disasters Series, Storms*, v. 2, p. 207-219, 1999.

- SILVA DIAS, M. A, F.; GRAMMELSBACHER, E. A. A POSSÍVEL OCORRÊNCIA DE TORNADO EM SÃO PAULO NO DIA 26 DE ABRIL DE 1991: UM ESTUDO DE CASO. *Revista Brasileira de Meteorologia*, v. 6, n. 2, p. 513-522, 1991.
- SILVA DIAS, M. A, F; MACHADO, Antonio Jaschke. The role of local circulations in summertime convective development and nocturnal fog in São Paulo, Brazil. *Boundary-Layer Meteorology*, v. 82, n. 1, p. 135-157, 1997.
- SILVA DIAS, M.A.F.; VIDALE, P.L. & BLANCO, C.M. Case study and numerical simulation of the summer regional circulation in São Paulo, Brazil. *Boundary-Layer Meteorology*, v. 74, n. 4, p. 371-388, 1995.
- SILVA DIAS, M. A. F., DIAS, J., CARVALHO, L. M. V., FREITAS, E. D., SILVA DIAS, P. L. Changes in extreme daily rainfall for São Paulo, Brazil. *Climatic Change*, 116(3-4): 705-722, 2013.
- TARIFA, JOSÉ ROBERTO; ARMANI, GUSTAVO. Os climas urbanos. Tarifa JR, Azevedo TR, organizadores. Os climas na cidade de São Paulo: teoria e prática. São Paulo: FFLCH/USP, p. 47-70, 2001.
- VELASCO, I. & FRITSH, J. M. Mesoscale Convective Complexes over the Americas. *Journal of Geophysical Research*, 92, 9591-9613, 1987.
- VEMADO, Felipe; PEREIRA FILHO, Augusto José. Severe weather caused by heat island and sea breeze effects in the metropolitan area of Sao Paulo, Brazil. *Advances in Meteorology*, v. 2016, 2016.
- VICENTE, E. C.; SANGIOLO, C. A.; PEREIRA FILHO, A. J. Características das precipitações convectivas intensas na area do radar meteorológico de São Paulo. In: *XII Congresso Brasileiro de Meteorologia*. 2002.

WEISMAN, Morris L.; KLEMP, Joseph B. Characteristics of isolated convective storms.

In: *Mesoscale meteorology and forecasting*. American Meteorological Society, Boston, MA, 1986. p. 331-358.

YOUNG, Carlos Eduardo Frickmann; AGUIAR, C.; SOUZA, E. Valorando Tempestades:

Custo econômico dos eventos climáticos extremos no Brasil nos anos de 2002–2012. *São Paulo: Observatório do Clima*, 2015.

ZIPSER, Edward J. et al. Where are the most intense thunderstorms on Earth?. *Bulletin of the*

American Meteorological Society, v. 87, n. 8, p. 1057-1071, 2006.